Probing the role of the Band 7 protein superfamily in the cyanobacterium *Synechocystis* sp. PCC 6803

Marko Boehm

Thesis submitted for the Degree of
Doctor of Philosophy of the University of London
and the Diploma of Imperial College

Division of Biology
Faculty of Natural Sciences
Imperial College London

2007

I hereby declare that this thesis, submitted in fulfilment of the requirements for the degree of Doctor of Philosophy of the University of London and the Diploma of Imperial College, represents my own work and has not been previously submitted to this or any other institute for any degree, diploma or other qualification.

_____

Marko Böhm

It is not what we don´t know that gets us into trouble.
It is what we know for sure, but just ain´t so.

Mark Twain (1835-1910)

Abstract

The Band 7 protein superfamily is found throughout nature and features the SPFH domain (**S**tomatin, **P**rohibitin, **F**lotillin and **H**flK/C) as a common motif. Despite intensive research, little is known about the functions of its member proteins. In *S. cerevisiae* mitochondria, prohibitin homologues form large, hetero-multimeric complexes with a FtsH protease and are implicated in the assembly of membrane protein complexes. Recently, the FtsH homologue (*slr0228*) found in the cyanobacterium *Synechocystis* sp. PCC 6803 has been shown to be important for the repair of the photosystem two (PSII) complex and the protection of the cell from the damaging effects of light. This thesis tests the hypothesis that the Band 7 proteins identified in the *Synechocystis* sp. PCC 6803 genome might interact with FtsH (Slr0228) and play an important physiological role in photoprotection, membrane protein assembly and PSII repair. Bioinformatic analyses revealed the presence of five Band 7 proteins in *Synechocystis* sp. PCC 6803, designated here as prohibitin (Phb) 1-5, that are only distantly related to other known prohibitin homologues and among each other. Immunoblotting experiments using monospecific polyclonal antisera, generated against *E. coli*-overexpressed protein, confirmed that Phb1 (*slr1006*), Phb2 (*slr1768*), Phb3 (*slr1128*) and Phb4 (*sll0815*) were membrane-anchored proteins that form large protein complexes. Membrane fractionation experiments revealed that Phb1 was present in the cytoplasmic and thylakoid membranes, whereas Phb2 and Phb3 were found mainly in the cytoplasmic membrane. Analyses using blue-native (BN) gel electrophoresis of specific single Band 7 gene inactivation mutants combined with immunoprecipitation experiments suggested that the complexes were homo-oligomeric. In the case of Phb3, single-particle electron microscopy experiments indicated that it forms a ring-like complex with a diameter of approximately 160 nm consisting of at least ten subunits. Co-immunoprecipitation experiments additionally revealed that Phb1 interacted with FtsH (slr0228) at low level, and possibly a subunit of the NDH-1 respiratory complex. Mutants lacking Phb2 seemed to be affected in phototaxis. A triple (ΔPhb1-3) and a quadruple (ΔPhb1-4) mutant were found not to be drastically impaired in their ability to repair PSII or to assemble photosynthetic and respiratory complexes. Thus, even though no physiological link between the Band 7 proteins of *Synechocystis* sp. PCC 6803 and the hypothesised role in photoinhibition could be established, this work provides the first detailed biochemical and mutational examination of Band 7 proteins in a cyanobacterium or any photosynthetic organism.

Acknowledgements

I sincerely thank my supervisor Prof. Peter Nixon for the opportunity to work on this interesting and challenging project. Throughout this work I experienced a good balance between academic guidance and freedom of research. I am deeply grateful for all that I have learned in your laboratory over the last four years.

I am very thankful for all the support and kindness I experienced from the members of the Nixon group, namely from Dr. Myles Barker, Dr. Emmanuel Franco, Dr. Mary Hamilton, Franck Michoux and Remco de Vries. Also, I would like to express my gratitude to all my colleagues in the Barber, Matthews, Nield and Saffell groups. All of you made my stay at Imperial College a pleasing memory and life experience.

I particularly appreciate the help and support I received during collaborations with colleagues from all over Europe. I am thankful for the help of Prof. Eva-Mari Aro, Dr. Uwe Kahmann, Dr. Josef Komenda, Dr. Jon Nield and Prof. Imre Vass. Special thanks go to Dr. Pengpeng Zhang who was a great help during my two-week stay at the University of Turku.

I thank the Division of Biology of the Imperial College London for the bursary I received to fund my research and life in London. In this context, I am also grateful for the references that Prof. Harry MacWilliams and Prof. Hugo Scheer provided, to help me get this bursary.

I am deeply indebted to my parents for their constant and loving support which always allowed me the luxury to let interest be my guide for the studies I pursued.

Finally, I thank Miriam for making me see life from a different perspective. Your support and love is an invaluable gift to me.

Table of contents

List of figures

List of tables

Abbreviations

1-D	one dimensional
2-D	two dimensional
A_0	chlorophyll 0
A_1	phylloquinone
A_X	absorbance at X (nm) wavelength
ADP	adenosine diphosphate
APS	ammonium persulphate
ATP	adenosine-5'-triphosphate
β-DM	n-dodecyl-β-D-maltoside
BisTris	bis(2-hydroxyethyl)-imino-tris(hydroxymethyl) methane
BN	blue-native
bp	base pairs
BSA	bovine serum albumin
cab	chlorophyll a/b binding
CF_0	chloroplast coupling factor 0
CF_1	chloroplast coupling factor 1
Chl	chlorophyll
COX	cytochrome oxidase
Ctp	C-terminal processing protease
CTP	cytosine-5'-triphosphate
cTP	chloroplastic transit peptide
Cyt b_{559}	cytochrome b_{559}
Cyt b_6f	cytochrome b_6f complex
DCBQ	2,6 dichloro-*p*-benzoquinone
DCMU	3-(3,4-dichlorophenyl)-1,1-dimethylurea
DegP	degradation protease P
DMSO	dimethyl sulfoxide
DNA	2'-deoxyribonucleic acid
DNP	1-3 dinitrophenylhydrazone
DNPH	2,4-dinitrophenylhydrazine
dNTP	2'deoxyribonucleoside triphosphate

ΔpH	proton gradient
DRM	detergent-resistant microdomains
EDTA	ethylenediaminetertraacetic acid
EM	electron microscopy
EtOH	ethanol
Fd	ferredoxin
Fe_{ci}	haem centre of cytochrome b_6
FeCN	ferricyanide
FNR	ferredoxin-NADP reductase
FPLC	fast protein liquid chromatography
FtsH	filament temperature sensitive H
g	gravitation, unit of gravity
GFP	green fluorescent protein
GST	glutathione *S*-transferase
GTP	guanine-5'-triphosphate
HF	high fidelity
Hfl	high frequency of lysogeny
HIR	hypersensitive induced reaction
His_X-tag	histidine tag (X represents the number of attached histidine residues)
HMW	high molecular weight
HSP	heat shock protein
HtrA	high temperature requirement A
hv	light
i-AAA	inter-membrane space facing mitochondrial FtsH family protease
IgG	immunoglobulin G
IPTG	isopropyl-ß-D-thiogalactopyranoside
kb	kilo base pairs
kDa	kilo Dalton
kV	kilo Volt
LB	Luria-Bertani medium
Lhca/b	light-harvesting complex a/b
LHCII	light-harvesting complex II
LMW	low molecular weight
M	molar

m-AAA	matrix facing mitochondrial FtsH family protease
MBP	maltose binding protein
MetOH	methanol
mRNA	messenger ribonucleic acid
mTP	mitochondrial targeting peptide
$NADP^+$	oxidised β-nicotinamide adenine dinucleotide phosphate
NADPH	reduced β-nicotinamide adenine dinucleotide phosphate
NDH	NADPH-dehydrogenase complex
NPQ	non-photochemical chlorophyll fluorescence quenching
NrtA	nitrate/nitrite transport system substrate-binding protein
OCP	orange carotenoid binding protein
OD_X	optical density at X (nm) wavelength
OEC	oxygen-evolving complex
P680	primary electron donor of photosystem II
P700	primary electron donor of photosystem I
PAA	polyacrylamide
PAGE	polyacrylamide gel electrophoresis
PCC	Pasteur Culture Collection
PBS	phosphate buffered saline
PC	plastocyanin
PCR	polymerase chain reaction
pD1	precursor D1 protein
PDB	protein data bank
Phe	pheophytin
PID	proliferation, ion and death
PQ	plastoquinone
PSI	photosystem I
PSII	photosystem II
Q_A	plastoquinone molecule bound to D2
Q_B	plastoquinone molecule bound to D1
qE	energy-dependent non-photochemical chlorophyll fluorescence quenching
qI	photoinhibition-related non-photochemical chlorophyll fluorescence quenching

qT	state-transition non-photochemical chlorophyll fluorescence quenching
qP	photochemical chlorophyll fluorescence quenching
RNA	ribonucleic acid
RNaseA	ribonuclease A
RO	reverse osmosis
ROS	reactive oxygen species
rpm	rounds per minute
RT	room temperature
Rubisco	ribulose 1,5-biphosphate carboxylase/oxygenase
S_{0-4}	manganese cluster water oxidation centre S-states 0-4
SbtA	sodium bicarbonate transporter A
SDS	sodium dodecyl sulphate
SPFH	stomatin, prohibitin, flotillin and HflK/C
TAE	tris-acetate-EDTA buffer
TCA	trichloroacetic acid
TE	tris-EDTA buffer
TEM	transmission electron microscopy
TEMED	N-N-N'-N'-tetramethylethylenediamine
TES	N-tris[hydroxymethyl]methyl-2-aminoethanesulfonic acid
TM	transmembrane
Tris	2-amino-2-hydroxy-methylpropane-1,3-diol
TTP	thymidine-5'-triphosphate
TW	terra (10^{12}) Watts
Tween-20	polyoxyethylene sorbitan monolaurate
UTR	untranslated region
UV	ultraviolet
v/v	volume per volume
VIPP1	vesicle inducing protein in plastids 1
w/v	weight per volume
WT	wild-type
WT-G	glucose-tolerant wild-type
X-Gal	5-bromo-4-chloro-3-indolyl-β-D-galactopyranoside

Chapter 1: General introduction

1.1 On the relevance of studying photosynthesis

The basis for the majority of life on planet Earth is dioxygen in the atmosphere, which began to accumulate after oxygenic photosynthesis was first exhibited by cyanobacteria (Blankenship and Hartman, 1998). Even though the geological circumstances under which the oxygen-rich atmosphere as we know it today has formed remain elusive, it is undisputed that it changed the course of evolution (Kerr, 2005). Chemical markers (Summons et al., 1999) and microfossil evidence (Kazmierczak and Altermann, 2002) suggest that oxygenic-photosynthesis-performing cyanobacteria occurred as early as 2.5-billion years ago. Since then this essential metabolic pathway has been conserved in cyanobacteria, algae and plants.

It is estimated that annually 100 billion tonnes of dry biomass, corresponding to an energy storage of approximately 100 TW-years, are produced by the intriguing conversion of light energy into biochemical energy, i.e. by photosynthesis (Barber, 2007). Nowadays, mankind in particular indirectly relies on photosynthesis for energy (biomass and fossil fuels), food and every-day materials. Furthermore, we are facing an urgent need to decrease our dependency on fossil fuels, since the supplies are ever-decreasing and their use for energy generation leads to the release of carbondioxide into the atmosphere and thus directly promotes global warming (Harries et al., 2001). Therefore, to generate the necessary 14 TW-years of energy that mankind requires annually (Barber, 2007), the exploitation of carbondioxide-neutral energy generated from water, wind and solar is on the rise. With a theoretically available annual global amount of 100,000 TW of solar energy (Barber, 2007), the sun outcompetes other alternative energy sources by far (water = ~ 4.6 TW; wind = 50 TW; de Winter and Swenson, 2006) and thereby offers the most promising solution to mankind's imminent energy and global warming problems.

Already part of this gigantic amount of energy is converted into biomass by photosynthesis, i.e. 100 TW-years on land that are stored as wood and fibre as well as 100 TW-years in the oceans that are directly fed into the food chain. However, to annually generate 20 TW-years of energy for mankind's consumption from biomass, given the rather low energy efficiency of biomass production at present, 30 % of the entire land mass of our planet would have to be cultivated (Barber, 2007). A similar

problem is encountered in the production of food for an ever-growing world population. For example, it has been calculated that the world rice production must increase annually by 1 % in order to meet future demands (Rosegrant et al., 1995). However, as the land suitable for agriculture is limited and to prevent environmental degradation and loss of biodiversity, the crucial part of any strategy to increase food production must come from greater yields on existing cropland, i.e. from an increase in the maximum yields of crops (Cassman, 1999; Khush and Peng, 1996; Tilman et al., 2002).

To increase the yields in biomass and from crops, it would be desirable to improve the efficiency of photosynthetic energy conversion (currently between 0.1 and 1%; Barber, 2007). One possible approach could be to limit a particular and long known aspect of photosynthesis, i.e. photoinhibition (see section 1.4; Ohad et al., 1984). Briefly, photoinhibition decreases the photosynthetic efficiency by causing irreversible damage to the PSII reaction centre due to excess light. Even though the influence of photoinhibition on photosynthetic losses has not yet been quantified, it could be significant where plants are exposed to constant high-light intensities in arid habitats (Horton, 2000).

Therefore, a good understanding of photosynthesis and specifically photoinhibition might help to increase biomass production and crop yields by providing the knowledge to genetically improve photosynthetic organisms. Furthermore, in the future, the knowledge from photosynthesis research might allow the development of an artificial energy-converting technology that exploits the principles of natural photosynthesis (Barber, 2007). In this study, the physiological role of the Band 7 proteins of *Synechocystis* sp. PCC 6803 was studied with a particular focus on their possible involvement in photoinhibition.

1.2 The model organism *Synechocystis* sp. PCC 6803

Synechocystis sp. PCC 6803 is a gram-negative, unicellular, non-nitrogen-fixing cyanobacterium and a ubiquitous inhabitant of freshwater. Since its genome has been completely sequenced (Kaneko et al., 1996) and because it is naturally transformable (Grigorieva and Shestakov, 1982), it is generally considered a useful tool for studying the genetics and biochemistry of cyanobacteria (Ikeuchi and Tabata, 2001). Moreover, *Synechocystis* sp. PCC 6803 contains photosynthetic components

and maintenance systems that are similar to those of chloroplasts, which make it an ideal model organism for photosynthesis research (Mullineaux, 1999). Another advantage to this particular field of science is the availability of different wild-type strains, one of which can be grown under photoheterotrophic growth conditions at the expense of glucose (Rippka et al., 1979; Williams, 1988).

1.3 Photosynthesis

1.3.1 General introduction to photosynthesis

Photosynthesis has been studied for several centuries and as early as 1779 Jan Ingenhousz discovered that light plays the key role. While a first basic equation that included all of the involved reactants could already be formulated by 1804, it took another 60 years to devise a minimal balanced chemical equation for photosynthesis (see Equation 1.1).

$$CO_2 + H_2O \Leftrightarrow (CH_2O) + O_2 \quad \textbf{(Equation 1.1)}$$

In 1931, Cornelis van Niel made an important contribution to photosynthesis research by proposing that both photosynthetic bacteria and plants exhibit similar metabolic processes in which a hydrogen donor (H_2A) is photodecomposed and where the released hydrogen is used in the dark for the enzymatically catalysed reduction of CO_2 to form carbohydrates (CH_2O; see Equation 1.2; Arnon, 1971).

$$2\,H_2A + CO_2 \Leftrightarrow (CH_2O) + 2A + H_2O \quad \textbf{(Equation 1.2)}$$

In general, two types of photosynthesis are distinguished, namely: oxygenic (i.e. aerobic) and anoxygenic (i.e. anaerobic). While the latter type is performed by green sulphur and purple bacteria, oxygenic photosynthesis is a characteristic feature of cyanobacteria, algae and plants. In the light-dependent reactions, protein complexes in the thylakoid membrane catalyse the splitting of water into oxygen, protons and electrons as well as the reduction of ferredoxin. The resulting electrons pass through the photosynthetic electron transport chain (see section 1.3.2) which ultimately leads to the generation of the high-energy compound ATP and the reduction equivalent NADPH (Arnon, 1971). In the light-independent reactions (also termed the Calvin-Benson cycle), the energy of ATP and the reducing power of NADPH contribute to the fixation of CO_2 into carbohydrates (see Figure 1.1; Calvin, 1962).

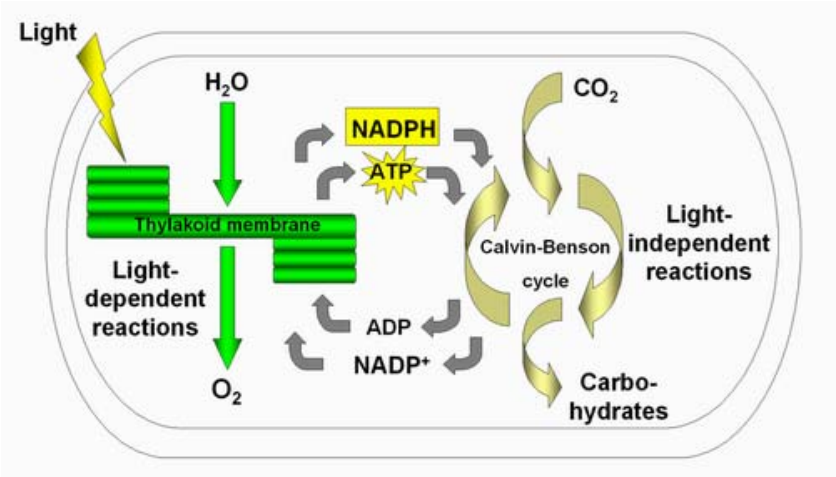

Figure 1.1: Schematic representation of oxygenic photosynthesis. The key reactants involved in the light-dependent and light-independent reactions of oxygenic photosynthesis are represented in this cartoon. For further details refer to text.

1.3.2 The linear electron transport of oxygenic photosynthesis

The capability of splitting water into oxygen, protons and electrons catalysed by the PSII protein complex is a unique feature of oxygenic photosynthesis. While dioxygen is being released as a by-product, the generated protons contribute to the generation of a pH gradient (ΔpH) across the thylakoid membrane, that is used to drive ATP production at the ATP synthase. The generated electrons on the other hand pass through a cascade of redox reactions from one protein complex of the photosynthetic electron transfer chain to another, namely from PSII to Cytochrome b_6f (Cyt b_6f) to PSI. Interestingly, the concept of electron flow between two photochemical systems in series, where the product of one become the substrate of the other, was already formulated in the 1960s (Hill and Bendall, 1960; Hill and Rich, 1983). While the absorption of photons at the PSII and PSI protein complexes elevates the electrons that are being fed into the photosystems to an energetically higher state and thereby drives the flow of electrons, the passage of electrons through the Cyt b_6f complex further increases the ΔpH at the thylakoid membrane by pumping protons from the stroma to the lumen. At PSI electrons are passed on to ferredoxin and in the subsequent reaction, catalysed by the ferredoxin-NADP reductase (FNR), $NADP^+$ is reduced to NADPH which can be used in the anabolic, carbohydrate-generating reactions of the Calvin-Benson cycle. This so-called Z-scheme of oxygenic photosynthesis is roughly outlined in Figure 1.2A, while detailed models of the protein complexes involved are shown in Figure 1.2B.

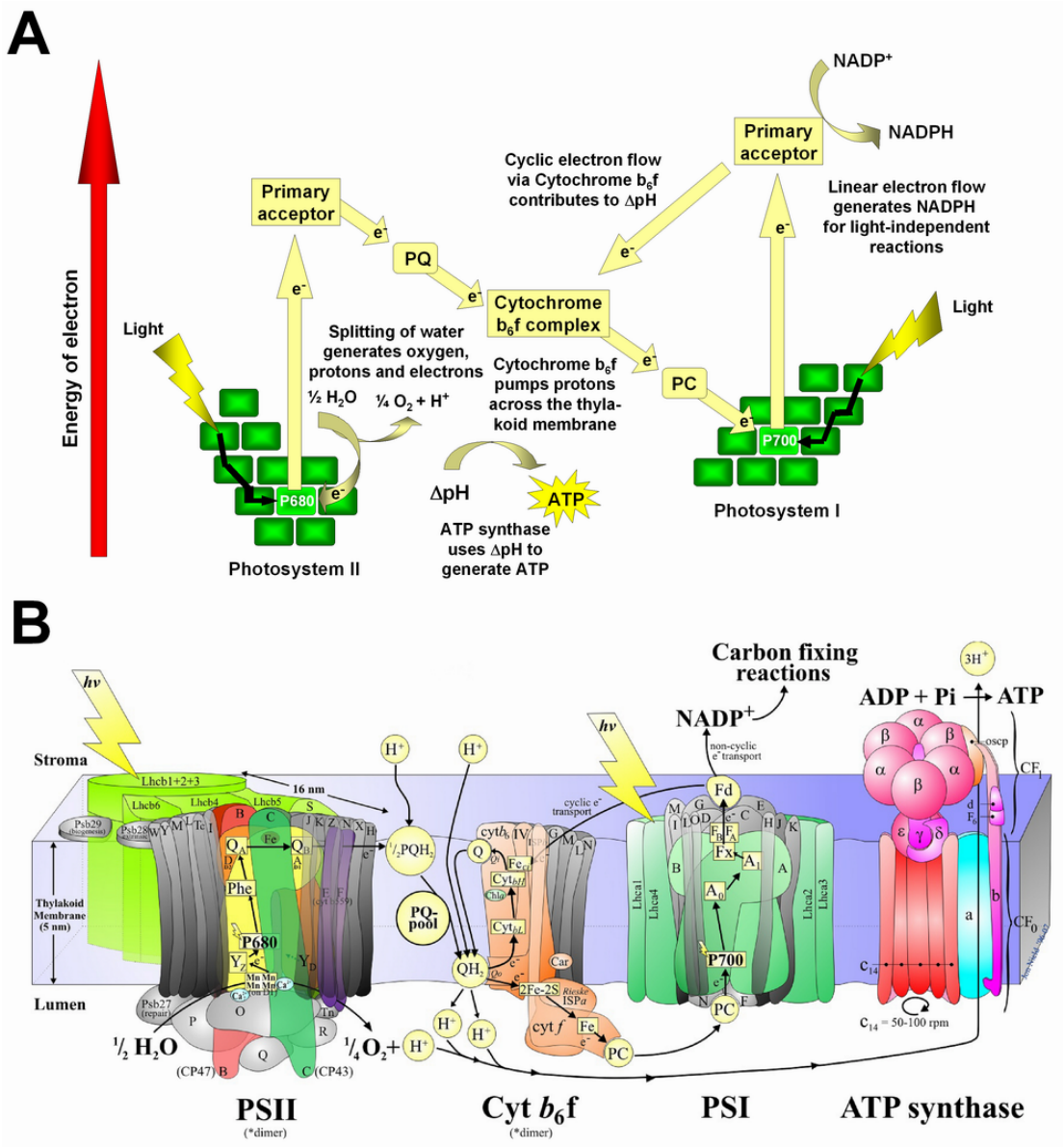

Figure 1.2: The electron transport chain of oxygenic photosynthesis in chloroplasts. (A) Schematic representation of the electron transport chain of oxygenic photosynthesis (Z-scheme). P680 and P700, primary electron donors of photosystem II and photosystem I respectively; e-, electron; PQ, plastoquinone; PC, plastocyanin. (B) Detailed model of the protein complexes (photosystem II, cytochrome b_6f, photosystem I) involved in the photosynthetic electron transport chain of higher plants and the ATP synthase, all of which are located in the thylakoid membrane. The protein complexes are labelled and their respective subunits annotated (e.g. A in PSII stands for PsbA and C in PSI stands for PsaC). Yellow arrows (hv) represent photons. The light-harvesting antennas of PSI and PSII are annotated as Lhca or Lhcb subunits respectively. PSII: Phe, pheophytin; Y_Z and Y_D, tyrosine Z and D; Q_A and Q_B, plastoquinone electron acceptors. Cytb$_6$f: Fe_{ci}, heme c_i of Cytb$_6$; Cyt b_H/Cyt b_L, cytochrome b high/low potential; Q, quinone molecule. PSI: A_0, chlorophyll 0; A_1, phylloquinone molecule; F_X/F_A/F_B, iron-sulphur centres; Fd, ferredoxin. ATP synthase: CF_0, chloroplast coupling factor 0; CF_1, chloroplast coupling factor 1. The figure in panel B was kindly provided by Dr. Jon Nield (Imperial College London, London, UK) (Nield (1997); updated 2006). For further details refer to text.

1.3.3 The major photosynthesis-related differences between chloroplasts and cyanobacteria

In both chloroplasts and cyanobacteria the light-dependent reactions of oxygenic photosynthesis, i.e. the photosynthetic electron transport chain, take place in the thylakoid membrane. However, even though the protein complexes involved (PSII, Cyt b_6f and PSI) share a remarkable functional and structural similarity, there are distinct differences in the arrangement of the thylakoid membranes (Andersson and Anderson, 1980; Mullineaux, 1999) and the components that act as the light-harvesting complexes for the reaction centres (Grossman et al, 1993; Grossman et al., 1995).

In chloroplasts, the thylakoid membrane is distinguished into disc-shaped stacks (grana or appressed lamellae) and interconnecting membranes (stroma or non-appressed lamellae) (Andersson and Anderson, 1980). This differentiation has functional implications, since a lateral heterogeneity of photosynthetic protein complexes can be observed, with the majority of PSII and light-harvesting protein complexes in the grana lamellae and PSI located to the stroma lamellae (Andersson and Anderson, 1980). The Cyt b_6f protein complex is evenly distributed (Allred and Staehelin, 1986). In *Synechocystis* sp. PCC 6803 on the other hand, the thylakoid membrane bilayer forms sheets following the periphery of the cell in three to ten concentric circles and converge at various sites near the cytoplasmic membrane (van de Meene et al., 2005). In general, the photosynthetic protein complex composition of cyanobacterial thylakoid membranes is rather homogenous, although a slight radial asymmetry, with more PSI protein complexes located to the outermost circles, has been detected (Sherman et al., 1994).

Another, fundamental difference is the type of antenna protein complex chloroplasts and cyanobacteria are using to maximise the amount of photons contributing to the photosynthetic electron transport chain (see Figure 1.3; Grossman et al., 1995). In chloroplasts, chlorophyll-a/b-containing integral thylakoid membrane proteins (light-harvesting complexes; LHCI for PSI and LHCII for PSII) function as antenna protein complexes (see Figure 1.3A), while phycobilisomes perform the light-harvesting in cyanobacteria (see Figure 1.3B). A phycobilisome is an assembly of biliproteins, where six biliprotein-rods are arranged in a fanlike-fashion around a central biliprotein-core. These antenna protein complexes are hydrophilic and peripherally attached to the stromal side of the thylakoid membrane, usually in close proximity to the photosystems (Grossman et al, 1993; Hankamer et al., 2001b).

1.3.4 The structure and function of PSII

Despite some fundamental differences associated with oxygenic photosynthesis between chloroplasts and cyanobacteria (see section 1.3.3), a structural comparison between the PSII complexes of spinach (Hankamer et al., 2001a) and *Thermosynechococcus elongatus* (Zouni et al., 2001) revealed striking similarities (Hankamer et al., 2001b).

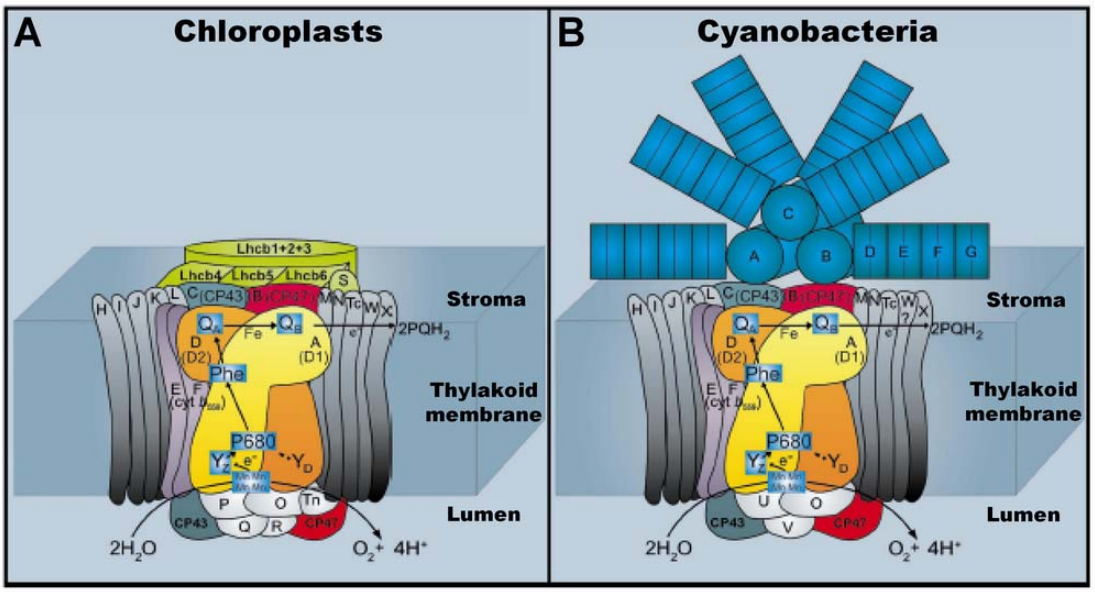

Figure 1.3: Detailed models of the PSII protein complexes of chloroplasts and cyanobacteria (adapted from Hankamer et al. (2001b)). (A) Schematic representation of a chloroplast PSII protein complex with a light-harvesting complex II (LHCII) antenna. (B) Schematic representation of a cyanobacterial PSII protein complex with an attached phycobilisome antenna. (A) and (B) The subunits and cofactors of the PSII protein complexes in both panels are labelled as in Figure 1.2. (A) It is noteworthy that the positioning of CP47 and the arrangement of the extrinsic subunits PsbO, PsbP, PsbQ and PsbR differs slightly from the more recent representation in Figure 1.2. (B) A to C represent allophycocyanin rods and D, E, F and G represent other phycobiliproteins. The electron transfer pathway from the splitting of water to the reduction of plastoquinone (PQH_2) is shown.

In both chloroplasts and cyanobacteria, the PSII protein complex consists out of more than 25 individual subunits (see Figure 1.3; Barber et al., 1997) and assembles into a dimer (see Figure 1.4; Hankamer et al., 2001b). Furthermore, the composition and arrangement of the major PSII core complex subunits, namely: D1, D2, Cyt b_{559}, CP43 and CP47, are remarkably similar (see Figure 1.3; Hankamer et al., 2001b). However, slight differences with respect to content and location of the low molecular mass (LMM) subunits have been noted (Hankamer et al., 2001b). The most evident differences are observed between the extrinsic subunits of the PSII protein complex

that make up the oxygen-evolving complex (OEC). In cyanobacteria the OEC is composed out of the PsbO (with an apparent molecular mass of 33-kDa), the PsbU (12-kDa) and the PsbV (cytochrome c_{550}; 13-kDa) subunits, while in chloroplasts the PsbU and the PsbV subunits have been replaced by the PsbP (23-kDa) and the PsbQ (17-kDa) subunits (see Figure 1.3; Shen and Inoue,1993; de las Rivas et al., 2004). Moreover, in chloroplasts, two additional extrinsic subunits, i.e. PsbR and $PsbT_n$, are reported to bind to the lumenal surface of the OEC (see Figure 1.3; Barber et al., 1997). However, even though the PsbP and PsbQ subunits have not been found to be associated with the OEC of the cyanobacterial PSII protein complex, cyanobacteria do encode respective homologues that may also bind to PSII (Kashino et al., 2002; de las Rivas et al., 2004; Thornton et al., 2004).

Only recently has the structure of the dimeric, hetero-multimeric PSII protein complex of the cyanobacterium *Thermosynechococcus elongatus* been solved by X-ray crystallography at a resolution of 3.5 angstrom (see Figure 1.4; Zouni et al., 2001; Ferreira et al., 2004). In that study, 16 integral membrane subunits with 35 transmembrane helices and three extrinsic, lumenal subunits could clearly be assigned to electron density. Characteristically, the PSII monomer displays a pseudo-twofold symmetry which relates the D1, CP47 and PsbI subunits to the D2, CP43 and PsbX subunits (see Figure 1.4B; Ferreira et al., 2004). Commonly, the D1/D2 heterodimer is referred to as the PSII reaction centre (RC) and most of the cofactors involved in primary charge separation and electron transfer are bound to these two subunits (Diner and Rappaport, 2002). The chlorophyll-binding proteins CP43 (PsbC; 14 chlorophylls) and CP47 (PsbB; 16 chlorophylls) serve as core antenna proteins, where CP43 is positioned on one side of the D1 protein, while CP47 flanks the D2 protein (see Figure 1.4B; Ferreira et al., 2004). Both the CP43 and CP47 subunits also interact via their lumenal loops with the extrinsic subunits PsbO, PsbU and PsbV of the oxygen-evolving complex (OEC) (Bricker and Franckel, 2002). The X-ray crystallography data further revealed that a cubane-like Mn_3CaO_4 cluster lies at the heart of the OEC of PSII with a fourth manganese ion peripherally attached (Ferreira et al., 2004). Functionally, the three extrinsic subunits (PsbO, PsbU and PsbV) provide the protein environment that stabilises the manganese cluster and maintains optimal levels of calcium and chloride ions which act as essential cofactors in the water oxidation reaction (Debus, 1992; de las Rivas et al., 2004).

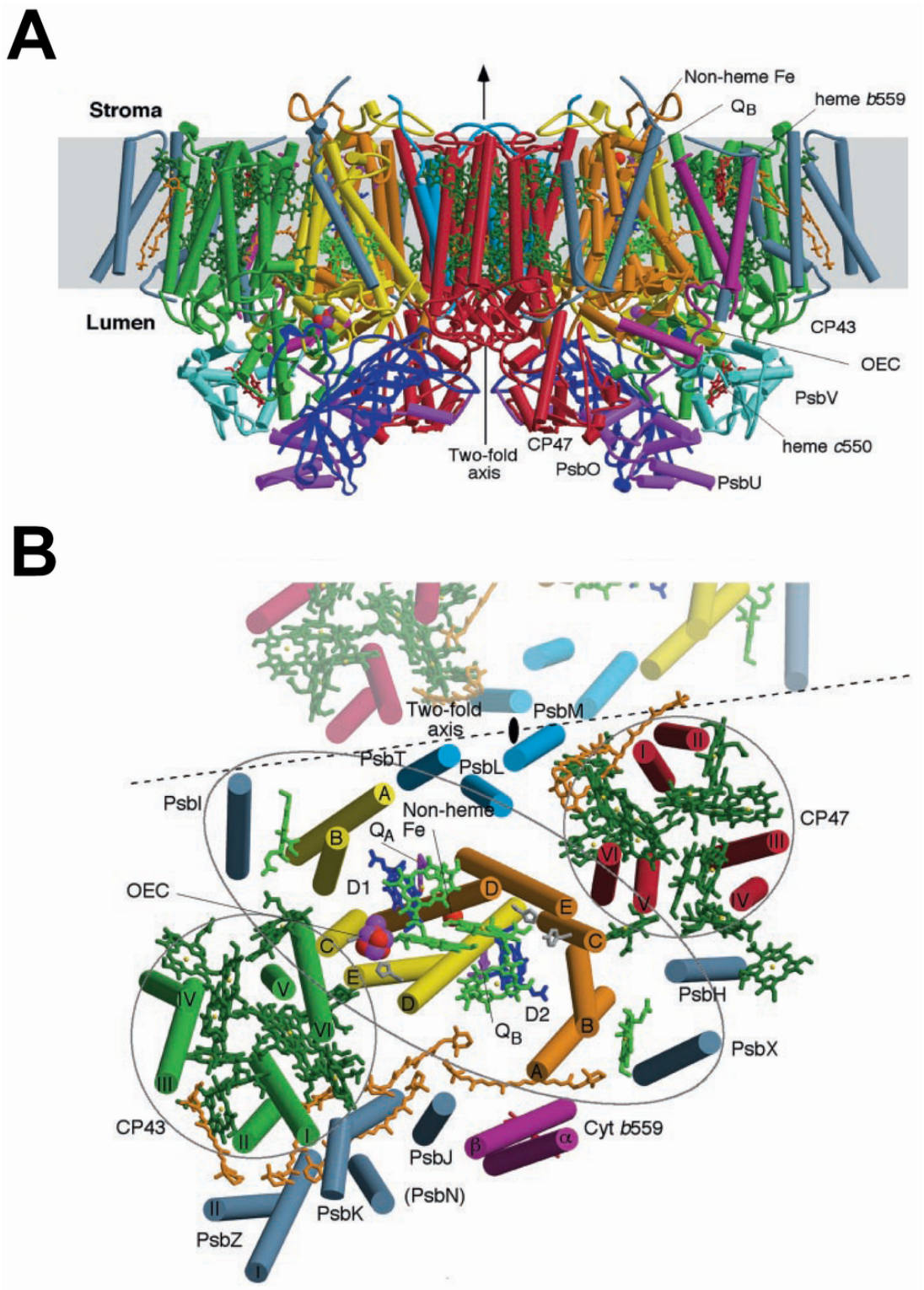

Figure 1.4: The structure of the cyanobacterial PSII complex (Ferreira et al., 2004). (A) Side-view ribbon diagram of a PSII dimer of *Thermosynechococcus elongatus*. The major PSII subunits and cofactors and the two-fold symmetry axis are labelled. Colouring: yellow, PsbA (D1); orange, PsbD (D2); red, PsbB (CP47); green, PsbC (CP43); blue, low molecular mass subunits; purple, Cytochrome b_{559}. (B) Top-view of one of the PSII monomers shown in panel A, where only the TM domains, chlorophylls (green), pheophytins (blue) and carotenoids (orange) are shown. The PSII subunits and cofactors are labelled and coloured as in panel A.

Interestingly, the assignment of three low-molecular-mass PSII subunits, namely PsbK as well as the α (PsbE) and β (PsbF) subunits of Cytochrome b_{559} (Ferreira et al., 2004), was in agreement with earlier studies (Zouni et al., 2001; Kamiya and Shen, 2003), while the positions of nine other low-molecular-mass subunits could be newly determined (see Figure 1.4B). Even though the PsbX protein was not present in the crystals of the preparation by Ferreira et al. (2004), it had previously been shown to be located adjacent to Cytochrome b_{559} (Cyt b_{559}) (Zouni et al., 2001; Kamiya and Shen, 2003). Both the PsbX and the PsbI subunits are believed to stabilise peripheral chlorophylls of the D1 (Chl_{ZD1}) and D2 (Chl_{ZD2}) proteins respectively (Ferreira et al., 2004). In accordance with their positions at the interface between the two PSII monomers the PsbL, PsbM and PsbT subunits have been implicated to be involved in PSII dimerisation (see Figure 1.4B; Ferreira et al., 2004; Iwai et al., 2004). The PsbJ, PsbK, putative PsbN (has only been tentatively assigned in the model) and PsbZ subunits are located at the periphery of CP43 (see Figure 1.4B) where these proteins have been suggested to aid the binding of carotenoids (Ferreira et al., 2004). The PsbH subunit is positioned between CP43, D2 and the PsbX subunit (see Figure 1.4B; Ferreira et al., 2004). Interestingly, inactivation of the PsbH subunit of *Synechocystis* sp. PCC 6803 lead to an increased sensitivity to high-light with a reduced rate of D1 turnover implying a role in the PSII repair cycle for this protein (Komenda and Barber, 1995).

The absorption of light at PSII and PSI drives the electron transport chain of oxygenic photosynthesis and provides the energy which is ultimately conserved in NADPH and ATP molecules (see Figure 1.1 and Figure 1.2). When a photon is absorbed by either the phycobilisome (Grossmann et al., 1995) or a core antenna protein (CP43 and CP47; Bricker and Franckel, 2002) of PSII, the resulting excitation energy is directly relayed towards P680 of the reaction centre. Here, at the reaction centre, the excited P680 state is delocalised over four chlorophylls (P_{D1}, P_{D2}, Chl_{D1} and Chl_{D2}) and initial primary charge separation occurs by the transfer of an electron from the D1-bound chlorophyll (Chl_{D1}) to pheophytin ($Pheo_{D1}$) leading to the formation of the the primary radical pair $P680^+/Pheo^-$ (Diner et al., 2001; Diner and Rappaport, 2002; Ferreira et al., 2004). Subsequently, the electron is passed on from the pheophytin radical ($Pheo^-$) to Q_A (a D2-bound plastoquinone) to the final electron acceptor Q_B (a D1-bound plastoquinone) (Diner and Rappaport, 2002; Ferreira et al., 2004). Once the thereby resulting Q_B^- semiquinone molecule has been reduced in the

same way by a second electron, it combines with two protons from the stroma to form plastoquinol (PQH_2) and is released into the thylakoid membrane (Trebst, 1978). Here the PQH_2 molecules accumulate to form the plastoquinone-pool which is used by the Cyt b_6f complex to pump protons across the membrane into the lumen and to reduce plastocyanin which then passes on the electrons to PSI (see section 1.3.2).

At the donor-side of PSII, primary charge separation results in an electron hole at P680 ($P680^+$) that needs to be filled, so that the photosynthetic electron transport chain remains functional. The necessary electron is provided by the OEC through performing the unique and remarkable feature of oxygenic photosynthesis, i.e. the water-splitting reaction. In the so called S-state cycle of the tetra-manganese cluster four electrons are extracted from two water molecules in four consecutive light-induced steps (Kok et al., 1970; Hoganson and Babcock, 1997; Barber, 2004). During each of these four steps one electron and one proton are extracted from the water molecules leaving dioxygen as a by-product at the end of the cycle. The S_0-state constitutes the ground state, where both water molecules are still fully reduced. When the system is in the S_1-state, the first electron has been transferred to tyrosine Z (Y_Z) and subsequently to $P680^+$ filling the electron hole, while the extracted proton contributes to the ΔpH that builds up across the thylakoid membrane (Hoganson and Babcock, 1997; Barber, 2004). Similarly, the S_2-, S_3- and S_4-states signify three further single extractions of an electron and a proton from those two water molecules. At the end of the cycle, in the S_4-S_0-transition, dioxygen is being released and two other water molecules enter the cycle.

1.4 Photoinhibition

Light is unique among the major climate variables in particular with respect to the possible speed and magnitude of its variation (Long et al., 1994). While in one moment the photosynthetic machinery of a leaf or cell can be exposed to intense illumination by the sun, in the next it can be in the shadow devoid of the energy light provides and vice versa. However, light usually represents a scarce resource for photosynthetic organisms and plants and cyanobacteria undertake a considerable effort to maximise the light available to photosynthesis by synthesising substantial amounts of antenna proteins. In most plants, the LHCII protein of the light-harvesting complex II of PSII can account for up to 50 % of the total thylakoid protein (Anderson, 1986),

while phycobilisome proteins of some cyanobacteria can make up up to 50 % of the soluble protein fraction of the cell (Grossmann et al., 1993). Nevertheless, even though light is essential for photosynthetic organisms, excess light causes damage to the photosynthetic reaction centre and in severe cases even to the cell itself. When excess light continuously stimulates the photosynthetic electron flow, free radicals and reactive oxygen species (ROS) are produced that can randomly react with surrounding proteins, pigments or lipids (Asada, 1999). However, the prime target in the thylakoid membrane is the D1 protein of the PSII reaction centre (Prasil et al., 1992; Aro et al., 1993b; Ohad et al., 1994) and several mechanisms for photoinhibition have been postulated (see section 1.4.1). In accordance with the complexity of the problem that light imposes, photosynthetic organisms have developed short- and long-term physiological responses to acclimate to the prevalent light conditions (see section 1.4.2), as well as a repair cycle that operates to re-establish the activity of damaged PSII (see section 1.5). In a situation where the protective mechanisms cannot completely avoid damage to the PSII reaction centre and the rate of damage exceeds the rate of PSII repair, the overall rate of photosynthesis declines, a phenomenon that is referred to as photoinhibition (Ohad et al., 1984).

1.4.1 Putative mechanisms for photoinhibition

Even though several theories that try to explain the underlying mechanisms of photoinhibition have been put forward within the last decades, the molecular details of photoinhibition *in vivo* are still unclear. Both the acceptor-side (see section 1.4.1.1) and the charge-recombination or low-light (see section 1.4.1.2) hypotheses are based on the damaging effects of singlet oxygen ($^1O_2$) (Vass et al., 1992; Keren et al., 1997). An alternative explanation, i.e. donor-side photoinhibition (see section 1.4.1.3), evolves around a non-functional OEC and a long-lived, highly oxidising $P680^+$ molecule (Chen et al., 1992). However, these three putative mechanisms are based on evidence from *in vitro* experiments on isolated PSII complexes or isolated thylakoid membranes (Nishiyama et al., 2006). Even though photodamage to PSII typically occurs before it is repaired, it is important to point out that the used *in vitro* material is impaired in the ability to repair damaged PSII and thus, it is unclear whether the observed effects mirror the situation in the living cell (Nishiyama et al., 2006). Nowadays, new methods that allow to separately monitor photodamage to and the

repair of PSII in both plants and cyanobacteria *in vivo* have been established (Gombos et al., 1994; Wada et al., 1994; Moon et al., 1995). As a result, it has recently been suggested that ROS are not directly responsible for photodamage to PSII, but rather inhibit its efficient repair and thereby contribute to photoinhibition in a two-step mechanism (see section 1.4.1.4; Hakala et al., 2005; Ohnishi et al., 2005).

1.4.1.1 The acceptor-side model for photoinhibition

Based on *in vitro* experiments, the acceptor-side model is one of the classic attempts to mechanistically explain photoinhibition (Vass et al., 1992; Barber and Andersson, 1992; Aro et al., 1993b; Long et al., 1994). Under strong illumination, the constant flow of electrons along the photosynthetic electron transport chain can lead to an over-reduced plastoquinone-pool, so that the possibility of a double reduction of the Q_A molecule is increased, leading to its dissociation from its binding site in the D2 protein (Styring et al., 1990; Vass et al., 1992). In that case, the excited electron of $Pheo^-$ of the primary radical pair ($P680^+/Pheo^-$) can not be passed on to Q_A and charge recombination, which results in an enhancement of P680 triplet states ($^3P680$), is more likely to occur (Vass et al., 1992). Under aerobic conditions, $^3P680$ molecules might transfer their energy to triplet oxygen ($^3O_2$) to produce singlet oxygen ($^1O_2$) which could then randomly react with the D1 protein of PSII leading to irreversible photodamage (see Figure 1.5). Interestingly, under anaerobic conditions, all these effects apart from the dissociation of the Q_A molecule from the D2 protein are reversible by the possible re-oxidation of the plastoquinones (Vass et al., 1992), so that this model fails to explain photoinhibition under anaerobic conditions (Hakala et al., 2005).

1.4.1.2 The charge-recombination model for photoinhibition

The charge-recombination or low-light model for photoinhibition (Keren et al., 1997) is conceptually similar to acceptor-side photoinhibition and refers to the observation that light-mediated damage of PSII and D1 protein turnover can also occur under low-light conditions (Mattoo et al., 1984). As a putative mechanism for this phenomenon, it has been suggested that excited electrons that have already been passed on to Q_A or even Q_B might flow as far back as to the S_2- or S_3-state of the S-state cycle of the OEC. Here, these electrons are believed to promote the formation of ROS that could then trigger D1 degradation (Keren et al., 1997).

1.4.1.3 The donor-side model for photoinhibition

The donor-side model is the second classic approach to explain photoinhibition based on *in vitro* evidence (Klimov et al., 1990; Barber and Andersson, 1992; Chen et al., 1992; Aro et al., 1993b; Long et al., 1994). At some point, the acidification of the lumen due to the establishing ΔpH across the thylakoid membrane is believed to inactivate OECs. Consequently, some electron holes that open upon the formation of the primary radical pair ($P680^+$/$Pheo^-$) cannot be filled and long-lived and highly oxidizing radicals such as $Y_Z^\bullet$ and $P680^+$ might form. Since these cofactor radicals have the capacity to extract electrons from their surrounding protein moiety, they could be the direct cause for the damage inflicted on the D1 protein in particular (see Figure 1.5) or the PSII protein complex as a whole (Klimov et al., 1990; Chen et al., 1992). It is noteworthy, that in contrast to the acceptor-side model, donor-side photoinhibition does not require oxygen.

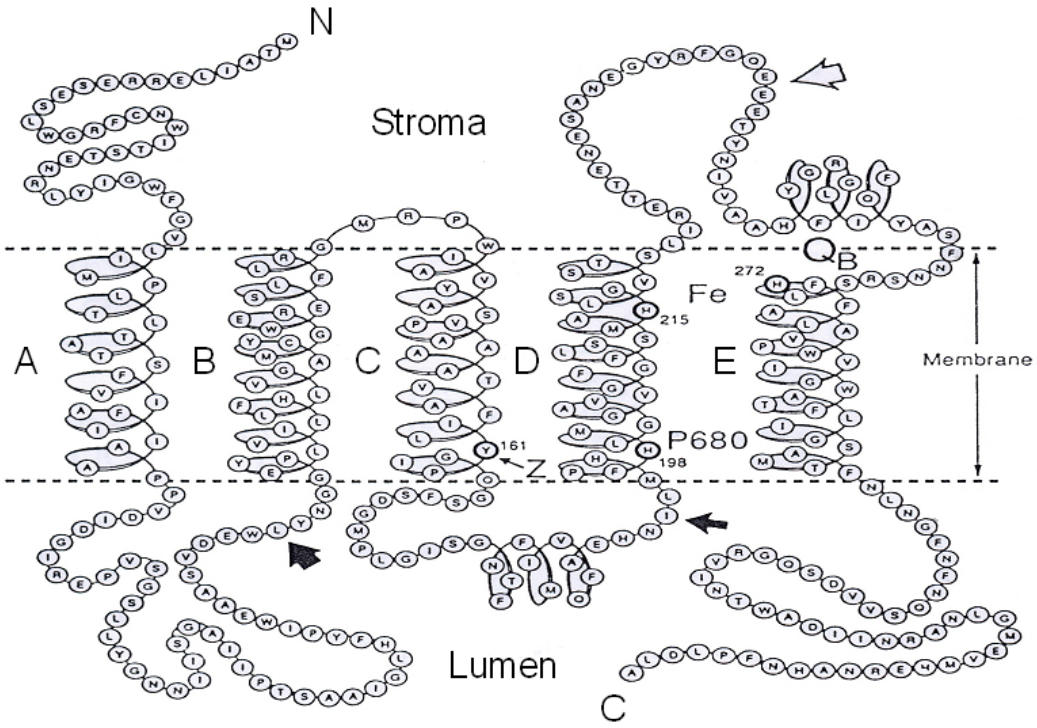

Figure 1.5: Schematic topology plot for the D1 protein of PSII (adapted from Barber and Andersson, 1992). This schematic drawing features the five transmembrane domains (A-E) that span the thylakoid membrane with the N-terminus facing the stromal and the C-terminus the lumenal side. Important components of the D1 protein are labelled: Tyrosine residue Z (Z); primary electron donor chlorophyll a (P680); Rieske iron-sulphur protein (Fe) and plastoquinone B binding pocket (Q_B). The white arrow marks the postulated cleavage site for acceptor-side photoinhibition. The black arrows indicate the postulated, cleavage sites for donor-side photoinhibition.

1.4.1.4 The two-step model for photoinhibition

While the acceptor-side (see section 1.4.1.1) and the charge-recombination or low-light (see section 1.4.1.2) models for photoinhibition attribute the light-mediated damage to PSII to the formation and action of ROS, the donor-side hypothesis (see section 1.4.1.3) holds an inactivation of the OEC of PSII responsible. However, these three, previously discussed putative models for photoinhibition are based on *in vitro* experiments on isolated PSII complexes or thylakoid preparations where photodamage to and repair of PSII complexes are typically impaired (Nishiyama et al., 2006). Thus, it is noteworthy that more recent *in vivo* studies on plants (Hakala et al., 2005) and cyanobacteria (Ohnishi et al., 2005) have lead to the formulation of another, two-step hypothesis for the underlying mechanisms of photoinhibition (Nishiyama et al., 2006).

Interestingly, previous studies have shown that photodamage to PSII is not due to the action of ROS (Hakala et al., 2005; Ohnishi et al., 2005), but that ROS rather inhibit the repair of PSII by suppressing the translation of proteins in general and of the D1 protein in particular (Nishiyama et al., 2001; Nishiyama et al., 2004). Additionally, the previously discussed models failed to conclusively explain the findings that photodamage to PSII occurs at any light intensity (Tyystjärvi and Aro, 1996), and that it can be observed even with an impaired electron flow (Allakhverdiev et al., 2005). In the recently hypothesised two-step model for photoinhibition, the primary damage is thought to be inflicted on the OEC of PSII by UV or strong blue light and that the subsequent absorption of light at photosynthetic pigments of the reaction centre leads to further, secondary damage (Onishi et al., 2005). More precisely, the primary damage event is believed to be the dislocation of manganese ions from the OEC upon the perception of light (Hakala et al., 2005), which is supported by the fact that the action spectrum of photodamage resembles those of model manganese compounds (Hakala et al., 2005; Onishi et al., 2005). The subsequent postulated mechanism is then similar to those formulated for the donor-side mechanism for photoinhibition, where long-lived and highly oxidizing $P680^+$ radicals are believed to inflict damage by randomly extracting electrons from their surroundings (see section 1.4.1.3). However, even though this theory manages to explain certain phenomena of photoinhibition that previous models failed to explain satisfactory, further studies are necessary to elucidate the exact mechanisms for primary and secondary damage.

1.4.2 Protective mechanisms against excess light

By definition, light constitutes an essential resource for photoautotrophs, although its absorption also inevitably inflicts damage on them (see section 1.4.1; Tyystjärvi and Aro, 1996; Asada, 1999). However, typically, light is in scarce supply for photoautotrophs and they undertake significant efforts to capture sufficient photons to drive the photosynthetic electron transport chain. Nevertheless, due to the possible, significant fluctuations in the availability of light (Long et al., 1994), it is impossible for them to have their photosynthetic machinery so precisely acclimated, that it can always use the entire amount of absorbed light energy. In a situation where a photoautotroph is acclimated to low light conditions and might suddenly experience high-light illumination or under constant high-light irradiation, it is vital that the organism can respond with a variety of short- and long-term mechanisms to minimise potential cellular damage (Long et al., 1994).

Usually, the light energy absorbed by photosynthetic pigments results in the excitation of chlorophyll molecules that can either pass on this energy for photochemistry, release it again by emitting light, i.e. chlorophyll fluorescence or by dissipating it as heat, referred to as non-photochemical quenching (NPQ). Apart from photochemistry, the processes that reduce chlorophyll fluorescence yields are considered as NPQ and divided according to their relaxation kinetics into three distinct categories, namely: energy-dependent quenching (qE; see section 1.4.2.1), state-transition quenching (qT; see section 1.4.2.2) and photoinhibitory quenching (qI; see section 1.4.2.3) (Müller et al., 2001). However, oxygenic photosynthetic organisms also direct excited electrons to alternative electron pathways where these electrons can be used for photochemistry other than the photosynthetic linear electron flow (see section 1.4.2.4). Furthermore, the production of ROS is an inevitable by-product of oxygenic photosynthesis and photoautotrophs maintain an inducible, efficient antioxidative system (see section 1.4.2.5; Asada, 1999). Physical responses, such as leaf (Abrams, 1990) or chloroplast (Brugnoli and Björkman, 1992) movement constitute obvious light avoidance strategies that cannot completely prevent, but do minimise potential damage (Kasahara et al., 2002).

1.4.2.1 The energy-dependent quenching (qE) of NPQ

In plants, energy-dependent quenching of chlorophyll fluorescence (qE) is the major contributor to non-photochemical quenching (NPQ) and constitutes the fastest

response to high-light conditions at a timescale of seconds (Horton and Ruban, 1992; Long et al., 1994; Demmig-Adams and Adams, 1996; Müller et al., 2001; Kanervo et al., 2005). Due to the water-splitting reaction at the OEC as well as the transfer of protons by the Cyt b_6f complex, photosynthetic electron transport leads to the formation of a ΔpH across the thylakoid membrane (see section 1.3.2). Under high-light illumination, electron transport is increased and the accompanying acidification of the chloroplast lumen results in the protonation and activation of the violaxanthin de-epoxidase which catalyses the conversion of violaxanthin to zeaxanthin via the intermediate antheraxanthin (Demmig-Adams and Adams, 1996). Zeaxanthin is a carotenoid capable of quenching the energy of excited chlorophyll molecules by absorbing their energy and subsequently dissipating it as heat (Demmig-Adams and Adams, 1996). Even though the extent of qE varies considerably from species to species, over 75 % of the absorbed photons can be dissipated as heat by some plants in this way (Demmig-Adams et al., 1996; Kanervo et al., 2005). Since the proximal antenna of PSII were found to only bind a small fraction of the total chlorophyll, but are enriched in the components of the xanthophyll cycle, it appears likely that the primary site for qE-mediated heat dissipation is in the antenna complexes (Demmig-Adams and Adams, 1996). In particular, protonation of the PsbS protein (see Figure 1.3A; a member of the chlorophyll a/b binding (cab) protein superfamily; note that cyanobacteria do not possess a PsbS homologue) and subsequent conformational changes in the LHCII have been implied to play a crucial role in qE (Ruban et al., 1993; Li et al., 2000). Even though the PsbS subunit of PSII has been identified as the likely site for qE in plants (Niyogi et al., 2005), the precise mechanism and some functional details of this NPQ component remain unresolved.

Interestingly, although cyanobacteria can synthesise zeaxanthin from β-carotene (Demmig-Adams and Adams, 1996), the fact that a dissipation of the ΔpH at the thylakoid membrane does not reduce their NPQ implies that they do not exhibit a chloroplast-like qE response (Campbell and Öquist, 1996). Nevertheless, in recent studies, ΔpH-independent antenna-related NPQ mechanisms that seem to enable cyanobacteria to dissipate excess excitation energy and quench chlorophyll fluorescence have been identified (Cadoret et al., 2004; Ihalainen et al., 2005; Wilson et al., 2006). These mechanisms seem to involve the CP43´ protein, the translation product of the *isiA* gene and a homologue of the PSII core antenna protein CP43 (Burnap et al., 1993). Typically, the expression of the CP43´ protein can be induced by

iron deficiency (Burnap et al., 1993; Yousef et al., 2003) as well as oxidative or high-light stress (Yousef et al., 2003; Havaux et al., 2005b), which leads to the formation of CP43´ rings around trimeric or monomeric PSI, where these rings act as peripheral antennas (Bibby et al., 2001a; Bibby et al., 2001b). Even though it has been proposed that CP43´ might also serve as an antenna protein for PSII (Tetenkin et al., 1998), a direct connection between PSII and CP43´ has never been reported (Ihalainen et al., 2005). A first mechanism, that has been observed in the early stages of iron depletion, is that blue-light converts CP43´ into an efficient excitation energy sink (Cadoret et al., 2004) and recent findings suggest that the orange carotenoid protein (OCP) might be the photoreceptor and mediator in this photoprotective energy dissipation mechanism (Ihalainen et al., 2005; Wilson et al., 2006). Interestingly, after prolonged iron starvation, also 'empty' CP43´ or IsiA rings (without PSI) are detected (Yeremenko et al., 2004), that could be demonstrated to represent strongly quenched states and might be involved in a second photoprotective mechanism (Ihalainen et al., 2005). While the blue-light inducible mechanism might serve to adjust the extra excitation energy that is provided by the CP43´ antenna rings (Cadoret et al., 2004), the CP43´ aggregates may be important for photoprotection under more severe iron depletion or oxidative stress conditions (Ihalainen et al., 2005).

1.4.2.2 The state transition quenching (qT) of NPQ

If excess light continuous to flow over a period of minutes, oxygenic photoautotrophs react by acclimating the size and positioning of their light-harvesting antennas (Anderson, 1986; Reuter and Müller, 1993; Melis,1999; Kanervo et al., 2005). In plants, the regulation of antenna size involves alteration of light-harvesting complex gene expression (Escoubas et al., 1995) and/or LHC protein degradation (Lindahl et al., 1995). Similarly, in cyanobacteria, the size of phycobilisomes is decreased and the gene expression of phycobilisome genes is modified in response to high-light stress (Reuter and Müller, 1993).

Another, short-term acclimation response that occurs within minutes of exposure to high-light is generally referred to as state transitions (Murata, 1969). Interestingly, while state transitions in plants and algae display a certain degree of similarity, although conceptually similar, the underlying molecular mechanisms seem to differ significantly in cyanobacteria (Mullineaux and Emlyn-Jones, 2004). Typically, state transitions constitute a shuttling of light-harvesting complexes from

one photosystem to another, and while transfer of antenna complexes from PSII to PSI corresponds to state 2, the reverse process is termed state 1 (Gal et al., 1997; Allen and Forsberg, 2001; Mullineaux and Emlyn-Jones, 2004; Kanervo et al., 2005). This redistribution of antenna complexes is believed to be mediated by the redox-state of the plastoquinone-pool, which, when reduced, leads to the activation of a protein kinase that then phosphorylates light-harvesting complexes (Gal et al., 1997; Allen and Forsberg, 2001; Kanervo et al., 2005). While in *Arabidopsis thaliana* and *Chlamydomonas reinhardtii* the STN7 and the Stt7 protein kinases have respectively been identified to be the likely LHCII phosphorylating enzymes (Bellafiore et al., 2005; Depege et al., 2003), it has not been proven that phosphorylation is required for phycobilisome transfer in cyanobacteria (Mullineaux and Emlyn-Jones, 2004). However, phosphorylation of LHCII protein complexes at PSII in the grana lamellae of chloroplasts triggers their migration towards the stroma lamellae, where they are ultimately transferred to PSI. Interestingly, even though it seems to be generally accepted that this migration is initiated and driven by electrostatic repulsion, alternatively, it has been suggested that conformational changes within the phosphorylated LHCII subunits might be another explanation (Allen, 1992).

Overall, the contribution of state transition quenching (qT) to NPQ in plants and cyanobacteria is considered without significance for photoprotection, while in algae qT plays an important role (Krause and Weis, 1991; Niyogi et al., 1999; Müller et al., 2001; Kanervo et al., 2005). More specifically, in plants, only 15 to 20 % of the LHCII trimers are involved in state transitions (Kanervo et al., 2005), so that this physiological response is only perceived as an elegant mechanism to balance the flux of excitation energy between the two photosystems. In *Chlamydomonas*, however, up to 80 % of the antenna complexes can participate in state transitions, so that a substantial redistribution of light-harvesting complexes might increase the performance of PSI and thereby act as a switch from linear to cyclic electron transfer (see section 1.4.2.4; Kanervo et al., 2005). Initially, qT was also believed to play an important role in NPQ of cyanobacteria, since, in contrast to plants, there was little evidence for qE in these organisms and because their NPQ closely correlated with state 2 transition (see section 1.4.2.2; Campbell and Öquist, 1996). However, in the meantime, it could be revealed that state transitions in cyanobacteria are rather required for the acclimation to low-light conditions and play no role in the prevention of photodamage (Emlyn-Jones et al., 1999; Mullineaux and Emlyn-Jones, 2004).

1.4.2.3 The photoinhibitory quenching (qI) of NPQ

Even though oxygenic photoautotrophs have evolved a variety of response mechanisms to minimise oxidative damage under high-light conditions, photodamage to the photosynthetic apparatus is inevitable (Tyystjärvi and Aro, 1996). Typically, an exposure to prolonged, severe high-light stress leads to quenching of chlorophyll fluorescence and a decrease in the oxygen evolution capacity of PSII, a phenomenon referred to as photoinhibition (see section 1.4.1). Thus, photoinhibition contributes as photoinhibitory quenching (qI) to NPQ and characteristically displays the slowest relaxation kinetics of the three NPQ components (Long et al., 1994; Müller et al., 2001).

Generally, within hours after relief from the high-light stress, chlorophyll fluorescence and oxygen evolution capacity of PSII slowly recover due to the actions of an elaborate but efficient PSII repair mechanism (see section 1.5; Aro et al., 1993a; Nixon et al., 2005). Since the D1 protein of PSII binds most of the essential cofactors for primary charge separation (see Figure 1.3), this protein is particularly vulnerable to irreversible damage and constitutes the main target for light-induced damage (Nixon et al., 2005; Kanervo et al., 2005). Remarkably, while the majority of the PSII subunits appear to be recycled, the D1 protein of damaged PSII protein complexes is selectively and rapidly turned over, and newly synthesised copies are incorporated into reassembling PSII complexes (Aro et al., 1993a; Nixon et al., 2005). Furthermore, in plants, the PSII repair cycle operates in the stroma thylakoids and it has been suggested that non-functional PSII protein complexes, for which no repair sites are yet available, might 'linger' in the grana thylakoids where they could act as strong energy sinks and thereby protect their functional neighbours (Aro et al., 1993a; Kettunen et al., 1997; Lee et al., 2001; Matsubara and Chow, 2004; Kanervo et al., 2005).

Cyanobacteria on the other hand feature an additional acclimation mechanism to high-light and UV-B stress associated with the composition of their PSII protein complexes (Clarke et al., 1993; Campbell et al., 1998). While the *psbA* gene is typically present as a single copy in higher plants and algae (Zurawski et al., 1982), most cyanobacteria possess three copies of the *psbA* gene (Golden et al., 1986). For example, in *Synechococcus* sp. PCC 7942, these three *psbA* genes encode two D1 proteins, i.e. D1:1 (encoded by *psbA1*) and D1:2 (encoded by *psbA2* and *psbA3*) (Golden et al., 1986; Campbell et al., 1998). During acclimated growth, the D1:1 protein is primarily transcribed and incorporated into the PSII reaction centres. However, a shift to high-light conditions or exposure to UV-B leads to an increased

expression of the *psbA2* and *psbA3* genes, so that the D1:2 protein becomes preferentially incorporated into PSII complexes until the cells have acclimated to the new growth conditions (Golden et al., 1986; Clarke et al., 1993; Clarke et al., 1995; Campbell et al., 1998). The significance of exchanging the D1 protein of PSII is based on the fact that the D1:2 protein exhibits a faster rate of turnover, which increases photoinhibitory quenching (qI) and thus allows faster recovery from photodamage (Campbell et al., 1998; Komenda et al., 2000; Sippola and Aro, 2000).

1.4.2.4 Dissipation of energy into alternative electron pathways

The energy of photons absorbed at the light-harvesting complexes of PSII and PSI usually fuels photosynthetic linear electron transport (LET) that leads to the generation of NADPH and ATP which are used in the Calvin-Benson cycle to assimilate CO_2 and generate carbohydrates (see section 1.3.1). However, particularly under stress conditions, the absorbed energy might also be diverted into alternative electron pathways, which thereby help to reduce photodamage.

Photorespiration is one of these alternative metabolic pathways, that are capable of maintaining LET by diverting the absorbed light energy (Niyogi, 1999; Badger et al., 2000; Wingler et al., 2000). Typically, the ribulose-bisphosphate carboxylase/oxygenase (rubisco) enzyme fixes CO_2, but, particularly under CO_2 limiting conditions, it is also capable of using dioxygen as a substrate, to then form 2-phosphoglycolate and 3-phosphoglyceric acid (Wingler et al., 2000). In general, photorespiration is considered a wasteful, competitive process to CO_2 assimilation, although it provides metabolites for other metabolic processes and blocking it leads to photoinhibition and oxidative damage (Niyogi, 1999; Wingler et al., 2000). However, in cyanobacteria, photorespiration is less relevant due to different kinetic properties of their rubisco enzymes, which are mirrored in a reduced oxygenase activity at ambient oxygen levels that is even further decreased by the efficient carbon concentrating mechanisms that most cyanobacterial strains possess (Badger et al., 2000).

The water-water cycle (also known as the Mehler-ascorbate peroxidase reaction or pseudocyclic electron transport) is another alternative oxygen-dependent electron pathway that is typically used by plants during high-light stress (Asada, 1999; Asada, 2000; Badger et al., 2000; Kanervo et al., 2005). In this mechanism, electrons that have passed through the LET chain via the PQ pool are directly transferred from PSI to dioxygen. The resulting highly reactive superoxide radicals ($O_2^{\bullet -}$) are ultimately

converted into water and ascorbic acid by the actions of the superoxide dismutase and the ascorbate peroxidase. Thus, even though neither NADPH nor dioxygen are being generated in this water-water cycle, it maintains LET and contributes to the generation of ΔpH for ATP synthesis as well as to the qE chlorophyll fluorescence quenching mechanism.

Furthermore, cyclic electron transport (CET) pathways within PSII and around PSI have been proposed (Hanley et al., 1999; Munekage et al., 2004). CET within PSII occurs when long-lived $P680^+$ species are formed due to an impaired or inactive OEC that failed to fill the electron hole resulting from primary charge separation. Several different electron pathways have been proposed to prevent random oxidation by $P680^+$ (Thompson and Brudvig, 1988; Hillmann and Schlodder, 1995; Hanley, 1999), but the branched pathway, where electrons are passed from either Chl_Z or Cyt b_{559} to a carotenoid and then ultimately to the $P680^+$ cation, is currently the favoured one (Faller et al., 2001). When PSI excitation energy is dissipated via a CET pathway, reduced ferredoxin or NADPH pass on electrons to plastoquinone and subsequently to the Cyt b_6f complex, which contributes to the formation of ΔpH which in turn is also used for ATP synthesis (see Figure 1.2A) and down-regulation of PSII activity by the qE mechanism (see section 1.4.2.1) (Munekage et al., 2004; Shikanai et al., 2002; Kanervo et al., 2005). Overall, while CET within PSII has not been proven and only been reported feasible in cyanobacteria (Vasil´ev et al., 2003), PSI CET-mediated ATP synthesis appears to also play an important role for ATP synthesis in these organisms (Kanervo et al., 2005).

Chlororespiration represents another alternative electron pathway, and cross-talk between the photosynthetic and respiratory electron transport chains is possible via the PQ-pool, which is shared as a common link (Berry et al., 2002; Peltier and Cournac, 2002). In higher plants (*A. thaliana*) and green algae (*C. reinhardtii*), chlororespiratory enzymes have been detected, but the role of chlororespiration remains unclear (Peltier and Cournac, 2002). Cyanobacteria also possess chlororespiratory enzymes and electrons could be fed into the PQ-pool by the actions of the NDH-1 and NDH-2 protein complexes that oxidise NADPH and NADH respectively, as well as by the succinate dehydrogenase that oxidises succinate (Cooley and Vermaas, 2001). However, for photoprotection the oxidation of the PQ-pool by terminal oxidases which transfer electrons to oxygen to form water and thereby constitute alternative electron sinks might be more relevant. In cyanobacteria, the

cytochrome c oxidase (CtaI) represents the major terminal oxidase and is being reduced by the Cyt b_6f complex (Howitt and Vermaas, 1998), while the Cytochrome bd type oxidase can directly obtain electrons from the PQ pool (Berry et al., 2002). Nevertheless, in the light, because of the comparatively low rates of electron flow of chlororespiration relative to that of photosynthesis, these alternative electron routes probably play only a minor role in photoprotection (Peltier and Cournac, 2002).

1.4.2.5 Protection against reactive oxygen species (ROS)

Since the excitation energy of absorbed photons might be transferred from chlorophyll molecules of the light-harvesting complexes to dioxygen, there is a constant source for damaging singlet oxygen ($^1O_2$) (Knox and Dodge, 1985; Zolla and Rinalducci, 2002). Furthermore, oxygen might act as a final electron acceptor of the photosynthetic electron transport chain at the donor-side of PSI (see section 1.4.2.4) and thereby form superoxide radicals ($O_2^{\bullet -}$) which could then be converted into hydrogen peroxide (H_2O_2) and into hydroxyl radicals (•OH) (Asada, 1999). Thus, even though a direct involvement of ROS as the damage-inducing component in photo-inhibition can probably be excluded (Hakala et al., 2005; Nixon et al., 2005; Ohnishi et al., 2005), thylakoid membrane proteins, including the PSII protein complex, and other cellular components are still prone to ROS-mediated oxidative damage.

As protection, both plants and cyanobacteria possess efficient, inducible antioxidative systems, i.e. the ROS-scavenging enzymes superoxide dismutase and ascorbate peroxidase that reduce the levels of various ROS to tolerable levels by a water-water cycle (see section 1.4.2.4; Asada, 1999; Kim and Suh, 2005). Moreover, certain antioxidants such as β-carotene and α-tocopherol aid to minimise cellular damage even under non-stress conditions (Asada, 1999; Havaux et al., 2005a). Generally, cyanobacteria and algae display a higher H_2O_2 tolerance compared to higher plants which is mirrored by their capability to actively excrete H_2O_2 and because they possess certain ROS-resistant enzymes (Takeda et al., 1995; Tamoi et al., 1998; Badger et al., 2000).

1.5 The PSII repair cycle

Light is essential to oxygenic photoautotrophs, but also causes damage at any intensity, that is hence inevitable (Tyystjärvi and Aro, 1996). The main target for

irreversible photodamage, particularly under high-light conditions, is the PSII protein complex in the thylakoid membrane, more specifically its D1 reaction centre subunit that holds the majority of cofactors involved in primary charge separation (see Figure 1.3; Prasil et al., 1992; Aro et al., 1993b; Ohad et al., 1994). In order to counteract this damage, eukaryotic photoautotrophs, i.e. chloroplast-containing plants and algae (see section 1.5.1) as well as cyanobacteria (see section 1.5.2) have evolved efficient PSII repair cycles whose molecular details are, despite intensive research, still elusive (Aro et al., 1993a; Melis, 1999; Kanervo et al., 2005; Nixon et al., 2005). It is noteworthy, that particularly the proposed mechanisms for D1 degradation are controversial and differ significantly between the PSII repair cycles that have been described for chloroplasts and cyanobacteria. Therefore, the two-protease model based on *in vitro* evidence (see section 1.5.3; Aro et al., 1993b) and the FtsH-only model derived from *in vivo* experiments (see section 1.5.4; Nixon et al., 2005) that aim to explain D1 protein degradation will be presented in detail.

1.5.1 The PSII repair cycle in chloroplasts

The PSII repair cycle in chloroplasts constitutes an elaborate and efficient mechanism to restore the functional status of photodamaged PSII, but it must be noted that the presented schemes for the underlying mechanisms, particularly for D1 degradation, have been largely based on *in vitro* evidence (Aro et al., 1993b; Melis, 1999; Kruse, 2001). However, once a PSII protein complex has been inactivated by one of the putative mechanisms of photoinhibition (see section 1.4.1), a cascade of events occurs to counteract the damage and to minimise the effect of photoinhibition (see Figure 1.6).

Initially, the LHCII antenna complexes of photodamaged PSII-LHCII supercomplexes detach, and reversible N-terminal phosphorylation of certain PSII core proteins (D1; D2; CP43 and PsbH) leads to ‘trapped’ PSII dimers (Ikeuchi et al., 1987; Kruse et al., 1997; Kruse, 2001). The term ‘trapped’ PSII dimers refers to the fact these phosphorylated protein complexes remain in the grana lamellae, while the key events of the PSII repair cycle take place in the stroma lamellae (Barbato et al., 1992; Aro et al., 1993b). Interestingly, non-functional, phosphorylated PSII dimers have been implied to contribute to non photochemical quenching of chlorophyll fluorescence by acting as strong energy sinks and to thereby protect their functional neighbours (Lee et

al., 2001; Matsubara and Chow, 2004; Kanervo et al., 2005). It has also been postulated that the reversible phosphorylation of PSII dimers aims to prevent premature complex disassembly and D1 degradation, to enable a tight coordination between the rates of D1 protein degradation and synthesis (Aro et al., 1993a; Koivuniemi et al., 1995; Rintamäki et al., 1996). It is noteworthy, that recent mutagenesis studies in *A. thaliana* revealed that the reversible phosphorylation of PSII subunits might not be essential for PSII repair (Bonardi et al., 2005), although this finding is not in contradiction with the current model for the eukaryotic PSII repair cycle (see Figure 1.6). It should also be mentioned that LHC phosphorylation is not involved in the PSII repair cycle, but is rather associated with another light-mediated acclimation response, i.e. the redistribution of excitation energy between the two photosystems during state transitions (see section 1.4.2.2; Gal et al., 1997). Both the protein kinases that catalyse the phosphorylation events to induce state transitions and to promote the formation of 'trapped PSII dimers' are themselves regulated by the redox state of the PQ pool (Bennett, 1983; Kruse, 2001). In agreement with the postulated functional role of reversible phosphorylation in the PSII repair cycle, dephosphorylation of the phosphorylated subunits of 'trapped' PSII dimers has been found to be a prerequisite for the removal and degradation of damaged D1 proteins (Aro et al., 1993b; Koivuniemi et al., 1995; Rintamäki et al., 1996). This dephosphorylation triggers the monomerisation of 'trapped' PSII dimers, the dissociation of their CP43 core antenna protein as well as their extrinsic OEC subunits and the subsequent migration of both the CP43 protein and the remainder of the monomeric PSII complex to the stroma lamellae (Barbato et al., 1992; Aro et al., 1993b; Kruse et al., 1997; Kruse, 2001; Kanervo et al., 2005).

Once the RC47 subcomplex has reached the stroma lamellae, synchronised replacement, i.e. removal and proteolytic degradation of the damaged D1 protein coordinated with the integration of a newly synthesised copy of D1, occurs. Based on *in vitro* evidence, the initial concept for the removal and subsequent proteolytic breakdown of the D1 protein has been suggested to be catalysed by two different proteases that belong to the DegP and FtsH protease families respectively (Lindahl et al., 2000; Haußühl et al., 2001). While the DegP2 protease has been suggested to perform the initial cleavage at the stromal loop between helices D and E (see Figure 1.5) that results in the formation of 23- and 10-kDa proteolytic fragments, the role of the FtsH protease has been postulated to further degrade the 23-kDa fragment (Lindahl

et al., 2000; Haußühl et al., 2001). However, it is under debate whether this two-protease mechanism for the degradation of the D1 protein is physiologically relevant (Nixon et al., 2005), since results from *in vivo* experiments on cyanobacteria (Silva et al., 2003) and more recent findings on higher plants (Bailey et al., 2001; Bailey et al., 2002; Huesgen et al., 2006) rather favour the FtsH-only model (see section 1.5.2 and section 1.5.4; Nixon et al., 2005).

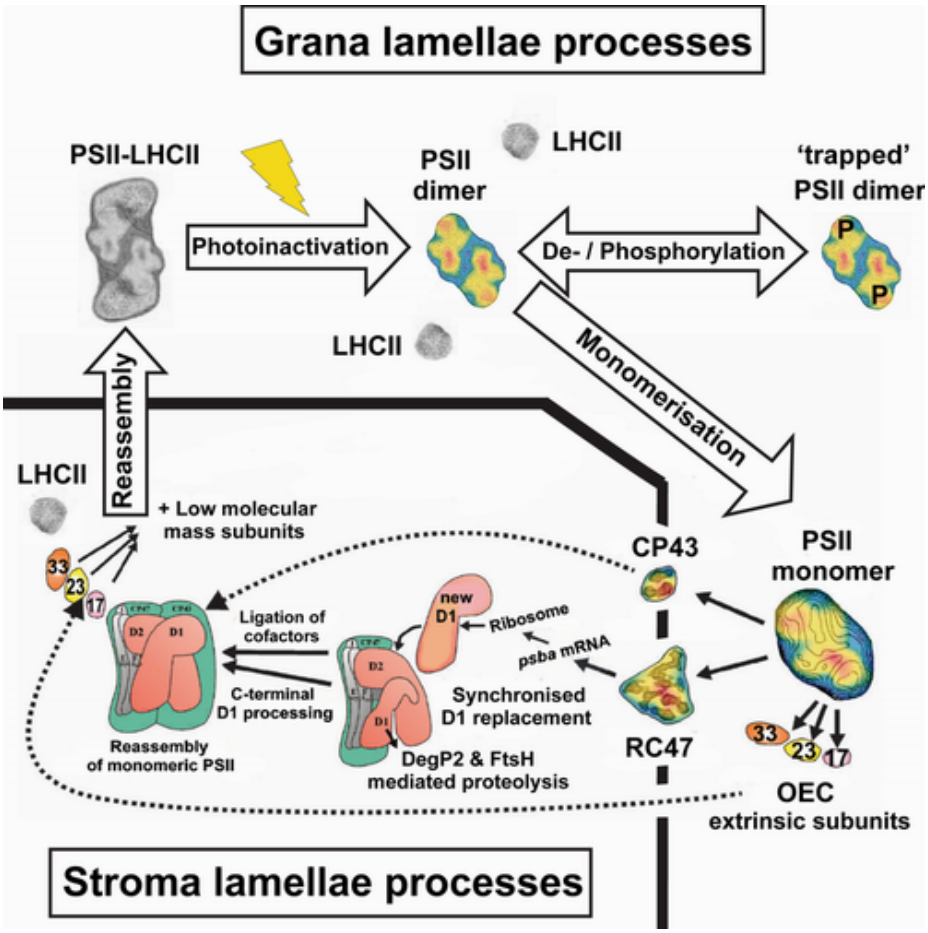

Figure 1.6: Model for the PSII repair cycle in chloroplasts (kindly donated by Dr. J. Nield and Dr. P. Silva; adapted from Kruse (2001)). The steps of the PSII repair cycle in chloroplasts are distinguished into grana and stroma lamellae processes. For a detailed description of this hypothetical model refer to the text in this section. The "P" in the drawing for the "trapped" PSII dimer represents the phosphorylation of certain PSII core subunits. 33, 23 and 17 symbolise the extrinsic subunits of the oxygen-evolving complex (OEC) PsbO, PsbP and PsbQ respectively. RC47 signifies a PSII core complexes lacking CP43. DegP2 and FtsH are the proteases that have been suggested to mediate D1 protein removal and degradation in the two-protease model.

Typically, higher plants and algae contain one *psbA* gene (Zurawski et al., 1982) for which gene expression is light-controlled at the level of translation (Fromm et al., 1985; Jensen et al., 1986; Klein et al., 1988). Therefore, *psbA*-mRNA is

generally abundant (Klein and Mullet, 1987) and readily available for the immediate initiation of precursor D1 protein (pD1) synthesis under photoinhibitory conditions. After targeting of the D1 nascent chain/ribosome complex to the stroma lamellae by the chloroplast signal recognition particle cpSRP54, co-translational insertion of the pD1 protein into the thylakoid membrane assisted by the cpSecY translocation channel can commence (Herrin and Michaels, 1985; Nilsson et al., 1999; Zhang et al., 2001b). After the insertion of the first two transmembrane domains, elongation of the pD1 protein is stalled and the cpSecY translocation channel opens laterally to allow association of pD1 with the RC47 receptor complex (Adir et al., 1990; Zhang et al., 2000; Aro et al., 2005; Rokka et al., 2005). Generally, a slow rate of pD1 elongation and occasional pausing of the ribosome during the insertion process are believed to allow pD1 to exit the translocation channel and to permit the re-ligation of cofactors like chlorophylls and carotenoids (Kim et al., 1991; Aro et al., 1993b; Aro et al., 2005). Following pD1 translation termination, a C-terminal extension is rapidly cleaved off the precursor protein by the lumenal CtpA protease, and the CP43 protein, other low molecular mass PSII subunits, the PsbO extrinsic subunit as well as the manganese ions can assemble to form monomeric PSII (Marder et al., 1984; Jensen et al., 1986; Bowyer et al., 1992; Aro et al., 1993b; Anbudurai et al., 1994; Zhang et al., 2000; Suorsa et al., 2004; Aro et al., 2005; Rokka et al., 2005). It has been postulated that the PSII monomers then migrate back to the grana lamellae for dimerisation and binding of the LHCII complex prior to the final assembly steps, i.e. binding of the extrinsic subunits PsbP and PsbQ as well as the calcium and chloride ions that stabilise the manganese cluster (Aro et al., 1993b; Hashimoto et al., 1997; Aro et al., 2005). However, at the end of the PSII repair cycle stands the re-established functional PSII-LHCII protein complex in the grana lamellae.

1.5.2 The PSII repair cycle of cyanobacteria

Another model has been devised for the cyanobacterial PSII repair cycle and is based on the schemes that have been postulated for chloroplasts as well as on additional results from *in vivo* experiments (see Figure 1.7; Aro et al., 1993b; Silva et al., 2003; Nixon et al., 2005).

In cyanobacteria, functional PSII protein complexes prevail as a dimers in the thylakoid membrane. Upon irreversible PSII photoinactivation, it has been suggested

that consequential conformational changes signal for the need to remove the damaged D1 subunit. However, prior to a synchronised D1 replacement, i.e. removal and degradation of the damaged D1 protein as well as the integration of a newly synthesised copy, the protein is made accessible by monomerisation and partial disassembly of the damaged PSII protein complex. Then, after processing of the newly integrated D1 protein, rebinding of various other PSII subunits and once PSII has reassembled into its dimeric form, photoactivation of the manganese cluster occurs to completes the repair cycle and PSII is functional once more.

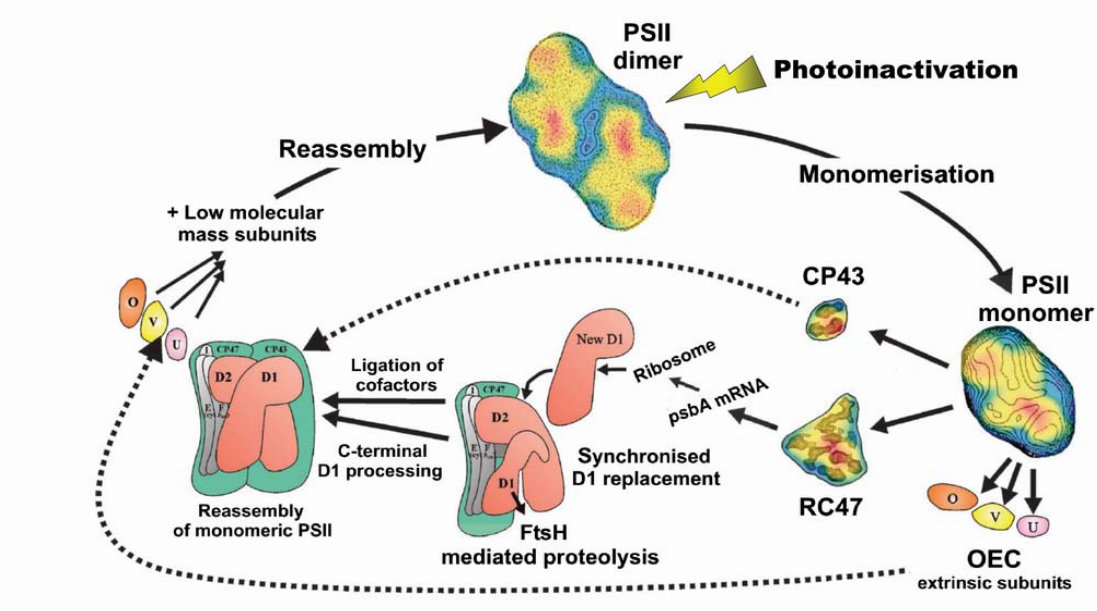

Figure 1.7: Model for the PSII repair cycle of cyanobacteria (kindly donated by Dr. J. Nield and Dr. P. Silva; adapted from Nixon et al. (2005)). The various steps of the cyanobacterial PSII repair cycle are depicted in this hypothetical model for which the description can be found in the text. O, V and U symbolise the extrinsic subunits of the oxygen -evolving complex (OEC) PsbO, PsbV and PsbQ respectively. RC47 signifies a PSII core complexes lacking CP43. In this model, only the FtsH protease is suggested to mediate D1 protein removal and degradation.

The D1 protein and its synchronised replacement also plays the central role in the cyanobacterial PSII repair cycle, while the majority of the at least 25 other PSII subunits is being recycled (Nixon et al., 2005). Although the exact molecular mechanisms for D1 removal and degradation are still subject to intense research, it has been postulated that these processes are catalysed by the FtsH protease only, a concept that seems to be also applicable to the PSII repair cycle in chloroplasts (see section 1.5.4; Nixon et al., 2005). Regarding the integration mechanism for newly synthesised D1 protein, it is the working hypothesis of this work (see section 1.7) and has been postulated that cyanobacterial Band 7 proteins might be involved (Silva et al., 2002;

Nixon et al., 2005). Briefly, cyanobacterial Band 7 proteins or prohibitin homologues (Tavernarakis et al., 1999) might protect newly synthesised copies of D1 or other PSII subunits from the degradation by the FtsH protease by shielding them prior to their incorporation into reassembling PSII complexes (see Figure 1.9).

Despite experimental evidence implying that PSII synthesis, assembly and repair might occur in the plasma membrane (Smith and Howe, 1993; Zak et al., 2001; Keren et al., 2005), it is still unclear whether these processes actually happen within that cellular compartment (Nixon et al., 2005). However, in early studies, the D1 protein of PSII could be identified in both the thylakoid and the plasma membrane, while the inner antenna proteins CP43 and CP47 were only found in the thylakoid membrane (Smith and Howe, 1993). Already at that time, it has been postulated that PSII subunits within the plasma membrane constitute either mistargeted proteins, or that certain PSII assembly or repair steps might occur there (Smith and Howe, 1993). Later, it could be shown that the D1, D2, Cyt b_{559} and PsbO subunits are present in the plasma membrane, incorporate respective pigments and that a hetero-multimeric PSII protein complex assembles in that lipid bilayer (Zak et al., 2001). More recently, evidence that these PSII protein complexes are capable of primary charge separation, i.e. electron transfer from $Y_Z \rightarrow P_{680} \rightarrow$ Pheo $\rightarrow Q_A$, but do not possess a functionally assembled donor-side, could be provided (Keren et al., 2005). Interestingly, also the enzyme that catalyses C-terminal processing of the precursor D1 protein (CtpA) was found to be solely present in the plasma membrane, providing further evidence for the hypothesis that PSII assembly or repair might occur there (Zak et al., 2001).

At this point, it is noteworthy that the thylakoid and plasma membrane are most likely physically discontinuous (Liberton et al., 2006), and that thereby lateral migration of protein complexes from one membrane to the other might not be possible. Consequently, since functional PSII protein complexes are definitely located in the thylakoid membrane, there would have to be a vesicle-mediated shuttling mechanism from the plasma to the thylakoid membrane, if the plasma membrane was the site for PSII biogenesis or repair. Intriguingly, the potential importance of vesicular transport for the development and possibly maintenance of cyanobacterial thylakoid membranes has been demonstrated by studies on a mutant in which a homologue of the vesicle-inducing protein in plastids (VIPP1) had been inactivated leading to a lack of photosynthesis and few thylakoid membranes (Huang et al., 2002a; Kroll et al., 2001; Westphal et al., 2001).

An alternative explanation for the mentioned experimental evidence (Smith and Howe, 1993; Zak et al., 2001; Keren et al., 2005) might be that other types of membrane system, apart from thylakoid and plasma membranes, exist in cyanobacteria and co-purified with the respective plasma membrane fractions investigated in those studies (Nixon et al., 2005). In this context, it is interesting to mention the so-called thylakoid centres, i.e. cylindrical structures of 50 to 1000 nm in length and 40 to 50 nm in diameter that can be found at some thylakoid membrane sheet convergence sites in close proximity to the plasma membrane (Kunkel, 1982; van de Meene, 2006). The function of these cyanobacterial structural features are still unknown, but they have been shown to be associated with the plasma membrane, while a continuity between thylakoid centres and membranes could not be confirmed (van de Meene, 2006). Intriguingly, in that study, occasional connections between the thylakoid and plasma membrane have been observed and were suggested to possibly represent a static situation of an otherwise dynamic, transient fusion between the two membrane systems (van de Meene et al., 2006).

Finally, it must be noted that despite the often suggested role of ROS as the photoinhibition-inducing compound, it now seems more likely that ROS interferes and inhibits the PSII repair cycle by suppressing protein translation in general and that of the D1 protein in particular (Nishiyama et al., 2001; Nishiyama et al., 2004; Hakala et al., 2005; Ohnishi et al., 2005).

1.5.3 The two-protease model for D1 protein degradation

The exact molecular mechanisms underlying the degradation of the D1 protein are still unclear, although, over the past decades, based on *in vitro* studies, a two-protease model has been devised, where initial cleavage sites for the acceptor- and donor-side photoinhibition mechanisms (see section 1.4.1.1 and section 1.4.1.3; Greenberg et al., 1987; Barbato et al., 1991; Shipton and Barber 1991; Salter et al., 1992; de las Rivas et al., 1992a; Aro et al., 1993b; Miyao, 1994) as well as responsible proteases (Lindahl et al., 2000; Haußühl et al., 2001; Adam and Ostersetzer, 2001) have been suggested.

For the acceptor-side photoinhibition mechanism a putative cleavage site has been postulated in the Q_B binding pocket of the D1 protein in the stromal loop between transmembrane (TM) domains four and five (see Figure 1.5; Greenberg et al., 1987;

Salter et al., 1992) Interestingly, some studies have reported 23-kDa and 16 kDa-fragments (Salter et al., 1992; Miyao, 1994), while other experimental evidence points towards 23-kDa and 10 kDa-fragments (de las Rivas et al., 1992a). With respect to the donor-side photoinhibition mechanism, one initial cleavage site has been reported between the luminal loop connecting TM domains one and two of the D1 protein, while another site has been proposed between the luminal loop connecting TM domains three and four (see Figure 1.5; Barbato et al., 1991; Barber and Andersson, 1992). There seems to be less certainty about the resulting protein fragments and while 24 and 10-kDa fragments have been reported consistently in several studies (Barbato et al., 1991; Shipton and Barber, 1991; de las Rivas et al., 1992a; Miyao, 1994), other intermediate size fragments: 17 and 14 kDa (Shipton and Barber, 1991) or 16 kDa respectively (Miyao, 1994) have been observed.

Initial *in vitro* experiments on spinach thylakoid membranes demonstrated that the degradation of the D1 protein is likely to be catalysed enzymatically, since during the exposure to low temperature and high-light illumination D1 degradation was initiated but not completed, while a subsequent incubation in the dark at room-temperature allowed its completion (Aro et al., 1990). Ever since, a multitude of mechanisms for the initial cleavage step have been proposed, including: autoproteolysis (on the donor-side; Shipton and Barber, 1991), the involvement of a serine-type protease with CP43 as a likely candidate (acceptor-side; Salter et al., 1992) and ROS-mediated cleavage (acceptor and donor-side; Miyao, 1994; Lupinkova and Komenda, 2004). Later, another *in vitro* study provided experimental evidence suggesting that the degradation of the D1 protein in chloroplasts is a two-step process that involves a primary GTP-dependent cleavage event by a serine-type protease followed by a secondary ATP- and zinc-dependent breakdown of the resulting fragments mediated by an FtsH protease (Spetea et al., 1999). Interestingly, further *in vitro* experiments on the primary proteolytic event (Spetea et al., 2000) were consistent with the earlier finding that the stroma exposed loop of the D1 protein between TM domain four and five contains an initial cleavage site of D1 degradation (Greenberg et al., 1987; Salter et al., 1992). Finally, the DegP2 protease from the DegP/HtrA family of *A. thaliana* could be identified to be capable of degrading the D1 protein *in vitro* into 23-kDa fragments in a GTP-stimulated manner (Haußühl et al., 2001). In another study, it could further be shown that an FtsH protease of *A. thaliana* is able to degrade

23-kDa fragments of photoinactivated PSII core complexes *in vitro* in an ATP-dependent fashion (Lindahl et al., 2000).

This experimental evidence culminated into the two-protease model for the proteolytic breakdown of the D1 protein during the PSII repair cycle, where a primary cleavage event in the Q_B-binding pocket (see Figure 1.5) by the serine-type DegP2 protease is proposed to be followed by the degradation of the resulting fragments, at least in part, by an FtsH protease (Lindahl et al., 2000; Haußühl et al., 2001; Adam and Clarke, 2002). However, it must be emphasised that the schemes of this two-protease model for D1 protein degradation are based on *in vitro* experiments and that particularly the role of the DegP2 protease *in planta* is still under dispute (see section 1.5.4; Bailey et al., 2001; Bailey et al., 2002; Huesgen et al., 2006).

1.5.4 The FtsH-only model for D1 protein degradation

Even though the molecular details of D1 degradation are also in cyanobacteria not yet completely understood, intriguingly, an FtsH protease of *Synechocystis* sp. PCC 6803 has been reported to also be involved in the early stages of the PSII repair cycle (Silva et al., 2003) and recently an 'FtsH-only' model based on *in vivo* experiments has been proposed (Nixon et al., 2005). Several lines of evidence have lead to the formulation of this alternative FtsH-only model, which seems to be also applicable to the PSII repair cycle of chloroplasts (Bailey et al., 2001; Bailey et al., 2002; Silva et al., 2003; Nixon et al., 2005; Huesgen et al., 2006).

The cyanobacterium *Synechocystis* sp. PCC 6803 possesses four FtsH homologues (designated *slr0228*, *sll1463*, *slr1390* and *slr1604*; Kaneko et al., 1996; Kaneko and Tabata, 1997; Sokolenko et al., 2002), and while *slr1390* and *slr1604* are essential for cell growth, viable gene inactivation mutants can be constructed for *slr0228* and *sll1463* (Mann et al., 2000). Remarkably, inactivation of the *slr0228* FtsH homologue leads to a high-light sensitive mutant with an increased susceptibility to photoinhibition, indicating an impaired PSII repair cycle (Silva et al., 2003). Specifically, pulse-chase analyses with and without the protein synthesis inhibitor lincomycin demonstrated that full-length D1 protein was stabilised even under constant high-light irradiance and no accumulation of D1 breakdown fragments could be observed (Silva et al., 2003).

Interestingly, *in vivo* studies on the *A. thaliana var2-2* mutant that lacks its FtsH2 protease, performed after, but published earlier than the work by Silva et al. (2003), yielded supporting experimental evidence for the 'FtsH-only' model (Bailey et al., 2001; Bailey et al., 2002). It could be shown that the *var2-2* mutant was more susceptible to photoinhibitory damage in comparison to the wild-type and that in the presence of the protein inhibitor lincomycin the proteolytic breakdown of the D1 protein was inhibited without an accumulation of primary D1 cleavage fragments (Bailey et al., 2002). More recently, in another *in vivo* study on an *A. thaliana* mutant that lacks the DegP2 protease, it could be observed that the mutant displays a similar rate of D1 protein degradation in comparison to the wild-type, implicating several redundant D1 protein degradation pathways (Huesgen et al., 2006), or refuting the earlier proposed two-protease model under physiological conditions. In this context, it is noteworthy that three potential members of the DegP/HtrA family, termed HtrA (*slr1204*), HhoA (*sll1679*) and HhoB (*sll1427*), have been identified in *Synechocystis* sp. PCC 6803 (Kaneko et al., 1996; Sokolenko et al., 2002) and although their inactivation appeared to confer a sensitivity to high-light illumination to a respective triple mutant (Silva et al., 2002), oxygen evolution and pulse-chase analyses did not reveal an impaired PSII repair cycle (Barker et al., 2006).

This accumulated evidence from *in vivo* experiments on cyanobacteria as well as *A. thaliana* supports the 'FtsH-only' model for D1 removal and degradation during the PSII repair cycle (Nixon et al., 2005). However, even though the model for a two-step mechanism for D1 degradation with an initial cleavage event catalysed by a DegP/HtrA protease can probably be refuted in cyanobacteria, it is still possible that the DegP2 protease might play a role in the PSII repair cycle of chloroplast, since the involvement of the DegP2 protease might have evolved after the divergence of chloroplasts and cyanobacteria (Nixon et al., 2005; Huesgen et al., 2006).

1.6 Towards formulating a working hypothesis

FtsH proteases belong to a conserved class of ATP-dependent proteinases, also referred to as AAA-proteases (ATPases associated with various cellular activities), that have been implied to function in a membrane-embedded quality control system in bacteria, chloroplasts and mitochondria (Langer et al., 2000). The cyanobacterium *Synechocystis* sp. PCC 6803 contains four FtsHs (see section 1.5.4; Sokolenko et al.,

2002) of which specifically the Slr0228 FtsH homologue could be shown to be involved in the early steps of the cyanobacterial PSII repair cycle (see section 1.5.4; Silva et al., 2003) and, more recently, in the quality control of the PSII protein complex (Komenda et al., 2006; Kamata et al., 2005). An interesting feature of the FtsH protease of *E. coli* (see section 1.6.1) and the m-AAA protease of *S. cerevisiae* (see section 1.6.2) is that these particular AAA proteases have been reported to be associated with and to be negatively regulated by Band 7 proteins (Kihara et al., 1996; Steglich et al., 1999). Remarkably, an InterPro database search in 09/2006 returned 1655 assigned Band 7 proteins from all taxonomic groups that have been grouped into the Band 7 protein superfamily, which can be further distinguished into five distinct protein subfamilies, namely: stomatins, prohibitins, flotillins and HflKs and HflCs (see section 1.7; InterPro entry: Band_7; accession number: IPR001107; Tavernarakis et al., 1999). Interestingly, five of these Band 7 proteins could be identified in *Synechocystis* sp. PCC 6803, and, given the role of the Slr0228 FtsH homologue in the cyanobacterial PSII repair cycle, a working model has been developed that connects these proteins (see section 1.6.3).

1.6.1 The FtsH homologue of *E. coli* and the HflK/C protein complex

Initial studies on an *E. coli* mutant associated the ftsH gene with a **f**ilamentous (cell-division-defect) and **t**emperature-**s**ensitive phenotype (Santos and de Almeida, 1975). Later, it could be shown that the investigated mutant carried two mutations, where the filamentous phenotype could be attributed to the *ftsI* gene, while the *ftsH* gene was responsible for the growth defect (Ogura et al., 1991; Begg et al., 1992). Nowadays, the FtsH homologue of *E. coli* is recognised as a cytoplasmic membrane-bound protease (Ogura and Wilkinson, 2001) that possesses two N-terminal TM domains and a large C-terminal cytosolic region that contains an AAA-ATPase domain (Krzywda et al., 2002; Niwa et al., 2002) as well as a Zn^{2+}-metallo protease active-site motif (Akiyama and Ito, 2000; Akiyama and Ito, 2001). Functionally, FtsH contributes to cellular regulation at the level of protein stability and to a proteolytic quality control system by catalysing the rapid elimination of harmful proteins (Ito and Akiyama, 2005). So far σ^{32} (Herman et al., 1995), λ cII (Kihara et al., 1997), λ cIII (Herman et al., 1997), λ Xis (Leffers and Gottesman, 1998), LpxC (Ogura et al.,

1999), SecY (Akiyama et al., 1996b), ATPase F_0 subunit a (Akiyama et al., 1996a) and YccA (Kihara et al., 1998) have been identified as FtsH substrates.

Since the FtsH protease of *E. coli* is involved in the proteolytic degradation of at least three bacteriophage λ proteins, it has been postulated that another important biological role of FtsH might be to affect the development and life cycle of infecting genetic systems by degrading their key regulatory molecules (Ito and Akiyama, 2005). Upon infecting *E. coli*, the λ cII protein plays a key role in the lysis (viral replication and cell lysis) versus lysogeny (chromosomal integration) decision for the bacteriophage λ (Herskowitz and Hagen, 1980; Gottesman et al., 1981). The unstable and rapidly degraded λ cII protein is a transcriptional activator of the λ cI phage repressor and an integrase protein, which both favour the lysogenic pathway, hence high levels of the λ cII promote lysogeny (Banuett et al., 1986). Interestingly, in *hflA* (Hoyt et al., 1982; Banuett et al. 1986) and *hflB* mutants (Banuett et al., 1986) a stabilisation of the λ cII protein could be observed that lead to a **h**igh-**f**requency **l**ysogenisation phenotype (Friedman et al., 1984). Furthermore, the *hflA/hflB* double mutant displayed an additive effect which suggested two independent pathways for the observed phenomenon (Banuett et al., 1986). *In vitro* studies revealed that HflB was responsible for the degradation of the λ cII protein, whereas the HflA proteins interacted with HflB to determine its substrate specificity (Kihara et al., 1997). While the *hflB* gene could later be shown to be an allele of the *ftsH* gene (Herman et al., 1993), the *hflA* locus was found to encode an operon of three genes (*hflX-hflK-hflC*). HflX is a putative GTP-binding protein, while the HflK and HflC proteins can be found in the cytoplasmic membrane (Zorick and Echols, 1991), where they form a hetero-multimeric protein complex (Cheng et al., 1988; Kihara and Ito, 1998) that interacts with FtsH (Saikawa et al., 2004).

Another, well-studied proteolytic process catalysed by the FtsH homologue of *E. coli* is the degradation of the integral cytoplasmic membrane protein SecY, as a part of a quality control mechanism that operates to maintain membrane functionality by preventing the accumulation of highly toxic, unassembled protein subunits (Kihara et al., 1995). The SecY protein spans the cytoplasmic membrane ten times and forms a hetero-trimeric protein complex with the SecE and SecG subunits (Brundage et al., 1990; Douville et al., 1994) that acts as an ATP dependent protein translocase during protein secretion across the cytoplasmic membrane (Schatz and Beckwith, 1990; Ito, 1996; Mori and Ito, 2001). In contrast to a stable, assembled SecYEG complex,

unassembled SecY subunits are rapidly degraded with a half life of less than 2 min (Matsuyama et al., 1990; Taura et al., 1993). Interestingly, a mutant form of the SecY protein, SecY24 is already efficiently degraded at 42 °C, supposedly due to weakened interactions with the SecE subunit (Baba et al., 1994). Both excess SecY and SecY24 proteins were found to be stabilised in a mutant with a compromised FtsH activity (Kihara et al., 1995). Studies in a *hflK/hflC* double deletion mutant reported an enhanced degradation of the SecY protein in this genetic background, which suggested a negative regulatory effect of the HflK/C protein complex on FtsH-mediated membrane-bound protein degradation (Kihara et al., 1996).

In mutants in which the interaction between HflK/C and FtsH was impaired due to the removal of a periplasmic region within the FtsH protease, the λ cII protein was stabilised, whereas no effect on the SecY protein degradation could be observed *in vivo* (Akiyama et al., 1998). In another experiment, a mutant form of the YccA protein, a membrane-bound substrate of FtsH, selectively interfered with the degradation of other membrane-bound substrates by forming a complex with the FtsH/HflK/C protein complex. Moreover, it could be shown that the HflK/C protein complex was required for this inhibition by YccA (Kihara et al., 1998). These findings suggested that the degradation pathways for membrane-bound and soluble substrates are in part different from each other and that the HflK/C protein complex appears to be involved in the differentiation.

HflK and HflC proteins are Band 7 proteins (Tavernarakis et al., 1999) that only exist in bacteria (293 HflKs and 271 HflCs; in 05/2007; InterPro database). Summarising the experimental evidence from studies on *E. coli*, the HflK and HflC Band 7 proteins are found in the plasma membrane (Zorick and Echols, 1991) where they form a large, hetero-multimeric protein complex (Cheng et al., 1988) that has been reported to interact with the FtsH protease and to be able to negatively regulate its activity (Kihara et al., 1996).

1.6.2 The m-AAA protease of *S. cerevisiae* and the prohibitin complex

Similar to chloroplasts, mitochondria are eukaryotic, intracellular organelles that originated from an endosymbiotic event where a eukaryotic cell engulfed and incorporated a proteobacterium (Gray, 1989; Gray et al., 1999). As a consequence, the

mitochondrial matrix is surrounded by two distinct lipid bilayers, where the outer mitochondrial membrane is of eukaryotic origin and contains largely membrane transport proteins, while the inner mitochondrial membrane results from the prokaryotic endosymbiont and is the main site for biological energy production (Benz, 1990; Gray et al., 1999; Saraste, 1999; Logan, 2005). Intriguingly, the inner mitochondrial membrane has one of the highest protein contents among cellular membranes and the biogenesis of its various protein complexes, like those of the respiratory chain or the ATP-synthase, require a precise coordination of various protein translocases and assembly factors (Arnold and Langer, 2002). Interestingly, a proteolytic quality control system that is capable of selectively removing unassembled, potentially harmful proteins and that features two AAA proteases which expose their catalytic sites on alternative sides of the inner mitochondrial membrane as well as a chaperone-like prohibitin complex as its key components, has been identified in yeast mitochondria (see Figure 1.8; Langer, 2000; Arnold and Langer, 2002).

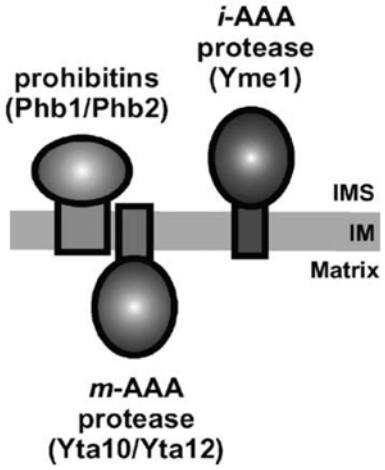

Figure 1.8: Schematic representation of the key components of the proteolytic quality control system in the inner mitochondrial membrane of *S. cerevisiae* (adapted from Arnold and Langer, 2002). Two AAA proteases are embedded in the inner mitochondrial membrane (IM). The m-AAA protease exhibits its catalytic site to the matrix, while that of the i-AAA protease faces the intermembrane space (IMS). The chaperone-like prohibitin complex that contains prohibitin 1 (Phb1) and prohibitin 2 (Phb2) is associated with the m-AAA protease (see text for further details).

It is noteworthy, that this proteolytic quality control system in the inner mitochondrial membrane of *S. cerevisiae* represents so far the best-understood functional model for the prohibitin complex (Arnold and Langer, 2002) and provides crucial insights to subsequent studies that aim to investigate prohibitin homologues in other organisms. As key components, two AAA proteases, namely: the m-AAA (Yta10/Yta12) and i-AAA (Yme1) proteases, are responsible for the proteolytic breakdown of target proteins (Arnold and Langer, 2002), while the prohibitin complex has been reported to negatively regulate the activity of the m-AAA protease (Steglich et al., 1999).

The significance of this quality control system is demonstrated by the fact that a double deletion mutant that lacks both of the AAA proteases displays a lethal phenotype (Lemaire et al., 2000; Leonhard et al., 2000). A deletion of the prohibitin genes on the other hand only causes an accelerated degradation of non-assembled membrane proteins by the m-AAA protease, while in a genetic background where also the m-AAA protease is deleted, the respective mutant exhibits a slow growing phenotype (Steglich et al., 1999). Interestingly, evidence from co-immunoprecipitations experiments on *S. cerevisiae* revealed that of the two AAA proteases only the m-AAA protease physically interacts with the prohibitin complex (Steglich et al., 1999). Furthermore, pulse-chase analyses were performed on a mutant in which distinct nuclear-encoded subunits of the respiratory chain protein complexes, i.e. COX4 (subunit 4 of the cytochrome c oxidase) and Atp10p (a subunit of the F_0 moiety of the ATPase complex) as well as the two prohibitin homologues had been deleted (Steglich et al., 1999). Typically, in Δcox4 (Nakai et al., 1994) or Δatp10 (Tzagoloff et al., 2004) mutants, the other non-assembled, mitochondrial-encoded subunits of the respective protein complex are already prone to proteolytic breakdown. In this study, however, it could be observed that the additional deletion of either of the prohibitins lead to an even higher decrease in the half-life time of certain known m-AAA protease substrates, e.g. Cox3p or Atp6p (Arlt et al., 1996; Guelin et al, 1996; Steglich et al., 1999). Interestingly, the half-life time of the Cox2p subunit, which is degraded by the i-AAA protease (Nakai et al, 1995), did not appear to change significantly in that study (Steglich et al., 1999).

However, in another study, not only the Cox3p protein, but also the Cox2p subunit of the cytochrome oxidase c, co-migrated with the prohibitin complex on 2-D SDS PAGE gels and could be co-immunoprecipitated with an antibody directed against the Phb1p protein (Nijtmans et al., 2000). Moreover, the pulse-chase analysis data further indicated that the observed interactions between the translation products and the prohibitin complex must be relatively stable, since even after 40 min some labelled Cox3p subunit could still be detected to be co-migrating with the prohibitin complex (Nijtmans et al., 2000). This experimental evidence suggests that the prohibitin complex of *S. cerevisiae* stabilises newly synthesised mitochondrial translation products by binding them prior to their incorporation into the respective protein complexes and thereby has a negative regulatory effect on the m-AAA protease activity (Nijtmans et al., 2000). This postulated function of the prohibitin protein

complex as a membrane-associated chaperone/'holdase' is supported by a small but significant sequence homology with chaperonins of the GroEL/Hsp60-class (Nijtmans et al., 2000).

So far the studies on the prohibitin complex in the inner mitochondrial membrane of *S. cerevisiae* have not only provided the best experimental evidence for the function of this intriguing protein complex (Steglich et al., 1999; Nijtmans et al., 2000), but also for its structure (Back et al, 2002; Tatsuta et al., 2005). The two prohibitin homologues of *S. cerevisiae*, designated Phb1p and Phb2p, are anchored to the inner mitochondrial membrane via an N-terminal TM domain, expose their C-termini to the intermembrane space and are the only constituents of the prohibitin complex that features an apparent molecular mass between 1 and 2 MDa (Coates et al., 1997; Berger and Yaffe, 1998; Steglich et al., 1999; Nijtmans et al., 2000). However, both proteins exhibit an interdependence *in vivo*, where neither of the two prohibitins accumulates nor can the prohibitin complex assemble, if one of the two subunits has been deleted (Berger and Yaffe, 1998). The combined results from a mass spectrometry approach on chemically crosslinked prohibitin complexes (Back et al, 2002) and a single-particle electron microscopic analysis (Tatsuta et al., 2005) suggests that this protein complex has a molecular mass of 1.0 to 1.4 MDa (without detergent and lipid) and should be composed out of 16 to 20 subunits of both Phb1p (31 kDa) and Phb2p (35 kDa) which are arranged in an alternating manner.

With respect to the biogenesis of the prohibitin complex, it could be revealed that both of the nucleus-encoded subunits are targeted to the mitochondria by unconventional, non-cleavable targeting sequences at their N-termini (Tatsuta et al., 2005). Their insertion into the inner mitochondrial membrane is then mediated by the Tim23-translocase (Tatsuta et al., 2005), a protein translocon that is typically required for the import of proteins destined for the mitochondrial matrix, but which is also capable of protein insertion into the inner mitochondrial membrane (Paschen *et al*., 2000; Jensen and Dunn, 2002). After integration of the Phb1p and Phb2p proteins into the inner mitochondrial membrane, the two prohibitins assemble into 120-kDa intermediate complexes that later form the larger, ring-shaped protein complexes (Tatsuta et al., 2005). Interestingly, conserved C-terminal coiled-coil regions that are present in both subunits are required for the proper assembly of the prohibitin complex (Tatsuta et al., 2005).

1.6.3 Working model for the synchronised replacement of the D1 protein in the cyanobacterial PSII repair cycle

The experimental evidence on the cyanobacterial PSII repair cycle (see section 1.5.2 and section 1.5.4) as well as on the functional interactions between certain Band 7 proteins and AAA proteases in *E. coli* (see section 1.6.1) and *S. cerevisiae* (see section 1.6.2) culminated in the unifying hypothesis and working model of this work that is presented in this section (see Figure 1.9; Silva et al., 2002; Nixon et al., 2005).

Initially, the Slr0228 FtsH homologue of *Synechocystis* sp. PCC 6803 has been found to be involved in the early steps of the cyanobacterial PSII repair cycle and could be shown to be responsible for the removal and degradation of the D1 protein during its synchronised replacement (Silva et al., 2003; Nixon et al., 2005; Komenda et al., 2006). Based on what is known about the FtsH homologue of *E. coli* (Akiyama and Ito, 2003) and AAA proteases in mitochondria (Langer, 2000) a general model for the FtsH catalysed degradation of the D1 protein in cyanobacteria has been proposed (Silva et al., 2003; Nixon et al., 2005). In this model, damaged D1 is translocated in an ATP dependent manner through a central pore in the ring-like, hexameric FtsH complex, and during the translocation process this D1 protein is successively degraded at the catalytic Zn^{2+} centre (Nixon et al., 2005). In *E. coli*, FtsH-mediated proteolysis can occur from either end of the substrate (Chiba et al. 2002) including newly generated ends from an endoproteolytic cleavage (Shotland et al., 2000) and is highly processive (Akiyama, 2002). Taking into account that the catalytic Zn^{2+} centre of the FtsH protease is likely to be located on the stromal side of the membrane (Lindahl et al, 1996) the degradation of the D1 protein is probably initiated from stroma-exposed regions such as the cleavage site in Q_B binding pocket or the N-terminus (see Figure 1.5; Nixon et al., 2005). However, Nixon and colleagues favour general destabilisation of the PSII protein complex and particularly the D1 subunit by accumulating photodamage in conjunction with an accessible N-terminus to be the triggering signal for FtsH-mediated proteolysis (Nixon et al., 2005). Substrate recognition could be mediated by interacting TM domains or a highly conserved 81-amino-acid sequence of the FtsH protease that is located on the luminal side (Bailey et al, 2002; Nixon et al., 2005).

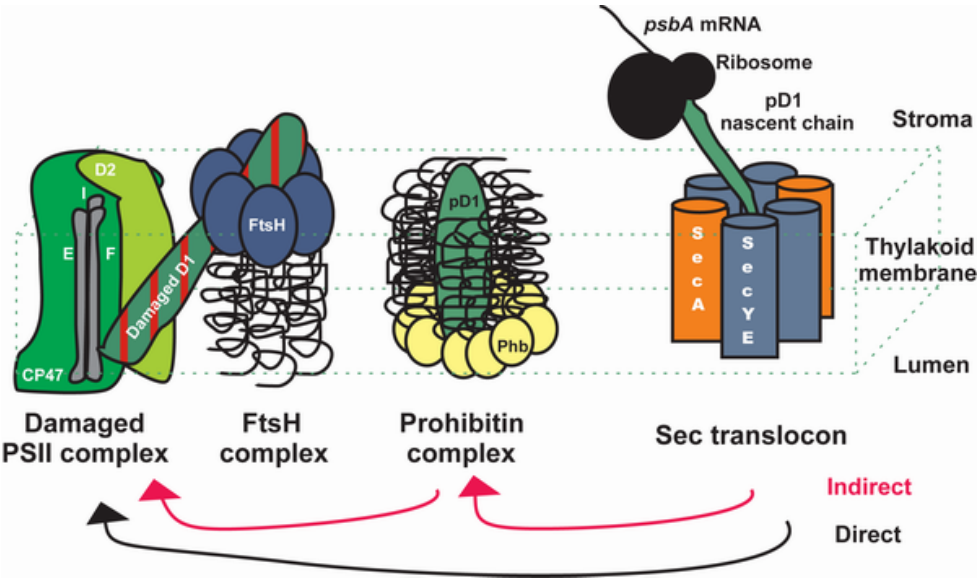

Figure 1.9: Schematic representation of the synchronised replacement of the D1 protein during the cyanobacterial PSII repair cycle (adapted from Silva et al., 2002). This schematic drawing depicts the postulated key components and pathways for the synchronised replacement of the D1 protein during the cyanobacterial PSII repair cycle: damaged and disassembled PSII complex (PSII monomer consisting out of D2, PsbE, PsbF, PsbI, CP47 and damaged D1), FtsH complex, prohibitin complex, newly synthesised copy of the D1 protein (pD1) and Sec translocon (consisting out of SecYE and SecA). The direct (from the Sec translocon into the reassembling PSII complex) and the indirect (via the prohibitin complex) routes for D1 insertion are indicated. This model is based on the chaperone/'holdase' hypothesis for the prohibitin homologues of *S. cerevisiae* (Nijtmans et al., 2000; Arnold and Langer, 2002). For further details see text.

The second constitutive process of synchronised D1 replacement during the PSII repair cycle is the integration of a newly synthesised D1 subunit into the thylakoid membrane and subsequently into a reassembling PSII complex. In chloroplasts, the targeting of the D1 nascent chain/ribosome complex to the thylakoid membrane is mediated by the chloroplast signal recognition particle cpSRP54 (Nilsson et al.,1999), while co-translational membrane insertion of the elongating pD1 protein (Zhang et al., 1999) is facilitated by a cpSecY translocon (see section 1.5.1; Roy and Barkan, 1998; Zhang et al., 2001). A slow rate of pD1 elongation and occasional pausing is believed to allow the assembly of various D1 cofactors and the integration into the PSII receptor complex consisting out of at least D2, Cyt b_{559} (i.e. PsbE and PsbF), PsbI and possibly CP47 (Zhang et al., 2000; Rokka et al., 2005). Interestingly, the Alb3 protein (a homologue of the bacterial YidC and mitochondrial Oxa1p protein) has been postulated to be involved in the Sec-dependent, co-translational membrane insertion of pD1 through the cpSecYE translocon (Samuelson et al., 2000; Scotti et al.,

2000; Eichacker and Henry, 2001), where it might act as a membrane-bound chaperone (Kuhn et al., 2003).

Since only little is known about pD1 integration into the thylakoid membrane in cyanobacteria, the working model of this study is mainly based on the schemes developed for chloroplasts in this respect. Consequently a similar, SecYE-mediated, co-translational integration mechanism is postulated to occur during the synchronised replacement of the D1 protein during the cyanobacterial PSII repair cycle (see Figure 1.9; Silva et al., 2002; Nixon et al., 2005). A SecY homologue has been identified in both the thylakoid and plasma membrane of *Synechococcus* PCC 7942 (Nakai et al., 1993) and also *Synechocystis* sp. PCC 6803 contains the genes for the necessary components for Sec-dependent translocation, i.e. SecY, SecE, SecG and SecA (Kaneko et al., 1996; Robson and Collinson, 2006). Moreover, *Synechocystis* sp. PCC 6803 possesses a single *alb3* gene (*slr1471*), that, intriguingly, has been shown to be essential for cell viability and thylakoid biogenesis (Spence et al., 2004). However, given the role of the Slr0228 FtsH protease in *Synechocystis* sp. PCC 6803 and the experimental evidence on the physical and functional interactions between the FtsH and HflK/C complexes in *E. coli* (Kihara et al., 1996; Saikawa et al., 2004) as well as of the m-AAA protease and the prohibitin complex in *S. cerevisiae* (Steglich et al., 1999; Nijtmans et al., 2000), an involvement of the Band 7 homologues (HflK/C and prohibitins are members of the Band 7 protein family; see section 1.7; Tavernarakis et al., 1999) of *Synechocystis* sp. PCC 6803 in the cyanobacterial PSII repair cycle has been hypothesised (see Figure 1.9; Silva et al., 2002; Nixon et al., 2005). More specifically, in this work, the Band 7 proteins and in particular the identified Slr1106 prohibitin homologue of *Synechocystis* sp. PCC 6803 are postulated to form a complex that binds newly synthesised pD1 protein after its insertion into the thylakoid membrane and prior to its incorporation into reassembling PSII complexes, thereby protecting it from potential, premature proteolytic breakdown by the Slr0228 FtsH protease. It appears feasible that newly synthesised pD1 is either incorporated indirectly via a possible Band 7 or prohibitin complex into reassembling PSII, or alternatively, as postulated for the chloroplast, directly from the Sec translocon. So far, it could be clearly demonstrated that the D1 protein constitutes a substrate for the Slr0228 FtsH protease of *Synechocystis* sp. PCC 6803, and there is additional experimental evidence that this protease might also be involved in the degradation of the D2, CP43 and CP47 subunits of PSII (Silva et al., 2003; Komenda et al., 2006).

Consequently, it might be possible, that potential Band 7 protein complexes not only protect pD1, but also other PSII subunits, or yet unidentified proteins in a similar way as hypothesised in the working model of this work. Initial supportive, experimental evidence for the presented working model came from the finding that the Slr1106 prohibitin homologue of *Synechocystis* sp. PCC 6803 could be identified in a PSII-His-tag preparation (Silva et al., 2001).

1.7 On the individual subfamilies of Band 7 proteins

The Band 7 superfamily of proteins has been recognised to comprise five distinct protein subfamilies that share an N-terminal SPFH domain, termed after the initials of the respective, constituting subfamilies: **s**tomatins, **p**rohibitins, **f**lotillins, **H**flCs and HflKs, as a conserved and characteristic sequence motif (Tavernarakis et al., 1999). Interestingly, stomatins, prohibitins and to a relatively lesser extent flotillins represent highly conserved protein families that have been found in a large variety of organisms ranging from prokaryotes to higher eukaryotes (Tavernarakis et al., 1999; Nijtmans et al., 2002; Rivera-Milla et al., 2005), while HflC and HflK homologues have only been identified in bacteria (InterPro database; http://www.ebi.ac.uk/interpro/; HflC entry = IPR010200; HflK entry = IPR010201). Despite intensive research, only little is known about the molecular functions of Band 7 proteins, particularly in prokaryotes, but, intriguingly, in *H. sapiens*, stomatins have been associated with the haemolytic disease overhydrated hereditary stomatocytosis (Lande et al., 1982), prohibitins with cancer (Coates et al., 2001) and flotillins with Alzheimer's disease (Kokubo et al., 2000; Girardot et al., 2003), implying that the Band 7 proteins might be involved in crucial cellular processes.

1.7.1 The stomatin subfamily of Band 7 proteins

The stomatin subfamily of Band 7 proteins is rather diverse and already in the first published phylogenetic analysis, in the work that reported on the discovery of the SPFH domain (Tavernarakis et al., 1999), eukaryotic stomatins have been distinctly distinguished from prokaryotic stomatins (p-stomatin; Nadimpalli et al., 2000).

The human homologue has been characterised as a 31-kDa integral membrane protein that exhibits a hairpin-loop topology, where both the N- and C-terminus face

the cytoplasm (Salzer et al., 1993). Furthermore, this protein has been shown to assemble into homo-oligomeric protein complexes that contain between 9 to 12 stomatin monomers and whose oligomerisation might be mediated by the C-termini of the assembling subunits (Snyers et al., 1998).

With regards to its function, in humans, the stomatin protein has been found to be absent in very leaky erythrocytes associated with the rare human haemolytic anaemia overhydrated hereditary stomatocytosis (OHSt), where the red blood cells assume a mouth-shaped morphology due to an impaired osmotic competence of their cellular membrane (Lande et al., 1982; Stewart, 1997; Fricke et al., 2003; Stewart, 2004). However, intriguingly, the stomatin gene could never be found to be mutated and the stomatin protein is found to be expressed in all other cell types, thus, it appears as if the protein is somehow lost during erythrocyte maturation in the affected individuals (Fricke et al., 2003; Stewart, 2004). In accordance with these findings, a later study, found that stomatin knock-out mice did not display the OHSt phenotype, implying a more elaborate cause for triggering of the abnormal erythrocyte morphology, and even though it is likely that the stomatin protein does play a part in this disease (Fricke et al, 2004), its precise role in the pathogenesis remains elusive (Zhu et al., 1999; Fricke et al., 2003; Stewart, 2004). Interestingly, supportive experimental evidence for a possible involvement of stomatins in ion channel regulation comes from studies on the nematode *C. elegans*, where the MEC-2 stomatin homologue has been implied to regulate the MEC-4 and MEC-10 ion channels that are required for mechanosensation (Huang et al., 1995; Goodman et al., 2002; Price et al., 2004). Specifically, it has been postulated that the MEC-2 stomatin homologue might form a link between the cytoskeleton and the MEC-4 as well as the MEC-10 ion channels respectively, transducing mechanical stimuli to the channel and thereby triggering its response (Huang et al., 1995; Tavernarakis and Driscoll, 1997). Intriguingly, the stomatin as well as the flotillin Band 7 homologues of *H. sapiens* have been identified as major components of erythrocyte lipid rafts, where they form independent protein complexes that might act as scaffolding components on the cytoplasmic side of the cell (Salzer and Prohaska, 2001). Furthermore, human stomatin has been found to interact with and possibly modulate the activity of the GLUT-1 glucose transporter that mediates the insulin-independent glucose transport (Zhang et al., 1999a, Zhang et al., 2001a).

In prokaryotes, apart from the observation that in some bacterial strains stomatin-like genes (*p-stomatin*) might form an operon with *nfed* genes that encode a probable serine-type protease (Green et al., 2004), very little is known about the function of prokaryotic stomatins. The identification of such operons in that study lead to the assumption that these transcriptional units might reflect the fact that both gene products are destined for a common function, in particular, to act as a proteolytic system to regulate the activity of certain ion channels (Green et al., 2004; Stewart, 2004).

In summary, even though experimental evidence supports the notion for an involvement of the stomatins in ion channel regulation, the overall understanding of the functional role of eukaryotic stomatins remains elusive, while even less is known about that of the prokaryotic homologues.

1.7.2 The prohibitin subfamily of Band 7 proteins

Prohibitins, as members of the Band 7 protein superfamily, have been found to be evolutionary conserved (McClung et al., 1995) with homologues in organisms ranging from prokaryotes (Banuett and Herskowitz, 1987) to higher eukaryotes (Nuell et al., 1991). Despite intensive research, little is known on the actual function of these intriguing proteins, although they could be linked to a multitude of important cellular processes, such as cellular signalling and transcriptional control (Terashima *et al*., 1994; Montano *et al*., 1999; Sun *et al*., 2004), apoptosis (van der Heiden *et al*., 2002; Fusaro *et al*., 2003), cellular senescence (McClung *et al*., 1992; Coates *et al*., 1997; Coates *et al*., 2001; Piper *et al*., 2002), early development of *C. elegans* (Artal-Sanz *et al*., 2003) or mitochondrial biogenesis (Berger and Yaffe, 1998; Steglich *et al*., 1999; Nijtmans *et al*., 2000; Artal-Sanz *et al*., 2003).

The best understood functional and structural model for prohibitins, that formed the basis of the working model for this study (see section 1.6.3), is that of the prohibitin complex in yeast mitochondria (see section 1.6.2). Briefly, in *S. cerevisiae*, two prohibitin homologues form a hetero-multimeric, ring-like protein complex that is located to the inner mitochondrial membrane where it negatively regulates the activity of the m-AAA protease by shielding possible substrates of that protease from potential proteolytic breakdown (Steglich et al., 1999; Nijtmans et al., 2000; Nijtmans et al., 2002; Tatsuta et al., 2005). Remarkably, non-dividing yeast cells (G_0 arrest) of a

double mutant strain in which both the *phb1* and *phb2* genes have been deleted, appear to lose respiration competence, emphasising the importance of the prohibitin complex for the functional maintenance of the mitochondrial respiratory chain (Piper et al., 2002).

Early studies associated mutations in the human prohibitin gene with sporadic breast cancer and consequently implied that the protein acted as a tumour suppressor (Sato et al., 1992). However, a subsequent study identified that there was a separate, second gene locus in the region previously attributed to the *PHB1* gene and that *PHB1* was not involved in affecting susceptibility to inherited breast cancer (Black and Solomon, 1993). There is different experimental evidence that microinjected *PHB1* mRNA inhibits the progression of the cell cycle into S-phase, an effect that could later be determined to result from the 3'-untranslated region (UTR) of the mRNA by an unknown mechanism (Nuell et al., 1991; Jupe et al., 1996). Finally, even though there is little evidence to substantiate a direct role for the human prohibitin protein to act as a tumour suppressor, several studies have identified this protein to be a possible marker for cancer, since it seems to be overexpressed in various tumour cell lines in comparison to their normal cell counterparts (Byrjalsen et al., 1999; Nijtmans et al., 2002; Wang et al., 2004).

Furthermore, prohibitin has been established as a vascular marker of adipose tissue that might represent a future target for drugs that aim to treat obese patients. In an initial study, a peptide motif (CKGGRAKDC) could be shown to associate with prohibitin and lead to an ablation of white fat (Kolonin et al., 2004).

In comparison to the rather extensive amount of knowledge that had been accumulated on other eukaryotic prohibitins at the beginning of this project, the respective plant homologues appeared almost neglected. At the time, it had only been reported that the *A. thaliana* prohibitin homologue is abundant in all tissues and located to a mitochondrial membrane (Snedden and Fromm, 1997). It is even more remarkable that no study on prokaryotic prohibitins had been published.

1.7.3 The flotillin subfamily of Band 7 proteins

Interestingly, flotillin has been independently discovered three times and is therefore also known as reggie protein or as epidermal surface antigen (ESA), however, the most commonly used name is flotillin (Schroeder et al., 1994; Schulte et

al., 1997; Bickel et al., 1997). In an initial phylogenetic analysis of Band 7 proteins, the flotillin homologues of *H. sapiens*, *D. melanogaster* and *B. subtilis* grouped together and were assigned as the flotillin subfamily of Band 7 proteins (Tavernarakis et al., 1999). More recently, this flotillin subfamily has been further distinguished into the flotillins, Bacteria flotillin-like, Plant flotillin-like and Fungi flotillin-like (Rivera-Milla et al., 2005).

Generally, flotillins are best-characterised in metazoans, where they constitute a well-conserved protein family that is typically represented by two homologous proteins, i.e. flotillin-1/reggie-2 and flotillin-2/reggie-1 (Bickel et al., 1997; Volonte et al., 1999; Malaga-Trillo et al., 2002). In humans, flotillin-1 and flotillin-2 are single copy genes that encode 47-kDa proteins with the SPFH domain of unknown function at their N-terminus and a characteristic flotillin domain consisting out of several glutamic acid/alanine (EA) repeats which probably promote the formation of coiled-coil structures at their C-terminus (Schroeder et al., 1994; Bickel et al., 1997; Tavernarakis et al., 1999; Edgar and Polak, 2001). Furthermore, the flotillins of *H. sapiens* have been found predominantly in the plasma membrane, where they are anchored by acylation and form high-order homo- and probably hetero-oligomeric protein complexes (Salzer and Prohaska, 2001; Neumann-Giesen et al., 2004; Langhorst et al., 2005).

Intriguingly, the profound evolutionary conservation of flotillins (Malaga-Trillo et al., 2002) suggests an involvement in an important cellular function, but even though these proteins have been implied to participate in various cellular processes such as signal transduction, vesicle trafficking and cytoskeleton rearrangement (Langhorst et al., 2005), their precise function is still largely unknown. Nevertheless, it seems to be clear that flotillins are components of lipid rafts (Salzer and Prohaska, 2001; Morrow and Parton, 2005), where they might provide specialised platforms for the recruitment of certain multi-protein complexes (Langhorst et al., 2005; Rivera-Milla et al., 2005). It is noteworthy, that there is evidence for an involvement of flotillins in the pathogenesis of neurodegenerative diseases such as Parkinson's and Alzheimer's disease (Kokubo et al., 2000; Langhorst et al., 2005). Furthermore, since different pathogens can enter cells via lipid rafts (Simons and Ehehalt, 2002), given the presence of flotillins in them, it has been postulated and experimental evidence supports this notion that flotillins might be involved in pathogen entry, e.g. for the malaria parasite *Plasmodium falciparum* (Samuel et al., 2001).

The flotillin homologues of plants, bacteria and fungi display a rather low similarity to the metazoan flotillins, a fact that is mirrored in their assignment as flotillin-like proteins (Borner et al., 2005; Rivera-Milla et al., 2005). In fact, it has even been suggested that the flotillin-like proteins outside the animal kingdom might have evolved independently and any similarities would consequently be the result of convergent evolution (Rivera-Milla et al., 2005). Overall, only very little is known about the flotillin-like proteins. However, the YuaG protein of *B. subtilis* has been implied to be involved in detoxification and the production of antimicrobial compounds (Huang et al., 1999), while a flotillin-like protein of *A. thaliana* has been identified in detergent-resistant membranes providing potential evidence for lipid rafts in the plant plasma membrane (Borner et al., 2005).

1.7.4 The HflC and HflK subfamilies of Band 7 proteins

In this work, the HflC and HflK proteins have been considered to belong to two, distinct Band 7 protein subfamilies based on phylogenetic evidence of this study (see section 3.6) and Tavernarakis et al. (1999). Interestingly, members of both the HflC and HflK subfamilies have only been identified in bacteria.

The hetero-multimeric HflK/C protein complex has been well-characterised (Kihara et al., 1996; Saikawa et al., 2004) and the obtained results on its functional role contributed to the generation of the working model of this study (see section 1.6). Briefly, in *E. coli*, the HflK/C protein complex plays a role in the lysis/lysogeny decision after bacteriophage λ infection and in a quality control mechanism that operates to maintain membrane functionality by associating with and negatively regulating the activity of the FtsH protease (see section 1.6.1).

It is noteworthy, that the HflK/C protein complex could be demonstrated to physically interact with the FtsH protease in the plasma membrane of *E. coli*, where the proteins form a large HflK/C-FtsH protein complex with an apparent molecular mass of about 1 MDa (Saikawa et al., 2004). With respect to the structure of the HflK/C protein complex itself, it has been shown to be anchored via the N-terminal TM domains of its constituent HflC and HflK subunits in the plasma membrane and to expose the respective C-terminal domains to the periplasmic space (Kihara and Ito, 1998). Interestingly, both proteins exhibit interdependency and deletion of the one leads to the destabilisation of the other (Kihara et al., 1996).

1.8 Project aims

Since cyanobacterial Band 7 proteins had not been subjected to a detailed analysis before and generally only very little was known about Band 7 proteins in prokaryotes, the aim of this work was to probe the role of potential Band 7 proteins of *Synechocystis* sp. PCC 6803. While one focus lay on the investigation of the physiological relevance of these proteins, another was on the identification and characterisation of possible Band 7 protein complexes. The hypothesised involvement of a previously identified prohibitin homologue in the synchronised replacement of the D1 protein, especially during the PSII repair cycle, was a particular focus. With respect to the working model (see Figure 1.9), a further aim was to identify potential physical or functional interactions between the Band 7 proteins and the Slr0228 FtsH homologue. In order to achieve these aims, the following objectives were defined:

- Identification of cyanobacterial Band 7 homologues.
- Identification of higher plant Band 7 homologues and probing for a potential association of these proteins with the chloroplast (presence or function).
- Bioinformatic analyses with a focus on the Band 7 proteins of *Synechocystis* sp. PCC 6803 (e.g. phylogenetic relationships and protein properties).
- Generation of single and multiple Band 7 gene inactivation mutants to:
    - test whether the Band 7 proteins are essential for cell viability.
    - reveal potential phenotypes under distinct growth conditions.
    - test the involvement of prohibitins in the PSII repair cycle.
    - study the characteristics of possible prohibitin complexes.
- Raising and affinity-purification of polyclonal antibodies against the Band 7 proteins of *Synechocystis* sp. PCC 6803.
- Identification and characterisation of possible Band 7 protein complexes *in vivo* with an emphasis on their:
    - subcellular localisation and possible membrane association.
    - size and stochiometry.
    - molecular architecture.
    - potential interaction partners.

Chapter 2: Materials and methods

2.1 Bioinformatic tools

The programs, internet-based servers and databases that were used for the bioinformatic analyses of the Band 7 proteins in this study are listed below. The specific settings for these tools can be found in the respective result chapter.

Protein and gene databases:

BLAST (Release 2.2.14; Altschul et al., 1990) (http://www.ncbi.nlm.nih.gov/BLAST/)
CyanoBase (Version 2006.9.12; Nakamura et al., 1998) (http://www.kazusa.or.jp/cyanobase/)
UniProt (Release 8.8; Bairoch et al., 2005) (http://www.ebi.uniprot.org/index.shtml)

Protein family databases:

InterPro (Release 13.0; Mulder et al., 2003) (http://www.ebi.ac.uk/interpro/)
PFAM (Version 20.0; Bateman et al., 2004) (http://www.sanger.ac.uk/Software/Pfam/)
PROSITE (Release 19.36; Hulo et al., 2004; Sigrist et al., 2002) (http://us.expasy.org/prosite/)
SPRINT (PRINTS-S Version 16.0; Attwood et al., 2003) (http://umber.sbs.man.ac.uk/dbbrowser/sprint/)

Protein properties prediction servers:

EXPASY (Wilkins et al., 1999) (http://us.expasy.org/tools/)

Multiple sequence alignment and phylogenetic tree generation:

Biology WorkBench (Version 3.2) (http://seqtool.sdsc.edu/CGI/BW.cgi#!)
CLUSTALW (WorkBench 3.2 environment) (Thompson et al., 1994; Gonnet et al., 1992)
Drawgram/PHYLIP (WorkBench 3.2 environment) (Felsenstein, 1989)

Protein targeting prediction server:

ChloroP (Version 1.1; Emanuelsson et al., 1999) (http://www.cbs.dtu.dk/services/ChloroP/)
Predotar (Version 1.03; Small et al., 2004) (http://urgi.infobiogen.fr/predotar/predotar.html)
TargetP (Version 1.1; Emanuelsson et al., 2000) (http://www.cbs.dtu.dk/services/TargetP/)

Other databases:

NCBI database (http://www.ncbi.nlm.nih.gov/)

2.2 *E. coli* strains and growth conditions

2.2.1 *E. coli* strains

The *E. coli* DH5α strain was used to propagate plasmid DNA and the BL21-Gold(DE3)pLysS and Rosetta(DE3) strains for protein expression (see Table 2.1).

Table 2.1: *E. coli* strains.

Strain	Genotype	Reference/Supplier
DH5α	F^-, *endA1*, *deoR*, *hsdR17*(r_K^- m_K^+), sup*E44*, *thi-1*, *recA1*, *gyrA96*, (NaI^1), *relA1*, Δ(*lacZYA-argF*)U169, (*m80lacZ*ΔM15), λ^-	Hanahan (1983)
BL21-Gold(DE3)pLysS	derivation of *E. coli* B strain; F^-, *ompT*, *hsdS*$_B$(r_B- m_B-), *dcm*$^+$, *gal*, λ(DE3), *endA*, *Hte*, [pLysS Cam^r]	Weiner et al. (1994) Stratagene
Rosetta(DE3)	derivation of *E. coli* B strain; F^-, *ompT*, *hsdS*$_B$(r_B^- m_B^-), *dcm*$^+$, *gal*, *lacY1*, *λ*(DE3), *endA*, *Hte*, [pRARE (argU, argW, ileX, glyT, leuW, proL) Cam^r]	Novy et al. (2001) Novagen

2.2.2 *E. coli* growth conditions

E. coli cells in liquid Luria-Bertani (LB) medium (1 % (w/v) NaCl, 1 % (w/v) bacto-tryptone, 0.5 % (w/v) yeast extract) (Sambrook et al., 1989) were grown on an orbital shaker (Innova 4400 incubator-shaker, New Brunswick Scientific, UK) at 37 °C and 200 rpm. Cells grown on solid LB 1.8 % (w/v) agar plates were incubated in a static incubator (Astell Hearsen, UK) at 37 °C. For long term storage cells were resuspended in liquid LB medium containing 15 % (v/v) glycerol, flash frozen in liquid nitrogen and kept at –80 °C (Sambrook et al., 1989). Antibiotics for selective growth in both liquid and solid LB medium were used at the following concentrations: ampicilin (AMP; 50-100 μg ml^{-1}), carbenicilin (CARB; 50 μg ml^{-1}), chloramphenicol (CAM; 30 μg ml^{-1}), erythromycin (ERM; 200 μg ml^{-1}), gentamycin (GENT; 10 μg ml^{-1}), kanamycin (KAN; 50 μg ml^{-1}) and spectinomycin (SPEC; 50 μg ml^{-1}).

2.3 Cyanobacterial strains and growth conditions

2.3.1 Cyanobacterial strains

The *Synechocystis* sp. PCC 6803 wild-type strain (WT) was supplied by the Pasteur Culture Collection of Cyanobacteria (Pasteur Institute, Paris, France). Another,

glucose-tolerant *Synechocystis* sp. PCC 6803 strain (GT) (Williams, 1988) was a gift from Dr. J. K. Williams (Dupont, Delaware, USA). These strains and derivatives produced in this study are listed in Table 2.2. Aliquots from already grown liquid cultures of *Thermosynechococcus elongatus* (TE) were kindly provided by Prof. James Barber's group (Imperial College London, London, UK).

Table 2.2: Cyanobacterial strains.

#	Strain name	Description	Reference
		***Synechocystis* sp. PCC 6803 (WT)**	
1	WT	PCC 6803 wild-type strain	Stanier (1973)
2	ΔPhb1-WT	WT strain in which *slr1106* was disrupted by a kanamycin-resistance cassette	this work
3	ΔPhb2-WT	WT strain in which *slr1768* was disrupted by a chloramphenicol-resistance cassette	this work
4	ΔPhb3-WT	WT strain in which *slr1128* was disrupted by a spectinomycin-resistance cassette	this work
		***Synechocystis* sp. PCC 6803 glucose-tolerant (GT)**	
5	GT	PCC 6803 wild-type glucose-tolerant strain	Williams (1988)
6	ΔPhb1	GT strain in which *slr1106* was disrupted by a kanamycin-resistance cassette	this work
7	Phb1-His	GT strain in which a C-terminal His_8-tag was added to *slr1106*; selective marker was a chloramphenicol-resistance cassette	this work
8	ΔPhb2	GT strain in which *slr1768* was disrupted by a chloramphenicol-resistance cassette	this work
9	Phb2-His	GT strain in which a C-terminal His_8-tag was added to *slr1768*; selective marker was a kanamycin-resistance cassette	this work
10	ΔPhb3	GT strain in which *slr1128* was disrupted by a spectinomycin-resistance cassette	this work
11	Phb3-His	GT strain in which a C-terminal His_8-tag was added to *slr1128*; selective marker was a kanamycin-resistance cassette	this work
12	ΔPhb4	GT strain in which *sll0815* was disrupted by a spectinomycin-resistance cassette	this work
13	Phb4-His	GT strain in which a C-terminal His_8-tag was added to *sll0815*; selective marker was a chloramphenicol-resistance cassette	this work
14	ΔPhb5	GT strain in which *sll1021* was disrupted by a chloramphenicol-resistance cassette	this work
15	ΔPhb1-3	GT triple mutant strain in which the following genes were disrupted by antibiotic-resistant cassettes: *slr1106* (KAN^R), *slr1768* (CAM^R) and *slr1128* ($SPEC^R$)	this work
16	ΔPhb1-4	GT quadruple mutant strain in which the following genes were disrupted by antibiotic-resistant cassettes: *slr1106* (KAN^R), *slr1768* (CAM^R), *slr1128* ($SPEC^R$) and *sll0815* (ERM^R)	this work
17	Δ0228	GT strain in which *slr0228* (*ftsH*) was disrupted by an erythromycin-resistance cassette	this work

Table 2.2 continued

#	Strain name	Description	Reference
		***Synechocystis* sp. PCC 6803 glucose-tolerant**	
18	Δ0228 / ΔPhb1-3	GT quadruple mutant strain in which the following genes were disrupted by antibiotic-resistant cassettes: *slr1106* (KAN^R), *slr1768* (CAM^R), *slr1128* ($SPEC^R$) and *slr0228* (*ftsH*) (ERM^R)	this work
19	ΔCP43	GT strain in which *sll0851* (*psbC*) was disrupted by an erythromycin-resistance cassette	this work
20	ΔCP43 / Δ Phb1-3	GT quadruple mutant strain in which the following genes were disrupted by antibiotic-resistant cassettes: *slr1106* (KAN^R), *slr1768* (CAM^R), *slr1128* ($SPEC^R$) and *sll0851* (*psbC*) (ERM^R)	this work
21	M55	GT strain in which *sll0223* (*ndhB*) was disrupted by a kanamycin-resistance cassette	Ogawa (1991)
22	TD41	GT D1 triple mutant strain in which the following genes were disrupted by antibiotic-resistant cassettes: *slr1181* (*psbA1*) (CAM^R), *slr1311* (*psbA2*) (KAN^R) and *sll1867* (*psbA3*) ($SPEC^R$)	Nixon et al. (1992)
23	CP47His / TD41	TD41 mutant strain (see 24) in which a C-terminal His_6-tag was added to *slr0906* (*psbB*)	Nixon (unpublished data)
24	0228-GST	GT strain in which a C-terminal GST-tag was added to *slr0228* (*ftsH*)	Barker (unpublished data)
		Thermosynechococcus elongatus	
25	TE	BP-1 wild-type strain	Yamaoka et al. (1978)

2.3.2 Cyanobacterial growth conditions

2.3.2.1 Routine growth conditions

All *Synechocystis* sp. PCC 6803 strains were cultivated on BG-11 1.5 % (w/v) agar plates (BG-11 basic mineral medium (Stanier et al., 1971), supplemented with 0.3 % (w/v) sodium thiosulphate, 10 mM N-tris[hydroxymethyl]methyl-2-aminoethanesulfonic acid (TES-KOH) pH = 8.2 (Hihara and Ikeuchi, 1997) and 1.5 % (w/v) agar, added separately after autoclaving; 5 mM of glucose was added where applicable (Williams, 1988)). Plates were restreaked every two to four weeks. Liquid BG-11 cultures (5 mM N-tris[hydroxy-methyl]methyl-2-aminoethanesulfonic acid (TES-KOH) pH = 8.2; 5 mM of glucose was added where applicable) were either grown in sterile, air-filter capped tissue culture flasks on an orbital shaker incubator (Innova 2100 shaker, New Brunswick Scientific, UK) at 100 rpm or in glass vessels bubbled with sterile air on a magnetic stirrer. The air used for bubbled cultures was sterilised by passage through a copper sulphate solution and a 0.2-μm pore filter (Midisart 2000, Sartorius Limited, UK). The strains were incubated in a temperature-controlled room set at 29 °C and illuminated with an incident fluorescent white light

intensity of ~10 µE m^{-2} s^{-1} (on plates) and 20 to 70 µE m^{-2} s^{-1} (in liquid cultures). For long term storage, cells from fresh plates or liquid cultures were suspended in 1 ml of liquid BG-11 supplemented with 15 % (v/v) glycerol, flash frozen in liquid nitrogen and kept at –80 °C. Where ne-cessary, antibiotics were added at the indicated levels: kanamycin (KAN; 50 µg ml^{-1}), chloramphenicol (CAM; 10 to 30 µg ml^{-1}), erythromycin (ERM; 10 µg ml^{-1}), gentamycin (GENT; 5 µg ml^{-1}) and spectinomycin (SPEC; 25 to 50 µg ml^{-1}).

2.3.2.2 Motility assay

A liquid *Synechocystis* sp. PCC 6803 culture that had reached an OD_{730} of ~ 0.5 was diluted to an OD_{730} of 0.1 and 10 µl drops of the diluted culture were inoculated onto BG-11 1.5 % (w/v) agar plates. The plates were left to incubate at 29 °C under diffuse light illumination at ~15 µE m^{-2} s^{-1} for 10 to 14 days and then photographed (Canon PowerShot Pro 1, Canon, UK).

2.3.2.3 Abiotic stress and photoheterotrophic growth conditions

Synechocystis sp. PCC 6803 strains on plates or in liquid cultures were exposed to various abiotic and photoheterotrophic stress conditions (see Table 2.3).

Table 2.3: Abiotic and photoheterotrophic stress conditions.

Stress condition	Light intensity [µE m^{-2} s^{-1}]	Temperature [°C]	[Chemical] [µM]	BG-11 growth medium type
High-light	100	29	None	Agar
Low temperature	20	22	None	Liquid
Hydrogen peroxide	20	29	10 - 40	Liquid
DCMU	20	29	10	Liquid

Plate assays were performed with freshly restreaked cells on BG-11 1.5 % (w/v) agar plates containing 5 mM glucose where applicable. After a period of seven to ten days cell growth was photographed (Canon PowerShot Pro 1, Canon, UK). Liquid culture assays were inoculated in duplicate or triplicate from a liquid starter culture with an initial OD_{730} of 0.4 to 0.5 that was diluted to an OD_{730} of approximately 0.05. Horizontally agitated tissue culture flasks with air-filter caps were used for all growth experiments. Cell density was assessed every day for a period of seven to ten days and graphs were plotted of cell density against time on a semi-logarhythmic scale.

2.3.3 Estimation of cell concentration of liquid *E. coli* and *Synechocystis* sp. PCC 6803 cultures

The optical density of liquid *E. coli* cultures was determined at 600 nm (OD_{600}), whereas the optical density of liquid *Synechocystis* sp PCC 6803 cultures was measured at 730 nm (OD_{730}). In both cases a 250-µl quartz or a 1-ml disposable cuvette was used with a Shimadzu spectrophotometer (UV-1601, Shimadzu, Japan). An OD_{730} of 0.25 for *Synechocystis* sp PCC 6803 corresponds to approximately 1x 10^8 cells ml^{-1} (Williams, 1988).

2.4 Molecular biology techniques

2.4.1 Standard buffers and solutions

Standard buffers and solutions were prepared unless otherwise stated according to Sambrook et al (1989). Reverse osmosis (RO) filtered water (Neptune model L993162, Purite Limited, UK) was routinely used to prepare all buffers and solutions. Chemicals and organic solvents were analytical grade reagents and purchased from Amersham Biosciences UK Limited; BDH Laboratory Supplies Limited, UK; Boehringer, Germany; Fisher Scientific Limited, UK; Merck Chemicals Limited, UK; Rose Chemicals Limited, UK and Sigma Aldrich Company Limited, UK. Where necessary buffers, solutions, media and other materials were sterilised by autoclaving for at least 40 min at 121 °C (130 kPa), or in case of thermo labile reagents by filtration through 0.2-µm syringe tip or bottle top filters (Schleicher & Schuell MicroScience GmbH, Germany). Antibiotics were prepared using RO water except for chloramphenicol and erythromycin which were dissolved in 100 % (v/v) ethanol. The photosystem II inhibitor 3-(3,4-dichlorophenyl)-1,1-dimethylurea (DCMU) was prepared in 100 % (v/v) ethanol. Both antibiotics and DCMU were kept as frozen stocks and stored at -20 °C until required.

2.4.2 Vectors and recombinant plasmids

Commercially available *E. coli* vectors that have been used for cloning and subsequent directed mutagenesis and expression in this work are shown in Table 2.4. Details about the antibiotic-resistance cassettes that were used as selective markers are given in Table 2.5. The recombinant plasmids that were generated in this work are

shown in Table 2.6 and their construction is outlined in the respective result chapters. Stocks of vectors and recombinant plasmids were maintained in bacterial cultures stored liquid LB medium supplemented with 15 % (v/v) glycerol at –80 °C or as DNA plasmids in RO water at –20 °C.

Table 2.4: Commercially available *E. coli* vectors used in this work.

Vector	Purpose	Supplier	Reference
pBluescript II KS(+)	Cloning	Stratagene, UK	Short et al. (1988)
pGEM-T Easy	Cloning	Promega Corporation, USA	Marcus et al. (1996)
pET-16b	Expression	Merck Biosciences, UK	Studier and Moffatt (1986)

Table 2.5: Antibiotic-resistance cassettes used in this work. The quoted accession numbers are for the mentioned vectors and refer to the NCBI nucleotide database. The exact origin of the gentamycin cassette was unknown. However, sequence data suggested it was derived from the *aaC(3)-Ia* gene found on p1658/97.

Vector	Antibiotic-resistance cassette	Accession #	Reference
pDC039	Chloramphenicol (*catI*) from pACYC184	X06403	Rose (1988)
pRL425	Erythromycin (*ermC*) from pE194	NC_005908	Elhai and Wolk (1988)
pCP47His-tagGENT	Gentamycin (*aaC(3)-Ia*) from p1658/97	NC_004998	Zienkiewicz et al. (unpublished data); Miriagou et al. (2005)
pDC057	Kanamycin (*aphI*) from pUC4K	X06404	Taylor and Rose (1988)
pSPEC	Spectinomycin (*aadA1*) from pHP45-omega	K02163	Prentki and Krisch (1984)

Table 2.6: Recombinant plasmids that were used in this work. Names of the recombinant plasmids contain a reference to the *Synechocystis* sp. PCC 6803 incorporated genes, where PHB1 refers to *slr1106*, PHB2 to *slr1768*, PHB3 to *slr1128*, PHB4 to *sll0815*, PHB5 to *sll1021* and CP43 to *sll0851* (*psbC*). Abbreviations for selective markers as well as for potential affinity-purification tags of resulting proteins, are also included in the names. The generation of each recombinant plasmid is briefly outlined in the description column. Selective markers are indicated and mentioned primers can be found in Table 2.7. Multiple cloning site (MCS).

#	Plasmid name	Description
		Cloning plasmids
1	pPHB2	*slr1768*, amplified with primers 3 and 5, inserted into the MCS of the pGEM-T Easy vector (AMP^R)
2	pPHB2-TM	*Δ1-225slr1768*, amplified with primers 16 and 5, inserted into the MCS of the pGEM-T Easy vector (AMP^R)
3	pPHB3	*slr1128*, amplified with primers 6 and 7, inserted into the MCS of the pGEM-T Easy vector (AMP^R)

Table 2.6 continued

#	Plasmid name	Description
		Cloning plasmids
4	pPHB3-TM	*Δ1-150slr1128*, amplified with primers 17 and 7, inserted into the MCS of the pGEM-T Easy vector (AMP^R)
5	pPHB4	*sll0815*, amplified with primers 8 and 9, inserted into the MCS of the pGEM-T Easy vector (AMP^R)
6	pPHB5	*sll1021*, amplified with primers 10 and 11, inserted into the MCS of the pGEM-T Easy vector (AMP^R)
7	pPHB5-TM	*Δ1-300sl1021*, amplified with primers 18 and 11, inserted into the MCS of the pGEM-T Easy vector (AMP^R)
8	pCP43	*Δ1-316sll0851* plus 602 bp downstream sequence, amplified with primers 14 and 15, inserted into the MCS of the pGEM-T Easy vector (AMP^R)
		Mutagenesis plasmids
9	pPHB1KAN	provided by Prof. Peter Nixon; *slr1106*, amplified with primers 1 and 2, inserted into the MCS of the pBluescript II KS(+) vector with a kanamycin-resistance cassette inserted at the NaeI site, 236 bp into the coding sequence (AMP^R, KAN^R)
10	pPHB2CAM	provided by Prof. Peter Nixon; *slr1768*, amplified with primers 4 and 5, inserted into the MCS of the pGEM-T Easy vector with a chloramphenicol-resistance cassette inserted at the EcoNI site, 256 bp into the coding sequence (AMP^R, CAM^R)
11	pPHB3CAM	plasmid #3 with a chloramphenicol-resistance cassette inserted at the MscI site, 238 bp into the coding sequence (AMP^R, CAM^R)
12	pPHB3SPEC	plasmid #3 with a spectinomycin-resistance cassette inserted at the MscI site, 238 bp into the coding sequence (AMP^R, $SPEC^R$)
13	pPHB4ERM	plasmid #5 with an erythromycin-resistance cassette inserted at the HindIII site, 317 bp into the coding sequence (AMP^R, ERM^R)
14	pPHB4GENT	plasmid #5 with a gentamycin-resistance cassette inserted at the HindIII site, 317 bp into the coding sequence (AMP^R, $GENT^R$)
15	pPHB4SPEC	plasmid #5 with a spectinomycin-resistance cassette inserted at the HindIII site, 317 bp into the coding sequence (AMP^R, $SPEC^R$)
16	pPHB5CAM	plasmid #6 with a chloramphenicol-resistance cassette inserted at the HpaI site, 836 bp into the coding sequence (AMP^R, CAM^R)
17	pPHB5ERM	plasmid #6 with an erythromycin-resistance cassette inserted at the HpaI site, 836 bp into the coding sequence (AMP^R, ERM^R)
18	pPHB5GENT	plasmid #6 with a gentamycin-resistance cassette inserted at the HpaI site, 836 bp into the coding sequence (AMP^R, $GENT^R$)
19	pCP43ERM	plasmid #8 was linearised with HindIII and SmaI and an erythromycin-resistance cassette inserted (AMP^R, ERM^R)
		Expression plasmids
20	pET16bPHB2	*slr1768*, excised from plasmid #1, inserted in between the BamHI and NdeI sites of the pET16b vector (AMP^R)
21	pET16bPHB2-TM	*Δ1-225slr176*, excised from plasmid #2, inserted in between the BamHI and NdeI sites of the pET16b vector (AMP^R)
22	pET16bPHB3	*slr1128*, excised from plasmid #3, inserted in between the BamHI and NdeI sites of the pET16b vector (AMP^R)
23	pET16bPHB3-TM	*Δ1-150slr1128*, excised from plasmid #4, inserted in between the BamHI and NdeI sites of the pET16b vector (AMP^R)
24	pET16bPHB4	*sll0815*, excised from plasmid #5, inserted in between the BamHI and NdeI sites of the pET16b vector (AMP^R)
25	pET16bPHB5	*sll1021*, excised from plasmid #6, inserted in between the BglII and NdeI sites of the pET16b vector (AMP^R)

Table 2.6 continued

#	Plasmid name	Description
		Expression plasmids
26	pET16bPHB5-TM	*Δ1-300sll1021*, excised from plasmid #7, inserted in between the BglII and NdeI sites of the pET16b vector (AMP^R)
		Tagging plasmids
27	pPHB1HIS	*slr1106* with the coding sequence of an His_8-tag before the stop codon plus 565 bp downstream sequence in the pGEM-T Easy vector (AMP^R)
28	pPHB1HISCAM	plasmid #27 with a chloramphenicol-resistance cassette inserted at the MscI site, 189 bp downstream of the *phb1* gene (AMP^R, CAM^R)
29	pPHB2HIS	*slr1768* with the coding sequence of an His_8-tag before the stop codon plus 556 bp downstream sequence in the pGEM-T Easy vector (AMP^R)
30	pPHB2HISKAN	plasmid #29 with a kanamycin-resistance cassette inserted at the MscI site, 267 bp downstream of the *phb2* gene (AMP^R, KAN^R)
31	pPHB3HIS	*slr1128* with the coding sequence of an His_8-tag before the stop codon plus 576 bp downstream sequence in the pGEM-T Easy vector (AMP^R)
32	pPHB3HISKAN	plasmid #31 with a kanamycin-resistance cassette inserted at the SmaI site, 101 bp downstream of the *phb3* gene (AMP^R, KAN^R)
33	pPHB4HIS	*sll0815* with the coding sequence of an His_8-tag before the stop codon plus 543 bp downstream sequence in the pGEM-T Easy vector (AMP^R)
34	pPHB4HISCAM	plasmid #33 with a chloramphenicol-resistance cassette inserted at the MscI site, 105 bp downstream of the *phb4* gene (AMP^R, CAM^R)

2.4.3 DNA transformation of cells

2.4.3.1 Preparation of chemically competent E. coli cells

A single *E. coli* colony from a freshly restreaked plate was inoculated into 2.5 ml liquid LB medium and incubated overnight under constant shaking at 37 °C. The next day a starter culture was inoculated into 250 ml liquid LB medium. The optical density at 600 nm (OD_{600}) was monitored, until the culture reached an OD_{600} of ~0.5. The cells were then pelleted by centrifugation (JA-14; 4,500 g, 10 min, 4 °C) and resuspended in 100 ml ice-cold TFB1 (100 mM RbCl, 50 mM $MnCl_2$, 30 mM potassium acetate, 10 mM $CaCl_2$, 15 % (v/v) glycerol, pH = 5.8, filter sterile). The cell suspension was kept on ice for 5 min and pelleted again (JA-14; 4,500 g, 10 min, 4 °C). The resulting cell pellet was resuspended in 10 ml of ice-cold TFB2 (10 mM MOPS pH = 6.5, 75 mM $CaCl_2$, 10 mM RbCl, 15 % (v/v) glycerol, pH = 6.5 filter sterile) and incubated on ice for 30 min. Subsequently the cells were aliquotted, flash frozen in liquid nitrogen and stored at –80 °C.

2.4.3.2 Transformation of chemically competent E. coli cells

For one transformation reaction, 100 µl of chemically competent *E. coli* cells were thawed on ice, gently mixed with ~1 µg of plasmid DNA and incubated for 20

min on ice. The cells were heat shocked for 45 s at 42 °C and incubated for 2 min on ice. 800 µl of liquid LB medium were added and the cells incubated for 1 hour under vigorous shaking at 37 °C. Then 200 µl of the mix were directly plated onto LB 1.8 % (w/v) agar plates supplemented with a suitable antibiotic selection and if applicable 0.5 mM isopropyl-β-D-thiogalactopyranoside (IPTG) and 80 µg ml^{-1} 5-bromo-4-chloro-3-indolyl-β-D-galactoside (X-Gal). The plates were incubated at 37 °C overnight.

2.4.3.3 Transformation of Synechocystis sp. PCC 6803

Synechocystis sp. PCC 6803 cells were transformed with recombinant plasmid DNA according to the protocol described by Williams (1988) and Nixon et al. (1992). Recipient cells that were grown in liquid BG-11 medium (5 mM glucose and antibiotic selection where applicable) were harvested in exponential growth phase (OD_{730} < 1) by centrifugation (centrifuge model Allegra 6R, Beckman Coulter Limited, UK; GH-3.8 rotor; 2,000 g, 15 min, 29 °C) and resuspended in fresh BG-11 medium yielding a cell suspension with a final OD_{730} of ~5.0. For each transformation reaction 200 µl of the concentrated cell suspension were mixed with 1 to 10 µg of recombinant plasmid DNA. The mixture was incubated at 29 °C, continuous white light illumination (~ 5 µE m^{-2} s^{-1}) for 4 to 6 h and occasional agitation. The transformation mix was plated in duplicate onto 2 µm cellulose nitrate membrane filters (Schleicher & Schuell MicroScience GmbH, Germany) placed on a BG-11 1.5 % (w/v) agar plate (5 mM glucose where applicable). After 48 h under continuous white light illumination ~10 µE m^{-2} s^{-1} the filter was transferred to a new plate containing suitable antibiotic(s). Resistant colonies appeared after seven to ten days. Transformants were restreaked at least three times, until PCR analyses were performed to test for segregation.

2.4.4 Extraction and purification of DNA

2.4.4.1 Mini plasmid DNA preparation from E. coli

Mini plasmid DNA preparations from *E. coli* were performed according to the method described in Birnboim and Doly (1979). A single colony was used to inoculate 5 ml of liquid LB medium containing the appropriate antibiotic(s) and the cells were incubated overnight at 37 °C under vigorous shaking. Cells of the 1.5-ml culture were harvested by centrifugation in a microfuge (model 5410, Eppendorf AG, Germany) at maximum speed for 1 min. The harvested cells were resuspended in 100 µl of ice-cold

cell resuspension solution (25 mM Tris/HCl pH = 8.0, 10 mM EDTA, 50 mM glucose, 20 mg ml^{-1} RNaseA (19101; Qiagen Limited, UK)) and after adding 100 µl of freshly prepared cell lysis solution (0.2 M NaOH; 1 % (w/v) SDS), the mixture was left for 5 min at room temperature. 100 µl of ice-cold 3 M potassium acetate solution (pH = 4.8) were added to neutralise the lysate and after mixing the sample properly, it was left for 5 min on ice. The precipitate was spun down in a microfuge at maximum speed for 10 min and the supernatant transferred to a new tube. 600 µl of ice-cold 100 % ethanol were added and left for 20 min at –20 °C to allow DNA precipitation. The DNA was pelleted in a microfuge at maximum speed for 5 min and the pellet was washed with 70 % (v/v) ethanol. The DNA pellet was air dried until all the ethanol had evaporated and was resuspended in 50 µl of nuclease-free RO water. The obtained plasmid DNA was stored at –20 °C.

2.4.4.2 Midi plasmid DNA preparation from E. coli

Midi plasmid DNA preparations from *E. coli* were performed using the Qiagen-Plasmid-Midi-Kit (Qiagen Limited, UK) according to the manufacturer's instructions (see Qiagen Plasmid Purification Handbook 11/1998, p. 13ff). The air-dried plasmid DNA pellet was resuspended in 500 µl nuclease-free RO water and stored at –20 °C.

2.4.4.3 Estimation of DNA concentration and quality

The concentration and quality of plasmid DNA midi preparations were determined with a Shimadzu spectrophotometer (UV-1601, Shimadzu, Japan) at a wavelength of 260 nm (A_{260}). An A_{260} of 1.0 is equivalent to a concentration of approximately 50 µg ml^{-1} of double-stranded DNA, 33 µg ml^{-1} of single-stranded DNA or 40 µg ml^{-1} RNA (Sambrook et al., 1989). The degree of contamination in the preparations could be estimated by measuring the A_{260}/A_{280} ratio. A value between 1.8-2.0 suggested a clean sample, whereas lower values indicated the presence of contaminants. The concentration and quality of mini plasmid DNA preparations were visually estimated after agarose gel electrophoresis and UV illumination (BioDoc-IT™ System; UVP;CA; USA)(VideoGraphicPrinter UP-890CE; Sony; Japan). The signal for the DNA with the unknown concentration was compared to the intensity of a marker DNA with a known DNA concentration.

2.4.4.4 Total cellular DNA extraction from Synechocystis sp. PCC6803

Total cellular DNA extractions from *Synechocystis* sp. PCC 6803 were performed according to the phenol-chloroform extraction method devised by Dr. Josef Komenda (Institute of Microbiology, Trebon, Czech Republic). A pea-sized glob of *Synechocystis* sp. PCC 6803 cells from a BG-11 agar plate or the pellet of a 1-ml aliquot of a liquid culture were resuspended in 200 µl of TE buffer (10 mM Tris/HCl pH = 8.0, 1 mM EDTA) and 200 µl of phenol were added. The suspension was hand-extracted twice for 20 s and centrifuged in a microfuge (model 5410, Eppendorf AG, Germany) at maximum speed for 5 min. The aqueous phase was transferred to a new tube and one volume of chloroform was added. The mix was hand extracted for 30 s and centrifuged in a microfuge at maximum speed for 5 min. The aqueous phase was transferred to a new tube and a tenth sample volume of 3 M sodium acetate (pH = 4.8) together with two volumes of 96 % (v/v) ethanol were added and mixed by vortexing. To allow DNA precipitation the sample was left at –20 °C overnight. The DNA was pelleted in a microfuge at maximum speed for 30 min and the obtained pellet was washed with 70 % (v/v) ethanol, resuspended in 100 µl nuclease-free RO water and stored at –20 °C.

2.4.5 DNA manipulations

2.4.5.1 Agarose gel electrophoresis

Agarose gel electrophoresis allows the separation of DNA fragments according to their sizes. Gels were prepared with molecular grade agarose (Bioline, UK; final [0.5-1.5 % (w/v)]) dissolved in Tris-acetate-EDTA buffer (TAE; 40 mM Tris-acetate, 1 mM EDTA pH = 8.0) and Ethidium bromide DNA stain (final [1 µg ml^{-1}]). Samples were loaded in the wells after the addition of 6x loading buffer (40 % (w/v) sucrose, 0.25 % (w/v) bromophenol blue; final [1x]). The gels were run in TAE-buffer at 80 to 100 V in a Bio-Rad horizontal Mini-sub cell (70 mm width; Bio-Rad Laboratories Limited, UK) or a Flowgen horizontal gel apparatus (150 mm width; Flowgen Limited, UK). DNA could be visualised by using a UV transilluminator and photographs were taken (BioDoc-IT™ System; UVP;CA; USA)(VideoGraphicPrinter UP-890CE; Sony; Japan). To estimate the size of unknown DNA fragments a DNA marker (2-log DNA marker ladder, N3200S; New England Biolabs Limited, UK) was loaded in one lane of

each agarose gel, which contained fragments of the following sizes (in kb): 10.0, 8.0, 6.0, 5.0, 4.0, 3.0, 2.0, 1.5, 1.2, 1.0, 0.9, 0.8, 0.7, 0.6, 0.5, 0.4, 0.3, 0.2 and 0.1.

2.4.5.2 DNA purification from agarose gels

DNA fragments from agarose gels were purified using the Qiagen gel extraction kit (Qiagen Limited, UK) according to the manufacturer's instructions. DNA was eluted from the spin column with two times 15 µl of nuclease-free RO water and stored at –20 °C.

2.4.5.3 Amplification of DNA fragments by polymerase chain reaction (PCR)

2.4.5.3.1 DNA polymerase enzymes

The thermo stable DNA polymerases used in this study were: BIOTAQ (BIO-21040; Bioline Limited, UK), BIO-X-ACT (BIO-21049; Bioline Limited, UK) and PHUSION (F-530L; New England Biolabs Limited, UK). BIOTAQ DNA polymerase was used for routine screening of *Synechocystis* sp. PCC 6803 segregation and both BIO-X-ACT and PHUSION DNA polymerases were used to amplify DNA fragments for high fidelity cloning and overlap extension. BIO-X-ACT DNA polymerase produced sticky-ended and PHUSION DNA polymerase blunt-ended PCR products.

2.4.5.3.2 Conditions for standard PCR

Either the Techne Touchgene Gradient (FTGrad2D; Techne Ltd., UK) or the Techne Techgene (FTGene5D; Techne Ltd., UK) PCR machine was used to amplify a desired DNA fragment using total cellular DNA extractions from *Synechocystis* sp. PCC 6803 (or other DNA templates) and primers listed in Table 2.7. A typical 50 µl reaction mixture, in which the 2.5 units of BIOTAQ or 2 units of BIO-X-ACT DNA polymerase were used, contained: 5 µl of 1x reaction buffer (dependent on the DNA polymerase; as supplied by Bioline Limited, UK; for BIOTAQ: 10x concentrate NH_4 buffer: 160 mM $(NH_4)_2SO_4$, 670 mM Tris/HCl pH = 8.8, 0.1 % (v/v) Tween-20; for BIO-X-ACT: 10x OptiBuffer and 5x HiSpec reagent: no information about their composition available), 2 µl of 20 mM dNTP mixture (ABgene, UK; final [0.2 mM] for each nucleotide: dATP, dCTP, dGTP and dTTP), 1.5 to 4 µl 50 mM $MgCl_2$ (Bioline, UK; final [1.5 – 4 mM]), 1 µl of 50 µM forward primer (MWG Biotech, Germany; final [1 µM]), 1 µl of 50 µM reverse primer (MWG Biotech, Germany; final

[1 µM]) and ~ 100 ng template DNA. This reaction mixture was made up to 50 µl with sterile RO water, mixed and briefly centrifuged. The lid of the PCR machine was heated during the program to prevent sample evaporation and condensation in the lid of the tube. A standard PCR program consisted of an initial denaturation step at 94 °C for 3 min and 30 subsequent cycles of 94 °C for 30 sec (denaturation), from 46 to 60 °C for 30 sec (primer annealing) and 72 °C for 1 to 6 min (primer extension; 1 min per 1 kb). The final extension step was performed at 72 °C for 10 min. The reaction mixture and the PCR program were varied when the standard procedure did not yield an optimum amplification.

2.4.5.3.3 PCR conditions for the PHUSION DNA polymerase

In order to quickly amplify high fidelity, blunt-ended DNA fragments, PHUSION DNA polymerase was used in PCRs, that varied from the standard PCRs in the following parameters. The typical reaction mixture had a volume of 20 µl and contained 0.4 units of PHUSION DNA polymerase, 4 µl of 5x PHUSION HF buffer (as supplied by New England Biolabs Limited, UK; no information about its composition available), 0.8 µl of 20 mM dNTP mixture (ABgene, UK; final [0.2 mM] for each nucleotide: dATP, dCTP, dGTP and dTTP), 0.4 µl of 50 µM forward primer (MWG Biotech, Germany; final [1 µM]), 0.4 µl of 50 µM reverse primer (MWG Biotech, Germany; final [1 µM]) and ~ 100 ng template DNA. This reaction mixture was made up to 20 µl with sterile RO water, mixed and briefly centrifuged. The PCR program consisted of an initial denaturation step at 98 °C for 30 s and 30 subsequent cycles of 98 °C for 7 s (denaturation), from 46 to 60 °C for 15 sec (primer annealing) and 72 °C for 15 s to 1.5 min (primer extension; 15-30 s per 1 kb). The final extension step was performed at 72 °C for 5 min. The reaction mixture and the PCR program were varied when the standard procedure did not yield an optimum amplification.

2.4.5.3.4 PCR conditions for overlap extension

Overlap extension PCRs (Horton et al., 1993) were performed to introduce the coding sequence for an His_8-tag at the 3' end of a target gene. Initial PCRs (PCR 1 and 2) using total cellular DNA extractions from *Synechocystis* sp. PCC 6803 as DNA template were set up using the same reagents and parameters as for a standard, high fidelity cloning PCR with the BIO-X-ACT DNA polymerase, but with a few alterations as listed below. PCR 1 contained a forward primer that had the same

sequence as the 5' end of the target gene. The reverse primer in PCR 1 was designed to bind directly upstream of the site for sequence insertion, containing the sequence for insertion at its 5' end together with the STOP codon of the target gene and three bases that were complementary to parts of the forward primer in PCR 2. PCR 2 contained the forward primer that shared at its 5' end six complementary bases to the reverse primer in PCR 1 (in which these bases preceded the sequence for insertion), the sequence for insertion and at its 3' end the STOP codon as well as the sequence directly downstream of the site for sequence insertion. The reverse primer in PCR 2 was designed to anneal ~600 bp downstream of the target gene. The PCR program for PCR 1 and 2 consisted of an initial denaturation step at 94 °C for 5 min and 30 cycles of 94 °C for 30 s (denaturation), 45 °C for 30 sec (primer annealing) and 72 °C for 2 min (primer extension). The final extension step was performed at 72 °C for 10 min. The resulting PCR fragments were separated by agarose gel electrophoresis and gel extracted to be used as DNA templates in a final PCR (PCR 3). PCR 3 was set up using the same reagents and parameters as for a standard, high fidelity cloning PCR with the BIO-X-ACT DNA polymerase, but in this reaction mixture 2 µl of each gel purified PCR products from PCR 1 and PCR 2 were used as DNA template and the forward primer was the same as the one used in PCR 1 while the reverse primer was the same as the one in PCR 2.

Table 2.7: Oligonucleotide primers used in this project. All oligonucleotide primers that have been used in this work were purchased from MWG Biotech, Germany. Primers 1-11 were used for cloning and general purposes. Primers 12-15 were used to confirm the segregation of mutants. Primers 16 to 18 were used to omit the TM domain coding sequences of the respective genes for expression constructs. Primers 19-31 were used in the process of His_8-tagging Band 7 proteins. Primers 32 and 33 were used in sequencing reactions.

#	Name	Primer sequence
1	*slr1106*-Fw	5´- GGGCTCGAGATGAGCAAACAATCCTTT –3´ XhoI
2	*slr1106*-Rev	5´- GGGGGATCCCTAGTTAGCCAGGTCAGTTAG –3´ BamHI
3	*slr1768*-Fw	5´- GCCCATATGGGTGCTGTTATCTCGGCGATC –3´ NdeI
4	*slr1768*-Fw-II (Remco)	5´- ACCGGATCCATGGGTGCTGTTATCTCGGCGATC –3´ BamHI
5	*slr1768*-Rev	5´- GGGGGATCCTTAGGGGTCCGACATGATAATGGG -3´ BamHI
6	*slr1128*-Fw	5´- GCCCATATGGAAGCCTTTTTTCTCTTCTTTCTCGTC –3´ NdeI
7	*slr1128*-Rev	5´- GGGGGATCCCTAAACTGCCCGATGGCGGTCTAC -3´ BamHI

Table 2.7 continued

#	Name	Primer sequence
8	*sll0815*- Fw	5´- GCCCATATGGCACGACAAGCTCGCTATCAA –3´ NdeI
9	*sll0815*-Rev	5´- GGGGGATCCTCAACTATCCGATGTTATTTTTTC -3´ BamHI
10	*sll1021*- Fw	5´- GCCCATATGCAAAGTAAATTTTGGTTTGAATTTCTCC –3´ NdeI
11	*sll1021*-Rev	5´- GGGAGATCTCTAAATTTCCTCCGGGGAAAAATT -3´ BglII
12	*slr0228*-Fw (Paulo)	5´- GGGGGATCCTATGAAATTTTCCTGGAGA -3´ BamHI
13	*slr0228*-Rev (Paulo)	5´- GGGCTCGAGAGTTGGGGAATTAACTG –3´ XhoI
14	CP43-1000 fw (Remco)	5´- ATATTTTCCCCTTCTTCGTAGTAGGGGTGC -3´
15	CP43-1000 rev (Remco)	5´- CTGCCATTAAAGAATTGGCTAAAGAAGCAGGTC -3´
16	*slr1768*-TM-Fw	5´- GCCCATATGACTCCCCTTACCTCTGGGGTT –3´ NdeI
17	*slr1128*-TM-Fw	5´- GCCCATATGATTTTGGATCGGGTCGTTTTT –3´ NdeI
18	*sll1021*-TM-Fw	5´- GCCCATATGTTTAAAAAAGAGCAAATGGTGATT –3´ NdeI
19	*slr1106*-HIS-1	5´- CCGCTAGTGATGGTGATGGTGATGGTGATGGTTAGCCAGGTCAGTTAGGTTAAA –3´
20	*slr1106*-HIS-2	5´- GCTAACCATCACCATCACCATCACCATCACTAGCGGCAGCGGGGAAGTTATAGG –3´
21	*slr1106*-down	5´- CCAATGGCCCTTACCTGTCCTGGATTA –3´
22	*slr1768*-HIS-1	5´- GGGTTAGTGATGGTGATGGTGATGGTGATGGGGGTCCGACATGATAATGGGCAA –3´
23	*slr1768*-HIS-2	5´- GACCCCCATCACCATCACCATCACCATCACTAACCCAACCCTGCGGCGGCATGG –3´
24	*slr1768*-down	5´- TTAACCCCCATTCCAAACTTTGCA –3´
25	*slr1128*-HIS-1	5´- TGCCTAGTGATGGTGATGGTGATGGTGATGAACTGCCCGATGGCGGTCTACCTT –3´
26	*slr1128*-HIS-2	5´- GCAGTTCATCACCATCACCATCACCATCACTAGGCAGTTAGCTTGGGGGCTGGG –3´
27	*slr1128*-down	5´- AAAAATGTTGTAATGTTGGACATTGGG –3´
28	*sll0815*-HIS-1	5´- ATTTCAGTGATGGTGATGGTGATGGTGATGACTATCCGATGTTATTTTTTCTGA –3´
29	*sll0815*-HIS-2	5´- GATAGTCATCACCATCACCATCACCATCACTGAAATTCAGCAAATTAAAATCTG –3´
30	*sll0815*-down	5´- TTGGCCCTACTACCCACCAACCAATCC –3´
31	His-Primer	5´- GTGATGGTGATGGTGATGGTGATG –3´
32	M13-Fw	5´- GTAAAACGACGGCCAGTGA -3´
33	M13-Rev	5´- GGAAACAGCTATGACCATG -3´

2.4.5.4 Restriction endonuclease digestion

Restriction endonuclease digestions were performed under suitable conditions as recommended by the enzyme manufacturer's instructions (New England Biolabs Limited, UK). Generally, approximately 1 µg of DNA was digested in 15 µl with 10 to 20 units of restriction endonuclease in the recommended buffer with acetylated bovine

serum albumin (BSA; as supplied by New England Biolabs Limited, UK; final [100 µg ml^{-1}]) at the optimum temperature in 1.5 hours.

2.4.5.5 Ammonium acetate DNA precipitation

Ammonium acetate precipitation is a suitable method for the purification of DNA from restriction endonuclease digestions and PCR products 1.6 volumes of 7.5 M ammonium acetate and eight volumes of 100 % (v/v) ethanol were added to the sample and the mixture was incubated for 15 min at –80 °C. The DNA was pelleted in a microfuge at maximum speed for 5 min and the supernatant discarded. The DNA was then washed in 70 % (v/v) ethanol and centrifuged again. Finally, the pellet was air dried, until all the ethanol had evaporated and resuspended in an appropriate volume of nuclease-free RO water.

2.4.5.6 Removal of 5' overhangs from DNA

In order to be able to insert a blunt-ended DNA fragment into a 5' overhang restriction site, it was necessary to convert the sticky ends into blunt-ends before the ligation reaction. The Klenow enzyme fragment of the *E. coli* DNA polymerase I was used for this purpose. Each reaction mixture contained 5 µl 10x restriction endonuclease buffer 2 (as supplied by New England Biolabs Limited, UK; 10x NEB buffer 2: 500 mM NaCl, 100 mM Tris/HCl pH = 7.9, 100 mM $MgCl_2$, 10 mM dithiothreitol), 5 µl 10x BSA (1:10 dilution of 100x BSA as supplied by New England Biolabs Limited, UK; final [100 µg ml^{-1}]), 1 µl dNTP-mix (20 mM; ABgene, UK), 1 unit of Klenow polymerase (Promega Corp., USA), ~150 ng of DNA and RO water was added to a final volume of 50 µl. The reaction mixture was incubated for 15 min at room temperature and afterwards heat inactivated for 20 min at 75 °C.

2.4.5.7 DNA ligation

DNA fragments were inserted into various recipient vectors using Quick DNA ligase according to the manufacturer's instructions (New England Biolabs Limited, UK). Excess insert fragment was provided and in most cases the insert/vector molar ratio was 4:1. The reaction mixture was incubated for 15 min at RT.

2.4.5.8 DNA Sequencing

The sequencing of plasmid DNA was performed by ABC Sequencing, Imperial College London, London, UK. The reaction mixture that was send off contained: ~ 1 µg of plasmid DNA, 12.5 pmol of a relevant primer and was made up to 12 µl with nuclease-free RO water.

2.5 Microarray analysis

The presented microarray data and the method with which it was obtained was kindly provided by Dr. Iwane Suzuki (National Institute for Basic Biology, Okazaki, Japan). *Synechocystis* sp. PCC 6803 (GT) was grown in liquid BG-11 medium under continuous light at 70 µE m^{-2} s^{-1} with an aeration of 1 % (v/v) CO_2/air at 34 °C. At an OD_{730} of 0.3 to 0.5 the cells, which had been growing for 12 to 16 h after inoculation into fresh BG-11 medium, were placed for 20 min under various stress conditions: salt stress (0.5 M NaCl), hyperosmotic stress (0.5 M sorbitol), heat stress (shift from 34 °C to 44 °C), oxidative stress (0.25 mM H_2O_2), cold stress (shift from 34 °C to 22 °C) and high-light stress (shift from 70 µE m^{-2} s^{-1} to 500 µE m^{-2} s^{-1}) before RNA was isolated for microarray analysis. *Synechocystis* DNA microarrays (Cyano-CHIP) were purchased from TaKaRa Bio Co. Ltd. (TaKaRa Bio Co. Ltd., Japan), and the analyses were performed as described previously (Suzuki et al. 2001; Kanesaki et al. 2002). All experiments were performed with CyanoCHIP version 1.6, which included 3074 out of the 3264 genes on the *Synechocystis* chromosome, and results were quantified with the IMAGENE version 5.5 program (BioDiscovery, USA). Changes in the levels of transcripts of individual genes relative to the total level of mRNA were calculated after normalisation by reference to the total intensity of signals from all genes with the exception of genes for rRNAs.

2.6 Analysis of *Synechocystis* sp. PCC 6803

2.6.1 Electron microscopy of *Synechocystis* sp. PCC 6803

2.6.1.1 Ultra-thin sections of Synechocystis sp. PCC 6803 cells

Electron microscopy of ultra-thin sections of *Synechocystis* sp. PCC 6803 cells was kindly performed by Dr. Uwe Kahmann (Centre for ultrastructural diagnostics,

Bielefeld, Germany). *Synechocystis* sp. PCC 6803 cells were grown in liquid BG-11 medium, until the culture reached an OD_{730} of 0.8. A 10-ml aliquot of the culture was harvested (centrifuge model Allegra 6R, Beckman Coulter Limited, UK; GH-3.8; 2,000 g, 15 min, 4 °C) and the cell pellet rinsed three times with electron microscopy buffer (EM buffer; 50 mM potassium phosphate buffer pH = 7.0 (Sambrook et al, 1989). Cells were fixed in 2.5 % (w/v) glutaraldehyde (Serva, Germany) in EM buffer for 60 min, washed three times with EM buffer and subsequently treated with 2 % (w/v) OsO_4 in RO water. Dehydration of the sample was performed in a graded acetone series (15 %, 30 %, 45 %, 60 %, 75 %, 90 % and 3x 100 % (v/v) acetone in RO water, 20 min for each dilution) and by an incubation in 100 % acetone for 60 min. After dehydration the samples were embedded stepwise in Transmit EM resin (TAAB Laboratories Equipment, UK) (acetone/Transmit (1:1) for 20 min and acetone/Transmit (1:2) for 14 h). After the next 6 h incubation the pure Transmit was changed tree times and for better infiltration the samples were evaporated under vacuum. Subsequently, the samples were filled into plastic capsules and left to polymerise for 16 h at 70 °C. Ultrathin sections of 60 to 70 nm were made with a diamond knife (DuPont, Germany) on an Ultracut (Ultracut E; Reichert, Germany) and placed onto 400 mesh gold grids. As far as possible steps were performed at 4 °C. Samples were then stained with 2 % (w/v) aqueous uranyl acetate for 15 min followed by 2 % (w/v) aqueous lead citrate for 15 min. Preparations were examined on a Hitachi H500 electron microscope at 75 kV.

2.6.1.2 Surface analysis of whole cells

Transmission electron microscopy (TEM) was used under the supervision of Dr. Jon Nield (Imperial College London, London, UK) to visualise the surface of *Synechocystis* sp. PCC 6803 cells. Liquid BG-11 cultures of *Synechocystis* sp. PCC 6803 were grown under routine growth conditions to an OD_{730} of ~0.5 and 10 µl droplets of undiluted cells were negatively stained with 2 % (w/v) uranyl acetate (pH = 4.5) on carbon-coated copper electron microscope (EM) grids via the droplet method devised by Harris and Agutter (1970). Cells were imaged on Kodak SO-163 film (Eastman Kodak Company, USA) at RT using a Phillips CM100 electron microscope (Royal Philips Electronics, The Netherlands). Micrographs were taken at 100 kV and a typical defocus of 2 µm. Micrographs displaying no discernible astigmatism or drift

were scanned with a Nikon LS9000 Super Coolscan densitometer (Nikon Ltd., UK) with an initial step size of 6.35 µm.

2.6.2 [^{35}S]-L-methionine pulse-labelling and pulse-chase analysis of *Synechocystis* sp. PCC 6803 cells

[^{35}S]-L-methionine pulse-labelling and pulse-chase analyses of *Synechocystis* sp. PCC 6803 cells were performed as described by Tichy et al. (2003) and Komenda et al. (2005).

2.6.2.1 [^{35}S]-L-methionine pulse-labelling of Synechocystis sp. PCC 6803 cells

A *Synechocystis* sp. PCC 6803 liquid culture was grown under routine growth conditions and its chlorophyll a concentration was determined as described in section 2.7.1.3 (optimum chlorophyll a concentration was considered to be between 5 and 6 µg ml^{-1}). Cells for 300 µg of chlorophyll a were spun down in two Falcon tubes (centrifuge model Allegra 6R, Beckman Coulter Limited, UK; GH-3.8; 2,000 g, 15 min, 30 °C) and each resulting cell pellet was gently resuspended in 1 ml of fresh BG-11 medium. The cells were transferred into a new 1.5 ml screw cap Eppendorf tube and washed twice with fresh BG-11 medium (spun down in a microfuge at maximum speed for 2 min and resuspended in fresh BG-11 medium). After the washing steps, the total volume in each tube was adjusted to 1 ml and the pellets were thoroughly resuspended. The cells were then equally distributed (0.5-ml aliquots) into four prepared pulse-chase glass vials that already contained 0.5 ml of fresh BG-11 medium. This lead to four pulse-chase glass vials each containing 1 ml of cell suspension with a chlorophyll a concentration of 75 µg ml^{-1}. The vials were kept in a four place, temperature controlled water jacket at 30 °C by a Grant Y6 circulating water bath (Grant Instruments Limited, UK) on a Selotec P6 shaking platform (Selotec GmbH, Germany) to allow equilibration of the cells at 30 °C for 30 min at an incident fluorescent white light intensity of 250 µE m^{-2} s^{-1}. After the 30 min equilibration time, the samples were pooled and 20 µCi radioactive [^{35}S]-L-methionine (Amersham Biosciences, UK) were added. The samples were equally divided again into the four glass vials and incubated for 30 min under the same conditions as before. After pulse-labelling the *Synechocystis* sp. PCC 6803 cells, the radioactive [^{35}S]-L-methionine was

removed by transferring the samples to new screw cap Eppendorf tubes and washing them three times with plain BG-11 medium (spun down in a microfuge at maximum speed for 2 min and resuspended in fresh BG-11 medium; supernatants containing low-level radioactive waste were disposed of in an appropriate sink).

2.6.2.2 [^{35}S]-L-methionine pulse-chase analysis of Synechocystis sp. PCC 6803 cells

For the [^{35}S]-L-methionine pulse-chase analysis, the washed samples from the pulse-labelling experiment were pooled, 100 µl of 180 mM unlabeled L-methionine were added (final [~4.5 mM]) and the cells were equally divided into the four glass vials again. The samples were incubated at 30 °C at an incident fluorescent white light intensity of 250 µE m^{-2} s^{-1} for 5 min before a 1-ml aliquot was removed from the pooled sample and shock frozen in a screw cap tube (t = 0 min). The light intensity was now raised to 1000 µE m^{-2} s^{-1} and other aliquots were taken in the same manner after 45, 90 and 180 min. The samples were stored at –80 °C until membrane extracts were generated by small-scale membrane isolations which could be used for 1-D or 2-D SDS-PAGE. The obtained gels were dried on Whatman paper using a gel dryer (Model 583; Bio-Rad Laboratories Limited, UK) and exposed to either a X-Ray film (SuperRX, X-Ray Film, 100 NIF, 18x24 cm; Fuji medical, UK) or to a Phosphorimager plate (BAS MP 2040; Fuji, UK) for 1 to 10 days. The film was developed according to the manufacturer's instructions, while the Phosphorimager plate was read in a Phosphorimager reader (Fuji Film Scanner FLA-5000; Fuji, UK) operated with the Image Reader FLA 5000 Version 3.0 software (Fuji, UK). Phosphorimager results were quantified using the AIDA software Version 3.28 (Raytest, Germany).

2.6.3 Oxygen measurements in liquid *Synechocystis* sp. PCC 6803 cultures

The amount of oxygen dissolved in a liquid culture was assessed with a Hansatech DW2 oxygen electrode (Hansatech instruments Ltd., UK) linked to a computer managed by a Oxy-Lab 1 control box (Hansatech Instruments Limited, UK). The temperature of the DW2 chamber was controlled by a Grant W14 circulating water bath (Grant Instruments Limited, UK). Before measuring different whole cell

samples the electrode needed to be calibrated according to the manufacturer's instructions.

2.6.3.1 Oxygen evolution measurements of whole cells

The activity of PSII of *Synechocystis* sp. PCC 6803 was assessed by means of oxygen evolution in liquid cultures with a chlorophyll a concentration between 2 and 5 μg ml^{-1}. Measurements required the use of 2 mM 2,6 dichlorobenzoquinone (DCBQ; Eastman Kodak Co., USA; in EtOH), a photosystem II Q_A electron acceptor and 1 mM potassium ferricyanide ($K_3Fe(CN)_6$), a DCBQ oxidising agent. Both reagents were added under stirring to the cell suspension to a total volume of 1 ml into the DW2 chamber. After stabilisation of the signal in the dark, cells were exposed to actinic light illumination at 800 μE m^{-2} s^{-1} for 2 min and oxygen evolution was recorded.

2.6.3.2 Photoinhibition analysis

100 ml starter cultures of wild-type *Synechocystis* sp. PCC 6803 and the mutant of interest were grown and inoculated into 1000 ml of culture medium under routine growth conditions. Photoinhibition analyses could be performed when the large cultures had grown to an OD_{730} of ~0.8 and sufficient cells to yield 200 to 300 ml of cell suspension with a chlorophyll a concentration of 10 to 25 μg ml^{-1} could be harvested (GH- 3.8; 2,000 g, 15 min, 30 °C). The harvested cells were resuspended in fresh BG-11 medium and placed in a sterile 500 ml glass crystallisation dish to be incubated at 30 °C for 1 h under continuous white light illumination with an intensity of 100 μE m^{-2} s^{-1}. Cultures were agitated by a magnetic stirrer and kept at 30 °C by a shallow circulatory water bath connected to a Julabo F12 heater/cooler unit (Julabo Labortechnik GmbH, Germany). A 1-kW halogen lamp in conjunction with a transparent heat sink was used as the light source. After the equilibration period, each of the wild-type and mutant cell suspensions was equally split, 100 μg ml^{-1} lincomycin (a protein synthesis inhibitor; in MetOH) added to one aliquot of each strain and the light intensity was raised to 1200 μE m^{-2} s^{-1}. A 3-ml sample that was taken every hour for six hours (without significantly reducing the culture depth) and diluted with fresh BG-11 medium to 5 μg ml^{-1} chlorophyll a before oxygen evolution was measured. Two 1-ml aliquots of the diluted samples were flash frozen in liquid nitrogen and stored at -80 °C for later chlorophyll a concentration determination. Finally, the

oxygen evolution rates were calculated in terms of μmol oxygen mg chlorophyll a $^{-1}$ h^{-1} and the normalised rates (t=0 corresponds to 100 %) were plotted as a function of time.

2.7 Protein biochemistry techniques

All protein biochemistry techniques were performed on ice or at 4 °C and where necessary under dim light conditions, in order to minimise protein damage.

2.7.1 Cell fractionation techniques in *Synechocystis* sp PCC 6803

Crude cyanobacterial membrane isolations were performed using glass bead breakage and differential centrifugation as described by Tichy et al. (2003).

2.7.1.1 Small-scale membrane isolation

Synechocystis sp. PCC 6803 cells were pelleted from a 50-ml culture (centrifuge model Allegra 6R, Beckman Coulter Limited, UK; GH-3.8; 2,000 g, 15 min, 4 °C) or from a previously harvested 50-ml culture (microfuge; 9,000 g, 2 min, 4 °C) and washed once with 1 ml ice cold buffer A (25 mM Tris/HCl pH = 7.5, 1 mM ε-amino caproic acid). The cells where then resuspended in 500 μl of ice cold buffer A and transferred to a new 2-ml Eppendorf tube to which ~200 μl of glass beads (200-300 μm; Sigma Aldrich Company Limited, UK) were added. The mixture was vortexed (strong vortexer obtained from Dr. Josef Komenda, Institute of Microbiology, Trebon, Czech Republic) for 1 min, placed on ice for 1 min and this process was repeated one more time. Once the glass beads had settled at the bottom of the tube, the supernatant was transferred to another tube. To maximise the yield, the glass beads were washed once with 1 ml of buffer A and the liquid was transferred to the new tube. The pooled supernatants were centrifuged (microfuge; 7,000 g, 1 min) to pellet unbroken cells. The supernatant was transferred to a new Eppendorf tube and centrifuged again (microfuge; 12,000 g, 20 min, 4 °C). The blue supernatant was kept separately and the pellet containing the thylakoid and plasma membranes was resuspended in 100 μl of an appropriate buffer: e.g. in ACA buffer (750 mM ε-amino caproic acid, 50 mM BisTris/HCL pH = 7.0, 0.5 mM EDTA) for blue-native gel electrophoresis and immunoprecipitations or in storage buffer (50 mM Tricine/NaOH

pH = 7.5, 600 mM sucrose, 30 mM $CaCl_2$ and 1 M betaine). The chlorophyll a content was determined and the sample flash frozen in liquid nitrogen to be kept –80 °C.

2.7.1.2 Large-scale membrane isolation

Synechocystis sp. PCC 6803 cells were pelleted from a 1000-ml culture (centrifuge model J2-21; Beckman Coulter Limited, UK; JA-14 rotor; 6,000 g, 15 min, 4 °C) or from a previously harvested 1000-ml culture (centrifuge model Allegra 6R, Beckman Coulter Limited, UK; GH-3.8; 2,000 g, 15 min, 4 °C) and resuspended in a 50-ml Falcon tube with 15 ml ice cold buffer A (25 mM Tris/HCL pH = 7.5, 1 mM ε-amino caproic acid). Glass beads (200-300 μm; Sigma Aldrich Company Limited, UK) were added to the 10 ml mark of the tube and the mixture was vortexed for 2 min, placed on ice for 1 min and this process was repeated twice. Once the glass beads had settled at the bottom of the tube, the supernatant was transferred to a new 50-ml Falcon tube. To maximise the yield, the glass beads were washed several times with altogether ~35 ml of buffer A and the liquid was transferred to the new tube. The pooled supernatants were centrifuged (centrifuge model Allegra 6R, Beckman Coulter Limited, UK; GH-3.8; 2,000 g, 15 min, 4 °C) to pellet unbroken cells. The supernatant was transferred into two type Ti70 ultracentrifugation tubes and centrifuged (ultracentrifuge model L-70; Beckman Coulter Limited, UK; Ti70 rotor; 100,000 g, 30 min, 4 °C). The blue supernatant was kept separately and the pellet containing the thylakoid and plasma membranes was resuspended in ~5 ml of storage buffer (50 mM Tricine/NaOH pH = 7.5, 600 mM sucrose, 30 mM $CaCl_2$ and 1 M betaine). The chlorophyll a content was determined and the sample flash frozen in liquid nitrogen to be kept –80 °C. Typically, 5 ml crude membranes with a chlorophyll a concentration of 0.5 μg μl^{-1} were obtained, corresponding to a yield of ~40 %.

2.7.1.3 Determination of chlorophyll a concentration

The chlorophyll a concentration of both liquid *Synechocystis* sp. PCC 6803 cultures and of isolated crude membrane isolations were estimated, typically in duplicates, by the method of Lichtenthaler and Welburn (1983). In case of a liquid culture, 1 ml of cells was centrifuged (microfuge; 9,000 g, 1 min, RT) and the pellet resuspended in 1 ml of 100 % methanol. Crude membrane extracts were either diluted 100 or 200 times by adding 10 or 5 μl to 990 or 995 μl 100 % methanol respectively. Chlorophyll a was extracted for 5 min and the sample subsequently centrifuged

(microfuge; maximum speed, 1 min, RT). The sample was transferred to a 1-ml disposable cuvette and measured with a Shimadzu spectrophotometer (UV-1601, Shimadzu, Japan) calibrated with 100 % methanol between the wavelengths of 600 and 800 nm. The chlorophyll a content was then estimated using the formula: $(A_{666}-A_{750})$ x 12.61 = [chlorophyll a] in μg ml^{-1}.

2.7.1.4 Determination of protein concentration

The protein concentration of a sample was determined with the Bio-Rad *DC* protein assay (Bio-Rad Laboratories Limited, UK) according to the manufacturer's instructions (assay volume was reduced fourfold). ACA buffer is not compatible with this protein concentration determination method.

2.7.2 Differential protein extraction of membranes

Small-scale crude membrane isolations were performed from *Synechocystis* sp. PCC 6803 cells and five equal amounts corresponding to approximately 20 μg chlorophyll a were pelleted in a microfuge (maximum speed, 20 min, 4 °C). Subsequently, the pellets were resuspended in 100 μl of various buffers: buffer B (control; 25 mM Tris/HCL pH = 7.5, 1 mM ε-amino caproic acid, 1 M sucrose), two aliquots in extraction buffer (20 mM Tricine pH = 8.0), one aliquot in extraction buffer with 2 M NaCl, pH = 8.0 and one aliquot in 20 mM CAPS, pH = 12.0. To determine the chlorophyll a concentration of the samples for later analyses an aliquot of 10 μl was taken. The rest of the sample was incubated for 15 min at RT and those samples for differential membrane isolation were treated twice with a freeze (30 min at –80 °C) and thaw (20 min at RT) cycle. After the freeze thaw treatment, samples were pelleted in a benchtop ultracentrifuge (ultracentrifuge model T-100; Beckman Coulter Limited, UK; TLA 120.1; 100,000 g, 20 min, 4 °C). The supernatant was removed and kept as the soluble fraction, whereas the pellet was resuspended in 90 μl of buffer B as the pellet fraction. Equal amounts of the soluble and the pellet fractions corresponding to 1 μg of chlorophyll a after the initial resuspension were analysed by 1-D SDS-PAGE and immunoblotting analyses.

2.7.3 Two-phase partitioning of a crude *Synechocystis* sp. PCC 6803 membrane isolation

Plasma and thylakoid membrane isolations generated by two-phase partitioning (Norling et al., 1994) for 1-D SDS-PAGE and immunoblotting analyses were kindly provided by Prof. Eva-Mari Aro's group (University of Turku, Turku, Finland) (Zhang et al., 2004).

2.7.4 Detection of oxidised proteins of *Synechocystis* sp. PCC 6803

In order to qualitatively compare the levels of protein oxidation in wild-type and mutant *Synechocystis* sp. PCC 6803 cells, an OxyBlot kit was used as described in the manufacturer's instructions (Chemicon International, Canada). This kit was based on the immunochemical detection of protein carbonylation (as an indicator for oxidative stress) after derivatisation of proteins with 2,4-dinitrophenylhydrazine (DNPH) (Levine et al., 1990; Shacter et al., 1994). 25-ml aliquots from liquid cultures were harvested and small-scale membrane isolations (see section 2.7.1.1) were performed. Protein concentrations for soluble fractions were determined by the DC protein assay (see section 2.7.1.4). For crude membrane fractions the chlorophyll a concentration was determined to ensure that the same amounts of protein were processed (1 μg μl^{-1} of chlorophyll a corresponds to ~12 μg μl^{-1} of protein). 7 μg of protein for soluble fractions and 10 μg of protein for the membrane fractions were derivatised and analysed using 1-D SDS-PAGE followed by immunoblotting. Immunodetection of DNP residues was performed as described in the OxyBlot instruction manual, although blots were treated as described in section 2.7.9.

2.7.5 Size exclusion using fast protein liquid chromatography (FPLC)

Proteins and protein complexes from *Synechocystis* sp. PCC 6803 and *Thermosynechococcus elongatus* membrane isolations were separated according to their sizes on a Superose 6 column (Amersham Pharmacia, UK; kindly provided by Prof. Paul Freemont's group, Imperial College London, London, UK) using an ÄKTA FPLC setup (Amersham Pharmacia, UK; kindly provided by Prof. Steve Matthew's group, Imperial College London, London, UK). Large-scale membrane isolations were

washed with 30 ml 2x phosphate-buffered saline (PBS; 1x PBS: 150 mM NaCl, 7.5 mM Na_2HPO_4, 2.5 mM NaH_2PO_4) and pelleted in an ultracentrifuge (ultracentrifuge model L-70; Beckman Coulter Limited, UK; Ti70 rotor; 100,000 g, 30 min, 4 °C). The pellets were resuspended in a small volume of 2x PBS and the chlorophyll a concentrations were adjusted to 100 µg in 270 µl 2x PBS. The samples were solubilised with 30 µl 10 % (w/v) n-dodecyl-β-maltoside (β-DM) for 10 min on ice and unsolubilised material was pelleted by centrifugation (microfuge; maximum speed, 10 min, 4 °C). The supernatants were loaded from an 250 µl loading loop onto the Superose 6 column and the runs performed at RT controlled by an ÄKTA FPLC unit (2x PBS supplemented with 0.05 % (w/v) β-DM running buffer, flow rate at 0.4 ml min^{-1}, 500 µl fractions and high pressure alarm set at 1.25 MPa). The fractions were collected automatically by a FRAP-950 fraction collector (Amersham Pharmacia, UK) and subsequently analysed by 1-D SDS-PAGE and immunoblotting. The following proteins were run as marker proteins using the same conditions and setup as for the samples: Dextran Blue 2000 (2 MDa; eluted after 7.76 ml), Thryoglobulin (669 kDa; eluted after 12.34 ml) (both from high molecular weight marker kit for FPLC; Amersham Pharmacia, UK) and Amylase (200 kDa; eluted after 15.14 ml) (high molecular weight marker kit for FPLC; Sigma Aldrich Company Limited, UK).

2.7.6 Continuous sucrose-density gradient centrifugation

Proteins and protein complexes from *Synechocystis* sp. PCC 6803 and *Thermosynechococcus elongatus* membrane isolations were separated according to their sizes by continuous sucrose-density centrifugation. Large-scale membrane isolations were washed with 30 ml buffer A (25 mM Tris/HCL pH = 7.5, 1 mM ε-amino caproic acid) and pelleted in an ultracentrifuge (ultracentrifuge model L-70; Beckman Coulter Limited, UK; Ti70 rotor; 100,000 g, 30 min, 4 °C). The pellets were resuspended in a small volume of ACA buffer (750 mM ε-amino caproic acid, 50 mM BisTris/HCl pH = 7.0, 0.5 mM EDTA) and the chlorophyll a concentrations were adjusted to 100 µg in 400 µl ACA buffer. The samples were then solubilised with 45 µl 10 % (w/v) n-dodecyl-β-maltoside (β-DM) for 10 min on ice and unsolubilised material was pelleted by centrifugation (microfuge; maximum speed, 10 min, 4 °C). The supernatants were directly loaded onto previously prepared, ice cold 0.1 to 1.8 M or 0 to 1.5 M continuous sucrose-density gradients (in 20 mM MES/KOH pH = 6.0, 20

mM $CaCl_2$, 20 mM $MgCl_2$, 0.5 M betaine, 0.03 % (w/v) β-DM) and centrifuged (ultracentrifuge model L-70; Beckman Coulter Limited, UK; SW40 rotor; 190,000 g, 16 h, 4 °C). After centrifugation, the gradients were photographed (Canon PowerShot Pro 1, Canon, UK), fractionated into 1-ml fractions using a Gilson pipette, and then analysed further by 1-D SDS-PAGE and immunoblotting.

2.7.7 Protein precipitations

2.7.7.1 Acetone protein precipitation

In order to precipitate proteins from a sample, four times the sample volume of ice-cold, 100 % acetone were added, the mixture vortexed and incubated for 60 min at -20 °C. Precipitated proteins were pelleted in a microfuge (maximum speed, 10 min, RT) and resuspended in an appropriate volume of a desired buffer.

2.7.7.2 Trichloroacetic acid (TCA) protein precipitation

Samples resuspended in buffers that contained non-compatible reagents with the acetone protein precipitation (e.g. sucrose), were precipitated by TCA protein precipitation. A sample volume of 20 % (w/v) TCA was added to the sample, vortexed and incubated for 20 min at -20 °C. Precipitated proteins were pelleted in a microfuge (maximum speed, 10 min, RT), washed in two sample volumes (or 500 µl) of ice-cold, 100 % acetone and resuspended in an appropriate volume of a desired buffer.

2.7.8 Polyacrylamide gel electrophoresis (PAGE)

Polyacrylamide gel electrophoresis (PAGE) was performed to separate complex protein mixtures according to their size differences into distinctive bands in a polyacrylamide gel matrix (Laemmli, 1970).

2.7.8.1 One-dimensional sodium dodecyl sulphate gel electrophoresis (1-D SDS-PAGE)

Samples for 1-D SDS-PAGE analyses were prepared by adding 1x or 2x SDS sample buffer (2x concentrate: 125 mM Tris/HCL pH = 6.8, 4 % (w/v) SDS, 20 % (v/v) glycerol, 0.1 % (w/v) bromophenol blue and 10 % (v/v) β- mercaptoethanol added freshly before each use; final [1x]) and incubation of the mixture (a) for 5 min at

95 °C for *E. coli* total cell extracts or (b) 45 min at RT for cyanobacterial soluble or membrane fractions. Unsolubilised material was pelleted in a microfuge (maximum speed, 10 min, RT) and samples were either flash frozen in liquid nitrogen for storage at –20 °C or loaded into the stacking gel wells at maximum volumes of 15 µl for 15-well gels or 25 µl for 10-well gels. The gels were self cast, 0.75 mm thick and routinely run in the Bio-Rad Mini-PROTEAN III vertical gel system (Bio-Rad Laboratories Limited, UK). The separation gel was typically a 10 or 12.5 % (w/v) continuous polyacrylamide (PAA; from a 40 % acrylamide/bisacrylamide = 37.5/1 stock solution), 6 M urea, 0.375 M Tris/HCl pH = 8.9, 0.01 % (v/v) N,N,N',N' tetramethylenediamine (TEMED); 0.1 % (w/v) ammonium persulphate (APS) SDS-PAGE gel. To obtain well focused protein bands, it proved crucial to adjust the pH of the separation gel solution to 8.9 again prior to adding TEMED and APS. A 5 % (w/v) PAA (from a 40 % acrylamide/bisacrylamide = 37.5/1 stock solution) stacking gel containing 0.125 M Tris/HCl pH = 6.8, 0.01 % (v/v) TEMED and 0.1 % (w/v) APS was poured on top of the separation gel. The gels were run at RT with a constant voltage of 100 to 130 Volts for a period of 2 to 3 h using a Bio-Rad PowerPac Basic (Bio-Rad Laboratories Limited, UK) in a variant of the Laemmli running buffer (25 mM Tris, 190 mM glycine, 0.1 % (w/v) SDS, pH = 8.3) (Laemmli, 1970). The obtained gels were either stained with Coomassie (see 2.7.8.4) or silver (see 2.7.8.5) or used for immunoblotting analyses (see 2.7.9).

2.7.8.2 One-dimensional blue-native polyacrylamide gel electrophoresis (1-D BN-PAGE)

The method for BN-PAGE analysis (Schägger and von Jagow, 1991; Schägger et al., 1994) was adapted for cyanobacteria (personal communication with Dr. Pengpeng Zhang, University of Turku, Turku, Finland) to routinely separate protein complexes from *Synechocystis* sp. PCC 6803 and *Thermosynechococcus elongatus* membrane isolations under native conditions according to their molecular masses. Both freshly prepared membrane isolations (see section 2.7.1.1) and frozen samples in storage buffer (50 mM Tricine/NaOH pH = 7.5, 600 mM sucrose, 30 mM $CaCl_2$ and 1 M betaine) could be used for BN-PAGE analysis. Enough sample for subsequent analyses (20 to 70 µg of protein determined with DC protein assay (see section 2.7.1.4) or 2 to 7 µg of chlorophyll a determined as described in section 2.7.1.3 per gel lane) were washed in 500 µl washing buffer (50 mM BisTris pH = 7.0, 330 mM sorbitol)

and centrifuged in a microfuge (maximum speed, 10 min, 4 °C). The pellet was carefully resuspended in 10 µl resuspension buffer (50 mM BisTris pH = 7.0, 40 % (v/v) glycerol, 250 µg ml^{-1} Pefabloc, 10 mM $MgCl_2$, 0.01 U ml^{-1} RNase-free DNase RQ1 (Promega, USA)) and left on ice for 10 min to settle. The volume of the resuspended sample was then measured using a pipette and after transferring it to a new tube, the same volume solubilisation buffer (50 mM BisTris pH = 7.0, 40 % (v/v) glycerol, 250 µg ml^{-1} Pefabloc, 10 mM $MgCl_2$, 0.01 U ml^{-1} RNase-free DNase RQ1 (Promega, USA), 3 % (w/v) β-DM)) was added. For solubilisation, the sample was incubated for 10 min on ice and another 10 min at RT avoiding illumination at all times. Unsolubilised material was pelleted in a microfuge (maximum speed, 15 min, 4 °C) and one tenth of sample volume sample buffer (200 mM BisTris pH = 7.0, 75 % (w/v) sucrose, 1 M ε-amino caproic acid and 5 % (w/v) Serva blue G) was added prior to loading usually 22 µl of the sample per gel lane. The gels were self cast, 0.75 mm thick and routinely run in the Bio-Rad Mini-PROTEAN III vertical gel system (Bio-Rad Laboratories Limited, UK) or Hoefer Mighty Small mini-vertical unit (Hoefer, USA). Typically, a 5 to 12.5 % (w/v) continuous polyacrylamide gradient separation gel was poured using a self-made gradient maker (kindly provided by Dr. Jane Saffell's group, Imperial College, London, London, UK) standing on a magnetic stirrer with the outlet tube connected to a Watson-Marlow SciQ 400 peristaltic pump (Watson-Marlow Bredel Incorporated, USA). The heavier 12.5 % (w/v) polyacrylamide (PAA; from a 48 % (w/v) acrylamide/1.5 % (w/v) bisacrylamide = 32/1 stock solution) containing 50 mM BisTris/HCL pH = 7.0, 500 mM ε-amino caproic acid and 20 % (v/v) glycerol was loaded into the chamber closest to the outlet tube. The lighter 5 % (w/v) PAA, 50 mM BisTris/HCL pH = 7.0, 500 mM ε-amino caproic acid and 5 % (v/v) glycerol gel solution was loaded in the other chamber. Both gel solutions were stirred by equal, small stirrer bars and 0.05 % (v/v) TEMED and 0.015 % (w/v) APS were added before the gel solutions were allowed to flow in between the glass plates to form a continuous polyacrylamide gradient gel matrix. A 4 % (w/v) PAA, 50 mM BisTris/HCL pH = 7.0, 500 mM ε-amino caproic acid stacking gel was poured on top of the separation gel and a 10 lane comb was inserted to form the sample wells. The anode buffer (50 mM BisTris/HCL pH = 7.0), coloured cathode buffer (50 mM Tricine, 15 mM BisTris/HCL pH = 7.0, 0.02 % (w/v) Coomassie Brilliant Blue G) and colourless cathode buffer (50 mM Tricine, 15 mM BisTris/HCL pH = 7.0) were precooled at 4 °C. The gels were run for ~5.5 h at 4 °C with a

gradually from 50 to 200 V increasing voltage using a Bio-Rad PowerPac Basic (Bio-Rad Laboratories Limited, UK). After the blue-coloured buffer front had reached the middle of the gel, the upper coloured cathode buffer was replaced by the uncoloured cathode buffer. The gels resulting from this procedure will be referred to as first dimensions and were either stained with Coomassie (see section 2.7.8.4), used for immunoblotting analyses (see section 2.7.9) or processed further when 2-D SDS gel analyses (see section 2.7.8.3) were performed.

2.7.8.3 Two-dimensional SDS-PAGE (2-D SDS-PAGE)

The successive application of 1-D BN-PAGE and SDS-PAGE as a second dimension divided separated protein complexes from the first dimension into their subunits in the second dimension. 1-D BN-PAGE was performed as described in section 2.7.8.2 and the gel was cut into its individual lanes to be further used in 2-D SDS-PAGE analyses. Initially, the protein complexes in the first dimension gel slice had to be solubilised for 60 min at RT in Laemmli SDS sample buffer (0.5 M Tris/HCl pH = 6.8, 6 M urea, 23 % (v/v) glycerol, 20 % (w/v) SDS) supplemented with 5 % (v/v) β-mercaptoethanol. The gel for the second dimension was self cast, 1 mm thick, contained 12.5 or 14 % (w/v) PAA, but was otherwise poured in the same way as a 1-D SDS-PAGE gel (see section 2.7.8.1). The stacking gel however did not have wells but consisted out of a 5 mm layer gel matrix, so that the solubilised first dimension gel strip could still be placed on top of it. A piece of Whatman paper, soaked with 10 µl of low molecular weight marker (Amersham Pharmacia, UK) or prestained protein marker (New England Biolabs Limited, UK) was slipped in between the glass plates before the gel strip was then sealed in between the glass plates using 0.5 % (w/v) agarose in running buffer (25 mM Tris/HCl, 190 mM glycine, 0.1 % (w/v) SDS, pH = 8.3). The gel was run at RT with a constant voltage of 100 to 130 Volts for a period of 2 to 3 h using a Bio-Rad PowerPac Basic (Bio-Rad Laboratories Limited, UK) in a variant of the Laemmli running buffer (25 mM Tris, 190 mM glycine, 0.1 % (w/v) SDS, pH = 8.3) (Laemmli, 1970). The obtained gels were either stained with Coomassie Blue (see section 2.7.8.4) or silver (see section 2.7.8.5) or used for immunoblotting analyses (see section 2.7.9).

2.7.8.4 Coomassie-brilliant-blue-R-250-staining of polyacrylamide (PAA) gels

Gels were incubated for at least two hours, but preferably overnight, under gentle shaking in staining solution (40 % (v/v) ethanol, 10 % (v/v) acetic acid and 0.2 % (w/v) Coomassie-brilliant-blue-R-250). Background as well as stained proteins could be destained by incubation in the first destaining solution (40 % (v/v) ethanol and 10 % (v/v) acetic acid). Incubating the gel in the second destaining solution (10 % (v/v) acetic acid) would not destain proteins, but would eventually completely remove any background staining. The stained gels were dried between two cellophane layers (Bio-Rad Laboratories Limited, UK) or on Whatman paper using a gel dryer (Model 583; Bio-Rad Laboratories Limited, UK).

2.7.8.5 Silver staining of polyacrylamide (PAA) gels

PAA gels were silver-stained when the sensitivity of the Coomassie staining method described in section 2.7.8.4 proved to be insufficient. The method devised by Blum et al. (1987) is summarised in Table 2.8.

Table 2.8: Silver staining protocol for PAA gels.

Step	Solution composition	Amount per 200 ml solution	Incubation time
Fix	40 % (v/v) methanol	80 ml	90 min
	10 % (v/v) acetic acid	20 ml	
Wash	30 % (v/v) ethanol	60 ml	3x 20 sec
Pretreat	0.02 % (w/v) sodium thiosulphate ($Na_2S_2O_3$ 5x H_2O)	0.04 g	1 min
Wash	RO water	n/a	3x 20 sec
Stain	0.2 % (w/v) silvernitrate ($AgNO_3$)	0.4 g	20 min
	0.02 % (v/v) formaldehyde (from 37 % (w/v) stock solution)	40 µl	
Wash	RO water	n/a	3x 20 sec
Develop	3 % (v/v) sodium carbonate (Na_2CO_3)	6 g	by eye
	0.05 % (w/v) formaldehyde (from 37 % (w/v) stock solution)	100 µl	
	2 % (v/v) pretreat stock solution	4 ml	
Stop	0.5 % (w/v) glycine	1 g	10 min
Wash	RO water	n/a	2x 30 min

2.7.8.6 Protein molecular weight markers for PAGE

The protein molecular weight markers that were used in this work are listed in the following Table 2.9.

Table 2.9: Protein molecular weight markers. Low molecular weight calibration kit for SDS-PAGE (LMW; Amersham Biosciences, UK), prestained protein marker (PPM; broad range; New England Biolabs Limited, UK) and high molecular weight calibration kit for native electrophoresis (HMW; Amersham Biosciences, UK). Maltose binding protein (MBP).

LMW		PPM		HMW	
Protein	Size [kDa]	**Protein**	**Size [kDa]**	**Protein**	**Size [kDa]**
Phosphorylase b	97.0	MBP-β-galactosidase	175.0	Thyroglobulin	669.0
Albumin	66.0	MBP-paramyosin	83.0	Ferritin	440.0
Ovalbumin	45.0	Glutamic dehydrogenase	62.0	Catalase	232.0
Carbonic anhydrase	30.0	Aldolase	47.5	Lactate dehydrogenase	140.0
Trypsin inhibitor	20.1	Triosephosphate isomerase	32.5	Bovine serum albumin	66.4
α-Lactalbumin	14.4	β-lactoglobulin A	25.0		
		Lysozyme	16.5		
		Aprotinin	6.5		

2.7.9 Immunoblotting analysis

1-D SDS-PAGE, 1-D BN-PAGE or 2-D SDS-PAGE gels were used for immunoblotting analyses using either a semidry setup (2117 Multiphor II, electrophoresis unit; LKB Bromma AB, Sweden) (Bjerrum und Schäfer-Nielsen, 1986) or a tank blot method (TransBlot; Bio-Rad Laboratories Limited, UK) (Burnette, 1981; Towbin et al., 1979). Protein transfer was performed for at least 90 min in transfer buffer (3 mM Na_2CO_3, 10 mM $NaHCO_3$ and 20 % (v/v) methanol) onto nitrocellulose membrane (Trans Blot, Transfer medium nitrocellulose membrane, 0.2 µm; Bio-Rad Laboratories Limited, UK). In case of the semidry setup the current to be used was calculated using the following formula: size of gel in cm^2 x 0.7 = current to be used in mA, whereas the TransBlot tank method was used with a constant current of 400 mA. After the proteins were blotted, the nitrocellulose membrane was blocked for 1 h with 1x PBS-T (150 mM NaCl, 7.5 mM Na_2HPO_4, 2.5 mM NaH_2PO_4 and 0.1 % (v/v) Tween 20) supplemented with 5 % (w/v) milk powder (Waitrose, UK). The membrane was then briefly washed with 1x PBS-T and incubated overnight at 4 °C on

a rocking shaker with a primary antibody of choice (listed in Table 2.10). On the following day the membrane was washed three times for 20 min with 1x PBS-T and subsequently incubated for 1 h at RT with the appropriate secondary antibody (anti-rabbit IgG, horse radish peroxidase conjugate or anti-mouse IgG, horse radish peroxidase conjugate, 1:10000 dilution in 1x PBS-T; Amersham Pharmacia, UK). Unbound secondary antibody was removed by washing the membrane three times for 10 min with 1x PBS-T and two times for 10 min with 1x PBS. To obtain the optimum chemiluminescent signal, it was important to omit Tween 20 from the last two washing steps, as the detergent seemed to inhibit the peroxidase activity. The secondary antibody was detected by the enhanced chemiluminescence procedure (ECL; Durrant, 1990; Schneppenheim et al., 1991). The membrane was incubated for 1 min in a 1:1 mixture of ECL reagent A (100 mM Tris/HCl pH = 8.3, 0.4 mM p-coumaric acid (90 mM stock solution in DMSO), 2.5 mM luminol (250 mM stock solution in DMSO)) and ECL reagent B (100 mM Tris/HCl pH = 8.3, 100 mM H_2O_2), put into an A4 reinforced pocket and exposed to a X-Ray film (SuperRX, X-Ray Film, 100 NIF, 18x24 cm; Fuji medical, UK) for 1 sec to 10 minutes. The film was developed according to the manufacturer's instructions. Dry membranes were stored between Whatman paper at RT and could be probed again with another antibody if necessary. Antibodies could also be removed from the membrane by incubating the membrane for 30 min at 50 °C in stripping buffer (100 mM β-mercaptoethanol, 2 % (w/v) SDS, 62.5 mM Tris/HCl pH = 6.8).

Table 2.10: Primary antibodies used in this work. Amino acids (AA), second region of homology (SRH; AAA^+ ATPase domain of FtsH), transmembrane domain (TM), 2,4-dinitrophenylhydrazone (DNP).

Antibody name	Antigen	Binding site	Working dilution	Secondary antibody	Source
αPHB1 (#32)	*Synechocystis* sp. PCC 6803 Slr1106	Slr1106	1:5,000	αrabbit	P. Nixon
αPHB1 (purified)	*Synechocystis* sp. PCC 6803 Slr1106	Slr1106	1:1,000	αrabbit	this work
αPHB2-1 (Seqlab 8-1)	*Synechocystis* sp. PCC 6803 Slr1768	Slr1768 without TM	1:5,000	αrabbit	this work
αPHB2-1 (purified)	*Synechocystis* sp. PCC 6803 Slr1768	Slr1768 without TM	1:1,000	αrabbit	this work
αPHB2-2 (Seqlab 8-2)	*Synechocystis* sp. PCC 6803 Slr1768	Slr1768 without TM	1:5,000	αrabbit	this work
αPHB3-1 (Seqlab 8-3)	*Synechocystis* sp. PCC 6803 Slr1128	Slr1128 without TM	1:5,000	αrabbit	this work
αPHB3-1 (purified)	*Synechocystis* sp. PCC 6803 Slr1128	Slr1128 without TM	1:1,000	αrabbit	this work

Table 2.10 continued

Antibody name	Antigen	Binding site	Working dilution	Secondary antibody	Source
αPHB3-2 (Seqlab 8-4)	*Synechocystis* sp. PCC 6803 Slr1128	Slr1128 without TM	1:5,000	αrabbit	this work
αPHB4-1 (Seqlab 8-5)	*Synechocystis* sp. PCC 6803 Sll0815	Sll0815	1:5,000	αrabbit	this work
αPHB4-1 (purified)	*Synechocystis* sp. PCC 6803 Sll0815	Sll0815	1:5,000	αrabbit	this work
αPHB4-2 (Seqlab 8-6)	*Synechocystis* sp. PCC 6803 Sll0815	Sll0815	1:5,000	αrabbit	this work
αPsaD	*Chlamydomonas reinhardtii* PsaD	PsaD	1:5,000	αrabbit	J-D Rochaix
αD1 (#304-F)	*Pisum sativum* PsbA	PsbA last 29 AA	1:5,000	αrabbit	P. Nixon
αCP43 (P6)	*Chlamydomonas reinhardtii* PsbC	PsbC	1:5,000	αrabbit	P. Nixon
αPsbO (33 kDa)	*Pisum sativum* PsbO	PsbO	1:5,000	αrabbit	J. Barber
αNdhI (#184 FB)	*Tobacco nicotiana* NdhI	NdhI	1:3,000	αrabbit	P. Nixon
αNdhJ (#182 FB)	*Tobacco nicotiana* NdhJ	NdhJ	1:3,000	αrabbit	P. Nixon
αSbtA	*Synechocystis* sp. PCC 6803 SbtA	SbtA AA 184-203	1:200,000	αrabbit	T. Ogawa
αNrtA	*Synechococcus* sp. PCC 6942 NrtA	NrtA	1:5,000	αrabbit	T. Omata
αFtsH	*Escherichia coli* FtsH	SRH	1:5,000	αrabbit	T. Ogura
α0228	*Synechocystis* sp. PCC 6803 Slr0228	Loop between TMs	1:5,000	αrabbit	J. Komenda
α1604	*Synechocystis* sp. PCC 6803 Slr1604	Loop between TMs	1:5,000	αrabbit	J. Komenda
αGST	*Schistosoma japonicum* GST	GST	1:20,000	αrabbit	G-7781 Sigma Aldrich
αHIS	His_6 motif	His_6 motif	1:3,000	αmouse	DIA 900 Dianova
αDNP	dinitrophenylhydrazone	dinitrophenyl-hydrazone moieties	1:150	αrabbit	Chemicon International
αRabbit IgG	n/a	rabbit derived antibodies	1:10.000	n/a	Amersham Pharmacia
αMouse IgG	n/a	mouse derived antibodies	1:10.000	n/a	Amersham Pharmacia

2.7.10 Polyclonal antibody serum generation

Polyclonal antibody sera from *E. coli*-overexpressed proteins were generated in rabbit by Seqlab (Seqlab, Germany) during a three-month immunisation procedure and subsequently affinity-purified.

2.7.10.1 Small-scale protein overexpression in E. coli

To test protein expression using a distinct combination of recombinant plasmid DNA and *E. coli* expression strain, a 25-ml LB medium culture was grown at 37 °C under constant shaking at 200 rpm until it reached an OD_{600} of ~0.5. The culture was then divided in two 10-ml aliquots and expression was induced in one of the aliquots (+) by adding isopropyl-β-D-thiogalactopyranoside (IPTG, final [1 mM]), whereas the other aliquot remained uninduced (-). After a three-hour incubation at 37 °C and constant shaking, a 1-ml aliquot was taken from each culture to determine the final OD_{600}. The rest of the cells were pelleted (GH-S 3.8; 2,000 g, 15 min, RT) and resuspended in X µl 50 mM Tris/HCl pH = 7.5, where X = final OD_{600} of the culture x 100, so that 10 µl cell suspension corresponded to an OD_{600} of 0.1. To assess whether the desired protein had been produced, total cell extracts from the induced and uninduced cultures were analysed by 1-D SDS-PAGE and compared.

2.7.10.2 Large-scale protein overexpression in E. coli

After a recombinant plasmid DNA and *E. coli* expression strain combination had been determined, the desired protein was expressed on a large-scale for purification. A 1000-ml LB medium culture was grown at 37 °C under constant shaking until it reached an OD_{600} of ~0.5. Protein expression was induced by the addition of IPTG (final [1 mM]). After a three-hour incubation at 37 °C and constant shaking, the final OD_{600} was determined and a 1-ml aliquot taken to test protein expression as described in section 2.7.10.1. The rest of the cells were harvested (JA-14 rotor; 6,000 g, 15 min, 4 °C), flash frozen in liquid nitrogen and stored at –80 °C.

2.7.10.3 E. coli cell lysis and inclusion body purification

E. coli cells were lysed and inclusion bodies purified using the bug buster procedure (Merck Biosciences, UK) according to the manufacturer's instructions (TB245 11/99).

2.7.10.4 Purification of overexpressed protein

E. coli-overexpressed protein, from recombinant plasmid DNA derived from a pET16b vector, contained an N-terminal, His_6-tag that could be used for a batch method purification with Ni^{2+}-charged chelating sepharose (Amersham Pharmacia, UK). The inclusion bodies obtained from the bug buster procedure (see section

2.7.10.3) were solubilised for 60 min on ice in binding buffer (20 mM Tris/HCl pH = 7.9, 0.5 M NaCl, 6 M guanidium hydrochloride) and the solubilised sample was filtered through a 0.2 µm syringe tip filter (Schleicher & Schuell MicroScience GmbH, Germany). The filtered sample was incubated overnight at 4 °C on a torture wheel with 5 ml of Ni^{2+} charged FastFlow chelating sepharose (Amersham Pharmacia, UK; the resin was charged according to the manufacturer's instructions). After the incubation, the sample was washed with 25-ml aliquots of washing buffers containing an increasing imidazole concentration (20 mM Tris/HCl pH = 7.9, 0.5 M NaCl, 6 M guanidium hydrochloride and imidazole concentrations from 5 mM (used twice), 20 mM and 100 mM). Bound protein was eluted with elution buffer (20 mM Tris/HCl pH = 7.9, 0.5 M NaCl, 6 M guanidium hydrochloride, 300 mM imidazole) and the sample dialysed overnight at 4 °C against 1x PBS (150 mM NaCl, 7.5 mM Na_2HPO_4, 2.5 mM NaH_2PO_4) using Spectra/Por 1 dialysis tubing (MWCO ~6 to 8 kDa; Spectrum, UK). The dialysate was centrifuged (centrifuge model Allegra 6R, Beckman Coulter Limited, UK; GH-3.8; 2,000 g, 30 min, 4 °C) to collect precipitated protein. Pelleted protein was resuspended in 500 µl of 1x PBS buffer and solubilised by adding 300 µl 10 % (w/v) SDS (final SDS [3.8 % (w/v)]). Samples for 1-D SDS-PAGE were taken during the procedure (samples containing guanidium hydrochloride had to be acetone precipitated and were resuspended in 50 mM Tris/HCl pH = 7.5).

2.7.10.5 Seqlab immunisation procedure

Two 1-ml aliquots of each overexpressed protein (125 µl of resuspended and solubilised protein (see section 2.7.10.4) with an additional 875 µl of 1x PBS; final SDS [~ 0.47 (w/v) %]) were send off for the immunisation procedure (see Table 2.11) that was performed by Seqlab (Seqlab, Germany).

Table 2.11: Seqlab immunisation protocol (3 months).

Day	Procedure
0	first injection of 100 to 500 µg of antigen (extraction of > 5 ml preimmune serum)
21	second injection of 100 µg of antigen
35	first bleeding (extraction of 10 – 20 ml serum)
49	third injection of 100 µg of antigen
63	second bleeding (extraction of 10 – 20 ml serum)
77	fourth injection of 100 µg of antigen
98	final bleeding (extraction of > 50 ml serum)

Each antigen was injected into two rabbits and the final bleeding sera were send back after the three month immunisation protocol. Preimmune serum, first and second bleeds were sent back for testing purposes shortly after they had been extracted.

2.7.10.6 Polyclonal antibody serum purification procedure

Polyclonal antibodies were affinity-purified in a batch method with *E. coli*-overexpressed antigen coupled to CNBr-activated sepharose (Amersham Biosciences, UK). For the purification of one polyclonal antibody serum, 1 g CNBr-activated sepharose was resuspended and swollen in 10 ml 1 mM HCl in an Econo-Pac chromatography column (Bio-Rad Laboratories Limited, UK). Additives to the resin were washed away at a low pH with 250 ml of 1 mM HCl and an immediate neutralisation with 250 ml of coupling solution (0.1 M $NaHCO_3$, 0.5 M NaCl and 0.1 % (w/v) SDS; pH = 8.3). Both solutions were sucked through the resin by either a peristaltic (Watson-Marlow Bredel Incorporated, USA) or a water-vacuum pump. 5 mg of the respective antigen were diluted in coupling solution to a final concentration of 2.5 mg protein ml^{-1} and incubated with the washed resin on an end-over-end rotation wheel at RT overnight. Free CNBr-binding sites were blocked by incubating the resin in 10 ml of 1 M Tris/HCl pH = 7.9 at RT for 1 h on an end-over-end rotation wheel. Subsequently, the resin was washed with 50 ml 1x PBS-T (150 mM NaCl, 7.5 mM Na_2HPO_4, 2.5 mM NaH_2PO_4 and 0.1 % (v/v) Tween 20) and could now either be used directly or be stored at 4 °C (for long term storage, 3 mM sodium azide was added). To purify the polyclonal antibody serum, typically 5 ml of serum were diluted with 5 ml 2x PBS-T and incubated with the prepared antigen resin on an end-over-end rotation wheel at 4 °C overnight. The flow through was captured and the resin was washed with 30 ml 1x PBS-T. To elute the bound antibodies, the resin was first washed under alkaline conditions with 5 ml 0.2 M glycine pH = 11.0, neutralised by washing with 10 ml 1x PBS-T and then washed under acidic conditions with 5 ml 0.2 M glycine pH = 2.4. The eluates of both the alkaline and acidic washes were immediately neutralised with 1.5 ml 1 M Tris/HCl pH = 8.3 and 0.8 mg bovine serum albumin (BSA) were added per ml of eluate. Both eluates were then dialysed separately overnight at 4 °C against 1x PBS (150 mM NaCl, 7.5 mM Na_2HPO_4, 2.5 mM NaH_2PO_4) using Spectra/Por 1 dialysis tubing (MWCO ~6 to 8 kDa; Spectrum, UK). After the dialysis step, 0.01 % (w/v) sodium azide were added to prevent

bacterial contamination and both the alkaline and acidic elutes were stored away in small aliquots at –80 °C. Subsequently, the eluates were tested for their purity and specificity by immunoblotting ananlysis on *Synechocystis* sp. PCC 6803 crude membranes. Usually, the acidic eluates produced better antibody signals and had a higher antibody titer (data not shown).

2.7.11 Protein purifications from *Synechocystis* sp. PCC 6803

Proteins and His-tagged proteins from *Synechocystis* sp. PCC 6803 were purified using Ni-NTA magnetic agarose beads (Qiagen Limited, UK; see section 2.7.11.1) and immunoprecipitation with affinity-purified polyclonal antibodies covalently crosslinked to Protein A sepharose (see section 2.7.11.2.2).

2.7.11.1 Ni-NTA magnetic agarose beads purification

His-tagged proteins from *Synechocystis* sp. PCC 6803 were purified on a small-scale using Ni-NTA magnetic agarose beads (Qiagen Limited, UK). The sample from a large-scale membrane isolation (see section 2.7.1.2) that was used for the purification procedure, contained 200 µg chlorophyll a in 1 ml storing solution (50 mM sodium phosphate buffer pH = 8.0 (Sambrook et al., 1989), 15 % (v/v) glycerol). To this 6 µl of 1 M imidazole (final ~[5 mM]), 72 µl of 5 M sodium chloride (NaCl, final ~[300 mM]) were added before solubilising the sample for 10 min on ice with 120 µl 10 % (w/v) β-DM (final ~[1 % (w/v)]). After solubilisation the sample was centrifuged in a microfuge (maximum speed, 10 min, 4 °C) and the supernatant transferred to a new tube. Ni-NTA magnetic agarose beads were properly resuspended and an aliquot of 50 µl was added to the solubilised membrane extract to be incubated on a torture wheel for 2 h at 4 °C. After the incubation, the sample was placed into a magnetic separator (Qiagen Limited, UK) for 1 min and the supernatant removed. The beads were washed once in various 500 µl washing buffer aliquots (50 mM sodium phosphate buffer pH = 8.0 (Sambrook et al., 1989), 300 mM sodium chloride, 0.04 % (w/v) β-DM) each supplemented with an increasing concentration of imidazole (5 mM, 20 mM, 50 mM, 100 mM and 250 mM). Finally, the sample was eluted in 500 µl elution buffer (50 mM sodium phosphate buffer pH = 8.0 (Sambrook et al., 1989), 300 mM sodium chloride, 0.04 % (w/v) β-DM, 500 mM Imidazole). Samples for 1-D SDS-PAGE analysis were taken during the procedure.

2.7.11.2 Immunoprecipitation

Polyclonal antibody sera and affinity-purified antibodies were either directly used for immunoprecipitation experiments following a protocol devised by Dr. Josef Komenda (Institute of Microbiology, Trebon, Czech Republic; see section 2.7.11.2.2; personal communication) or after they had been covalently crosslinked to Protein A sepharose (see section 2.7.11.2.1).

2.7.11.2.1 Covalent crosslinking of antibodies to Protein A sepharose

Various antibody sera and affinity-purified antibodies were covalently crosslinked using dimethylpimelimidate (DMP) to Protein A sepharose (PC-A10; Generon, UK). Typically, 2 mg of antibody could be coupled to 1 ml of wet Protein A beads, but in this work antibodies were supplied in excess. 1 ml of resuspended Protein A beads was washed three times in a 2-ml Eppendorf tube in borate buffer (0.2 M boric acid pH = 9.0). The beads were made up to a volume of 1 ml in borate buffer and the desired antibody (maximum of 500 µl antibody serum) was added to be incubated on a torture wheel for at least 60 min at RT. The beads were spun down in a microfuge (7000 g, 2 min, RT), the supernatant removed and the beads transferred to a 15-ml Falcon tube in which they were washed in 10 ml borate buffer. After pelleting the beads (centrifuge model Allegra 6R, Beckman Coulter Limited, UK; GH-3.8; 2,000 g, 10 min, RT) and resuspending them in fresh 10-ml borate buffer, solid dimethylpimelimidate (DMP; final [20 mM]; 52 mg in 10 ml) was added and mixed on a torture wheel for 30 min at RT. The crosslinking reaction was stopped by washing the beads with 10 ml of 0.2 M ethanolamine pH = 8.0. Subsequently the beads were incubated on a torture wheel for further 2 h at RT in fresh 10-ml 0.2 M ethanolamine pH = 8.0. Finally, the beads were washed once with 0.2 M glycine pH = 2.4 to elute unbound antibodies and then washed twice in 1x PBS prior to being stored at 4 °C in 1x PBS supplemented with 3 mM sodium azide. Binding and crosslinking efficiency of the antibodies to the beads was tested by 1-D SDS-PAGE and immunoblotting.

2.7.11.2.2 Immunoprecipitation of *Synechocystis* sp. PCC 6803 proteins

Proteins or protein complexes of *Synechocystis* sp. PCC 6803 were immuno-precipitated from freshly prepared small-scale crude membrane isolations (see section 2.7.1.1). Sufficient Protein A sepharose (PC-A10; Generon, UK; typically 200 µl per immunoprecipitation reaction) was prepared by three consecutive washes in TNE

buffer (50 mM Tris/HCl pH = 7.5, 300 mM NaCl, 2 mM EDTA (from stock solution 0.5 M EDTA pH = 7.0 adjusted with NaOH)). Membranes containing 40 µg of chlorophyll a resuspended in 100 µl ACA buffer (750 mM ε-amino caproic acid, 50 mM BisTris/HCL pH = 7.0, 0.5 mM EDTA) were solubilised by adding 8 µl of 10 % (w/v) β-DM and incubation for 10 min on ice. Unsolubilised material was pelleted in a microfuge (maximum speed, 10 min, 4 °C) and the supernatant was transferred into a new tube containing 400 µl of ACA buffer to which 2.5 µl of 10 % (w/v) β-DM were added (final β-DM [0.1 % (w/v)]). To avoid non-specific protein interaction with Protein A sepharose, 30 µl of Protein A sepharose in TNE buffer were added and the assay was mixed on a torture wheel for 30 min at 4 °C. The Protein A sepharose was pelleted in a microfuge (7000 g, 1 min, 4 °C) and the supernatant transferred into a new tube. The selected antibody was either added as antibody serum (typically 10 to 20 µl) or as to Protein A beads coupled antibody (typically 50 to 100 µl). The assay was then mixed on a torture wheel for 1 h or overnight at 4 °C. If antibodies had been applied as serum, 50 µl of Protein A sepharose had to be added and incubated on a torture wheel for 60 min at 4 °C to capture the antibody-protein conjugates. However, the protein-antibody-Protein A sepharose conjugates were pelleted in a microfuge (7000 g, 1 min, 4 °C) and the supernatant was kept for 1-D SDS-PAGE analysis. The pellet was washed twice with 1 ml TNE buffer supplemented with 0.1 % (w/v) β-DM and once with 1 ml TNE buffer. After pelleting the washed beads (7000 g, 1 min, 4 °C), they were transferred quantitatively with ~100 µl TNE buffer into a new 0.5 ml tube, that had been pierced at the bottom with a syringe needle. The tube was put into a 2 ml tube and the lid was carefully closed. A small TNE buffer droplet formed at the bottom of the tube, while the beads stayed inside. The small tube was then also pierced at the top and both tubes were centrifuged (7000 g, 1 min, 4 °C), so that the large tube collected the flow through. The colour of the Protein A sepharose changed from opaque to white as it went dry and the captured antibody-protein or protein only complexes could be eluted either under native conditions (incubation with ~40 µl 0.2 M glycine pH = 2.4, 0.1 % (w/v) β-DM for 5 min at RT, which was subsequently centrifuged into 40 µl 1 M BisTris pH = 7.0, 20 % (v/v) glycerol for neutralisation) or under denaturing conditions (incubation with 80 µl 1x SDS sample buffer: 62.5 mM Tris/HCL pH = 6.8, 2 % (w/v) SDS, 10 % (v/v) glycerol, 0.05 % (w/v) bromophenol blue and 5 % (v/v) β- mercaptoethanol for 5 min at 50 °C). Samples were used for 1-D SDS and 1-D BN-PAGE and immunoblotting analyses.

2.7.12 Electron microscopy and single-particle analysis of *Synechocystis* sp. PCC 6803 protein complexes

Electron microscopy and single-particle analysis of *Synechocystis* sp. PCC 6803 protein complexes were performed in collaboration with Dr. Jon Nield (Imperial College London, London, UK). Samples were negatively stained with 2 % (w/v) uranyl acetate (pH = 4.5) on carbon-coated copper electron microscope (EM) grids via the droplet method devised by Harris and Agutter (1970). In order to obtain an even distribution of protein complexes across the carbon support surface, a dilution series was made for each sample over several grids. Imaging was performed on Kodak SO-163 film (Eastman Kodak Company, USA) at RT using a Philips-FEI Tecnai 12 EM (Royal Philips Electronics, The Netherlands) operating at 120 kV and 27,500x, as maintained by the Centre of Biomolecular Electron Microscopy at Imperial College London. Only the micrographs with minimal astigmatism and drift, based on post-scanning image analysis, after scanning into the computing environment using a Nikon LS9000 CoolScan densitometer (Nikon Ltd., UK) operating at a step size of 6.35 μm, were chosen. Finally, after calculating each micrograph's power spectrum, seven micrographs, for which the first minimum was calculated to be in the 20 to 22.5 Å spatial resolution range, remained and were chosen for further image analysis. A dataset consisting of all possible single-particles (3,708 image locations, each a pixel box of 160x160 pixels) was compiled using automatic selection in 'boxer', a module of the EMAN software package (Version 1.7; Ludtke et al., 2004). All subsequent image processing was performed using the Imagic-5 environment (Image Science GmbH, Berlin) with protein visualised as white and stain as black. No correction was made for the contrast transfer function (CTF). The single-particle image locations were analysed at a sampling frequency of 2.31 Å on the specimen scale. Reference-free alignment using a soft-edged circular mask applied to each image, followed by multivariate statistical analyses, gave initial 2-D class averages that were then iteratively refined in order to obtain the final averages shown (van Heel at al., 1996; Ruprecht and Nield, 2001). A clear subpopulation, consisting of 499 particles, was identified and assigned as 'top views' i.e. the largest 2-D projection observed. This was then processed *de novo* to give further refined class averages.

Chapter 3: Bioinformatic analysis of the Band 7 superfamily of proteins

In this chapter, bioinformatic tools were used to identify and analyse Band 7 proteins of cyanobacteria, in particular those of *Synechocystis* sp. PCC 6803 and *Thermosynechococcus elongatus*. The main aims were to assess how related the identified proteins were to each other and more importantly how similar they were to other Band 7 proteins with a known function. The latter was essential to evaluate whether parallels could be drawn between previously described Band 7 proteins and those that had been newly identified in this work. Moreover, attempts were made to assess whether the predicted Band 7 proteins of higher plants had the potential to be targeted to chloroplasts and to perhaps be involved in photosynthesis.

3.1 Defining the Band 7 superfamily of proteins

According to the PFAM (protein family) database, the Band 7 superfamily of proteins consists of proteins that contain either the Band 7 domain (PROSITE; PDOC00977; see section 3.1.1) or display high BLAST scores when compared to known Band 7 proteins (PFAM database entry PF01145). In the literature, such proteins have been implied to share the **SPFH** domain as a common motif, named after the initials of the respective protein subfamilies: **s**tomatins, **p**rohibitins, **f**lotillins and **H**flK/C homologues (Tavernarakis et al., 1999). While defining sequence motifs for the stomatin (see section 3.1.2) and prohibitin (see section 3.1.3) subfamilies are listed in the SPRINT database (http://www.bioinf.manchester.ac.uk/dbbrowser/sprint/), no such motifs can be found for the flotillin or HflK/C subfamilies in that database.

3.1.1 The Band 7 domain

The Band 7 domain is a regular expression for Band 7 proteins, i.e. stomatins, that has been defined in the PROSITE database (http:// www.expasy.ch/ prosite/; accession number: PDOC00977 or PS01270; created 11/1997; see Table 3.1). It is derived from a 29 amino acid region of the human Band 7 protein (also known as 7.2B or stomatin; Gallagher and Forget, 1995) and is located about 110 residues after the transmembrane domain of the protein.

Table 3.1: The Band 7 domain. This expression is characteristic for stomatins and was taken from the PROSITE database (accession number: PDOC00977 or PS01270).

Consensus sequence motif
R-x(2)-[LIV]-[SAN]-x(6)-[LIV]-D-x(2)-T-x(2)-W-G-[LIVT]-[KRH]-[LIV]-x-[KRA]-[LIV]-E-[LIV]-[KRQ]

3.1.2 Defining sequence motifs for the stomatin family

The sequence motif that defines the stomatin family of proteins is a 7-element fingerprint (for more details see: SPRINT database entry: Stomatin; accession number: PR00721) that is drawn from conserved regions, spanning virtually the full alignment length, of an initial alignment of ten stomatin homologue sequences which includes: Sto-1, Sto-2, Sto-3, Sto-4, Mec-2 and Unc-1 of *Caenorhabditis elegans*, three stomatins of *Mus musculus* (annotated Ban7_Mouse, MMEMPEPB7 and MMU17297) and human stomatin isoform A (source: SPRINT database).

3.1.3 Defining sequence motifs for the prohibitin family

The sequence motif that defines the prohibitin family of proteins is a 7-element fingerprint (for more details see: SPRINT database entry: Prohibitin; accession number: PR00679) that is drawn from the central portion of an initial alignment of seven prohibitin homologue sequences which includes: BAP37 of *Mus musculus*; prohibitin 2 of *Caenorhabditis elegans*; prohibitin of rat; prohibitin of human; prohibitin 1 and 2 of *Saccharomyces cerevisiae* and prohibitin of *Drosophila melanogaster* (source: SPRINT database).

3.2 Identification of Band 7 proteins

In order to identify the Band 7 proteins of *Synechocystis* sp. PCC 6803 and *Thermosynechococcus elongatus*, the InterPro protein family database was searched. The search revealed 1655 assigned Band 7 proteins in all taxonomic groups (InterPro entry: Band_7; accession number: IPR001107). Furthermore, these proteins of the Band 7 protein superfamily were distinguished into five subfamilies: stomatins (729 members; accession number: IPR001972; see Figure 3.2 B) prohibitins (220 members; accession number: IPR000163; see Figure 3.2 A), flotillins (66 members; accession

number: IPR004851), HflCs (200 members; accession number: IPR010200) and HflKs (214 members; accession number: IPR010201). It was noteworthy that almost all stomatins, prohibitins, HflCs and HflKs were Band 7 proteins, whereas only 66 out of 90 flotillins were considered to belong to the Band 7 protein superfamily. Taxonomy plots, taken from the InterPro database, showed the distribution of Band 7 proteins among actual and artificial taxonomic groups (see Figure 3.1.). Remarkably, the same database search had been performed a year earlier and since then the outcome had changed significantly (compare Figure 3.1 A and B). Moreover, closer examinations of the Band 7 proteins in cyanobacteria revealed the presence of five Band 7 homologues in *Synechocystis* sp. PCC 6803 and two in *Thermosynechococcus elongatus*.

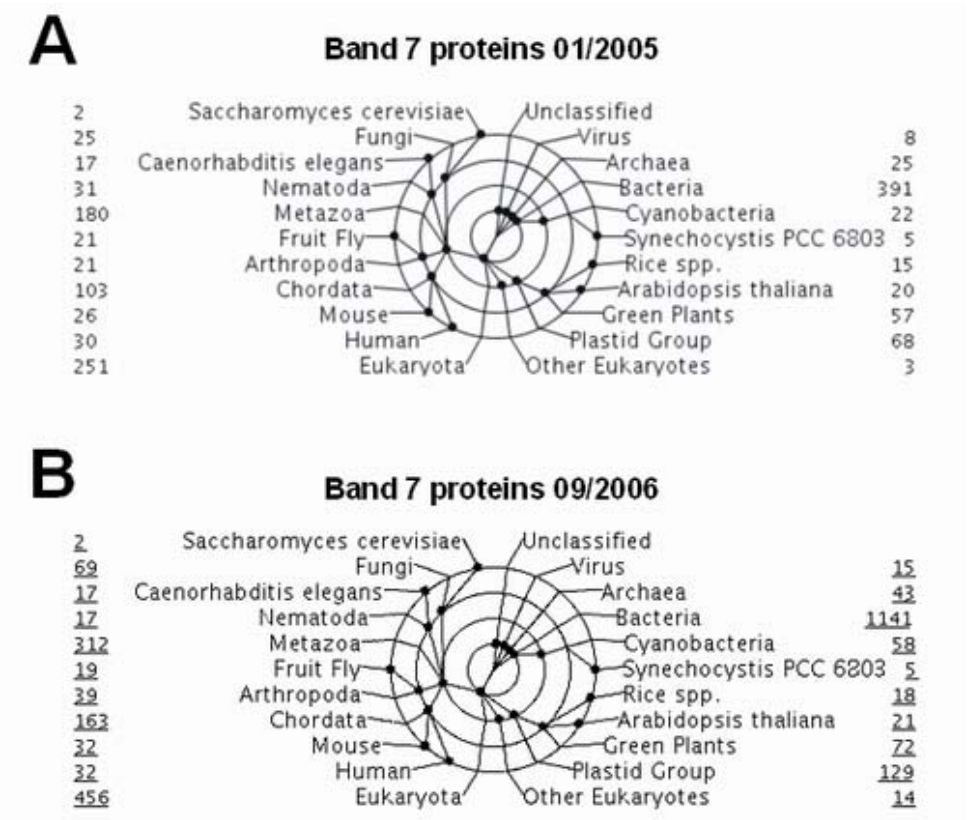

Figure 3.1: Taxonomy plots for the Band 7 protein superfamily (taken from the InterPro database). Taxonomy plots for the Band 7 protein superfamily (A) 01/2005 and (B) 09/2006. This display aims to provide a 'at a glance' view of the taxonomic range of the sequences associated with the chosen InterPro database entry and the number of sequences associated with each lineage. The circular display has the taxonomy-tree root as its centre. The model organisms selected populate the outer most circle. Nodes of the taxonomy-tree are placed on the inner circles. Radial lines lead to the description for each node. No significance is attached to the position of the node on a particular inner-circle, other than convenience, though some attempt had been made to group nodes. The nodes themselves are either true taxonomy nodes and have a NCBI taxonomy number or are artificial nodes created for this display; of which there are three: 'Unclassified', 'Other Eukaryota' (Non-Metazoa) and the 'Plastid Group'.

The overall number of Band 7 proteins had increased more than two fold from 668 in 01/2005 to 1655 in 09/2006, which was most likely due to the rise in amount of available sequence information. Consistent with this, the number of Band 7 proteins in for example *Caenorhabditis elegans* (17 in 01/2005 and 17 in 09/2006) or *Arabidopsis thaliana* (20/21) did not change, whereas in groups in which the amount of sequence information had drastically increased since 2005, such as in bacteria (391/1141), so did the number of Band 7 proteins. Interestingly for this study, more members of the Band 7 protein superfamily had also been found in cyanobacteria (22/58) and the so called plastid group (68/129). The distribution of prohibitins and stomatins among various taxonomic groups is presented in Figure 3.2 A and B.

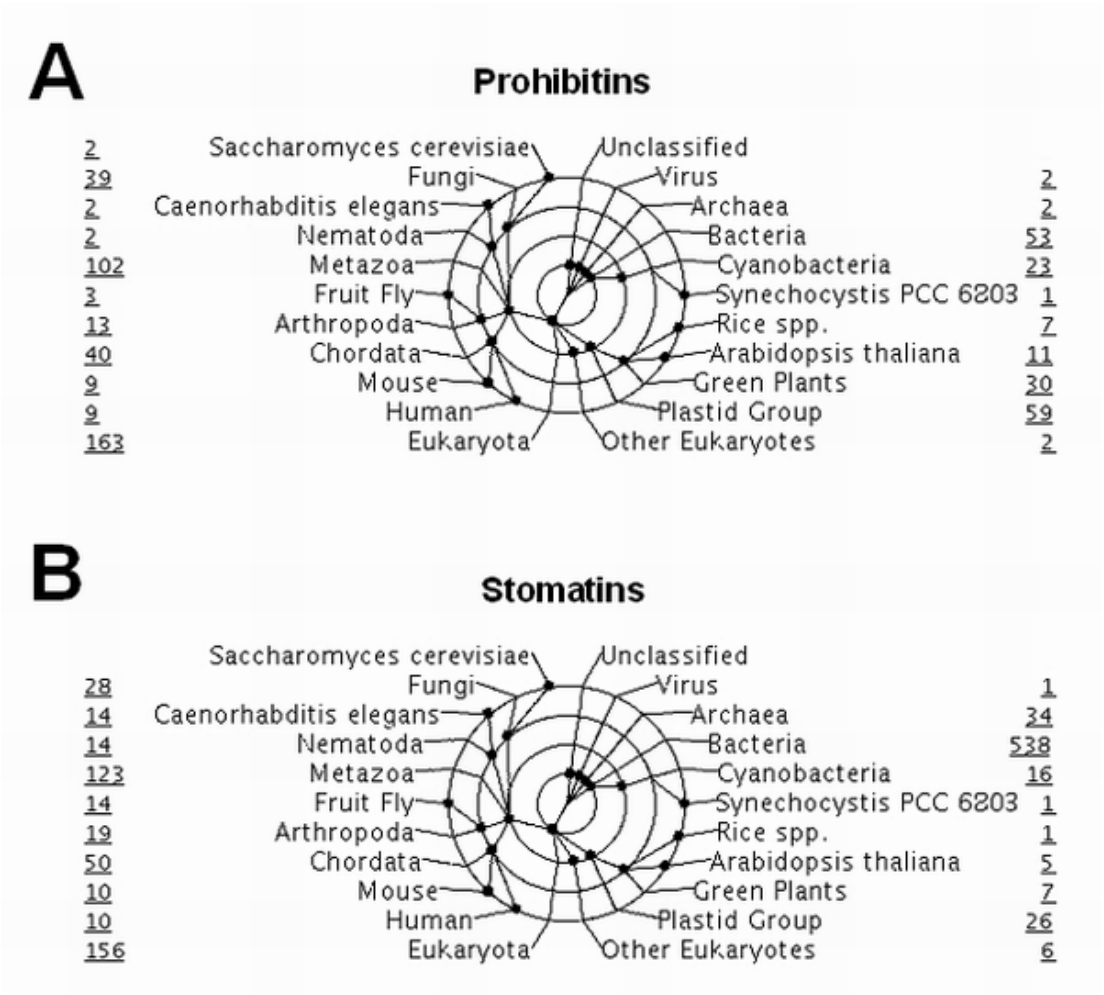

Figure 3.2: Taxonomy plots for the prohibitin and stomatin protein families (taken from the InterPro database). Taxonomy plot for (A) the prohibitin and (B) the stomatin protein families, both taken from the InterPro database in 09/2006. This display aims to provide a 'at a glance' view of the taxonomic range of the sequences associated with the chosen InterPro database entry and the number of sequences associated with each lineage. More information about the principle of the taxonomy plot is given in the legend of Figure 3.1.

After retrieving additional information from the InterPro database on the five identified Band 7 proteins of *Synechocystis* sp. PCC 6803 (see Figure 3.1), the one prohibitin homologue (see Figure 3.2 A) could be identified as Slr1106, while the one stomatin homologue (see Figure 3.2 B) is the Slr1128 protein. The other three identified Band 7 proteins of *Synechocystis* sp. PCC 6803 (Slr1768, Sll0815 and Sll1021) did not clearly belong to any one of the five subfamilies of the Band 7 protein superfamily. In *Thermosynechococcus elongatus*, the InterPro database listed one of the two identified Band 7 proteins as a member of the prohibitin family (Tlr1760), while the other protein (Tlr2184) was an assigned stomatin.

3.3 Analysis of the Band 7 proteins of cyanobacteria

3.3.1 Note on the nomenclature

As the Band 7 proteins that have been identified in *Synechocystis* sp. PCC 6803 and *Thermosynechococcus elongatus* were the focus of this work, a nomenclature was put into place to make these proteins stand out. Initially, the prohibitin homologue of *Synechocystis* sp. PCC 6803 (Slr1106) had been of particular interest and consequently the other identified Band 7 proteins were termed '**p**ro**h**i**b**itins' (abbreviated Phb) and numbered according to their chronological finding from one to five (see Table 3.2). Similarly, the Band 7 proteins of *Thermosynechococcus elongatus* were termed Phb1 and Phb2 with the prefix TE added to the respective protein. This nomenclature was put into place from the very beginning of this work and might be somewhat misleading, particularly in the case of the stomatin homologues, which were termed Phb3 (Slr1128 of *Synechocystis* sp. PCC 6803) and TE_Phb2 (Tlr2184 of *Thermosynechococcus elongatus*).

Originally, the term prohibitin derived from the observation that these proteins seemed to inhibit DNA synthesis and would thereby prohibit cell cycle progression (McClung et al., 1989). Later studies, however, assigned this effect to the 3' untranslated region (3'-UTR) of the prohibitin messenger RNA (Jupe et al., 1996), while another study found the prohibitin homologues in the mitochondria of *S. cerevisiae* to act as chaperones (Steglich et al., 1999; Nijtmans et al. 2000). It was then suggested to keep the original phb abbreviation for prohibitins, as this had already been established in the literature, but to adjust the meaning to "**p**rotein that **h**olds **b**adly folded subunits" (Nijtmans et al. 2002).

Table 3.2: Nomenclature of the Band 7 proteins of *Synechocystis* sp. PCC 6803 and *Thermosynechococcus elongatus*. The names of the Band 7 genes (CyanoBase) and proteins (CyanoBase and nomenclature of this work) of *Synechocystis* sp. PCC 6803 and *Thermosynechococcus elongatus* are listed in this Table. Sequence information can retrieved from the UniProt database. The 'Remarks' column indicates which subfamily the respective protein is assigned to (InterPro database).

Organism	Gene name	Protein names	UniProt accession #	Remarks
Synechocystis sp. PCC 6803	*slr1106*	Slr1106 or Phb1	P72754	prohibitin
	slr1768	Slr1768 or Phb2	P73049	none
	slr1128	Slr1128 or Phb3	P72655	stomatin
	sll0815	Slr0815 or Phb4	P74042	none
	sll1021	Slr1021 or Phb5	P72929	none
Thermosynechococcus elongatus	*tlr1760*	Tlr1760 or TE_Phb1	Q8DI32	prohibitin
	tlr2184	Tlr2184 or TE_Phb2	Q8DGX8	stomatin

3.3.2 Properties of selected cyanobacterial Band 7 proteins

Certain protein properties can be calculated from primary protein structures, e.g. the molecular mass, the isoelectric point (pI) and transmembrane domains (TMs). The calculations were carried out for the identified Band 7 proteins of *Synechocystis* sp. PCC 6803 and *Thermosynechococcus elongatus* (see Table 3.3).

Table 3.3: Properties of selected cyanobacterial Band 7 proteins. The properties of selected cyanobacterial Band 7 proteins like molecular mass (MM), isoelectric point (pI) (both http://www.expasy.ch/tools/pi_tool.html) and the number of transmembrane (TM) domains (http://www.ch.embnet.org/software/TMPRED_form.html) were calculated and are listed in the Table below.

Protein name	UniProt accession #	Length		Calculated MM [kDa]	pI	Expected TM-domains
		[bp]	[aa]			
Phb1	P72754	849	282	30.57	5.21	1
Phb2	P73049	897	298	32.83	5.58	2
Phb3	P72655	966	321	35.73	5.55	1
Phb4	P74042	795	264	30.37	8.36	none
Phb5	P72929	2022	673	74.42	5.08	1
TE_Phb1	Q8DI32	864	287	31.55	5.32	1
TE_Phb2	Q8DGX8	963	320	35.68	5.55	1

The analysed Band 7 proteins had similar molecular masses of about 30 kDa, except for Phb5, which had a molecular mass of 74 kDa. The isoelectric points for these proteins were in the range from 5.1 to 5.6 making them acidic proteins and only Phb4 had an isoelectric point of 8.4 with basic properties. Most of the Band 7 proteins were predicted to possess one N-terminal transmembrane domain, except for Phb2 (two TMs) and Phb4 (no TM) of *Synechocystis* sp. PCC 6803.

3.3.3 Identification and phylogenetic analysis of cyanobacterial Band 7 proteins

An InterPro database search identified 58 cyanobacterial Band 7 proteins (see Figure 3.1) that were distributed among 20 different strains (see Table 3.4) and for which a phylogenetic tree was generated (see Figure 3.3).

Table 3.4: Cyanobacterial Band 7 proteins. Cyanobacterial strains are listed alphabetically. The B/P/S column shows the number of proteins in the respective strain that are according to the InterPro database either other Band 7 proteins (B) or assigned prohibitins (P) or stomatins (S). The accession numbers originate from the UniProt database and proteins marked in bold were used for the comparative phylogenetic analysis (see Figure 3.5).

#	Strain	B/P/S	other Band 7 accession #s	Prohibitin accession #s	Stomatin accession #s
1	*Anabaena* sp. PCC 7120	6/1/2	Q8YNN6 Q8YNN8 Q8YYV3	Q8YXC0	Q8YP15 Q8YU82
2	*Anabaena variabilis* PCC 7937	7/2/2	**Q3M448** **Q3MDB5** **Q3MDB6**	**Q3M310** **Q3M8Q8**	**Q3M7Z0** **Q3MG56**
3	*Anabaena variabilis*	1/0/1	none	none	Q44559
4	*Crocosphaera watsonii*	3/1/1	**Q4C2E9**	**Q4CB16**	**Q4BYA2**
5	*Gloeobacter violaceus*	3/1/1	**Q7NJI8**	**Q7NJI7**	**Q7NIK9**
6	*Prochlorococcus marinus*	1/1/0	none	**Q7VDA2**	none
7	*Prochlorococcus marinus* sub. pastoris CCMP1378	1/1/0	none	**Q7V2J4**	none
8	*Prochlorococcus marinus* NATL2A	1/1/0	none	**Q46GU0**	none
9	*Prochlorococcus marinus* MIT 9312	1/1/0	none	**Q31C51**	none
10	*Prochlorococcus marinus* MIT 9313	2/1/1	none	**Q7V750**	**Q7V674**
11	*Synechococcus* sp. CC9605	2/2/0	none	Q3AHV3 Q3AM84	none
12	*Synechococcus* sp. CC9902	2/2/0	none	Q3AWH5 Q3AZS3	none
13	*Synechococcus* sp. JA-2-3B'a(2-13)	5/3/1	**Q2JMY3**	**Q2JKS9** **Q2JMD1** **Q2JMY4**	**Q2JPG5**
14	*Synechococcus* sp. JA-3-3AB	3/1/1	Q2JUX9	Q2JUY0	Q2JUC9
15	*Synechococcus* sp. PCC 6301	3/0/1	Q5N1M2 Q5N1M3	none	Q5N1D7
16	*Synechococcus* sp. PCC 7942	3/0/1	**Q54704** **Q54705**	none	**Q31KH7**
17	*Synechococcus* sp. WH8102	2/2/0	none	**Q7U503** **Q7U5Z1**	none
18	*Synechocystis* sp. PCC 6803	5/1/1	**Slr1768 (P73049)** **Sll0815 (P74042)** **Sll1021 (P72929)**	**Slr1106 (P72754)**	**Slr1128 (P72655)**
19	*Thermosynechococcus elongatus* BP-1	2/1/1	none	**Tlr1760 (Q8DI32)**	**Tlr2184 (Q8DGX8)**
20	*Trichodesmium erythraeum* IMS101	5/1/2	**Q119N4** **Q119N5**	**Q114E5**	**Q113W9** **Q10X38**
		Total	**19**	**23**	**16**

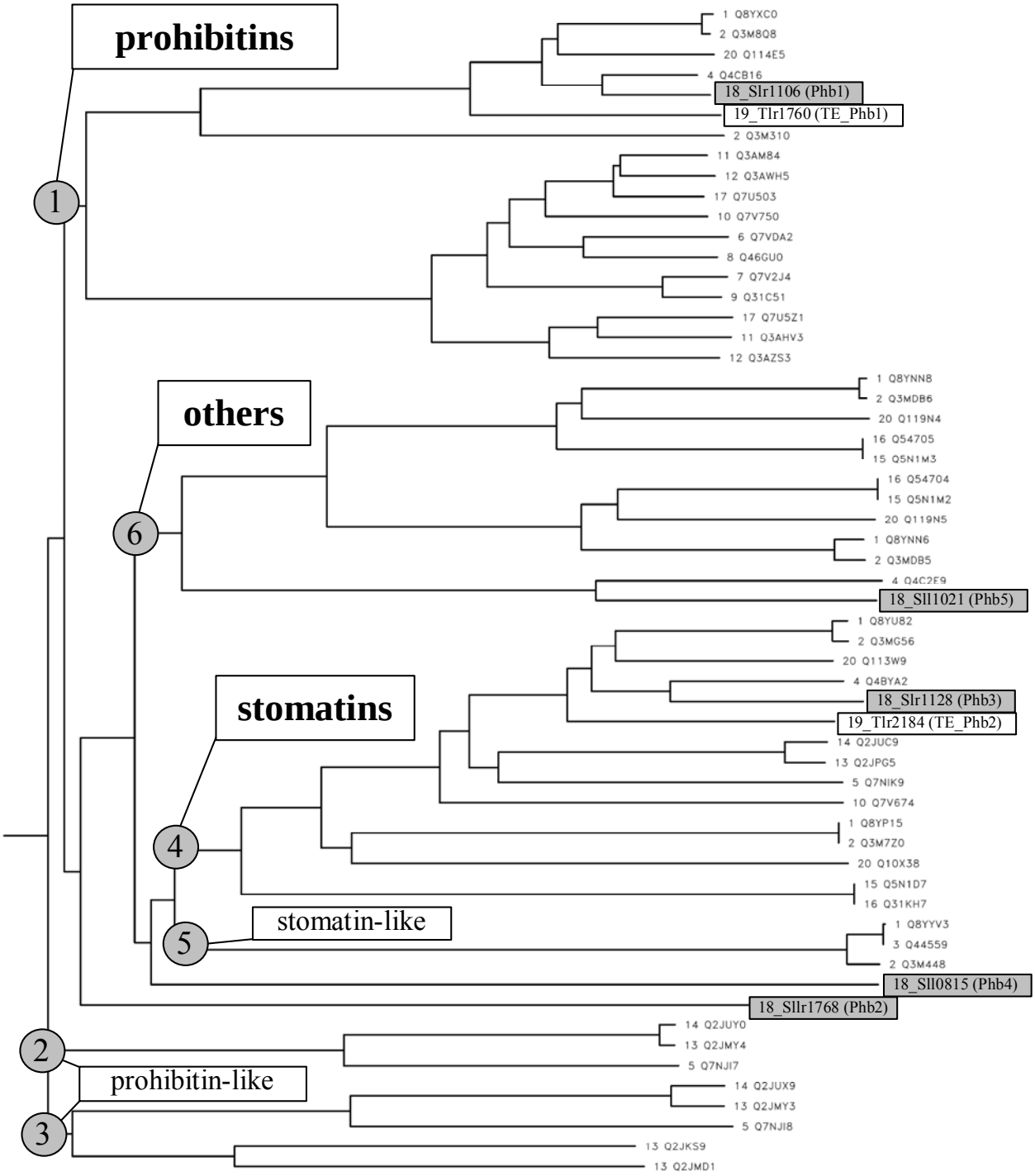

Figure 3.3: Phylogenetic analysis of cyanobacterial Band 7 proteins. A phylogenetic tree for all cyanobacterial Band 7 proteins was drawn using the workbench server (http://seqtool.sdsc.edu/CGI/BW.cgi#!). The 58 Band 7 protein sequences (see Table 3.4) were aligned by the CLUSTALW multiple sequence alignment tool (default settings) from which a PHYLIP rooted phylogenetic tree was drawn (default settings). Each protein is labelled with a number (according to the strain number in Table 3.4) followed by its UniProt accession number. Relevant branching points are marked from 1 to 6 and labelled as references. The Band 7 proteins of *Synechocystis* sp. PCC 6803 (grey boxes) and *Thermosynechococcus elongatus* (white boxes) are highlighted and labelled with their protein names rather than the UniProt accession numbers.

Most of the cyanobacterial Band 7 proteins were either assigned prohibitins (23) or stomatins (16) (see Table 3.4) and none of the remaining 19 proteins was an assigned flotillin, HflC or HflK homologue (InterPro database). Analysing the phylogenetic tree (see Figure 3.3), most of the Band 7 proteins of cyanobacteria were found in three categories: prohibitins, stomatins and others. These categories were assigned in accordance with the information retrieved from the InterPro database on the constitutive proteins. The prohibitins formed the largest category with 18 members and branched off at node 1. Only the five assigned prohibitin homologues of *Gloeobacter violaceus* (#5_Q7NJI7), *Synechococcus* sp. JA-2-3B'a(2-13) (#13_Q2JKS9, #13_Q2JMD1 and #13_Q2JMY4) and *Synechococcus* sp. JA-3-3AB (#14_QJUY0) branched off earlier at nodes 2 and 3. Interestingly, other Band 7 proteins of the same strains #14_Q2JUX9 of *Synechococcus* sp. JA-3-3AB, #13_Q2JMY3 of *Synechococcus* sp. JA-2-3B'a(2-13) and #5_Q7NJI8 of *Gloeobacter violaceus*, were also found in these branches. Given the genetic background and the fact that these branches contained assigned prohibitins, the proteins in branches 2 and 3 were considered 'prohibitin-like' proteins. The second category, branching off at node 4, contained almost all assigned stomatins. Only one exception (#3_Q44559 of *Anabaena variabilis*) was found in branch 5 together with two proteins of two other *Anabaena* strains (#1_Q8YYV3 of *Anabaena* sp. PCC 7120 and #2_Q3M448 of *Anabaena variabilis* PCC 7937). As with the 'prohibitin-like' proteins, given the genetic background and the assignment of #3_Q44559 as a stomatin, the other two proteins were considered 'stomatin-like'. The third category contained most of the remaining Band 7 proteins and was referred to as the 'Others' category (branching off at node 6; including #18_Sll1021 of *Synechocystis* sp. PCC 6803). No relationship was observed between the #18_Slr1768 or the #18_Sll0815 proteins of *Synechocystis* sp. PCC 6803 with any other cyanobacterial Band 7 protein.

3.4 The Band 7 proteins of higher plants

Approximately 1.5 billion years ago a cyanobacterium has been incorporated into a eukaryotic cell, and over time developed into the chloroplasts of higher plants (Gray, 1989; Douglas, 1998). This event is referred to in the endosymbiont theory and represents an evolutionary link between cyanobacteria and higher plants. Thus, it was particularly interesting to include the Band 7 homologues of higher plants in the

bioinformatic analyses performed in this chapter. At first, these Band 7 proteins had to be identified by searching the InterPro database (see section 3.4.1). Subsequently, the potential of the identified proteins to be targeted to chloroplasts was assessed by using various targeting prediction servers (see section 3.4.2). Finally, a phylogenetic analysis was performed in order to assess the relationships of the Band 7 proteins of higher plants among each other (see section 3.4.3).

3.4.1 Identification of the Band 7 proteins of higher plants

An InterPro database search revealed 72 Band 7 proteins (see Figure 3.1B) that were found in 19 higher plants species (see Table 3.5). *A. thaliana* alone contained 21 Band 7 homologues (5 other Band 7 proteins/11 prohibitins/5 stomatins) and other species with many Band 7 proteins were *Oryza sativa* (Japonica cultivar-group) (16/6/1) and *Zea mays* (9/4/1). Apparently, Band 7 proteins were present in dicotyledons as well as in monocotyledons spanning the taxonomic spectrum. Interestingly, only a small proportion of Band 7 proteins of higher plants was assigned to be stomatin homologues and already five out of the total seven were found in *A. thaliana*. Another observation was that the potato species *Solanum dimissum* contained an unassigned Band 7 protein (#36_Q6L4B0), whereas its close relative *Solanum tuberosum* contained an assigned prohibitin homologue (#37_Q38M64).

3.4.2 Targeting of the Band 7 proteins of higher plants

The identified Band 7 proteins of higher plants were tested for their potential to be targeted to chloroplasts using the targeting prediction servers ChloroP, TargetP (Emanuelsson et al., 1999; Emanuelsson et al., 2000) and Predotar (Small, 2004) (see Table 3.6). In order to test the reliability of the targeting prediction servers, three *A. thaliana* control proteins were included in the analysis: PsbA (D1 protein of PSII; plastid-encoded), PsbO (33-kDa protein of the oxygen-evolving complex; nuclear-encoded) and the succinate dehydrogenase subunit 1 (mitochondrial protein; nuclear-encoded). The PsbA protein did not yield a result, because it does not need to be targeted to chloroplasts, whereas the localisation of the PsbO and the succinate dehydrogenase proteins was assigned correctly. However, ChloroP predicted a chloroplast transit peptide for both of these proteins, which raised doubts whether the tool could discriminate between chloroplast transit and mitochondrial-targeting peptides.

Table 3.5: The Band 7 proteins of higher plants. Higher plant species are listed alphabetically and numbering resumes from Table 3.4. For more details about the columns see the legend of Table 3.4. Proteins marked in bold were used in the comparative phylogenetic analysis (see Figure 3.5). Coloured backgrounds indicate potential targeting to chloroplasts (green) or mitochondria (red) according to the targeting prediction analyses performed in section 3.4.2. The two coloured background for #29_Q1T6H8 protein indicates contradicting predictions (see Table 3.6).

#	Species	B/P/S	other Band 7 accession #s	Prohibitin accession #s	Stomatin accession #s
21	*Arabidopsis thaliana*	21/11/5	Q84TE3 Q9CAR7 Q9FHM7 Q9FM19 Q9ZQ87	**O04331** **O49460** **Q3EDJ1** **Q8LBC7** **Q9FFH5** **Q9LY99** **Q9SIL6** Q9LK25 Q8LA39 Q9ZNT7 Q84WL7	**Q8LDI0** **Q93VP9** **Q9T082** Q9LVW0 Q9SRH6
22	*Brassica napus*	1/1/0	none	**Q9AXM0**	none
23	*Capsicum annuum*	1/0/0	Q5GI04	none	none
24	*Cicer arietinum*	1/0/0	Q9ZRU2	none	none
25	*Cucumis sativus*	1/0/0	Q6UNT3	none	none
26	*Hordeum vulgare* var. distichum	4/0/0	Q8H1V3 Q8H1V4 Q8H1V5 Q8H1V6	none	none
27	*Lotus japonicus*	1/0/0	Q5KSB6	none	none
28	*Lupinus polyphyllus*	1/0/0	P16148	none	none
29	*Medicago truncatulla*	4/0/0	**Q1T6H1** **Q1T6H8** **Q1T6H9** Q1SBN2	none	none
30	*Nicotiana benthamiana*	2/2/0	none	**Q45Q23** **Q45Q24**	none
31	*Nicotiana tabacum*	1/1/0	none	**O04361**	none
32	*Oryza sativa*	2/1/0	Q94JS7	**Q25A95**	none
33	*Oryza sativa* (Japonica cultivar-group)	16/6/1	Q8S1F1 Q8S1F0 Q8H918 Q7XEB7 Q6ZIV7 Q6L4S3 Q6K550 Q6ATM4 Q5VNU2	**Q6AVQ4** **Q6EP40** **Q6MWE2** **Q75HF7** **Q75HG8** **Q7EYR6**	**Q7EZD2**
34	*Pennisetum ciliare*	1/0/0	Q9ATP0	none	none
35	*Petunia hybrida*	2/2/0	none	**Q4ZGM7** **Q5ECI7**	none
36	*Solanum dimissum*	1/0/0	Q6L4B0	none	none
37	*Solanum tuberosum*	1/1/0	none	**Q38M64**	none
38	*Triticum aestivum*	2/1/0	Q70AI7	**Q84VJ0**	none
39	*Zea mays*	9/4/1	Q9FS40 Q9M582 Q9M583 Q9M584	**Q9M586** **Q9M587** **Q9M588** **Q9M589**	**Q9M585**
		Total	**35**	**30**	**7**

Analysing the results for the Band 7 proteins of higher plants revealed that the majority of the proteins did not possess a chloroplast transit peptide and was neither predicted to be targeted to chloroplasts nor to mitochondria. However, ChloroP predicted 15 Band 7 proteins of various plant species to possess a chloroplast transit peptide. For three of these proteins (#21_O04331, #30_Q45Q24 and #31_O04361) a low-scoring chloroplast transit peptide was predicted by ChloroP, although Predotar made no prediction and TargetP indicated that these three proteins followed the secretory pathway with a medium reliability (RC of 2 and 3). For the other twelve Band 7 proteins that were predicted to possess a chloroplast transit peptide, a targeting prediction had either been made by TargetP, by Predotar or by both of the targeting prediction tools. In eight other cases, ChloroP did not predict a chloroplast transit peptide, whereas TargetP or Predotar had indicated the protein to be either targeted to the chloroplast or to the mitochondrium. Had TargetP made a localisation prediction, the proteins were indicated to be targeted to mitochondria with the weakest possible reliability (RC of 5). When Predotar had made a localisation prediction, it was also a low scoring chloroplastic or mitochondrial-targeting peptide. Looking closer at the localisation predictions, the Predotar server had only in the case of #21_Q9LY99 of *A. thaliana* made an alternative prediction and indicated that the protein might follow the secretory pathway as a possible route. The TargetP server also made no predictions for many proteins, but twenty Band 7 proteins were assigned to the secretory pathway. Another observation was that both targeting prediction servers did not always agree with each other and in the case of #29_Q1T6H8 of *Medicago truncatulla* even contradicted each other.

Overall the TargetP software predicted eleven proteins to be targeted to mitochondria, and only three to chloroplasts. The Predotar server predicted seven proteins to be targeted to mitochondria and six to chloroplasts. In general, the calculated targeting scores appeared to be rather low, although when both tools were in agreement with each other, the scores were relatively higher. This could be observed for the following proteins: #21_Q93VP9, #21_Q9T082, #29_Q1T6H1, #33_Q7EZD2 and #39_Q9M585 (targeted to mitochondria) and #33_Q8S1F0 (targeted to the plastid). The proteins that were predicted to be targeted to chloroplasts included unassigned Band 7 proteins (#26_Q8H1V6, #29_Q1T6H8, #33_Q5VNU2, #33_Q6ATM4 and #33_Q8S1F0) and more importantly, with respect to the initial objective of this analysis, three assigned prohibitins (#32_Q25A95, #33_Q6MWE2 and #39_Q9M587).

Table 3.6: Targeting of the Band 7 proteins of higher plants. The protein targeting prediction servers ChloroP, TargetP and Predotar were used to analyse the 71 Band 7 proteins of higher plants. Proteins were named as described before in the phylogenetic analyses (see legend Figure 3.3) and their lengths are given in amino acids (AA). Scores for chloroplast transit peptides (cTP) and mitochondrial-targeting peptides (mTP); chloroplast transit peptide yes or no (Y/N); predicted location (Loc) where C is chloroplast (green background), M is mitochondrion (red background) and S is secretory pathway; Reliability classes (RC) from 1 to 5, where 1 indicates the strongest prediction. *Succinate dehydrogenase (SDH).

#	Protein name	Length [AA]	ChloroP		TargetP				Predotar		
			cTP	Y/N	cTP	mTP	Loc	RC	cTP	mTP	Loc
1	21_O04331	277	0.521	Y	0.118	0.021	S	2	0.02	0.03	-
2	21_O49460	288	0.440	-	0.026	0.156	-	3	0.00	0.02	-
3	21_Q3EDJ1	221	0.434	-	0.043	0.504	-	4	0.00	0.14	-
4	21_Q84TE3	316	0.434	-	0.075	0.388	-	4	0.00	0.01	-
5	21_Q84WL7	279	0.488	-	0.024	0.039	S	1	0.01	0.03	-
6	21_Q8LA39	288	0.440	-	0.026	0.156	-	3	0.00	0.02	-
7	21_Q8LBC7	279	0.492	-	0.039	0.035	S	1	0.01	0.03	-
8	21_Q8LDI0	401	0.563	Y	0.046	0.672	M	2	0.06	0.17	-
9	21_Q93VP9	411	0.573	Y	0.298	0.704	M	3	0.03	0.36	M
10	21_Q9CAR7	286	0.435	-	0.064	0.100	-	2	0.00	0.01	-
11	21_Q9FFH5	278	0.453	-	0.008	0.172	S	4	0.00	0.02	-
12	21_Q9FHM7	292	0.431	-	0.150	0.141	-	3	0.00	0.01	-
13	21_Q9FM19	286	0.438	-	0.044	0.089	-	3	0.01	0.01	-
14	21_Q9LK25	279	0.488	-	0.024	0.039	S	1	0.01	0.03	-
15	21_Q9LVW0	401	0.563	Y	0.046	0.672	M	2	0.06	0.17	-
16	21_Q9LY99	249	0.469	-	0.010	0.437	S	4	0.00	0.25	S
17	21_Q9SIL6	286	0.441	-	0.010	0.167	-	4	0.00	0.01	-
18	21_Q9SRH6	285	0.448	-	0.033	0.177	-	3	0.00	0.01	-
19	21_Q9T082	515	0.573	Y	0.298	0.704	M	3	0.03	0.36	M.
20	21_Q9ZNT7	286	0.473	-	0.022	0.124	S	2	0.00	0.01	-
21	21_Q9ZQ87	356	0.440	-	0.037	0.472	-	3	0.00	0.01	-
22	22_Q9AXM0	290	0.441	-	0.023	0.131	-	4	0.00	0.01	-
23	23_Q5GI04	285	0.436	-	0.079	0.100	-	3	0.01	0.01	-
24	24_Q9ZRU2	286	0.432	-	0.055	0.194	-	2	0.00	0.01	-
25	25_Q6UNT3	284	0.436	-	0.073	0.159	-	2	0.01	0.01	-
26	26_Q8H1V3	284	0.437	-	0.045	0.152	-	2	0.01	0.01	-
27	26_Q8H1V4	287	0.438	-	0.079	0.117	-	3	0.01	0.01	-
28	26_Q8H1V5	284	0.439	-	0.045	0.121	-	2	0.01	0.01	-
29	26_Q8H1V6	288	0.449	-	0.125	0.081	S	4	0.20	0.01	C
30	27_Q5KSB6	286	0.441	-	0.039	0.114	-	2	0.01	0.01	-
31	28_P16148	184	0.427	-	0.046	0.144	-	2	0.00	0.01	-
32	29_Q1SBN2	361	0.528	Y	0.486	0.536	M	5	0.00	0.01	-
33	29_Q1T6H1	190	0.508	Y	0.481	0.570	M	5	0.07	0.60	M
34	29_Q1T6H8	260	0.531	Y	0.716	0.320	C	4	0.37	0.82	M
35	29_Q1T6H9	472	0.433	-	0.026	0.248	-	3	0.00	0.42	M
36	30_Q45Q23	290	0.449	-	0.020	0.231	-	4	0.00	0.01	-
37	30_Q45Q24	279	0.501	Y	0.114	0.096	S	3	0.05	0.05	-
38	31_O04361	279	0.501	Y	0.119	0.097	S	3	0.05	0.05	-
39	32_Q25A95	284	0.482	-	0.053	0.032	S	1	0.21	0.02	C
40	32_Q94JS7	284	0.437	-	0.034	0.127	-	2	0.01	0.01	-
41	33_Q5VNU2	288	0.458	-	0.082	0.095	S	3	0.22	0.01	C
42	33_Q6ATM4	374	0.571	Y	0.942	0.024	C	2	0.02	0.01	-
43	33_Q6AVQ4	283	0.445	-	0.003	0.242	S	4	0.01	0.02	-
44	33_Q6EP40	282	0.478	-	0.049	0.104	S	3	0.16	0.06	-
45	33_Q6K550	287	0.437	-	0.064	0.122	-	2	0.01	0.01	-

Table 3.6 continued

#	Protein name	Length [AA]	ChloroP		TargetP				Predotar		
			cTP	Y/N	cTP	mTP	Loc	RC	cTP	mTP	Loc
46	33_Q6L4S3	288	0.434	-	0.033	0.126	-	3	0.01	0.01	-
47	33_Q6MWE2	287	0.481	-	0.037	0.039	S	1	0.21	0.02	C
48	33_Q6ZIV7	284	0.437	-	0.034	0.127	-	2	0.01	0.01	-
49	33_Q75HF7	420	0.430	-	0.064	0.246	-	3	0.00	0.16	-
50	33_Q75HG8	551	0.426	-	0.053	0.310	-	3	0.00	0.03	-
51	33_Q7EYR6	289	0.458	-	0.020	0.583	-	5	0.01	0.05	-
52	33_Q7EZD2	377	0.508	Y	0.167	0.967	M	1	0.01	0.86	M
53	33_Q8H918	292	0.433	-	0.119	0.116	S	5	0.00	0.01	-
54	33_Q8S1F0	311	0.505	Y	0.454	0.070	C	5	0.20	0.01	C
55	33_Q8S1F1	314	0.436	-	0.165	0.122	-	2	0.02	0.01	-
56	34_Q9ATP0	283	0.445	-	0.048	0.129	-	2	0.01	0.01	-
57	35_Q4ZGM7	145	0.447	-	0.085	0.376	M	5	-	-	-
58	35_Q5ECI7	279	0.496	-	0.106	0.111	S	4	0.02	0.04	-
59	36_Q6L4B0	292	0.432	-	0.141	0.097	-	4	0.00	0.01	-
60	37_Q38M64	296	0.458	-	0.029	0.254	-	3	0.00	0.01	-
61	38_Q70AI7	215	0.442	-	0.111	0.273	-	3	-	-	-
62	38_Q84VJ0	273	0.447	-	0.004	0.362	S	4	0.00	0.02	-
63	39_Q9FS40	284	0.435	-	0.040	0.113	-	2	0.01	0.01	-
64	39_Q9M582	287	0.440	-	0.086	0.085	-	3	0.01	0.01	-
65	39_Q9M583	284	0.440	-	0.063	0.106	-	2	0.01	0.01	-
66	39_Q9M584	284	0.435	-	0.040	0.113	-	2	0.01	0.01	-
67	39_Q9M585	394	0.528	Y	0.076	0.954	M	1	0.02	0.74	M
68	39_Q9M586	289	0.453	-	0.007	0.499	M	5	0.00	0.13	-
69	39_Q9M587	282	0.514	Y	0.063	0.117	S	4	0.29	0.07	C
70	39_Q9M588	284	0.482	-	0.034	0.036	S	1	0.19	0.01	-
71	39_Q9M589	289	0.472	-	0.020	0.530	M	5	0.01	0.04	-
Control proteins											
72	21_P83755 PsbA	352	0.432	-	0.015	0.495	-	4	-	-	-
73	21_P23321 PsbO	332	0.570	Y	0.839	0.195	C	2	0.97	0.08	C.
74	21_O82663 SDH* subunit 1	634	0.551	Y	0.271	0.882	M	2	0.00	0.43	M.

3.4.3 Phylogenetic analysis of the Band 7 proteins of higher plants

As before for the cyanobacterial Band 7 proteins, a phylogenetic analysis was performed with solely the Band 7 proteins of higher plants, in order to assess the relationships of these proteins among each other (see Figure 3.4). In this context, it was worthy of note that a previous phylogenetic study had identified another category of Band 7 proteins, apart from stomatins, prohibitins, flotillins, HflCs or HflKs, that had been assigned as 'plant defence' (Nadimpalli et al., 2000). In that study the 'plant defence' category included three Band 7 proteins of *Zea mays* which are induced during the hypersensitive reaction (HR) of this plant. Plant hypersensitive reaction is a defence response to pathogen infection involving rapid, localised cell death and induction of many pathogenesis-related proteins (Heath, 2000). Since then, higher

plant Band 7 proteins of *Hordeum vulgare* (Rostoks et al., 2003) and *Oryza sativa* (Japonica cultivar-group) (Takahashi et al., 2003) have also been shown to be involved in the HR plant defence mechanism. Consequently, the 'plant defence' category of Band 7 proteins was introduced in this phylogenetic analysis, although no specific sequence motifs that distinguished the members of this category could be found in the databases.

Analysing the generated phylogenetic tree for the Band 7 proteins of higher plants (see Figure 3.4), the majority of proteins could be found in three categories: prohibitins, stomatins and others or plant defence. The prohibitins formed the largest category, branching off at node 1 and contained all 30 assigned prohibitin homologues. A smaller group of Band 7 proteins branched off at node 2, but did not contain any assigned prohibitins and could therefore not be related to this protein family. All but one of the assigned stomatins were grouped together branching off at node 3. The Band 7 proteins of *Medicago truncatulla* (#29_Q1T6H8, #29_Q1T6H1, and #29_Q1T6H9) branched off at node 4 and seemed to be related to the stomatins, although they had not been assigned as such according to the InterPro database. One assigned *A. thaliana* stomatin (#21_Q9SRH6; indicated with an arrow) and other *A. thaliana* Band 7 proteins (#21_Q9CAR7, #21_Q9FHM7 and #21_Q9FM19; indicated with arrows) had been related to plant defence proteins in earlier phylogenetic analyses (data not shown) and could be found in heterologous clusters together with other or plant defence proteins (see clusters C and E). Cluster C seemed to contain the Band 7 plant defence proteins of dicotyledons represented by #21_Q9CAR7 of *A. thaliana* and #27_Q5KFB6 of *Lotus japonicus*, which was a reported HIR protein (Hakozaki et al., 2004). The small clusters A, B and D contained the Band 7 proteins of the monocotyledons: *Zea mays*, *Oryza sativa* (Japonica cultivar-group) and *Hordeum vulgare*, where the barley homologue was always the most distant relative. Both the maize and the barley Band 7 proteins had previously been reported to be involved in the HIR plant defence mechanism (Nadimpalli et al., 2000; Rostoks et al., 2003). Interestingly, the Band 7 protein #36_Q6L4B0 of *Solanum dimissum* was found in cluster E, whereas the Band 7 protein #37_Q38M64 of another, closely related potato species *Solanum tuberosum* had been assigned to be a prohibitin homologue and grouped accordingly in branch 1.

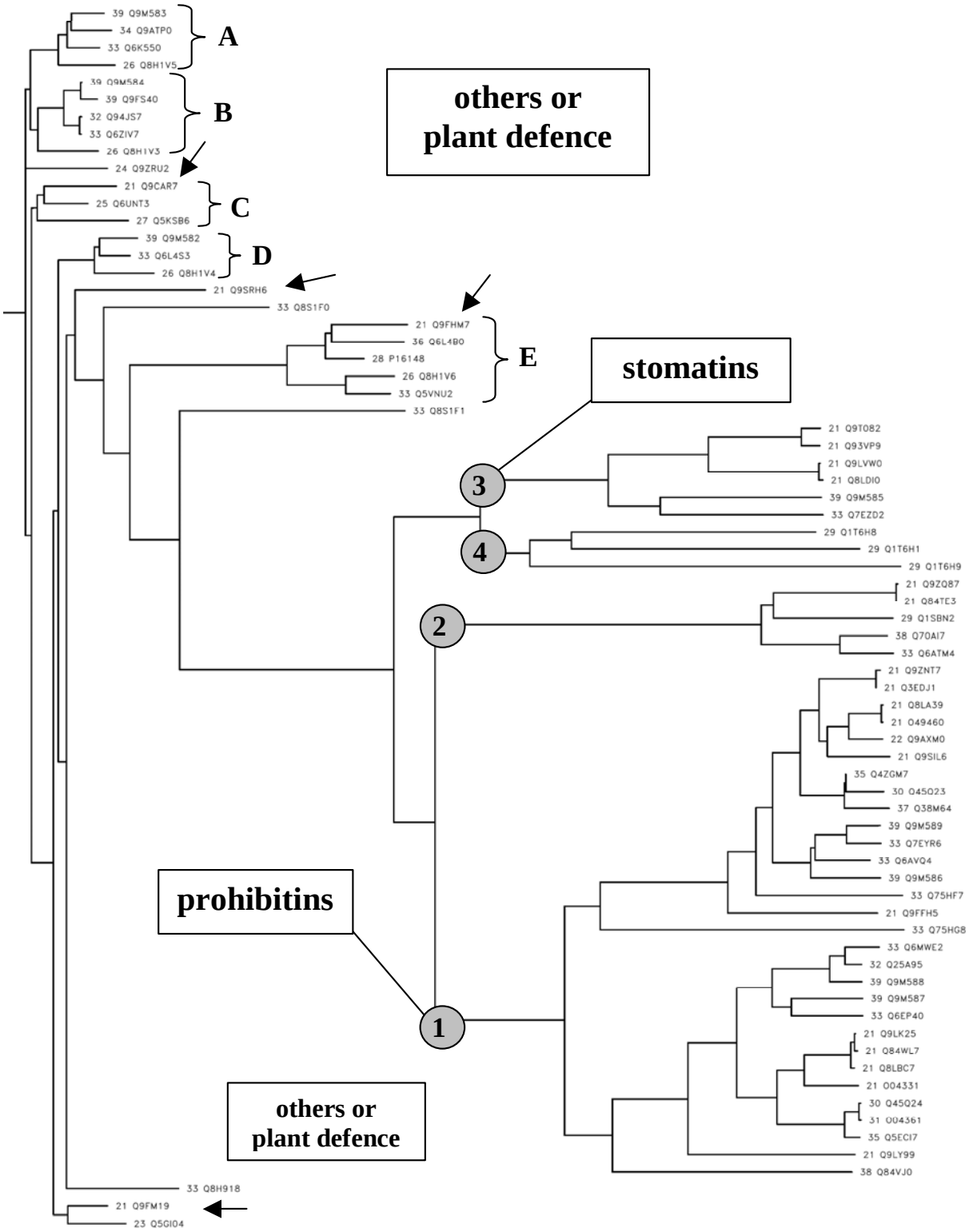

Figure 3.4: Phylogenetic analysis of the Band 7 proteins of higher plants. A phylogenetic tree was generated for the 71 Band 7 proteins of higher plants (see Table 3.5; sequence information for #33_Q7XEB7 is not available) as described in the legend of Figure 3.3. Relevant branching points are marked from 1 to 4 and labelled as references. A to E indicate clusters of Band 7 proteins of which some had previously been reported to be involved in plant defence (A, B and D; Nadimpalli et al., 2000). Arrows point at proteins which had been shown to group with plant defence proteins in previous phylogenetic analyses (unpublished data).

3.5 Other relevant Band 7 proteins

Prior to the comparative phylogenetic analysis of the Band 7 proteins of cyanobacteria and higher plants, the InterPro database was searched for additional proteins that could be relevant in such an analysis (see Table 3.7). As the Band 7 superfamily of proteins consists of the five protein subfamilies: prohibitins, stomatins, flotillins HflCs and HflKs (Tavernarakis et al., 1999), representatives of each of these subfamilies were chosen to be included. The Band 7 domain has first been identified in the stomatin homologue of *Homo sapiens* (#42_P27105; see section 3.1.1), which was therefore included in the analysis together with the human prohibitin (#42_P35232 = Prohibitin 1 and #42_Q99623 = Prohibitin 2) and flotillin (#42_O75955 = Flotillin 1 and #42_Q6FG43 = Flotillin 2) homologues.

Although Band 7 proteins have been extensively studied in many organisms, most information about their function and biochemistry has come from studies on the prohibitin homologues of *S. cerevisiae* and the HflK/C proteins of *E. coli*. Consequently, the Band 7 proteins of these lower eukaryotic (*S. cerevisiae*) and prokaryotic (*E. coli*) organisms were also included in the subsequent comparative phylogenetic analysis. The two prohibitin homologues of *S. cerevisiae* (#43_P40961 = Prohibitin 1 and #43_P50085 = Prohibitin 2; InterPro database) had revealed the best insights into the function of prohibitins. It had been found that the two proteins form a hetero-multimeric protein complex which acts as a membrane-bound chaperone to shield the subunits of newly assembling respiratory protein complexes from degradation by an AAA-type protease (Steglich et al., 1999; Nijtmans et al., 2000). In *E. coli*, six members of the Band 7 protein family could be identified and while none of them belonged to the prohibitin subfamily, the proteins YbbK (#41_P0AA53), YhdA (#41_Q9F507) and HflK (#41_P0ABC7) contained stomatin motifs. Furthermore, two Band 7 proteins of *E. coli* were assigned HflC (#41_P0ABC3) and HflK (#41_P0ABC7) homologues that belonged to the equally termed protein subfamilies which only exist in bacteria. The Band 7 homologue Ybbk and the HflK/C proteins were particularly interesting, because they had previously been shown to physically interact with the AAA-type FtsH protease of *E. coli* (Saikawa et al., 2004; Chiba and Akiyama, 2006). Furthermore, two flotillin-like proteins from a plant species (#21_Q501E6 of *A. thaliana*; not listed as a flotillin in the InterPro database, but identified as such by Borner et al. (2005)) and a prokaryote (#40_O32076 of *Bacillus subtilis*) respectively were included in the analysis. Although eukaryotic

flotillins are lipid raft-associated integral membrane proteins that are believed to be involved in the formation of specific platforms for the recruitment of multiprotein complexes, their functional role still remains largely enigmatic (Langhorst et al., 2005; Morrow and Parton, 2005). As prokaryotes lack cholesterol (Tannert et al., 2003) and are therefore unlikely to contain lipid raft domains (Morrow and Parton, 2005), the function of prokaryotic flotillin homologues is even less clear. In the end, altogether 15 additional and relevant proteins were identified and included in the subsequent comparative phylogenetic analysis (see Table 3.7 and Figure 3.5).

Table 3.7: Other relevant Band 7 proteins. The organisms are listed alphabetically and numbering resumes from Table 3.5. Proteins marked in bold were used in the comparative phylogenetic analysis (see Figure 3.5). (*) The Q501E6 protein of *A. thaliana* is not an assigned Band 7 protein according to the InterPro database, but had been identified as a flotillin-like protein in the literature (Borner et al., 2005).

#	Species	other Band 7 accession #s	Prohibitin accession #s	Stomatin accession #s
21	Arabidopsis thaliana (*)	**Q501E6**	none	none
40	*Bacillus subtilis*	**O32076**	none	none
41	*Escherichia coli*	**P0ABC3** **P77306** **Q93D69**	none	**P0AA53** **Q9F507** **P0ABC7**
42	*Homo sapiens*	**O75955** **Q6FG43**	**P35232** **Q99623**	**P27105**
43	*Saccharomyces cerevisiae*	none	**P40961** **P50085**	none
		7	**4**	**4**

3.6 Comparative phylogenetic analysis of Band 7 proteins

The phylogenetic analysis of cyanobacterial Band 7 proteins had already shown that Slr1106 (Phb1) of *Synechocystis* sp. PCC 6803 and Tlr1760 (TE_Phb1) of *Thermosynechococcus elongatus* were prohibitins with related proteins in other cyanobacterial strains (see Figure 3.3). The same was true for the assigned stomatins, Slr1128 (Phb3) of *Synechocystis* sp. PCC 6803 and Tlr2184 (TE_Phb2) of *Thermosynechococcus elongatus*. However, the other three Band 7 proteins of *Synechocystis* sp. PCC 6803: Slr1768 (Phb2), Sll0815 (Phb4) and Sll1021 (Phb5), did not clearly belong to any other known Band 7 subfamily and only Sll1021 had been found to be grouping in a so far unassigned category, together with other cyanobacterial Band 7 proteins. In order to assess the relationships between the Band 7 proteins of cyanobacteria, higher plants and selected other organisms and to possibly

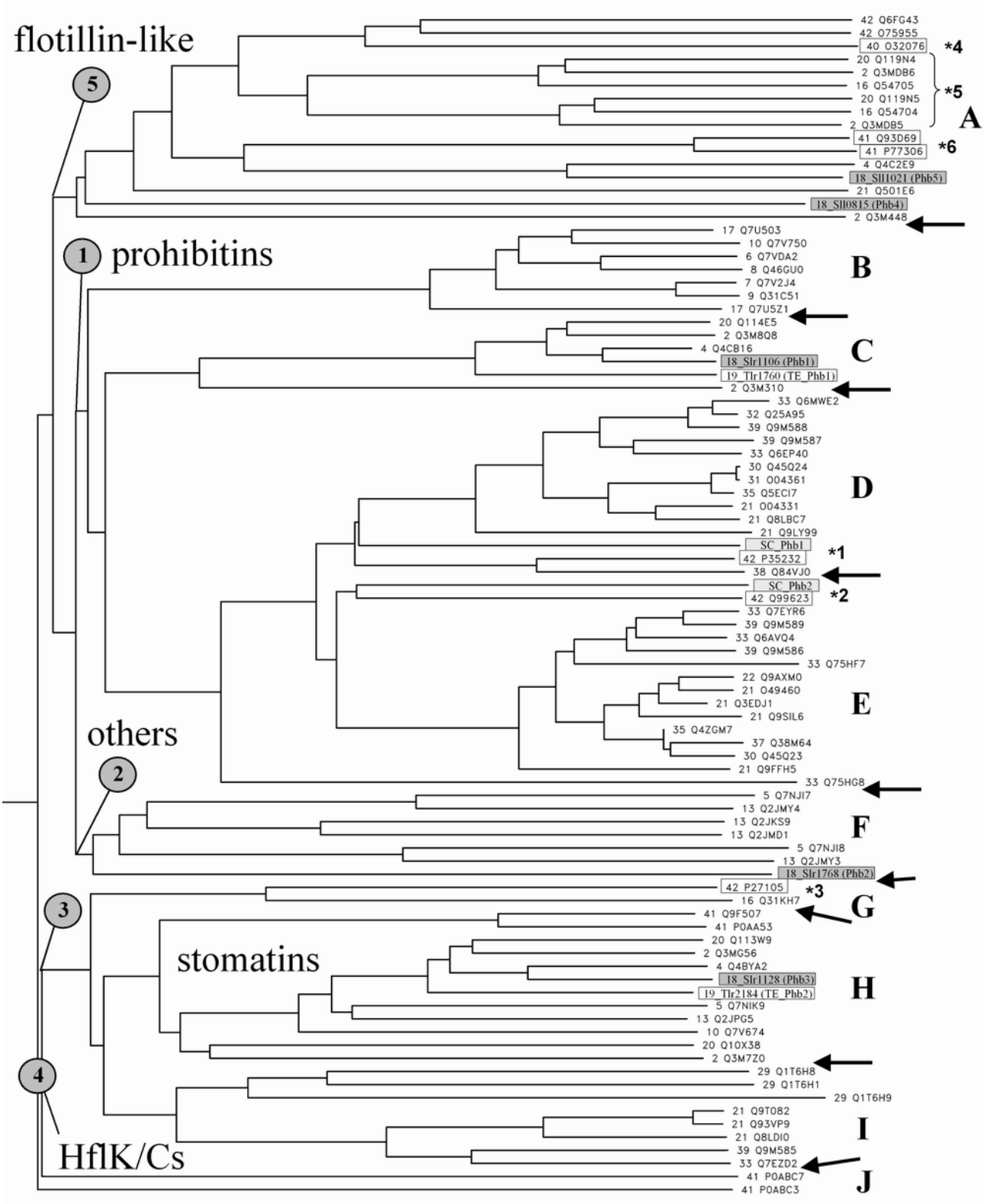

Figure 3.5: Comparative phylogenetic analysis of Band 7 proteins. A phylogenetic tree was generated for 90 selected Band 7 proteins (see text) as described in the legend of Figure 3.3. Proteins are labelled with a number (according to the species number in the Tables 3.4, 3.5 and 3.7) followed by its UniProt accession number. Relevant branching points are marked from 1 to 5 and labelled as references. Arrows indicate a border between protein subcategories which were referred to as A to J (see text). Proteins of special interest are boxed and the numbered asterisks mark proteins of interest that are specifically referred to in the text.

assign the three unassigned Band 7 proteins of *Synechocystis* sp. PCC 6803 to a specific category of Band 7 proteins with perhaps a known function, a comparative phylogenetic analysis was performed (see Figure 3.5).

Due to the restrictions implied by the CLUSTALW alignment tool, not all 1655 Band 7 proteins could be analysed and the subset was limited to 100 protein sequences. Therefore, the Band 7 proteins of the cyanobacterial strains # 1, #3, #11, #12, #14 and #15 were ignored, because they were represented by homologues of other, closely related strains (compare Table 3.4 and Figure 3.3). As for the Band 7 proteins of higher plants, initially all the proteins that had been found in the branches 1 to 4 of Figure 3.4, except for those proteins that had another, closely related homologue in the same species, were supposed to be included in this phylogenetic analysis. However, a preliminary analysis had shown that the proteins found in branch 2 of Figure 3.4, did not exhibit any relationship towards the cyanobacterial or the other included proteins (data not shown), so that the subset was reduced again by removing these proteins from the final comparative phylogenetic analysis. Moreover, the proteins that had been found in the smaller clusters (see Figure 3.4) and seemed to be associated with plant defence were also ignored, because an earlier phylogenetic analysis had revealed no evidence for a relationship between these and the Band 7 proteins of cyanobacteria (unpublished data). Thus, including the other relevant Band 7 proteins (see Table 3.7), a subset total of 90 Band 7 proteins was analysed in this comparative phylogenetic analysis (see Figure 3.5).

Analysing the generated phylogenetic tree, five major categories of proteins could be distinguished: prohibitins (1), 'others' (2), stomatins (3), HflK/Cs (4) and flotillin-like (5). Each of the specifically denominated categories was named after the constituent proteins and some categories were further divided into smaller subcategories that were referred to as A to J. The largest category was that of the prohibitins, found in branch 1 and consisting out of the subcategories B to E, with 43 members, although 47 assigned prohibitins had been included in this analysis. The four assigned prohibitin homologues that were not found in the subcategories B to E were those of *Synechococcus* sp. strain JA-2-3B'a(2-13) (#13_Q2JMY3; #13_Q2JK59; #13_Q2JMD1) and of *Gloeobacter violaceus* (#5_Q7NJI7), which could be found in branch 2 in subcategory F instead. Together with #5_Q7NJI8 of *Gloeobacter violaceus*, #13_Q2JMY3 of *Synechococcus* sp. strain JA-2-3B'a(2-13) and Slr1768 (Phb2) of *Synechocystis* sp. PCC 6803, these proteins were assigned to as the 'others'

subcategory, as the relationship to the prohibitins appeared to be only of a minor nature. Looking at the various prohibitin subcategories, subcategory B and C contained the prohibitin homologues of cyanobacteria. Both of these subcategories appeared to be rather independent of each other, as the respective branches had separated rather early on, while the individual member proteins of these subcategories exhibited stronger relationships. The prohibitin homologues of *Synechocystis* sp. PCC 6803 (Slr1106) and *Thermosynechococcus elongatus* (Tlr1760) were both found in subcategory C. The prohibitin homologues of higher plants were identified in subcategory D and E, together with the two prohibitins #43_P40961 (SC_Phb1) and #43_P50085 (SC_Phb2) of *S. cerevisiae* and those of *Homo sapiens* #42_P35232 (Prohibitin 1) and #42_Q99623 (Prohibitin 2) (*1 and *2). It was noteworthy, that the prohibitin homologues of higher plants, yeast and human formed the two subcategories D and E, with representatives of each organism in each of the two branches. Similarly, prohibitin homologues of #21 *Arabidopsis thaliana*, #30 *Nicotiana benthamiana*, #33 *Oryza sativa* (Japonica cultivar-group), #35 *Petunia hybrida* and #39 *Zea mays* could be found in each of the two subcategories. The plant prohibitin homologue #33_Q75HG8 of *Oryza sativa* (Japonica cultivar-group) however, branched off rather early from these subcategories and appeared to be only a distantly related member of the prohibitin family. Interestingly, the prohibitin homologues of monocotyledons and dicotyledons seemed to group separately in each of the two subcategories D and E.

The second largest category, containing subcategories G, H and I (branch 3), was that of the stomatins with 22 members, although only 20 assigned stomatins had been included in this analysis. One of the proteins that had been assigned as a stomatin by the InterPro database was #41_POABC7 (HflK) of *E. coli*, which possessed stomatin domains, but ultimately is a HflK homologue. This protein could be found in branch 4 and subcategory J together with the HflC homologue #41_POABC3 of *E. coli*. It is noteworthy that HflK and HflC of *E. coli* did not exhibit any phylogenetic relationship to each other. Going back to analysing the stomatin subcategories, it was observed that three Band 7 proteins of #29 *Medicago truncatulla* were found in subcategory I, although they were non-stomatins according to the InterPro database. Overall, the stomatins could roughly be divided into three subcategories (G, H and I), that generally seemed to be less related among each other, as the respective branches split earlier than it was observed for the prohibitins (compare subcategories H with B and C and I with E). In subcategory H, a cyanobacterial stomatin #16_Q31KH7 of

Synechococcus sp. PCC 7942 was found to group together with human stomatin (#42_P27105), which together branched off early from the other stomatins (*3). Plant stomatins could be identified in subcategory I and it was again observed that the stomatins of mono- and dicotyledons were found in separate branches. The largest stomatin subcategory (subcategory H) contained all cyanobacterial stomatins, as well as the assigned stomatins #41_Q9F507 and #41_P0AA53 of *E. coli*, even though these two proteins branched off earlier from the cyanobacterial stomatin homologues.

Interestingly, the proteins that had been found to group together in branch 6 of Figure 3.3 and had then been assigned as the 'others' subcategory, were found to group as well in this phylogenetic analysis (branch 5; subcategory A) and displayed relationship to the flotillins which had been included in this comparative phylogenetic analysis. Because subcategory A, which had 16 Band 7 protein members, contained the flotillin homologues of *Homo sapiens* (#42_Q6FG43 and #42_O75955) and *Bacillus subtilis* (#40_O32076)(*3), the whole subcategory was assigned as the 'flotillin-like' subcategory. In general this category appeared rather heterogeneous, but it was interesting to note that six cyanobacterial Band 7 proteins, two of each #2 *Anabaena variabilis* PCC7937, #16 *Synechococcus* sp. PCC7942 and #20 *Trichodesmium erythraeum* IMS101, were found with one protein of each strain in two branches (*5). Additionally, #18_Sll1021 of *Synechocystis* sp. PCC 6803, #4_Q4C2E9 of *Crocosphaera watsonii* and to some degree even the Band 7 proteins #41_Q93D69 and #41_P77306 of *E. coli* (*6) seemed to be related to these flotillin-like Band 7 proteins. Moreover, the flotillin-like protein of *Arabidopsis thaliana* (#21_Q501E6; Borner et al., 2005) could be found in subcategory A, as well as #18_Sll0815 of *Synechocystis* sp. PCC 6803 and #2_Q3M448 of *Anabaena variabilis* PCC 7937, although these proteins appeared to be only rather distantly related to the other flotillins and flotillin-like proteins.

Summarising the results of this comparative phylogenetic analysis, it could be noted that cyanobacterial Band 7 proteins in general, and those of *Synechocystis* sp. PCC 6903 in particular, were in most cases only distantly related to the Band 7 proteins of higher plants. While prohibitin homologues appear to be more conserved among each other, stomatins and flotillins appear to be rather diverse protein families. The most interesting finding in this analysis however was, that some cyanobacterial Band 7 proteins (among them Sll1021 and maybe Sll0815 of *Synechocystis* sp. PCC 6803) exhibited a certain phylogenetic relationship to flotillin homologues. The other

Band 7 protein Slr1768 of *Synechocystis* sp. PCC 6803, could not be clearly assigned to a particular Band 7 protein subfamily.

3.7 Discussion

In this section, the targeting prediction results for the Band 7 proteins of higher plants are discussed and compared to relevant results from the literature (see section 3.7.1). Furthermore, the identification of cyanobacterial Band 7 proteins in general (see section 3.7.2) and also the properties of the Band 7 proteins of *Synechocystis* sp. PCC 6803 and *Thermosynechococcus elongatus* in particular (see section 3.7.3) are discussed. Moreover, the observed phylogenetic relationships of cyanobacterial Band 7 proteins among themselves (see section 3.7.4) and with Band 7 proteins of other organisms (see section 3.7.6) is touched upon. Additionally, views on the evolution of the Band 7 domain from the literature are presented (see section 3.7.5).

3.7.1 Targeting of the Band 7 proteins of higher plants

Most of what is known about the function and localisation of Band 7 proteins has come from studies of *H. sapiens*, *C. elegans*, *S. cerevisiae* and *E. coli*. In comparison very little is known about Band 7 proteins of other prokaryotes and higher plants. However, some of the Band 7 proteins of the following plants (mostly their prohibitin homologues) have been studied to some extent: *Arabidopsis thaliana*, *Nicotiana benthamiana*, *Nicotiana tabacum*, *Oryza sativa*, *Petunia hybrida* and *Zea mays* (Snedden and Fromm, 1997; Ahn et al., 2006; Takahashi et al., 2003; Chen et al., 2005; Nadimpalli et al., 2000). As the working hypothesis of this work was that the prohibitin homologues of *Synechocystis* sp. PCC 6803 are involved in the PSII repair cycle (see Figure 1.9), it was relevant to test whether the predicted Band 7 proteins of higher plants have the potential to be targeted to chloroplasts and thereby to perhaps be involved in photosynthesis. Two approaches can be used to determine whether a protein is targeted to a particular compartment of the cell. One is to search the primary structure of a protein of interest for specific targeting signal sequences (Rusch and Kendall, 1995; Schatz and Dobberstein 1996) with targeting prediction servers (Emanuelsson, 2000; Small et al., 2004), while the other is to identify the compartment(s) in which the protein resides experimentally (Snedden and Fromm,

1997; Takahashi et al., 2003; Ahn et al., 2006). In this section, the used targeting prediction servers are briefly discussed (see section 3.7.1.1) and the results that were generated with them are compared to findings in the literature (see section 3.7.1.2).

3.7.1.1 Targeting prediction servers

The Band 7 proteins of higher plants were analysed for their potential to be targeted to chloroplasts using the following, three targeting prediction servers: ChloroP, TargetP and Predotar (see Table 3.6).

The ChloroP prediction server is a 'neural network' that can discriminate between chloroplastic transit peptides (cTPs) and non-cTPs. In a test set of 715 *A. thaliana* protein sequences, it has achieved a sensitivity of around 0.9 (i.e. 90 % of cTPs were found) and a specificity of 0.6 (i.e. 60 % of the predicted cTPs were correct) (Emanuelsson, 1999). Thus, the ChloroP prediction server can be considered useful for screening Band 7 proteins of higher plants for putative chloroplast proteins. However, one problem associated with the ChloroP prediction server is that it cannot discriminate very efficiently between cTPs and mitochondrial-targeting peptides (mTPs). Even though the ChloroP prediction server can be used individually, it is also an integral part of the TargetP prediction server which differentiates between secretory proteins, mitochondrial proteins, chloroplast proteins, and everything else.

The TargetP prediction server has achieved an overall prediction accuracy of 85.3 % on a test set of 940 plant protein sequences and generally predicts signal peptides for the secretory pathway with high sensitivity (0.91) and specificity (0.95) but performs less well on chloroplast transit peptides (0.85 and 0.69) and mitochondrial-targeting peptides (0.82 and 0.90) (Emanuelsson, 2001).

The Predotar prediction server is designed to deal with plant protein sequences and addresses the chloroplast/mitochondrion sorting problem. The level of overall prediction accuracy for the Predotar prediction server is 84.8 % on the same plant test set that has been used to test the accuracy for the TargetP prediction server (Emanuelsson, 2001). Although both the TargetP and the Predotar prediction servers achieve a similar level of accuracy, their performances vary slightly and therefore the sequences of the Band 7 proteins of higher plants were analysed using both prediction servers.

3.7.1.2 Targeting prediction servers versus findings in the literature

The targeting prediction results of the TargetP and Predotar prediction servers are graphically represented in Table 3.5. In the following discussion, the individual targeting prediction scores for mentioned Band 7 proteins are largely neglected and no distinction is made which program predicted their localisation. Results on the subcellular localisation of higher plant Band 7 proteins from the literature that are referred to in this section are summarised in Table 3.8.

Table 3.8: Reported subcellular localisations of higher plant Band 7 proteins. The 'method' column indicates the applied technique for the identification of the subcellular localisation of a particular higher plant Band 7 protein in the respective study. Mass spectrometry (MS), GFP-tagging of the respective protein and subsequent confocal microscopy (GFP). (*) See text for more details.

Protein name & organism	Band 7 type	Found in	Method	Reference
#21_Q9T082 (*A. thaliana*)	stomatin	mitochondria	MS	Millar et al., (2001)
			MS	Kruft et al., (2001)
#21_Q9LVW0 (*A. thaliana*)	stomatin	mitochondria	MS	Kruft et al., (2001)
#21_Q93VP9 (*A. thaliana*)	stomatin	detergent-resistant membranes	MS	Borner et al., (2004)
#21_O04331 (*A. thaliana*)	prohibitin	mitochondria	cell fractionation *	Snedden and Fromm, (1997)
			MS	Kruft et al., (2001)
			MS	Millar et al., (2001)
#21_O49460 (*A. thaliana*)	prohibitin	mitochondria	MS	Millar et al., (2001)
#21_Q9LK25 (*A. thaliana*)	prohibitin	mitochondria	MS	Millar et al., (2001)
#21_Q9SIL6 (*A. thaliana*)	prohibitin	mitochondria	MS	Millar et al., (2001)
#21_Q9ZNT7 (*A. thaliana*)	prohibitin	**mitochondria**	MS	Millar et al., (2001)
#21_Q9ZNT7 or #21_Q3EDJ1 (*A. thaliana*)	prohibitin	**chloroplast envelope**	MS	Kleffmann et al., (2004)
#21_Q84WL7 or #21_Q9LK25 (*A. thaliana*)	prohibitin	chloroplast envelope	MS	Kleffmann et al., (2004)
#32_Q25A95 (*O. sativa*)	prohibitin	mitochondria	GFP	Takahashi et al., (2003)
#35_Q4ZGM7 (*P. hybrida*)	prohibitin	mitochondria	indirect respiration *	Chen et al., (2006)
#35_Q5ECI7 (*P. hybrida*)	prohibitin	mitochondria	indirect respiration *	Chen et al., (2006)
#31_O04361 (*N. tabacum*)	prohibitin	BY-2 plastids	MS	Baginsky et al., (2004)
#30_Q45O23 (*N. benthamiana*)	prohibitin	mitochondria	GFP	Ahn et al., (2006)
#30_Q45O24 (*N. benthamiana*)	prohibitin	mitochondria	GFP	Ahn et al., (2006)

Interestingly, such a representation of the results suggested that almost all of the assigned stomatins of higher plants were localised to mitochondria (except for #21_Q9SRH6). Remarkably, this Band 7 protein had already been suggested not to belong to the stomatins because of the results of the phylogenetic analysis (see Figure 3.4) and given the combined evidence, it seemed likely that this proteins had been falsely assigned as a stomatin in the InterPro database. Otherwise, the observation that stomatins localise to mitochondria is supported by the literature: the Band 7 proteins #21_Q9T082 (Millar et al., 2001) and #21_Q9LVW0 and #21_ Q9T082 (both Kruft et al., 2001) have also been found in the mitochondria of *A. thaliana* by proteomic approaches. It is worthy of note, that all the Band 7 proteins of *Medicago truncatulla* had been predicted to be localised to mitochondria and were also rather closely related to the stomatins in the phylogenetic analysis (compare Figure 3.4). This emphasised the assumption that the Band 7 proteins of *Medicago truncatulla* might in fact rather be stomatins than other Band 7 proteins. Interestingly, another stomatin homologue of *A. thaliana* (#21_Q93VP9) has also been identified in the literature, where it is found to be enriched in detergent-resistant membranes (Borner et al., 2005). This result is particularly interesting, because in other eukaryotes, stomatins have been reported to be associated with lipid rafts (Salzer and Prohaska, 2001; Mairhofer et al., 2002; Morrow and Parton, 2005; Umlauf et al. 2006) where their function is suggested to be an involvement in ion channel gating (Sedensky et al., 2001; Price et al., 2004; Stewart, 2004). Summarising the targeting prediction server results and the findings in the literature, it appears unlikely that the stomatins of higher plants, are directly involved in photosynthesis-related processes.

In contrast to the rather confident mitochondrial localisation predictions for the stomatins, the chloroplastic localisation predictions all obtained low scores no matter which of the prediction server had given the result. Overall, eight Band 7 proteins were predicted to be targeted to chloroplasts, while five of these proteins were assigned other Band 7 proteins. Thus, more important for this study were the three prohibitin homologues (#32_Q25A95, #33_Q6MWE2 and #39_Q9M587) that, according to the Predotar prediction server, had the potential to be targeted to chloroplasts. Interestingly, these three prohibitin homologues of the monocotyledons *Oryza sativa* and *Zea mays* had previously been found to group closely in the phylogenetic analysis (see Figure 3.4). Contradictory to the targeting prediction result, the prohibitin homologue of *Oryza sativa* (#32_Q25A95) has already been associated with

mitochondria. Green fluorescent protein (GFP) tagged prohibitin has been transiently introduced into *Allium cepa* epidermal cells, where the GFP protein could be observed in mitochondria by confocal microscopy (Takahashi et al., 2003). However, no experimental evidence is available on the prohibitin homologue #39_Q9M587 of *Zea mays*. Interestingly, TargetP predicted one prohibitin homologue of *Petunia hybrida* (#35_Q4ZGM7) to be localised to mitochondria. This finding is in agreement with the literature; although no direct evidence exists for a mitochondrial localisation, both prohibitin homologues of this species have been implied to have an effect on respiration (Chen et al., 2005). One protein that had not been assigned to be targeted to chloroplasts by the targeting prediction servers (TargetP or Predotar), but was predicted by the ChloroP server to posses a chloroplastic transit peptide, was the prohibitin homologue of *Nicotiana tabacum* (#31_O04361). The same was true for the closely related prohibitin homologue of *Nicotiana benthamiana* (#30_Q45O24). Interestingly, a proteomic approach has identified #31_O04361 in undifferentiated heterotrophic plastids (tobacco bright yellow-2 cell culture plastids) as an integral membrane protein (Baginsky et al., 2004). In another study the prohibitin homologues of *Nicotiana benthamiana* (#30_Q45O23and #30_ Q45O24) were found to be targeted to mitochondria by expressing each of the full-length prohibitin homologues together with GFP as fusion proteins and subsequent confocal microscopy (Ahn et al., 2006). However, potential artefacts due to transient expression cannot be completely excluded.

Some of the Band 7 proteins of *A. thaliana*, which had not been assigned to mitochondria or the chloroplasts by the TargetP or Predotar prediction servers in this study, have been identified in the literature. The first report on the localisation of a plant Band 7 protein was that of the #21_O04331 prohibitin homologue of *A. thaliana* which was immunochemically identified in the mitochondria-enriched fraction of a subcellular fractionation assay (Snedden and Fromm, 1997). More recent studies have applied proteomic approaches and also identified some Band 7 proteins of *A. thaliana* in different organelles. For example, proteome analyses of mitochondrial proteins of *A. thaliana* have identified the prohibitin homologue #21_O04331 (Kruft et al., 2001), while five Band 7 proteins of *A. thaliana* are identified in another study (#21_O04331, #21_O49460, #21_Q9LK25, #21_Q9SIL6, **#21_Q9ZNT7**) (Millar et al., 2001). A further proteomic analysis of the chloroplast proteome of *A. thaliana* has found two prohibitin homologues (At1g03860 and At3g27280) in the envelope fraction of

chloroplasts, while in the same study TargetP has assigned these proteins to the secretory pathway (Kleffmann et al., 2004). Unfortunately, the accession numbers that were listed in the literature were not unambiguous and when the proteins corresponding to the accession numbers At1g03860 and At3g27280 were looked up in the SwissProt database, At1g03860 yielded #21_Q3EDJ1 and **#21_Q9ZNT7**, while At3g27280 returned #21_Q84WL7 and #21_Q9LK25 respectively. Thus, surprisingly, experimental data (Millar et al., 2001 and Kleffmann et al., 2004) suggests that the prohibitin homologues **#21_Q9ZNT7** of *A. thaliana* might be found in both mitochondria and chloroplasts. Even though dual targeting events, i.e. the targeting of a certain protein to both chloroplasts or mitochondria, has been reported in the literature (Akashi et al., 1998 and Menand et al., 1998), this phenomenon is suggested to be quite rare. Consequently, either the **#21_Q9ZNT7** prohibitin homologue of *A. thaliana* exhibits dual targeting, or it has to be considered that this proteins is a potential contaminant and therefore a false positive in the results of one of the two studies by Millar et al. (2001) or Kleffmann et al. (2004).

Summarising the obtained results, although the prediction servers TargetP and Predotar gave correct predictions for the control proteins and have been shown to assign proteins to the correct locations with a high degree of accuracy in the literature, the fact that the results from both prediction servers did not necessarily agree with each other in this study, left an element of doubt about the validity of the obtained results. However, the targeting prediction analysis and evidence in the literature gave some indications that some Band 7 proteins of higher plants and more importantly certain prohibitin homologues might be targeted to chloroplasts. Therefore, considering both bioinformatic and experimental data, the possibility that certain prohibitin homologues of higher plants might be involved in photosynthesis-related processes cannot be completely ruled out.

3.7.2 Identification of cyanobacterial Band 7 proteins

In this work, 58 cyanobacterial Band 7 proteins have been identified, which was significantly more than the 22 Band 7 proteins which had been found in previous database searches (see Figure 3.1). This increase could be attributed to the increasing amount of available sequence information. According to the National Centre for Biotechnology Information (NCBI) 10 complete genome sequences were available for

cyanobacteria in 01/2005 and this number has increased to 19 in 09/2006, with another 28 cyanobacterial genomes in the process of being sequenced. Therefore, most of the previously unknown Band 7 proteins were newly identified proteins in cyanobacterial strains whose genome had been newly sequenced, rather than newly assigned Band 7 proteins in strains whose genome sequence had already been known. However, the assignment of Band 7 proteins seems to be under constant revision, as the number of Band 7 proteins also varies slightly in those organisms whose genome had already been completely sequenced at the time of the previously performed database search, such as *A. thaliana*, *H. sapiens* and *M. musculus*. When the distribution of the Band 7 proteins among the various taxonomic groups was investigated, it became apparent that in bacteria and archaea significantly more Band 7 proteins were assigned stomatins (538 and 34) than prohibitins (53 and 2). However, in cyanobacteria (16 stomatins and 23 prohibitins) and higher plants (7 stomatins and 30 prohibitins), this relationship seemed to be reversed. In other eukaryotic organisms the number of the Band 7 proteins that were assigned stomatins and prohibitins seemed to be more equal (compare Figure 3.2). Even though these differences were obvious, no conclusions could yet be drawn from these observations.

3.7.3 Properties of selected cyanobacterial Band 7 proteins

Analysing the properties of the Band 7 proteins of *Synechocystis* sp. PCC 6803 and *Thermosynechococcus elongatus* (see Table 3.3), the expected N-terminal transmembrane domains suggested that these proteins might be membrane-associated. Interestingly, the two prohibitin homologues of *S. cerevisiae* also feature N-terminal transmembrane domains and have similar molecular masses (SC_Phb1 = 31.47 kDa and SC_Phb2 = 34.40 kDa; compare to Table 3.3). Together the prohibitin homologues of *S. cerevisiae* form membrane-associated, large, hetero-multimeric and ring-like structures (Steglich et al., 1999; Back et al., 2002; Tatsuta et al., 2005). Human stomatin is also known to possess N-terminal transmembrane domains (Stewart et al., 1992) and to form large, multimeric protein complexes (Snyers et al., 1998). Therefore, it seems possible that the prohibitin and stomatin homologues of *Synechocystis* sp. PCC 6803 and *Thermosynechococcus elongatus* might form similar large, multimeric protein complexes.

3.7.4 Phylogenetic relationships between cyanobacterial Band 7 proteins

After having discussed identification and properties of cyanobacterial Band 7 proteins, this section focuses on the relationships between the proteins that have emerged from the phylogenetic analysis performed in this work (see Figure 3.3).

Initially, while comparing the numbers of Band 7 proteins, or members of the respective protein subfamilies, that were identified in the individual cyanobacterial strains, it became apparent, that no generalisation could be made on how many Band 7 proteins a cyanobacterium would possess, as this number appeared to differ even between closely related strains. For example, *Anabaena variabilis* PCC 7937 possessed seven Band 7 proteins, whereas in the closely related *Anabaena variabilis* strain only one Band 7 protein had been identified. Even though it had been observed earlier that cyanobacteria seemed to have more prohibitins than stomatins, three strains possessed a stomatin homologue, but not any assigned prohibitin homologues (*Anabaena variabilis*, *Synechococcus* sp. PCC 6301 and *Synechococcus* sp. PCC 7942). These observations are likely to be intrinsic features of the respective cyanobacterial strains, as the general identification of the Band 7 and their assignment to the various subfamilies of proteins in the InterPro database appears to be mostly correct and once a genome has been completely screened, the assignments do not seem to change much during subsequent revisions (compare Figure 3.1A and Figure 3.1B).

Looking at the phylogenetic analysis of cyanobacterial Band 7 proteins (see Figure 3.3), it could be observed that the Band 7 proteins of genetically closely related strains were found in the same branches (e.g. for the three *Anabaena* strains #1, #2 and #3 or for some *Synechococcus* strains #13 and #14 or #15 and #16). However, these close relationships could clearly be attributed to the similar genetic backgrounds of the respective cyanobacterial strains. Traditionally, cyanobacteria are classified by morphology into five sections, referred to by the numerals I to V (Chroococcales, Pleurocapsales, Oscillatoriales, Nostocales and Stigonematales) (Boone et al., 2001). However, the sections Chroococcales, Pleurocapsales, Oscillatoriales are not necessarily supported by phylogenetic studies and a slightly different classification scheme is found on the NCBI website (http://www.ncbi.nlm.nih.gov/Taxonomy/Browser/wwwtax.cgi?mode=Undef&id=1117&lvl=3&p=mapview&p=has_linkout&p=blast_url&p=genome_blast&lin=f&keep=1&srchmode=1&unlock). Considering the classification schemes, it was an interesting observation that the Band 7 proteins of

Synechocystis sp. PCC 6803 and *Thermosynechococcus elongatus* (members of the Chroococales) seemed to bear some relationship to the Band 7 proteins of the *Anabaena* strains (#1 to #3) (members of the Nostocales) rather than to those of the *Synechococcus* strains (#11 to #17) (members of the Chroococales). In agreement with the classification schemes, however, were the observed relationships between the Band 7 proteins of *Crocosphaera watsonii* and those of *Synechocystis* sp. PCC 6803 (both members of Chroococales). Although *Crocosphaera watsonii* only possessed three Band 7 proteins, all of them seemed to group with a homologue of *Synechocystis* sp. PCC 6803. This was true for the prohibitin and stomatin homologues as well as for Phb5 (Sll1021) which had been found in the 'others' category. No homologues for the #18_ Slr1768 (Phb2) and the #18_ Sll0815 (Phb4) proteins of *Synechocystis* sp. PCC 6803 were found in *Crocosphaera watsonii*, which emphasised the particularity of these proteins. Especially interesting was the finding of the third, large category of cyanobacterial Band 7 proteins which had preliminarily been labelled as the 'others' category and which consisted out of twelve unassigned Band 7 proteins with a yet unknown function or homology. Interesting in this category was that the #4_Q4C2E9 Band 7 protein of *Crocosphaera watsonii* had a similar molecular mass (77 kDa) compared to the #18_Sll1021 (Phb5) protein of *Synechocystis* sp. PCC 6803 (75 kDa), while the other members of this category had molecular masses between 42 and 51 kDa (data not shown).

3.7.5 Evolution of the Band 7 domain

Several studies have addressed the phylogenetic relationships between the Band 7 proteins. Some of these studies include a comparative phylogenetic analysis of the Band 7 proteins of all the five subfamilies (stomatins, prohibitins, flotillins, HflCs and HflKs) from different organisms, while the focus usually lies on one of these subfamilies: stomatins (Tavernarakis et al., 1999), plant defence proteins (Nadimpalli et al., 2000) and flotillins (Rivera-Milla et al., 2005). The relationships between the prohibitin subfamily of proteins however, have been analysed in other studies, that rather focus on experimental data, while evolutionary coherences are only covered to a lesser extent (Chen et al., 2005; Ahn et al., 2006).

Tavernarakis et al. (1999) initially identified a common motif in five protein families: stomatins, prohibitins, flotillins, HflCs and HflKs using stomatin sequences

for PSI-BLAST searches. The identified conserved region was subsequently named the SPFH domain, which is commonly used as a synonym to Band 7 domain. In the phylogenetic analysis of that study, archaeal stomatins were observed to be highly homologous to eukaryotic stomatins, and are therefore suggested to be the prokaryotic members of the stomatin family (p-stomatins). As p-stomatins were found in almost all of the archaeal genomes that had been sequenced at the time, but only in a minority of bacterial genomes, it was suggested that Archaea and Eukarya shared a common ancestor that contained a stomatin homologue, from which horizontal gene transfer occurred to specific bacterial lineages. Interestingly, a later publication postulated that p-stomatins are linked to the *nfed* gene, which bears a conserved, probable serine protease motif (Green at al., 2004). In that study, *p-stomatin* genes were found adjacent to *nfed* genes in 19 different prokaryotes, of which 12 belonged to the Bacteria and 7 to the Archaea. This suggests that the assumption by Tavernarakis et al. (1999), that p-stomatins were of archaeal origin and only occur in specific bacteria due to horizontal gene transfer, is most likely wrong. However, Green at al. (2004) postulate that the p-Stomatin/Nfed membrane-bound proteolytic system is indeed of an ancient origin, as these proteins can be found in both Bacteria and Archaea, but has evolved through general vertical rather than horizontal gene transfer. This conclusion is supported by the finding that the GC contents of the *p-stomatin*/*nfed* gene sequences are similar to those of the originating organisms (Green at al., 2004).

Already in the study by Tavernarakis et al. (1999), a second, distinct, prokaryotic stomatin protein subfamily is identified that forms a separate branch apart from the other protein families and contains Slr1128 (Phb3) of *Synechocystis* sp. PCC 6803 and Ybbk of *E. coli* (see also subcategory H in Figure 3.5). It is worthy of note that this category of proteins was neither assigned or recognised as stomatins (Tavernarakis et al., 1999), nor were any of its members found to form an operon with the *nfed* gene (Green at al., 2004). Thus, it appears that this second group of prokaryotic stomatins has evolved independently of the so called p-stomatins.

In the study by Tavernarakis et al. (1999), the biochemical activities of the Band 7 protein subfamilies: HflC and HflK of *E. coli* and prohibitin of eukaryotes were recognised to be remarkably conserved. While HflC and HflK interact with and regulate the activity of the FtsH protease of *E. coli* (Kihara et al., 1996), the prohibitin homologues of *S. cerevisiae* have been shown to interact with and regulate the activity of a m-AAA protease in mitochondria (Steglich et al., 1999). Thus, it is suggested that

the region around the SPFH domain is important for complex formation with membrane-associated proteases and that Band 7 proteins in general might be involved in regulating membrane-associated protein turnover.

A study by Nadimpalli et al. (2000) which had been published shortly after the article by Tavernarakis et al. (1999) also reported on the existence of a superfamily of proteins which contained prohibitins, stomatins and plant defence response proteins, which has been called the PID (proliferation, ion and death) superfamily of proteins. The comparative phylogenetic analysis of that study distinguishes four major categories of proteins, namely the stomatins, prohibitins, HflK/C and HIR (hypersensitive induced reaction = plant defence proteins). Due to the identified sequences and structural similarities that were found in all of the proposed member proteins and the fact that stomatin has been suggested to act to regulate potassium ion channels (Stewart, 1997), the authors conclude that the conserved function of this superfamily of proteins might be ion channel regulation.

A more recent study focuses on the flotillin Band 7 subfamily of proteins (Rivera-Milla et al., 2005) and contradicts the assumption by Tavernarakis et al. (1999) that the proteins that contain the SPFH domain originate from a common ancestor and share functional homology, but that the observed relations are rather a consequence of convergent evolution. These claims are based on the observation that the members of different Band 7 subfamilies exhibit only very low sequence similarities (e.g. 19 % between human prohibitin-1 and stomatin) which are moreover largely found, in contrast to the definition of the SPFH domain (which states that it is located at the N-terminus of proteins), at the C-termini of the respective proteins. Thus, a closer phylogenetic analysis was performed in that study which revealed that there is no evidence for homology within the Band 7 protein superfamily apart from rather general sequence affinities. Even though the study strongly opposes the relationships between the Band 7 protein subfamilies and a common ancestor that is implicated by Tavernarakis et al. (1999), it observes that apparently all Band 7 family members seem to be involved in the formation of scaffolds in detergent-resistant microdomains (DRM).

In summary, the evidence given in the study by Rivera-Milla et al. (2005) strongly suggests that observed, weak phylogenetic relationships between Band 7 protein subfamilies are probably due to convergent evolution of the SPFH domain. However, it should be mentioned that the proteins within individual Band 7 protein

subfamilies probably evolved through divergent evolution. Therefore, because it is demonstrated that an overinterpretation of a comparative phylogenetic analysis of Band 7 proteins can be misleading when conclusions are drawn between proteins of different Band 7 subfamilies (Rivera-Milla et al., 2005), it still seems justified to perform comparative phylogenetic analyses in order to categorise Band 7 proteins of interest into the different protein subfamilies and to draw conclusions from the relationships between proteins within the same Band 7 subfamily.

3.7.6 Comparative phylogenetic analysis of Band 7 proteins

Even though some phylogenetic analyses of Band 7 proteins have already been published (Tavernarakis et al., 1999; Nadimpalli et al., 2000; Chen et al., 2005; Rivera-Milla et al, 2005), cyanobacterial and higher plant Band 7 proteins have not yet been compared in detail. In accordance with the results obtained by Rivera-Milla et al. (2005), which suggested that phylogenetic relationships between the Band 7 protein subfamilies were most likely the result of convergent evolution rather than due to a common ancestor, the discussion of the comparative phylogenetic analysis presented in this work (see Figure 3.5) focuses on the relationships that were observed within the individual Band 7 protein subfamilies.

In a previous study, the plant prohibitin homologues of *Arabidopsis thaliana, Nicotiana tabacum*, *Oryza sativa*, *Petunia hybrida* and *Zea mays* together with the prohibitin homologues of *H. sapiens* and *S. cerevisiae* have been subjected to a comparative phylogenetic analysis that identified two categories of prohibitin homologues (Chen et al., 2005). That result is consistent with the observation of the two branches (subcategories D and E in Figure 3.5), which contain the prohibitins homologues of higher plant as well as the prohibitin homologues of *H. sapiens* and *S. cerevisiae*, in this study. As each of the two branches contains one of the *S. cerevisiae* prohibitin homologues, which have been shown to form hetero-multimeric protein complexes together (Steglich et al., 1999), it seems possible that the prohibitin homologues of higher plants also form similar complexes. Furthermore, it can be speculated that in plant species that possess more than two prohibitin homologues, different combinations of prohibitin homologues from each of the two branches could form a multitude of hetero-multimeric prohibitin complexes, that would appear highly flexible in composition and feature an adaptable specificity for potential substrates or

interaction partners. Interestingly, although the cyanobacterial prohibitin homologues do not group within the two previously mentioned branches (subcategories D and E in Figure 3.5), they can be found in two other, distinct branches (subcategories B and C in Figure 3.5), both of which however contain the prohibitin homologues of different cyanobacterial strains. In the literature, the prohibitin homologues of *H. sapiens* (Ikonen et al., 1995), *S. cerevisiae* (Berger and Yaffe, 1998) and of some higher plants (Takahashi et al., 2003; Ahn et al., 2006) have been reported to be localised to mitochondria. Taking these two observations and the implications on the evolution of the Band 7 superfamily by Rivera-Milla et al. (2005) into account, it appears possible that cyanobacterial prohibitin homologues evolved independently of the prohibitin homologues found in subcategories D and E in Figure 3.5 and that the classification into the prohibitin subfamily might have to be attributed to convergent evolution.

Similarly, cyanobacterial stomatins seem to have evolved independently. The facts that the stomatin homologue Slr1128 (Phb3) of *Synechocystis* sp. PCC 6803 and Ybbk of *E. coli* did not group with eukaryotic or p-stomatins (Tavernarakis et al., 1999) and that p-stomatins form an operon with the *nfed* gene (Green et al., 2004), which could not be observed for cyanobacterial stomatin homologues, supported this assumption.

An interesting observation from the comparative phylogenetic analysis in this work was that some cyanobacterial Band 7 proteins grouped together with flotillins and flotillin-like proteins from other organisms. Flotillin homologues are highly conserved among metazoans (Malaga-Trillo et al., 2002), can be found in detergent-resistant microdomains (DRM) and are thought to be involved in cell-cell recognition, adhesion and signalling events (Langhorst et al., 2005). Even though it has been reported that these proteins are absent from plants, fungi and bacteria and the InterPro database did not list any flotillins for higher plants or cyanobacteria, recently flotillin-like proteins have been identified in these organisms (Rivera-Milla et al., 2005). However, the results of Rivera-Milla et al. (2005) suggest that the flotillin and flotillin-like proteins have different genetic origins and only the necessity to occupy a functional niche is assumed to have lead to the development of seemingly homologous proteins. Nevertheless, it is an important observation that Sll1021 of *Synechocystis* sp. PCC 6803, in particular, and other cyanobacterial Band 7 proteins, can be related to these flotillin-like proteins. This conclusion has not yet been reflected by assignments in the databases.

Summarising these conclusions, it appears that the relationships that are suggested by the common nomenclature and the assignment to the same Band 7 protein subfamilies does not always correlate with phylogenetic evidence. Particularly, the cyanobacterial prohibitin and stomatin homologues do not seem to be related to the prohibitin and stomatin homologues of other organisms, not even to those of higher plants and furthermore appear to have evolved independently. The observed, little sequence similarities among these Band 7 protein subfamilies can most likely be contributed to limited convergent evolution rather than to a common ancestor. In contrast to the observations for cyanobacterial prohibitin and stomatin homologues, the phylogenetic relationships between the flotillin-like proteins of cyanobacteria and higher plants appear to be stronger and a further, more detailed investigation might conclude that these proteins shared a common ancestor. Consequently, given the phylogenetic evidence, it seems even more important to investigate the role of the Band 7 proteins of *Synechocystis* sp. PCC 6803 or *Thermosynechococcus elongatus* unbiased from the observations that have been gained from other, well-studied organisms like *H. sapiens* or *S. cerevisiae*.

Chapter 4: Probing the physiological relevance of the Band 7 proteins

In this chapter, the generation of various Band 7 gene inactivation mutants and experiments to elucidate the physiological relevance of the Band 7 proteins of *Synechocystis* sp. PCC 6803 are described. Generally, mutants constitute an important tool in biological studies to test whether a certain gene of interest is involved in a particular process. Usually, random mutations are introduced into the genome of an organism to trigger an obvious phenotype. The subsequent aim is then to identify the specific site of mutation, in order to link the affected gene to the observed phenotype. In this work, however, a ΔPhb1-4 quadruple mutant strain was generated by site-directed mutagenesis (see section 4.1.1), in the hope of identifying an obvious phenotype for the generated mutant in comparative growth analyses (see section 4.1.3) or by studying its morphology by electron microscopy (see section 4.1.4). Another important question addressed in this chapter is whether the Band 7 proteins of *Synechocystis* sp. PCC 6803 are involved in the PSII repair cycle that operates to replace the D1 protein of photodamaged PSII reaction centre core complexes (see section 4.2). Furthermore, since the prohibitin homologues of *S. cerevisiae* have been reported to have a positive effect on the stability of unassembled respiratory protein complex subunits (Nijtmans et al., 2000), it was tested whether an inactivation of the Band 7 genes would affect respiratory NDH-1 complexes in *Synechocystis* sp. PCC 6803 (see section 4.3). The last section of this chapter examines cell motility of Band 7 gene inactivation mutants that were generated in the genetic background of the *Synechocystis*. sp. PCC 6803 wild-type (WT) strain (see section 4.4). In contrast to the routinely used, only slightly motile *Synechocystis*. sp. PCC 6803 wild-type glucose-tolerant (GT) strain, the wild-type (WT) strain displays a certain degree of motility on BG-11 agar plates.

4.1 Investigating the ΔPhb1-4 quadruple mutant strain

Initially, the generation of a ΔPhb1-4 quadruple mutant is described (see section 4.1.1). Subsequently, microarray data on the *Synechocystis*. sp. PCC 6803 wild-type GT strain provided by Dr. Iwane Suzuki (National Institute for Basic

Biology, Okazaki, Japan) is presented (see section 4.1.2). This data was analysed in order to be able to focus on those environmental stress conditions that might reveal a potential phenotype of the ΔPhb1-4 quadruple mutant strain in comparative growth analyses (see section 4.1.3). Finally, the morphology of the *Synechocystis*. sp. PCC 6803 wild-type GT and the quadruple mutant strains are compared (see section 4.1.4).

4.1.1 Generation of the ΔPhb1-4 quadruple mutant strain

Synechocystis sp. PCC 6803 gene inactivation mutants are routinely generated by transforming cyanobacterial cells with plasmid DNA constructs that contain the gene of interest disrupted by an antibiotic-resistance cassette (Williams, 1988). Following transformation, the antibiotic-resistance cassette is integrated into the genome within the target gene via double homologous recombination, which subsequently leads to the disruption and inactivation of the respective gene.

Thus, in order to generate a ΔPhb1-4 quadruple inactivation mutant strain, four consecutive site-directed mutagenesis steps with four different plasmid DNA constructs were necessary. Two of these DNA constructs (pPHB1KAN and pPHB2CAM) had previously been generated in the laboratory (see Figure 4.1A1 and Figure 4.1B1), so that only the DNA constructs to inactivate the *phb3* and *phb4* genes remained to be produced (see Figure 4.1C1 and Figure 4.1D1). As the first step, the *phb3 (slr1128)* and *phb4* (*sll0815*) Band 7 genes were amplified by PCR from *Synechocystis* sp. PCC 6803 wild-type GT genomic DNA using BIOXACT DNA polymerase and specific primers. The used primers contained additional restriction enzyme sites (*slr1128*-Fw (NdeI); *slr1128*-Rev (BamHI); *sll0815*-Fw (NdeI) and *sll0815*-Rev (BamHI)) to be able to excise the respective gene for religation into other recipient vectors if necessary. The obtained PCR DNA fragments were inserted into the multiple cloning site of the pGEM-T easy vector. In general, antibiotic-resistance cassettes were excised from their parental vectors with blunt-end producing restriction enzymes. Thus, after linearising the newly generated vectors (pPHB3 with MscI; pPHB4 with HindIII), they were blunted in a Klenow reaction where necessary. Subsequently, the antibiotic-resistance cassettes were inserted ($SPEC^R$ into pPHB3; ERM^R into pPHB4) to obtain the final plasmid DNA constructs: pPHB3SPEC and pPHB4ERM. Prior to the transformation of the *Synechocystis* sp. PCC 6803 cells, all plasmid DNA constructs

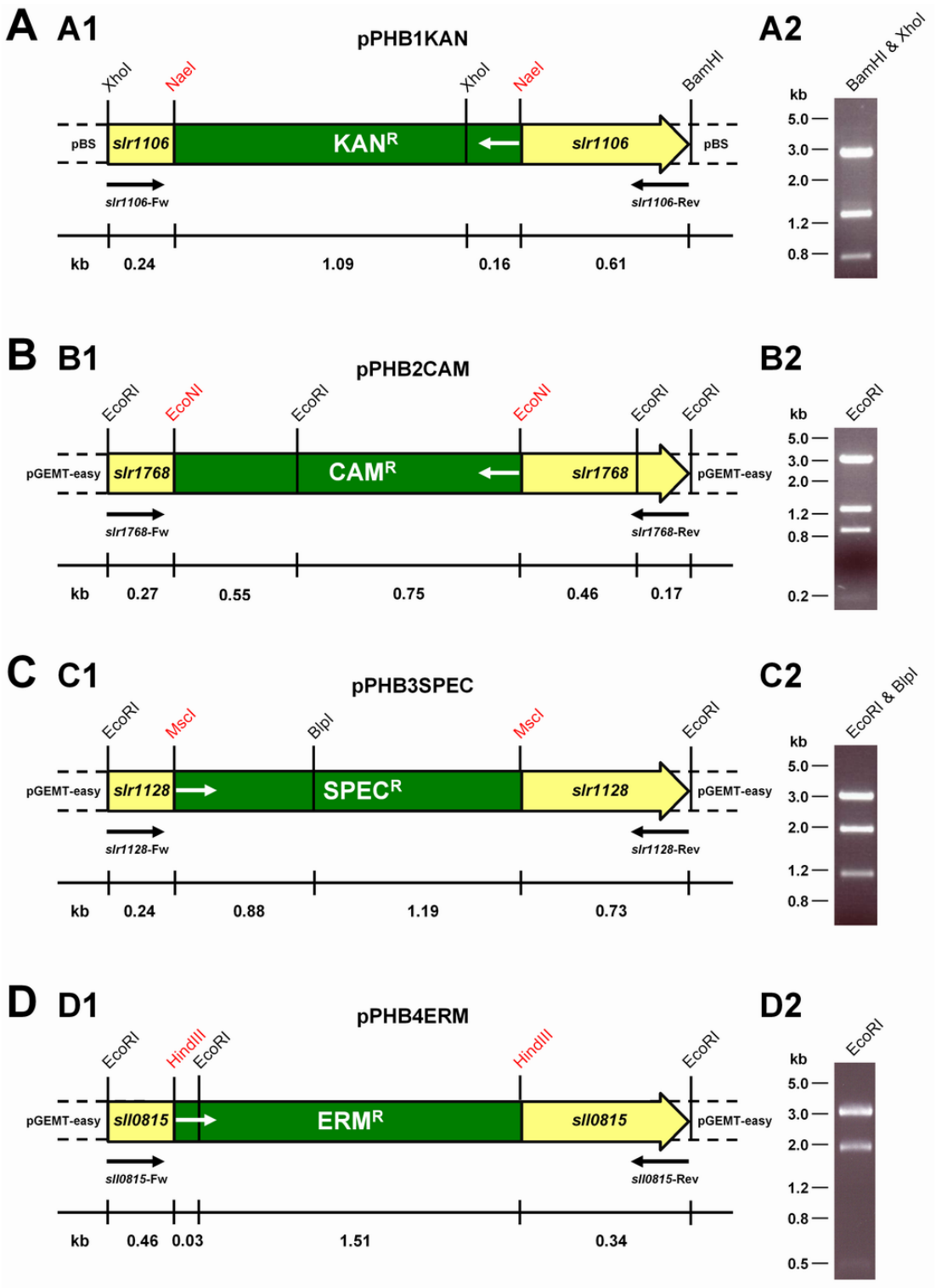

Figure 4.1: Plasmid DNA constructs to inactivate the Band 7 genes. (A1 to D1) Partial schematic representations and (A2 to D2) analytical restriction digestions of plasmid DNA constructs: (A) pPHB1KAN, (B) pPHB2CAM, (C) pPHB3SPEC and (D) pPHB4ERM. The pPHB1KAN and pPHB2CAM DNA constructs were kindly provided by Prof. Peter Nixon, while the pPHB3SPEC and pPHB4ERM DNA constructs were generated in this work (see text). (A1 to D1) The partial schematic representations are not to scale. The Band 7 genes are represented as arrows and annotated, while the flanking vector regions of the pBluescript II KS(+) (pBS) or the pGEM-T easy vectors are indicated as dashed lines. Restriction **(Legend continued!)**

Legend Figure 4.1 continued:
sites that were introduced by the used primers (represented by the arrows underneath) are marked in black. Restriction sites that were used to insert the antibiotic-resistance cassettes (KAN^R, CAM^R, $SPEC^R$ and ERM^R; marked in green; direction of transcription is indicated by the white arrows) are marked in red. (A1) the *phb1* gene (*slr1106*; 849 bp) was disrupted by a kanamycin-resistance cassette (KAN^R) that was inserted at the NaeI site at position 236. (B) The *phb2* gene (*slr1768*; 897 bp) was disrupted by a chloramphenicol-resistance cassette (CAM^R) that was inserted at the EcoNI site at position 265. (C) The *phb3* gene (*slr1128*; 966 bp) was disrupted by a spectinomycin-resistance cassette ($SPEC^R$) inserted at the MscI site at position 238. (D) The *phb4* gene (*sll0815*; 795 bp) was disrupted by an erythromycin-resistance cassette (ERM^R) inserted at the HindIII site at position 458. The lengths of the DNA fragments (in kb) in between the respective restriction sites are indicated on the line underneath of each partial schematic representation. (A2 to D2) Analytical restriction digestions using the indicated restriction enzymes on the plasmid DNA constructs used to inactivate the Band 7 genes.

were subjected to an analytical restriction digestion (see Figure 4.1A2 to Figure 4.1D2). pPHB1KAN was digested with BamHI and XhoI, which yielded the expected 2.95-kb DNA fragment of the pBluescript II KS(+) vector and two other DNA fragments of the following sizes: 1.33 and 0.77 kb. pPHB2CAM was digested with EcoRI, which yielded the expected 3.0-kb DNA fragment of the pGEM-T easy vector and three other DNA fragments of the following sizes: 1.19, 0.82 and 0.17 kb. pPHB3SPEC was usually digested with BlpI and EcoRI, which yielded the expected 3.0-kb DNA fragment of the pGEM-T easy vector and two other DNA fragments of the following sizes: 1.12 and 1.92 kb. pPHB4ERM was digested with EcoRI, which yielded the expected 3.0-kb DNA fragment of the pGEM-T easy vector and two other DNA fragments of the following sizes: 0.47 and 1.85 kb.

After it had been confirmed that the correct DNA constructs were generated, they were transformed in four consecutive site-directed mutagenesis steps, initially into *Synechocystis* sp. PCC 6803 wild-type GT cells, and subsequently into the completely segregated mutant cells of the previous transformation. Resulting transformants of each site-directed mutagenesis step were grown on selective plates to enforce segregation, of which the progress was monitored by PCR analyses. Finally, in order to test whether the ΔPhb1-4 quadruple gene inactivation mutant had completely segregated, the Band 7 genes of this strain and a wild-type control were amplified in a PCR analysis with the respective forward and reverse primers (see Table 2.7). The primers amplified the Band 7 genes of the *Synechocystis* sp. PCC 6803 wild-type strain (*phb1* = 849 bp; *phb2* = 897 bp; *phb3* = 966 bp and *phb4* = 795 bp), while significantly

larger DNA fragments (Band 7 gene plus the antibiotic-resistance cassette; *phb1KAN* = ~2.05 kb; *phb2CAM* = ~2.20 kb; *phb3SPEC* = ~2.97 kb and *phb4ERM* = ~2.30 kb) were amplified in the ΔPhb1-4 quadruple mutant strain. The *phb5* gene, was amplified as a ~2.0 kb DNA fragment (which corresponded to the size of the wild-type *phb5* gene) in both the wild-type control and in the quadruple mutant strain, as it had not been disrupted by an antibiotic-resistance cassette. Consequently, since no more wild-type Band 7 gene DNA fragments for the *phb1*, *phb2*, *phb3* and *phb4* genes could be detected in the tested ΔPhb1-4 quadruple mutant strain (see Figure 4.2), a completely segregated and viable mutant had been generated.

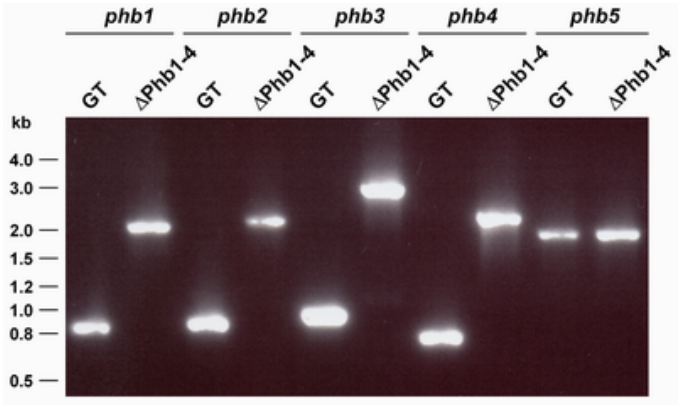

Figure 4.2: Segregation confirmation of the ΔPhb1-4 quadruple mutant. The results of the PCR analyses in which the Band 7 genes (*phb1*, *phb2*, *phb3*, *phb4* and *phb5*) were amplified with specific primers from genomic DNA isolated from the *Synechocystis* sp. PCC 6803 wild-type GT and the ΔPhb1-4 quadruple mutant strains.

4.1.2 Microarray analysis of *Synechocystis* sp. PCC 6803 genes

Prior to performing comparative growth experiments, microarray data on selected *Synechocystis* sp. PCC 6803 wild-type GT genes (see Table 4.1), kindly provided by Dr. Iwane Suzuki (National Institute for Basic Biology, Okazaki, Japan), was analysed to be able to focus on those growth conditions that appeared to affect the transcription levels of the Band 7 genes the most. Analysing the provided microarray data revealed that the induction ratios (IR) of the Band 7 homologues did not seem to vary dramatically under the tested stress conditions. Preliminary controls for this microarray analysis had indicated that the limit of experimental deviation corresponds to as much as a two-fold difference in the relative levels of expression (Suzuki et al., 2004). Consequently only genes that demonstrated a more than two-fold induction or repression were considered to have changed significantly.

Analysing the obtained microarray data, only the exposure to oxidative (0.25 mM H_2O_2) or cold stress (34 °C to 22 °C) seemed to have minor effects on the expression of some Band 7 genes. Under oxidative stress conditions, the *phb1* (IR =

2.89) and the *phb3* (IR = 3.13) genes were upregulated, while the *phb4* gene was slightly downregulated (IR = 0.37). When the cells were subjected to cold stress, the expression of the *phb4* gene (IR = 4.48) was upregulated, while the *phb3* gene (IR = 0.43) and the *phb5* gene (IR = 0.46) were slightly downregulated. The exposure to high-light intensities (500 µE m^{-2} sec^{-1}), only caused a slight downregulation of the expression of the *phb5* gene (IR = 0.45).

Table 4.1: Microarray analysis data of selected genes of the *Synechocystis* sp. PCC 6803 wild-type GT strain. Changes in the induction ratio (IR) of the Band 7 genes (*slr1106*, *slr1768*, *slr1128*, *sll0815* and *sll1021*), the *ftsH* gene (*slr0228*) and the three *psbA* genes (*psbA1*, *psbA2*, *psbA3*) of the *Synechocystis* sp. PCC 6803 wild-type GT strain, that were observed under the following stress conditions: salt (0.5 M NaCl), hyperosmolarity (0.5 M sorbitol), heat (34 °C to 44 °C), oxidative (0.25 mM H_2O_2), cold (34 °C to 22 °C) and high-light (70 µE m^{-2} sec^{-1} to 500 µE m^{-2} sec^{-1}) are summarised in this table. Cells had been exposed to the indicated stress conditions for a period of 20 min prior to the isolation of RNA. Upregulated genes (induction ratios > 2.0) are highlighted red, while downregulated genes (induction ratios < 0.5) are highlighted blue.

		Stress condition					
Gene	**Synonym**	**Salt** 0.5 M NaCl	**Hyperosmolarity** 0.5 M sorbitol	**Heat** 34 to 44 °C	**Oxidative** 0.25 mM H_2O_2	**Cold** 34 to 22 °C	**High-light** 70 to 500 µE m^{-2} sec^{-1}
slr1106	*phb1*	0.94	1.63	0.63	2.89	1.39	0.77
slr1768	*phb2*	0.53	0.92	1.08	1.37	0.55	0.88
slr1128	*phb3*	0.51	1.63	1.18	3.13	0.43	0.72
sll0815	*phb4*	0.96	1.72	0.80	0.37	4.48	1.30
sll1021	*phb5*	0.62	0.56	1.03	0.81	0.46	0.45
slr0228	*ftsH*	1.75	1.95	2.09	6.93	2.60	2.06
slr1181	*psbA1*	1.13	1.54	2.32	1.50	1.26	1.29
slr1311	*psbA2*	1.80	1.48	2.85	2.05	1.44	1.67
sll1867	*psbA3*	1.78	1.51	1.42	2.66	1.77	1.37

Because of the working model (see Figure 1.9), which hypothesised that the Band 7 homologues of *Synechocystis* sp. PCC 6803 protect newly synthesised D1 protein from the degradation by the Slr0228 FtsH protease prior to its incorporation into reassembling PSII complexes, the microarray data on the *ftsH* and *psbA* genes was also considered. Interestingly, transcription of the *ftsH* gene was significantly induced under almost all the tested stress conditions: heat (IR = 2.09), oxidative (IR = 6.93), cold (IR = 2.60) and high-light (IR = 2.06), while the induction that occurred under hyperosmolaric stress (IR = 1.95) just failed to reach the threshold level. Only some of the *psbA* genes *psbA1* (IR = 2.32) and *psbA2* (IR = 2.85), were affected by heat stress,

whereas oxidative stress seemed to induce the transcription of the *psbA2* (IR = 2.05) and *psbA3* (IR = 2.66) genes. The other stress conditions did not seem to affect the transcription levels of the *psbA* genes significantly. Summarising the analysed microarray data, only cold and oxidative stress displayed significant effects on the transcription of the Band 7 genes and would therefore be the first stress conditions to be analysed in the subsequent comparative growth analyses.

4.1.3 Comparative growth analyses under different environmental conditions

In order to identify a potential phenotype, comparative growth analyses were performed between the *Synechocystis* sp. PCC 6803 wild-type GT and the ΔPhb1-4 quadruple mutant strains under different environmental stress conditions (see Figure 4.3). Because of the conclusions that were drawn from the microarray data (see section 4.1.2), the focus of these experiments was directed on cold (see Figure 4.3B) and oxidative stress (see Figure 4.3C). Additionally, as results in the literature suggested that Band 7 homologues might have an effect on respiratory protein complexes and thereby on respiration itself (Steglich et al., 1999; Nijtmans et al, 2000; Chen et al., 2005), a comparative growth analysis was performed under photoheterotrophic growth conditions, in order to increase the energetic dependency of the cells on respiration (see Figure 4.3D). As an impaired electron transport chain has been related to increased levels of reactive oxygen species (ROS) (Kowaltowski and Vercesi, 1999), the level of damaged, i.e. oxidised proteins of the cells grown under photoheterotrophic growth conditions was also qualitatively assessed (see Figure 4.4).

Initially, however, growth of the *Synechocystis* sp. PCC 6803 wild-type GT and the ΔPhb1-4 quadruple mutant strains was compared under standard laboratory growth conditions, i.e. in liquid BG-11 cultures grown in filter-capped tissue-culture flasks under gentle agitation at 29 °C and at a light intensity of 20 $\mu E\ m^{-2}\ s^{-1}$ fluorescent, white light. The resulting growth curves, where the measured optical density at 730 nm (OD_{730}) was plotted against time on a semi-logarithmic scale, were almost identical. While both strains exhibited exponential growth between day 1 and 2, the growth rate decreased thereafter and once in stationary phase (after day 4), the measured OD_{730} of the cultures remained at similar levels (see Figure 4.3A).

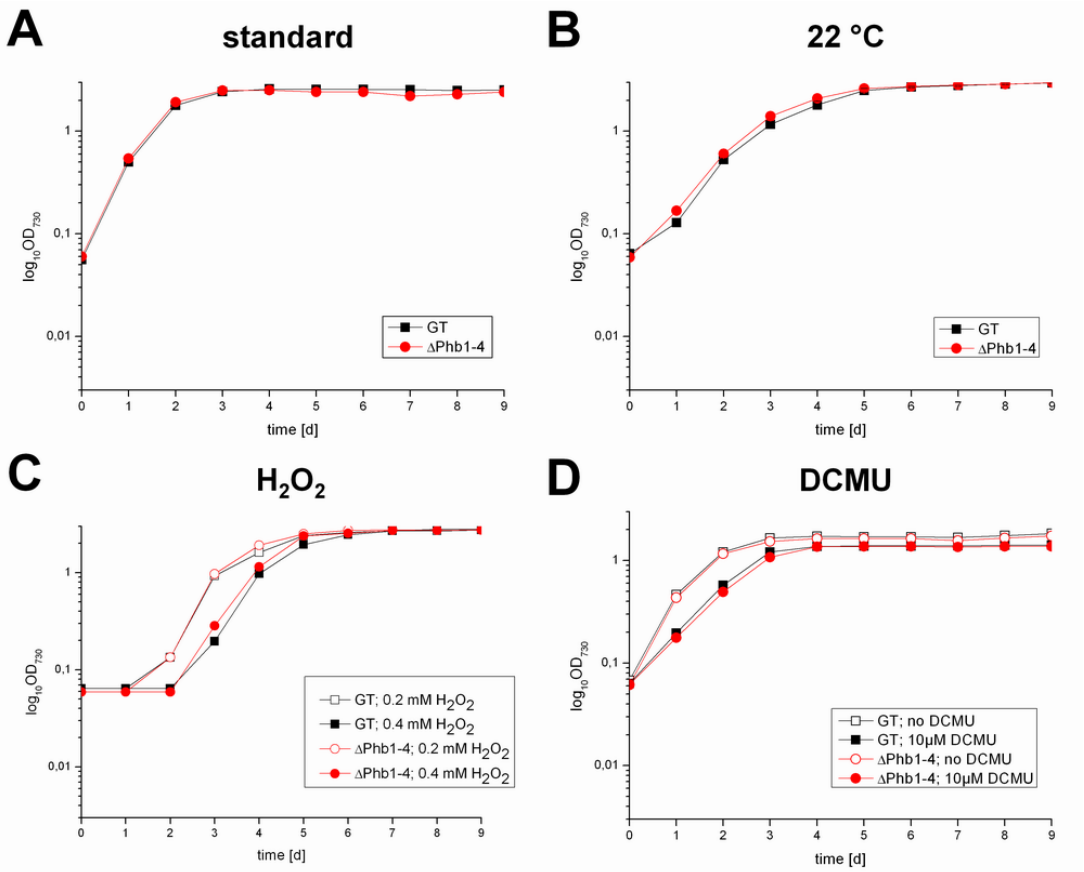

Figure 4.3: Comparative growth analyses of the *Synechocystis* sp. PCC 6803 wild-type GT and the ΔPhb1-4 quadruple mutant strains under different environmental conditions. Growth of the *Synechocystis* sp. PCC 6803 wild-type GT and the ΔPhb1-4 quadruple mutant strains was monitored under different environmental stress conditions, such as: (A) standard laboratory growth conditions, (B) cold stress at 22 °C, (C) oxidative stress with 0.2 and 0.4 M H_2O_2 in the liquid BG-11 culture medium and (D) under photoheterotrophic growth conditions with 10 µM DMCU in the liquid BG-11 culture medium. Growth of the cultures was assessed by measuring the optical density of the liquid cultures at 730 nm (OD_{730}).

When both strains were grown at a lower temperature (at 22 °C), while the other growth parameters were kept as under standard laboratory growth conditions, their growth rate seemed to be equally affected and stationary phase was only reached after six instead of three days. However, no severe or obvious phenotype of the ΔPhb1-4 quadruple mutant strain could be triggered by lowering the temperature (see Figure 4.3B). Analysing the growth curves for the liquid cultures of both strains grown under oxidative stress (0.2 or 0.4 mM H_2O_2), no significant differences in the growth characteristics could be observed between the wild-type GT and the ΔPhb1-4 quadruple mutant strains. After a two (0.2 mM H_2O_2) or three (0.4 mM H_2O_2) day lag phase, due to the increased oxidative stress, both strains appeared to reach stationary phase after six days. Even though slight differences in the growth curves could be

detected during exponential growth, these effects appeared to be of only a minor nature and overall the corresponding graphs had a sigmoid shape that appeared to be rather similar. Consequently, oxidative stress applied by adding H_2O_2 to the culture medium did also not seem to trigger a severe or obvious phenotype in the ΔPhb1-4 quadruple mutant strain (see Figure 4.3C).

In the literature, prohibitin Band 7 homologues of various organisms have been linked to respiratory processes. While the prohibitin homologues of *S. cerevisiae* have been reported to play a role in the maintenance of respiratory protein complexes (Steglich et al., 1999; Nijtmans et al, 2000), silencing of the prohibitin genes in the flowers of *Petunia hybrida* resulted in a higher rate of respiration in the effected tissue (Chen et al., 2005). Thus, it appeared worthwhile to expose the ΔPhb1-4 quadruple mutant strain to environmental conditions in which the cells were forced to rely more on energy generated by respiration. Consequently, *Synechocystis* sp. PCC 6803 wild-type GT and ΔPhb1-4 quadruple mutant liquid cultures were supplied with DCMU (a PSII electron transfer inhibitor; final concentration 10 μM), glucose (final concentration 5 mM) and light, so that photoheterotrophic growth conditions prevailed. In addition to generating growth curves for both strains under these conditions, the degree of oxidative stress, i.e. oxidised and damaged proteins in the wild-type GT and the ΔPhb1-4 quadruple mutant cells at different time points, was assessed biochemically with the OxyBlot kit (Chemicon International, Canada) (see Figure 4.4). This kit uses 2,4-dinitrophenylhydrazine (DNPH) to derivatise carbonyl groups of proteins that have been oxidised by ROS or other free radicals and then detects the introduced DNP moieties with a specific antibody. However, although a lower total cell density in stationary phase could be detected for the liquid cultures in this experiment, which was even further reduced in the samples that were incubated with DCMU, no significant differences could be observed between the *Synechocystis* sp. PCC 6803 wild-type GT and the ΔPhb1-4 quadruple mutant strains (see Figure 4.3D).

The samples for the subsequent qualitative analysis of the levels of oxidised and therefore damaged proteins in both strains were taken directly from the cultures of this growth experiment. Crude membrane isolations and soluble fractions of both strains were generated and analysed according to the manufacturer's instructions. The silver-stained gels showed that the samples had been loaded more or less equally. Also, the observed protein patterns for the *Synechocystis* sp. PCC 6803 wild-type GT and the ΔPhb1-4 quadruple mutant strains appeared to be similar in the corresponding

samples (see Figure 4.4A1 and Figure 4.4B1). The immunoblot that was probed with the αDNP antibody allowed only qualitative statements on the levels of oxidised proteins within the analysed samples. However, it was obvious that the levels of damaged proteins appeared to be higher in the samples that had been treated with DCMU than in those that had not been exposed to the PSII inhibitor (see Figure 4.4A2 and Figure 4.4B2). Nevertheless, no significant differences could be detected between the two strains, which suggested that the inactivation of the *phb1*, *phb2*, *phb3* and *phb4* genes did not lead to significantly increased levels of oxidative stress in the ΔPhb1-4 quadruple mutant strain.

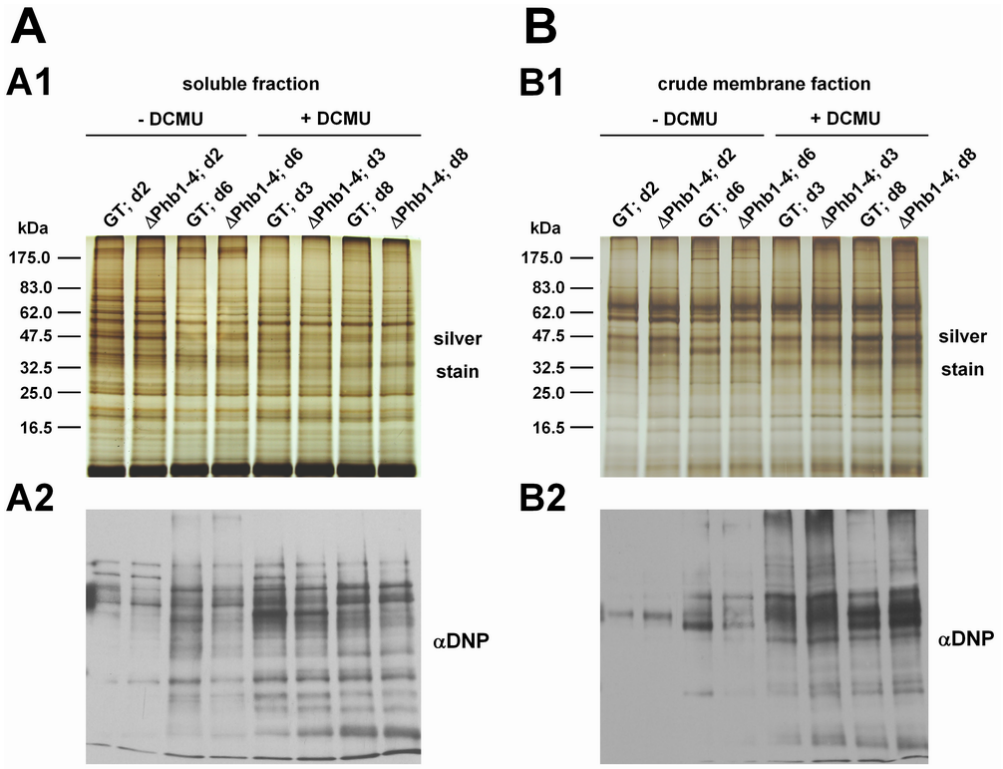

Figure 4.4: Assessment of oxidised proteins of the *Synechocystis* sp. PCC 6803 wild-type GT and the ΔPhb1-4 quadruple mutant strains. In order to determine the levels of oxidised and therefore damaged proteins in the (A) soluble and (B) crude membrane fraction of the *Synechocystis* sp. PCC 6803 wild-type GT (GT) and the ΔPhb1-4 quadruple mutant (ΔPhb1-4) strains, the OxyBlot kit procedure was performed according to the manufacturer's instructions. Samples were taken from a growth experiments that had been performed with (+) and without (-) the presence of 10 µM DCMU (see Figure 4.3D) at different, indicated time points (at day 2 (d2) and day 6 (d6) for cultures without DCMU and at day 3 (d3) and day 8 (d8) for cultures with DCMU). 7 µg of protein for the soluble fractions and 10 µg of protein for the crude membrane fractions were derivatised and loaded on 1-D SDS-PAGE gels. (A1 and B1) One gel was silver-stained, while another was immunoblotted and probed with the provided αDNP antibody.

4.1.4 The morphology of the ΔPhb1-4 quadruple mutant strain

Initially, immunogold-labelling experiments on the *Synechocystis* sp. PCC 6803 wild-type GT and the ΔPhb1-4 quadruple mutant strains with specific, purified antibodies were to be performed, in order to elucidate the localisation of the Band 7 proteins. Immunogold-labelling and electron microscopy were kindly performed by Dr. Uwe Kahmann (University of Bielefeld, Bielefeld, Germany). However, the respective Band 7 proteins were insufficiently labelled, so that the obtained data was inconclusive and the proteins could not be assigned to a specific cellular location (data not shown). Nevertheless, some electron micrographs, taken of unlabelled *Synechocystis* sp. PCC 6803 wild-type GT and ΔPhb1-4 quadruple mutant cells grown under standard laboratory growth conditions, allowed to compare some basic features of the morphology of both strains (see Figure 4.5).

The electron micrographs in panels A1 and A2 (13,000x magnification) and those in panels B1 and B2 (28,500x magnification) were taken of different regions of the generated ultra-thin sections. Panels A3 and B3 each show a selected, single (A3) *Synechocystis* sp. PCC 6803 wild-type cell (GT) from panel A2 and (B3) ΔPhb1-4 quadruple mutant cell from panel B1 (large red arrows) that have been further magnified *in silico*. Generally, cells of various developmental stages were found on the electron micrographs, but overall the morphology of both strains did not appear to differ significantly. In both cases, regular, spherical cells as well as dividing cells, that were constricted in the middle and would yield two individual daughter cells (small red arrows) were observed. Also, the typical arrangement of pairs of thylakoid membranes, that form sheets in concentric circles following the periphery of the cell were detected (large white arrows). Typical cyanobacterial inclusions such as carboxysomes (small white arrows), polyhydroxyalkanoate (PHA) granules (large black arrows) and polyphosphate bodies (small black arrows) were also present in the cells of both strains. These cytoplasmic components were identified from reference to previously assigned inclusions (van de Meene et al., 2006). Overall, no severe phenotype could be detected on the electron micrographs, that were obtained from cells grown under standard laboratory growth conditions. However, in order to reveal or exclude a potential, more subtle effect on the morphology of *Synechocystis* sp. PCC 6803 by the inactivation of the Band 7 genes, a more detailed examination of a larger data set and higher resolution micrographs would be necessary.

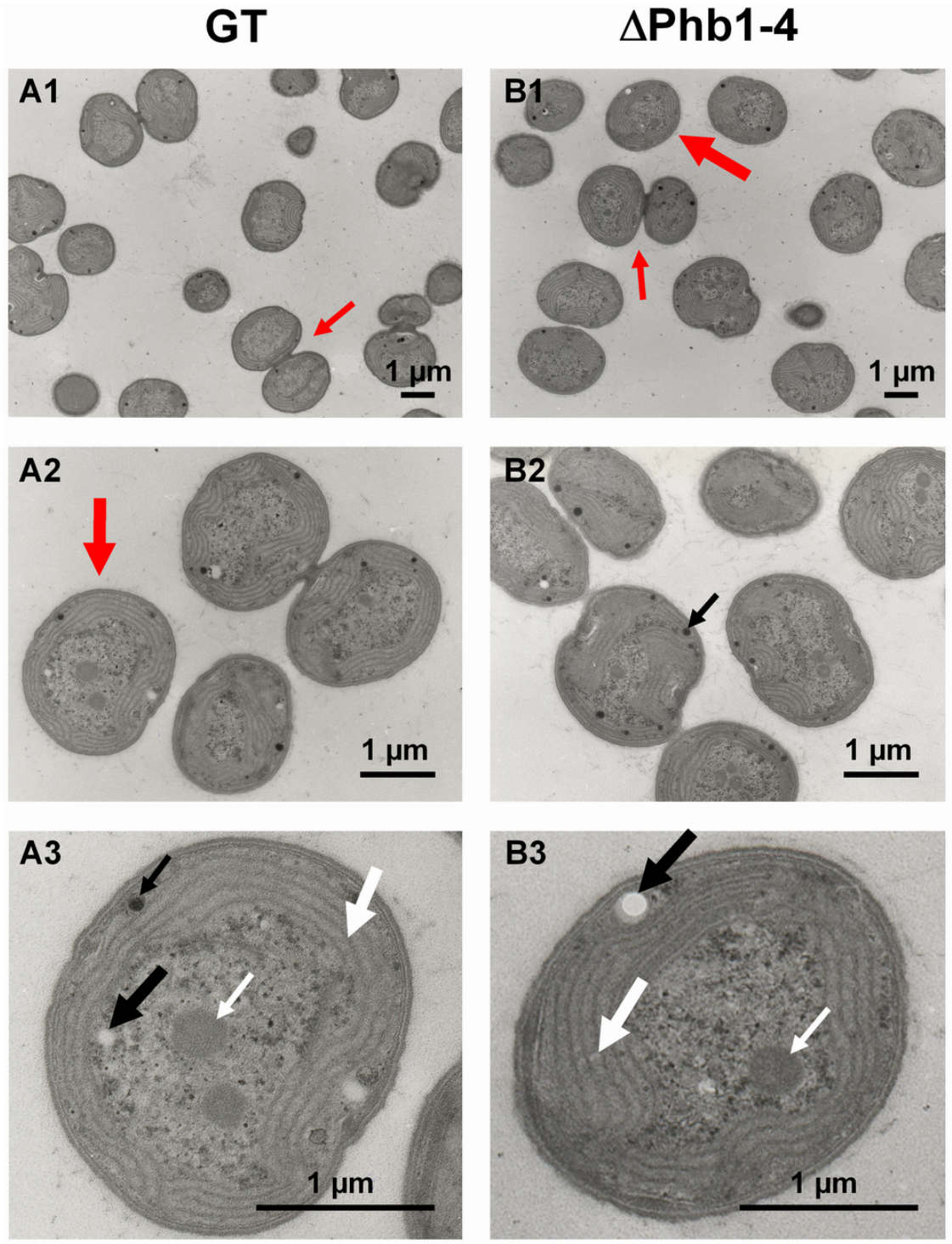

Figure 4.5: Electron micrographs of *Synechocystis* sp. PCC 6803 wild-type GT and ΔPhb1-4 quadruple mutant cells. Electron micrographs of ultra-thin sections of (A1 to A3) *Synechocystis* sp. PCC 6803 wild-type GT and (B1 to B3) ΔPhb1-4 quadruple mutant (ΔPhb1-4) cells were taken at a magnification of (A1 and B1) 13.000x and (A2 and B2) 28.500x. (A3 and B3) A wild-type GT and a ΔPhb1-4 quadruple mutant cell (marked with large red arrows in A2 and B1) were further magnified *in silico*. Some dividing cells are marked (small red arrows). The following inclusions are also marked: Thylakoid membrane (large white arrow), carboxysome (small white arrow), polyhydroxyalkanoate (PHA) granule (large black arrow) and polyphosphate body (small black arrow). The scale bars represent 1 µm, as indicated.

4.2 The Band 7 proteins and the PSII repair cycle

The working hypothesis of this project (see Figure 1.9) was based on the findings that the prohibitin homologues of *S. cerevisiae* interact with the mitochondrial m-AAA protease and negatively regulate its activity (Steglich et al., 1999, Nijtmans et al., 2000). This negative regulation results in the protection of newly synthesised, mitochondrial, membrane protein complex subunits prior to their integration into assembling respiratory protein complexes (Nijtmans et al., 2000). A similar regulatory interaction between large HflK/C Band 7 protein complexes and a FtsH homologue has also been observed in *E. coli* (Kihara et al., 1996; Saikawa et al., 2004). The finding, that the cyanobacterial Slr0228 FtsH homologue (also an AAA-type protease) is involved in the early stages of the PSII repair cycle (Silva et al., 2003), initiated the research of this work, which aims to test the hypothesis whether Band 7 proteins of *Synechocystis* sp. PCC 6803 might interact and regulate the Slr0228 protease. Analogous to the situation in *S. cerevisiae*, it was hypothesised that the Band 7 proteins of *Synechocystis* sp. PCC 6803 might interact with the Slr0228 FtsH protease and protect one of its potential substrates, specifically newly synthesised D1 protein, prior to its incorporation into reassembling PSII complexes during the PSII repair cycle (Silva et al., 2002).

In order to test this hypothesis, various biochemical and physiological assays were performed. Initially, an affinity-purified preparation of enriched PSII complexes was probed for the presence of Band 7 proteins (see Figure 4.6). In another experiment, the *Synechocystis* sp. PCC 6803 wild-type GT, the ΔPhb1-4 quadruple mutant and the Δ0228 mutant strains were exposed to an elevated level of illumination (see Figure 4.7). Additionally, the selective turnover of the D1 protein, which is a key process and hallmark of the PSII repair cycle (Aro et al., 1993a), was monitored in various *Synechocystis* sp. PCC 6803 mutant strains. These strains were: the *Synechocystis* sp. PCC 6803 wild-type GT, the ΔPhb1-3 triple mutant (see Figure 4.8), the ΔPhb1-4 quadruple mutant (see Figure 4.12) and the PSII assembly defective mutants ΔCP43 and ΔCP43/ΔPhb1-3 (see Figure 4.10), as well as the Δ0228 and Δ0228/ΔPhb1-3 mutant strains, that were impaired in the degradation of photodamaged D1 protein (see Figure 4.11). Finally, a photoinhibition experiment was performed in order to assess the functionality of the PSII repair cycle in the ΔPhb1-4 quadruple mutant strain (see Figure 4.12).

4.2.1 Band 7 proteins in a PSII-enriched fraction

In order to test the result of an earlier experiment, that Band 7 proteins co-purified with PSII complexes of *Synechocystis* sp. PCC 6803 (Silva and Nixon, 2001), an independently generated, affinity-purified fraction of PSII complexes was probed for Band 7 proteins. This new fraction was kindly provided by Ms. Elisa Corteggiani Carpinelli in Prof. James Barber's group (Imperial College London, London, UK) and had been purified by affinity chromatography using Ni-NTA superflow affinity resin (Qiagen Limited, UK) from crude membrane isolations of the *Synechocystis* sp. PCC 6803 HT-3A strain (a strain with a His_6-tagged CP47 protein; Bricker et al., 1998; Corteggiani Carpinelli, 2006). The absorption spectrum obtained from this PSII-enriched fraction corresponded to a spectrum that would be expected for PSII core complexes (data not shown). Subsequently, the sample was separated on a 1-D SDS PAGE gel and probed with various antibodies (see Figure 4.6).

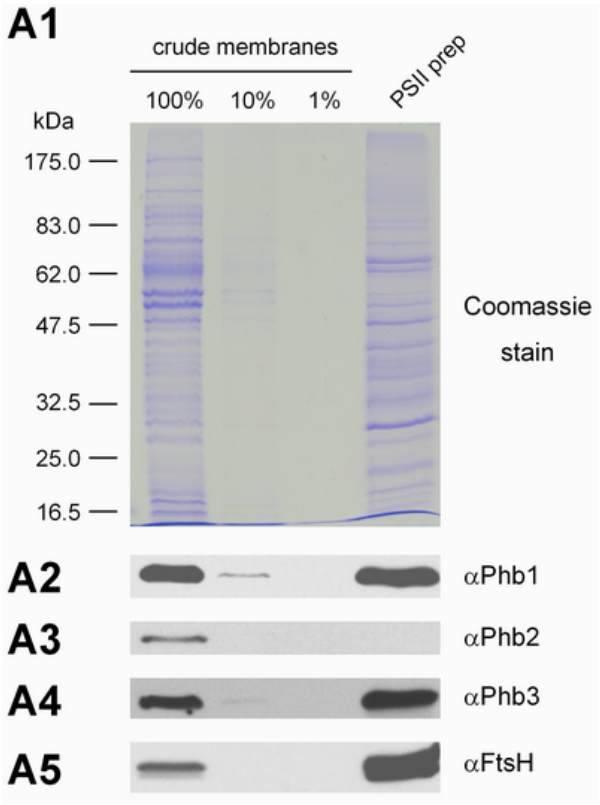

Figure 4.6: Immunoblotting analysis of a PSII-enriched fraction. A PSII-enriched fraction, obtained by Ni-NTA affinity chromatography from a crude mem-brane isolation of the *Synechocystis* sp. PCC 6803 HT-3A mutant strain, was kindly provided by Ms Elisa Corteggiani Carpinelli. The amounts of crude membrane sample (100 %) and the enriched PSII fraction (PSII prep) that were loaded in the lanes of a 1-D SDS PAGE gel corresponded to 1 µg of chlorophyll a, while the dilution series of the crude membranes (10 and 1 %) contained accordingly less. One of the obtained gels was (A1) Coomassie-stained, while others (A2 to A5) were used for immunoblotting analyses with the indicated antibodies.

The Coomassie-stained 1-D SDS PAGE gel revealed that the analysed PSII preparation also contained many other proteins in addition to PSII protein core complex subunits and could therefore only be considered a PSII-enriched fraction. However, when the protein pattern of this preparation was compared to the protein

pattern for crude membranes, it became obvious that unidentified proteins had clearly been enriched by the purification process. Nevertheless, no assignments of specific proteins to particular bands could be made (see Figure 4.6A1). The performed immunoblots showed that the Phb1 and Phb3 Band 7 proteins were still present in the PSII-enriched fraction (see Figure 4.6A2 and Figure 4.6A4), while the Phb2 protein was depleted from the sample (see Figure 4.6A3). The immunoblot that had been probed with an αFtsH antibody that is able to detect all four FtsH homologues of *Synechocystis* sp. PCC 6803, gave a stronger signal in the PSII preparation than in the crude membrane sample, which indicated that the FtsH proteases seemed to be enriched in the PSII preparation (see Figure 4.6A5). Overall, the fact that the Phb1 and Phb3 Band 7 proteins could be found in the PSII-enriched fraction, encouraged further investigations into the possible involvement of Band 7 proteins in the PSII repair cycle.

4.2.2 Growth of the ΔPhb1-4 quadruple mutant strain under high-light conditions

Even though the microarray analysis data did not indicate increased transcript levels of the Band 7 genes under high-light conditions (see Table 4.1), a possible involvement of the Band 7 proteins in the PSII repair cycle was tested in a growth assay. In this experiment, *Synechocystis* sp. PCC 6803 wild-type GT, the ΔPhb1-4 quadruple mutant and the Δ0228 mutant strains were incubated on BG-11 agar plates under either standard laboratory or under high-light growth conditions (see Figure 4.7).

Visual inspection showed that all strains grew equally well under the standard laboratory growth conditions. Under high-light growth conditions, the *Synechocystis* sp. PCC 6803 wild-type GT and the ΔPhb1-4 quadruple mutant strains were both viable and showed the same extent of growth and pigmentation phenotype, while the Δ0228 mutant strain did not tolerate the prolonged exposure to high-light intensities and died. In the Δ0228 mutant strain, the Slr0228 FtsH protease is inactivated, which renders this strain light sensitive because of its inability to remove photodamaged D1 protein (Silva et al, 2003) and possibly also other membrane components. Thus, due to its impaired PSII repair cycle, the Δ0228 mutant strain represents the positive control of this experiment. In general, the PSII repair cycle did not seem to be affected whether the cells had been grown on BG11 or on BG11 plus glucose plates, although

the cells grown on BG11 plus glucose plates seemed to grow better and looked healthier, i.e. greener (compare Figure 4.7A1 and 4.7B1 as well as Figure 4.7A2 and 4.7B2). Additionally, the prolonged exposure to higher light intensities seemed to equally affect the *Synechocystis* sp. PCC 6803 wild-type GT and the ΔPhb1-4 quadruple mutant strains, as they appeared more yellowish towards the end of the experiment (see Figure 4.7A2 and Figure 4.7B2). Summarising the results of this experiment, it could be concluded that an inactivation of the four Band 7 genes *phb1*, *phb2*, *phb3* and *phb4*, did not appear to have a severe effect on cell viability under photoinhibitory growth conditions. Nevertheless, further experiments had to be performed on the ΔPhb1-4 quadruple mutant strain, in order to thoroughly investigate the possibility of a more subtle effect on the PSII repair cycle.

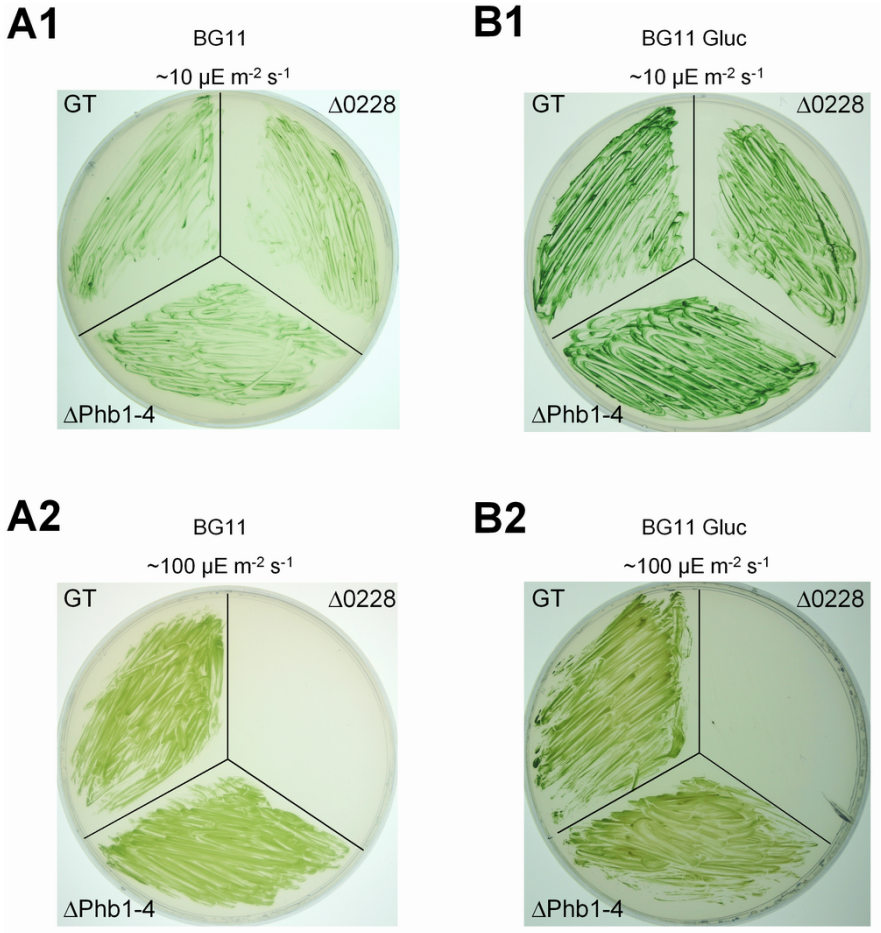

Figure 4.7: Growth of the ΔPHB1-4 quadruple mutant strain under standard laboratory or high-light growth conditions. Cells of the *Synechocystis* sp. PCC 6803 wild-type GT, the ΔPhb1-4 quadruple mutant and the Δ0228 mutant strains were grown on (A1 and A2) BG-11 agar plates or on (B1 and B2) BG-11 agar plates supplemented with 5 mM glucose. While (A1 and B1) were exposed to a light intensity of ~10 µE m^{-2} s^{-1}, (A2 and B2) were subjected to a higher light intensity of ~100 µE m^{-2} s^{-1}. The respective conditions and strains are indicated.

4.2.3 Pulse-labelling experiments with various Band 7 mutants

A repair cycle operates and selectively turns over the D1 protein of PSII (Aro et al., 1993a), which is the main target for light-induced damage by reactive oxygen species (ROS) (Asada, 1999). The selective turnover of the D1 protein can be conveniently monitored *in vivo* by using the pulse-chase radiolabelling technique (Mattoo et al., 1984). Thus, cyanobacterial cells were incubated with [^{35}S]-labelled methionine (pulse period), so that *de novo* synthesised proteins were radioactively labelled. After removal of the radioactive methionine, the cells were exposed to photoinhibitory conditions, i.e. high-light intensities of ~1000 μE m^{-2} s^{-1}, for a prolonged period of time in the presence of unlabelled methionine (chase period). During this incubation period, due to the fast (Mattoo et al., 1984) and selective turnover of the D1 protein (Aro et al., 1993a), the initially strong radioactive signal for the D1 protein in autoradiograms decreases. Consequently, to investigate further the possible involvement of the Band 7 protein in the PSII repair cycle, this method was applied to the following *Synechocystis* sp. PCC 6803 strains: the *Synechocystis* sp. PCC 6803 wild-type GT, the ΔPhb1-3 triple (see Figure 4.8), the ΔPhb1-4 quadruple (see Figure 4.12) as well as the PSII assembly defective mutants ΔCP43 and ΔCP43/ΔPhb1-3 (see Figure 4.10) and the Δ0228 and Δ0228/ΔPhb1-3 mutant strains with an impaired degradation of the D1 protein (see Figure 4.11). The ΔCP43, ΔCP43/ΔPhb1-3, Δ0228 and Δ0228/ΔPhb1-3 mutant strains were generated in this work (see section 4.2.3.2). As the functionality of the PSII repair cycle could be assessed by comparatively monitoring the turnover of the D1 protein in the *Synechocystis* sp. PCC 6803 wild-type GT and a mutant strain of interest, this assay had the potential to reveal the possible involvement of the Band 7 proteins in the PSII repair cycle.

4.2.3.1 Comparative pulse-chase analysis of the ΔPhb1-3 triple mutant

Initially, the selective turnover of the D1 protein was analysed in a comparative pulse-chase experiment with the *Synechocystis* sp. PCC 6803 wild-type GT and the ΔPhb1-3 triple mutant strains. Crude isolated membranes of samples taken during the pulse-chase experiments, were analysed on 1-D SDS and 1-D BN PAGE gels, which were subsequently processed into autoradiograms (see Figure 4.8).

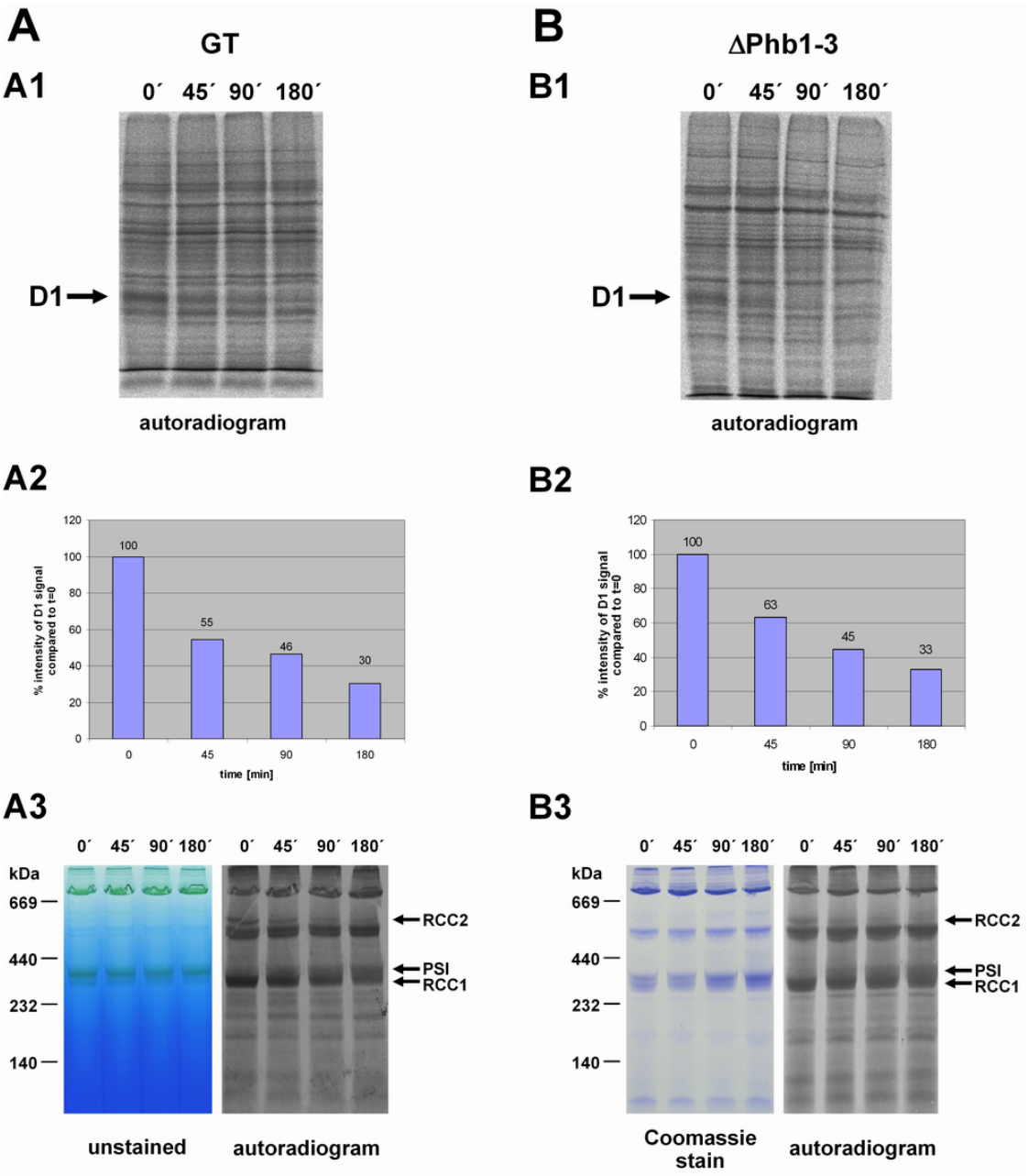

Figure 4.8: Comparative pulse-chase analysis of the *Synechocystis* sp. PCC 6803 wild-type GT and the ΔPhb1-3 triple mutant strains. Pulse-chase analyses were performed on the (A) *Synechocystis* sp. PCC 6803 wild-type GT and the (B) ΔPhb1-3 triple mutant strains. Crude membranes were isolated from aliquots taken after the pulse period and the subsequent chase period at time points: 0´, 45´, 90´ and 180´. The isolated membranes were separated by 1-D SDS and 1-D BN PAGE. (A1 and B1) The 1-D SDS PAGE gels were dried in order to generate autoradiograms on which the signal for the D1 protein is indicated (arrow). The autoradiograms were developed using a Phosphorimager and (A2 and B2) D1 signals were quantified using the AIDA software and plotted. The generated values for the indicated time points were plotted as percentage of the D1 signal intensity compared to the value at t = 0. (A3 and B3) The Coomassie-stained gels and the resulting autoradiograms of the 1-D BN PAGE analyses. The positions of PSII monomers (RCC1) and dimers (RCC2) as well as for PSI monomers (PSI) are indicated.

The autoradiograms of the 1-D SDS PAGE gels showed equally rapid and selective turnover of the D1 protein in both of the tested strains (compare Figure 4.8A1 and Figure 4.8B1, D1 protein marked with a black arrow). An estimation of the D1 protein signal intensities with the naked eye suggested, that most of the radioactively labelled D1 protein was selectively degraded during the 180 min chase period, while most of the other protein bands displayed equal signal intensities in the 0 and 180 min sample lanes. Unfortunately, other PSII subunits of the reaction centre core (RCC), such as D2, CP43 and CP47, could not be assigned to specific signal bands and only additional immunoblotting analyses would allow such assignments. Thus, the presented pulse-chase analyses only focuses on the turnover of the D1 protein, for which an attempt was made to quantify the observed signal intensities. Due to the partially high background in the respective regions of the gel, the obtained values for the D1 signal intensities were considered to be qualitative rather than absolute. Nevertheless, the generated values confirmed the observation that was already made with the naked eye. In the *Synechocystis* sp. PCC 6803 wild-type GT strain, after an initial rapid decrease of the D1 protein signal intensity to 55 % after 45 min, the signal continued to decrease, but at a slower rate. Thus, after 90 min 46 % and after 180 min 30 % of the initial signal intensities could still be detected (see Figure 4.8A2). The D1 protein of the ΔPhb1-3 triple mutant was degraded at a similar rate. Again, after an initial rapid decrease of the D1 protein signal intensity to 63 % after 45 min, the signal continued to decrease at a slower rate. Thus, after 90 min 45 % and after 180 min 33 % of the initial signal intensities could still be detected (see Figure 4.8B2). The remaining 30 and 33 percent respectively of the initial signals intensities could probably be considered as background (see Figure 4.8A1 and Figure 4.8B1). Summarising the data obtained from the 1-D SDS autoradiogram, the observed protein patterns and quantified signal intensities for the D1 protein appeared to be rather similar in the compared strains.

The same seemed to be true for the autoradiograms that were obtained from the 1-D BN PAGE analysis (compare Figure 4.8A3 and Figure 4.8B3). Unfortunately, the Coomassie-stained 1-D BN PAGE gel of the *Synechocystis* sp. PCC 6803 wild-type GT samples had not been documented, so that only the ‘unstained’ gel (with some residual Coomassie stain from the running buffer) can be shown. The 1-D BN PAGE gels showed that the lanes were equally loaded, but no apparent differences in the protein complex profiles could be observed between the two strains. This was also true

for the resulting autoradiograms, where the selective turnover of PSII monomers (RCC1) and dimers (RCC2) could be monitored (the assignment of protein complexes is according to Tichy et al., 2003 and Herranen et al., 2004), but no apparent differences between the strains were spotted. No attempt was made to quantify the obtained signals of these 1-D BN PAGE analyses. Overall, the presented analyses did not suggested that an inactivation of the *phb1*, *phb2* and *phb3* genes influences the selective turnover of the D1 protein in the ΔPhb1-3 mutant.

4.2.3.2 Generation of mutants with accelerated or impaired D1 protein turnover

In order to study a possible effect of the inactivation of Band 7 genes on the turnover of the D1 protein in detail, not only the ΔPhb1-3 triple mutant strain was subjected to pulse-labelling and pulse-chase analyses, but also mutants in which the turnover of the D1 protein was either accelerated or impaired. A mutant that features an accelerated, selective turnover of the D1 protein, is the ΔCP43 mutant strain (Rögner et al., 1991), in which the CP43 protein encoding gene (*psbC*) is inactivated. Although the levels of CP47, D1 and D2 proteins are significantly decreased (Vermaas et al., 1988), this strain still forms reduced amounts (not exceeding 20 % of wild-type levels) of RC47 complexes (PSII core complexes lacking CP43) (Rögner et al., 1991, Komenda et al., 2004). Intense radiolabelling of the D1 protein indicates a high degree of selective turnover and the observation that the majority of this protein is found in RC47 complexes suggests, that this protein complex might be the predominant site of selective D1 protein replacement (Komenda et al., 2004). The converse effect, i.e. impaired D1 protein turnover, has been linked to the inactivation of the Slr0228 FtsH protease. This protease has been shown to be involved in the early steps of the PSII repair cycle (Silva et al., 2003), and its inactivation leads to significantly increased levels of PSII assembly intermediates and unassembled PSII protein subunits in mutants that are incapable of properly assembling PSII complexes (Komenda et al., 2006).

In this section, the generation of the ΔCP43, the ΔCP43/ΔPhb1-3, the Δ0228 and the Δ0228/ΔPhb1-3 mutant strains are described. The used plasmid DNA construct to inactivate the *psbC* gene (*sll0851*) was generated in this work (see Figure 4.9A), while the p0228ERM plasmid to inactivate the Slr0228 FtsH protease was kindly

provided by Prof. Peter Nixon (data not shown). The PCR analyses to confirm the segregation of the generated mutants are shown in Figure 4.9B and Figure 4.9C.

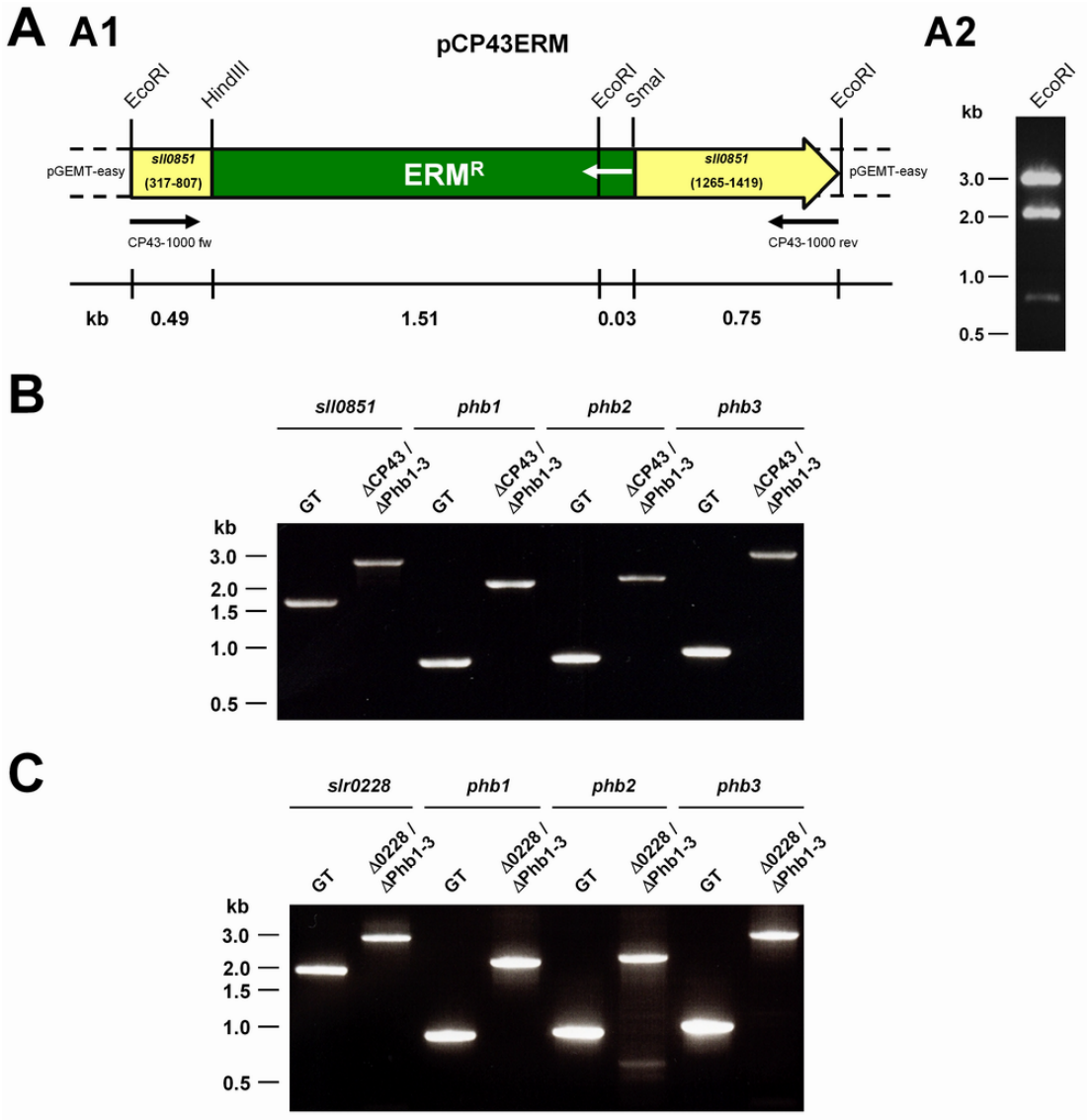

Figure 4.9: Generation of mutants with an accelerated or impaired D1 protein turnover. (A1) Partial schematic representation and (A2) analytical restriction digestion of the pCP43ERM plasmid DNA construct that was used to inactivate the *psbC* (*sll0851*) gene. The pCP43ERM DNA construct was generated in this work (see text). (A1) The partial schematic representations is not to scale. For a detailed explanation of the used annotations, see the legend of Figure 4.1. A part of the *psbC* (*sll0851*) gene (317-1419) was inserted into the pGEM-T easy vector. After linearisation of the resulting pCP43 vector with HindIII and SmaI (excised a DNA fragment from bp 808 to 1264 of the *sll0851* sequence), an erythromycin-resistance cassette (ERM^R) was inserted. (A2) Analytical restriction digestion of the pCP43ERM plasmid DNA construct with the EcoRI restriction enzyme. (B and C) Segregation confirmation of the (B) ΔCP43/ΔPhb1-3 and the (C) Δ0228/ΔPhb1-3 mutant strains. PCR analyses in which the respective genes (*sll0851*, *slr0228*, *phb1*, *phb2* and *phb3*) were amplified with specific primers (see text) from genomic DNA isolated from the *Synechocystis* sp. PCC 6803 wild-type GT and the indicated mutant strains.

To generate the pCP43ERM plasmid DNA construct with which the *psbC* gene could be inactivated, a part of the *sll0851* gene plus some of its downstream sequence (*sll0851* from bp 317 to 1419 plus 602 bp downstream sequence) was amplified in a PCR reaction from *Synechocystis* sp. PCC 6803 wild-type GT genomic DNA using the BIOXACT DNA polymerase and specific primers (CP43-1000fw and CP43-1000rev). The obtained PCR DNA fragment was inserted into the multiple cloning site of the pGEM-T easy vector. The newly generated vector (pCP43) was then linearised with SmaI and HindIII (excising roughly 450 bp), blunted in a Klenow reaction and then the erythromycin-resistance cassette (ERM^R; excised with EcoRV and SmaI) inserted, to obtain the final pCP43ERM plasmid DNA construct. Prior to transforming *Synechocystis* sp. PCC 6803 cells with this DNA construct, the pCP43ERM vector was subjected to an analytical restriction digestion with EcoRI (see Figure 4.9A2), which yielded an expected 3.0-kb DNA fragment of the pGEM-T easy vector and two other DNA fragments of the following sizes: 2.0 and 0.78 kb. After it was confirmed that the pCP43ERM DNA construct was correctly generated, this and the p0228ERM construct were used to transform the *Synechocystis* sp. PCC 6803 wild-type GT and the ΔPhb1-3 triple mutant cells.

The resulting transformants were grown on selective plates to enforce segregation, of which the progress was monitored by PCR analyses. To test whether the generated mutants were completely segregated, the respective, inactivated genes were amplified from DNA isolated from the newly generated strains and a wild-type control in PCR analyses using the corresponding forward and reverse primers (see Table 2.7). The used primers amplified the respective genes of the *Synechocystis* sp. PCC 6803 wild-type strain (*sll0851* = ~1.70 kb; *slr0228* = ~1.88 kb; *phb1* = 849 bp; *phb2* = 897 bp; *phb3* = 966 bp), while significantly larger DNA fragments (same sequence than in the wild-type plus the antibiotic-resistance cassette; *sll0851ERM* = ~2.78 kb; *slr0228ERM* = ~2.60 kb; *phb1KAN* = ~2.05 kb; *phb2CAM* = ~2.20 kb; *phb3SPEC* = ~2.97 kb) were amplified in the generated mutant strains. Since no more DNA fragments, that would correspond to the sizes of the respective *sll0851* (*psbC*), *slr0228* (*ftsH*), *phb1*, *phb2* and *phb3* wild-type genes, could be detected in the tested mutant strains (see Figure 4.9B and Figure 4.9C), completely segregated and viable mutants were generated. The results of the PCR analyses for the single ΔCP43 and the Δ0228 inactivation mutants, are for the inactivated genes in principle similar to those obtained and shown in Figure 4.9B and Figure 4.9C and are not shown.

4.2.3.3 Pulse-chase analyses of mutants with an accelerated D1 protein turnover

Due to the inactivation of the *psbC* gene, the ΔCP43 and the ΔCP43/ΔPhb1-3 mutants were unable to assemble functional PSII monomers (RCC1) and dimers (RCC2) and feature an accelerated D1 protein turnover (Komenda et al., 2004). Crude isolated membranes of the samples that were taken during the pulse-chase experiments, were analysed on 1-D SDS and 1-D BN PAGE gels, which were subsequently processed into autoradiograms (see Figure 4.10).

The autoradiograms resulting from the 1-D SDS PAGE gels, showed equally rapid and selective turnover of the D1 protein in both of the tested strains (compare Figure 4.10A1 and Figure 4.10B1; D1 protein marked with a black arrow). Already an estimation of the D1 protein signal intensities with the naked eye suggested, that the majority of the radioactively labelled D1 protein was selectively degraded after 45 min, while most of the other protein bands displayed equal signal intensities in the 0 and 180 min sample lanes. Other PSII subunits, such as D2 or CP47 could not be assigned to specific signal bands and therefore, the presented results focus on the turnover of the D1 protein, for which an attempt was made to quantify the observed signal intensities. Due to the partially high background in the respective regions of the gel, the obtained values for the D1 signal intensities were considered to be qualitative rather than absolute. Nevertheless, the generated values confirmed the observation that had been made with the naked eye. Most, if not all of the D1 protein was turned over after 45 min in both strains and the remaining signal intensity of 20 to 25 percent could probably be assigned to background signal (see Figure 4.10A2 and Figure 4.10B2). Summarising this data, it could be shown that a mutant with accelerated D1 protein turnover was generated, but the observed protein patterns and quantified signal intensities for the D1 protein appeared to be rather similar in the compared strains. Analysing the Coomassie-stained 1-D BN PAGE gels showed, that the lanes of the respective gels were equally loaded and apart from the fact that no PSII monomers and dimers could be detected, no significant differences could be observed between the two strains. In the 1-D BN autoradiograms however, slight differences were detectable (compare Figure 4.10A3 and Figure 4.10B3). First of all, a comparison of the autoradiograms of the PSII assembly defective mutants with that of the *Synechocystis* sp. PCC 6803 wild-type GT strain (see Figure 4.8A3) revealed an increase in the amounts of RC47 protein complexes. This protein complex appeared to be intensely

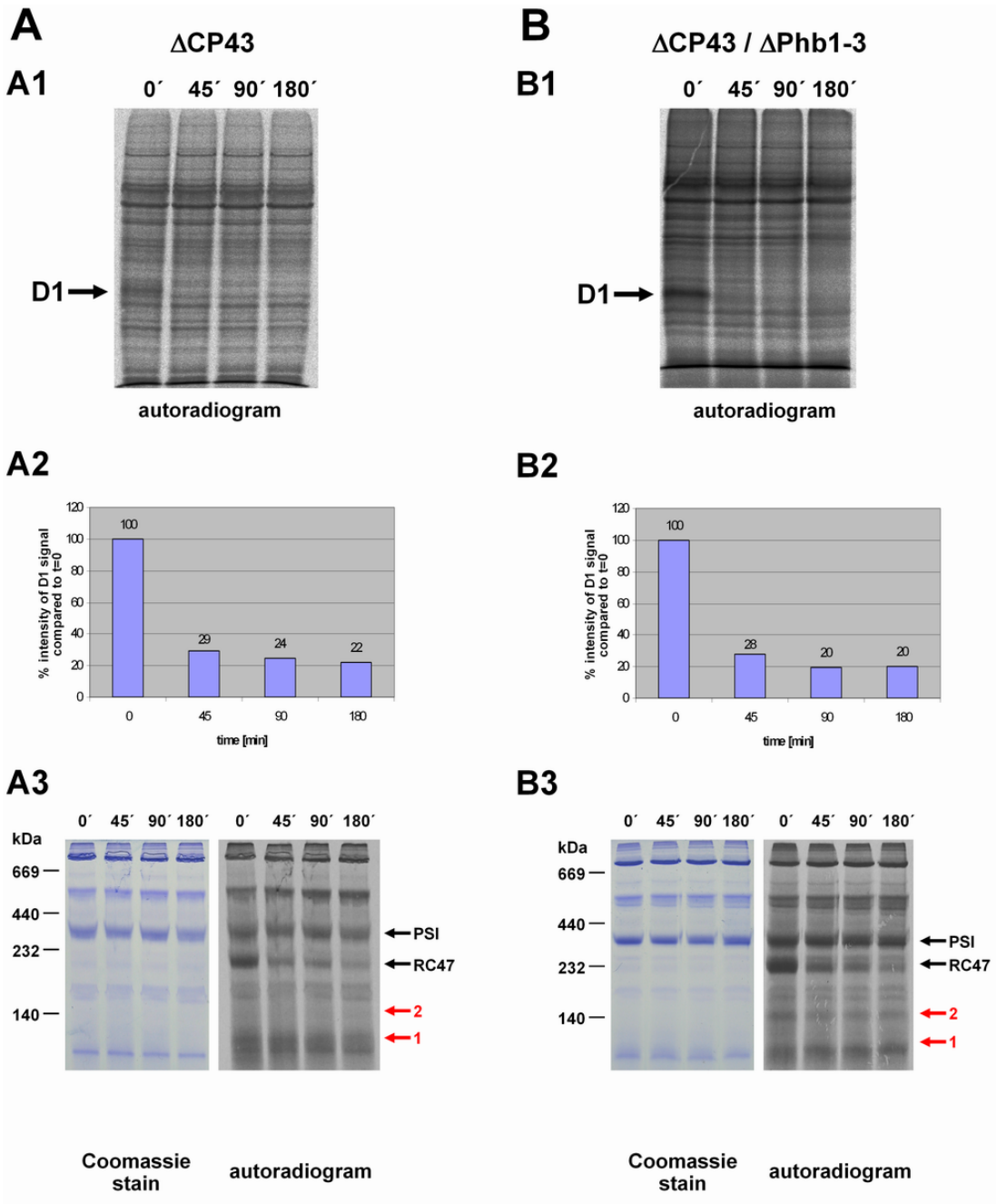

Figure 4.10: Pulse-chase analyses of *Synechocystis* sp. PCC 6803 mutant strains with an accelerated D1 protein turnover. Pulse-chase analyses were performed on the (A) ΔCP43 and the (B) ΔCP43/ΔPhb1-3 mutant strains. For a more detailed description of the performed analysis, see the legend of Figure 4.8. (A3 and B3) The positions of the PSI monomers (PSI) and the RC47 protein complex (RC47; PSII core complexes lacking CP43) are indicated. Unidentified proteins or protein complexes of interest are mentioned in the text and marked in red with (1) and (2).

labelled in both mutants at time point 0´, while the corresponding radioactive signals at later time points decreased rapidly. In the *Synechocystis* sp. PCC 6803 wild-type GT strain, the RC47 protein complex is not as distinctly labelled and therefore none of the observed bands was assigned to this particular PSII protein complex (compare Figure

4.8A3). Interestingly, an unidentified protein complex that was smaller than 140 kDa (indicated with a red 1) appeared to be present or more intensely labelled in the ΔCP43 mutant, while it was absent in the ΔCP43/ΔPhb1-3 mutant. Additionally, an unidentified protein complex that was larger than 140 kDa (indicated with a red 2) appeared to be present or more intensely labelled in the ΔCP43/ΔPhb1-3 mutant, while it was absent in the ΔCP43 mutant. Unfortunately, as the identities of both of these unassigned protein complexes could not be revealed, no conclusions could be drawn from the observed differences. Summarising the presented pulse-chase analysis data, the inactivation of the *phb1*, *phb2* and *phb3* genes did not appear to influence the turnover of the D1 protein, while it seemed to affect the expression (presence or absence) or the turnover rate (intensity of labelling) of two unidentified protein complexes.

4.2.3.4 Pulse-chase analyses of mutants with an impaired D1 protein turnover

As the Slr0228 FtsH protease has been shown to be involved in the early stages of the PSII repair cycle (Silva et al., 2003), inactivation of this protein, in both the Δ0228 and the Δ0228/ΔPhb1-3 mutant strains, resulted in an impaired D1 protein turnover. Thus, since according to the working model of this study (see Figure 1.9) the D1 protein should not be degraded in these genetic backgrounds, general dynamics of protein complexes, that might possibly display differences in the two mutant strains due to the inactivation of the Band 7 genes, were investigated. Crude isolated membranes of the samples that were taken during the pulse-chase experiments, were analysed on 1-D SDS and 1-D BN PAGE gels, which were subsequently processed into autoradiograms (see Figure 4.11).

In the cases of the Δ0228 and the Δ0228/ΔPhb1-3 mutant strains, the D1 protein could not as easily be detected in the autoradiograms from the 1-D SDS PAGE gels as in the previous analyses, because here the D1 protein was not selectively turned over and the corresponding signal did not stand out (see Figure 4.11A1 and Figure 4.11B1, D1 protein region marked with a black arrow). Therefore, no attempt was made to quantify the rate of D1 protein turnover and also the other PSII subunits of the reaction centre core (RCC), such as D2, CP43 and CP47, remained unassigned. Therefore, the only conclusion that could be drawn from this analysis was that a

mutant with impaired D1 protein turnover had been generated. Interestingly, already the Coomassie-stained 1-D BN PAGE gels revealed slight differences in the observed protein complex patterns between the two strains (compare Figure 4.11A2 and Figure 4.11B2). An unidentified protein complex could be observed in the 232 kDa region in the Δ0228 mutant (marked with a red 2), while this protein complex did not seem to be present in the Δ0228/ΔPhb1-3 mutant. However, the rest of the protein complex pattern on the Coomassie-stained 1-D BN PAGE gels appeared to be rather similar.

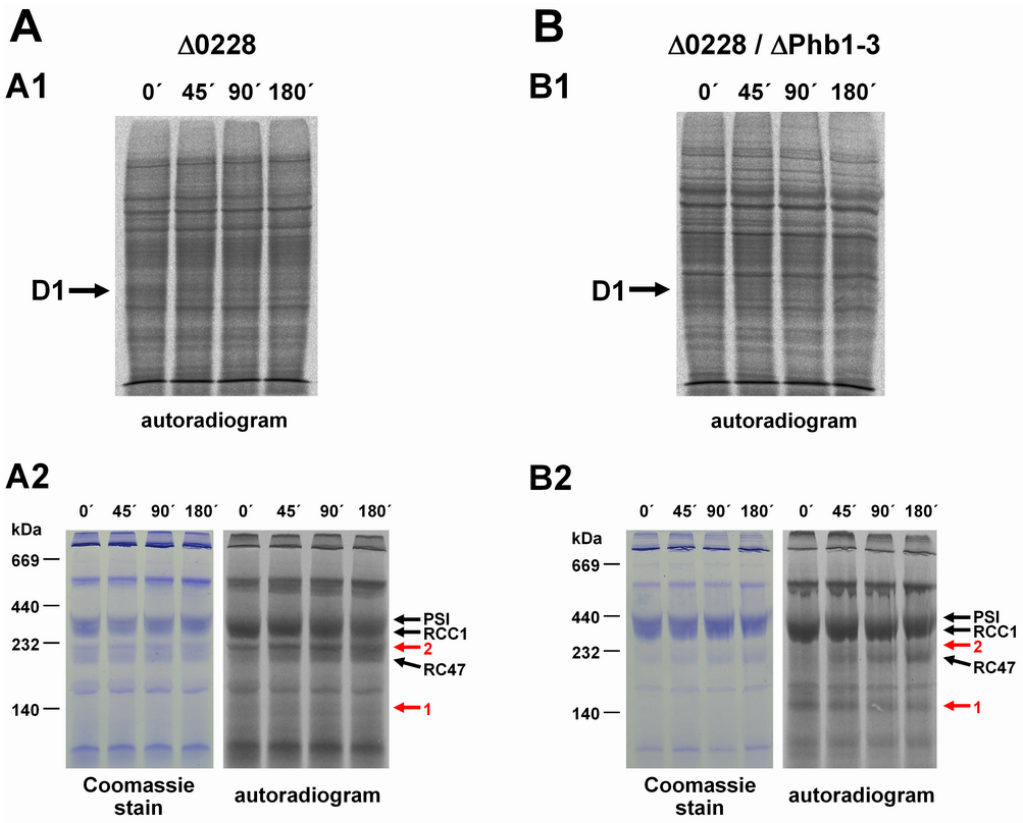

Figure 4.11: Pulse-chase analyses of *Synechocystis* sp. PCC 6803 mutant strains with an impaired D1 protein turnover. Pulse-chase analyses were performed on the (A) Δ0228 and the (B) Δ0228 in ΔPhb1-3 mutant strains. For a more detailed description of the performed analysis, see the legend of Figure 4.8. (A2 and B2) The positions of the PSI monomer (PSI), the PSII monomers (RCC1) and the RC47 protein complex (RC47, PSII core complexes lacking CP43) are indicated. Unidentified proteins or protein complexes of interest are mentioned in the text and marked in red with (1) and (2).

Analysing the corresponding autoradiograms revealed that no PSII dimers (RCC2; compare Figure 4.8A3) could be detected, while the radioactive signal for PSII monomers (RCC1) seemed to decrease with time. At the same time the intensity of a radioactive signal, that was assigned to the RC47 protein complex, appeared to increase correspondingly. However, the decrease of the signal for PSII monomers was

partly masked by the signal for monomeric PSI complexes (PSI) that could be found slightly higher in the same region. The absence of the previously mentioned, unidentified protein complex in the 232 kDa region (marked with a red 2) in the Δ0228/ΔPhb1-3 mutant compared to the Δ0228 mutant became more obvious in the autoradiogram. Additionally, a signal for another unidentified protein complex in the 140 kDa region could be detected in the Δ0228/ΔPhb1-3 mutant, while it did not appear in the autoradiogram of the Δ0228 mutant. No attempt was made to quantify the obtained signals of the 1-D BN PAGE analyses. Overall, the presented analyses did not suggest, as expected, that the inactivation of the *phb1*, *phb2* and *phb3* genes influenced the turnover of the D1 protein in the Δ0228/ΔPhb1-3 mutant. Interestingly, the expression (presence or absence) or the turnover rate (intensity of labelling) of two unidentified protein complexes appeared to be affected in the Band 7 gene inactivation mutant.

4.2.3.5 Comparative pulse-chase and pulse labelling analyses of the ΔPhb1-4 quadruple mutant

As not only a ΔPhb1-3 triple mutant was generated in this work, but also a ΔPhb1-4 quadruple mutant, comparative pulse-chase and pulse-labelling analyses of this mutant and the *Synechocystis* sp. PCC 6803 wild-type GT strain were performed. The pulse-chase experiment was analysed by 1-D SDS PAGE and audiography as described before, while the pulse labelling samples were subjected to 2-D SDS PAGE analyses and subsequent audiography in collaboration with Dr. Josef Komenda (Institute of Microbiology, Trebon, Czech Republic) as described by Komenda et al. (2004). For the 1-D SDS PAGE gels, crude membranes were isolated of the samples taken during the pulse-chase experiments and the resulting gels were processed into autoradiograms (see Figure 4.12).

These autoradiograms showed equally rapid and selective turnover of the D1 protein in both of the tested strains (compare Figure 4.12A1 and Figure 4.12B1, D1 protein marked with a black arrow). An estimation of the D1 protein signal intensities with the naked eye suggested, that most of the radioactively labelled D1 protein was selectively degraded during the 180 min chase period, while most of the other protein bands displayed equal signal intensities in the 0 and 180 min sample lanes. Unfortunately, the other PSII reaction centre core (RCC) subunits remained unassigned and the presented pulse-chase analysis only focuses on the turnover of the D1 protein.

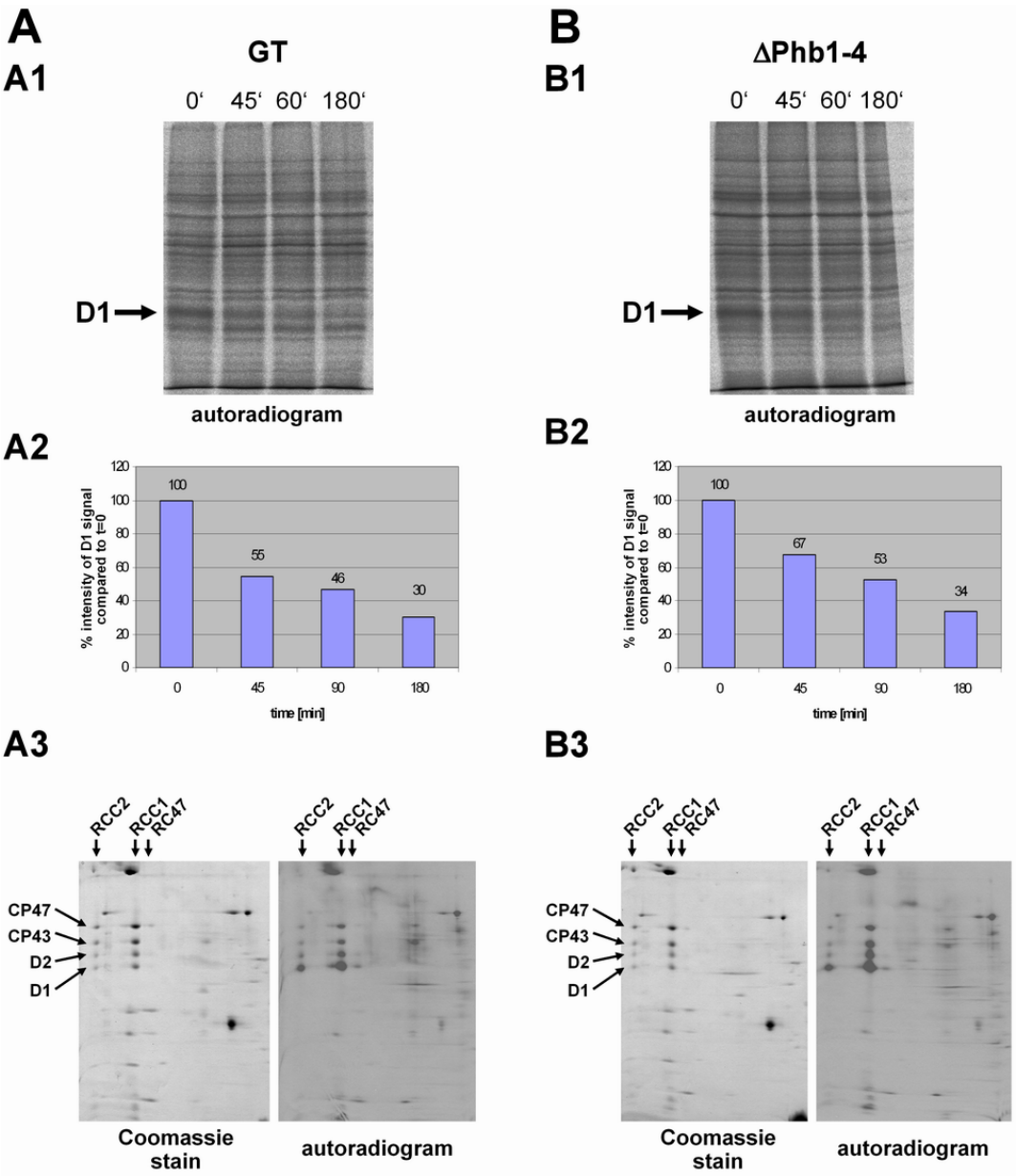

Figure 4.12: Comparative pulse-chase and pulse-labelling analyses of the *Synechocystis* sp. PCC 6803 wild-type GT and the ΔPhb1-4 quadruple mutant strains. Pulse-chase and pulse-labelling analyses were performed on the (A) *Synechocystis* sp. PCC 6803 wild-type GT and the (B) ΔPhb1-4 quadruple mutant strains and a more detailed description of the performed analysis can be found in the legend of Figure 4.8. (A3 and B3) Coomassie-stained gels and resulting autoradiograms of the 2-D SDS PAGE analyses of the pulse labelling experiments that were performed in collaboration with Dr. Josef Komenda (Institute of Microbiology, Trebon, Czech Republic) as described by Komenda et al. (2004). The positions of PSII dimers (RCC2), PSII monomers (RCC1) and RC47 protein complexes (RC47, PSII core complexes lacking CP43) are indicated.

Furthermore, a strip of tape, that was used to fix the gel in the Phosphorimager cassette, had blocked part of the signal in the autoradiogram of the ΔPhb1-4 quadruple mutant and consequently, the quantification of the signal intensities had to be

performed on only one half of each lane. Due to the partially high background in the respective regions of the gel, the obtained values for the D1 signal intensities were considered to be qualitative rather than absolute. Nevertheless, the generated values confirmed the observation that was made with the naked eye. In the *Synechocystis* sp. PCC 6803 wild-type GT strain, after an initial rapid decrease of the D1 protein signal intensity to 55 % after 45 min, the signal continued to decrease, but at a slower rate. Thus, after 90 min 46 % and after 180 min 30 % of the initial signal intensities could still be detected (see Figure 4.8A2). The D1 protein of the ΔPhb1-4 quadruple mutant was degraded at a similar rate. Again, after an initial rapid decrease of the D1 protein signal intensity to 67 % after 45 min, the signal continued to decrease, but at a slower rate. Thus, after 90 min 53 % and after 180 min 34 % of the initial signal intensities could still be detected (see Figure 4.8B2). The remaining 30 and 34 percent respectively of the initial signals intensities could probably be considered as background (see Figure 4.8A1 and Figure 4.8B1). Summarising the data obtained from the 1-D autoradiogram, the observed protein patterns and quantified signal intensities for the D1 protein appeared to be rather similar in both of the compared strains.

Analysing the Coomassie-stained 2-D SDS PAGE gels and the resulting autoradiograms, that were generated from the pulse labelling samples, no significant differences could be observed between the two strains (compare Figure 4.12A3 and Figure 4.12B3). For either strain, PSII dimers (RCC2), PSII monomers (RCC1) and RC47 (RC47) protein complexes could be detected in the gels as well as in the resulting autoradiograms. Overall, the presented analyses did not suggested that the inactivation of the *phb1*, *phb2*, *phb3* and *phb4* genes influences the turnover of the D1 protein in the ΔPhb1-4 mutant.

4.2.4 PSII repair assay with the ΔPhb1-4 quadruple mutant strain

In order to assay the functioning of the PSII repair cycle in the *Synechocystis* sp. PCC 6803 wild-type GT and the ΔPhb1-4 quadruple mutant strains, a photoinhibition analysis was performed. In this experiment, cyanobacterial cells are exposed to an illumination with high-light intensities (~1200 μE m^{-2} s^{-1}) for a prolonged period of time. At various time points, samples are taken and the ability of whole cells to evolve oxygen, as an indirect mean of measuring PSII activity, is assessed with a Hansatech DW2 oxygen electrode (Hansatech instruments Ltd., UK).

In this analysis, the measured rates of oxygen evolution (µmol oxygen mg chlorophyll a $^{-1}$ h^{-1}) were normalised to the values at t=0 as 100 % for each of the samples respectively and plotted against time (see Figure 4.13).

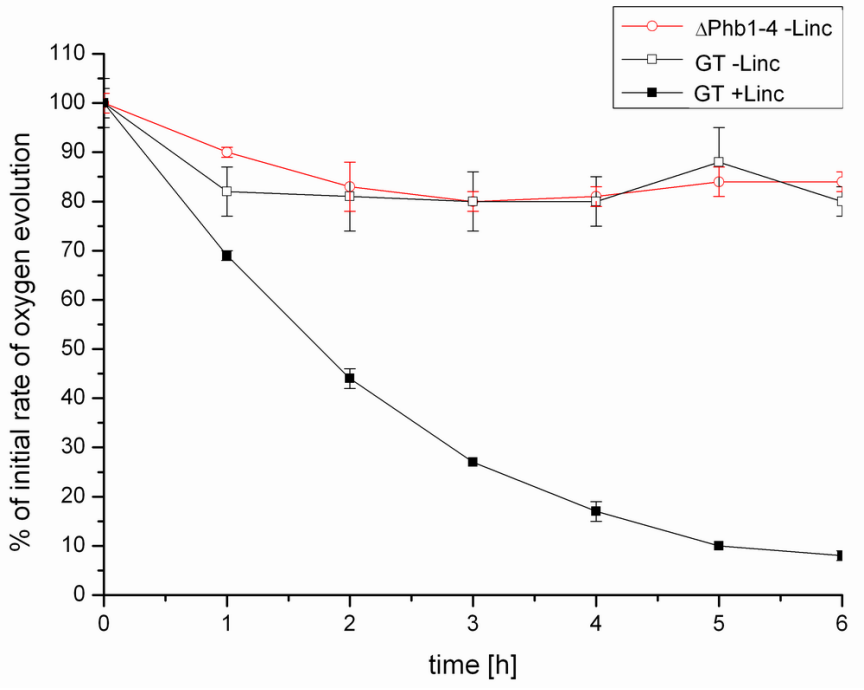

Figure 4.13: Photoinhibition analysis of the *Synechocystis* sp. PCC 6803 wild-type GT and the ΔPhb1-4 quadruple mutant strains. A photoinhibition analysis was performed on the *Synechocystis* sp. PCC 6803 wild-type GT (black lines) and the ΔPhb1-4 quadruple mutant (red line). Cells at a chlorophyll a concentration of ~20 µg ml^{-1} were exposed to a light intensity of ~1200 µE m^{-2} s^{-1} over a period of six hours. Oxygen evolution of whole cells was measured in the presence (closed symbols) or absence (open symbols) of lincomycin (100 µg ml^{-1}; a protein synthesis inhibitor) at the indicated time points in the presence of 2,6 dichlorobenzoquinone (DCBQ) and $K_3Fe(CN)$. The oxygen evolution rates (µmol oxygen mg chlorophyll a $^{-1}$ h^{-1}) were normalised (for each sample the t=0 value as 100%) and plotted as a function of time. The initial, absolute rates of oxygen evolution for the respective strains were as follows: 324 (ΔPhb1-4 –Linc), 316 (GT –Linc) and 350 (GT +Linc) (all in µmol oxygen mg chlorophyll a $^{-1}$ h^{-1}).

Analysis of the obtained data showed that the PSII repair cycle of both the *Synechocystis* sp. PCC 6803 wild-type GT and the ΔPhb1-4 quadruple mutant strains were functional. After an initial drop to an oxygen evolution rate that was around 80 % of the initially measured rate, both strains managed to maintain a high level of oxygen evolution thereafter, even after prolonged exposure to photodamage-inducing light intensities. Due to the multitude of antibiotic-resistance cassettes that were introduced to generate the ΔPhb1-4 quadruple mutant, this strain was insensitive to lincomycin and no antibiotic control was performed for this strain. However, the measured oxygen

evolution rate for the *Synechocystis* sp. PCC 6803 wild-type GT strain that had been incubated with lincomycin decreased steadily and due to a blocked *de novo* protein synthesis that rendered the PSII repair cycle impaired, the strain could not recover the loss of PSII activity. Overall the observed decrease of the oxygen evolution rate appeared to be similar in both the wild-type GT and the ΔPhb1-4 quadruple mutant strain, indicating that the inactivation of the *phb1*, *phb2*, *phb3* and *phb4* genes did not seem to influence the PSII repair cycle drastically.

4.3 The Band 7 proteins and NDH-1 complexes

The working hypothesis of this work is based on the model for the PHB complex (proteins that hold badly folded subunits; prohibitin homologues) of *S. cerevisiae*, which has been shown to be involved in the biogenesis of respiratory chain protein complexes (Nijtmans et al., 2002). In yeast, the prohibitin homologues are associated with the mitochondrial m-AAA protease and negatively regulate its activity by binding potential substrates (Steglich et al., 1999), e.g. newly synthesised subunits of the cytochrome c oxidase (COX) (Nijtmans et al., 2000). The m-AAA protease has been shown to be involved in the splicing of transcripts of mitochondrial genes that encode essential respiratory chain protein complex subunits and the post-translational control of the assembly of respiratory protein complexes (Arlt et al., 1998). Together, the m-AAA protease and prohibitins are part of a quality-control mechanism that operates in *S. cerevisiae* to avoid mistakes during respiratory protein complex assembly and thereby maintains the integrity of the inner mitochondrial membrane (Langer et al., 2001; Nijtmans et al., 2002). Respiration in cyanobacteria is complex and a multitude of protein complexes is involved in primary oxidoreduction (Peschek et al., 2004). The NAD(P)H dehydrogenase complexes (NDH-1 and NDH-2) and the succinate dehydrogenase oxidise NAD(P)H or succinate and feed electrons into the plastoquinone (PQ) pool (Cooley and Vermaas, 2001). From the PQ pool, which is shared by photosynthetic and respiratory pathways (Aoki and Katoh, 1983), electrons can be passed on to PSI, alternative oxidases or terminal oxidases (Berry et al., 2002). Several terminal oxidases have been identified in cyanobacteria, but the cytochrome aa_3-type cytochrome c oxidase (CtaI) is the major terminal oxidase where oxygen is reduced to water (Howitt and Vermaas, 1998). However, after having tested the working hypothesis and the possible involvement of Band 7 proteins in the PSII repair

cycle, the results from *S. cerevisiae* in the literature suggested to conduct further experiments to test whether Band 7 protein might be linked to respiratory processes. Initially, immunoprecipitation experiments with antibodies directed against protein subunits of the NDH-1 complex were performed on various *Synechocystis* sp. PCC 6803 strains (see section 4.3.1). Furthermore, NDH-1 protein complex dynamics were examined in a comparative 2-D SDS PAGE analysis (see section 4.3.2).

4.3.1 Immunoprecipitation of NDH-1 complex subunits

The aim of this initial immunoprecipitation experiment was to test whether the Band 7 proteins would co-immunoprecipitate with NDH-1 protein complex subunits. Therefore, unpurified and polyclonal antibodies, directed against the NdhI and NdhJ subunits of NDH-1 protein complexes, as well as the Phb1 protein of *Synechocystis* sp. PCC 6803, that were all readily available in the laboratory, were used on crude membrane isolations of various *Synechocystis* sp. PCC 6803 strains (see Figure 4.14). The ΔPhb1-4 quadruple mutant and the M55 mutant, in which the *ndhB* gene had been inactivated and which therefore could not assemble functional NDH-1 protein complexes (Ogawa, 1991a), were used as controls.

On the Coomassie-stained 1-D SDS PAGE gel, only the bands of the eluted antibodies could be detected, while no immunoprecipitated proteins could be observed (see Figure 4.14A1). The immunoblot that was probed with the αPhb1 antibody, revealed that the Phb1 protein could be immunoprecipitated with the αPhb1 antibody from *Synechocystis* sp. PCC6803 wild-type GT isolated crude membranes (see Figure 4.14A2). More interestingly however, the Phb1 protein appeared to co-immunoprecipitate with the NdhI subunit of NDH-1 protein complexes when the αNdhI antibody was used. Even though the observed antibody signal was slightly weaker than in the eluate corresponding to the αPhb1 antibody, this signal seemed to be specific, as the Phb1 protein was neither found in the eluate obtained from the ΔPhb1-4 quadruple mutant nor in the one of the M55 mutant. Additionally, the αPhb1 antibody yielded very weak signals for the eluates that had been obtained with the αNdhJ antibody used on *Synechocystis* sp. PCC6803 wild-type GT and M55 isolated crude membranes. Because these similarly weak signals were detected in both eluates, the antibody signal were probably unspecific. It is noteworthy that these immunoprecipitations were performed with unpurified, polyclonal antibody sera.

Unfortunately, the immunoblots that were probed with the αNdhI and αNdhJ antibodies on the eluates were inconclusive (data not shown).

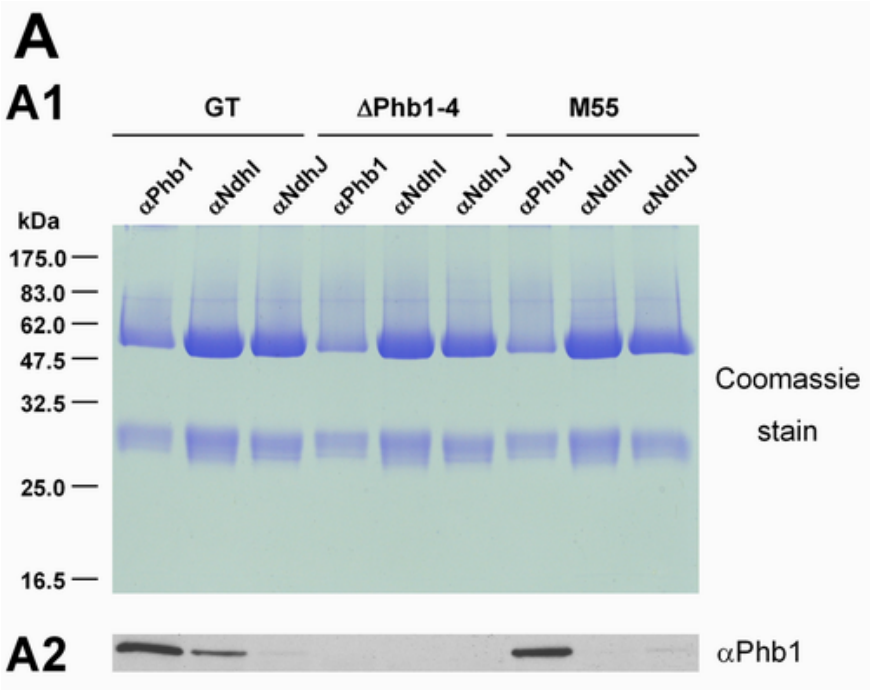

Figure 4.14: Immunoprecipitation experiment on crude membrane isolation of various *Synechocystis* sp. PCC 6803 strains using the αNdhI, αNdhJ and αPhb1 antibodies. Crude membrane isolations of the *Synechocystis* sp. PCC 6803 wild-type GT, the ΔPhb1-4 quadruple mutant and the M55 strain were used in an immunoprecipitation experiment with the indicated antibodies (αPhb1, αNdhI and αNdhJ). 15 µl of the immunoprecipitations (the samples had been eluted in 70 µl 1x SDS sample buffer) were loaded in the respective lanes. (A1) One 1-D SDS PAGE gel was Coomassie-stained, while (A2) another was used for an immunoblotting analysis with the αPhb1 antibody.

However, the control immunoblots that were performed on the crude membrane isolations of the used strains with the αNdhI, αNdhJ and αPhb1 antibodies yielded the following, expected results (data not shown). The NdhI and NdhJ proteins were detected in the *Synechocystis* sp. PCC6803 wild-type GT and the ΔPhb1-4 quadruple mutant strains, while they could not be detected in the M55 crude membranes. The Phb1 protein could be detected in the *Synechocystis* sp. PCC6803 wild-type GT and the M55 mutant strains, while it was not present in the ΔPhb1-4 quadruple mutant. Summarising these results, it appeared possible that the Phb1 prohibitin homologue of *Synechocystis* sp. PCC6803, could specifically be associated with the NdhI protein either directly or indirectly via another subunit of the NDH-1 protein complex.

4.3.2 Assembly and inducibility of NDH-1 complexes

After it became apparent that an inactivation of Band 7 genes did not seem to affect oxygen consumption (data not shown), the chaperone function of the prohibitin homologues of *S. cerevisiae* (Nijtmans et al., 2000) suggested to test whether the Band 7 proteins of *Synechocystis* sp. PCC 6803 might influence NDH-1 protein complex dynamics. NDH-1 protein complexes have been shown to be an extremely dynamic group of membrane protein complexes and four of them have been annotated in the literature: NDH-1L, NDH-1M, NDH-1S_1 NDH-1S_2 (Herranen et al., 2004). Interestingly, NDH-1 protein complexes are not only involved in respiratory processes, but also in the cyclic electron transport around PSI (Mi et al., 1992). Another important function of NDH-1 protein complexes is their involvement in carbon acquisition (Ogawa et al., 1991a; Ogawa et al., 1991b; Badger and Price, 2003). The NDH1-L protein complex is constitutively expressed and has been shown to be a prerequisite for photoheterotrophic growth, which suggests that this protein complex is involved in cellular respiration (Zhang et al., 2004). The NDH1-M protein complex has been implied to be involved in cyclic electron transport around PSI, while NDH1-S protein complexes have been shown to be part of the inorganic carbon (C_i) concentrating mechanism (CCM) (Zhang et al., 2004). An interesting feature of NDH1-S protein complexes is, that they can be induced by shifting a *Synechocystis* sp. PCCC 6803 culture from a high (3 % (v/v)) to a low (air level) CO_2-containing environment (Zhang et al., 2004). Conversely, the NDH-1S protein complexes involved in CCM do not seem to be subject to immediate proteolytic breakdown when a culture is shifted from a low to a high CO_2 level containing environment (Zhang, personal communication). Therefore, in order to study a possible effect of Band 7 proteins on the dynamics of NDH-1S protein complexes, the focus was limited to the assembly and inducibility of NDH-1S protein complexes by altering the CO_2 levels at which the cultures were grown. The following 2-D SDS PAGE analysis was performed in collaboration with Dr. Pengpeng Zhang in Prof. Eva-Mari Aro´s group (University of Turku, Turku, Finland) (see Figure 4.15).

Analysing the corresponding, silver-stained 2-D SDS PAGE gels, similar protein profiles were observed for both strains for each of the tested CO_2 condition. The only obvious difference in the protein patterns were two additional spots in close proximity to the region that corresponded to the high-molecular-mass region of the first dimension in the *Synechocystis* sp. PCCC 6803 wild-type GT strain (circled in

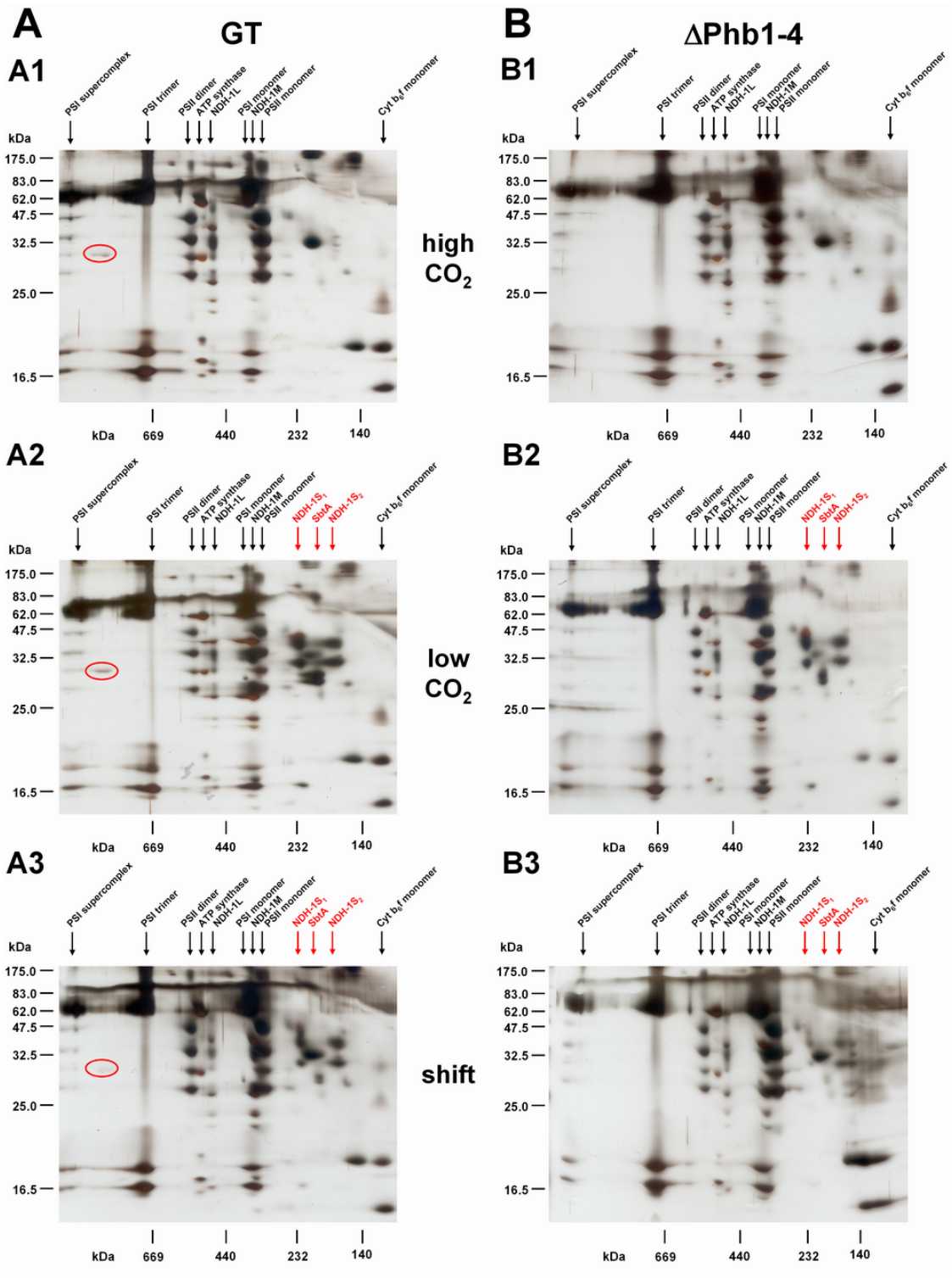

Figure 4.15: Comparative 2-D SDS PAGE analysis of the *Synechocystis* sp. PCC 6803 wild-type GT and the ΔPhb1-4 quadruple mutant strains under different CO_2 growth conditions. Crude membranes of (A) the *Synechocystis* sp. PCC 6803 wild-type GT and (B) the ΔPhb1-4 quadruple mutant strains were isolated and separated by 2-D SDS PAGE. Cells were grown under standard laboratory growth conditions, except for a change in the pH of the liquid BG-11 media (pH = 7.5 instead of 8.2) and different CO_2 conditions. The CO_2 conditions under which the liquid cultures were grown were as follows: (A1 and B1) at high CO_2 (3 % (v/v) CO_2 in air), (A2 and B2) at low CO_2 (air level) and (A3 and B3) with a **(Legend continued!)**

Legend Figure 4.15 continued:
shift from high CO_2 (3 % (v/v) CO_2 in air) to low CO_2 (air level). An amount of crude isolated membranes corresponding to 5 µg chlorophyll a were separated in each lane of a 5 to 12.5 % BN PAGE linear gradient gel. The gel strips for the second dimension SDS PAGE gels were incubated for 30 min in solubilisation buffer, transferred and run on 14 % SDS PAGE gels that were subsequently silver-stained. The positions of various protein complexes are indicated with arrows (see also in the text). Protein complexes that were induced by the change of the CO_2 level, are indicated in red. The position of the Phb3 protein (Slr1128) is marked with a red circle.

red). These protein spots could be assigned to the Phb3 (Slr1128) protein, because of an identification in an earlier mass spectrometry approach (Herranen et al., 2004). Additionally, the 2-D SDS PAGE analyses of the single Band 7 gene inactivation mutants confirmed this assignment, as this protein spot was only missing in the ΔPhb3 mutant strain (data not shown). When the cells were grown in an environment with high CO_2 levels, all major membrane protein complexes could be observed: PSI supercomplexes, trimers and monomers, PSII dimers and monomers, ATP synthase, NDH-1L, NDH-1M and the cytochrome b_6f monomer (see Figure 4.15A1 and Figure 4.15B1; assignment of protein complexes according to Zhang et al., 2004). Growing the cells at low CO_2 levels lead to a protein profile in which all the previously mentioned membrane protein complexes, plus three additional protein complexes (NDH-$1S_1$, NDH-$1S_2$ and SbtA) could be detected (see Figure 4.15A2 and Figure 4.15B2). The 2-D SDS PAGE gels that were obtained for the cultures shifted from high to low CO_2 levels, displayed the same protein pattern as the ones that were grown under low CO_2 levels (see Figure 4.15A3 and Figure 4.15B3). Unfortunately, the means to quantify the obtained protein spot patterns were limited to an estimation with the naked eye. Thus, even though the patterns of corresponding 2-D SDS PAGE gels were very similar, the intensities of the silver-stained subunits of the NDH-$1S_1$, NDH-$1S_2$ and SbtA protein complexes appeared to be slightly different in the ΔPhb1-4 quadruple mutant when compared to the *Synechocystis* sp. PCCC 6803 wild-type GT strain (compare Figure 4.16A2 to Figure 4.16B2 and Figure 4.16A3 to Figure 4.16B3). For cells grown at low CO_2 level, this effect can possibly be attributed to a shorter developing step in the silver staining procedure, as other protein spots also appeared to be stained weaker. Analysing the gel for the ΔPhb1-4 quadruple mutant after a shift in the CO_2 levels, the abundance of NDH-$1S_1$, NDH-$1S_2$ and SbtA protein complexes appeared to be slightly decreased, while other protein complexes seemed to be equally or only slightly less well stained. Consequently, these results suggest that an

inactivation of the *phb1*, *phb2*, *phb3* and *phb4* genes might influence the dynamics of the CCM protein complexes NDH-1S_1, NDH-1S_2 and SbtA. Although inducibility in general is not affected, the actual amounts of newly induced proteins complexes might be slightly decreased in the ΔPhb1-4 quadruple mutant. Nevertheless, further experiments and immunoblotting analyses to quantify the induction of the NDH-1S protein complexes would be necessary to test the indication that is given by this 2-D SDS PAGE analysis.

4.4 Cell motility of single Band 7 gene inactivation mutants

The *Synechocystis* sp. PCC 6803 wild-type strain is, in contrast to the glucose-tolerant strain that has mainly been used in this study, motile and can exhibit positive as well as negative phototaxis (Choi et al., 2000). The cyanobacterial cells display a twitching movement (Ng et al., 2003) that is mediated by type IV pili (Bhaya et al., 1999). Thus, in order to test whether Band 7 proteins might affect cell motility, single Band 7 gene inactivation mutants were generated in the genetic background of the *Synechocystis* sp. PCC 6803 wild-type strain. The generated mutants were subsequently tested for complete segregation (see Figure 4.16A), subjected to a plate assay (see Figure 4.16B) and some of them were used for a cell surface analysis by electron microscopy (see Figure 4.16C).

Initially, the single Band 7 gene inactivation mutants ΔPhb1-WT, ΔPhb2-WT and ΔPhb3-WT had to be generated in the genetic background of the motile *Synechocystis* sp. PCC 6803 wild-type strain. For the transformation of the wild-type cells, the same plasmid DNA constructs that were used for the generation of the ΔPhb1-4 quadruple mutant strain were used (see Figure 4.1). Subsequently, PCR analyses were performed on the obtained transformants to confirm complete segregation using the respective forward and reverse primers (see Table 2.7). In the *Synechocystis* sp. PCC 6803 wild-type strain, DNA fragments corresponding to the Band 7 genes were amplified (*phb1* = 849 bp; *phb2* = 897 bp and *phb3* = 966 bp), while significantly larger DNA fragments (Band 7 gene plus the antibiotic-resistance cassette; *phb1KAN* = ~2.05 kb; *phb2CAM* = ~2.20 kb and *phb3SPEC* = ~2.97 kb) were amplified in the respective single Band 7 gene inactivation mutant strains. Since no more wild-type Band 7 gene DNA fragments for the *phb1*, *phb2* and *phb3* genes could

be detected in the tested mutant strains (see Figure 4.16A), completely segregated and viable mutants were generated.

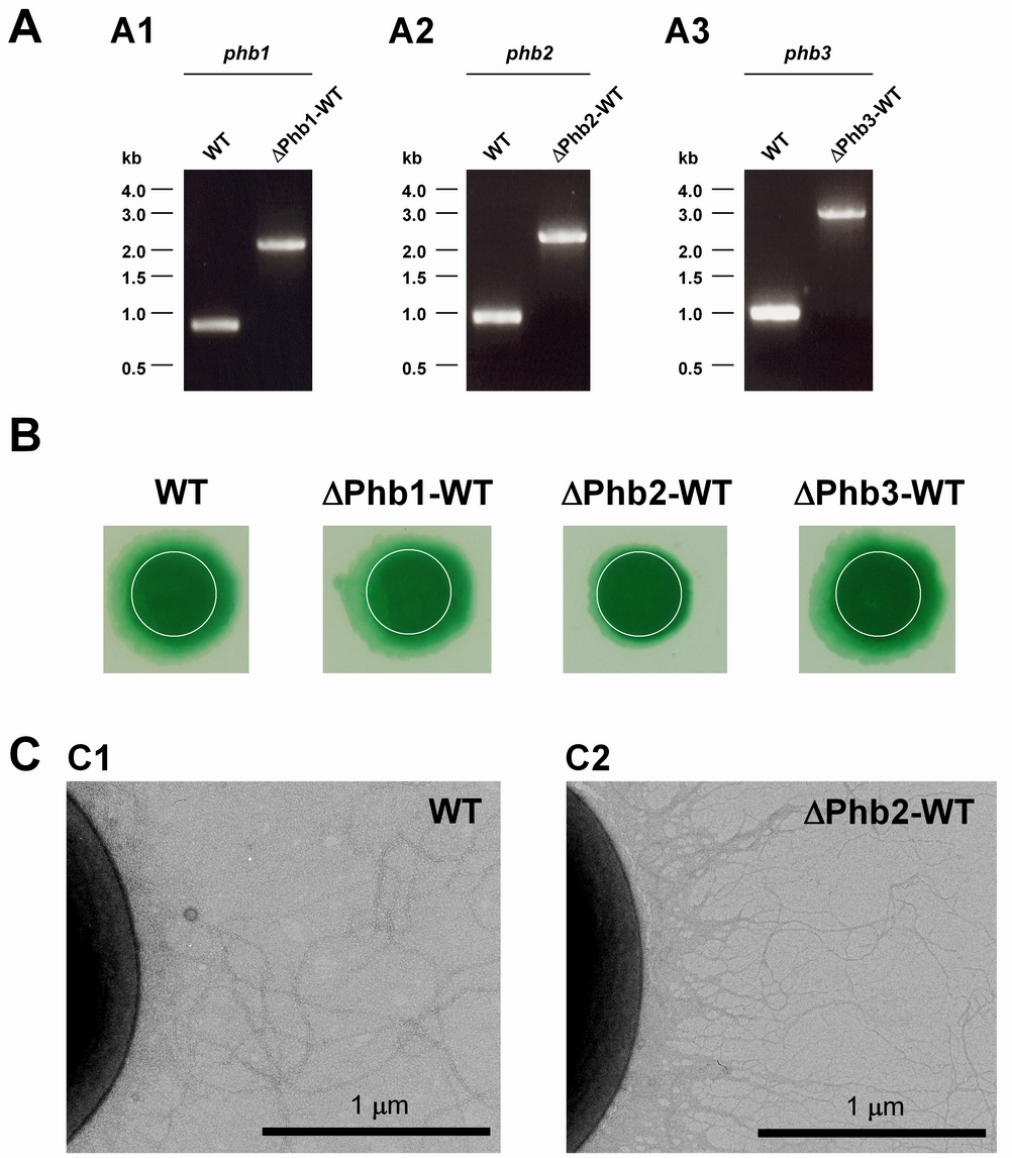

Figure 4.16: Cell motility of the *Synechocystis* sp. PCC 6803 wild-type and single Band 7 gene inactivation mutant strains. Possible effects of an inactivation of individual Band 7 genes on cell motility were assessed in the *Synechocystis* sp. PCC 6803 ΔPhb1-WT, ΔPhb2-WT and ΔPhb3-WT mutant strains. (A) The results of PCR analyses using specific primers (see text) to test for the segregation of the single Band 7 gene inactivation mutants (A1) ΔPhb1-WT, (A2) ΔPhb2-WT and (A3) ΔPhb3-WT. (B) Cell motility was assessed from 10 µl aliquots of diluted, liquid cell cultures that were spotted onto standard BG-11 agar plates and incubated under diffuse light for approximately ten days. (C) Inversed electron micrographs of the cell surface of the (C1) *Synechocystis* sp. PCC 6803 wild-type and the (C2) ΔPhb2-WT mutant strains. Black scale bars represent 1 µm as indicated.

The generated mutants were then subjected to a cell motility plate assay, where droplets of diluted, liquid cultures were spotted onto standard BG-11 agar plates. After

an incubation period of approximately ten days under diffuse illumination, the appearance of the droplets was imaged and the apparent cell motility of the different strains compared. While the cells of the *Synechocystis* sp. PCC 6803 wild-type, the ΔPhb1-WT and the ΔPhb3-WT strains appeared to be equally motile, because of the with similarly large and diffuse edges of the initially round drops, the motility of the ΔPhb2-WT mutant strain seemed to be decreased (see Figure 4.16B). Although this effect could only be qualitatively observed, the results could be repeated several times from independently grown liquid cultures.

Thus, in order to test whether this effect was due to a morphological change in the cell surface or the piliation of the ΔPhb2-WT mutant strain, a few electron micrographs were taken of the *Synechocystis* sp. PCC 6803 wild-type and the ΔPhb2-WT mutant strains by transmission electron microscopy (see Figure 4.16C). Analysing the obtained and inverted electron micrographs, it became apparent that the ΔPhb2-WT mutant did possess pili, which however appeared to be slightly different to the pili of the *Synechocystis* sp. PCC 6803 wild-type strain. The representative region of the cell surface of the ΔPhb2-WT mutant appeared to be slightly darker, which suggested that the mutant might possess more pili in close proximity to the cell surface (~300 nm) that were also more densely arranged. However, it needs to be emphasised that only a few cells had been imaged in this preliminary surface analysis, so that it was important not to over interpret this data. Summarising these results, the inactivation of the *phb2* gene in the ΔPhb2-WT mutant appeared to negatively influence cell motility. Still the mutant strain did possess pili, but some differences in piliation were detectable between the *Synechocystis* sp. PCC 6803 wild-type and the mutant cells. Nevertheless, a more detailed cell surface analysis with a larger sample size and additional biochemical assays would be necessary to draw further conclusions on the nature of this phenotype.

4.5 Discussion

The experiments discussed in this section were performed to investigate the physiological relevance of the Band 7 proteins, in particular the Phb1 prohibitin homologue, of *Synechocystis* sp. PCC 6803. Consequently, the obtained results will predominantly be compared to the literature in which other prohibitin homologues have been studied. Initially, the focus will be on a variety of growth experiments and

other more general assays to probe the function of the Band 7 proteins (see section 4.5.1). In the later sections, the possible involvement of the Band 7 proteins of *Synechocystis* sp. PCC 6803 in the PSII repair cycle (see section 4.5.2) and their potential effects on NDH-1 protein complex dynamics (see section 4.5.3) will be touched upon. Finally, the results will be discussed addressing the question whether the Phb1 prohibitin homologue might act as a molecular chaperone in *Synechocystis* sp. PCC 6803 (see section 4.5.4).

4.5.1 Investigating the physiological role of the Band 7 proteins

Overall, a variety of experiments was performed to probe the physiological role of the Band 7 proteins of *Synechocystis* sp. PCC 6803, and in the following sections the more general approaches, such as microarray data and comparative growth analyses (see section 4.5.1.1) as well as morphology assessment and motility assays (see section 4.5.1.2) will be discussed.

4.5.1.1 Microarray data and comparative growth analyses

DNA microarray analyses allow simultaneous monitoring of the transcript levels of thousands of genes (Watson et al., 1998; DeRisi and Iyer, 1999). By changing one factor of the environmental growth conditions and by then monitoring and comparing the effect on the transcript level of a gene of interest in a respective mutant with the wild-type strain, a particular, potential stress condition can be identified under which this mutant might display a distinct phenotype. In this work, microarray data (see Table 4.1; kindly provided by Dr. Iwane Suzuki, National Institute for Basic Biology, Okazaki, Japan) was analysed, in order to narrow down the number of environmental stress conditions that were to be tested in comparative growth analyses.

The obtained data consisted out of the induction ratios (IR) for the transcript levels for the Band 7 proteins of the *Synechocystis* sp. PCC 6803 wild-type GT strain under the following environmental stress conditions: salt (0.5 M NaCl), hyperosmolarity (0.5 M sorbitol), heat (34 to 44 °C), oxidative (0.25 mM H_2O_2), cold (34 to 22 °C), high-light (70 to 500 µE m^{-2} sec^{-1}). However, apparently, only oxidative and cold stress seemed to significantly affect the transcript levels of the Band 7 proteins (i.e. IR > 2 or IR < 0.5), so that *Synechocystis* sp. PCC 6803 wild-type GT and ΔPhb1-4 quadruple mutant liquid BG-11 cultures were subjected to these particular

stress conditions. In the literature, a multitude of microarray data analyses focusing on different environmental stress conditions, i.e. salt stress and hyperosmolarity (Kanesaki et al., 2002), high-light illumination (Hihara et al., 2001), low CO_2 levels (Wang et al., 2004) or light to dark transition (Gill et al., 2002) are available, but in none of these studies were the transcription levels of the Band 7 proteins of *Synechocystis* sp. PCC 6803 mentioned to be significantly affected.

Prior to discussing the results of the comparative growth analyses (see Figure 4.3), it is worthy of note that all of these experiments were performed with the glucose-tolerant *Synechocystis* sp. PCC 6803 wild-type GT and mutant strains grown in liquid BG-11 medium (pH = 8.2) which was always supplemented with 5 mM glucose. Under standard laboratory growth conditions (see section 2.3.2.1), glucose-tolerant *Synechocystis* sp. PCC 6803 cells grew significantly slower when glucose was omitted from the culture medium and furthermore the cells seemed to exhibit a different pigmentation (data not shown). However, the same glucose-tolerant *Synechocystis* sp. PCC 6803 strains could be grown without the addition of glucose in liquid BG-11 medium (pH = 7.5) that was bubbled with or incubated in air that contained 3 % (v/v) CO_2 (data not shown). In the literature, it has been shown that *Synechocystis* sp. PCC 6803 grows significantly slower under low (air level) CO_2 conditions. Furthermore, it has been reported that cell growth (at low CO_2 levels and without additional glucose) is dependent on the efficiency of CO_2 uptake, which itself is influenced by the prevalent pH of the culture medium (Zhang et al., 2004). This dependency on the pH results from the fact, that in cyanobacteria, four distinct inorganic carbon (Ci) acquisition systems have been reported (Ogawa and Kaplan, 2003), two of which mediate the uptake of CO_2 (Ohkawa et al., 2000; Shibata et al., 2001; Maeda et al., 2002), while the other two promote HCO_3^- uptake (Shibata et al., 2002; Omata and Ogawa, 1986; Omata et al., 1999) (at pH = 8.3 Ci is mostly present as HCO_3^-, while at pH = 7.5 Ci exists mainly as CO_2). Therefore, the inability to grow well without supplemented glucose in the culture medium was not due to a general incompetence of the strains, but most likely due to insufficient C_i availability under the prevalent laboratory growth conditions.

Focussing on the performed comparative growth analyses, no phenotype could be observed between the *Synechocystis* sp. PCC 6803 wild-type GT and the ΔPhb1-4 quadruple mutant strains, when the strains were subjected to cold stress, oxidative stress or photoheterotrophic growth conditions. In the literature, no effect of cold stress

on Band 7 mutants has been reported and it is unknown whether this question has been specifically addressed, while studies on *S. cerevisiae* and *Nicotiana benthamiana* have investigated the effects of oxidative stresses, in particular, on prohibitin mutants (Coates et al., 1997; Piper and Bringloe, 2002; Ahn et al., 2006). However, due to the information on the function of the prohibitins that was respectively available at the time, the underlying rationale of the experiments varied slightly. The starting point of earlier studies on *S. cerevisiae* seemed to be the implicated role of prohibitins in senescence (Jazwinski, 1996), which ultimately revealed a decreased replicative life span of the ΔPhb1 and the ΔPhb2 single mutants, as well as for the ΔPhb1-2 double mutant in comparison to the wild-type (Coates et al., 1997; Berger and Yaffe, 1998). In this work, the viability of *Synechocystis* sp. PCC 6803 wild-type GT and the ΔPhb1-4 quadruple mutant cells was also assessed by plating out 10 µl aliquots (directly and diluted) of those cells that had been used for the photoheterotrophic growth experiment (see Figure 4.3D). Unfortunately, an initial finding that the cell viability appeared to be decreased under photoheterotrophic growth conditions in the ΔPhb1-4 quadruple mutant (data not shown) could not be repeated in another independently performed experiment. Still, it might be worthwhile to repeat the experiment under more carefully controlled growth conditions and apply different techniques to assess and quantify cell viability, e.g. life/dead stains for bacterial cells and subsequent confocal microscopy analysis (e.g. with BacLight™ Bacterial Viability Kits, Molecular Probes, Eugene, USA; Taghi-Kilani et al., 1996). However, since resistance to a variety of stresses has been shown to correlate with life span in *S. cerevisiae* (Kennedy et al., 1996), yeast prohibitin mutants have been subjected to oxidative stress. Initially, no increased sensitivity towards oxidative stress induced by H_2O_2, Paraquat or tertiary-butyl hydroperoxide could be observed when one or both of the prohibitin homologues of *S. cerevisiae* were inactivated (Coates et al., 1997; Piper and Bringloe, 2002).

In more recent studies, the effect of oxidative stress on prohibitin mutants was investigated (Ahn et al., 2006), because the prohibitins have been shown to be involved in the assembly of oxidative phosphorylation complexes (Steglich et al., 1999; Nijtmans et al., 2000). An impaired maintenance of the respiratory chain has been shown to lead to an increased production of reactive oxygen species (ROS; Lenaz et al., 2002) and thus to a decreased tolerance to oxidative stress. Interestingly, in contrast to the mentioned earlier findings, the inactivation of each of the prohibitin homologues of *Nicotiana benthamiana* has been shown to increase the sensitivity of

the cells to oxidative stresses (Ahn et al., 2006). In that study, the sensitivity to the applied oxidative stresses was assessed by measuring ion leakage from leaf discs (Kim et al., 2003), which is a reported indicator for cell death (Mitsuhara et al., 1999). Remarkably, the effect of H_2O_2 (10 mM) was the least effective, while the cells exhibited stronger sensitivity to other oxidative stress inducing agents, i.e. Paraquat (1 mM; Gonzalez-Polo et al., 2004), Antimycin A (100 µM; Maxwell et al., 1999) and Salicylic acid (100 µM; Rao and Davis, 1999) (Ahn et al., 2006).

In this work, an OxyBlot was performed (see Figure 4.4) to qualitatively assess whether the ΔPhb1-4 quadruple mutant exhibits an increased level of oxidative damage due to a potentially impaired respiratory chain protein complex maintenance. However, no indications could be found that this strain might be subject to elevated levels of oxidative stress. Nevertheless, it might be worthwhile to try and adapt a different approach that uses 2′,7′-dichlorodihydrofluorescin diacetate (H_2DCFDA; Molecular Probes, Eugene, USA) followed by confocal microscopy (Bethke and Jones, 2001; Ahn et al., 2006) to quantitatively assess intracellular ROS levels in *Synechocystis* sp. PCC 6803, even though this technique has not yet been applied to cyanobacteria. H_2DCFDA is a nonfluorescent, cell permeable agent that becomes fluorescent when the acetate groups are removed by intracellular esterases and when oxidation by ROS occurs within the cell.

Summarising these observations, the discussed experiments have failed to elucidate the role of the Band 7 proteins of *Synechocystis* sp. PCC 6803 and except for the observed effects on the transcript level of some of the Band 7 proteins under cold (Phb3, Phb4 and Phb5) and oxidative stress (Phb1, Phb3 and Phb4), no insights on their physiological relevance could be gained. Interestingly, even in the literature contradictory results on the effect of oxidative stress on prohibitin mutants have been reported, where initial studies on *S. cerevisiae* indicate no increased sensitivity (Coates et al., 1997; Piper and Bringloe, 2002) while experiments on higher plants demonstrate an increase in sensitivity (Ahn et al., 2006).

4.5.1.2 Morphology and motility

The morphological data presented in this chapter was generated during immunogold-labelling experiments that had been performed to determine the localisation of the Band 7 proteins of *Synechocystis* sp. PCC 6803. Since the immunolabelling of the proteins turned out to be unsatisfactory for an unambiguous

assignment of the respective Band 7 proteins to either the plasma or thylakoid membrane (data not shown), some electron micrographs of unlabelled cells were used for a morphological comparison between the wild-type and the ΔPhb1-4 quadruple mutant strains (see Figure 4.5). Unfortunately, no obvious differences in the morphology could be detected in the cells from different developmental stages. However, the sample size of the analysed cells was too small and the method (observation with the naked eye) too crude to detect a subtle phenotype.

Interestingly, when the motility of single Band 7 gene inactivation mutants was investigated in the *Synechocystis* sp. PCC 6803 wild-type strain, the ΔPhb2-WT mutant appeared to be affected and exhibited a decreased motility. Motility studies on *Synechocystis* sp. PCC 6803 have to be performed in the wild-type strain, since the glucose-tolerant strain does not display motility due to a 1-bp frame-shift mutation in the *spkA* gene (a serine/threonine protein kinase that regulates and is essential for motility) (Kamei et al., 2001; Panichkin et al., 2006; see also section 5.7.2.1). Later, two-phase partitioning localisation experiments revealed that the Phb2 Band 7 protein (Slr1768) was solely present in the plasma membrane of *Synechocystis* sp. PCC 6803 (see Figure 5.5B), which would be plausible for a protein that affects cellular motility. In the literature, the transcript level of Phb2 (and also of Phb1) has been found to be increased in a *slr2100* (a potential cGMP phosphodiesterase) inactivation mutant after an exposure for 15 min with UV-B illumination (Cadoret et al., 2005). Even though no experimental evidence is given in that study, both the Phb1 and the Phb2 proteins have been postulated to be part of a protective mechanism (more specifically for PSII repair) whose expression is upregulated as a response to the applied UV-B stress. However, even though this assumption is in accordance with the working hypothesis of this work (see Figure 1.9), the evidence accumulated in this work does not support this hypothesis (see section 4.5.2). Nevertheless, it is a noteworthy observation that the transcript level of the Phb2 protein is increased in a mutant with an inactivated cyclic nucleotide phosphodiesterase (these enzymes are responsible for the degradation of either the second messenger cAMP or cGMP), since cAMP and its receptor (Sycrp1) have been shown to be required for cell motility of *Synechocystis* sp. PCC 6803 (Terauchi and Ohmori, 1999; Yoshimura et al., 2002). However, the *slr2100* gene has been postulated to encode a cGMP phosphodiesterase in the study by Cadoret et al. (2005), it would be interesting to investigate whether the Phb2 transcript levels are also affected in a cAMP phosphodiesterase or cAMP cyclase mutant strain.

In this work, cell motility was not only assessed qualitatively, but the affected ΔPhb2-WT mutant strain was also investigated by transmission electron microscopy (see Figure 4.16). The twitching movement (Ng et al., 2003) of *Synechocystis* sp. PCC 6803 wild-type cells is mediated by cell surface appendages that are termed type IV pili (Bhaya et al., 1999). Unfortunately, due to the small sample size, the observed piliation of both the *Synechocystis* sp. PCC 6803 wild-type and the ΔPhb2-WT mutant cannot be considered to be representative and thus it remains unclear whether piliation and/or cell surface structure of the two strains do really exhibit differences.

Nevertheless, the presented data suggests that the Phb2 protein might be involved in a cell motility related signalling pathway. The morphological study of the ΔPhb1-4 quadruple mutant strain on the other hand did not reveal any obvious effects on the physiology or morphology of the inactivated Band 7 proteins.

4.5.2 The potential role of Band 7 proteins in the PSII repair cycle

The main aim of this project was to test the possible involvement of the Band 7 proteins, in particular that of the Phb1 prohibitin homologue, of *Synechocystis* sp. PCC 6803 in the PSII repair cycle. This PSII repair mechanism (see Figure 1.7) operates to counteract a decline in photosynthetic performance that oxygenic photosynthetic organisms experience when they are exposed to excessive light illumination (Aro et al., 1993a; Aro et al., 1993b). The working hypothesis of this study postulates that the prohibitin homologue of *Synechocystis* sp. PCC 6803 physically shields newly synthesised copies of the D1 protein prior to their incorporation into reassembling PSII complexes from the degradation by a FtsH protease (see Figure 1.9; Silva et al., 2002). This model is based on the findings on the prohibitins of *S. cerevisiae* (Steglich et al., 1999; Nijtmans et al., 2000) as wells as on the discovery that the Slr0228 FtsH protease is involved in the early stages of the PSII repair cycle (Silva et al., 2003). Interestingly, in a preliminary experiment, the Phb1 prohibitin homologue was detected in a His-tagged PSII preparation from *Synechocystis* sp. PCC 6803 (Silva and Nixon, 2001). A multitude of experiments, such as: high-light growth assay (see Figure 4.7), pulse-labelling and pulse-chase analyses (see Figure 4.8, Figure 4.10 to Figure 4.12) as well as a photoinhibition experiment (see Figure 4.13) were performed to test the working model and will be discussed in this section.

Initially, to repeat the experiment by Silva and Nixon (2001), a sample containing affinity-purified His_6-tagged PSII protein complexes from *Synechocystis* sp. PCC 6803 (kindly provided by Miss Elisa Corteggiani Carpinelli) was used in an immunoblotting analysis and probed with various Band 7 antibodies (see Figure 4.6). Unfortunately, the provided sample was not very pure and could only be considered as a PSII-enriched fraction. However, the absorption spectra corresponded to a spectrum that would be expected for PSII core complexes (an absorption peak at 674 nm; data not shown), so that the purity of the analysed sample was only of minor concern. Despite the lack of an αD1 immunoblot and the same analysis performed on a similarly prepared sample from the wild-type strain, it is interesting to note that both the Phb1 prohibitin homologue and the Phb3 protein of *Synechocystis* sp. PCC 6803 could be identified in this PSII preparation.

In the literature, the Phb3 and Phb5 proteins of *Synechocystis* sp. PCC 6803 have been identified in an affinity-purified preparation of the ScpD-His_6 protein together with major PSII components as well as FtsH (Yao et al., 2007). ScpD is a member of the cyanobacterial, small CAB-like proteins (CAB = chlorophyll a/b binding proteins) and has been postulated to associate with damaged PSII complexes, in order to serve as a temporary pigment reservoir while PSII components are being repaired (Yao et al., 2007). Unfortunately, in that study, also no immunochemical evidence is presented that would rule out the possibility of an unspecific binding of the Phb3 and the Phb5 proteins to the used Ni^{2+}-column.

It is noteworthy that in later experiments of this work the Phb3 protein has been shown to unspecifically bind to Ni-NTA magnetic beads (see Figure 5.16A) and to be localised to the plasma membrane (see Figure 5.5B). Therefore, it appears likely that the Phb3 protein is neither associated with PSII protein complexes nor with the ScpD protein. Since no unspecific interaction with a Ni^{2+}-resin have been observed for the Phb1 and Phb5 protein respectively (in case of the Phb5 protein, no antibody was available to test this), it is possible that Phb1 might be associated with PSII, while Phb5 might be interacting with ScpD. Nevertheless, an element of doubt remains due to the lack of the necessary controls and the precise roles of the Phb1 or Phb5 Band 7 proteins that might be implicated by the observed interactions with PSII complexes or ScpD respectively remain to be elucidated.

Although there was no microarray data to indicate that the transcript levels of the Band 7 proteins were significantly affected by illumination with high-light intensities (only

that of Phb5 seemed to be reduced to 45 %; see Table 4.1; Hihara et al., 2001), a plate assay was performed to assess the growth of the ΔPhb1-4 quadruple mutant under high-light conditions (see Figure 4.7). While the Δ0228 control strain, in which the PSII repair cycle is impaired due to an inactivation of the Slr0228 FtsH homologue (Silva et al., 2003), died under the prolonged exposure to high-light intensities in this experiment, the ΔPhb1-4 quadruple mutant appeared to be unaffected and was viable. Similarly, a ΔPhb1-3+5 quadruple mutant strain remained viable in this experiment (data not shown), so that none of the Band 7 proteins appears to be essential for the survival of *Synechocystis* sp. PCC 6803 under high-light conditions.

Subsequently, pulse-labelling and pulse-chase analyses were performed to monitor selective D1 protein turnover, a key process and hallmark of the PSII repair cycle (Aro et al., 1993a), in various multiple Band 7 gene inactivation mutants. Although the ΔPhb1-3 triple mutant, the ΔPhb1-4 quadruple mutant and Band 7 gene inactivation mutants with accelerated or impaired PSII turnover were investigated, no apparent abnormalities in the turnover of the D1 protein or PSII complexes could be observed. However, a few unidentified protein complexes in the lower-molecular-mass region (<232 kDa) could be observed to be affected in the experiments where the Band 7 mutants with accelerated or impaired PSII turnover were investigated (see Figure 4.10 and Figure 4.11). Nevertheless, an assignment of any of these unidentified protein complexes would be largely speculation.

Interestingly, due to their involvement in a membrane-embedded quality control system (see section 1.6.2) the deletion of the Phb1 and Phb2 prohibitin homologues in a yeast strain that also lacks the m-AAA protease (by an inactivation of its subunits, either Yta10 or Yta12) leads to a severe growth defect (Steglich et al., 1999). In this study on the other hand, a viable Δ0228/ΔPhb1-3 *Synechocystis* sp. PCC 6803 quadruple mutant strain could be generated (see section 4.2.3.2) that did not display an apparent phenotype under normal laboratory growth conditions (data not shown). Thus, even though later experiments in this study demonstrate a low-level physical interaction between the Phb1 prohibitin and Slr0228 FtsH homologues of *Synechocystis* sp. PCC 6803 (see Figure 5.20), the potential functional interactions between the two proteins do not appear to be essential for the growth of the cyanobacterium. However, it is worthy of note that *Synechocystis* sp. PCC 6803 possesses three other FtsH homologues (Sll1463, Slr1390 and Slr1604) which might be able to compensate for the inactivation of the Slr0228 homologue in the

Δ0228/ΔPhb1-3 quadruple mutant. In a previous study, the Slr1390 and Slr1604 FtsH homologues of *Synechocystis* sp. PCC 6803 have been shown to be essential for cell growth (Mann et al., 2000) and it appears to be worthwhile to examine the possible interactions between these three other FtsH homologues and the Band 7 proteins.

A photoinhibition analysis was performed to assess whether the PSII repair cycle operates and remains functional under prolonged exposure to high-light intensities in the ΔPhb1-4 quadruple mutant strain (see Figure 4.13). In this assay, the functioning of the PSII repair cycle is assessed indirectly by measuring the oxygen evolution of whole cells. Again, no difference between the wild-type and the ΔPhb1-4 quadruple mutant could be observed, and after a slight initial decrease in oxygen evolution in both strains, it remained relatively stable thereafter at 80 % of the initial oxygen evolution rates.

Summarising the presented data, it could not be shown that the Phb1, Phb2, Phb3 and Phb4 Band 7 proteins of *Synechocystis* sp. PCC 6803 play an important role in the PSII repair cycle under the tested conditions. Therefore, the hypothesised working model of this work is not supported by experimental data with regards to D1 protein stabilisation, even though it is still possible that the Band 7 proteins of *Synechocystis* sp. PCC 6803 interact with and exhibit a chaperone activity for other, yet unidentified proteins.

4.5.3 The Band 7 proteins and NDH-1 protein complexes

The initial working hypothesis of this work was based on the assumption that the prohibitin homologues of *Synechocystis* sp. PCC 6803 and *S. cerevisiae* act analogously. In yeast, two prohibitin isoforms form a large hetero-multimeric protein complex that acts as a chaperone and protects newly synthesised copies of respiratory protein complex subunits (e.g. Cox2p and Cox3p) from the degradation by the m-AAA protease (Steglich et al., 1999; Nijtmans et al., 2000). Initially, the possible involvement of the Phb1 prohibitin homologue and the Band 7 proteins in the PSII repair cycle of *Synechocystis* sp. PCC 6803 was investigated, because previously the Slr0228 FtsH protease, also an AAA-type protease, has been shown to be involved in D1 protein degradation and thus to play an important role in this photo-protective mechanism (Silva et al., 2003). However, since no evidence in support of this working model could be found, an alternative hypothesis, that the Band 7 proteins might rather

be functionally associated with respiratory protein complexes of *Synechocystis* sp. PCC 6803, was investigated by immunoprecipitation (see Figure 4.14) and 2-D SDS PAGE analyses (see Figure 4.15). The focus of these experiments was directed on NDH-1 protein complexes, because specific antibodies for the NdhI and NdhJ subunits were readily available in the lab (Burrows et al., 1998) and the dynamics of NDH-1 protein complexes is well described in the literature (Herranen et al., 2004; Zhang et al., 2004).

The results from the immunoprecipitation analysis suggested that the Phb1 protein might specifically interact with the NdhI subunit, since the Phb1 protein could be immunoprecipitated with the αNdhI antiserum, and was absent from the immunoprecipitate of the αNdhJ antibody. However, it must be mentioned, that the used αNdhI and αNdhJ antisera were polyclonal and unpurified. Unfortunately, the immunoblots that were performed to demonstrate that the αNdhI and αNdhJ antisera immunoprecipitated their respective cognate subunits and to test whether the two Ndh subunits were present in the immunoprecipitate of the αPhb1 antibody were inconclusive. Since both the NdhI and NdhJ subunits can be found in the soluble subcomplex of the NDH-1M and the NDH-1L protein complexes (Battchikova et al., 2005), apart from the possibility that the αNdhJ antibody does not immunoprecipitate the NdhJ subunit, it remains elusive why a potential Phb1 prohibitin chaperone complex would only associate with the NdhI subunit and not with the NdhJ subunit. However, this analysis gives a first indication towards a possible interaction between a Band 7 protein and a NDH-1 protein complex subunit in *Synechocystis* sp. PCC 6803, but additional immunoprecipitation analyses with preferably purified αNdh antibodies are necessary to substantiate this finding.

In another experiment, 2-D SDS PAGE protein profiles of the *Synechocystis* sp. PCC 6803 wild-type GT and the ΔPhb1-4 quadruple mutant strains cultured under different CO_2 conditions were generated (see Figure 4.15), in order to study the dynamics of the protein complexes involved in the inorganic carbon (C_i) concentrating mechanism (CCM). NDH-1S protein complexes have been shown to be part of the CCM (Zhang et al., 2004) and while the induction of these complexes only takes a few hours at low C_i (Omata and Ogawa, 1985), once the complexes are induced, C_i uptake capacity remains high for several days (Benschop et al., 2003). Interestingly, the Slr0228 FtsH protease has been shown to be required for the induction of NDH-1S and

SbtA protein complexes that are involved in the CCM. Even though the precise role of Slr0228 is yet unclear, it seems conceivable that the protease might be involved in a CCM protein complex inducing signalling pathway, since these protein complexes fail to accumulate in the absence of the Slr0228 FtsH protease (Zhang, personal communication). In a previous DNA microarray study, where the global gene expression pattern upon C_i limitation was assessed in *Synechocystis* sp. PCC 6803, the transcript level of the Slr0228 FtsH protease has been found to be increased (2.39 fold), while no effect on the Band 7 transcripts has been reported (Wang et al., 2004). Analysing the generated 2-D SDS PAGE protein profiles, the CCM protein complexes were clearly inducible in both the *Synechocystis* sp. PCC 6803 wild-type and the ΔPhb1-4 quadruple mutant strains. However, in the obtained protein profile for the ΔPhb1-4 quadruple mutant that was subjected to a shift from high to low CO_2 level, it seemed as if the relative abundances of the newly induced NDH-1S_1, NDH-1S_2 and SbtA CCM protein complexes were slightly reduced in comparison to wild-type (compare Figure 4.15A3 and Figure 4.15B3). When the corresponding protein profiles for the Band 7 single mutants were analysed, the CCM protein complexes were found to have been induced to apparently wild-type levels (data not shown). Therefore, a proper quantification of the effect that seems to be apparent to the naked eye for the ΔPhb1-4 quadruple mutant would be necessary in order to be able to exclude a staining artefact of the gel. The fact that the CCM protein complexes seem to be induced to wild-type levels in the Band 7 single mutants and not in the ΔPhb1-4 quadruple mutant, might be attributed to possible redundancy of the Band 7 proteins, although, given the distant phylogenetic relationships among them (see Figure 3.3), this appears unlikely. In *S. cerevisiae*, the interaction between the prohibitin complex and respiratory protein complex subunits has been demonstrated using pulse-chase and subsequent 2-D SDS PAGE analyses on yeast strains that overexpress the prohibitin complex (Nijtmans et al., 2000). In this work, the Phb1 prohibitin and Slr0228 FtsH homologues of *Synechocystis* sp. PCC 6803 are shown to be interacting at low levels (<3 %; see Figure 5.20). Thus, it appears to be crucial for further studies to significantly increase the abundance of the Band 7 protein complexes in *Synechocystis* sp. PCC 6803, or to improve the sensitivity of the applied methods, to be able to identify possible interaction partners of the Band 7 proteins.

In summary, these experiments show that the NdhI subunit of NDH-1M or NDH-1L protein complexes might be associated directly or indirectly with the Phb1

prohibitin homologue of *Synechocystis* sp. PCC 6803. However, further experiments are necessary to substantiate this initial indication that Band 7 proteins of *Synechocystis* sp. PCC 6803 might act as chaperones on certain NDH-1 or other respiratory protein complex subunits.

4.5.4 Evidence for a chaperone activity of the Phb1 prohibitin homologue of *Synechocystis* sp. PCC 6803

Since the prohibitin complex of *S. cerevisiae* has been shown to act as a chaperone on newly synthesised respiratory protein complex subunits (Nijtmans et al., 2000), it has been hypothesised that a possible Phb1 prohibitin complex in *Synechocystis* sp. PCC 6803 might also display such a chaperone activity (Silva et al., 2002). However, in the previous chapter, cyanobacterial prohibitin homologues have been shown to be only distantly related to the prohibitins of yeast (see section 3.6). While in this work, the Phb1 protein could not be shown to act as a chaperone in the PSII repair cycle, some evidence could be gathered that the Phb1 protein might be associated with the NdhI subunit of NDH-1 protein complexes (see Figure 4.14). Furthermore, it appeared that an inactivation of the *phb1*, *phb2*, *phb3* and *phb4* Band 7 genes in the ΔPhb1-4 quadruple mutant might negatively affect the accumulation of CCM protein complexes after a downshift in the CO_2 levels (see Figure 4.15). Even though these observations need to be investigated further, they represent first hints for a chaperone activity of the Phb1 protein of *Synechocystis* sp. PCC 6803.

In this context, it is noteworthy that yeast two hybrid data (provided by Prof. Satoshi Tabata, Kazusa DNA Research Institute, Kisarazu, Japan; data not shown) revealed that the Phb1 protein might interact with the Slr1918 protein, which contains a DnaJ domain at its N-terminus (InterPro database). 40-kDa heat shock proteins (Hsp40; also termed DnaJ) are crucial partners for 70-kDa heat shock proteins (Hsp70, also termed DnaK) chaperones and their J-domain is involved in mediating the interaction with (Han et al., 2007) and regulating the activity of the interacting Hsp70 protein (Karzai and MacMacken, 1996; Walsh et al, 2004 and Qiu et al., 2006). However, there is also evidence that some members of the DnaJ protein family might be chaperones in their own right (Gamer et al., 1996). Hsp70 chaperones are involved in the folding of nascent polypeptide chains, rescue of misfolded proteins, translocation of polypeptide chains through membranes, assembly and disassembly of

protein complexes and the control of the biological activity of folded regulatory proteins (Han and Christen, 2004). According to the CyanoBase database (http://bacteria.kazusa.or.jp/cyano/) *Synechocystis* sp. PCC 6803 possesses three assigned DnaK proteins (Sll1932, Sll0058, Sll0170) and one DnaK-like protein (Slr0086). Furthermore, three assigned DnaJ proteins (Sll0897, Sll1933 and Slr0093) and two proteins that are assigned DnaJ-like proteins (Sll1384 and Sll1666) could be identified in *Synechocystis* sp. PCC 6803 by a search of the same database. Typically, a DnaJ or DnaJ-like protein contains one to four of the following regions: a 70-residue N-terminal domain (J-domain), a 30-residue glycine-rich region (G-domain), a central domain containing repeats of a CxxCxGxG motif (the CRR-domain) and a 120-170 residue C-terminal region (InterPro database; accession number: IPR012724; Cheetham and Caplan, 1998), while only the J-domain seems to be completely conserved in all of the DnaJ protein family members (Martinez-Yamout et al., 2000). DnaJ proteins are subdivided into 3 types, depending on the degree of conservation: Type I = full domain conservation with DnaJ; Type II = J- and G-domains conserved; Type III = only the J-domain conserved (Cheetham and Caplan, 1998). The DnaJ protein family is extremely diverse in sequence and function (Cheetham and Caplan, 1998), and apparently, Slr1918 of *Synechocystis* sp. PCC 6803 represents a Type III DnaJ protein. An alignment of the Phb1 prohibitin homologue with the four DnaK and DnaK-like proteins of *Synechocystis* sp. PCC 6803 did not reveal any significant sequence similarities between the proteins (data not shown). Thus, since no sequence homology between the Phb1 and the Hsp70 (DnaK) proteins in *Synechocystis* sp. PCC 6803 could be identified, it remains unclear if the Phb1 protein does really interact with the Slr1918 protein and what the functional implications for this potential chaperone system might be. However, it would be interesting to generate a *slr1918* gene inactivation mutant, in order to perform biochemical assays and to test whether there is an interaction between the two proteins.

Previously, it has been reported that the Phb1 and Phb2 prohibitin homologues of *S. cerevisiae* exhibit a small, but significant sequence homology to Hsp60 chaperones (Nijtmans et al., 2000). A prominent member of the Hsp60 chaperone family is the GroEL protein of *E. coli* which forms a large, soluble protein complex that consists out of two stacked, heptameric rings, each containing a central cavity (Xu et al., 1997). In *E. coli*, GroEL in combination with its cochaperonine GroES and ATP facilitates protein folding by providing an environment that stabilises the native state

and furthermore, it has been suggested that this chaperone complex might also unfold misfolded proteins (Zahn et al., 1996). However, again, it needs to be emphasised that the Phb1 prohibitin homologue of *Synechocystis* sp. PCC 6803 is only distantly related to the prohibitin homologues of *S. cerevisiae* (see section 3.6). Additionally, a CyanoBase database search (http://bacteria.kazusa.or.jp/cyano/) revealed that *Synechocystis* sp. PCC 6803 already possesses two Hsp60 homologues (*sll0416* and *slr2076*). These two proteins could be shown to display some sequence homology to the GroEL protein of *E. coli*, while in the same phylogenetic analysis no relationships between the Band 7 proteins of *Synechocystis* sp. PCC 6803 and the Hsp60 homologues could be observed (data not shown). Given these observations, it seems unlikely that the Band 7 proteins of *Synechocystis* sp. PCC 6803 display a functional homology to the Hsp60 protein family.

Overall, the functional role and physiological relevance of the Phb1 prohibitin homologue in particular and the Band 7 proteins of *Synechocystis* sp. PCC 6803 in general remains enigmatic. Nevertheless there are some indications that the Phb1 protein might act as a chaperone in the cyanobacterium, but further experiments are necessary to follow up on these initial findings.

Chapter 5: Characterisation of Band 7 proteins and their complexes

To be able to identify cyanobacterial Band 7 proteins for subsequent characterisation, polyclonal antibodies were raised against *E. coli*-overexpressed Band 7 proteins of *Synechocystis* sp. PCC 6803 (see section 5.1.1 and section 5.1.2). The antibodies were affinity-purified and used to identify Band 7 proteins in crude membrane isolations of *Synechocystis* sp. PCC 6803 and *Thermosynechococcus elongatus* (see section 5.1.3). Then cyanobacterial Band 7 proteins were analysed with regards to membrane association and localisation (see section 5.2.2), while an analysis of the identified Band 7 protein complexes focused on their sizing and the identification of possible interaction partners (see section 5.2.3 to section 5.2.5). A further aim of this study was to characterise Band 7 protein complexes structurally. Consequently, C-terminal His_8-tags were added to the Phb1, Phb2, Phb3 and Phb4 proteins of *Synechocystis* sp. PCC 6803 to facilitate their purification (see section 5.3). One subsequent affinity-purification used Ni-NTA magnetic agarose beads (see section 5.4.1), but only an immunoprecipitation approach with purified antibodies coupled to Protein A sepharose beads (see section 5.4.2) yielded material of sufficient quality and quantity for a single-particle analysis of Phb3 protein complexes (see section 5.5). Furthermore, immunoprecipitates generated from crude membrane isolations of the 0228-GST-tagged strain were probed with Band 7 antibodies to investigate possible interactions between Band 7 proteins and the Slr0228 FtsH homologue (see section 5.6).

5.1 Generation and testing of purified, polyclonal antibodies

One aim of this work was to produce polyclonal antibodies directed against the Band 7 proteins of *Synechocystis* sp. PCC 6803. Previously, a polyclonal antibody specific for the Phb1 protein had been generated (P. Nixon, unpublished data), so that only the expression constructs to overexpress the remaining four Band 7 proteins of *Synechocystis* sp. PCC 6803 in *E. coli* needed to be synthesised (see Figure 5.1 and Figure 5.2A). The overexpressed proteins (see Figure 5.2B) were affinity-purified (see Figure 5.2C) and used for the immunisation of rabbits. Finally, the generated

polyclonal antibody sera were also affinity-purified and tested on *Synechocystis* sp. PCC 6803 and *Thermosynechococcus elongatus* crude membrane isolations (see Figure 5.3).

5.1.1 Generation of expression constructs

Initially, four Band 7 genes of *Synechocystis* sp. PCC 6803 (*phb2*, *phb3*, *phb4* and *phb5*) were amplified from genomic DNA isolated from the wild-type GT strain in a standard PCR reaction with the BIO-X-ACT DNA polymerase and specific primers. The obtained fragments were cloned into the pGEM-T Easy vector and after excision

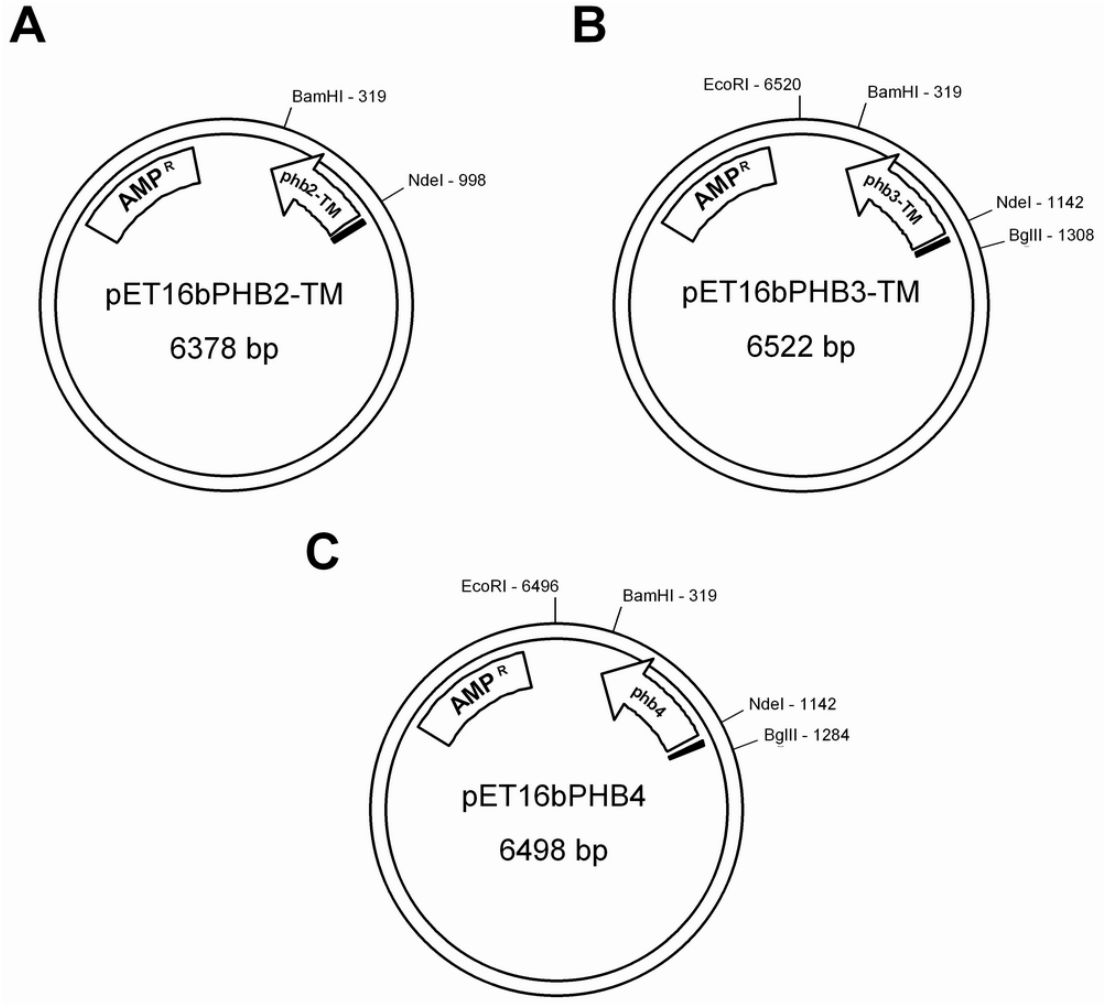

Figure 5.1: Schematic representation of expression constructs. The expression constructs (A) pET16bPHB2-TM, (B) pET16bPHB3-TM and (C) pET16bPHB4 were schematically drawn. The restriction enzymes that were used to insert the PCR fragments and for the analytical restriction digestions (see Figure 5.2A) are indicated. Direction of transcription is indicated by an arrow-like representation of the gene. The coding sequence for the N-terminal His_{10}-tag of the resulting protein is marked as a black box.

with the respective restriction enzymes (*phb2*, *phb3* and *phb4* with BamHI and NdeI and *phb5* with BglII and NdeI; restriction sites had been introduced by the previously used primers) inserted into the pET16b expression vector, which had been linearised with BamHI and NdeI restriction enzymes (BamHI and BglII produce compatible ends) (see Figure 5.1). The pET16b expression vector adds a His_{10}-tag at the N-termini of expressed proteins, which was a prerequisite for the intended affinity-purification procedure. Even though various bacterial strains were tested, it was not possible to overexpress full-length Phb2, Phb3 and Phb5 proteins. Consequently, truncated versions of the respective genes, in which the coding sequences for the N-terminal TM domains had been deleted (*Δ1-225phb2*, *Δ1-150phb3* and *Δ1-300phb5*), were amplified, subcloned and inserted into the pET16b expression vector as described for the full-length fragments (see Figure 5.1). Deletion of TM domains allowed overexpression of the truncated versions of the Phb2 and Phb3 proteins (Phb2-TM and Phb3-TM), whereas the Phb5 protein could still not be overexpressed. No more attempts were made to obtain the Phb5 protein and the antibody generation for this protein was not carried further. Analytical restriction digestions were performed on the final expression constructs pET16bPHB2-TM, pET16bPHB3-TM and pET16bPHB4 (see Figure 5.2A). The expression construct pET16bPHB2-TM could be linearised with a single cut of the restriction enzymes BamHI or NdeI, while both restriction enzymes together excised the expected 680 bp fragment. The expression constructs pET16bPHB3-TM and pET16bPHB4 could be linearised with a single cut of the restriction enzymes BglII or EcoRI, while both restriction enzymes together excised the expected 1310 and 1284 bp fragments respectively. Moreover, the sequencing of all expression constructs (ABC sequencing, Imperial College London, London, UK) confirmed that no mutation had been introduced during the cloning process (data not shown).

5.1.2 Expression and purification of antigens

In order to identify the combinations of expression constructs and bacterial strains with which the proteins of interest could be expressed, small-scale expression experiments were performed and resulting whole cell extracts were analysed using 1-D SDS PAGE (data not shown). While full-length Phb4 protein (~30 kDa) was readily expressed, the Phb2 and Phb3 proteins could only be expressed as truncated versions

without their TM domains (Phb2-TM (~25 kDa) and Phb3-TM (~30 kDa)) in the BL21-Gold(DE3)pLysS *E. coli* strain (see Figure 5.2B). Expression of the Phb5 protein could not be achieved from any tested combination of expression construct and bacterial strain. Generally, expression constructs were expressed constitutively in the Rosetta(DE3) *E. coli* strain (data not shown), while the expression of the same construct was usually inducible with IPTG in the BL21-Gold(DE3)pLysS *E. coli* strain (see Figure 5.2B).

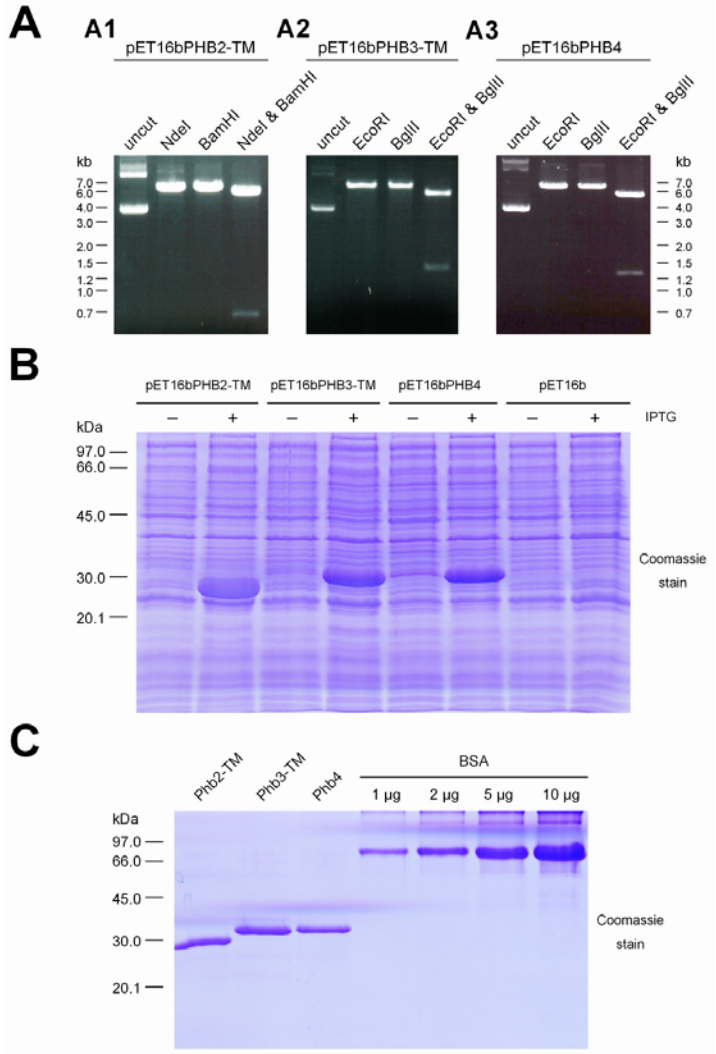

Figure 5.2: Antigen generation. Various stages of the antigen generation procedure are shown. (A) Analytical restriction digestions of the expression constructs (A1) pET16bPHB2-TM, (A2) pET16bPHB3-TM and (A3) pET16bPHB4. (B) Protein expression of various expression constructs in the BL21-Gold(DE3)pLysS *E. coli* strain assessed in the absence (-) and presence (+) of IPTG. Whole cell extracts of an amount of cells corresponding to an OD_{600} of 0.1 (in 10-µl aliquots) were loaded in the lanes of an 1-D SDS PAGE gel. (C) A small aliquot of the purified overexpressed proteins (total volumes were 800 µl) was diluted (1:20) and 1 µl of the dilution was analysed by 1-D SDS PAGE. All gels were Coomassie-stained. Phb2-TM (~25 kDa), Phb3-TM (~30 kDa) and Phb4 (~30 kDa). Internal BSA standards (1 µg, 2 µg, 5 µg and 10 µg) were loaded on the gel to estimate the amounts of generated antigen.

Therefore, the latter strain was used to overexpress the Phb2-TM, Phb3-TM and Phb4 proteins on a large-scale for the subsequent quantitative purification (see Figure 5.2C). The overexpressed proteins formed inclusion bodies and were purified using the bug buster procedure (data not shown). The purified inclusion bodies were then solubilised in binding buffer (containing 6 M guanidium hydrochloride) and the proteins of interest quantitatively bound overnight to a Ni^{2+}-charged resin in a batch method. Following various washing steps with buffers containing an increasing concentration of imidazole, proteins were eluted with 300 mM imidazole. During an overnight dialysis step against 1x PBS, proteins in the eluate precipitated and were pelleted. The obtained protein pellets were resuspended in 500 µl 1x PBS and solubilised by the addition of 300 µl 10 % (w/v) SDS (total [3.75 % (w/v)]). A 1-D SDS PAGE analysis of the purified and diluted antigens revealed that the samples were rather pure and by comparison of the Coomassie-stained bands of the antigens with the internal standard with the naked eye, suggested that the loaded amounts of antigen corresponded to roughly 2 µg of protein. Consequently, each 1000-ml *E. coli* culture had yielded approximately 32 mg of target protein (see Figure 5.2C).

5.1.3 Testing the purified antibodies

10 mg of each purified antigen were sent to Seqlab (Göttingen, Germany) for the immunisation of two rabbits. After the completion of a three-month immunisation protocol, the generated polyclonal antibody sera were received, affinity-purified (using antigen columns; antigens coupled to CNBr activated sepharose) and tested for their specificity. Although two independent antibody sera against each antigen were produced and tested, only one of each was used for the purification of specific antibodies. It must be noted, that unless stated otherwise, all the presented results generated with Band 7 protein antibodies (henceforth indicated by αPhb1 to αPhb4), resulted from the purified antibody sera of αPhb1, αPhb2-1, αPhb3-1 and αPhb4-1.

Initially, the newly generated and purified antibodies (αPhb2, αPhb3 and αPhb4) were tested on the overexpressed and purified antigens (Phb2-TM, Phb3-TM and Phb4) (see Figure 5.3A). As the purified antibodies solely recognised their respective antigens, while the corresponding preimmune sera did not show cross reactions with the antigens (data not shown), it could be deduced that specific antibodies had been raised and purified.

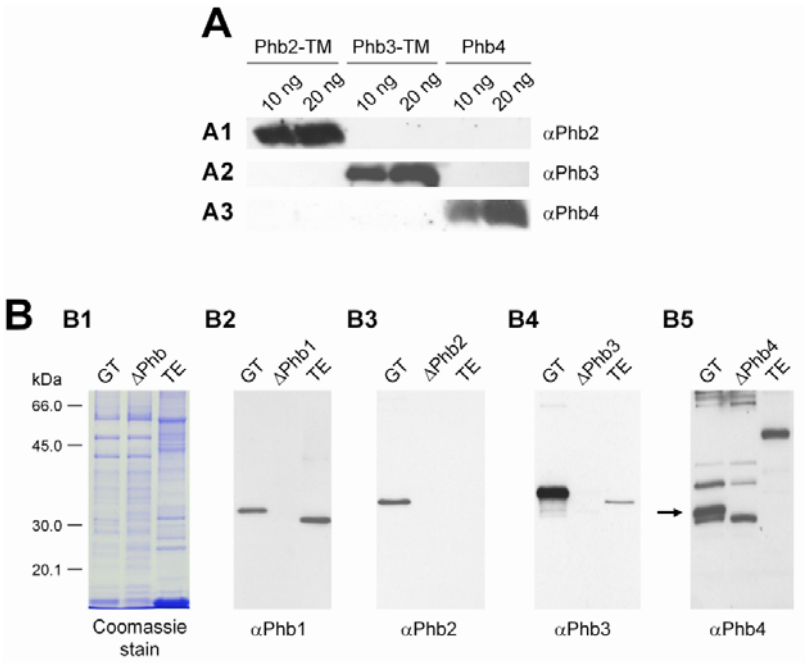

Figure 5.3: Testing the purified, polyclonal antibodies. Immunoblotting analysis using the generated and purified, polyclonal antibodies (A) on the various antigens and (B) on crude cyanobacterial membrane isolations. (A) 10 and 20 ng of each overexpressed antigen (Phb2-TM, Phb3-TM and Phb4) were loaded on a 1-D SDS PAGE gel. The resulting immunoblots were probed with purified antibodies: (A1) αPhb2, (A2) αPhb3 and (A3) αPhb4. (B) Crude membrane isolations were performed on the *Synechocystis* sp. PCC 6803 wild-type GT strain (GT), prohibitin inactivation mutants (ΔPhb1 to ΔPhb4) and *Thermosynechococcus elongatus* (TE). The amount that was loaded on a 1-D SDS PAGE gel corresponded to 1 µg chlorophyll a. The gels were (B1) Coomassie-stained or transferred to a nitrocellulose membrane and probed with the purified antibodies: (B2) αPhb1, (B3) αPhb2, (B4) αPhb3 and (B5) αPhb4.

Next, the purified antibodies were tested on crude cyanobacterial membrane isolations. As a preliminary experiment had shown that cyanobacterial Band 7 proteins were membrane-associated (data not shown), crude membranes were isolated from *Synechocystis* sp. PCC 6803 wild-type GT (GT), various prohibitin inactivation mutants (ΔPhb1 to ΔPhb4) and *Thermosynechococcus elongatus* (TE) and used for immunoblotting analyses with the purified antibodies (see Figure 5.3B). The purified αPhb1 antibodies recognised one protein with an approximate molecular mass of about 30 kDa in *Synechocystis* sp. PCC 6803 wild-type GT, while no signals were observed for the ΔPhb1 inactivation mutant. Thus, the observed signal could be attributed to the Phb1 protein of *Synechocystis* sp. PCC 6803. In *Thermosynechococcus elongatus* also one protein with an apparent, slightly lower molecular mass was detected, but no ΔPhb1 inactivation mutant was available to confirm the identity of this protein. The purified αPhb2 antibodies recognised one protein with an approximate molecular mass

of about 32 kDa in *Synechocystis* sp. PCC 6803 wild-type GT, while no signals were observed in the ΔPhb2 inactivation mutant. Thus, the observed signal could be attributed to the Phb2 protein of *Synechocystis* sp. PCC 6803. In *Thermosynechococcus elongatus* no protein was detected by the purified antibodies. The purified αPhb3 antibodies recognised one protein with an approximate molecular mass of about 35 kDa in *Synechocystis* sp. PCC 6803 wild-type GT, while no signals were observed in the ΔPhb3 inactivation mutant. Thus, the observed signal could be attributed to the Phb3 protein of *Synechocystis* sp. PCC 6803. In *Thermosynechococcus elongatus* also one protein with a slightly lower molecular mass and a relatively weaker antibody signal than for the protein detected in *Synechocystis* sp. PCC 6803 could be observed. Unfortunately, no ΔPhb3 inactivation mutant was available to confirm the identity of this protein. The purified αPhb4 antibodies were not very specific and recognised several proteins in *Synechocystis* sp. PCC 6803 wild-type GT and all but one signal could also be detected in the ΔPhb4 inactivation mutant. Thus, the purified antibodies recognised the Phb4 protein of *Synechocystis* sp. PCC 6803, however the non-specificity and the proximity of unspecific cross reactions rendered this antibody almost useless for the intended analyses. Unfortunately, the αPhb4-2 antibody serum displayed similar, unspecific cross reactions (data not shown) and could therefore not be considered an appropriate alternative. In *Thermosynechococcus elongatus* the purified αPhb4 antibodies recognised one protein with a relatively high molecular mass of about 50 kDa. Although no ΔPhb4 inactivation mutant was available this signal was unspecific, because no homologue had been reported for the Phb4 protein in this organism. In each case, the respective preimmune sera had been used as control (data not shown) and it could be confirmed that the observed signals of the purified antibodies resulted from antibodies that had been raised during the immunisation procedure.

5.2 Characterisation of cyanobacterial Band 7 proteins and their complexes

The previous section demonstrated that the purified antibodies specifically identified cyanobacterial Band 7 proteins and were therefore appropriate tools to characterise these proteins and their complexes in *Synechocystis* sp. PCC 6803 and

Thermosyne-chococcus elongatus. In a first experiment the expression of Band 7 proteins of both the *Synechocystis* sp. PCC 6803 wild-type and the *Synechocystis* sp. PCC 6803 wild-type GT strains were compared (see Figure 5.4A). Then the expression of Band 7 proteins was probed in the generated single Band 7 gene inactivation mutants (see Figure 5.4B). A differential protein extraction was performed to address the question whether the Band 7 proteins of *Synechocystis* sp. PCC 6803 were peripheral or integral membrane proteins (see Figure 5.5A). To allocate the Band 7 proteins of *Synechocystis* sp. PCC 6803 to either the thylakoid or plasma membrane, a two-phase partitioning experiment followed by immunoblotting was performed (see Figure 5.5B). Finally, the protein complexes of *Synechocystis* sp. PCC 6803 and *Thermosynechococcus elongatus* were separated and analysed under native conditions by FPLC (see Figure 5.6), sucrose-density gradient centrifugation (see Figure 5.7) and 1-D BN PAGE (see Figure 5.8 and Figure 5.10) followed by immunoblotting.

5.2.1 Expression of Band 7 proteins in *Synechocystis* sp. PCC 6803

In a first experiment, the expression of Band 7 proteins was compared between the *Synechocystis* sp. PCC 6803 wild-type and the *Synechocystis* sp. PCC 6803 wild-type GT strains (see Figure 5.4A). In another analysis, the expression of Band 7 proteins was probed in various Band 7 gene inactivation mutants (see Figure 5.4B).

The protein profiles of crude membrane isolations of both the *Synechocystis* sp. PCC 6803 wild-type (WT) and the glucose-tolerant (GT) strains were observed on a silver-stained 1-D SDS PAGE gel, but did not seem to differ significantly (see Figure 5.4A1). Both strains were grown under similar conditions, the only difference being that the media in which the GT strain was grown contained 5 mM glucose. On the silver-stained gel, the only obvious differences detected with the naked eye, were three distinct, but unidentified protein bands in the *Synechocystis* sp. PCC 6803 wild-type strain (marked with an arrow). Immunoblotting analyses revealed that the Phb1, Phb2 and Phb3 proteins were almost equally expressed in both strains. However, the expression level of the SbtA protein, a sodium-dependent bicarbonate transporter located in the plasma membrane of *Synechocystis* sp. PCC 6803 (see Figure 5.5B), was significantly elevated in the wild-type strain when compared to the glucose-tolerant strain. The expression levels of the D1 thylakoid membrane protein of PSII did not differ between both strains.

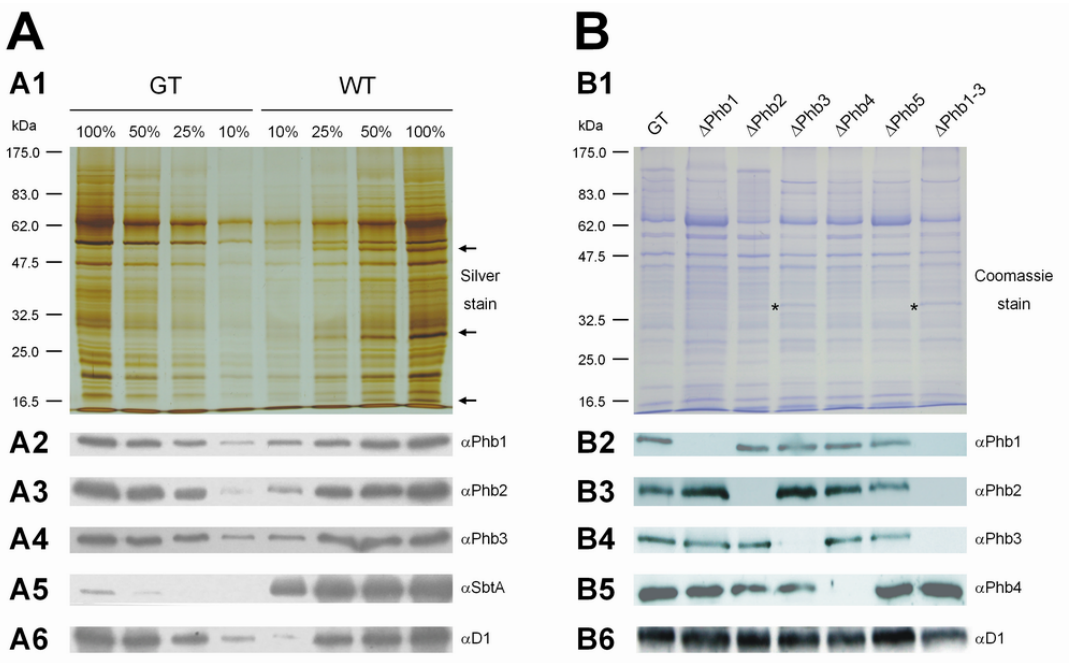

Figure 5.4: Expression of Band 7 proteins of *Synechocystis* sp. PCC 6803. The expression of Band 7 proteins of *Synechocystis* sp. PCC 6803 was assessed in (A) the wild-type (WT; grown in liquid BG-11) and the glucose-tolerant (GT; grown in liquid BG-11 supplemented with 5 mM glucose) strains and (B) in various Band 7 gene inactivation mutant strains. (A and B) Crude membrane isolations were performed on the various strains and an amount corresponding to 1 µg of chlorophyll a (100 %) was loaded in each lane of a 1-D SDS PAGE gel, while respectively less was loaded in the dilution series. One gel of each analysis was (A1) silver-stained or (B1) Coomassie-stained. (A1) Arrows indicate proteins that were present in the *Synechocystis* sp. PCC 6803 wild-type strain, but not in the glucose-tolerant strain. (B1) Asterisks indicate a protein band that seemed to be linked to the inactivation of the *phb3* gene. (A2 to A6 and B2 to B6) Immunoblots were probed with indicated antibodies.

In the analysis of the various Band 7 gene inactivation mutants, only minor differences could be detected in the protein profiles (see Figure 5.4B1). However, one additional protein with an apparent molecular mass of about 35 kDa could be observed in the ΔPhb3 and in the ΔPhb1-3 triple inactivation mutants, but remained unidentified and could not always be reproduced. Nevertheless, the immunoblotting analysis demonstrated that the disruption of a gene with an antibiotic-resistance cassette lead to the disappearance of the signal for the respective Band 7 protein. Thus, the results of the PCR analyses performed to test the segregation of the inactivation mutants were confirmed at the protein level. In the crude membrane isolations of the *Synechocystis* sp. PCC 6803 glucose-tolerant strain all the Phb1, Phb2, Phb3 and Phb4 Band 7 proteins could be detected. In the inactivation mutants the respective proteins that were insertionally inactivated were not present, while the expression of the other Band 7 proteins did not seem to be affected. Probing an immunoblot with the D1 antibody

showed that the lanes of the gels had been loaded equally and that the proteins had been transferred properly onto the nitrocellulose membrane.

5.2.2 Membrane association and localisation of Band 7 proteins

In order to test whether the Band 7 proteins of *Synechocystis* sp. PCC 6803 were peripheral or integral membrane proteins, a differential membrane protein extraction procedure (Breyton et al., 1994) and immunoblotting was performed (see Figure 5.5A). The respective membrane in which a Band 7 protein resides was determined by two-phase partitioning followed by immunoblotting (see Figure 5.5B).

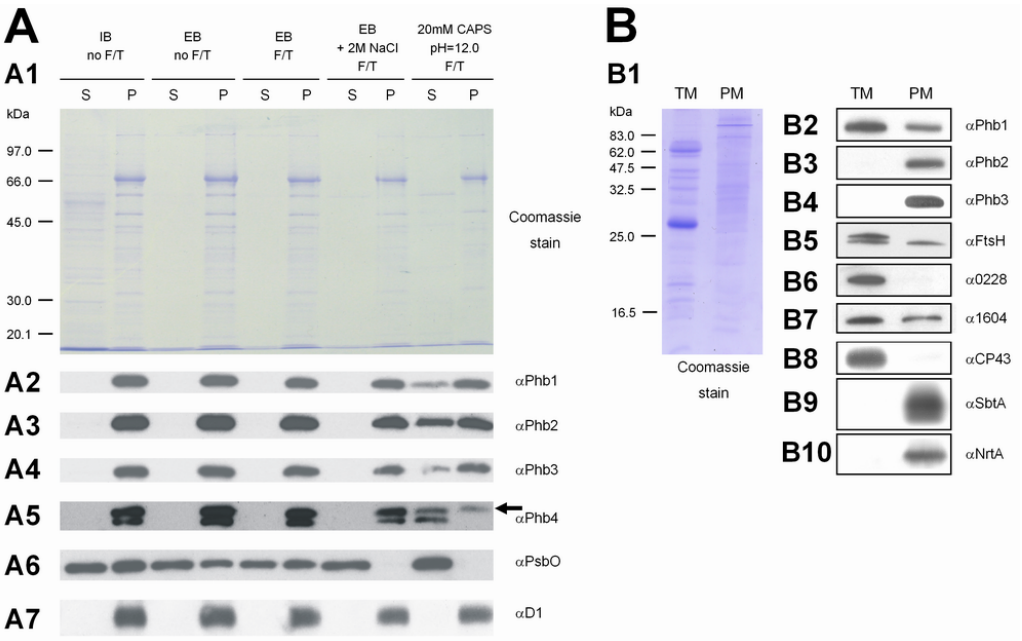

Figure 5.5: Membrane association and localisation of Band 7 proteins of *Synechocystis* sp. PCC 6803. (A) A differential membrane protein extraction and (B) a two-phase partitioning experiment were performed on crude membrane isolations of the *Synechocystis* sp. PCC 6803 wild-type GT strain. (A) Crude membrane isolations of the *Synechocystis* sp. PCC 6803 wild-type GT strain were washed in various buffers: isolation buffer (IB), extraction buffer (EB), 2 M NaCl in EB and 20 mM CAPS pH = 12.0. Membranes were pelleted in an ultracentrifuge either directly (no F/T) or after two consecutive freeze/thaw (F/T) cycles and separated into a soluble (S) and a pellet (P) fraction. Aliquots corresponding to an amount of 1 µg of chlorophyll a were loaded in each lane. One gel was (A1) Coomassie-stained, while (A2 to A7) other gels were used for immunoblotting analyses with various, indicated antibodies. (A5) The antibody signal corresponding to the Phb4 protein is indicated by an arrow. (B) Crude membrane isolations of the *Synechocystis* sp. PCC 6803 wild-type GT strain were separated into thylakoid (TM) and plasma membrane (PM) fractions by two-phase partitioning. Aliquots corresponding to an amount of 5 µg of protein were loaded in each lane. One gel was (B1) Coomassie-stained, while other gels were used for (B2 to B10) immunoblotting analyses with various, indicated antibodies.

The TMPRED server had predicted that most of the Band 7 proteins of *Synechocystis* sp. PCC 6803, except for the Phb4 protein, possessed at least one TM domain (see Table 3.3). To test this, a differential membrane protein extraction procedure was performed on crude membrane isolations, in order to assess whether these proteins were peripheral or integral membrane proteins (see Figure 5.5A). Crude *Synechocystis* sp. PCC 6803 wild-type GT membranes were isolated, resuspended in different buffers and treated in various, indicated ways. At the end of each treatment, the sample was pelleted in an ultracentrifuge and fractionated into a soluble (i.e. the supernatant) and a pellet fraction that were analysed by 1-D SDS PAGE and immunoblotting. The generated blots were probed with antibodies directed against cyanobacterial Band 7 proteins, as well as with control antibodies that recognised the following proteins: the peripheral PsbO protein (the 33-kDa protein of the oxygen-evolving complex of photosystem II; should be readily extracted) and the integral membrane PsbA protein (the D1 protein of the photosystem II reaction centre; should not be extracted). It is important to mention, that the upper signal of the doublet αPhb4 antibody signal (indicated with an arrow) corresponds to the Phb4 protein (see Figure 5.3B5). When the crude membrane isolations were resuspended in isolation buffer without a freeze/thaw (F/T) treatment, approximately equal amounts of the PsbO protein could be found in the soluble and the pellet fractions. The Band 7 and D1 proteins however, were exclusively found in the pellet fraction. The observations that had been made for the treatment with isolation buffer, were also made for the treatment with extraction buffer without and with F/T cycles. Under slightly harsher, but still rather mild extraction conditions, i.e. resuspension in extraction buffer with 2 M NaCl and F/T cycles, the PsbO protein was completely extracted from the membranes and was solely found in the soluble fraction. The D1 and the Band 7 proteins however, were still associated with their respective host membrane and could entirely be found in the pellet fraction. As the extraction conditions became harsher, i.e. 20 mM CAPS pH = 12.0 and F/T cycles, the PsbO protein was again completely extracted from the membranes, and the Band 7 proteins could also be extracted to varying degrees from the membranes under these conditions. Only the D1 protein could not be extracted from the membranes, even under the harsh extraction conditions. In conclusion, the Phb1, Phb2, Phb3 and Phb4 Band 7 proteins of *Synechocystis* sp. PCC 6803 are probably integral membrane proteins that are, however, only weakly associated to their respective host membrane.

A two-phase partitioning experiment followed by immunoblotting analyses (see Figure 5.5B) allowed to determine whether the Band 7 and other proteins of interest reside in the thylakoid, in the plasma or in both membranes. The separated membranes were kindly provided by Prof. Eva-Mari Aro's group (University of Turku, Turku, Finland). Unfortunately, the purified membranes were a scarce material, so that no dilution series could be included on the gels and the antibody signals could not be quantitatively compared. However, analysing the immunoblots, the Phb1 protein of *Synechocystis* sp. PCC 6803 could be found in both the thylakoid and plasma membrane (see Figure 5.5B2), with a slightly larger proportion residing in the thylakoid membrane. The Phb2 and Phb3 proteins were exclusively found in the plasma membrane (see Figure 5.5B3 and Figure 5.5B4). Other proteins that were relevant to this work included FtsH protease homologues, so that some immunoblots were probed with available antibodies against these proteins. The αFtsH antibody is directed against all four FtsH homologues of *Synechocystis* sp. PCC 6803 and previous analyses had attributed the upper band of the doublet antibody signal to the Slr0228 FtsH homologue (data not shown). Therefore, the Slr0228 protein seemed to exclusively reside in the thylakoid membrane, while other FtsH homologues appeared to be also present in the plasma membrane (see Figure 5.5B5). This was supported by the findings with other specific antibodies directed against the Slr0228 and Slr1604 FtsH homologues. The α0228 antibody gave a signal that was exclusively found in the thylakoid membrane (see Figure 5.5B6), whereas the α1604 antibody detected the Slr1604 protein in both, the thylakoid and plasma membrane (see Figure 5.5B7). Three control immunoblots were performed to assess the degree of purity of the used membranes. The CP43 protein is an integral part of the PSII core complex and a marker for the thylakoid membrane (see Figure 5.5B8). Both, the SbtA (a sodium-dependent bicarbonate transporter) and the NrtA (a nitrate transporter) proteins are markers for the plasma membrane (see Figure 5.5B9 and Figure 5.5B10). The tested control proteins were exclusively found in the expected membrane fractions, but the lack of a dilution series impeded an estimation on the purity of the used membranes.

5.2.3 Characterisation of Band 7 protein complexes using FPLC

Fast protein liquid chromatography (FPLC) was one of the protein separation techniques used in conjunction with immunoblotting analyses to study the Band 7

protein complexes of *Synechocystis* sp. PCC 6803 and *Thermosynechococcus elongatus* (see Figure 5.6).

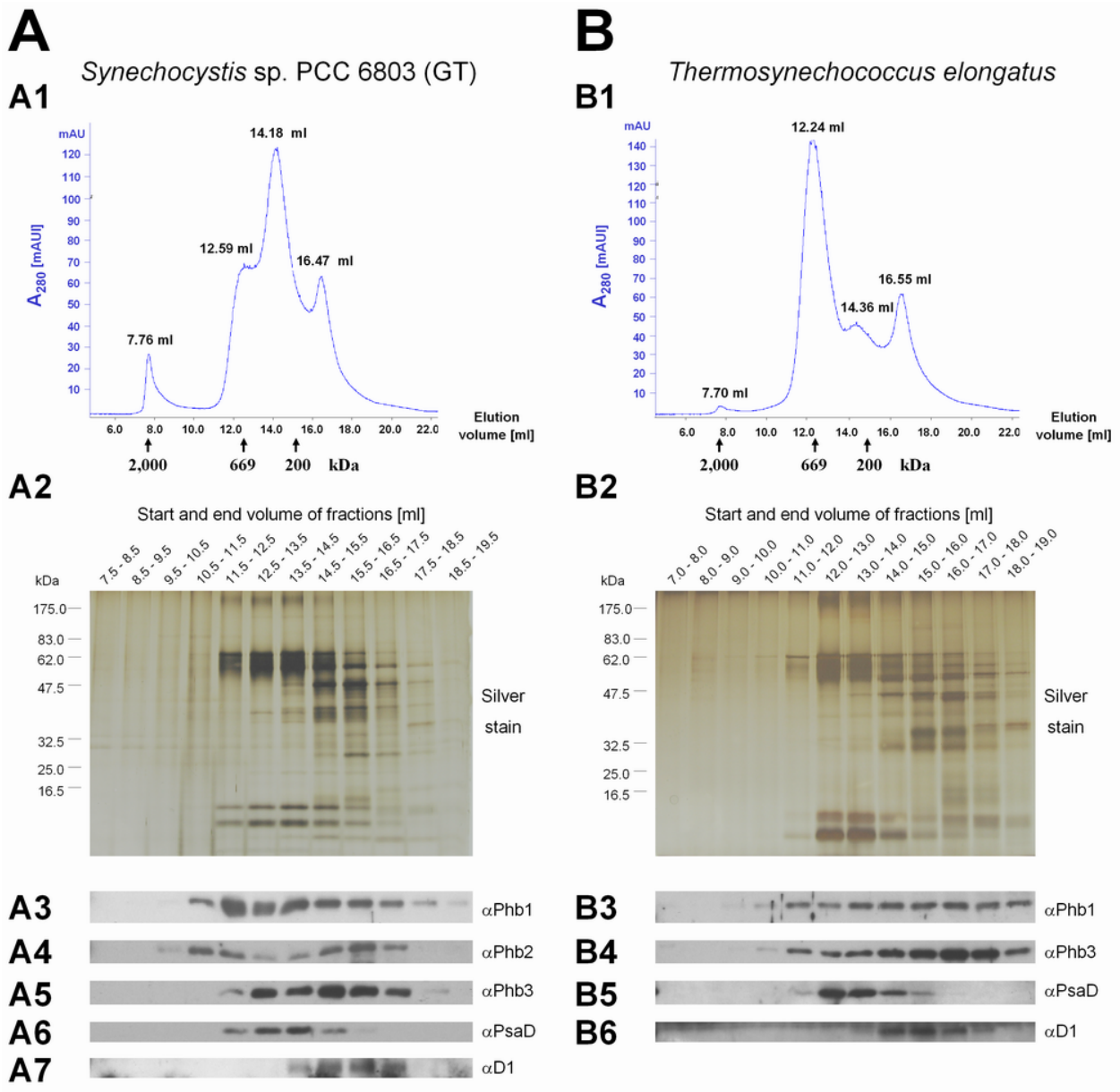

Figure 5.6: Separation of cyanobacterial protein complexes by FPLC. Crude membrane isolations of (A) *Synechocystis* sp. PCC 6803 wild-type GT and (B) *Thermosynechococcus elongatus* were separated by FPLC and analysed by immunoblotting. (A1 and B1) Absorption spectra of the eluate recorded at 280 nm. Marker proteins were run separately and respective elution peaks are indicated as little arrows underneath the X-axis: 2,000 kDa at 7.76 ml, 669 kDa at 12.34 ml and 200 kDa at 15.14 ml. Elution volumes of sample peaks are also indicated. 500-µl fractions of the samples were collected and 7.5-µl aliquots of each fraction were analysed on a 1-D SDS PAGE gel. One gel each was (A2 and B2) silver-stained, while other gels were used for (A3 to A7 and B3 to B6) immunoblotting analyses with various antibodies.

Crude membranes were isolated from *Synechocystis* sp. PCC 6803 wild-type GT and *Thermosynechococcus elongatus* and solubilised proteins and protein complexes were separated according to their sizes on a Superose 6 column (Amersham Biosciences, UK). The resulting fractions were immunochemically analysed with various antibodies. Initially, a set of marker proteins was analysed in three separate FPLC runs to be able to roughly size the Band 7 protein complexes (data not shown). The void volume of the column, i.e. the volume which has to pass from sample injection until the first proteins of the sample elute, was determined using Blue Dextran (molecular mass ~2,000 kDa). In this case, the void volume corresponded to 7.76 ml, as the peak for Blue Dextran could be detected in the A_{280} absorption spectrum after this volume had passed through the column. Thryoglobulin (669 kDa) was detected when 12.34 ml had passed through the column, while 15.14 ml had to pass through until the amylase protein (200 kDa) could be detected. These elution times are indicated underneath the X-axis as reference (see Figure 5.6A1 and Figure 5.6B1).

When the recorded A_{280} absorption spectrum of the FPLC run of crude membrane isolation of *Synechocystis* sp. PCC 6803 wild-type GT was analysed (see Figure 5.6A1), the first peak, corresponding to the void volume of the column, was detected after 7.76 ml. Three other peaks were observed after 12.59 ml, 14.18 ml and 16.47 ml respectively, of which the one in the middle (after 14.18 ml) had the highest absorption reading (120 mAU), while the two side peaks displayed similar absorption readings (~70 mAU). The majority of proteins in this sample were possibly the two photosystems, I and II, in their various compositional states. PSI typically adopts a trimeric (~900 kDa) and monomeric (~300 kDa) form, while PSII can be found as dimers (~650 kDa) and monomers (~325 kDa). Therefore, it was likely that the three peaks represent mainly these protein complexes, although a distinct correlation between a specific peak and particular photosystem complexes could not be attributed. However, the silver-stained 1-D SDS PAGE gel (see Figure 5.6A2) and the immunoblots that were probed with the αPsaD and αD1 antibodies (see Figure 5.6A6 and Figure 5.6A7) supported the conclusion that subunits of the photosystems made up the majority of the analysed proteins. More important for this work, were the immunoblotting analyses for the Band 7 proteins of *Synechocystis* sp. PCC 6803 (see Figure 5.6A3 to Figure 5.6A5). These proteins were found to form large protein complexes that started to elute after 10.5 ml (Phb1), 9.5 ml (Phb2) and 11.5 ml (Phb3)

respectively. This was a first indication that the Band 7 proteins of *Synechocystis* sp. PCC 6803 formed large protein complexes with an apparent molecular mass of more than 669 kDa. However, for all assayed Band 7 proteins a tailing antibody signal through almost all the fractions could be observed, so that it was impossible to distinguish whether the Band 7 proteins prevail as one or more distinct protein complexes.

The A_{280} absorption spectrum of the FPLC run of crude *Thermosynechococcus elongatus* membranes (see Figure 5.6B1) displayed a similar pattern to the one observed for *Synechocystis* sp. PCC 6803 (see Figure 5.6A1). The first peak, corresponding to the void volume of the column (after 7.70 ml; <10 mAU), was smaller than the first observed peak for *Synechocystis* sp. PCC 6803 (after 7.76 ml; <30 mAU). However, similarly, three other peaks were detected, eluting at 12.24 ml (140 mAU), 14.36 ml (~50 mAU) and 16.55 ml (~60 mAU). All of the observed peaks eluted slightly earlier and the first of the three peaks had the highest absorption reading, while the middle and the last peak reached similar, but relatively low absorption readings. Also in this sample, the majority of the proteins most likely originate from the two photosystems in their various compositional forms, which was supported by the silver-stained 1-D SDS PAGE gel (see Figure 5.6B2) and the immunoblots probed with the αPsaD and αD1 antibodies (see Figure 5.6B5 and Figure 5.6B6). More important for this work however, were the immunoblotting analyses for the two Band 7 proteins of *Thermosynechococcus elongatus* (TE_Phb1 and TE_Phb2), which started to elute after 10 ml. This was a first indication that the Band 7 proteins of *Thermosynechococcus elongatus* form large protein complexes with an apparent molecular mass of more than 669 kDa. However, similarly to the FPLC analysis of crude membrane isolations of *Synechocystis* sp. PCC 6803 the tailing antibody signals made it impossible to distinguish whether these Band 7 proteins prevailed as one or more distinct protein complexes.

5.2.4 Characterisation of Band 7 protein complexes using sucrose-density gradient centrifugation

Sucrose-density gradient centrifugation was one of the protein separation techniques used in conjunction with immunoblotting analyses to study the Band 7 protein complexes of *Synechocystis* sp. PCC 6803 and *Thermosynechococcus*

elongatus (see Figure 5.7). Crude cyanobacterial membrane isolations were generated and solubilised proteins and protein complexes were separated according to their sizes on a linear sucrose-density gradient. The gradient was centrifuged in an ultracentrifuge overnight and fractionated into 1-ml fractions which were subsequently analysed by 1-D SDS PAGE and immunoblotting using various antibodies.

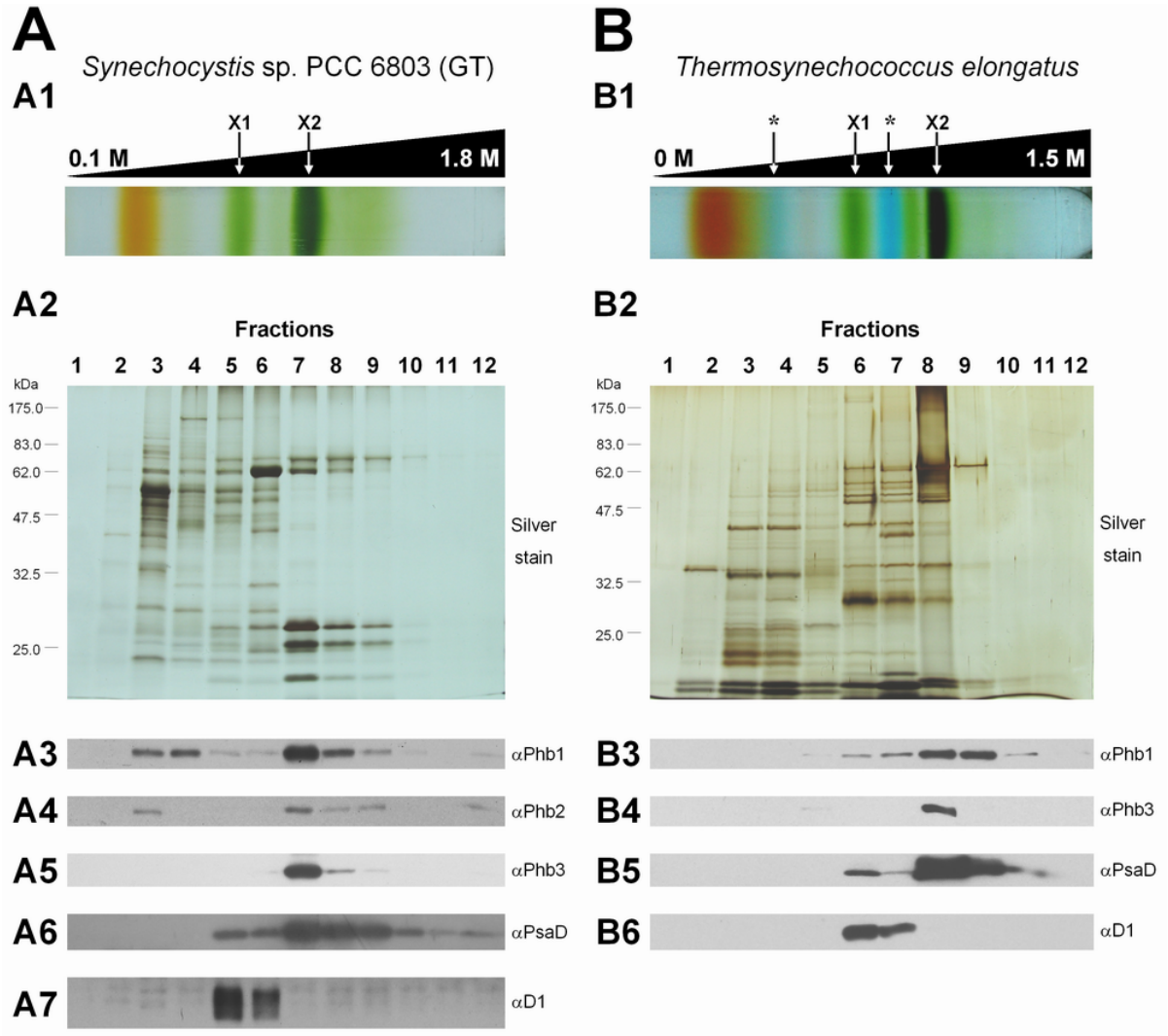

Figure 5.7: Separation of cyanobacterial protein complexes by sucrose-density gradient centrifugation. Crude membrane isolations of (A) *Synechocystis* sp. PCC 6803 wild-type GT and (B) *Thermosynechococcus elongatus* were separated on a linear (A) 0.1 to 1.8 M or a (B) 0 to 1.5 M sucrose-density gradient by centrifugation and analysed by immunoblotting. X1 indicates the band that most likely contained PSI and PSII monomers, while X2 marks the band in which mainly PSI trimers were expected. The two asterisks mark bands that contain contaminating phycobilisomes from the soluble fraction of the crude membrane isolation. The gradients were fractionated into 1-ml fractions and 7.5-µl aliquots of each fraction were analysed on a 1-D SDS PAGE gel. One gel each was (A2 and B2) silver-stained, while other gels were used for (A3 to A7 and B3 to B6) immunoblotting analyses with various, indicated antibodies.

As a note on the presentation of the sucrose gradients, small protein complexes can be found to the left, while bigger protein complexes migrated to the bottom of the centrifugation tube and can be found to the right. The sucrose gradients are roughly aligned with the silver-stained 1-D SDS PAGE gels, so that one can approximately estimate which fraction of the gradients was analysed in which lane of the gel.

Analysing the linear 0.1 to 1.8 M sucrose gradient of crude membrane isolations of *Synechocystis* sp. PCC 6803 wild-type GT (see Figure 5.7A1), three major bands could be distinguished. The first band had a yellowish colour which resulted from carotenoids and was found at the low-molecular-mass end (fractions 2 and 3). Unfortunately, no protein markers were run on a separate sucrose-density gradient, so that only internal references could be used to estimate the molecular masses of the protein complexes of interest. Such internal references were the two green bands (marked X1 and X2) which could be observed in the sucrose gradient. The first green band probably represented monomeric PSI and PSII (marked X1; fractions 5 and 6) with a molecular mass of ~300 kDa, while the more intensely coloured green band most likely contained trimeric PSI (marked with X2; fractions 7 and 8) with a molecular mass of ~900 kDa. The silver-stained 1-D SDS PAGE gel (see Figure 5.7A2) and the immunoblots with αPsaD and αD1 (see Figure 5.7A6 and Figure 5.7A7) supported these assignments. The immunoblot analyses for the Phb1, Phb2 and Phb3 Band 7 proteins of *Synechocystis* sp. PCC 6803 revealed a more distinct pattern for the Band 7 protein complexes than previously observed in the immunoblotting analysis of the FPLC run (see Figure 5.6A). The most intense antibody signal for the Phb1 protein could be found in fraction 7, together with trimeric PSI. Moreover, a progression of this signal into the high-molecular-mass region in fractions 8 and 9 could be observed. Additionally, the Phb1 protein of *Synechocystis* sp. PCC 6803 could be found the low-molecular-mass region in fractions 3 and 4. A similar pattern was observed for the Phb2 protein of *Synechocystis* sp. PCC 6803, a low-molecular-mass signal in fraction 3 with an antibody signal in fraction 7 that progressed into the high-molecular-mass region in fractions 8 and 9. The Phb3 protein of *Synechocystis* sp. PCC 6803 displayed no signal in the low-molecular-mass region and the majority of this protein was present in fraction 7 with a progressing signal into the high-molecular-mass region in fractions 8 and 9. The results of this analysis indicated that the Phb1, Phb2 and Phb3 Band 7 proteins of *Synechocystis* sp. PCC 6803 form large protein complexes with a molecular mass of 900 kDa and above.

Both, the linear 0 to 1.5 M sucrose gradient of the crude membrane isolation of *Thermosynechococcus elongatus* (see Figure 5.7B1) and the gradient previously described for *Synechocystis* sp. PCC 6803 displayed similar patterns. In the case of *Thermosynechococcus elongatus*, the first band at the low-molecular-mass end of the gradient (fractions 2 and 3) also resulted from carotenoids and had a darker yellowish colour. Furthermore, similarly two green bands (marked X1 and X2) were observed in the gradient and were taken as internal references containing the same kind of photosynthetic protein complexes as previously described for *Synechocystis* sp. PCC 6803 (X1, fractions 6, ~300 kDa; X2, fraction 8, ~900 kDa). The silver-stained 1-D SDS PAGE gel (see Figure 5.7B2) and the immunoblots with αPsaD and αD1 (see Figure 5.7B5 and Figure 5.7B6) supported this. Several blue bands were detected in this sucrose gradient (see asterisks in Figure 5.7B1), which could be attributed to contaminating phycobilisomes of the crude membrane isolation. The immunoblot analyses for the TE_Phb1 (αPhb1) and TE_Phb2 (αPhb3) Band 7 proteins of *Thermosynechococcus elongatus* revealed a more distinct pattern for the protein complexes than could be observed in the immunoblotting analysis of the FPLC run (see Figure 5.6B). The most intense antibody signals for the TE_Phb1 protein could be found in fractions 8 and 9 in which trimeric PSI could be found. The antibody signal progressed a little into the high-molecular-mass region into fraction 10, as well as it tailed into the low-molecular-mass region of fractions 6 and 7. No antibody signals for the TE_Phb1 protein were detected in the low-molecular-mass region. The TE_Phb2 protein of *Thermosynechococcus elongatus* was only detected in fraction 8 together with trimeric PSI. The results of this analysis indicated that the TE_Phb1 and TE_Phb2 Band 7 proteins of *Thermosynechococcus elongatus* form large protein complexes with a molecular mass of 900 kDa or above.

Overall, the sucrose gradients only allowed a rough estimation of the molecular masses of cyanobacterial Band 7 protein complexes; however with a better resolution than had previously been obtained by FPLC.

5.2.5 Characterisation of Band 7 protein complexes using BN PAGE

Blue-native polyacrylamide gel electrophoresis (BN PAGE) was another protein separation technique used in conjunction with immunoblotting analyses to study cyanobacterial Band 7 protein complexes (see Figure 5.8). Crude membrane

isolations were generated of *Synechocystis* sp. PCC 6803 and *Thermosynechococcus elongatus*, solubilised proteins and protein complexes separated according to their sizes on linear gradient 1-D BN PAGE gels which were blotted and probed with various antibodies.

5.2.5.1 BN PAGE analyses of Synechocystis sp. PCC 6803 strains

The *Synechocystis* sp. PCC 6803 wild-type GT and various Band 7 gene inactivation mutants were analysed by 1-D BN PAGE and immunoblotting (see Figure 5.8) to study Band 7 protein complexes. Additionally, the effects of an inactivation of a Band 7 protein on other Band 7 and FtsH protein complexes were assessed.

Crude membrane isolations were generated from various *Synechocystis* sp. PCC 6803 GT strains and separated on 5 to 12.5 % (w/w) PAA linear gradient BN PAGE gels. No obvious differences could be observed in the protein complex pattern of the various strains on an unstained BN PAGE gel (see Figure 5.8A). The αD1 antibody recognised a similar pattern of monomeric and dimeric PSII complexes in all strains, which indicated that the PSII complexes did not seem to be noticeably affected by an inactivation of either the Phb1, Phb2, Phb3 or Phb4 genes (see Figure 5.8B). Analysing the immunoblots in which antibodies directed against the Band 7 proteins were used (see Figure 5.8C to Figure 5.8E), a consistent pattern could be observed in each lane. For the Phb1 protein, several signals in the high-molecular-mass region could be detected, where the uppermost signal represented the strongest. Unfortunately, the largest marker protein of the used protein marker was thryoglobulin with a molecular mass of 669 kDa, so that none of the detected Band 7 protein complexes could be sized more accurately than before. However, the largest Phb1 protein complex appeared to have a molecular mass significantly larger than 669 kDa, while a signal for another Phb1 protein complex population was observed as a relatively broad signal in the area of 669 kDa. In order to achieve maximum resolution of the high-molecular-mass region, the bottom of the gel had been intentionally run off which might have contributed to the fact that no Band 7 protein complexes with a molecular mass of lower than 440 kDa could be detected. Interestingly, the same Phb1 protein complex profile was detected in the single Band 7 gene inactivation mutants, in which Phb2, Phb3 and Phb4 had been inactivated respectively. The lanes for the Phb1 (ΔPhb1), the triple (ΔPhb1-3) and quadruple (ΔPhb1-3) Band 7 gene inactivation mutants demon-

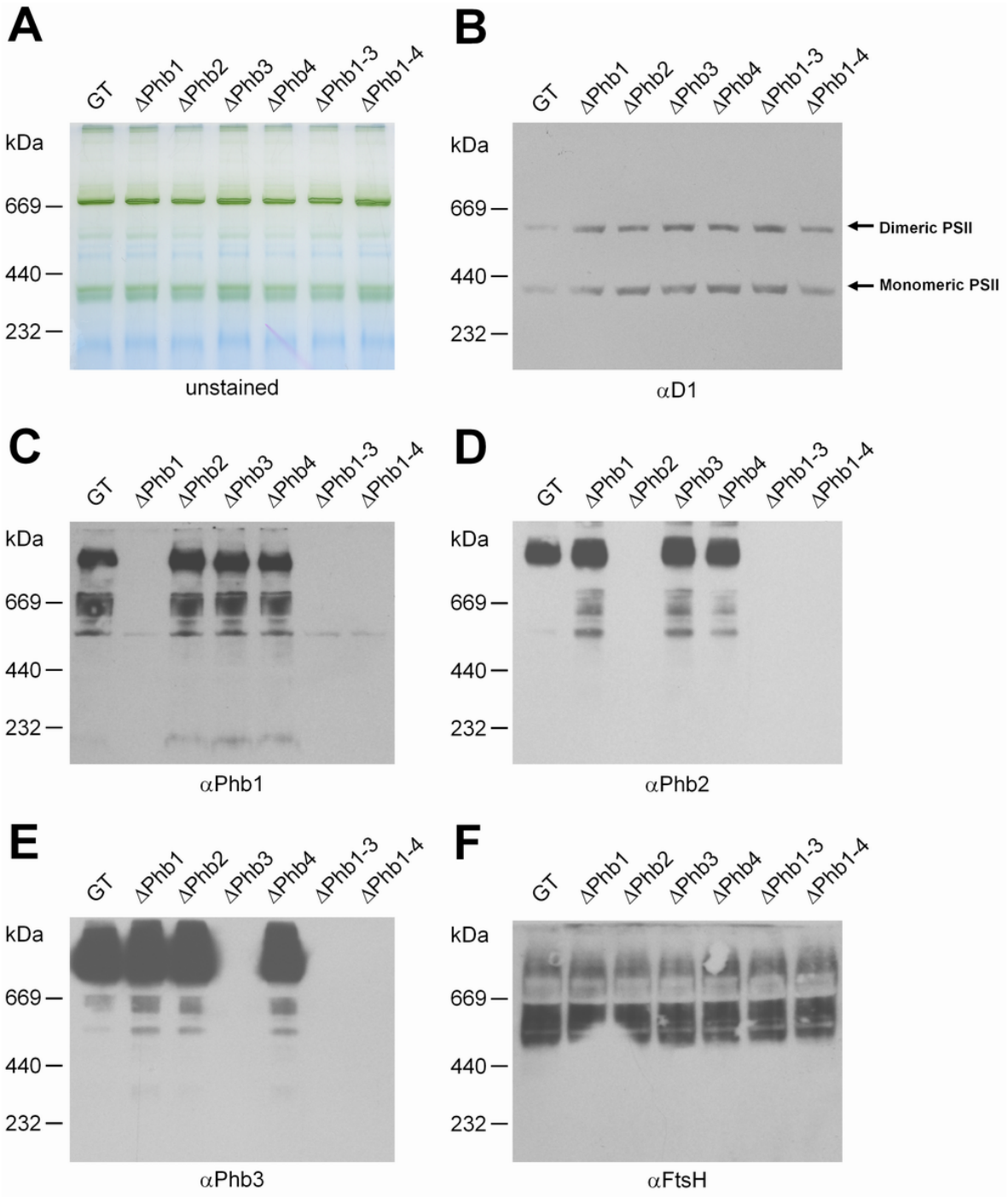

Figure 5.8: Separation of protein complexes of *Synechocystis* sp. PCC 6803 using 1-D BN PAGE. Crude membrane isolations of various *Synechocystis* sp. PCC 6803 GT strains were separated by 1-D BN PAGE. Samples corresponding to an amount of 1 µg chlorophyll a were loaded in the lanes of 5 to 12.5 % (w/w) PAA linear gradient BN PAGE gels. (A) One unstained gel and (B to F) subsequent immunoblotting analyses with various, indicated antibodies are shown. (B) The positions of monomeric and dimeric PSII complexes are marked with arrows.

strated that the observed signals of the αPhb1 antibody were specific for the Phb1 protein complexes. The immunoblots that were performed with the αPhb2 and αPhb3 antibodies, yielded similar results. The most intense signal in both cases was in the

high-molecular-mass region, well above the 669 kDa marker band and several weaker signals could be detected underneath in between 500 and 669 kDa.

These 1-D BN PAGE analyses suggested that the Phb1, Phb2 and Phb3 Band 7 homologues form independent complexes. This observation also seemed to be true for the Phb4 protein (data not shown) and was further supported by immunoprecipitation results (see Figure 5.9). In an immunoprecipitation experiment performed with antibodies that were covalently crosslinked to sepharose A beads, the used αPhb1, αPhb2 and αPhb3 antibodies precipitated their respective cognate subunit, while the respective other Band 7 proteins did not co-purify.

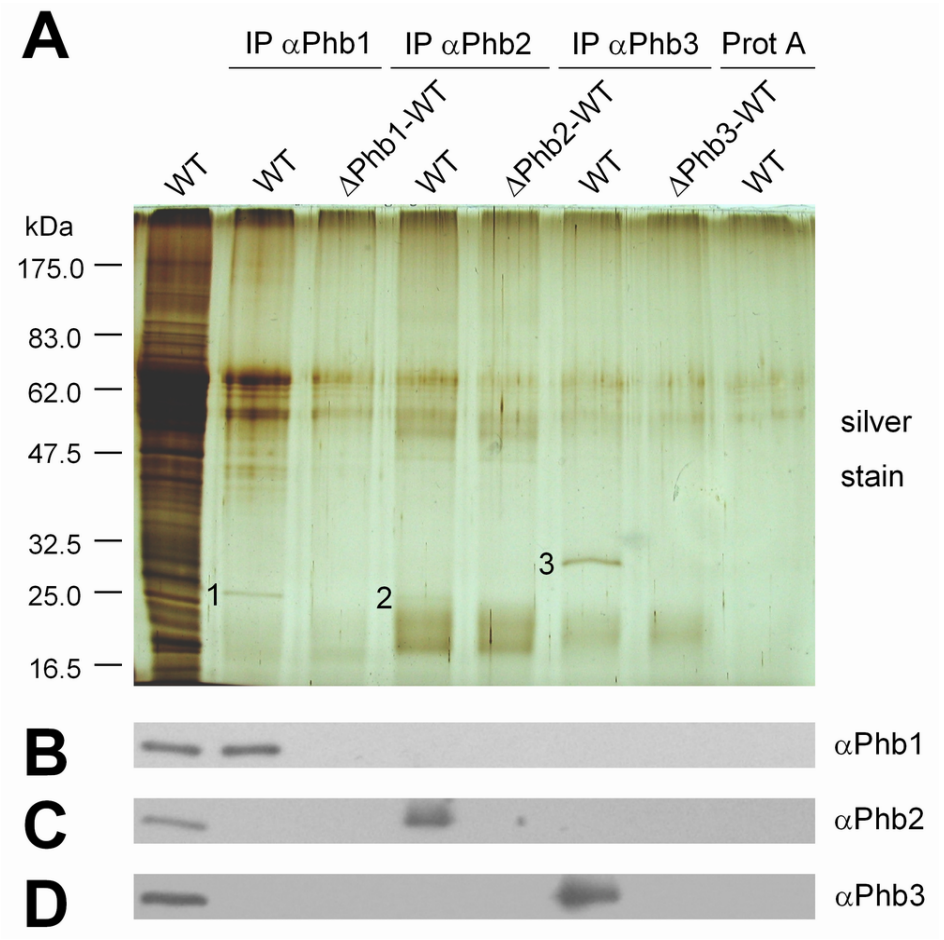

Figure 5.9: Immunoprecipitation of Band 7 proteins of *Synechocystis* sp. PCC 6803 (WT). Crude membrane isolations of *Synechocystis* sp. PCC 6803 wild-type (WT) and various Band 7 gene inactivation mutant strains were used for an immunoprecipitation experiment with the indicated antibodies covalently crosslinked to sepharose A beads. An amount of crude membrane isolation of the *Synechocystis* sp. PCC 6803 wild-type (WT) strain corresponding to 1 µg of chlorophyll a was loaded in one lane (WT), while 20 µl of the immunoprecipitations (the samples had been eluted in 100 µl 1x SDS sample buffer) were loaded in the other lanes. Precipitated (1) Phb1, (2) Phb2 and (3) Phb3 proteins could be visualised by silver staining and are marked. (B to D) Generated immunoblots were probed with the indicated antibodies.

One immunoblot of the 1-D BN PAGE analysis of crude membrane isolations of the *Synechocystis* sp. PCC 6803 wild-type GT and the various Band 7 gene inactivation mutants was probed with the αFtsH antibody and a broad antibody signal in between the 669 and 440 kDa marker bands indicated that the FtsH homologues form high-molecular-mass protein complexes (see Figure 5.7F). Interestingly, the observed pattern for the FtsH protein complexes did not seem to be affected in any of the single or multiple Band 7 gene inactivation mutants, suggesting a lack or low levels of FtsH/Band 7 protein supercomplexes.

5.2.5.2 BN PAGE analyses of Thermosynechococcus elongatus

Thermosynechococcus elongatus crude membranes were isolated and analysed by 1-D BN PAGE followed by immunoblotting (see Figure 5.10), to study the Band 7 and possible FtsH homologue protein complexes. Unfortunately, no inactivation mutants of either the Band 7 or FtsH homologues were available for this cyanobacterial strain.

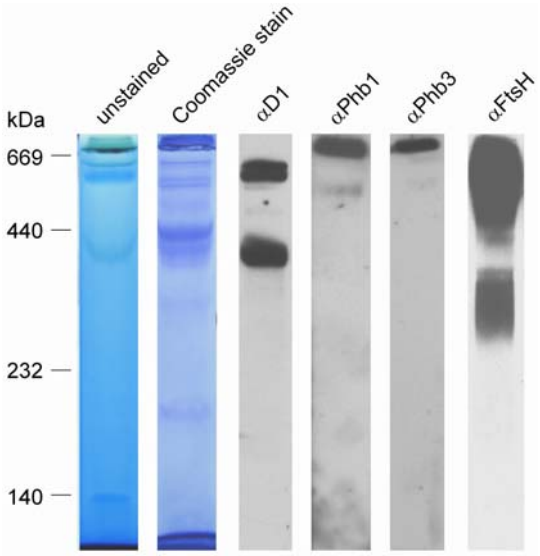

Figure 5.10: Separation of protein complexes of *Thermosynechococcus elongatus* by 1-D BN PAGE. Crude membranes of *Thermosynechococcus elongatus* were separated by 1-D BN PAGE. Samples corresponding to an amount of 1 µg chlorophyll a were loaded in the lanes of an 8 % (w/w) PAA BN PAGE gel. One unstained and a Coomassie-stained gel strip as well as immunoblotting analyses with various antibodies are shown.

The 1-D BN PAGE analysis of crude *Thermosynechococcus elongatus* membranes was performed on a 8 % (w/w) PAA BN PAGE gel that lacked the resolution of a BN gradient gel in the high-molecular-mass region (see Figure 5.8). However, the protein complexes in the sample could be separated and distinct antibody

signal bands were obtained in the subsequent immunoblotting analyses. The αD1 antibody detected two PSII bands in the analysed sample, of which the uppermost band ,just below the 669 kDa marker band, probably contained PSII dimers. The other band was below the 440 kDa protein marker band and represented the antibody signal for PSII monomers. Both the TE_Phb1 and TE_Phb2 proteins formed high-molecular-mass protein complexes, that had a size of more than 669 kDa. In the case of the TE_Phb1 protein, a second, significantly weaker antibody signal band was detected in between the 669 and 440 kDa markers. No low-molecular-mass complexes or monomers were observed for either the TE_Phb1 or the TE_Phb2 proteins. When an immunoblot was probed with the αFtsH antibody, two larger protein complex populations could be observed. One was represented by a broad antibody signal in between the 669 and 440 kDa protein marker bands (similar to that observed for *Synechocystis* sp. PCC 6803), while the second signal could be found right in between the 440 and 232 kDa marker bands.

5.3 His_8-tagging of Band 7 proteins of *Synechocystis* sp. PCC 6803

The Band 7 proteins Phb1, Phb2, Phb3 and Phb4 of *Synechocystis* sp. PCC 6803 were His_8-tagged to facilitate subsequent purification attempts. Consequently, plasmid DNA constructs for the transformation of *Synechocystis* sp. PCC 6803 were generated (see section 5.3.1) and the segregation of the mutants was confirmed by PCR analyses (see section 5.3.2). The expression of the His_8-tagged proteins was assessed by 1-D SDS PAGE followed by immunoblotting (see section 5.3.3).

5.3.1 Generation of transformation plasmid DNA constructs

The transformation plasmid DNA constructs to produce His_8-tagged Phb1, Phb2, Phb3 and Phb4 protein *Synechocystis* sp. PCC 6803 mutants were generated by overlap extension PCR (see Figure 5.11). For each Band 7 protein, two PCR reactions were performed using genomic *Synechocystis* sp. PCC 6803 wild-type GT DNA and specific primers to obtain two DNA fragments ("HIS I" and "HIS II"; see Figure 5.11B and Figure 5.12). The *phbX*-HIS I and *phbX*-HIS II primers (X = 1 to 4) shared some complementary DNA sequence and were used to introduce a His_8-tag before the

STOP codon of the respective gene (see Figure 5.11A). In a third PCR reaction, the generated "HIS I" and "HIS II" fragments were mixed and used as template DNA with specific primers to generate another DNA fragment ("HIS I + II"; see Figure 5.11C and Figure 5.12) that was subsequently ligated into the pGEM-T easy vector. After antibiotic-resistance cassettes were inserted as selective markers into the vectors, the generation of the final plasmid DNA constructs was complete (pPHB1HISCAM, pPHB2HISKAN, pPHB3HISKAN and pPHB4HISCAM; see Figure 5.13A and Figure 5.13B).

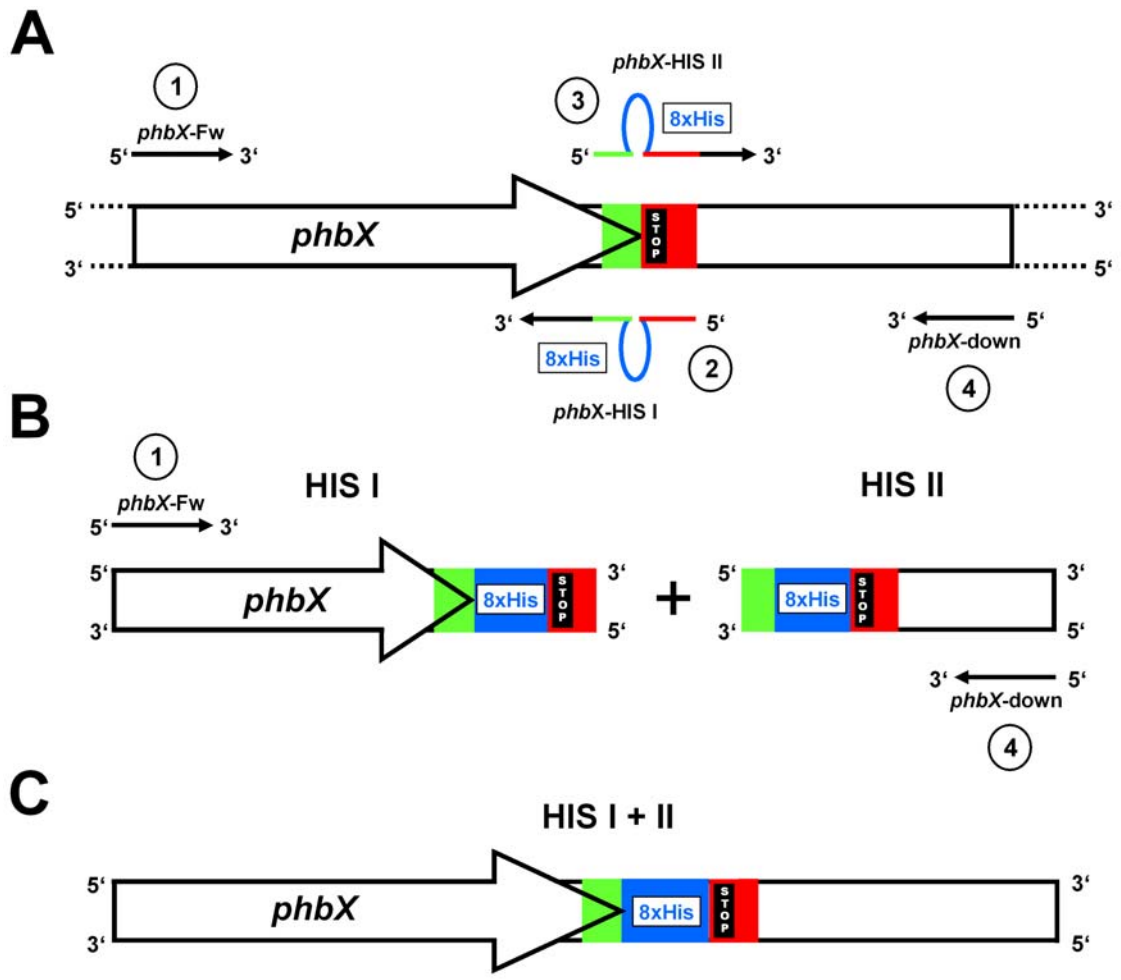

Figure 5.11: Schematic representation of an overlap extension PCR procedure. (A) Two sets of specific primers (1 and 2; 3 and 4) were used on genomic *Synechocystis* sp. PCC 6803 wild-type GT DNA to generate (B) two DNA fragments ("HIS I" and "HIS II"). Because primers 2 and 3 share complementary DNA sequences (represented in green, blue and red), the coding sequence of an His_8-tag (blue) is introduced before the stop codon (STOP) of a gene of interest (*phbX*). In a third PCR reaction, in which a mixture of the "HIS I" and "HIS II" DNA fragments is used as template DNA together with primers 1 and 4, (C) one large "HIS I + II" DNA fragment is obtained which can be cloned into a recipient vector and can be processed further.

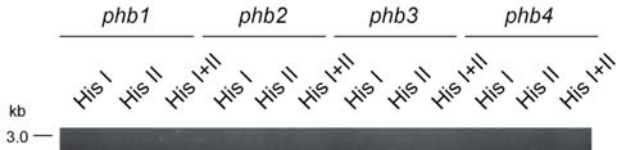

	Expected fragment size [bp]			
	phb1	*phb2*	*phb3*	*phb4*
His I	876	923	993	822
His II	598	590	610	577
His I+II	1428	1477	1567	1363

Figure 5.12: DNA fragments from the overlap extension PCRs. The DNA fragments "HIS I", "HIS II" and "HIS I + II" of the Band 7 genes *phb1*, *phb2*, *phb3* and *phb4* that were obtained from the overlap extension PCR procedure. The table underneath the gel lists the expected sizes of the respective DNA fragments. For more details see text.

The DNA fragments that were obtained from the three overlap extension PCRs are shown in Figure 5.12. The coding sequence of a His_8-tag was introduced before the STOP codon of the Band 7 genes with the phbX-HIS I (primer 2) and phbX-HIS II primers (primer 3) in all "HIS I" and "HIS II" DNA fragments respectively. The "HIS I" DNA fragments had the size of the amplified Band 7 genes plus 27 bp (24 bp for the His_8-tag and an additional 3-bp overlap). Consequently, the sizes for the *phb1*, *phb2*, *phb3* and *phb4* "HIS I" DNA fragments were 876, 923, 993 and 822 bp respectively. The sizes of the "HIS II" DNA fragments depended on the annealing site of the *phbX*-down primer (primer 4) in the downstream region of the respective Band 7 gene. The "HIS I + II" DNA fragments, that resulted from the third overlap extension PCR reaction, had the following sizes: *phb1* (1428 bp), *phb2* (1477 bp), *phb3* (1567 bp) and *phb4* (1363 bp). However, all the sizes of the obtained DNA fragments were listed in Figure 5.12. The "HIS I + II" DNA fragments were then ligated into the pGEM-T easy vector and after insertion of the antibiotic-resistance cassettes as selective markers, analytical EcoRI restriction digestions were performed on the final plasmid DNA constructs (see Figure 5.13A). The EcoRI restriction enzyme excised the initially inserted DNA fragment and yielded a 2997 bp fragment (the pGEM-T easy vector) and various DNA fragments depending on the inserted DNA (see Figure 5.13B): pPHB1HISCAM (1789 and 1009 bp), pPHB2HISKAN (1935 and 760 bp), pPHB3HISKAN (2784 bp) and pPHB4HISCAM (1558 and 1164 bp). The analytical EcoRI restriction digestion confirmed that the correct plasmid DNA constructs were generated, which could then be used for the transformation of *Synechocystis* sp. PCC 6803 wild-type GT cells. Additionally, the 0228-GST strain, a *Synechocystis* sp. PCC 6803 glucose-tolerant strain in which the FtsH protease (*slr0228*) had been GST-tagged, was transformed with the generated constructs, although the obtained transformants were not used in this work.

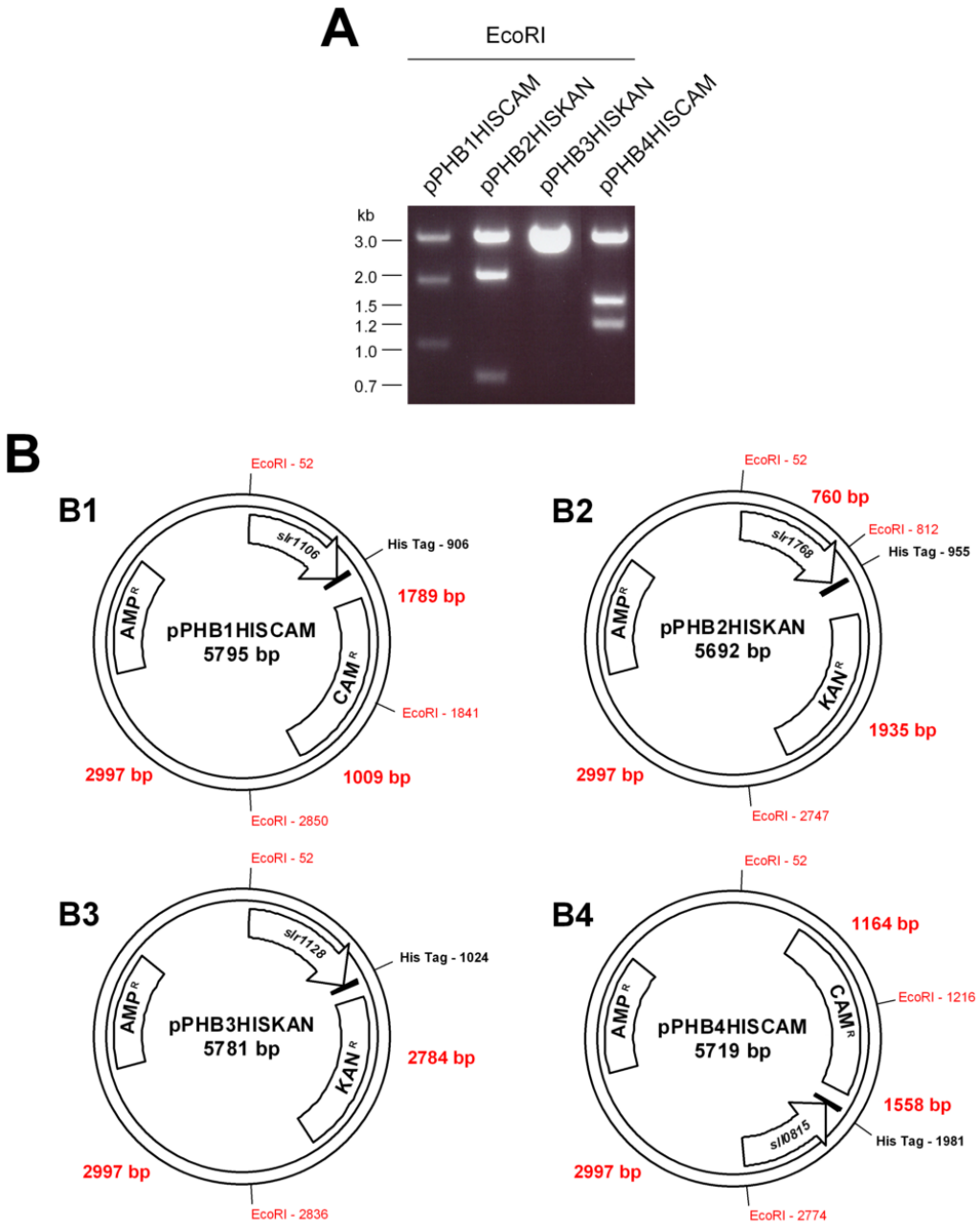

Figure 5.13: Transformation plasmid DNA constructs to generate His_8-tagged Band 7 protein mutants. (A) EcoRI digests and (B) schematic representations of the final plasmid DNA constructs: pPHB1HISCAM, pPHB2HISKAN, pPHB3HISKAN and pPHB4HISCAM. EcoRI cut sites of the vectors and the sizes of the resulting DNA fragments are indicated in red. The position of the coding sequence for the His_8-tag (black box) is also indicated.

5.3.2 Segregation confirmation of His_8-tagged mutants

As *Synechocystis* sp. PCC 6803 possesses multiple copies of its genome, the progress of segregation of the His_8-tagged Band 7 protein mutants was monitored by PCR analyses. After several restreaks, complete segregation could be confirmed for the Phb1-His, Phb2-His, Phb3-His and Phb4-His mutants (see Figure 5.14).

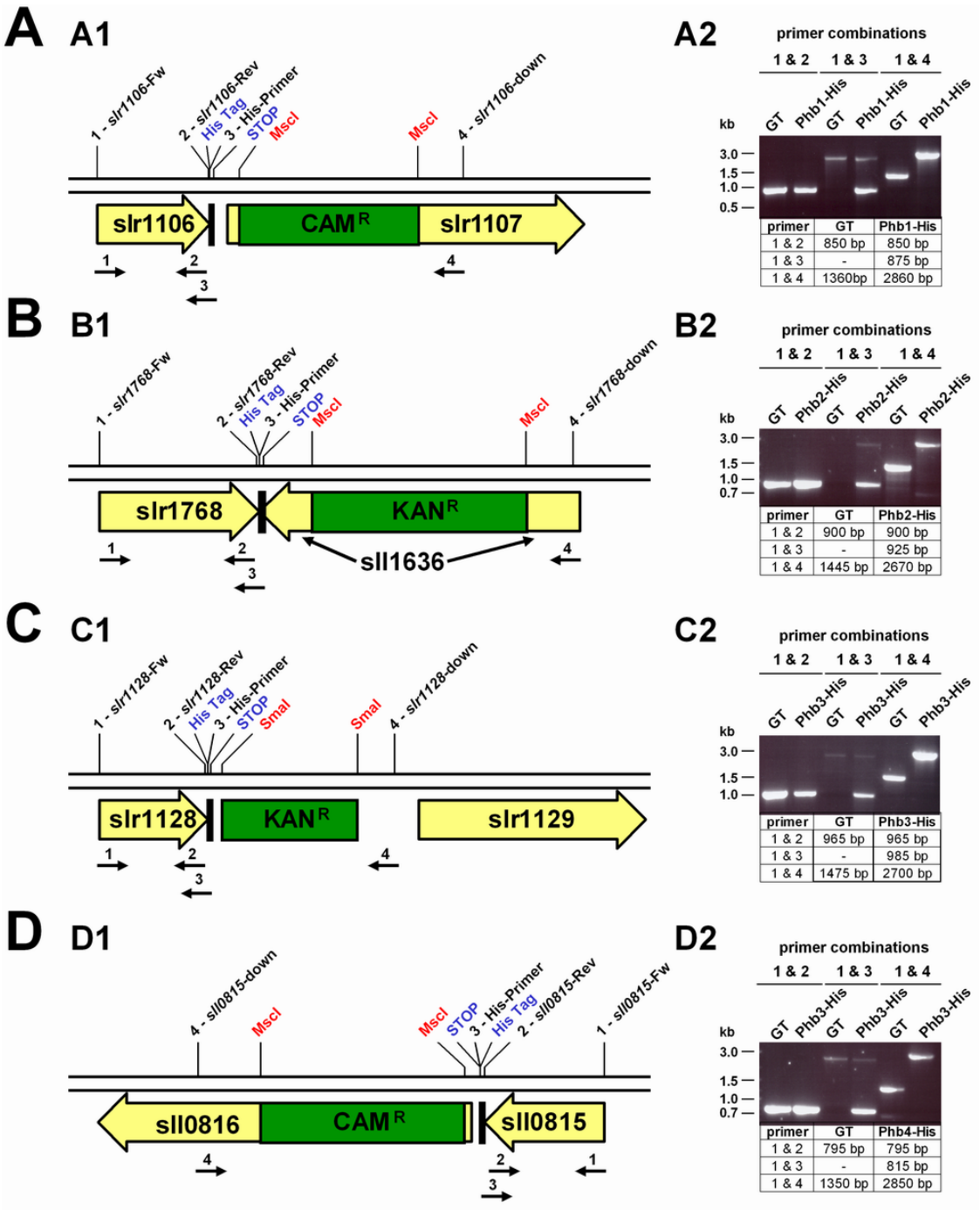

Figure 5.14: Segregation confirmation of the His_8-tagged Band 7 protein mutants. (A1 to D1) Schematic representations of the genomic DNA of the His_8-tagged Band 7 protein mutants in the region of the respective Band 7 gene. Gene names, His_8-tags (black boxes) and the restriction enzymes that were used to insert antibiotic-resistance cassettes (CAM^R and KAN^R) are annotated. Approximate annealing positions of the primers (1 to 4) used to confirm the segregation of the mutants are indicated and (A2 to D2) the results of the PCR analyses shown. The sizes of the expected DNA fragments are given in the tables underneath the photographed agarose gels.

Schematic representations of the genomic DNA in the region of the respective Band 7 gene of the His_8-tagged Band 7 protein mutants (see Figure 5.14A1 to Figure

5.14D1) indicated that some neighbouring genes had been disrupted by the insertion of antibiotic-resistance cassettes. The *slr1107* gene encoded an unknown protein and was disrupted in the Phb1-His mutant. The *sll1636* gene encoded a ferripyochelin binding protein and was disrupted in the Phb2-His mutant, while the *sll0816* gene encoded a probable oxidoreductase and was disrupted in the Phb4-His mutant. However, no phenotype seemed to result from the inactivation of these genes or the insertion of the His_8-tag coding sequence under standard laboratory growth conditions (data not shown). When PCR analyses were performed to test for complete segregation of the generated mutants (see Figure 5.14A2 to Figure 5.14D2), the *phbX*-Fw (primer 1; *slr1106*-FW, *slr1768*-Fw, *slr1128*-Fw and *sll0815*-Fw) and the *phbX*-Rev primers (primer 2; *slr1106*-Rev, *slr1768*-Rev, *slr1128*-Rev and *sll0815*-Rev) yielded DNA fragments of the same size in both the *Synechocystis* sp. PCC 6803 wild-type GT and the His_8-tagged Band 7 protein mutant strains. The *phbX*-Fw and His-primer (primer 3) amplified specific DNA fragments, that were slightly bigger than the respective Band 7 genes, only in the His_8-tagged Band 7 protein mutant strains. When the same primers were used on genomic DNA of *Synechocystis* sp. PCC 6803 wild-type cells, only unspecific bands with a higher molecular mass could be observed. The combination of the *phbX*-Fw and *phbX*-down (primer 4) primers lead to the amplification of DNA fragments which in the wild-type GT strain had a size of 1360 bp for the *slr1106*-down primer, 1445 bp for the *slr1768*-down primer, 1475 bp for the *slr1128*-down primer and 1350 bp for the *sll0815*-down primer. In the PhbX-His mutants, these DNA fragments were significantly bigger because of the insertion of antibiotic-resistance cassettes, so that a 2860 bp DNA fragment was obtained in the Phb1-His mutant, a 2670 bp DNA fragment in the Phb2-His mutant, a 2700 bp DNA fragment in the Phb3-His mutant and a 2850 bp DNA fragment in the Phb4-His mutant. Overall, the His_8-tagged Band 7 protein mutants were completely segregated and the His_8-tag coding sequence had been successfully introduced at the 3' end of the *phb1*, *phb2*, *phb3* and *phb4* Band 7 genes.

5.3.3 Expression analyses of His_8-tagged Band 7 proteins

After it had been shown that the generated His_8-tagged Band 7 protein mutants were completely segregated, it needed to be tested whether the respective His_8-tagged

Band 7 proteins would accumulate. Therefore, crude membrane isolations of the mutants were generated and immunoblotting analyses performed (see Figure 5.15).

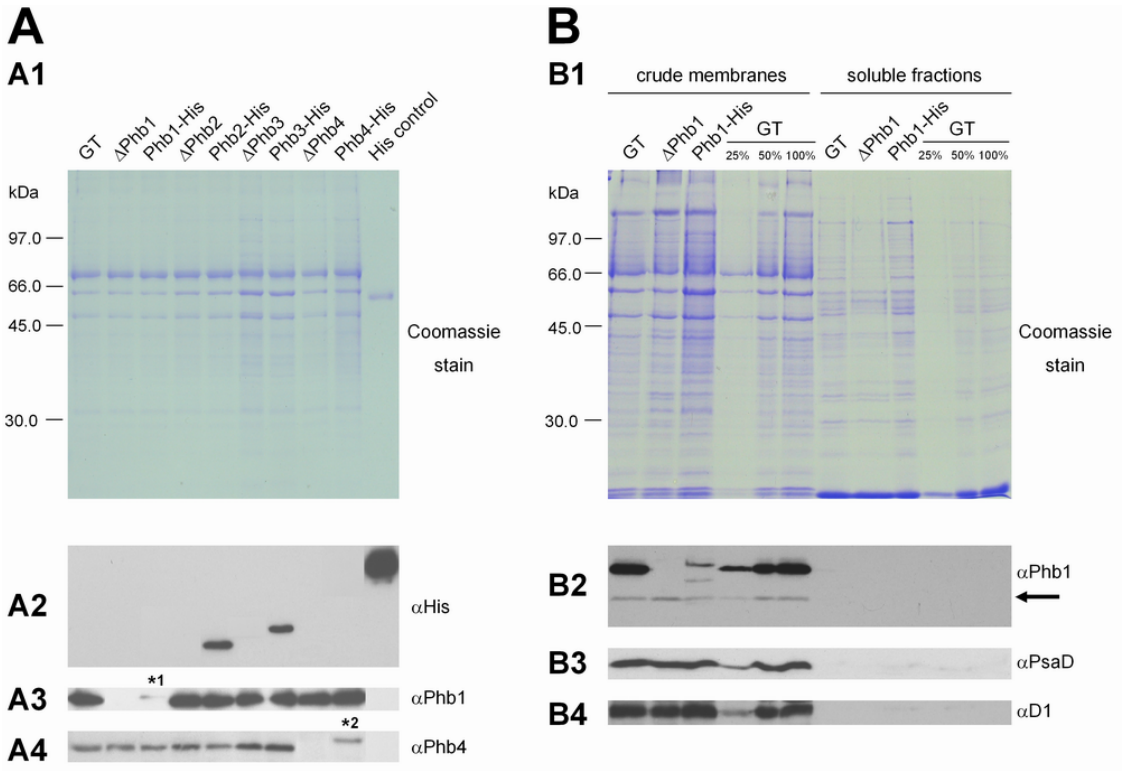

Figure 5.15: Protein expression analyses of His_8-tagged Band 7 protein mutants. (A) Assessment of the expression of His_8-tagged Band 7 proteins in all the generated Phb-His mutants. (B) Detailed expression analysis for the Phb1-His protein in the Phb1-His mutant strain. (A and B) Isolated crude membranes of the various strains (*Synechocystis* sp. PCC 6803 wild-type GT, Band 7 protein inactivation and His_8-tagged Band 7 protein mutant strains) were loaded on a 1-D SDS PAGE gel corresponding to (A) 0.5 µg chlorophyll a and 2 µl of the His control (His-tagged p53, as supplied by Dianova) or (B) 1 µg chlorophyll a (100 %) of the crude membrane fraction or to 12 µg protein (100 %) of the soluble fraction. Respectively less crude membrane and soluble fraction was loaded in the dilution series. (A1 and B1) One gel of each analysis was Coomassie-stained, while (A2 to A4 and B2 to B4) other gels were blotted and probed with various, indicated antibodies. (A3 and A4) The antibody signals for the Phb1-His (*1) and Phb4-His (*2) proteins are marked. (B2) An unspecific antibody signal in the αPhb1 panel is indicated with an arrow.

In a first analysis, the expression of Band 7 and His_8-tagged Band 7 proteins was tested in crude membrane isolations of *Synechocystis* sp. PCC 6803 wild-type GT, Band 7 protein inactivation and His_8-tagged Band 7 protein mutant strains (see Figure 5.15A). An immunoblot probed with the αHis antibody revealed that the Phb2 and Phb3 Band 7 homologues had been His_8-tagged and accumulated in the respective mutants. While also His-tagged p53 protein (His control; as supplied by Dianova) also

gave a strong signal, the Phb1 and Phb4 Band 7 proteins could not be detected with this antibody (see Figure 5.15A2). Thus, in order to test whether the Phb1 and Phb4 proteins had nevertheless been successfully His_8-tagged, and only failed to accumulate in amounts above the detection limit of the αHis antibody, similarly generated immunoblots were probed with the αPhb1 (see Figure 5.15A3) or αPhb4 antibody respectively (see Figure 5.15A4). In these immunoblotting analyses, it appeared as if the αPhb1 antibody signal in the Phb1-His (marked with *1) and the αPhb4 antibody signal in the Phb4-His mutant strain (marked with *2) respectively were slightly shifted towards a higher molecular mass in comparison to the antibody signal observed in the wild-type lane. Therefore, even though this suggested that both the Phb1 and the Phb4 protein had been His_8-tagged, in both cases the accumulation of the His_8-tagged Band 7 proteins appeared to be reduced, but no quantitative conclusions could be drawn.

The apparent instability of the Phb4-His protein was not investigated further, while another 1-D SDS PAGE and immunoblotting analysis was performed to assess the stability of the Phb1-His protein in more detail (see Figure 5.15B). In this analysis, more material was loaded in the lanes of the 1-D SDS PAGE gels and a dilution series for the wild-type GT strain, as well as for the soluble fractions of all strains were included. An important observation was that the Phb1 protein clearly seemed to be His_8-tagged, as the antibody signal in the lane corresponding to the Phb1-His strain was slightly shifted towards a higher molecular mass when compared to the wild-type. Additionally, a weaker antibody signal was detected for a protein that was smaller than the full-length Phb1 protein. Since this signal could not be detected in the wild-type or the ΔPhb1 inactivation mutant strains, it seemed likely that this signal represents a degradation product of the Phb1-His protein. No other degradation products could be detected in the Phb1-His mutant strain. Another antibody signal that corresponded to a protein with a lower molecular mass than full-length Phb1 was unspecific (marked with an asterisk). When the intensities of the αPhb1 antibody signals for the wild-type and Phb1-His strains were compared (estimated with the naked eye), it appeared that significantly less than 25 % of the wild-type Phb1 protein level was present in the Phb1-His strain. Interestingly, although the His_8-tag seemed to cause that the Phb1 protein could not accumulate, no degradation products could be observed in the soluble fraction of the Phb1-His strain (see Figure 5.15B1). The αPsaD (see Figure 5.15B2) and αD1 (see Figure 5.15B3) immunoblots were performed as loading controls.

5.4 Purification of Band 7 proteins of *Synechocystis* sp. PCC 6803

His_8-tags were introduced at the C-termini of the Phb1, Phb2, Phb3 and Phb4 Band 7 proteins of *Synechocystis* sp. PCC 6803, in order to facilitate the purification of their complexes. While the Phb1-His and Phb4-His Band 7 proteins did not accumulate to wild-type levels, the abundance of the His_8-tagged Phb2 and Phb3 proteins did not appear to be affected. Thus, an attempt was made to affinity-purify the tagged Band 7 proteins using Ni-NTA magnetic agarose beads (see section 5.4.1). Another approach to purify Band 7 protein complexes under near native conditions, was to immunoprecipitate them with purified antibodies coupled to Protein A sepharose beads (see section 5.4.2).

5.4.1 Purification of Band 7 proteins using magnetic beads

The His_8-tag that was introduced at the C-terminus of the *Synechocystis* sp. PCC 6803 Band 7 proteins could be used for an affinity-purification procedure with Ni-NTA magnetic agarose beads. This purification method proved to be rather quick and convenient, because washing and elution solutions could easily be removed from the tube without disturbing the sample, while the beads were held in place by a magnet. Initially, the procedure was tested on a crude membrane isolation from a *Synechocystis* sp. PCC 6803 TD41 strain that possessed a His_6-tagged CP47 protein (kindly provided by Prof. Peter Nixon; see Figure 5.16A). In the TD41 strain all three *psbA* genes are inactivated, so that PSII complexes cannot assemble properly. After the procedure had been tested successfully, it was applied on crude membrane isolations of *Synechocystis* sp. PCC 6803 strains in which the Phb1, Phb2 and Phb3 Band 7 proteins had been His_8-tagged (see Figure 5.16B).

In the initial test of the Ni-NTA magnetic beads affinity-purification procedure, not all the generated samples of the His_6-tagged CP47 protein purification were analysed (see Figure 5.16A). Nevertheless, an intensely stained protein band was detected in the 47-kDa region of the silver-stained 1-D SDS PAGE gel which suggested that His-tagged proteins could specifically be purified with this method (see Figure 5.16A1). An immunoblot that was probed with the αHis antibody identified the 47-kDa protein as CP47-His. A comparison of the pre- and postbinding samples suggested that the majority of the His_6-tagged CP47 protein had been captured by the

magnetic beads within the 2 h incubation period (see Figure 5.16A2). However, the CP43 protein, part of the PSII core complex, as well as the Phb1 and Phb2 Band 7 proteins, could not be detected in the eluate (see Figure 5.16A3 to Figure 5.16A5). However, since PSII complexes cannot assemble properly in the TD41 strain, it was not surprising that the CP43 protein did not co-purify with the CP47-His protein in this experiment. The Phb3 protein on the other hand was found in the eluate of the CP47-His protein purification, and since this protein was also found in the eluate of the control purification with a crude membrane isolation of the TD41 strain, the presence of the Phb3 protein could only be attributed to its unspecific binding to the magnetic beads (see Figure 5.16A6).

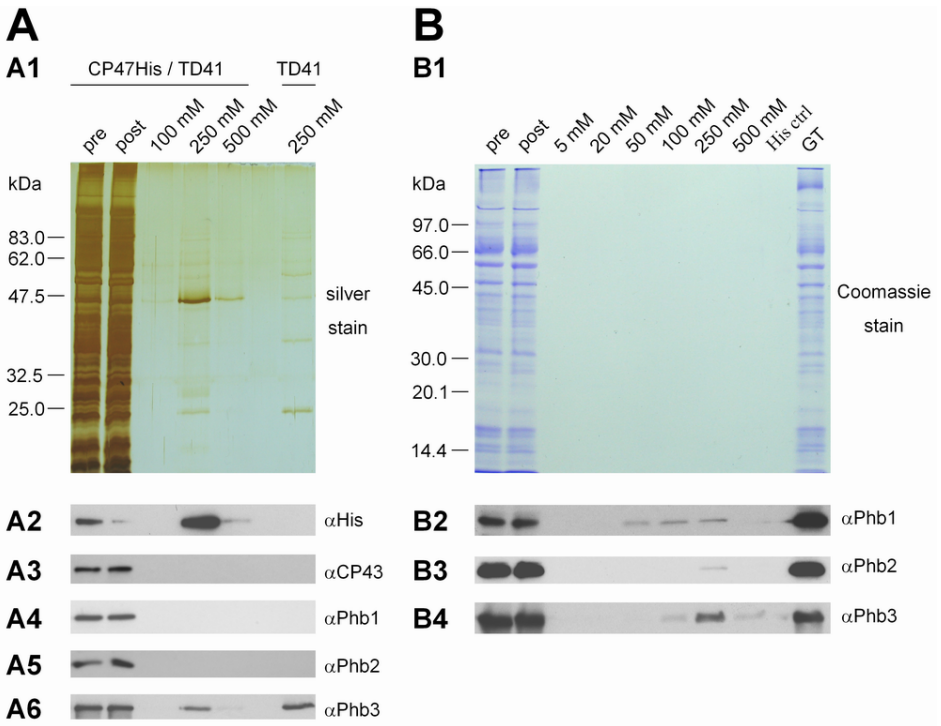

Figure 5.16: Purification of His_8-tagged Band 7 proteins using Ni-NTA magnetic beads. The samples of the Ni-NTA magnetic beads affinity-purifications of (A) His_6-tagged CP47 protein of the CP47-His/TD41 strain and (B) His_8-tagged Band 7 proteins of the Phb1-His, Phb2-His and Phb3-His strains, were analysed by 1-D SDS PAGE and immunoblotting. (A and B) The pre- and postbinding samples corresponded to an amount of 1 µg chlorophyll a, while only 7.5 µl of the 500 µl washing (5 mM, 20 mM, 50 mM, 100 mM Imidazole) and elution fractions (250 and 500 mM Imidazole) were loaded. Gels of each purification were (A1) silver- or (B1) Coomassie-stained or (A2 to A4 and B2 to B4) used for immunoblots with the indicated antibodies.

When the Ni-NTA magnetic beads affinity-purification procedure was performed on crude membrane isolations of the Phb1-His, Phb2-His and Phb3-His *Synechocystis* sp. PCC 6803 mutant strains, no protein bands could be detected on

Coomassie-stained 1-D SDS PAGE gels (see Figure 5.16B1). Immunoblotting analyses however, indicated that the His_8-tagged Phb1, Phb2 and Phb3 proteins had been captured by the Ni-NTA magnetic beads, although the antibody signals for the pre- and postbinding samples suggested that only a minority of His_8-tagged protein had been bound (see Figure 5.16B2 to Figure 5.16B4). Thus, due to the rather low binding efficiency and yield of His_8-tagged Band 7 protein with this method, a different purification approach was taken.

5.4.2 Purification of Band 7 proteins by immunoprecipitation

As the His_8-tagged Band 7 proteins could not be purified in sufficient quantity or quality using Ni-NTA magnetic agarose beads, an immunoprecipitation approach with antibodies coupled to Protein A sepharose beads was pursued. In order to be able to elute the complexes of the proteins of interest without contaminating antibodies, initially, purified polyclonal Band 7 antibodies were bound and covalently crosslinked to Protein A sepharose beads (see Figure 5.17A). In another immunoprecipitation experiment with non-crosslinked antibodies, the optimum incubation time to quantitatively capture the protein of interest from crude membrane isolations was determined (see Figure 5.17B). After the initial preparations were concluded, immunoprecipitations on crude membrane isolations of the *Synechocystis* sp. PCC 6803 wild-type GT and the ΔPhb1-4 quadruple mutant strains were performed. Captured Band 7 proteins were eluted under native and denaturing conditions and analysed by 1-D SDS PAGE, 1-D BN PAGE and immunoblotting (see Figure 5.18).

To generate sepharose beads that would specifically precipitate the proteins of interest without contaminating antibodies in the eluate, in a first step, purified polyclonal Band 7 antibodies were incubated with Protein A-coupled sepharose beads (pre- and post-binding samples) and in a second step covalently crosslinked (pre- and post-coupling samples) using the crosslinker dimethylpimelimidate (DMP). Subsequently, equal amounts of the pre- and post-binding and the pre- and post-coupling samples respectively were compared on a silver-stained 1-D SDS PAGE gel. This gel showed that roughly equal amounts of the samples had been loaded and antibody related protein bands could be observed in the pre-binding and pre-coupling samples in the region of approximately 50 kDa and in between the 25.0 and 32.5 kDa marker bands (see Figure 5.17A1). The αrabbit secondary antibody immunoblotting

analysis, that detected the heavy chains of rabbit antibodies, showed strong signals in the pre-binding and pre-coupling samples, while no signals could be detected in the post-binding and post-coupling samples (see Figure 5.17A2). Thus, this analysis demonstrated that the Band 7 antibodies had been quantitatively bound and coupled to Protein A sepharose beads.

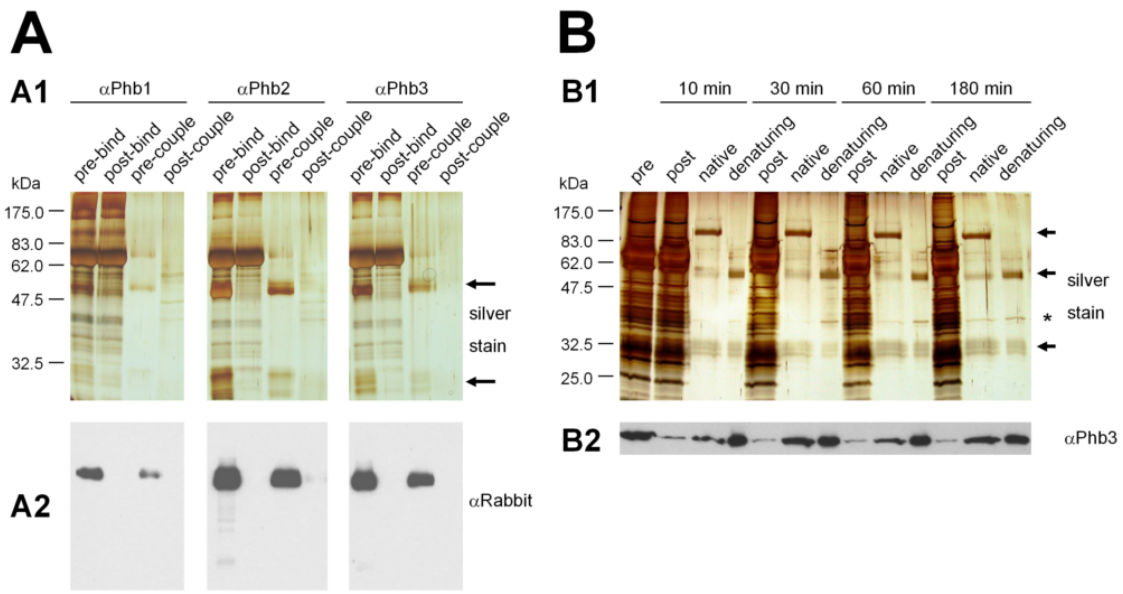

Figure 5.17: Preparation of purified Band 7 antibody-coupled Protein A sepharose beads and testing of the optimum incubation time for immunoprecipitations. (A) The binding and covalent coupling of purified Band 7 antibodies was tested by 1-D SDS PAGE and immunoblotting. Equal amounts of pre- and post binding and pre- and post coupling samples were loaded. (A1) One gel was silver-stained and antibody-related protein bands are marked with arrows. (A2) Another gel was blotted and incubated with secondary αrabbit antibody. (B) Immunoprecipitation analyses with varying incubation times of 10, 30, 60 and 180 min were performed on a crude membrane isolation of the *Synechocystis* sp. PCC 6803 wild-type GT strain with non-crosslinked, purified αPhb3 antibodies. Pre- and postbinding samples corresponded to an amount of 0.6 µg chlorophyll a per lane, while 15 µl of an 80 µl native elution and 5 µl of a 50 µl subsequent denaturing elution were loaded. (B1) One gel was silver-stained, antibody-related protein bands are marked with arrows and an asterisk marks the position of the immunoprecipitated Phb3 protein. (B2) Another gel was blotted and incubated with the αPhb3 antibody.

In another immunoprecipitation experiment, the optimum incubation time to capture the protein of interest from crude membrane isolations using non-crosslinked antibodies was determined. Thus, αPhb3 beads were incubated with crude *Synechocystis* sp. PCC 6803 wild-type GT membranes for 10, 30, 60 and 180 min. After the respective incubation time had elapsed, samples were washed and then eluted under native and then under denaturing elution conditions. On the 1-D SDS PAGE

gels, the post binding and both the native and denaturing elution samples were analysed. A silver-stained gel revealed, that under native elution conditions, 60 min incubation time seemed to be enough to capture sufficient Phb3 protein to yield a detectable protein band. Under denaturing elution conditions, the Phb3 protein bands were stronger and could be detected already after an incubation time of 30 min (see Figure 5.17B1; asterisk). When the corresponding immunoblot, that had been probed with the αPhb3 antibody, was analysed, it became apparent, that the Phb3 protein seemed to be depleted from all post samples. Even though no quantitative analysis could be performed on this immunoblot, this more sensitive method revealed that all native elution fractions seemed to contain the Phb3 protein in what looked like roughly similar amounts. The same seemed to be true for the eluates that had been obtained under denaturing elution conditions (see Figure 5.17B2). In the end, as a compromise to maximise binding efficiency and minimise protein complex degradation, an incubation time of 60 min was chosen for routine immunoprecipitations.

After the necessary antibody-coupled sepharose beads had been produced and the appropriate immunoprecipitation conditions determined, further experiments were performed to obtain purified Band 7 protein complexes for subsequent structural analyses. Crude membrane isolations of both the *Synechocystis* sp. PCC 6803 wild-type and the ΔPhb1-4 quadruple mutant strains were generated for immunoprecipitations with the previously produced αPhb1, αPhb2 and αPhb3 antibody-coupled sepharose beads. Native and consecutive denaturing elutions were analysed on both 1-D SDS and 1-D BN PAGE gels, which were also blotted and probed with the various Band 7 antibodies.

Interestingly, the Phb1, Phb2 and Phb3 Band 7 proteins appeared to be quantitatively eluted from the beads under native conditions in this analysis and could be visualised on a silver-stained 1-D SDS PAGE gel. Apparently, not enough material remained bound to the beads, so that no protein bands could be detected in the denaturing elution fractions. Both the Phb1 and Phb2 proteins yielded only relatively faint protein bands, while the Phb3 protein displayed a strong band (marked as 1, 2 and 3 on the gel respectively). Additionally, the elution fractions appeared to be rather clean and only a few contaminating protein bands could be observed (see Figure 5.18A1). The corresponding immunoblots underlined these observations (see Figure 5.18A2 to Figure 5.18A4). In order to test the eluates for intact or broken down Band 7 protein complexes, 1-D BN PAGE and immunoblotting analyses were performed.

Since only small amounts of protein had been detected on the silver-stained 1-D SDS PAGE gel, it was not surprising, that no protein complex bands could be detected on the Coomassie-stained 1-D BN PAGE gel (see Figure 5.18B1).

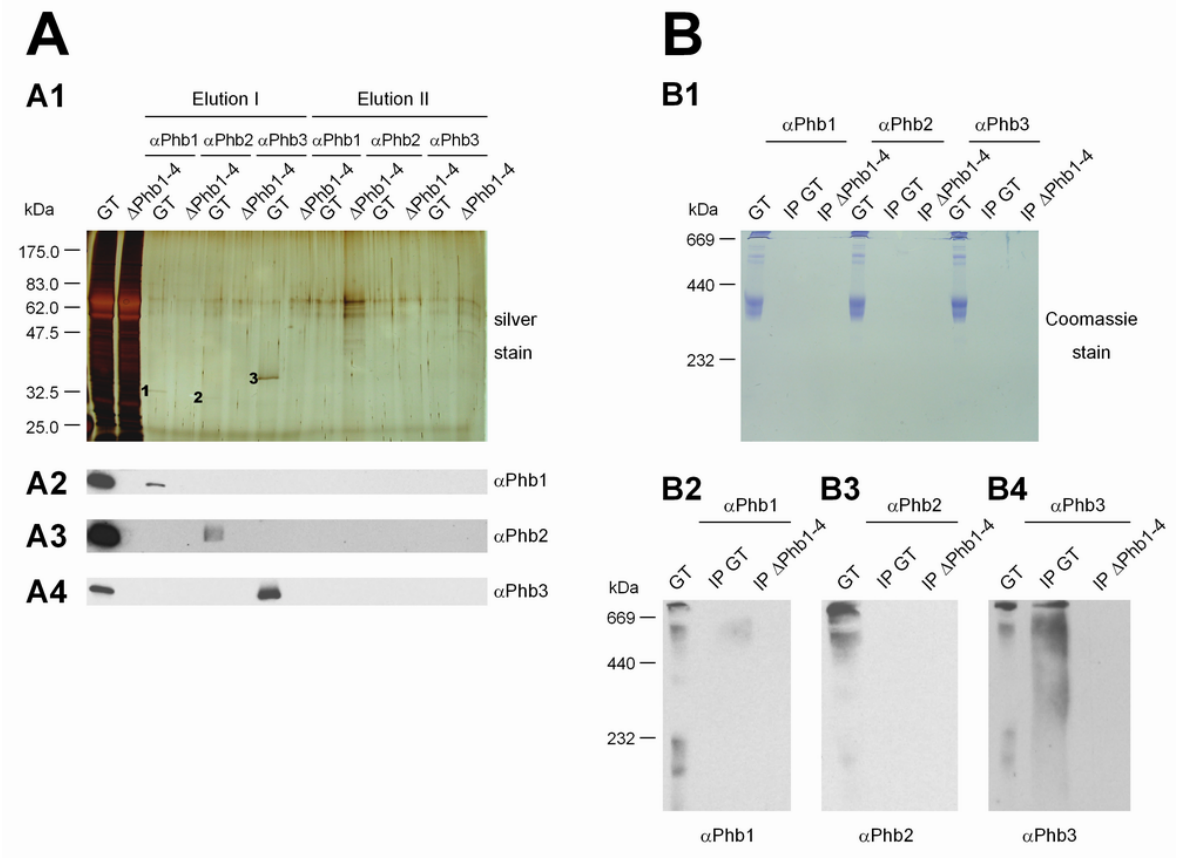

Figure 5.18: Analyses of immunoprecipitated Band 7 proteins of *Synechocystis* sp. PCC 6803. Immunoprecipitation analyses were performed on crude membrane isolations of the *Synechocystis* sp. PCC 6803 wild-type GT and the ΔPhb1-4 quadruple mutant strains with previously prepared αPhb1, αPhb2 and αPhb3 purified antibody-coupled Protein A sepharose beads. Captured proteins were eluted under native (elution I) and denaturing (elution II) conditions and analysed by (A) 1-D SDS PAGE, (B) 1-D BN PAGE followed by immunoblotting. (A) Crude membrane isolations of both strains that corresponded to an amount of 0.25 µg chlorophyll a were loaded per lane. 7.5 µl of a total volume of 100 µl native elution and 15 µl of a total volume of 110 µl denaturing elution were loaded on 1-D SDS PAGE gels. (A1) One gel was silver-stained and 1 to 3 indicated the protein bands that corresponded to the respective, immunoprecipitated Band 7 protein. (B) Crude membrane isolation of the *Synechocystis* sp. PCC 6803 wild-type GT strain corresponding to an amount of 1 µg chlorophyll a and aliquots of 15 µl of 55 µl solubilised native elution fractions were loaded the lanes of a 1-D BN PAGE gel. (A2 to A4 and B2 to B4) Other gels were used for immunoblotting analyses with indicated antibodies. (A and B) The type of antibody-coupled beads and the strain from which the crude membrane isolations originated used in the analyses are indicated.

However, the αPhb3 immunoblot displayed a discrete antibody signal band, that corresponded to an antibody signal obtained from crude wild-type membranes and

furthermore suggested that intact Phb3 protein complexes had been purified. As this signal smeared into the low-molecular-mass region, it could be assumed that the sample also contained Phb3 protein complex breakdown products (see Figure 5.18B4). Probably due to the low yields, no protein complexes could be detected in the eluates obtained with the αPhb1 and αPhb2 antibodies (see Figure 5.18B2 and Figure 5.18B3). The purified Phb3 protein complexes were then further analysed by transmission electron microscopy and yielded enough data for a single-particle analysis.

5.5 Single-particle analysis of Phb3 protein complexes of *Synechocystis* sp. PCC 6803

The native eluate of the immunoprecipitation experiment with αPhb3 sepharose beads and crude *Synechocystis* sp. PCC 6803 wild-type GT membranes contained purified Phb3 protein complexes that could be visualised under the transmission electron microscope (TEM) and were subsequently analysed by single-particle analysis (in collaboration with Dr. Jon Nield, Imperial College London, London, UK; van Heel et al., 2000). Many electron micrographs were taken over the course of several electron microscopy sessions and provided the dataset that gave the first low resolution (~3 nm) projections of the Phb3 protein complex of *Synechocystis* sp. PCC 6803 (see Figure 5.19) and of a stomatin protein complex in general. A representative region of one such electron micrograph that contained several Phb3 protein complexes, is shown in Figure 5.19A. In total, 3,708 single-particles belonging to the Phb3 protein complex were chosen from seven electron micrographs that were of sufficient quality to be included in this analysis. The visualised Phb3 protein complexes appeared to be randomly orientated on the carbon support and had a ring-like appearance. Even though an occasional trimeric PSI protein complex could be identified in the sample (data not shown), the overall structural homogeneity of the sample appeared to be high i.e. few contaminating protein complexes. Initially, 2-D class averages were calculated from all 3,708 single-particles using the reference-free alignment techniques (for more information, see review: Ruprecht and Nield, 2001), which ultimately allowed for the identification of a subpopulation of 499 single-particle 'top views', i.e. the largest Phb3 particle observed in terms of projection surface area. After a *de novo* iterative refinement of these 499 single-particles, 20 different class averages of the Phb3 protein

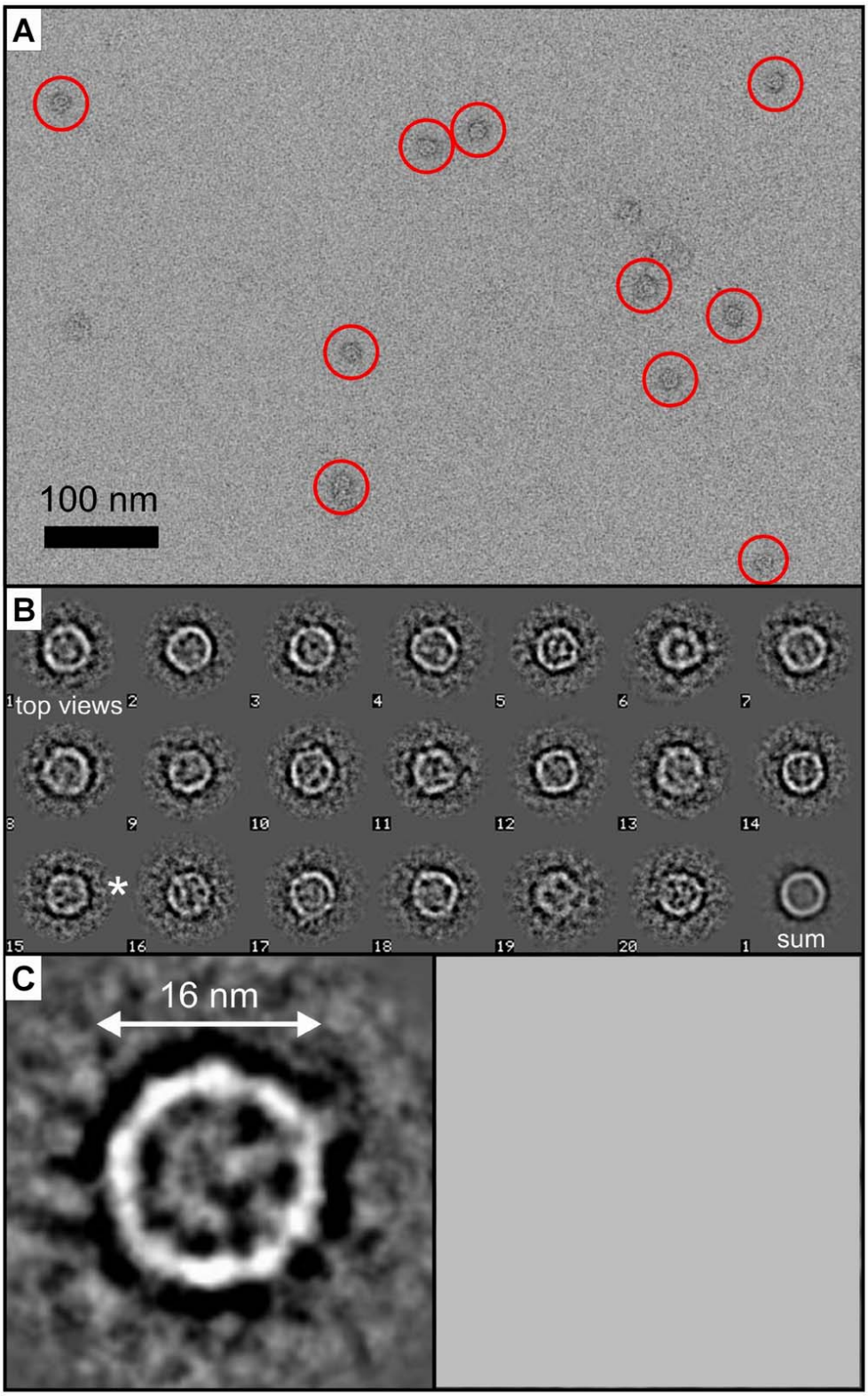

Figure 5.19: Single-particle analysis of Phb3 protein complexes of *Synechocystis* sp. PCC 6803. (A) Selected region of an electron micrograph that shows Phb3 protein complexes (circled in red). Scale bar represents 100 nm, as indicated. (B) A subpopulation of 499 particles (classified as the largest projections observed within a total of 3,708) was assigned as a 'top view' and was further classified into 20 classes, where (C) is a magnified class # 15, being ~16 nm in diameter. (A to C) Protein is shown as white and stain as black.

complexes were distinguished by this *in silico* method (see Figure 5.19B). In summary, the Phb3 protein complex appeared as a ring-like structure with an approximate diameter of about 16 nm. Although no definitive stochiometric conclusions could be drawn from these class averages, given the small subpopulation dataset extracted, an evaluation of the class averages # 15 suggested that the Phb3 protein complex might be composed of between ten to twelve Phb3 monomer subunits (see Figure 5.19C).

5.6 The Phb1 prohibitin and Slr0228 FtsH homologues of *Synechocystis* sp. PCC 6803 interact with each other

Prohibitin homologues have been shown to form large, membrane-bound protein complexes that interact with and seem to regulate FtsH protease homologues in *E. coli* (Kihara et al., 1996; Saikawa et al., 2004) and *S. cerevisiae* (Steglich et al., 1999). However, the results that had been obtained on the physiological relevance of the Band 7 proteins in this study, did not reveal a functional interdependence between the Band 7 proteins i.e. also the Phb1 prohibitin homologue and the Slr0228 FtsH protease of *Synechocystis* sp. PCC 6803 (see Chapter 4).

Nevertheless, various approaches were taken to test whether the two proteins physically interact with each other. Initially, eluates of immunoprecipitations with Band 7 antibody-coupled sepharose beads were probed for the presence of FtsH homologues with the αFtsH antibody (data not shown). Also the reciprocal experiment was performed, in which the eluates of immunoprecipitation experiments with the αFtsH antibody serum were probed with Band 7 antibodies (data not shown). Disappointingly, neither of these approaches gave evidence for a physical interaction between the Band 7 and FtsH homologues. However, as only little amounts of an unpurified αFtsH antibody serum were available, that was moreover only directed against *E. coli* FtsH homologues, ultimately, another approach was pursued. Crude membranes of a 0228-GST strain that contained a GST-tagged version of the Slr0228 FtsH protease together with αGST antibodies coupled to sepharose beads were used in an immunoprecipitation experiment and the resulting eluates were analysed by 1-D SDS PAGE and immunoblotting (see Figure 5.20). Additionally, a 1-D BN PAGE analysis of crude membranes of the *Synechocystis* sp. PCC 6803 wild-type and the Δ0228 mutant strains was performed, where the resulting gels were blotted and probed with the Band 7 and the αFtsH antibodies (see Figure 5.21).

The immunoprecipitation analysis with αGST antibodies coupled to protein A sepharose beads on both *Synechocystis* sp. PCC 6803 wild-type GT and 0228-GST crude membranes gave the first indication that the Phb1 protein and the Slr0228 FtsH protease do physically interact with each other. Already on the silver-stained 1-D SDS PAGE gel could the eluted 0228-GST protein be visualised (marked by an asterisk) in the 'bound' fraction of 0228-GST crude membranes. Another, unknown protein was detected in between the 62.0 and 83.0 kDa protein marker bands. Both of these proteins were neither present in the no AB controls or in the 'bound' fraction of wild-type GT crude membranes. Moreover, the washing steps seemed to effectively clean the sample, as only little contamination could be observed in wash 1, and no distinct contaminating protein bands could be detected in the washes 2 and 3 (see Figure 5.20A1). The αGST immunoblotting analysis confirmed the identity of the asterisk-marked protein as the 0228-GST FtsH protease. Because the αGST antibody did not yield a detectable antibody signal for the 10 % pre-binding sample, only a rough estimate of the binding efficiency of the 0228-GST protein can be given (~80 %), although it seems that the majority of the 0228-GST protein had been captured by the beads (see Figure 5.20A2). More importantly, the αPhb1 antibody yielded a signal in the 'bound' eluate indicating that the Phb1 protein co-immunoprecipitated with the 0228-GST protein. Furthermore, this interaction between the Phb1 and the 0228-GST proteins was found to be specific, as the Phb1 protein could neither be detected in the 'no AB' controls nor in the 'bound' fraction of the immunoprecipitation with the wild-type crude membrane isolation. Nevertheless, even though the interaction was specific, a comparison of the antibody signals in the 'bound' and 1 % pre-binding samples with the naked eye already suggested that only a very small fraction of the total Phb1 protein population co-immunoprecipitated with the 0228-GST FtsH protease (see Figure 5.20A3). Given an amount of crude thylakoid membranes that corresponded to 40 µg Chl a as starting material for the immunoprecipitation experiment, an estimated amount of ~80 % of the GST-tagged Slr0228 bound to the beads (compare Figure 5.20A2; 100 % and post lane), ~10 % of the eluate loaded, i.e. 12.5 µl of the total 120 µl and a signal intensity for the Phb1 protein in the bound fraction that would be expected for a sample that contained ~0.01 µg Chl a (compare Figure 5.20A3; bound and 1 % lane), it was calculated that only 0.3 % of the entire Phb1 protein population seemed to be associated with the Slr0228-GST protein under the prevailent experimental conditions. The Phb2 and Phb3 Band 7 proteins could not be detected in

the eluate of the immunoprecipitation with αGST coupled sepharose beads and crude 0228-GST membranes (see Figure 5.20A4 and Figure 5.20A5). It is noteworthy, that the αPhb2 and αPhb3 antibodies did not seem to react sensitively enough in this analysis, as no antibody signal could be observed in the 1 % pre-binding sample and only weak antibody signals were detected in the 10 % pre-binding samples. Ultimately however, excluding the possibility that Phb1 might interact with the GST-tag of the Slr0228-GST fusion protein, this analysis suggested that the Phb1 prohibitin and the Slr0228 FtsH homologues of *Synechocystis* sp. PCC 6803 physically interact with each other at very low levels under standard laboratory growth conditions.

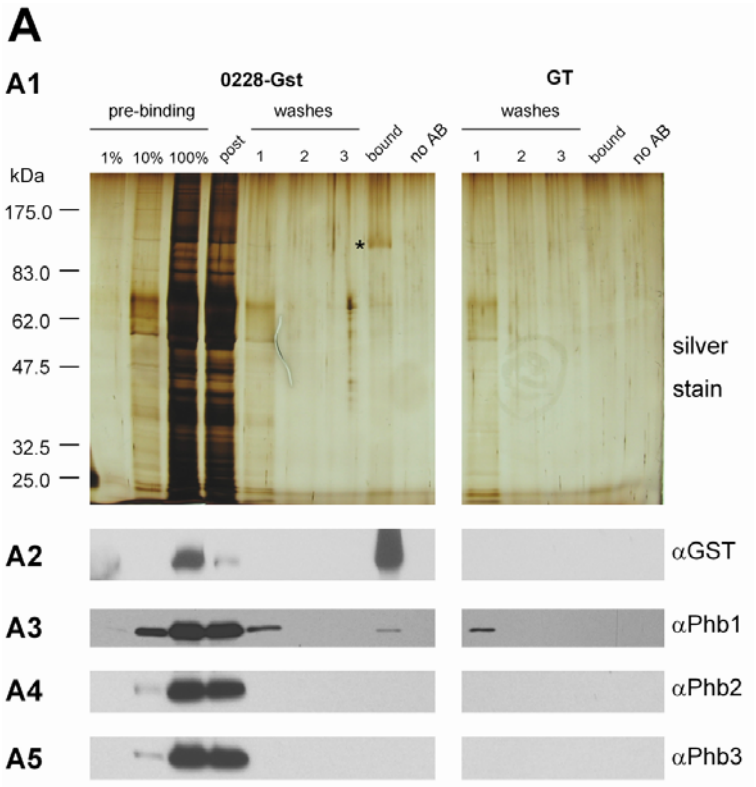

Figure 5.20: Analysis of immunoprecipitated GST-tagged FtsH. Immunoprecipitation analyses were performed on crude membrane isolations of the *Synechocystis* sp. PCC 6803 wild-type GT and the 0228-GST strains with previously prepared αGST antibodies coupled to Protein A (bound) and Protein A sepharose beads only (no AB). Captured proteins were eluted under native conditions and analysed on 1-D SDS PAGE gels that were (A1) silver-stained or (A2 to A5) immunoblotted with various antibodies. The 100 % sample of the dilution series and the post-binding sample contained crude 0228-GST membranes that corresponded to an amount of 0.5 µg chlorophyll a per lane, while the other dilution series samples contained respectively less. 6.25 µl aliquots of the three washing steps were solubilised with the same amount of 1x SDS sample buffer and loaded on the gel. The 'bound' and 'no AB' samples had been eluted into a volume of 60 µl that was solubilised with 60 µl of 1x SDS sample buffer. Both samples were loaded in 12.5 µl aliquots per lane. The asterisk (*) indicates the position of the 0228-GST protein on the gel.

In order to test the effect of inactivating the Slr0228 FtsH homologue on Band 7 protein complexes, a 1-D BN PAGE analysis followed by immunoblotting was performed on crude membrane isolations of the *Synechocystis* sp. PCC 6803 wild-type GT and the Δ0228 inactivation mutant strains. The unstained and the Coomassie-stained 1-D BN PAGE gel strips showed similar protein complex patterns in the high-molecular-mass region above the 440 kDa protein marker band. However, an additional protein complex (marked by *3) could be observed in the Δ0228 mutant strain in the molecular mass region of around the 232 kDa protein marker band, while two other protein complexes (marked by *1 and *2) below the 232 kDa protein marker band, that had been present in the wild-type strain, could not be detected in this strain (see Figure 5.21A1 and Figure 5.21A2).

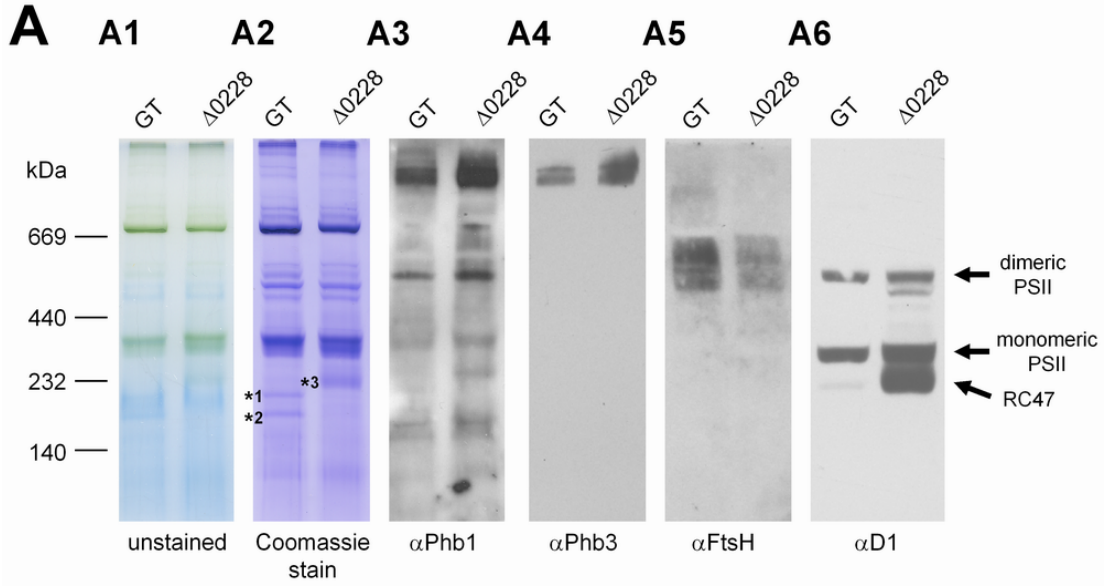

Figure 5.21: 1-D BN PAGE and immunoblotting analyses of the *Synechocystis* sp. PCC 6803 wild-type GT and the Δ0228 inactivation mutant strains. Crude membrane isolations of the *Synechocystis* sp. PCC 6803 wild-type GT and the Δ0228 inactivation mutant strains were separated by 1-D BN PAGE. Samples corresponding to an amount of 2 µg chlorophyll a were loaded in the lanes of 5 to 12.5 % (w/w) PAA linear gradient 1-D BN gels. (A1) One unstained, (A2) one Coomassie-stained gel strip (with protein complexes referred to in the text marked by asterisks) and (A3 to A6) subsequent immunoblotting analyses with indicated antibodies are shown. The positions of monomeric and dimeric PSII protein as well as RC47 protein complexes are indicated.

The immunoblotting analysis with the αD1 antibody yielded signals for both strains that could be attributed to monomeric and dimeric PSII (marked with arrows). Moreover, the additional protein complex that had been observed below monomeric

PSII on the Coomassie-stained 1-D BN PAGE gel, reacted with the αD1 antibody and was therefore identified as the RC47 protein complex (Komenda et al., 2006; see Figure 5.21A6). Unlike the PSII complexes, the protein complex pattern of the Band 7 proteins did not seem to be affected by the inactivation of the Slr0228 FtsH homologue. The high-molecular-mass protein complexes of the Phb1 Band 7 protein that were usually observed in 1-D BN PAGE immunoblotting analyses (see Figure 5.8), could still be found, although the background signal in this analysis were rather strong (see Figure 5.21A3). In the case of the Phb3 Band 7 protein, two distinct, previously unresolved antibody signals in the high-molecular-mass region could be detected in both strains (see Figure 5.21A4). When the immunoblot that had been probed with the αFtsH antibody was analysed, a broad antibody signal could be observed that started just below the 669 kDa protein marker band and tailed into the lower-molecular-mass-region to roughly 550 kDa. This broad antibody signal was detected in both strains, while it appeared to be slightly weaker in the Δ0228 mutant strain. In conclusion, it could be noted that given the very low level physical interaction between the Phb1 prohibitin and Slr0228 FtsH homologues, it is not surprising to find that the protein complex pattern of the tested Band 7 proteins was not affected by the inactivation of the Slr0228 FtsH homologue.

5.7 Discussion

The first part of this discussion deals with the generation of the purified, polyclonal Band 7 antibodies (see section 5.7.1), while the characterisation of the Band 7 proteins and their respective protein complexes in *Synechocystis* sp. PCC 6803 and *Thermosynechococcus elongatus* will be discussed afterwards (see section 5.7.2).

5.7.1 Generation of purified, polyclonal antibodies

In order to generate purified, polyclonal antibodies, the Band 7 proteins were overexpressed in *E. coli* and purified for their usage as antigens (see section 5.7.1.1). While the following immunisation procedure was performed by an external company (Seqlab, Göttingen, Germany), the resulting polyclonal antibody sera were purified and tested in this work. Relevant details of the final testing of the purified antibodies are briefly discussed (see section 5.7.1.2).

5.7.1.1 Overexpression of Band 7 proteins

Initially, expression constructs for full-length Band 7 proteins of *Synechocystis* sp. PCC 6803 were generated in the pET16b expression vector to be subsequently used in various *E. coli* expression strains. The important features of pET vectors for the overexpression of proteins in *E. coli* are that large quantities of the protein of interest can be obtained (more than 50 % of total cell protein), while the expression can be tightly controlled by different regulation mechanisms. The pET16b vector features a T7*lac* promoter as part of the transcription control mechanism and a N-terminal His_{10}-tag in combination with a factor Xa protease site that can be used during a subsequent affinity-purification. By using the pET16b vector, transcription to overexpress a protein of interest can only be initiated when T7 RNA polymerase is available. In this work, the expression constructs were transformed into the BL21-Gold(DE3)pLysS and Rosetta(DE3) *E. coli* bacterial strains, where T7 RNA polymerase is integrated into the bacterial genome by the bacteriophage DE3 under the control of the *lac*UV5 promoter (Studier and Moffat, 1986). Therefore, the addition of IPTG to the culture medium induces the expression of T7 RNA polymerase, so that transcription and subsequent expression of the protein of interest can begin. However, even in the absence of IPTG it is possible that the protein of interest is expressed at low level due to some background expression of the T7 RNA polymerase from the *lac*UV5 promoter. Thus, in order to prevent the transcription of the T7 RNA polymerase, glucose can be added to the growth medium (Grossman et al., 1998) or another expression strain (for example the BL21-Gold(DE3)pLysS *E. coli* expression strain) can be tested. The BL21-Gold(DE3)pLysS *E. coli* strain contains an additional plasmid that encodes the chloramphenicol acetyl transferase (confers chloramphenicol resistance), some rare tRNAs and more importantly the gene for T7 lysozyme. T7 lysozyme is a bifunctional enzyme that is on the one hand a natural inhibitor of the T7 RNA polymerase (Zhang and Studier, 1997; Huang et al., 1999) and on the other hand an enzyme that specifically cuts bonds within the peptidoglycan layer of the *E. coli* cell wall (Inouye et al., 1973). The latter property of the enzyme is beneficial for subsequent purification procedures, as lysis of the bacterial cells is facilitated. The Rosetta(DE3) *E. coli* expression strain is an alternative bacterial expression strain, that also provides rare tRNAs to the expression host. However in this work, the proteins of interest were constitutively expressed under standard laboratory growth conditions by the Rosetta strain (data not shown), so that the pLysS strain was used preferentially.

Even though the expression of full-length Band 7 proteins was attempted in different *E. coli* expression strains, only Sll0815 (Phb4) could be readily expressed. Interestingly, this protein is the only Band 7 protein that is not predicted to possess a TM domain and therefore, in another attempt to overexpress the Phb2, Phb3 and Phb5 proteins, the region that is predicted to encode the TM domains of these proteins was omitted. Subsequently, Phb2-TM and Phb3-TM could be expressed in amounts that could be detected with the naked eye on a Coomassie-stained 1-D SDS PAGE gel, while the Phb5 protein could still not be expressed, even as a truncated version. Nevertheless, as the bacterial cells that had been transformed with the constructs to express Phb5 or Phb5-TM were able to grow during the induction period (data not shown), it appears unlikely that the Phb5 protein does not accumulate due to a potential toxicity of the protein to the cells. However, it is noteworthy, that the Phb5 gene is the largest of the Band 7 genes of *Synechocystis* sp. PCC 6803 (*phb5* = 2022 bp; Phb5 = 74.4 kDa) and even after the truncation of the region that encodes the TM domain, the Phb5-TM expression product would still have been substantially large (*phb5-TM* = 1722 bp; Phb5-TM = 63.6 kDa). Thus, the problem lies in between transcription of the *phb5* or *phb5-TM* mRNA and the accumulation of the final expression product, so that the expression conditions could be altered until the Phb5 protein is expressed from the already generated expression constructs. However, it appears to be more advisable to chose an even smaller portion of the Phb5 protein, preferably a unique region, for the generation of a new expression construct. All the proteins that were successfully expressed in this work prevailed as inclusion bodies, which was advantageous, as these insoluble aggregates could be easily isolated by centrifugation and furthermore protected the proteins of interest from proteolytic degradation.

Overall, it remains enigmatic why the Phb2, Phb3 and Phb5 full-length and especially the Phb5-TM truncated version of the Band 7 proteins could not be overexpressed.

5.7.1.2 Testing the purified antibodies

After having affinity-purified the generated polyclonal antibody sera directed against the Phb1, Phb2, Phb3 and Phb4 Band 7 proteins of *Synechocystis* sp. PCC 6803, the purified antibodies were first tested on the used antigens and then on crude membrane isolations of *Synechocystis* sp. PCC 6803 and *Thermosynechococcus*

elongatus (see Figure 5.3). While the immunoblotting analysis on the antigens yielded the expected results and showed that only specific antibodies had been raised during the immunisation procedure, some details about the test results on the crude membrane isolations needed to be addressed.

In general, the purified antibodies were capable of specifically detecting their antigen in crude membrane isolations of *Synechocystis* sp. PCC 6803 and where possible even recognised their corresponding Band 7 homologue in *Thermosynechococcus elongatus*. However, even though TE_Phb1 (31.55 kDa) had a slightly larger predicted molecular mass than Phb1 (30.57 kDa), and TE_Phb2 (35.68 kDa) and Phb3 (35.73 kDa) possessed almost equal molecular masses, the positions of the antibody signals in the immunoblotting analysis did not reflect this fact. Thus, due to the exhibited, slightly increased electrophoretic mobility of the Band 7 proteins of *Thermosynechococcus elongatus*, it can be postulated that the protein of this thermophilic organism in general might not be completely unfolded under the prevalent denaturation conditions (1h at RT in 1x SDS sample buffer) and thereby the apparent molecular masses of the proteins could be influenced. However, more important was the observation that the purified αPhb1 antibody yields signals of equal intensities in the lanes that corresponded to the crude membrane isolations of *Synechocystis* sp. PCC 6803 and *Thermosynechococcus elongatus* respectively, while the two signals for the αPhb3 antibody exhibited significantly different intensities. A ClustalW alignment revealed that the TE_Phb1 (Tlr1760) protein contained 202 identical (70.4 %) and 40 similar (13.9 %) amino acids with an alignment score of 68 when compared to the Phb1 (Slr1106) protein (data not shown), whereas the same analysis revealed that the TE_Phb2 (Tlr2184) protein contained 197 identical (61.4 %) and 69 similar (21.5 %) amino acids with an alignment score of 60 when compared to the Phb3 (Slr1128) protein (data not shown). To put the quoted alignment scores into perspective, a ClustalW alignment of the D1 (PsbA) proteins of *Synechocystis* sp. PCC 6803 and *Thermosynechococcus elongatus* yielded an alignment score of 81. However, although the TE-Phb1 and Phb1 proteins appear slightly more conserved than the TE_Phb2 and Phb3 proteins, it is remarkable that that the TE_Phb2 protein was significantly less well recognised by the αPhb3 antibody in this immunoblotting analysis.

Finally, testing the αPhb4 antibody sera revealed that antibodies against the Phb4 protein of *Synechocystis* sp. PCC 6803 had been raised during the immunisation

procedure, but due to too many unspecific cross-reactions, that were in close proximity to the desired antibody signal, these antibodies were difficult to use. Apparently, the affinity-purification process had not been as successful as for the other antibodies and the rabbits that had been used in the immunisation procedure were possibly not chosen carefully enough.

Nevertheless, three potent and specific antibody sera against the Phb1, Phb2 and Phb3 proteins of *Synechocystis* sp. PCC 6803 and TE_Phb1 and TE_Phb2 of *Thermosynechococcus elongatus* could be used for subsequent analyses.

5.7.2 Characterisation of cyanobacterial Band 7 proteins and their complexes

5.7.2.1 Different Synechocystis sp. PCC 6803 wild-type strains

Synechocystis sp. PCC 6803 is a gram-negative, unicellular, non-nitrogen (N_2)-fixing, ubiquitous fresh water inhabiting cyanobacterium and one of the prokaryotic model organisms for photosynthetic research. There are two main reasons for the preferential use of this organism in genetic and physiological studies of photosynthesis: its natural competence for transformation with exogenous DNA (Grigorieva and Shestakov, 1982) and its ability to grow heterotrophically (Williams, 1998). Additionally, *Synechocystis* sp. PCC 6803 was overall the fourth organism and the first phototrophic organism whose genome has been completely sequenced (Kaneko et al., 1996).

Generally, four culture substrains of *Synechocystis* are mentioned in the literature ('PCC','ATCC','GT' and 'Kasuza'), all of which are derivatives of the so-called Berkeley strain 6803 (Stanier et al., 1971). Initially, all of the four substrains were believed to be the same and consequently listed and grouped under *Synechocystis* sp. PCC 6803 (Rippka and Herdman, 1992). However, differences in the genotypes that subsequently lead to slight phenotypic changes between the four substrains have been identified in various studies (Ikeuchi and Tabata, 2001). The apparent phenotypic differences are: motility in the *Synechocystis* sp. PCC 6803 wild-type strain, which cannot be observed in the ATCC or the GT strains; sensitivity to glucose, which is exhibited by both the *Synechocystis* sp. PCC 6803 and the ATCC strain, while the GT strain has been intentionally manipulated to grow under photoheterotrophic growth conditions; and it appears that the 'Kazusa' cannot be transformed with exogenous

DNA. In this work, the *Synechocystis* sp. PCC 6803 strain (Rippka et al., 1979) is referred to as the *Synechocystis* sp. PCC 6803 wild-type strain, which can be distinguished from the other substrains by its motility, displayed as either positive (in the PCC-P strain) or negative (in the PCC-N strain) phototaxis (Yoshihara et al., 2000). The other strain that was used in this work, was the *Synechocystis* sp. PCC 6803 wild-type GT strain, which is only slightly motile and has been shown to possess a slightly altered genotype. A comparison between the GT and ATCC 27184 *Synechocystis* substrains with the *Synechocystis* Berkeley strain 6803 attributes the decreased motility phenotype to a 1 bp frame shift mutation in the *spkA* gene (a eukaryotic-type, serine/threonin protein kinase) (Kamei et al., 2001). A deletion of a 154 bp fragment in the *slr2031* gene (Katoh et al., 1995) in the ATCC 27184 strain then lead to the generation of the strain that is now commonly referred to as the *Synechocystis* sp. PCC 6803 wild-type GT strain (Williams, 1988). After two further genetic manipulation steps (Okamoto et al., 1999; Bhaya et al., 2000), this strain became the 'Kazusa' strain which has been used to sequence the complete *Synechocystis* sp. PCC 6803 genome (Kaneko et al., 1996).

Even though the genetic backgrounds of the *Synechocystis* sp. PCC 6803 strains appear to be defined, spontaneous mutations, possibly promoted by unintended selective pressure even under standard laboratory growth conditions, have been reported in the literature (Hihara and Ikeuchi, 1997). Therefore, in order to assess a possible difference in the expression of Band 7 proteins under standard laboratory growth conditions in the *Synechocystis* sp. PCC 6803 wild-type and the *Synechocystis* sp. PCC 6803 wild-type GT strains, crude membrane were isolated, separated on 1-D SDS PAGE gels and probed with various antibodies. A comparison of the intensities of the obtained antibody signals suggested that the Phb1, Phb2 and Phb3 Band 7 proteins were equally expressed in the two strains. However, the immunoblot which had been probed with an αSbtA antibody showed an increased expression of this protein in the *Synechocystis* sp. PCC 6803 wild-type strain. The SbtA protein is a $Na^+/HCO3^-$ symporter (Shibata et al., 2002) involved in the uptake of CO_2 in *Synechocystis* sp. PCC 6803 and can be induced by Ci limitation (Zhang et al., 2004). Thus, the apparent relative overexpression of the SbtA protein in the *Synechocystis* sp. PCC 6803 wild-type strain can most likely be attributed to absence of glucose in the culture medium. The differences between the two strains that could be observed in the protein profiles

on the silver-stained 1-D SDS PAGE gels, do not seem to affect the expression of the Band 7 proteins.

In conclusion, the presented data indicates that the Band 7 proteins are equally expressed in both the *Synechocystis* sp. PCC 6803 wild-type and *Synechocystis* sp. PCC 6803 wild-type GT strains and that their expression does not appear to be altered by the lack or respectively presence of glucose in the culture medium.

5.7.2.2 Expression of tagged Band 7 proteins in Synechocystis sp. PCC 6803

During the course of this project, the Phb1, Phb2, Phb3 and Phb4 proteins of *Synechocystis* sp. PCC 6803 were His_8-tagged, in order to facilitate their subsequent purification (see section 5.3). Unfortunately, the addition of a C-terminal His_8-tag caused the Phb1 and Phb4 Band 7 proteins to be less abundant in the His_8-tagged protein mutant when compared to the non-His_8-tagged Phb1 and Phb4 proteins in the wild-type strain (see Figure 5.15A). A semi-quantitative approach to estimate the level of expression for the Phb1 protein revealed that roughly less than 25 % of the wild-type Phb1 protein could be detected in the His_8-tagged Phb1 protein mutant strain (see Figure 5.15B). Interestingly, the His_8-tagged Phb2 and Phb3 Band 7 proteins accumulated (see Figure 5.15A) and their abundance did not seem to have changed noticeable in the mutant strains (see Figure 5.16B).

Similarly, in an attempt to express the Phb1 and Phb3 proteins with GFP fused to their respective C-termini, the expected GFP-tagged proteins did not accumulate (data not shown). This finding was surprising, as previous studies that aimed to investigate the localisation of Band 7 homologues, have shown that the rice prohibitin (Takahashi et al., 2003) or the human stomatin (Umlauf et al., 2004) homologues can be fused to GFP and accumulate as stable fusion proteins. Nevertheless, although human GFP-tagged stomatin has even been shown to assemble into larger complexes (Umlauf et al., 2004), it can be envisaged that the C-terminal GFP might impose a steric hindrance during the assembly of potential Band 7 protein complexes which ultimately triggers the degradation of the GFP-tagged Band 7 proteins in *Synechocystis* sp. PCC 6803. Interestingly, the two prohibitin homologues of *S. cerevisiae* have been successfully His_6-tagged at their N-termini, while a C-terminal His_6-tag interfered with the formation of the prohibitin complex (Tatsuta et al., 2005). Moreover, genetic manipulations in the predicted C-terminal coiled-coil region of both the prohibitins of

S. cerevisiae and the human stomatin homologue have stressed the importance of the C-terminal domain for complex assembly and stability (Tatsuta et al., 2005; Umlauf et al., 2006). Furthermore, it seems important to remember that cyanobacterial Band 7 proteins have been shown to form large and possibly homo-multimeric protein complexes (see section 5.2.3 to section 5.2.5). Therefore, as for example the prohibitin complex of *S. cerevisiae* is believed to contain between 16 and 20 monomers of each the Phb1 and Phb2 prohibitin homologues (Tatsuta et al., 2005), the introduction of a large amount of positive charges originating from the histidine residues of a His_6-tag might indeed destabilise the Phb1 and Phb4 protein complexes of *Synechocystis* sp. PCC 6803 by electrostatic repulsion.

However, an earlier study that investigated the subcellular localisation of rat prohibitin by immunoelectron microscopy, has shown that if this protein is expressed with a C-terminal c-Myc-tag, it is targeted to the mitochondrion, while an N-terminal c-Myc-tag appears to interfere with the correct targeting and causes the protein to accumulate in the cytoplasm (Ikonen et al., 1995). In this case, the N-terminal c-Myc-tag seems to mask the N-terminal presequence of the prohibitin homologue that usually labels this protein to be targeted to the mitochondrion (Roise and Schatz, 1988; Ikonen et al., 1995).

In summary, although it appears very possible that the introduced C-terminal His_8- and GFP-tags of the cyanobacterial Band 7 proteins might interfere with the formation of the Band 7 protein complexes either by electrostatic repulsion or steric hindrance, it remains enigmatic at which level the accumulation of these tagged proteins is blocked and what triggers their proteolytic breakdown. In conclusion, although the Phb2 and Phb3 proteins had been successfully His_8-tagged at their C-terminus, it would probably have been more advisable to introduce the His_8-tag also at the N-terminus of the Band 7 proteins of *Synechocystis* sp. PCC 6803 or to use a different, preferably uncharged tag.

5.7.2.3 Membrane association and localisation of Band 7 protein complexes

In order to characterise a protein or protein complex of interest, one fundamental question is whether the protein or the constitutive protein subunit respectively is a soluble or a membrane proteins. This problem can be addressed bioinformatically using specific programs that search for approximately 20

hydrophobic residue stretches in the amino acid sequence of the respective protein that typically constitute possible TM domains and mediate membrane integration.

When the Band 7 proteins of *Synechocystis* sp. PCC 6803 and *Thermosynechococcus elongatus* were analysed in this way, in all but the Phb4 (Sll0815) protein at least one N-terminal TM domain could be identified (see Table 3.3). Nevertheless, even though TM domains could be identified and the results in the literature support the notion that the Band 7 proteins of *Synechocystis* sp. PCC 6803 are membrane proteins, ultimately biochemical assays had to provide absolute evidence. In an immunoblotting analysis performed on generated soluble and crude membrane fractions of *Synechocystis* sp. PCC 6803 and *Thermosynechococcus elongatus*, it was found that the Phb1, Phb2, Phb3 and Phb4 and TE_Phb1 and TE_Phb2 proteins were solely present in the crude membrane fraction (data not shown) and consequently can be considered membrane proteins.

Subsequently, further properties of the Band 7 proteins of *Synechocystis* sp. PCC 6803 were assessed, specifically: whether these proteins are peripheral or integral membrane proteins and in which specific membrane the protein complexes reside (see Figure 5.5). Initially, the degree to which the Band 7 proteins of *Synechocystis* sp. PCC 6803 were associated with their hosting membrane was assessed by differential membrane protein extraction (Breyton et al., 1994; see Figure 5.5A). The first observation from the obtained results was that all of the tested Band 7 proteins behaved roughly similar no matter which extraction treatment was applied. Under mild extraction conditions, such as incubation in isolation buffer without Freeze/Thaw (F/T) cycles or extraction buffer with or without F/T cycles, none of the Band 7 proteins could be extracted from the membranes, while an estimated 50 % of the peripheral control protein (PsbO of PSII) were extracted. Similarly, a treatment with 2 M NaCl in the extraction buffer (with F/T cycles), where electrostatic protein/protein interactions are perturbed, did not extract any of the Band 7 proteins from the membranes, while all of the PsbO protein was extracted. Previously, samples in a similar differential membrane protein extraction had been treated with extraction buffer containing 6.8 M urea (with F/T cycles) extracting an estimated 50 % of each of the Band 7 proteins from the membranes, while all of the PsbO and none of the intrinsic control protein (D1 of PSII) were extracted (data not shown). Urea is a chaotropic agent, i.e. an agent that can destabilise hydrogen bonding and hydrophobic interactions by increasing the lipophilicity of water (Hatefi and Hanstein, 1969), but can still be considered a mild

extraction agent. The Band 7 proteins were also only partly extracted (~50 %) by a treatment with 20 mM CAPS (pH = 12.0) (with F/T cycles), where electrostatic protein/protein interactions are affected by the alkaline pH. In conclusion, the Phb1, Phb2, Phb3 and Phb4 Band 7 proteins of *Synechocystis* sp. PCC 6803 are most likely integral membrane proteins that, however, appear to be only weakly associated via their N-terminal TM or hydrophobic domains to the host membrane.

Synechocystis sp. PCC 6803 is a unicellular, prokaryotic organism, that is surrounded by an outer membrane, a peptidoglycan layer and a plasma membrane. Additionally, this cyanobacterium contains intracellular thylakoid membranes, that harbour a multitude of protein complexes and are the main site for oxygenic photosynthesis (Gantt, 1994). Thus, in order to determine the subcellular location of a membrane protein of interest in *Synechocystis* sp. PCC 6803 biochemically, a method that fractionates crude membrane isolations of *Synechocystis* sp. PCC 6803 into plasma and thylakoid membrane fractions to a high degree of purity has been developed (Norling et al., 1998) by combining aqueous polymer two-phase partitioning (Albertsson, 1986) with sucrose density centrifugation. Previously, the Phb1, Phb2, Phb3 and Phb5 proteins of *Synechocystis* sp. PCC 6803 have been identified in the plasma membrane in a proteomic study that analysed a plasma membrane fraction generated in this way (Huang et al., 2002). Furthermore, the Slr0228 FtsH protease has been shown to be localised to the thylakoid membrane using two-phase partitioning (Komenda et al., 2006). Thus, considering the working model and a potential interaction between a Band 7 protein and the Slr0228 FtsH protease, it was necessary to test whether the Phb1 prohibitin homologue in particular or the other Band 7 proteins of *Synechocystis* sp. PCC 6803 might also be present in the thylakoid membrane. Consequently, pure thylakoid and plasma membrane fractions, generated by the two-phase partitioning method, were separated on 1-D SDS PAGE gels and the resulting immunoblots were probed with various antibodies (see Figure 5.5B). This experiment revealed that the Phb1 protein resides in both the plasma and the thylakoid membranes, while the Phb2 and Phb3 proteins were solely found in the plasma membrane (see Figure 5.5B).

With regards to the Phb1 prohibitin homologue of *Synechocystis* sp. PCC 6803, it is interesting to note that despite its localisation to the thylakoid membrane, this protein could not yet be shown to be involved in photosynthesis-related processes (see section 4.2). Additionally, it is remarkable that in most studies the investigated

prohibitin homologues have been reported to localise to the mitochondrion and not to the chloroplast (see section 3.4.2 and section 3.7.1). Consequently, these facts seem to support the assumption that any observed relationships between the prohibitin homologues of cyanobacteria and of higher plants are probably rather due to a convergent functional evolution of the SPFH domain than to a common ancestor (see section 3.6 and section 3.7.6; Rivera-Milla et al., 2006). As the Phb2 Band 7 protein of *Synechocystis* sp. PCC 6803 could not clearly be related to any other identified Band 7 protein (see Figure 3.5), the information that this protein is localised to the plasma membrane in itself does not reveal any insights into further characteristics or its molecular function. Interestingly, the Phb3 protein, which together with the other cyanobacterial stomatin homologues has been shown to be related to the YbbK protein (P0AA53) of *E. coli* (see Figure 3.5), is solely present in the plasma membrane. The YbbK protein has also been found to reside in the plasma membrane of *E. coli*, and protease accessibility assays furthermore reveal that the C-terminal domain of this protein is exposed to the cytoplasm (Chiba et al., 2006). However, the apparently less related human stomatin homologue, has been shown to expose both its N- and C-terminus to the cytoplasmic side of the membrane (Salzer et al., 1993). The topologies of the Phb1 and Phb2 prohibitin homologues of *S. cerevisiae* have also been investigated and it has been reported that both proteins are anchored to the inner mitochondrial membrane via an N-terminal TM domain exposing their C-termini to the intermembrane space (Steglich et al., 1999). Thus, it would have been interesting to assess the topological properties of the Band 7 proteins of *Synechocystis* sp. PCC 6803, in order to test whether the observed phylogenetic relationships are mirrored in this protein property, particularly in the case of the more closely related Phb3 and YbbK proteins. Unfortunately, the topological properties of the Band 7 proteins of *Synechocystis* sp. PCC 6803 were not assessed in this work.

Overall, even though no topological information has been gathered on the Band 7 proteins of *Synechocystis* sp. PCC 6803, it is important for further studies to have identified the subcellular localisation of the Phb1, Phb2 and Phb3 proteins.

5.7.2.4 Size and oligomeric nature of Band 7 protein complexes

5.7.2.4.1 Cyanobacterial Band 7 protein complexes

The results from the FPLC analysis indicated that the Band 7 protein complexes are at least 669 kDa in size, although an insufficient resolution of the high

molecular mass region and a rather crude discrimination into 500 µl fractions, did not allow a more precise evaluation of the Band 7 protein complex sizes. Furthermore, the immunoblotting analysis of the generated fractions suggested that under the prevalent FPLC running conditions the Band 7 protein complexes were subjected to degradation, as the proteins could be identified in almost all the fractions. Thus, it is noteworthy, that even though the used samples were prepared on ice, the actual FPLC run was performed at room temperature with a running buffer (2x PBS supplemented with 0.05 % (w/v) β-DM) that had not previously been optimised for the separation of protein complexes from crude cyanobacterial membrane isolations. However, as each FPLC run lasted only approximately 50 min and the Band 7 proteins had not been extracted from their host membranes by 2 M NaCl (see Figure 5.5A; 2x PBS contains ~300 mM NaCl) it remains unclear, why the protein complexes display this degree of fragility.

The protein complexes of a similarly prepared sample were separated by sucrose-density gradient centrifugation and it seemed that the Band 7 protein complexes were less prone to falling apart or being degraded, as they were found in a few distinct fractions. Nevertheless, in general, sucrose-density gradient centrifugation also features various disadvantages: longer duration of the separation process and prolonged exposure to the detergent used for solubilisation (16 h), imprecise fractionation and the lack of a molecular weight marker. Moreover, a certain degree of variability was added to the method in this work, because the used gradients had to be generated manually. However, despite the lack of a separate molecular weight marker, the presence of distinct and known internal bands allow an approximate evaluation of the Band 7 protein complex sizes, which in each case seemed to be at least 900 kDa.

Ultimately, in agreement with the literature, the best resolution in the high molecular mass region and identification of distinct protein complexes was achieved by BN PAGE followed by immunoblotting analysis (Schägger et al., 1994; Kashino, 2003). Various cyanobacterial Band 7 protein complex populations could be separated, but unfortunately, the largest protein in the used molecular weight marker was thryoglobulin, with a molecular mass of 669.0 kDa, so that despite the remarkable resolution, the identified protein complexes could still not be sized more precisely. Interestingly, in the immunoblotting analysis the intensities of the antibody signals were strongest for the largest, detected protein complexes, while smaller complexes were detected, but with significantly weaker signal intensities. Thus, the integrity and stability of the Band 7 protein complexes appeared to be least affected by the

conditions that prevailed during the BN PAGE analysis. Typically, BN PAGE is performed at a physiological pH of 7.0 to 7.5. The negative net charge, that is a prerequisite for electrophoretic protein separation, because it renders the protein complexes mobile in an electric field and where separation according to particle size is achieved by the sieving effect of a polyacrylamide gel matrix, is introduced into the protein complexes by Coomassie Brilliant Blue G-250 (Schägger and von Jagow, 1991). Moreover, the use of this anionic dye also diminishes artificial aggregation due to electrostatic repulsion of the negatively charged protein complexes (Krause, 2006).

It is important to note, that the initial sample preparation, i.e. crude membrane isolation and sample solubilisation, for each of the three applied protein separation techniques was the same. In each case, n-dodecyl-β-D-maltoside was the detergent of choice for sample solubilisation, as this nonionic detergent is generally used and has been shown to sufficiently solubilise membrane proteins while not causing dissociation of possible multimeric protein complexes in the sample (Musatov et al., 2000). 6-Aminocaproic acid, added with the ACA buffer, is reported to support the solubilisation process of membrane proteins with neutral detergents (Schägger and von Jagow, 1991).

However, for the sizing of protein complexes, it needs to be kept in mind that associated detergents can influence the apparent molecular mass of a protein complex in FPLC or BN PAGE analyses significantly (Nijtmans et al., 2002). Still, cyanobacterial Band 7 protein complexes are clearly multimeric as the molecular masses of the monomers have been calculated to be in the region of 30 to 36 kDa, except for Phb5 which has a calculated molecular mass of 75 kDa, so that the question whether the identified protein complexes are homo- or hetero-multimeric raised itself. Evidence from an immunoprecipitation experiment where the Phb1, Phb2 and Phb3 Band 7 proteins of *Synechocystis* sp. PCC 6803 did not co-immunoprecipitate (see Figure 5.9) and from a BN PAGE analysis on crude membrane isolations of single Band 7 gene inactivation mutants that showed no interdependence between the proteins (see Figure 5.8), suggested that these Band 7 proteins are most likely to form homo-multimeric protein complexes.

With regards to a comparison between the two investigated cyanobacterial strains, in both cases the Band 7 protein complexes appeared to be similarly large, while the ones of the thermophilic *Thermosynechococcus elongatus* appeared to be slightly more stable than those of *Synechocystis* sp. PCC 6803 (see Figure 5.7 and

Figure 5.10). This conclusion is based on the observations from the sucrose-density gradient centrifugation and the BN PAGE analysis, and even though this is in agreement with the expectations, it is possible that the intensities of the antibody signals on the presented immunoblots are slightly misleading, as the immunoblots for *Synechocystis* sp. PCC 6803 in the BN PAGE analysis are overexposed.

Summarising the results on the sizing and oligomeric nature of the Band 7 protein complexes of *Synechocystis* sp. PCC 6803 and *Thermosynechococcus elongatus*, it could be shown that cyanobacterial Band 7 proteins form large (>900 kDa) protein complexes that are likely to be homo-multimeric.

5.7.2.4.2 The Band 7 protein complexes of other organisms

Even though the comparative phylogenetic analysis in this study (see section 3.6) suggests that cyanobacterial prohibitin and stomatin homologues have evolved through convergent evolution rather than sharing a common ancestor with eukaryotic prohibitins and stomatins or with p-stomatins, some structural properties of other Band 7 protein complexes will be briefly described in this section.

The best studied example of a Band 7 protein complex is that of the prohibitin complex of *S. cerevisiae*, which has not only been characterised structurally (Berger and Yaffe, 1998; Back et al., 2002; Tatsuta et al., 2005), but to a certain extent also functionally (Steglich et al., 1999; Nijtmans et al., 2000). Two lines of evidence lead to the conclusion that the two prohibitin homologues (Phb1 and Phb2) of *S. cerevisiae* are the only constituents of this prohibitin complex (Berger and Yaffe, 1998; Nijtmans et al., 2000) that exhibits a molecular mass between 2 (Steglich et al, 1999) and 1 MDa (Nijtmans et al., 2000) and is localised to the mitochondrial inner membrane (Berger and Yaffe, 1998). Here, both prohibitin homologues are anchored via N-terminal hydrophobic regions (Berger and Yaffe, 1998) exposing tightly folded C-termini towards the intermembrane space (Steglich et al, 1999). While crosslinking experiments suggest that the complex consists out of hetero-dimeric Phb1/Phb2 building blocks (Back et al., 2002), a more recent, single-particle electron microscopy study revealed that the complex contains approximately 14 of these building blocks that are arranged in a ring-like structure mediated by the C-terminal coiled-coil regions of the these proteins (Tatsuta et al., 2005).

Another, well-characterised Band 7 protein complex, that has been linked to the prohibitin complex of *S. cerevisiae* by its similar function (Nijtmans et al., 2002), is

the HflK/C protein complex of *E coli*. The HflK and HflC proteins each contain a single N-terminal TM domain, that anchors them in the plasma membrane of *E. coli* where the proteins expose their C-termini to the periplasm (Kihara et al., 1997). Furthermore, it has been reported, that both proteins are interdependent, i.e. that they only accumulate when they are expressed together (Banuett and Herskowitz, 1987; Kihara and Ito, 1998). The HflK/C protein complex has been found to be associated with the FtsH protease of *E. coli* (Kihara et al., 1996) and a $(FtsH)_6(HflK/C)_6$ structure has been proposed with a molecular mass of 924 kDa for the two associated protein complexes, which is reported to agree with observed sedimentation behaviour in sucrose-density gradient centrifugation (Saikawa et al., 2004). Consequently, a potentially hexameric HflK/C protein complex would exhibit a molecular mass of about approximately 500 kDa (~83 kDa for the combined monomers).

Additionally, *E. coli* features another Band 7 protein (YbbK; P0AA53) that is partially characterised in the literature (Chiba et al., 2006). According to the InterPro database, YbbK is a stomatin homologue, but it does not group with either eukaryotic stomatins nor p-stomatins (Tavernarakis et al., 1999; see section 3.6), but can be found to group with the cyanobacterial stomatin homologues (see Figure 3.5). Structurally, YbbK has been found to form homo-oligomeric protein complexes, with an estimated molecular mass between 500 to 1000 kDa. YbbK has been shown to be anchored in the bacterial plasma membrane and in contrast to the HflK/C protein complex exposes its C-terminal domain to the cytoplasm (Chiba et al., 2006). Interestingly, this protein complex has also been reported to interact physically with the FtsH protease of *E. coli*, although the interaction does not appear to be stable and could only be observed when both proteins were co-expressed (Chiba et al., 2006).

Among eukaryotic stomatins, human stomatin is probably the best characterised. It has been shown to display an unusual topology, as the N-terminal hydrophobic domain is believed to form a putative 'hairpin loop', so that both a short N-terminal region and a larger C-terminal domain face the cytoplasm (Salzer et al., 1993). While within the epithelial plasma membrane stomatin has been reported to be organised in homo-oligomeric protein complexes that exhibit an apparent molecular mass of about 300 kDa (9 to 12 monomers) (Snyers et al., 1998), larger complexes in the range from 200 to 600 kDa have been observed in the plasma membrane of erythrocytes (Salzer and Prohaska, 2001). The oligomerisation of the stomatin monomers is dependent on the C-terminal region between amino acid 264 to 272 and

within this region, three amino acids are essential for the association of the proteins with detergent-resistant membranes (DRMs). The fact that human stomatin can be found in these DRMs, is another characteristic feature of the protein (Umlauf et al., 2006).

However, as already stated, cyanobacterial Band 7 proteins do not appear to be related to eukaryotic prohibitin or stomatin homologues as well as to the HflK and HflC proteins of *E. coli*, so that it is difficult to evaluate to what extent the knowledge about the described protein complexes will be applicable to the complexes that are formed by cyanobacterial Band 7 proteins.

5.7.2.5 Purification of Band 7 protein complexes

Initially, to facilitate the purification of Band 7 protein complexes of *Synechocystis* sp. PCC 6803, His_8-tags were introduced at the C-termini of the Phb1, Phb2, Phb3 and Phb4 proteins (see section 5.3). Unfortunately, this seemed to destabilise the Phb1-His and Phb4-His proteins and in case of the Phb1-His protein, its apparent expression level in the Phb1-His_8-tagged Band 7 protein mutant strain decreased to estimated less than 25 % of the wild-type level (see Figure 5.15B and section 5.7.2.2). Nevertheless, attempts were made to purify the Phb1-His, Phb2-His and Phb3-His protein complexes using Ni-NTA magnetic beads on crude membrane isolations. Immunoblots probed with the αPhb1, αPhb2 and αPhb3 antibodies indicated that the respective protein were purified (even the destabilised Phb1-His), but the proteins could not be detected by Coomassie staining on 1-D SDS PAGE gels. Consequently, the yields of this affinity-purification method were considered to be insufficient for a structural analyses (see Figure 5.16). Subsequently, another affinity-purification attempt with the ProPur IMAC kit yielded similar results, although this time, purified Phb3-His protein could be detected on a silver-stained 1-D SDS PAGE gel (data not shown). Nevertheless, the observed destabilisation of the Phb1 and Phb4 proteins (see Figure 5.15 and section 5.7.2.2) and the relatively low yields of the His_8-tag based affinity-purification methods (see Figure 5.16B) inspired a completely different purification approach.

As an alternative, purified Band 7 antibodies were covalently coupled to Protein A sepharose beads and subsequently used for the immunoprecipitation of Band 7 protein complexes of *Synechocystis* sp. PCC 6803 under native conditions. The utilisation of purified antibodies in a preparative immunoprecipitation procedure

proved to be ideal for a rapid purification of small amounts of protein complexes. Interestingly, an immunoblotting analysis after 1-D BN PAGE revealed that the eluate generated with αPhb3 coupled to the sepharose beads contained large Phb3 protein complexes (see Figure 5.18B) that were of sufficient quantity and quality to be used for structural studies (see section 5.5). Unfortunately, Phb1 and Phb2 Band 7 protein complexes of *Synechocystis* sp. PCC 6803 could still not be purified in sufficient amounts, although it appears possible that optimising or upscaling of the method would lead to the desired result.

In the literature, the only Band 7 protein complex that has been reported to have been purified and used for structural studies, is the prohibitin complex of *S. cerevisiae* (Tatsuta et al., 2005). In that study, prohibitin 1 has been N-terminally His_6-tagged, so that the resulting prohibitin complexes, which in *S. cerevisiae* are composed out of the two prohibitin homologues (Phb1 and Phb2), was still stable and accumulated. Furthermore, the yeast strain from which the prohibitin complexes has been purified, was genetically manipulated and contained a multicopy plasmid that encoded the Phb1 and Phb2 prohibitin homologues. Thus, expression of these two proteins was under the control of an inducible promoter and the protein levels could be increased as much as 20 times (Tatsuta et al., 2005). Unfortunately, no such method to overexpress a protein of interest in *Synechocystis* sp. PCC 6803 was available.

In summary, although there is still room for improvement for the purification of the Band 7 protein complexes of *Synechocystis* sp. PCC 6803, the immunoprecipitation purification protocol devised in this study, has proved to be a powerful tool. However, if the tagging strategy was reassessed (see section 2.7.2.2) and the purification procedures were optimised, it might be possible to produce sufficient and appropriate material, to properly characterise the Band 7 protein complexes of *Synechocystis* sp. PCC 6803.

5.7.2.6 Structural characterisation of Band 7 protein complexes

The Band 7 proteins of *Synechocystis* sp. PCC 6803 assemble mainly into large protein complexes (see section 5.2.3 to section 5.2.5) that allow a low resolution structural investigation by electron microscopy and single-particle analysis.

However, until Phb3 protein complexes of *Synechocystis* sp. PCC 6803 have been characterised in this study, the prohibitin complex of *S. cerevisiae* was the only structurally characterised Band 7 protein complex (Back et al., 2002; Tatsuta et al.,

2005). Initially, crosslinking, proteolytic digest and mass spectrometry of the prohibitin homologues of *S. cerevisiae*, formed the basis for the first suggestion on the molecular architecture of the prohibitin complex (Back et al., 2002). In that study, no Phb1 or Phb2 homo-dimers were identified and the subsequent prediction for the secondary and tertiary protein conformations, that takes the identified interaction sites into account, leads to the hypothesis for a structural Phb1/Phb2 hetero-dimeric building block. Furthermore, because of the previous findings that the prohibitin homologues of *S. cerevisiae* display functional and sequence homologies to HSP60 chaperones (Nijtmans et al., 2000); that the prohibitin complex acts as a chaperone for mitochondrial membrane proteins and the observed molecular mass of this protein complex (2 MDa, Steglich et al., 1999; 1 MDa, Nijtmans et al., 2000), a circular, barrel shaped structure with approximately 14 of the predicted building blocks was suggested (Back et al., 2002). Later, an electron microscopy and single-particle analysis approach, similar to the one performed in this study (see section 5.5), yielded the first low resolution data identifying ring-like prohibitin complexes that confirmed the initially predicted model and was the first structural characterisation of a Band 7 protein complex (Tatsuta et al., 2005). However, as the Phb1 prohibitin homologue of *Synechocystis* sp. PCC 6803 was only distantly related to the prohibitin homologues of *S. cerevisiae* and its molecular function remains to be determined, it is only speculation that this protein might also assemble into similar, ring-like structures.

In this study, although various purification methods were applied, only Phb3 protein complexes of *Synechocystis* sp. PCC 6803 could be purified in sufficient quantity and quality (see Figure 5.18) to be examined by electron microscopy (see Figure 5.19). Again, it is worthy of note that the Phb3 stomatin homologue of *Synechocystis* sp. PCC 6803 has been found to be only distantly related to eukaryotic stomatin or p-stomatin homologues, but to bear some phylogenetic relationship to the YbbK protein of *E. coli* (see section 3.6). However, the obtained results from the single-particle analysis indicated that the Phb3 protein forms also ring-like protein complexes with an approximate diameter of about 16 nm that contain possibly ten to twelve monomer subunits (see section 5.5). Considering the molecular mass of the Phb3 monomer (35.7 kDa), this oligomeric composition would correspond to a molecular mass between 360 and 430 kDa for the observed protein complexes, disregarding additional molecular mass added by associated detergent. This finding seems to agree with the molecular masses that have been reported for human stomatin

protein complexes which ranged from 300 kDa (9 to 12 monomers) (Snyers et al., 1998) to 200 to 600 kDa (Salzer and Prohaska, 2001). However, the calculated molecular mass for the Phb3 protein complexes stands in contrast to the apparent molecular mass on immunoblots of 1-D BN PAGE analyses of either crude *Synechocystis* sp. PCC 6803 membranes (see Figure 5.8) and even the sample used for the structural study itself (see Figure 5.18). Therefore, it has to be considered whether the Phb3 protein complexes observed in the single-particle analysis were contaminants or whether the molecular masses determined in both analyses resulted from artefacts. However, it appears unlikely that the observed protein complexes are contaminants, because of the single band on the silver-stained 1-D SDS PAGE gel that could be identified as the Phb3 protein (see Figure 5.18) and the apparent homogeneity of the sample analysed under the electron microscope (see Figure 5.19). Another explanation might be that the apparent molecular mass determined by 1-D BN PAGE results from artefacts (potentially aggregated Phb3 complexes), although the fact that such large molecular mass Phb3 protein complexes have been detected in different and independently performed experiments suggests otherwise (see sections 5.2.3 to section 5.2.5). The possibility that the apparent shift of the molecular mass of the Phb3 protein complexes into the high-molecular-mass region could be caused by associated detergents seems unlikely due to the significance of the difference, but cannot be entirely refuted. Thus, it remains unclear what causes this significant difference between the calculated and the observed apparent molecular masses of the Phb3 protein complexes in the two performed analyses.

Unfortunately, the YbbK protein, eukaryotic or p-stomatin homologues have not yet been characterised structurally, although a speculative model with structural implications on the molecular function of stomatins has been suggested. In that model, the stomatin protein is integrated into the plasma membrane via its N-terminal domain regulating an ion channel with a C-terminal 'ball' domain (Stewart, 1997). However, although stomatins homologues in vertebrates and *C. elegans* have been reported to be involved in the gating of ion channels (Stewart et al., 1992; Price et al., 2004), the implication that stomatins acts as a monomer is neither supported by the evidence that stomatins form large oligomeric protein complexes in the literature (Snyers et al., 1998; Salzer and Prohaska, 2001), nor by the findings in this work. Thus, keeping the phylogenetic distance between the Phb3 protein of *Synechocystis* sp. PCC 6803 and eukaryotic stomatin or p-stomatin homologues and the so far uncharacterised

molecular function of this protein in the cyanobacterium in mind, speculations on the function of this protein based on the structural evidence presented in this work do not seem justified. Nevertheless, the data presented in this work is the first structural characterisation with regards to the molecular architecture of a stomatin homologue.

5.7.2.7 On the interaction between Band 7 and FtsH homologues

This work is based upon the hypothesis that the Phb1 prohibitin homologue of *Synechocystis* sp. PCC 6803 interacts with the Slr0228 FtsH protease and negatively regulates its activity by physically shielding and thereby protecting certain membrane proteins from proteolysis (Silva et al., 2002). This hypothesis was formed analogously to the findings in *S. cerevisiae*, where the prohibitin complex interacts with the m-AAA protease and shields respiratory protein complex subunits from the degradation by this protease (Steglich et al., 1999; Nijtmans et al., 2000). Previously, Slr0228 of *Synechocystis* sp. PCC 6803 has been shown to be involved in the degradation of the D1 membrane protein of PSII in the PSII repair cycle (Silva et al., 2003). However, it is worthy of note that *Synechocystis* sp. PCC 6803 possesses three further FtsH homologues: Slr1604, Sll1463 and Slr1390 (CyanoBase database).

Since none of the performed functional assays in this work yielded any conclusive evidence for a dependency between the Band 7 proteins and the Slr0228 FtsH homologue of *Synechocystis* sp. PCC 6803 (see Chapter 4), different approaches had to be taken to investigate a possible interaction. Initially, two-phase partitioning followed by immunoblotting analyses (see Figure 5.5B) revealed that the Slr0228 FtsH homologue solely resides in the thylakoid membrane and thus co-localises in this subcellular compartment with the Phb1 protein. This indicates that an interaction between the Slr0228 FtsH protease and the Phb2 and Phb3 protein, which were only found to be present in the plasma membrane, appears unlikely. However, all of the Band 7 proteins might still interact with another FtsH homologue, since for example Slr1604 has been found in both the thylakoid and plasma membrane (see Figure 5.5B).

Even though additional evidence, e.g. apparent co-migration of Band 7 and FtsH proteins in a sucrose-density gradient (data not shown) and on 1-D BN PAGE gels (see Figure 5.8), the fact that the αFtsH antibody signal pattern for FtsH complexes did not seem to be affected by an inactivation of Band 7 genes (or the other way around; see Figure 5.8F and Figure 5.21) already suggested that a possible interaction could only be expected to be weak or at low level. Previously, the m-AAA

protease complex has been found to cofractionate with the prohibitin complex in a FPLC experiment, only when digitonin was used for the solubilisation of the sample, while the interaction was perturbed by Triton X-100 (Steglich et al., 1999). Consequently, immunoprecipitations, as a rapid and sensitive method, were performed to assess the possible interaction between Band 7 and FtsH homologues (however, samples were solubilised with n-dodecyl-β-D-maltoside). Initially, even though various antibodies were used, no evidence for such an interaction could be gathered. Ultimately, αGST antibodies were coupled to Protein A sepharose beads and used in an immunoprecipitation experiment on crude membrane isolations of the 0228-GST strain, a *Synechocystis* sp. PCC 6803 strain in which the Slr0228 FtsH homologue had been tagged with the GST protein. This approach seemed to provide the necessary sensitivity, as the Phb1 protein could specifically be found in the eluate. However, it cannot be excluded that the Phb1 protein might only be interacting with the GST-tag of the Slr0228-GST fusion protein. Nevertheless, an estimation of the intensity of the αPhb1 antibody signal in the bound fraction and a comparison with the signal that had been generated for Phb1 in the dilution series, lead to the assumption that roughly only 0.3 % of the Phb1 protein complex population might be associated with the 0228-GST FtsH homologue under standard laboratory growth conditions. Thus, in an attempt to increase the yield, it might be worthwhile to perform another immunoprecipitation and test digitonin as the detergent for sample solubilisation. Ultimately, this analysis still represents the first indication of an interaction between the two proteins in *Synechocystis* sp. PCC 6803.

Previously, the interaction between a Band 7 protein homologue and an FtsH homologue has only been reported for *S. cerevisiae* (Steglich et al., 1999) and *E. coli*. Interestingly, in *E coli*, two Band 7 protein complexes are associated with the FtsH protease, namely: HflK/C (Kihara et al., 1996; Saikawa et al., 2004) and YbbK (Chiba et al., 2006). In *S. cerevisiae*, the association of the prohibitin complex with the m-AAA protease has been demonstrated by co-immunoprecipitation, although the presented immunoblots suggest that in this organism the interaction occurs at a much higher level, as the proteins could be readily detected in the respective eluates. Unfortunately, no dilution series is included which would allow a quantitative evaluation (Steglich et al., 1999). In *E. coli*, the FtsH and HflK/C complexes were demonstrated to interact with each other by crosslinking and subsequent immunoprecipitation and moreover by co-purification in a Ni-NTA-agarose affinity

chromatography procedure performed on a His_6-Myc-tagged FtsH *E. coli* strain. The presented immunoblots for the affinity-purification procedure suggest that even though only a minority of the His_6-Myc-tagged FtsH protein seems to have bound to the column (<50 %), still a substantial amount of HflK/C protein complex co-purified (Kihara et al., 1996). Furthermore, the association between the HflK/C and FtsH protein complexes is demonstrated by immunoblots on the fractions of a sucrose density gradient that was performed on either a Δ*hflK-hflC* or a Δ*ftsh* deletion mutant strain, where the deletion of the HflK/C protein complex resulted in a shift of the FtsH protein complex towards the low-molecular-mass fractions and vice versa (Saikawa et al., 2004). Similarly, sucrose density gradient centrifugation was performed using an *E. coli* Δ*ftsh* deletion mutant strain to investigate whether the YbbK protein complex would be shifting towards the low-molecular-mass region of the gradient, but in this case, no effect of the FtsH deletion could be detected (Chiba et al., 2006). However, when *E. coli* cells expressing His_6-Myc-tagged FtsH where used for a Ni-NTA affinity-purification, the YbbK protein is found to co-purify in the eluate. Subsequently, the same procedure was performed on a His_6-Myc-tagged Δ236FtsH mutant strain (lacking a large part of its periplasmic region), in order to demonstrate that the previously observed co-purification was not due to unspecific binding. Interestingly, the YbbK protein was then absent from the eluate, suggesting an interaction between the two proteins mediated by the periplasmic domain of the FtsH protease (Chiba et al., 2006). It is worthy of note, that genetic manipulations of the used *E. coli* strains in that study allowed overexpression of both the YbbK and/or various FtsH derivates, which significantly increased the chances for the discovery of this apparently weak interaction.

In summary, although the potential functional interaction between the Phb1 prohibitin and Slr0228 FtsH homologues of *Synechocystis* sp. PCC 6803 remains to be determined, it could be shown that these two proteins specifically interact with each other physically at very low levels. Furthermore, despite the lack of direct evidence for interactions between other Band 7 proteins (e.g. Phb3) with other FtsH homologues, the localisation experiments that have been performed in this work do not exclude such possibilities. However, to identify such potential interactions, it would be beneficial to be able to overexpress either members of the involved protein families or to significantly improve the respective purification and detection techniques.

Chapter 6: Conclusions and future work

This work has investigated the Band 7 superfamily of proteins, more specifically its cyanobacterial members in *Synechocystis* sp. PCC 6803 and *Thermosynechococcus elongatus*, and has provided the first detailed analysis of prokaryotic Band 7 proteins. The working hypothesis, that the Phb1 prohibitin homologue of *Synechocystis* sp. PCC 6803 shields newly synthesised copies of the D1 protein from the degradation by the Slr0228 FtsH protease prior to their incorporation into reassembling PSII complexes, has been based on the finding that Slr0228 is involved in the early stages of the PSII repair cycle (Silva et al., 2003) and the assumption that Phb1 might act analogously to the prohibitins of *S. cerevisiae* (Nijtmans, et al., 2000; Silva et al., 2002). Consequently, the focus of the presented experiments is on the prohibitin homologue of *Synechocystis* sp. PCC 6803, but where possible, the other Band 7 proteins were included in the respective analyses. Since cyanobacterial Band 7 proteins have virtually not been studied previously and due to the diversity of the Band 7 superfamily of proteins, the experiments performed in this work range from bioinformatic analyses (see Chapter 3; see section 6.1) to physiological assays (see Chapter 4; see section 6.2) and to a biochemical and structural characterisation of Band 7 protein complexes (see Chapter 5; see section 6.4). In the subsequent sections, the most important results from the previous chapters will be briefly summarised, followed by an outlook on possible future work (see section 6.4).

6.1 Bioinformatic analyses of Band 7 proteins

An InterPro protein family database search for prohibitin homologues in *Synechocystis* sp. PCC 6803 and *Thermosynechococcus elongatus* identified five and two Band 7 proteins respectively (see Table 3.2). The five Band 7 proteins of *Synechocystis sp. PCC 6803* were one assigned prohibitin (Slr1106, Phb1), one assigned stomatin (Slr1128, Phb3) and one possible flotillin-like protein (Sll1021, Phb5), while the remaining two proteins (Slr1768, Phb2; Sll0815, Phb4) could not clearly be assigned to a particular subfamily of the Band 7 protein. The two Band 7 proteins of *Thermosynechococcus elongatus* were one assigned prohibitin (Tlr1760, TE_Phb1) and one assigned stomatin (Tlr2184, TE_Phb2). Typically, all of these proteins exhibited a calculated molecular mass of around 30 kDa (except for Phb5 of

Synechocystis sp. PCC 6803 with 74 kDa) and possessed one predicted N-terminal TM domain (except for Phb2 and Phb4 of *Synechocystis sp. PCC 6803* with two and none TM respectively) (see Table 3.3). A subsequent phylogenetic analysis of all identified, cyanobacterial Band 7 proteins demonstrated that these proteins form a diverse protein family that can be divided into the following, three main categories: prohibitin homologues, stomatin homologues and others (see Figure 3.3). Interestingly, while most of the cyanobacterial Band 7 proteins could be assigned to one of these categories, the Slr1768 and Sll0815 proteins of *Synechocystis sp. PCC 6803* could not clearly be grouped into any of them and none of the investigated cyanobacteria possessed a closely related homologue for these proteins.

Given the evolutionary link between higher plants and cyanobacteria (Gray, 1989; Douglas, 1998), the Band 7 proteins of higher plants were also bioinformatically analysed with a focus on their subcellular localisation (see section 3.4.2) and the phylogenetic relationships between them (see section 3.4.3). Taking the obtained targeting prediction results (see Table 3.6) and indications from the literature (Baginsky et al., 2004; Kleffman et al., 2004) into account, it could not be excluded that certain prohibitin homologues of higher plants might be located to chloroplasts. However, the majority of proteomics studies (Kruft et al., 2001; Millar et al., 2001) and also functional and biochemical assays in the literature (Snedden and Fromm, 1997; Takahashi et al., 2003; Ahn et al., 2006; Chen et al., 2006) provide evidence that, generally, prohibitin homologues of higher plants are located to mitochondria. A phylogenetic analysis indicated that the Band 7 proteins of higher plants can be distinguished into three categories: prohibitins, stomatins and 'others or plant defence' (see Figure 3.4). Interestingly, the prohibitin homologues could be found to group in two branches with representatives of most of the investigated species in both of these branches. Furthermore, only a few stomatin homologues could be identified in higher plants, while a multitude of Band 7 proteins appear to be involved in plant defence mechanisms (Nadimpalli et al., 2000).

A comparative phylogenetic analysis in this work emphasised that the Band 7 superfamily of proteins represents a diverse protein family (see Figure 3.5). Virtually no phylogenetic relationships could be observed between the prohibitin or stomatin homologues of cyanobacteria and higher plants, and no cyanobacterial Band 7 protein seems to display a phylogenetic relationship with the HflK/C homologues of *E. coli*. Interestingly, the prohibitins of *S. cerevisiae* and *H. sapiens* were found to group

together with the prohibitin homologues of higher plants. A multitude of cyanobacterial Band 7 proteins (previously grouped in the 'others' category, see Figure 3.3; among them Sll1021 of *Synechocystis sp. PCC 6803*) could now be associated with flotillin-like homologues, e.g. that of *B. subtilis*. Overall, the conclusions that can be drawn from results of this comparative phylogenetic analysis seem to be in accordance with those of a recently published phylogenetic analysis of the flotillin subfamily of proteins (Rivera-Milla et al., 2006). In that study, it is postulated that the relationships between proteins with a SPFH/Band 7 domain are less distinct than is implied by the grouping in the same protein superfamily and that therefore the observed sequence similarities are probably more likely the result of convergent rather than of divergent evolution.

6.2 The physiological relevance of the Band 7 proteins of *Synechocystis* sp. PCC 6803

Band 7 proteins have been implied to be involved in a multitude of physiological processes and the extent of knowledge about these proteins differs significantly according to each of its five protein subfamilies and the organism of interest. For example, members of the prohibitin subfamily of proteins have been found in many organisms ranging from prokaryotes (Banuett and Herskowitz, 1987) to higher eukaryotes (Nuell et al., 1991), and functionally these proteins have been linked to important processes, such as cellular signalling and transcriptional control (Terashima *et al*., 1994; Montano *et al*., 1999; Sun *et al*., 2004), apoptosis (Fusaro *et al*., 2003), cellular senescence (Coates *et al*., 2001; Piper *et al*., 2002), early development of *Caenorhabditis elegans* (Artal-Sanz *et al*., 2003) or mitochondrial biogenesis (Berger and Yaffe, 1998). However, the most detailed account on the function of prohibitin homologues has come from studies on *S. cerevisiae*, where these proteins have been shown to form a large hetero-multimeric protein complex that acts as a chaperone for respiratory, membrane protein complex subunits which are shielded from the degradation by the m-AAA protease (Steglich et al., 1999; Nijtmans et al., 2000).

In this work, a completely segregated and viable ΔPhb1-4 quadruple mutant strain (see Figure 4.1) and various other single and multiple Band 7 gene inactivation mutants (data not shown) have been generated. Prior to performing specific growth

experiments, the effects of various stress conditions on the transcript levels of the Band 7 proteins of *Synechocystis sp. PCC 6803* were investigated by an analysis of DNA microarray data, and cold as well as oxidative stress were identified to slightly, but significantly, affect the transcription of some of these genes (see Table 4.1). However, in the subsequent growth analyses, no decreased tolerance to cold (see Figure 4.3B) or oxidative stress (see Figure 4.3C) could be observed for the ΔPhb1-4 quadruple mutant. In the literature, an inactivation of prohibitins has been shown to lead to an impaired respiratory chain, the loss of respiratory competence and to ultimately to affect cell viability (Piper and Bringloe, 2002). Thus, to test the functioning of the respiratory chain in the ΔPhb1-4 quadruple mutant strain, this mutant was also grown under photoheterotrophic growth conditions, but no obvious phenotype could be triggered (see Figure 4.3D). Furthermore, the amounts of oxidised i.e. damaged proteins in the cells grown under these conditions did not seem to be increased (see Figure 4.4), while only inconclusive cell viability results could be generated (data not shown). Moreover, the ΔPhb1-4 quadruple mutant strain did not seem to exhibit any morphological differences in comparison to the wild-type strain (see Figure 4.5).

Subsequently, the working hypothesis, which assumes an involvement of the Phb1 prohibitin homologue as a chaperone in the PSII repair cycle of *Synechocystis* sp. PCC 6803, was tested using different experimental approaches. Interestingly, in a preliminary experiment, both the Phb1 (Slr1106) and Phb3 (Slr1128) proteins could be identified in a PSII-enriched fraction obtained by affinity-chromatography (see Figure 4.6), although the presence of Phb3 was most likely due to unspecific interactions between the protein and the used Ni-NTA resin. In a plate growth assay, it could be shown that the viability of the ΔPhb1-4 quadruple mutant strain was not impaired upon exposure to photoinhibitory growth conditions (see Figure 4.7). Also, the selective turnover of the D1 protein in the ΔPhb1-3 triple or ΔPhb1-4 quadruple mutant strains examined by pulse-labelling and pulse-chase analyses did not appear to be affected (see Figure 4.8 and Figure 4.12). Similar experiments performed on various, other Band 7 gene inactivation mutants with accelerated or impaired D1 protein turnover, only displayed minor differences in the protein complex pattern, mainly for unidentified but not for PSII protein complexes (see Figure 4.10 and Figure 4.11). Since the PSII repair cycle could be shown to be functional in the ΔPhb1-4 quadruple mutant strain in a photoinhibition assay (see Figure 4.13), it seemed unlikely that the

Phb1, Phb2, Phb3 and Phb4 proteins play a significant role in this protective mechanism of *Synechocystis sp. PCC 6803*.

As the Band 7 proteins could not be linked to the PSII repair cycle, it was tested whether these proteins might be functionally associated with the NDH-1 protein complexes of *Synechocystis sp. PCC 6803*, which are involved in respiration (Burrows et al., 1998) and inorganic carbon accumulation (Zhang et al., 2004). Interestingly, in an immunoprecipitation experiment, the Phb1 protein seemed to specifically co-immunoprecipitate with the NdhI subunit (see Figure 4.14), which can be found in the hydrophilic domain of NDH-1L and NDH-1M protein complexes (Zhang et al., 2005). Furthermore, typically, the expression of certain protein complexes that are involved in the inorganic carbon concentrating mechanism (CCM) of *Synechocystis sp. PCC 6803* (NDH-1S_1, NDH-1S_2 and SbtA) can be induced by low CO_2 conditions (i.e. air level; Zhang et al., 2004). Studying the dynamics of these CCM protein complexes, it could be shown that they are clearly inducible in the ΔPhb1-4 quadruple mutant strain (see Figure 4.15B1 and Figure 4.15B2). However, it appeared as if they were less abundant in the quadruple mutant compared to the wild-type when the cultures were shifted from high to low CO_2 conditions (see Figure 4.15B3 and Figure 4.15A3), but immunoblots with the respective αNdh antibodies on these gels would be necessary to quantify and compare the amounts of protein complexes and to thereby substantiate this initial observation.

In another set of experiments, cell motility of various single Band 7 gene inactivation mutants in the *Synechocystis sp. PCC 6803* wild-type background was investigated. Interestingly, while the ΔPhb1-WT and ΔPhb3-WT mutant strains did not exhibit an altered phenotype, inactivation of the *phb2* gene seemed to significantly decrease the ability of the mutant cells to move on the agar plates (see Figure 4.16B), although it could later be shown by electron microscopy that these cells possessed pili which are a prerequisite for cell motility (see Figure 4.16C).

Overall, the physiological relevance of the Band 7 proteins of *Synechocystis sp. PCC 6803* remains enigmatic. While it could be shown that they do not play a significant role in the PSII repair cycle, it is possible that they might be functionally linked to, and specifically to the dynamics of, NDH-1 protein complexes. The Phb2 protein on the other hand could be shown to be involved cell motility, probably in a related signalling pathway.

6.3 Characterisation of Band 7 proteins and their complexes in *Synechocystis* sp. PCC 6803

In Chapter 5, prior to the characterisation of Band 7 proteins and their complexes in *Synechocystis sp. PCC 6803*, it is described how polyclonal antibodies against the Band 7 proteins were generated, affinity-purified and tested (see section 5.1). At first, expression constructs to overexpress the Phb2-TM and Phb3-TM Band 7 protein fragments and the Phb4 Band 7 protein were generated (see Figure 5.1). Subsequently, the respective *Synechocystis sp. PCC 6803* proteins were overexpressed (see Figure 5.2B), affinity-purified (see Figure 5.2C) and used for the immunisation of rabbits. The obtained polyclonal antibody sera were then also affinity-purified and testing them revealed, that specific antibodies directed against the Phb2 and Phb3 proteins had been generated, while the αPhb4 antibody displayed a multitude of unspecific cross reactions (see Figure 5.3). It is worthy of note, that the αPhb1 antibody specifically detected the TE_Phb1 protein and that the αPhb3 antibody was similarly specific for the TE_Phb2 protein of *Thermosynechococcus elongatus*.

In another experiment, the expression of the Phb1, Phb2 and Phb3 Band 7 proteins in the *Synechocystis sp. PCC 6803* wild-type and glucose-tolerant strains was compared, but no obvious differences could be observed (see Figure 5.4). A differential membrane protein extraction experiment demonstrated that the Phb1, Phb2, Phb3 and Phb4 proteins are most likely integral membrane proteins, that are ,however, only weakly associated with their host membranes (see Figure 5.5A). The localisation of certain Band 7 and FtsH homologues was determined using two-phase partitioning and immunoblotting (see Figure 5.5B), with which it could be shown that the Phb1 protein can be found in both the thylakoid and plasma membrane, while the Phb2 and Phb3 proteins are solely present in the plasma membrane. The Slr0228 FtsH protease was shown to reside in the thylakoid membrane, while the Slr1604 FtsH homologue appeared to be localised in both membranes. The molecular masses of the Band 7 protein complexes of *Synechocystis sp. PCC 6803* and *Thermosynechococcus elongatus* were roughly determined by the application of various protein separation techniques in combination with immunoblotting, namely: FPLC (see Figure 5.6), sucrose-density gradient centrifugation (see Figure 5.7) and BN PAGE (see Figure 5.8 and Figure 5.10). In all of these experiments, it could be shown that the Phb1, Phb2 and Phb3 proteins of *Synechocystis sp. PCC 6803* and TE_Phb1 and TE_Phb2 proteins

of *Thermosynechococcus elongatus* form large protein complexes with an apparent molecular mass of significantly more than 669 kDa. Unfortunately, the precise molecular masses of these Band 7 protein complexes could not be determined, due to insufficient resolution or lack of suitable marker proteins. However, the BN PAGE analysis (see Figure 5.8) and an immunoprecipitation experiment (see Figure 5.10) suggested that the Phb1, Phb2 and Phb3 do not seem to interact with each other and probably form homo-multimeric protein complexes.

In order to facilitate the purification of the Band 7 proteins of *Synechocystis* sp. PCC 6803, the Phb1, Phb2, Phb3 and Phb4 proteins were C-terminally His_8-tagged (see section 5.3). While all the generated Phb-His mutant strains could be shown to be completely segregated and viable (see Figure 5.14), only the Phb2-His and Phb3-His proteins accumulated *in vivo* (see Figure 5.15A). Attaching the His_8-tag at the C-terminus of the Phb1 protein seemed to render this protein susceptible to proteolytic breakdown and less than 25 % of wild-type Phb1 protein levels were detected in the Phb1-His mutant strain (see Figure 5.15B). A subsequent affinity-purification approach for the Phb1-His, Phb2-His and Phb3-His proteins using Ni-NTA magnetic agarose beads failed to yield material of sufficient quantity and quality for structural analyses (see Figure 5.16). Thus, another purification approach had to be taken and by immunoprecipitation with purified antibodies covalently crosslinked to Protein A-coupled sepharose, enough Phb3 protein complexes suitable for electron microscopy and subsequent single-particle analysis could be obtained (see Figure 5.18). While, in principle, the Phb1 and Phb2 proteins could be immunoprecipitated (see Figure 5.18A), the yields were insufficient (see Figure 5.18B) for visualisation by electron microscopy (data not shown). The single-particle analysis of purified Phb3 protein complexes revealed that this protein forms ring-like structures with a diameter of approximately 16 nm, which possibly contain between ten to twelve individual Phb3 subunits (see Figure 5.19).

In another immunoprecipitation experiment, using αGST antibodies covalently crosslinked to Protein A-coupled sepharose and crude membranes from the 0228-GST strain, it could be shown that the Phb1 prohibitin and Slr0228 FtsH homologues of *Synechocystis* sp. PCC 6803 might be physically interacting with each other at very low levels (see Figure 5.20). However, it is possible that the Phb1 protein might only be associated with the GST-tag of the Slr0228-GST fusion protein. Previously, it had been shown by BN PAGE and immunoblotting that an inactivation of the Phb1

prohibitin or Slr0228 FtsH homologue did not significantly affect the respective protein complex pattern of either protein (see Figure 5.8 and Figure 5.21), which already indicated that a potential interaction would probably be low level.

6.4 Future work

In this work, the Band 7 proteins of *Synechocystis* sp. PCC 6803 and *Thermosynechococcus elongatus* have been partially characterised, but some major questions remain unanswered. Still, the most important aim for future studies will be to identify the physiological relevance of the individual Band 7 proteins of *Synechocystis* sp. PCC 6803. For this, a ΔPhb1-5 quintuple mutant should be generated and this mutant, or in case it cannot be made the ΔPhb1-4 quadruple mutant, should be subjected to a DNA microarray analysis, in order to identify particular proteins whose transcript levels might be affected by an inactivation of the Band 7 proteins. Furthermore, it could prove worthwhile to test the growth of *Synechocystis* sp. PCC 6803 Band 7 gene inactivation mutants under additional environmental stress conditions, other than those tested in this work, to identify potential phenotypes. Also, cell viability in liquid cultures should be assessed more thoroughly at different stages using quantitative and more sensitive approaches, such as life/death stains in combination with confocal microscopy.

For further biochemical studies, it would be beneficial to once more attempt to affinity-purify αPhb4 antibodies or to generate new polyclonal antibody sera directed against the Phb4 protein and the Phb5 protein, in order to then be able to identify all of the Band 7 proteins immunochemically. Once αPhb4 and αPhb5 antibodies have been raised and purified, the protein characteristics which have already been determined for the Phb1, Phb2 and Phb3 proteins in this work, such as subcellular localisation, possible membrane association and protein complex size, should be determined for both the Phb4 and the Phb5 protein. Using the available, purified antibodies, it appears to be worthwhile to improve or upscale the immunoprecipitation procedure with purified antibodies covalently crosslinked to Protein A-coupled sepharose, in order to obtain better yields and suitable material for further single-particle analyses. In this context, it might be useful to explore the addition of other, preferably small or uncharged tags to either the N- or C-terminus of the Band 7 proteins for different affinity-purification attempts.

Another main issue would be to identify potential interaction partners of the Band 7 proteins of *Synechocystis* sp. PCC 6803. This could be achieved by performing immunoprecipitation experiments on radioactively labelled cells, where potential bands in the autoradiograms would indicate possible interaction partners of the Band 7 proteins. Also, generated immunoprecipitates could be analysed by mass spectrometry in order to probe for co-purifying proteins. A further development of this approach would be to use cells which have been treated with chemical crosslinkers or where the crude membrane isolations have been solubilised with digitonin, so that potential protein/protein interactions might be better preserved and the chances of identifying potential interaction partners are improved. Specifically, it would be interesting to test whether the observed low level interaction between the Phb1 prohibitin and Slr0228 FtsH homologues could be significantly increased by either using a crosslinker or digitonin in the immunoprecipitation procedure.

Also, the possible physical and functional interactions with the NDH-1 protein complexes and the Band 7 proteins in *Synechocystis* sp. PCC 6803 need to be investigated further. It would be important to show that the NdhI subunit does indeed specifically interact with the Phb1 protein and that the NdhI and maybe also other NDH-1 protein complex subunits can be found in the eluate of an immunoprecipitation with the αPhb1 antibody and vice versa. For this, it will be necessary to utilise better, i.e. affinity-purified αNdh protein antibodies. Furthermore, NDH-1 protein complex subunit inactivation mutants, in which the proper assembly of the NDH-1 complexes is impaired, should also be included in these immunoprecipitation experiments, since the possibility that unassembled NDH-1 subunits interact with a prohibitin homologue might be increased in such a genetic background. Once further evidence for an interaction between the Phb1 prohibitin or possibly also other Band 7 homologues with NDH-1 protein complex subunits has been gathered, it needs to be elucidated what the functional implications are.

In general, it would immensely facilitate the purification of the Band 7 protein complexes and the identification of potential interaction partners, if an overexpression system for the Band 7 proteins was available for *Synechocystis* sp. PCC 6803. However, it should also be considered, whether potential interactions might possibly be better assessed in the thermophilic cyanobacterium *Thermosynechococcus elongatus* and maybe to utilise this strain for future purification and immuno-precipitation experiments.

Overall, with the information accumulated on the Band 7 proteins of *Synechocystis* sp. PCC 6803 in this study, the construction of a multitude of mutants, the generation of two specific Band 7 protein antibodies and the implementation of various biochemical techniques a substantial groundwork for future studies has been laid.

References

Abrams, M.D. (1990). Adaptations and responses to drought in *Quercus* species of North America. Tree Physiol. ***7***, 227-38.

Adam, Z. and Clarke, A.K. (2002). Cutting edge of chloroplast proteolysis. Trends Plant Sci. ***7***, 451-6.

Adam, Z. and Ostersetzer, O. (2001). Degradation of unassembled and damaged thylakoid proteins. Biochem. Soc. Trans. ***29***, 427-30.

Adir, N., Shochat, S., and Ohad, I. (1990). Light-dependent D1 protein synthesis and translocation is regulated by reaction center II. Reaction center II serves as an acceptor for the D1 precursor. J. Biol. Chem. ***265***, 12563-8.

Ahn, C.S., Lee, J.H., Reum-Hwang, A., Kim, W.T., and Pai, H.S. (2006). Prohibitin is involved in mitochondrial biogenesis in plants. Plant J. ***46***, 658-67.

Akashi, K., Grandjean, O., and Small, I. (1998). Potential dual targeting of an *Arabidopsis* archaebacterial-like histidyl-tRNA synthetase to mitochondria and chloroplasts. FEBS Lett. ***431***, 39-44.

Akiyama, Y. (2002). Proton-motive force stimulates the proteolytic activity of FtsH, a membrane-bound ATP-dependent protease in *Escherichia coli*. Proc. Natl. Acad. Sci. USA ***99***, 8066-71.

Akiyama, Y. and Ito, K. (2003). Reconstitution of membrane proteolysis by FtsH. J. Biol. Chem. ***278***, 18146-53.

Akiyama, Y. and Ito, K. (2001). Roles of homooligomerization and membrane association in ATPase and proteolytic activities of FtsH *in vitro*. Biochemistry ***40***, 7687-93.

Akiyama, Y. and Ito, K. (2000). Roles of multimerization and membrane association in the proteolytic functions of FtsH (HflB). EMBO J. ***19***, 3888-95.

Akiyama, Y., Kihara, A., and Ito, K. (1996a). Subunit a of proton ATPase F0 sector is a substrate of the FtsH protease in *Escherichia coli*. FEBS Lett. ***399***, 26-8.

Akiyama, Y., Kihara, A., Mori, H., Ogura, T., and Ito, K. (1998). Roles of the periplasmic domain of *Escherichia coli* FtsH (HflB) in protein interactions and activity modulation. J. Biol. Chem. ***273***, 22326-33.

Akiyama, Y., Kihara, A., Tokuda, H., and Ito, K. (1996b). FtsH (HflB) is an ATP-dependent protease selectively acting on SecY and some other membrane proteins. J. Biol. Chem. ***271***, 31196-201.

Albertsson, P.A. (1986). Partition of cells, particles and macromolecules. Wiley, New York, USA.

Allakhverdiev, S.I., Tsvetkova, N., Mohanty, P., Szalontai, B., Moon, B.Y., Debreczeny, M., and Murata, N. (2005). Irreversible photoinhibition of photosystem II is caused by exposure of *Synechocystis* cells to strong light for a prolonged period. Biochim. Biophys. Acta ***1708***, 342-51.

Allen, J.F. (1992). How does protein phosphorylation regulate photosynthesis? Trends Biochem. Sci. ***17***, 12-7.

Allen, J.F. and Forsberg, J. (2001). Molecular recognition in thylakoid structure and function. Trends Plant Sci. ***6***, 317-26.

Allred, D.R. and Staehelin, L.A. (1986). Spatial organization of the cytochrome b_6f complex within chloroplast thylakoid membranes. Biochim. Biophys. Acta ***849***, 94-103.

Altschul, S.F., Gish, W., Miller, W., Myers, E.W., and Lipman, D.J. (1990). Basic local alignment search tool. J. Mol. Biol. ***215***, 403-10.

Anbudurai, P.R., Mor, T.S., Ohad, I., Shestakov, S.V., and Pakrasi, H.B. (1994). The *ctpA* gene encodes the C-terminal processing protease for the D1 protein of the photosystem II reaction center complex. Proc. Natl. Acad. Sci. USA ***91***, 8082-6.

Anderson, J.M. (1986). Photoregulation of the composition, function, and structure of thylakoid membranes. Ann. Rev. Plant Physiol. *37*, 93-136.

Andersson, B. and Anderson, J.M. (1980). Lateral heterogeneity in the distribution of chlorophyll-protein complexes of the thylakoid membranes of spinach chloroplasts. Biochim. Biophys. Acta ***593***, 427-40.

Aoki, M. and Katoh, S. (1983). Size of plastoquinone pool functioning in photosynthetic and respiratory electron transport of *Synechococcus* sp. Plant and Cell Physiol. ***24***, 1379-86.

Arlt, H., Steglich, G., Perryman, R., Guiard, B., Neupert, W., and Langer, T. (1998). The formation of respiratory chain complexes in mitochondria is under the proteolytic control of the m-AAA protease. EMBO J. ***17***, 4837-47.

Arlt, H., Tauer, R., Feldmann, H., Neupert, W., and Langer, T. (1996). The YTA10-12 complex, an AAA protease with chaperone-like activity in the inner membrane of mitochondria. Cell ***85***, 875-85.

Arnold, I. and Langer, T. (2002). Membrane protein degradation by AAA proteases in mitochondria. Biochim. Biophys. Acta ***1592***, 89-96.

Arnon, D.I. (1971). The light reactions of photosynthesis. Proc. Natl. Acad. Sci. USA ***68***, 2883-92.

Aro, E.M., Hundal, T., Carlberg, I., and Andersson, B. (1990). *In vitro* studies on light-induced inhibition of photosystem II and D1-protein degradation at low-temperatures. Biochim. Biophys. Acta ***1019***, 269-75.

Aro, E.M., McCaffery, S., and Anderson, J.M. (1993a). Photoinhibition and D1 protein degradation in peas acclimated to different growth irradiances. Plant Physiol. ***103***, 835-43.

Aro, E.M., Suorsa, M., Rokka, A., Allahverdiyeva, Y., Paakkarinen, V., Saleem, A., Battchikova, N., and Rintamäki, E. (2005). Dynamics of photosystem II: A proteomic approach to thylakoid protein complexes. J. Exp. Bot. ***56***, 347-56.

Aro, E.M., Virgin, I., and Andersson, B. (1993b). Photoinhibition of photosystem II. Inactivation, protein damage and turnover. Biochim. Biophys. Acta ***1143***, 113-34.

Artal-Sanz, M., Tsang, W.Y., Willems, E.M., Grivell, L.A., Lemire, B.D., van der Spek, H., Nijtmans, L.G., and Sanz, M.A. (2003). The mitochondrial prohibitin complex is essential for embryonic viability and germline function in *Caenorhabditis elegans*. J. Biol. Chem. ***278***, 32091-9.

Asada, K. (2000). The water-water cycle as alternative photon and electron sinks. Philos. Trans. R. Soc. Lond. B. Biol. Sci. ***355***, 1419-31.

Asada, K. (1999). The water-water cycle in chloroplasts: Scavenging of active oxygens and dissipation of excess photons. Annu. Rev. Plant Physiol. Plant Mol. Biol. ***50***, 601-39.

Attwood, T.K., Bradley, P., Flower, D.R., Gaulton, A., Maudling, N., Mitchell, A.L., Moulton, G., Nordle, A., Paine, K., Taylor, P., Uddin, A., and Zygouri, C. (2003). PRINTS and its automatic supplement, prePRINTS. Nucleic Acids Res. ***31***, 400-2.

Baba, T., Taura, T., Shimoike, T., Akiyama, Y., Yoshihisa, T., and Ito, K. (1994). A cytoplasmic domain is important for the formation of a SecY-SecE translocator complex. Proc. Natl. Acad. Sci. USA ***91***, 4539-43.

Back, J.W., Sanz, M.A., de Jong, L., de Koning, L.J., Nijtmans, L.G., de Koster, C.G., Grivell, L.A., van der Spek, H., and Muijsers, A.O. (2002). A structure for the yeast prohibitin complex: Structure prediction and evidence from chemical crosslinking and mass spectrometry. Protein Sci. ***11***, 2471-8.

Badger, M.R. and Price, G.D. (2003). CO_2 concentrating mechanisms in cyanobacteria: Molecular components, their diversity and evolution. J. Exp. Bot. ***54***, 609-22.

Badger, M.R., von Caemmerer, S., Ruuska, S., and Nakano, H. (2000). Electron flow to oxygen in higher plants and algae: Rates and control of direct photoreduction (Mehler reaction) and rubisco oxygenase. Philos. Trans. R. Soc. Lond. B. Biol. Sci. ***355***, 1433-46.

Baginsky, S., Siddique, A., and Gruissem, W. (2004). Proteome analysis of tobacco bright yellow-2 (BY-2) cell culture plastids as a model for undifferentiated heterotrophic plastids. J. Proteome Res. ***3***, 1128-37.

Bailey, S., Silva, P., Nixon, P., Mullineaux, C., Robinson, C., and Mann, N. (2001). Auxiliary functions in photosynthesis: The role of the FtsH protease. Biochem. Soc. Trans. ***29***, 455-9.

Bailey, S., Thompson, E., Nixon, P.J., Horton, P., Mullineaux, C.W., Robinson, C., and Mann, N.H. (2002). A critical role for the Var2 FtsH homologue of *Arabidopsis thaliana* in the photosystem II repair cycle *in vivo*. J. Biol. Chem. ***277***, 2006-11.

Bairoch, A., Apweiler, R., Wu, C.H., Barker, W.C., Boeckmann, B., Ferro, S., Gasteiger, E., Huang, H., Lopez, R., Magrane, M., Martin, M.J., Natale, D.A., O'Donovan, C., Redaschi, N., and Yeh, L.S. (2005). The universal protein resource (UniProt). Nucleic Acids Res. ***33 Database Issue***, D154-9.

Banuett, F. and Herskowitz, I. (1987). Identification of polypeptides encoded by an *Escherichia coli* locus (hflA) that governs the lysis-lysogeny decision of bacteriophage lambda. J. Bacteriol. ***169***, 4076-85.

Banuett, F., Hoyt, M.A., McFarlane, L., Echols, H., and Herskowitz, I. (1986). HflB, a new *Escherichia coli* locus regulating lysogeny and the level of bacteriophage lambda cII protein. J. Mol. Biol. ***187***, 213-24.

Barbato, R., Friso, G., Rigoni, F., Dalla Vecchia, F., and Giacometti, G.M. (1992). Structural changes and lateral redistribution of photosystem II during donor side photoinhibition of thylakoids. J. Cell Biol. ***119***, 325-35.

Barbato, R., Shipton, C.A., Giacometti, G.M., and Barber, J. (1991). New evidence suggests that the initial photoinduced cleavage of the D1-protein may not occur near the PEST sequence. FEBS Lett. ***290***, 162-6.

Barber, J. (2007). Biological solar energy. Philos. Transact. A Math. Phys. Eng. Sci. ***365***, 1007-23.

Barber, J. (2004). Water, water everywhere, and its remarkable chemistry. Biochim. Biophys. Acta ***1655***, 123-32.

Barber, J. and Andersson, B. (1992). Too much of a good thing: Light can be bad for photosynthesis. Trends Biochem. Sci. ***17***, 61-6.

Barber, J., Nield, J., Morris, E.P., Zheleva, D., and Hankamer, B. (1997). The structure, function and dynamics of photosystem II. Physiol. Plant. ***100***, 817-27.

Barker, M., de Vries, R., Nield, J., Komenda, J., and Nixon, P.J. (2006). The Deg proteases protect *Synechocystis* sp. PCC 6803 during heat and light stresses but are not essential for removal of damaged D1 protein during the photosystem two repair cycle. J. Biol. Chem. ***281***, 30347-55.

Bateman, A., Coin, L., Durbin, R., Finn, R.D., Hollich, V., Griffiths-Jones, S., Khanna, A., Marshall, M., Moxon, S., Sonnhammer, E.L., Studholme, D.J., Yeats, C., and Eddy, S.R. (2004). The Pfam protein families database. Nucleic Acids Res. ***32 Database issue***, D138-41.

Battchikova, N., Zhang, P., Rudd, S., Ogawa, T., and Aro, E.M. (2005). Identification of NdhL and Ssl1690 (NdhO) in NDH-1L and NDH-1M complexes of *Synechocystis* sp. PCC 6803. J. Biol. Chem. ***280***, 2587-95.

Begg, K.J., Tomoyasu, T., Donachie, W.D., Khattar, M., Niki, H., Yamanaka, K., Hiraga, S., and Ogura, T. (1992). *Escherichia coli* mutant Y16 is a double mutant carrying thermosensitive *ftsH* and *ftsI* mutations. J. Bacteriol. ***174***, 2416-7.

Bellafiore, S., Barneche, F., Peltier, G., and Rochaix, J.D. (2005). State transitions and light adaptation require chloroplast thylakoid protein kinase STN7. Nature ***433***, 892-5.

Bennett, J. (1983). Regulation of photosynthesis by reversible phosphorylation of the light-harvesting chlorophyll a/b protein. Biochem J. ***212***, 1-13.

Benschop, J.J., Badger, M.R., and Dean Price, G. (2003). Characterisation of CO_2 and HCO_3- uptake in the cyanobacterium *Synechocystis* sp. PCC6803. Photosynth. Res. ***77***, 117-26.

Benz, R. (1990). Biophysical properties of porin pores from mitochondrial outer membrane of eukaryotic cells. Experientia ***46***, 131-7.

Berger, K.H. and Yaffe, M.P. (1998). Prohibitin family members interact genetically with mitochondrial inheritance components in *Saccharomyces cerevisiae*. Mol. Cell. Biol. ***18***, 4043-52.

Berry, S., Schneider, D., Vermaas, W.F., and Rögner, M. (2002). Electron transport routes in whole cells of *Synechocystis* sp. strain PCC 6803: The role of the cytochrome bd-type oxidase. Biochemistry ***41***, 3422-9.

Bethke, P.C. and Jones, R.L. (2001). Cell death of barley aleurone protoplasts is mediated by reactive oxygen species. Plant J. ***25***, 19-29.

Bhaya, D., Bianco, N.R., Bryant, D., and Grossman, A. (2000). Type IV pilus biogenesis and motility in the cyanobacterium *Synechocystis* sp. PCC6803. Mol. Microbiol. ***37***, 941-51.

Bhaya, D., Watanabe, N., Ogawa, T., and Grossman, A.R. (1999). The role of an alternative sigma factor in motility and pilus formation in the cyanobacterium *Synechocystis* sp. strain PCC6803. Proc. Natl. Acad. Sci USA ***96***, 3188-93.

Bibby, T.S., Nield, J., and Barber, J. (2001a). Iron deficiency induces the formation of an antenna ring around trimeric photosystem I in cyanobacteria. Nature ***412***, 743-5.

Bibby, T.S., Nield, J., and Barber, J. (2001b). Three-dimensional model and characterization of the iron stress-induced CP43'-photosystem I supercomplex isolated from the cyanobacterium *Synechocystis* PCC 6803. J. Biol. Chem. ***276***, 43246-52.

Bickel, P.E., Scherer, P.E., Schnitzer, J.E., Oh, P., Lisanti, M.P., and Lodish, H.F. (1997). Flotillin and epidermal surface antigen define a new family of caveolae-associated integral membrane proteins. J. Biol. Chem. ***272***, 13793-802.

Birnboim, H.C. and Doly, J. (1979). A rapid alkaline extraction procedure for screening recombinant plasmid DNA. Nucleic Acids Res. ***7***, 1513-23.

Bjerrum, O.J. and Schäfer-Nielson, C. (1986). Buffer systems and transfer parameters for semidry electroblotting with a horizontal apparatus. *In:* Dunn (ed), Electrophoresis. VCH publishers, Deerfield Beach, USA. 315-27.

Black, D.M. and Solomon, E. (1993). The search for the familial breast/ovarian cancer gene. Trends Genet. ***9***, 22-26.

Blankenship, R.E. and Hartman, H. (1998). The origin and evolution of oxygenic photosynthesis. Trends Biochem. Sci. ***23***, 94-7.

Blum, H., Beier, H., and Gross, H.J. (1987). Improved silver-staining of plant proteins, RNA and DNA in polyacrylamide gels. Electrophoresis ***8***, 93-9.

Bonardi, V., Pesaresi, P., Becker, T., Schleiff, E., Wagner, R., Pfannschmidt, T., Jahns, P., and Leister, D. (2005). Photosystem II core phosphorylation and photosynthetic acclimation require two different protein kinases. Nature ***437***, 1179-82.

Boone, D.R., Castenholz, R.W., and Garrity G. M. (2001). The Archaea and the deeply branching and phototrophic Bacteria. *In*: Bergey's Manual of Systematic Bacteriology, 2nd edition. Springer-Verlag, New York, USA.

Borner, G.H., Sherrier, D.J., Weimar, T., Michaelson, L.V., Hawkins, N.D., Macaskill, A., Napier, J.A., Beale, M.H., Lilley, K.S., and Dupree, P. (2005). Analysis of detergent-resistant membranes in *Arabidopsis*. Evidence for plasma membrane lipid rafts. Plant Physiol. ***137***, 104-16.

Bowyer, J.R., Packer, J.C., McCormack, B.A., Whitelegge, J.P., Robinson, C., and Taylor, M.A. (1992). Carboxyl-terminal processing of the D1 protein and photoactivation of water-splitting in photosystem II. Partial purification and characterization of the processing enzyme from *Scenedesmus obliquus* and *Pisum sativum*. J. Biol. Chem. ***267***, 5424-33.

Breyton, C., de Vitry, C., and Popot, J.L. (1994). Membrane association of cytochrome b_6f subunits. The Rieske iron-sulfur protein from *Chlamydomonas reinhardtii* is an extrinsic protein. J. Biol. Chem. ***269***, 7597-602.

Bricker, T.M. and Frankel, L.K. (2002). The structure and function of CP47 and CP43 in photosystem II. Photosynth. Res. ***72***, 131-46.

Bricker, T.M., Morvant, J., Masri, N., Sutton, H.M., and Frankel, L.K. (1998). Isolation of a highly active photosystem II preparation from *Synechocystis* 6803 using a histidine-tagged mutant of CP 47. Biochim. Biophys. Acta ***1409***, 50-7.

Brugnoli, E. and Björkman, O. (1992). Chloroplast movements in leaves: Influence on chlorophyll fluorescence and measurements of light-induced absorbance changes related to ΔpH and zeaxanthin formation. Photosynth. Res. ***32***, 23-35.

Brundage, L., Hendrick, J.P., Schiebel, E., Driessen, A.J., and Wickner, W. (1990). The purified *E. coli* integral membrane protein SecY/E is sufficient for reconstitution of SecA-dependent precursor protein translocation. Cell ***62***, 649-57.

Burnap, R.L., Troyan, T., and Sherman, L.A. (1993). The highly abundant chlorophyll-protein complex of iron-deficient *Synechococcus* sp. PCC7942 (CP43') is encoded by the *isiA* gene. Plant Physiol. ***103***, 893-902.

Burnette, W.N. (1981). "Western blotting": Electrophoretic transfer of proteins from sodium dodecyl sulfate-polyacrylamide gels to unmodified nitrocellulose and radiographic detection with antibody and radioiodinated Protein A. Anal. Biochem. ***112***, 195-203.

Burrows, P.A., Sazanov, L.A., Svab, Z., Maliga, P., and Nixon, P.J. (1998). Identification of a functional respiratory complex in chloroplasts through analysis of tobacco mutants containing disrupted plastid ndh genes. EMBO J. ***17***, 868-76.

Byrjalsen, I., Mose Larsen, P., Fey, S.J., Nilas, L., Larsen, M.R., and Christiansen, C. (1999). Two-dimensional gel analysis of human endometrial proteins: Characterization of proteins with increased expression in hyperplasia and adenocarcinoma. Mol. Hum. Reprod. ***5***, 748-56.

Cadoret, J.C., Demouliere, R., Lavaud, J., van Gorkom, H.J., Houmard, J., and Etienne, A.L. (2004). Dissipation of excess energy triggered by blue light in cyanobacteria with CP43' (IsiA). Biochim. Biophys. Acta ***1659***, 100-4.

Cadoret, J.C., Rousseau, B., Perewoska, I., Sicora, C., Cheregi, O., Vass, I., and Houmard, J. (2005). Cyclic nucleotides, the photosynthetic apparatus and response to a UV-B stress in the cyanobacterium *Synechocystis* sp. PCC 6803. J. Biol. Chem. ***280***, 33935-44.

Calvin, M. (1962). The path of carbon in photosynthesis. Science ***135***, 879-89.

Campbell, D., Eriksson, M.J., Öquist, G., Gustafsson, P., and Clarke, A.K. (1998). The cyanobacterium *Synechococcus* resists UV-B by exchanging photosystem II reaction-center D1 proteins. Proc. Natl. Acad. Sci. USA ***95***, 364-9.

Campbell, D. and Öquist, G. (1996). Predicting light acclimation in cyanobacteria from nonphotochemical quenching of photosystem II fluorescence, which reflects state transitions in these organisms. Plant Physiol. ***111***, 1293-8.

Cassman, K.G. (1999). Ecological intensification of cereal production systems: Yield potential, soil quality, and precision agriculture. Proc. Natl. Acad. Sci. USA ***96***, 5952-9.

Cheetham, M.E. and Caplan, A.J. (1998). Structure, function and evolution of DnaJ: Conservation and adaptation of chaperone function. Cell Stress Chaperones ***3***, 28-36.

Chen, G.X., Kazimir, J., and Cheniae, G.M. (1992). Photoinhibition of hydroxylamine-extracted photosystem II membranes: Studies of the mechanism. ***31***, 11072-83.

Chen, J.C., Jiang, C.Z., and Reid, M.S. (2005). Silencing a prohibitin alters plant development and senescence. Plant J. ***44***, 16-24.

Cheng, H.H., Muhlrad, P.J., Hoyt, M.A., and Echols, H. (1988). Cleavage of the cII protein of phage-lambda by purified HflA protease - Control of the switch between lysis and lysogeny. Proc. Natl. Acad. Sci. USA ***85***, 7882-6.

Chiba, S., Akiyama, Y., and Ito, K. (2002). Membrane protein degradation by FtsH can be initiated from either end. J. Bacteriol. ***184***, 4775-82.

Chiba, S., Ito, K., and Akiyama, Y. (2006). The *Escherichia coli* plasma membrane contains two PHB (prohibitin homology) domain protein complexes of opposite orientations. Mol. Microbiol. ***60***, 448-57.

Choi, J.S., Chung, Y.H., Moon, Y.J., Kim, C., Watanabe, M., Song, P.S., Joe, C.O., Bogorad, L., and Park, Y.M. (1999). Photomovement of the gliding cyanobacterium *Synechocystis* sp. PCC 6803. Photochem. Photobiol. ***70***, 95-102.

Clarke, A.K., Campbell, D., Gustafsson, P., and Öquist, G. (1995). Dynamic responses of photosystem II and phycobilisomes to changing light in the cyanobacterium *Synechococcus* sp. PCC 7942. ***197***, 553-62.

Clarke, A.K., Soitamo, A., Gustafsson, P., and Öquist, G. (1993). Rapid interchange between two distinct forms of cyanobacterial photosystem II reaction-center protein D1 in response to photoinhibition. Proc. Natl. Acad. Sci. USA ***90***, 9973-7.

Coates, P.J., Jamieson, D.J., Smart, K., Prescott, A.R., and Hall, P.A. (1997). The prohibitin family of mitochondrial proteins regulate replicative lifespan. Curr. Biol. ***7***, 607-10.

Coates, P.J., Nenutil, R., McGregor, A., Picksley, S.M., Crouch, D.H., Hall, P.A., and Wright, E.G. (2001). Mammalian prohibitin proteins respond to mitochondrial stress and decrease during cellular senescence. Exp. Cell Res. ***265***, 262-73.

Cooley, J.W. and Vermaas, W.F. (2001). Succinate dehydrogenase and other respiratory pathways in thylakoid membranes of *Synechocystis* sp. strain PCC 6803: Capacity comparisons and physiological function. J. Bacteriol. ***183***, 4251-8.

Corteggiani Carpinelli, E. (2006). Iron stress in cyanobacteria: Association of CP43′ with photosystem II. Master thesis, University of Padua, Italy.

de las Rivas, J., Andersson, B., and Barber, J. (1992). Two sites of primary degradation of the D1-protein induced by acceptor or donor side photo-inhibition in photosystem II core complexes. FEBS Lett. ***301***, 246-52.

de las Rivas, J., Balsera, M., and Barber, J. (2004). Evolution of oxygenic photosynthesis: Genome-wide analysis of the OEC extrinsic proteins. Trends Plant Sci. ***9***, 18-25.

de Winter, F. and Swenson, R.B. (2006). Dawn of the solar era: A wake-up call. Solar Today ***2***, 15-9.

Debus, R.J. (1992). The manganese and calcium ions of photosynthetic oxygen evolution. Biochim. Biophys. Acta ***1102***, 269-352.

Demmig-Adams, B. and Adams III, W.W. (1996). The role of xanthophyll cycle carotenoids in the protection of photosynthesis. Trends Plant Sci. ***1***, 21-6.

Depege, N., Bellafiore, S., and Rochaix, J.D. (2003). Role of chloroplast protein kinase Stt7 in LHCII phosphorylation and state transition in *Chlamydomonas*. Science ***299***, 1572-5.

deRisi, J.L. and Iyer, V.R. (1999). Genomics and array technology. Curr. Opin. Oncol. ***11***, 76-9.

Diner, B.A. and Rappaport, F. (2002). Structure, dynamics, and energetics of the primary photochemistry of photosystem II of oxygenic photosynthesis. Annu. Rev. Plant Biol. ***53***, 551-80.

Diner, B.A., Schlodder, E., Nixon, P.J., Coleman, W.J., Rappaport, F., Lavergne, J., Vermaas, W.F.J., and Chisholm, D.A. (2001). Site-directed mutations at D1-His198 and D2-His197 of photosystem II in *Synechocystis* PCC 6803: Sites of primary charge separation and cation and triplet stabilization. Biochemistry ***40***, 9265-81.

Douglas, S.E. (1998). Plastid evolution: Origins, diversity, trends. Curr. Opin. Genet. Dev. ***8***, 655-61.

Douville, K., Leonard, M., Brundage, L., Nishiyama, K., Tokuda, H., Mizushima, S., and Wickner, W. (1994). Band 1 subunit of *Escherichia coli* preportein translocase and integral membrane export factor P12 are the same protein. J. Biol. Chem. ***269***, 18705-7.

Durrant, I., Benge, L.C., Sturrock, C., Devenish, A.T., Howe, R., Roe, S., Moore, M., Scozzafava, G., Proudfoot, L.M., Richardson, T.C., and et, al. (1990). The application of enhanced chemiluminescence to membrane-based nucleic acid detection. Biotechniques ***8***, 564-70.

Edgar, A.J. and Polak, J.M. (2001). Flotillin-1: Gene structure: cDNA cloning from human lung and the identification of alternative polyadenylation signals. Int. J. Biochem. Cell Biol. ***33***, 53-64.

Eichacker, L.A. and Henry, R. (2001). Function of a chloroplast SRP in thylakoid protein export. Biochim. Biophys. Acta ***1541***, 120-34.

Elhai, J. and Wolk, C.P. (1988). A versatile class of positive-selection vectors based on the nonviability of palindrome-containing plasmids that allows cloning into long polylinkers. Gene ***68***, 119-38.

Emanuelsson, O., Nielsen, H., Brunak, S., and von Heijne, G. (2000). Predicting subcellular localization of proteins based on their N-terminal amino acid sequence. J. Mol. Biol. ***300***, 1005-16.

Emanuelsson, O., Nielsen, H., and von Heijne, G. (1999). ChloroP, a neural network-based method for predicting chloroplast transit peptides and their cleavage sites. Protein Sci. ***8***, 978-84.

Emanuelsson, O. and von Heijne, G. (2001). Prediction of organellar targeting signals. Biochim. Biophys. Acta ***1541***, 114-9.

Emlyn-Jones, D., Ashby, M.K., and Mullineaux, C.W. (1999). A gene required for the regulation of photosynthetic light harvesting in the cyanobacterium *Synechocystis* 6803. Mol. Microbiol. ***33***, 1050-8.

Escoubas, J.M., Lomas, M., La Roche, J., and Falkowski, P.G. (1995). Light intensity regulation of cab gene transcription is signaled by the redox state of the plastoquinone pool. Proc. Natl. Acad. Sci. USA ***92***, 10237-41.

Faller, P., Pascal, A., and Rutherford, A.W. (2001). Beta-carotene redox reactions in photosystem II: Electron transfer pathway. Biochemistry ***40***, 6431-40.

Felsenstein, J. (1989). PHYLIP phylogeny inference package (Version 3.2). Cladistics ***5***, 164-6.

Ferreira, K.N., Iverson, T.M., Maghlaoui, K., Barber, J., and Iwata, S. (2004). Architecture of the photosynthetic oxygen-evolving center. Science ***303***, 1831-8.

Fricke, B., Argent, A.C., Chetty, M.C., Pizzey, A.R., Turner, E.J., Ho, M.M., Iolascon, A., von During, M., and Stewart, G.W. (2003). The "stomatin" gene and protein in overhydrated hereditary stomatocytosis. Blood ***102***, 2268-77.

Fricke, B., Jarvis, H.G., Reid, C.D., Aguilar-Martinez, P., Robert, A., Quittet, P., Chetty, M., Pizzey, A., Cynober, T., Lande, W.F., Mentzer, W.C., During, M., Winter, S., Delaunay, J., and Stewart, G.W. (2004). Four new cases of stomatin-deficient hereditary stomatocytosis syndrome: Association of the stomatin-deficient cryohydrocytosis variant with neurological dysfunction. Br. J. Haematol. ***125***, 796-803.

Friedman, D.I., Olson, E.R., Georgopoulos, C., Tilly, K., Herskowitz, I., and Banuett, F. (1984). Interactions of bacteriophage and host macromolecules in the growth of bacteriophage lambda. Microbiol. Rev. ***48***, 299-325.

Fromm, H., Devic, M., Fluhr, R., and Edelman, M. (1985). Control of *psbA* gene expression: In mature *Spirodela* chloroplasts light regulation of 32-kd protein synthesis is independent of transcript level. EMBO J. ***4***, 291-5.

Fusaro, G., Dasgupta, P., Rastogi, S., Joshi, B., and Chellappan, S. (2003). Prohibitin induces the transcriptional activity of p53 and is exported from the nucleus upon apoptotic signaling. J. Biol. Chem. ***278***, 47853-61.

Gal, A., Zer, H., and Ohad, I. (1997). Redox-controlled thylakoid protein phosphorylation. News and views. Physiol. Plant. ***100***, 869-85.

Gallagher, P.G. and Forget, B.G. (1995). Structure, organization, and expression of the human band 7.2b gene, a candidate gene for hereditary hydrocytosis. J. Biol. Chem. ***270***, 26358-63.

Gamer, J., Multhaup, G., Tomoyasu, T., McCarty, J.S., Rudiger, S., Schonfeld, H.J., Schirra, C., Bujard, H., and Bukau, B. (1996). A cycle of binding and release of the DnaK, DnaJ and GrpE chaperones regulates activity of the *Escherichia coli* heat shock transcription factor sigma32. EMBO J. ***15***, 607-17.

Gantt, E. (1994). Supramolecular membrane organization. *In*: Bryant (ed), The molecular biology of cyanobacteria, pp. 119-38. Kluwer Academic Publishers, Dordrecht, The Netherlands.

Gill, R.T., Katsoulakis, E., Schmitt, W., Taroncher-Oldenburg, G., Misra, J., and Stephanopoulos, G. (2002). Genome-wide dynamic transcriptional profiling of the light-to-dark transition in *Synechocystis* sp. strain PCC 6803. J. Bacteriol. ***184***, 3671-81.

Girardot, N., Allinquant, B., Langui, D., Laquerriere, A., Dubois, B., Hauw, J.J., and Duyckaerts, C. (2003). Accumulation of flotillin-1 in tangle-bearing neurones of Alzheimer's disease. Neuropathol. Appl. Neurobiol. ***29***, 451-61.

Golden, S.S., Brusslan, J., and Haselkorn, R. (1986). Expression of a family of *psbA* genes encoding a photosystem II polypeptide in the cyanobacterium *Anacystis nidulans* R2. EMBO J. ***5***, 2789-98.

Gombos, Z., Wada, H., and Murata, N. (1994). The recovery of photosynthesis from low-temperature photoinhibition is accelerated by the unsaturation of membrane lipids: A mechanism of chilling tolerance. Proc. Natl. Acad. Sci. USA ***91***, 8787-91.

Gonnet, G.H., Cohen, M.A., and Benner, S.A. (1992). Exhaustive matching of the entire protein sequence database. Science ***256***, 1443-5.

Gonzalez-Polo, R.A., Rodriguez-Martin, A., Moran, J.M., Niso, M., Soler, G., and Fuentes, J.M. (2004). Paraquat-induced apoptotic cell death in cerebellar granule cells. Brain Res. ***1011***, 170-6.

Goodman, M.B., Ernstrom, G.G., Chelur, D.S., O'Hagan, R., Yao, C.A., and Chalfie, M. (2002). MEC-2 regulates *C. elegans* DEG/ENaC channels needed for mechanosensation. Nature ***415***, 1039-42.

Gottesman, S., Gottesman, M., Shaw, J.E., and Pearson, M.L. (1981). Protein degradation in *E. coli*: The *lon* mutation and bacteriophage lambda N and cII protein stability. Cell ***24***, 225-33.

Gray, M.W. (1989). The evolutionary origins of organelles. Trends Genet. ***5***, 294-9.

Gray, M.W., Burger, G., and Lang, B.F. (1999). Mitochondrial evolution. Science ***283***, 1476-81.

Green, J.B., Fricke, B., Chetty, M.C., von During, M., Preston, G.F., and Stewart, G.W. (2004). Eukaryotic and prokaryotic stomatins: The proteolytic link. Blood Cells Mol. Dis. ***32***, 411-22.

Greenberg, B.M., Gaba, V., Mattoo, A.K., and Edelman, M. (1987). Identification of a primary *in vivo* degradation product of the rapidly-turning-over 32-kD protein of photosystem II. EMBO J. ***6***, 2865-9.

Grigorieva, G. and Shestakov, S. (1982). Transformation in the cyanobacterium *Synechocystis* sp. 6803. FEMS Microbiol. Lett. ***13***, 367-70.

Grossman, A.R., Bhaya, D., Apt, K.E., and Kehoe, D.M. (1995). Light-harvesting complexes in oxygenic photosynthesis: Diversity, control, and evolution. Annu. Rev. Genet. ***29***, 231-88.

Grossman, A.R., Schaefer, M.R., Chiang, G.G., and Collier, J.L. (1993). The phycobilisome, a light-harvesting complex responsive to environmental conditions. Microbiol. Rev. ***57***, 725-49.

Grossman, T.H., Kawasaki, E.S., Punreddy, S.R., and Osburne, M.S. (1998). Spontaneous cAMP-dependent derepression of gene expression in stationary phase plays a role in recombinant expression instability. Gene ***209***, 95-103.

Guelin, E., Rep, M., and Grivell, L.A. (1994). Sequence of the AFG3 gene encoding a new member of the FtsH/Yme1/Tma subfamily of the AAA-protein family. Yeast ***10***, 1389-94.

Hakala, M., Tuominen, I., Keranen, M., Tyystjärvi, T., and Tyystjärvi, E. (2005). Evidence for the role of the oxygen-evolving manganese complex in photoinhibition of photosystem II. Biochim. Biophys. Acta ***1706***, 68-80.

Hakozaki, H., Endo, M., Masuko, H., Park, J.I., Ito, H., Uchida, M., Kamada, M., Takahashi, H., Higashitani, A., and Watanabe, M. (2004). Cloning and expression pattern of a novel microspore-specific gene encoding hypersensitive-induced response protein (LjHIR1) from the model legume, *Lotus japonicus*. Genes Genet. Syst. ***79***, 307-10.

Han, C., Chen, T., Li, N., Yang, M., Wan, T., and Cao, X. (2007). HDJC9, a novel human type C DnaJ/HSP40 member interacts with and cochaperones HSP70 through the J domain. Biochem. Biophys. Res. Commun. ***353***, 280-5.

Han, W. and Christen, P. (2004). cis-Effect of DnaJ on DnaK in ternary complexes with chimeric DnaK/DnaJ-binding peptides. FEBS Lett. ***563***, 146-50.

Hanahan, D. (1983). Studies on transformation of *Escherichia coli* with plasmids. J. Mol. Biol. ***166***, 557-80.

Hankamer, B., Morris, E., Nield, J., Carne, A., and Barber, J. (2001b). Subunit positioning and transmembrane helix organisation in the core dimer of photosystem II. FEBS Lett. ***504***, 142-51.

Hankamer, B., Morris, E., Nield, J., Gerle, C., and Barber, J. (2001a). Three-dimensional structure of the photosystem II core dimer of higher plants determined by electron microscopy. J. Struct. Biol. ***135***, 262-9.

Hanley, J., Deligiannakis, Y., Pascal, A., Faller, P., and Rutherford, A.W. (1999). Carotenoid oxidation in photosystem II. Biochemistry ***38***, 8189-95.

Harries, J.E., Brindley, H.E., Sagoo, P.J., and Bantges, R.J. (2001). Increases in greenhouse forcing inferred from the outgoing longwave radiation spectra of the Earth in 1970 and 1997. Nature ***410***, 355-7.

Harris, J.R. and Agutter, P. (1970). A negative staining study of human erythrocyte ghosts and rat liver nuclear membranes. J. Ultrastr. Res. ***33***, 219-32.

Hashimoto, A., Ettinger, W.F., Yamamoto, Y., and Theg, S.M. (1997). Assembly of newly imported oxygen-evolving complex subunits in isolated chloroplasts: Sites of assembly and mechanism of binding. Plant Cell ***9***, 441-52.

Hatefi, Y. and Hanstein, W.G. (1969). Solubilization of particulate proteins and nonelectrolytes by chaotropic agents. Proc. Natl. Acad. Sci. USA ***62***, 1129-36.

Haußühl, K., Andersson, B., and Adamska, I. (2001). A chloroplast DegP2 protease performs the primary cleavage of the photodamaged D1 protein in plant photosystem II. EMBO J. ***20***, 713-22.

Havaux, M., Eymery, F., Porfirova, S., Rey, P., and Dormann, P. (2005a). Vitamin E protects against photoinhibition and photooxidative stress in *Arabidopsis thaliana*. ***17***, 3451-69.

Havaux, M., Guedeney, G., Hagemann, M., Yeremenko, N., Matthijs, H.C.P., and Jeanjean, R. (2005b). The chlorophyll-binding protein IsiA is inducible by high-light and protects the cyanobacterium *Synechocystis* PCC6803 from photooxidative stress. FEBS Lett. ***579***, 2289-93.

Heath, M.C. (2000). Hypersensitive response-related death. Plant Mol. Biol. ***44***, 321-34.

Herman, C., Thevenet, D., d'Ari, R., and Bouloc, P. (1995). Degradation of sigma 32, the heat shock regulator in *Escherichia coli*, is governed by HflB. Proc. Natl. Acad. Sci. USA ***92***, 3516-20.

Herman, C., Thevenet, D., d'Ari, R., and Bouloc, P. (1997). The HflB protease of *Escherichia coli* degrades its inhibitor lambda cIII. J. Bacteriol. ***179***, 358-63.

Herranen, M., Battchikova, N., Zhang, P., Graf, A., Sirpio, S., Paakkarinen, V., and Aro, E.M. (2004). Towards functional proteomics of membrane protein complexes in *Synechocystis* sp. PCC 6803. Plant Physiol. ***134***, 470-81.

Herrin, D. and Michaels, A. (1985). The chloroplast 32 kDa protein is synthesized on thylakoid-bound ribosomes in *Chlamydomonas reinhardtii*. FEBS Lett. ***184***, 90-5.

Herskowitz, I. and Hagen, D. (1980). The lysis-lysogeny decision of phage lambda: Explicit programming and responsiveness. Annu. Rev. Genet. ***14***, 399-445.

Hihara, Y. and Ikeuchi, M. (1997). Mutation in a novel gene required for photomixotrophic growth leads to enhanced photoautotrophic growth of *Synechocystis* sp. PCC 6803. Photosynth. Res. ***53***, 243-52.

Hihara, Y., Kamei, A., Kanehisa, M., Kaplan, A., and Ikeuchi, M. (2001). DNA microarray analysis of cyanobacterial gene expression during acclimation to high light. Plant Cell ***13***, 793-806.

Hill, R. and Bendall, F. (1960). Function of the two cytochrome components in chloroplasts - A working hypothesis. Nature ***186***, 136-7.

Hill, R. and Rich, P.R. (1983). A physical interpretation for the natural photosynthetic process. Proc. Natl. Acad. Sci. USA ***80*** , 978-82.

Hillmann, B. and Schlodder, E. (1995). Electron transfer reactions in photosystem II core complexes from *Synechococcus* at low temperature - Difference spectrum of P680+ Q_A-/P680 Q_A at 77 K. Biochim. Biophys. Acta ***1231***, 76-88.

Hoganson, C.W. and Babcock, G.T. (1997). A metalloradical mechanism for the generation of oxygen from water in photosynthesis. Science ***277***, 1953-6.

Horton, P. (2000). Prospects for crop improvement through the genetic manipulation of photosynthesis: Morphological and biochemical aspects of light capture. J. Exp. Bot. ***51***, 475-85.

Horton, P. and Ruban, A.V. (1992). Regulation of photosystem II. Photosynth. Res. ***34***, 375-85.

Horton, R.M., Ho, S.N., Pullen, J.K., Hunt, H.D., Cai, Z., and Pease, L.R. (1993). Gene splicing by overlap extension. Methods Enzymol. ***217***, 270-9.

Howitt, C.A. and Vermaas, W.F. (1998). Quinol and cytochrome oxidases in the cyanobacterium *Synechocystis* sp. PCC 6803. Biochemistry ***37***, 17944-51.

Hoyt, M.A., Knight, D.M., Das, A., Miller, H.I., and Echols, H. (1982). Control of phage lambda development by stability and synthesis of cII protein: Role of the viral *cIII* and host *hflA*, *himA* and *himD* genes. Cell ***31*** , 565-73.

Huang, F., Parmryd, I., Nilsson, F., Persson, A.L., Pakrasi, H.B., Andersson, B., and Norling, B. (2002a). Proteomics of *Synechocystis* sp. strain PCC 6803: Identification of plasma membrane proteins. Mol. Cell. Proteomics ***1***, 956-66.

Huang, J., Villemain, J., Padilla, R., and Sousa, R. (1999). Mechanisms by which T7 lysozyme specifically regulates T7 RNA polymerase during different phases of transcription. J. Mol. Biol. ***293***, 457-75.

Huang, M., Gu, G., Ferguson, E.L., and Chalfie, M. (1995). A stomatin-like protein necessary for mechanosensation in *C. elegans.* Nature ***378***, 292-5.

Huang, X., Gaballa, A., Cao, M., and Helmann, J.D. (1999). Identification of target promoters for the *Bacillus subtilis* extracytoplasmic function sigma factor, sigma W. Mol. Microbiol. ***31***, 361-71.

Huesgen, P.F., Schuhmann, H., and Adamska, I. (2006). Photodamaged D1 protein is degraded in *Arabidopsis* mutants lacking the Deg2 protease. FEBS Lett. ***580***, 6929-32.

Hulo, N., Sigrist, C.J., Le Saux, V., Langendijk-Genevaux, P.S., Bordoli, L., Gattiker, A., de Castro, E., Bucher, P., and Bairoch, A. (2004). Recent improvements to the PROSITE database. Nucleic Acids Res. ***32 Database issue***, D134-7.

Ihalainen, J.A., d'Haene, S., Yeremenko, N., van Roon, H., Arteni, A.A., Boekema, E.J., van Grondelle, R., Matthijs, H.C.P., and Dekker, J.P. (2005). Aggregates of the chlorophyll-binding protein IsiA (CP43') dissipate energy in cyanobacteria. Biochemistry ***44*** , 10846-53.

Ikeuchi, M., Plumley, F.G., Inoue, Y., and Schmidt, G.W. (1987). Phosphorylation of photosystem II components, CP43 apoprotein, D1, D2, and 10 to 11 kilodalton protein in chloroplast thylakoids of higher plants. Plant Physiol. ***85***, 638-42.

Ikeuchi, M. and Tabata, S. (2001). *Synechocystis* sp. PCC 6803 - A useful tool in the study of the genetics of cyanobacteria. Photosynth. Res. ***70***, 73-83.

Ikonen, E., Fiedler, K., Parton, R.G., and Simons, K. (1995). Prohibitin, an antiproliferative protein, is localized to mitochondria. FEBS Lett. ***358***, 273-7.

Inouye, M., Arnheim, N., and Sternglanz, R. (1973). Bacteriophage T7 lysozyme is an N-acetylmuramyl-L-alanine amidase. J. Biol. Chem. ***248***, 7247-52.

Ito, K. (1996). The major pathways of protein translocation across membranes. Genes Cells ***1***, 337-46.

Ito, K. and Akiyama, Y. (2005). Cellular functions, mechanism of action, and regulation of FtsH protease. Annu. Rev. Microbiol. ***59***, 211-31.

Iwai, M., Katoh, H., Katayama, M., and Ikeuchi, M. (2004). PSII-Tc protein plays an important role in dimerization of photosystem II. Plant Cell Physiol. ***45***, 1809-16.

Jazwinski, S.M. (1996). Longevity, genes, and aging. Science ***273***, 54-9.

Jensen, K.H., Herrin, D.L., Plumley, F.G., and Schmidt, G.W. (1986). Biogenesis of photosystem II complexes: Transcriptional, translational, and posttranslational regulation. J. Cell Biol. ***103***, 1315-25.

Jensen, R.E. and Dunn, C.D. (2002). Protein import into and across the mitochondrial inner membrane: Role of the TIM23 and TIM22 translocons. Biochim. Biophys. Acta ***1592***, 25-34.

Jupe, E.R., Liu, X.T., Kiehlbauch, J.L., McClung, J.K., and dell'Orco, R.T. (1996). The 3' untranslated region of prohibitin and cellular immortalization. Exp. Cell Res. ***224***, 128-35.

Kaltwasser, M., Wiegert, T., and Schumann, W. (2002). Construction and application of epitope- and green fluorescent protein-tagging integration vectors for *Bacillus subtilis*. Appl. Environ. Microbiol. ***68***, 2624-8.

Kamata, T., Hiramoto, H., Morita, N., Shen, J.R., Mann, N.H., and Yamamoto, Y. (2005). Quality control of photosystem II: An FtsH protease plays an essential role in the turnover of the reaction center D1 protein in *Synechocystis* PCC 6803 under heat stress as well as light stress conditions. Photochem. Photobiol. Sci. ***4***, 983-90.

Kamei, A., Yuasa, T., Orikawa, K., Geng, X.X., and Ikeuchi, M. (2001). A eukaryotic-type protein kinase, SpkA, is required for normal motility of the unicellular cyanobacterium *Synechocystis* sp. strain PCC 6803. J. Bacteriol. ***183***, 1505-10.

Kamiya, N. and Shen, J.R. (2003). Crystal structure of oxygen-evolving photosystem II from *Thermosynechococcus vulcanus* at 3.7-A resolution. Proc. Natl. Acad. Sci. USA ***100***, 98-103.

Kaneko, T., Sato, S., Kotani, H., Tanaka, A., Asamizu, E., Nakamura, Y., Miyajima, N., Hirosawa, M., Sugiura, M., Sasamoto, S., Kimura, T., Hosouchi, T., Matsuno, A., Muraki, A., Nakazaki, N., Naruo, K., Okumura, S., Shimpo, S., Takeuchi, C., Wada, T., Watanabe, A., Yamada, M., Yasuda, M., and Tabata, S. (1996). Sequence analysis of the genome of the unicellular cyanobacterium *Synechocystis* sp. strain PCC6803. II. Sequence determination of the entire genome and assignment of potential protein-coding regions. DNA Res. ***3***, 109-36.

Kaneko, T. and Tabata, S. (1997). Complete genome structure of the unicellular cyanobacterium *Synechocystis* sp. PCC6803. Plant Cell Physiol. ***38***, 1171-6.

Kanervo, E., Suorsa, M., and Aro, E.M. (2005). Functional flexibility and acclimation of the thylakoid membrane. Photochem. Photobiol. Sci. ***4***, 1072-80.

Kanesaki, Y., Suzuki, I., Allakhverdiev, S.I., Mikami, K., and Murata, N. (2002). Salt stress and hyperosmotic stress regulate the expression of different sets of genes in *Synechocystis* sp. PCC 6803. Biochem. Biophys. Res. Commun. ***290***, 339-48.

Karzai, A.W. and McMacken, R. (1996). A bipartite signaling mechanism involved in DnaJ-mediated activation of the *Escherichia coli* DnaK protein. J. Biol. Chem. ***271***, 11236-46.

Kasahara, M., Kagawa, T., Oikawa, K., Suetsugu, N., Miyao, M., and Wada, M. (2002). Chloroplast avoidance movement reduces photodamage in plants. Nature ***420***, 829-32.

Kashino, Y. (2003). Separation methods in the analysis of protein membrane complexes. J. Chromatogr. B. Analyt. Technol. Biomed. Life Sci. ***797***, 191-216.

Kashino, Y., Lauber, W.M., Carroll, J.A., Wang, Q., Whitmarsh, J., Satoh, K., and Pakrasi, H.B. (2002). Proteomic analysis of a highly active photosystem II preparation from the cyanobacterium *Synechocystis* sp. PCC 6803 reveals the presence of novel polypeptides. Biochemistry ***41***, 8004-12.

Katoh, A., Sonoda, M., and Ogawa, T. (1995). A possible role of 154-base pair nucleotides located upstream of ORF440 on CO_2 transport of *Synechocystis* sp. PCC 6803 whose CP47 has been HIS-tagged. *In*: Mathis (ed), Photosynthesis: From light to biosphere, pp. 481-4. Kluwer Academic Publishers, Dordrecht, The Netherlands.

Kazmierczak, J. and Altermann, W. (2002). Neoarchean biomineralization by benthic cyanobacteria. Science ***298***, 2351

Kennedy, B.K., Austriaco, N.R. Jr, Zhang, J., and Guarente, L. (1995). Mutation in the silencing gene SIR4 can delay aging in *S. cerevisiae*. Cell ***80***, 485-96.

Keren, N., Berg, A., van Kan, P.J., Levanon, H., and Ohad, I.I. (1997). Mechanism of photosystem II photoinactivation and D1 protein degradation at low light: The role of back electron flow. Proc. Natl. Acad. Sci. USA *94*, 1579-84.

Keren, N., Liberton, M., and Pakrasi, H.B. (2005). Photochemical competence of assembled photosystem II core complex in cyanobacterial plasma membrane. J. Biol. Chem. ***280***, 6548-53.

Kerr, R.A. (2005). Earth science. The story of O_2. Science ***308***, 1730-2.

Kettunen, R., Pursiheimo, S., Rintamäki, E., van Wijk, K.J., and Aro, E.M. (1997). Transcriptional and translational adjustments of *psbA* gene expression in mature chloroplasts during photoinhibition and subsequent repair of photosystem II. Eur. J. Biochem. ***247***, 441-8.

Khush, G.S. and Peng, S. (1996). Breaking the yield frontier of rice. *In*: Reynolds, Rajaram, and McNab (eds), Increasing yield potential in wheat: Breaking the barriers. Mexico: CIMMYT 11-19.

Kihara, A., Akiyama, Y., and Ito, K. (1998). Different pathways for protein degradation by the FtsH/HflK/C membrane- embedded protease complex: An implication from the interference by a mutant form of a new substrate protein, YccA. J. Mol. Biol. ***279***, 175-88.

Kihara, A., Akiyama, Y., and Ito, K. (1995). FtsH is required for proteolytic elimination of uncomplexed forms of SecY, an essential protein translocase subunit. Proc. Natl. Acad. Sci. USA ***92***, 4532-6.

Kihara, A., Akiyama, Y., and Ito, K. (1997). Host regulation of lysogenic decision in bacteriophage lambda: Transmembrane modulation of FtsH (HflB), the cII degrading protease, by HflK/C (HflA). Proc. Natl. Acad. Sci. USA ***94***, 5544-9.

Kihara, A., Akiyama, Y., and Ito, K. (1996). A protease complex in the *Escherichia coli* plasma membrane: HflK/C (HflA) forms a complex with Ftsh (HflB), regulating its proteolytic activity against SecY. EMBO J. ***15***, 6122-31.

Kihara, A. and Ito, K. (1998). Translocation, folding, and stability of the HflK/C complex with signal anchor topogenic sequences. J. Biol. Chem. ***273***, 29770-5.

Kim, J., Klein, P.G., and Mullet, J.E. (1991). Ribosomes pause at specific sites during synthesis of membrane-bound chloroplast reaction center protein D1. J. Biol. Chem. ***266***, 14931-8.

Kim, J.H. and Suh, K.H. (2005). Light-dependent expression of superoxide dismutase from cyanobacterium *Synechocystis* sp. strain PCC 6803. Arch. Microbiol. ***183***, 218-23.

Kim, M., Ahn, J.W., Jin, U.H., Choi, D., Paek, K.H., and Pai, H.S. (2003). Activation of the programmed cell death pathway by inhibition of proteasome function in plants. J. Biol. Chem. ***278***, 19406-15.

Kleffmann, T., Russenberger, D., von Zychlinski, A., Christopher, W., Sjolander, K., Gruissem, W., and Baginsky, S. (2004). The *Arabidopsis thaliana* chloroplast proteome reveals pathway abundance and novel protein functions. Curr. Biol. ***14***, 354-62.

Klein, R.R., Mason, H.S., and Mullet, J.E. (1988). Light-regulated translation of chloroplast proteins. I. Transcripts of *psaA-psaB*, *psbA*, and *rbcL* are associated with polysomes in dark-grown and illuminated barley seedlings. J. Cell Biol. ***106***, 289-301.

Klein, R.R. and Mullet, J.E. (1987). Control of gene expression during higher plant chloroplast biogenesis. Protein synthesis and transcript levels of *psbA*, *psaA-psaB*, and *rbcL* in dark-grown and illuminated barley seedlings. J. Biol. Chem. ***262***, 4341-8.

Klimov, V.V., Shafiev, M.A., and Allakhverdiev, S.I. (1990). Photoinactivation of the reactivation capacity of photosystem II in pea subchloroplast particles after a complete removal of manganese. Photosynth. Res. ***23***, 59-65.

Knox, J.P. and Dodge, A.D. (1985). Singlet oxygen and plants. Phytochemistry ***24***, 889-96.

Koivuniemi, A., Aro, E.M., and Andersson, B. (1995). Degradation of the D1- and D2-proteins of photosystem II in higher plants is regulated by reversible phosphorylation. Biochemistry ***34***, 16022-9.

Kok, B., Forbush, B., and McGloin, M. (1970). Cooperation of charges in photosynthetic O_2 evolution-I. A linear four step mechanism. Photochem. Photobiol. ***11***, 457-75.

Kokubo, H., Lemere, C.A., and Yamaguchi, H. (2000). Localization of flotillins in human brain and their accumulation with the progression of Alzheimer's disease pathology. Neurosci. Lett. ***290***, 93-6.

Kolonin, M.G., Saha, P.K., Chan, L., Pasqualini, R., and Arap, W. (2004). Reversal of obesity by targeted ablation of adipose tissue. Nature Med. ***10***, 625-32.

Komenda, J. and Barber, J. (1995). Comparison of *psbO* and *psbH* deletion mutants of *Synechocystis* PCC 6803 indicates that degradation of D1 protein is regulated by the Q_B site and dependent on protein synthesis. Biochemistry ***34***, 9625-31.

Komenda, J., Barker, M., Kuvikova, S., de Vries, R., Mullineaux, C.W., Tichy, M., and Nixon, P.J. (2006). The FtsH protease, Slr0228, is important for quality control of photosystem II in the thylakoid membrane of *Synechocystis* PCC 6803. J. Biol. Chem. ***281***, 1145-51.

Komenda, J., Hassan, H.A., Diner, B.A., Debus, R.J., Barber, J., and Nixon, P.J. (2000). Degradation of the photosystem II D1 and D2 proteins in different strains of the cyanobacterium *Synechocytis* PCC 6803 varying with respect to the type and level of *psbA* transcript. Plant Mol. Biol. ***42***, 635-45.

Komenda, J., Reisinger, V., Müller, B.C., Dobakova, M., Granvogl, B., and Eichacker, L.A. (2004). Accumulation of the D2 protein is a key regulatory step for assembly of the photosystem II reaction center complex in *Synechocystis* PCC 6803. J. Biol. Chem. ***279***, 48620-9.

Kowaltowski, A.J. and Vercesi, A.E. (1999). Mitochondrial damage induced by conditions of oxidative stress. Free Radic. Biol. Med. ***26***, 463-71.

Krause, F. (2006). Detection and analysis of protein-protein interactions in organellar and prokaryotic proteomes by native gel electrophoresis: (Membrane) protein complexes and supercomplexes. Electrophoresis ***27***, 2759-81.

Krause, G.H. and Weis, E. (1991). Chlorophyll fluorescence and photosynthesis: The basics. Annu. Rev. Plant Physiol. Plant Mol. Biol. ***42***, 313-49.

Kroll, D., Meierhoff, K., Bechtold, N., Kinoshita, M., Westphal, S., Vothknecht, U.C., Soll, J., and Westhoff, P. (2001). VIPP1, a nuclear gene of *Arabidopsis thaliana* essential for thylakoid membrane formation. Proc. Natl. Acad. Sci. USA ***98***, 4238-42.

Kruft, V., Eubel, H., Jansch, L., Werhahn, W., and Braun, H.P. (2001). Proteomic approach to identify novel mitochondrial proteins in *Arabidopsis*. Plant Physiol. ***127***, 1694-710.

Kruse, O. (2001). Light-induced short-term adaptation mechanisms under redox control in the PSII-LHCII supercomplex: LHCII state transitions and PSII repair cycle. Naturwissenschaften ***88***, 284-92.

Kruse, O., Zheleva, D., and Barber, J. (1997). Stabilization of photosystem II dimers by phosphorylation: Implication for the regulation of the turnover of D1 protein. FEBS Lett. ***408***, 276-80.

Krzywda, S., Brzozowski, A.M., Verma, C., Karata, K., Ogura, T., and Wilkinson, A.J. (2002). The crystal structure of the AAA domain of the ATP-dependent protease FtsH of *Escherichia coli* at 1.5 A resolution. Structure ***10***, 1073-83.

Kuhn, A., Stuart, R., Henry, R., and Dalbey, R.E. (2003). The Alb3/Oxa1/YidC protein family: Membrane-localized chaperones facilitating membrane protein insertion? Trends Cell Biol. ***13***, 510-6.

Kunkel, D.D. (1982). Thylakoid centers - Structures associated with the cyanobacterial photosynthetic membrane system. Arch. Microbiol. ***133***, 97-9.

Laemmli, U.K. (1970). Cleavage of structural proteins during the assembly of the head of bacteriophage T4. Nature ***227***, 680-5.

Lande, W.M., Thiemann, P.V., and Mentzer, W.C.Jr. (1982). Missing band 7 membrane protein in two patients with high Na, low K erythrocytes. J. Clin. Invest. ***70***, 1273-80.

Langer, T. (2000). AAA proteases: Cellular machines for degrading membrane proteins. Trends Biochem. Sci. ***25***, 247-51.

Langer, T., Kaser, M., Klanner, C., and Leonhard, K. (2001). AAA proteases of mitochondria: Quality control of membrane proteins and regulatory functions during mitochondrial biogenesis. Biochem. Soc. Trans. ***29*** , 431-6.

Langhorst, M.F., Reuter, A., and Stuermer, C.A. (2005). Scaffolding microdomains and beyond: The function of reggie/flotillin proteins. Cell. Mol. Life Sci. ***62***, 2228-40.

Lee, H.-Y., Hong, Y.-N., and Chow, W.S. (2001). Photoinactivation of photosystem II complexes and photoprotection by non-functional neighbors in *Capsicum annuum* L. leaves. Planta ***212***, 332-342.

Leffers, G.G.Jr. and Gottesman, S. (1998). Lambda Xis degradation *in vivo* by Lon and FtsH. J. Bacteriol. ***180***, 1573-7.

Lemaire, C., Hamel, P., Velours, J., and Dujardin, G. (2000). Absence of the mitochondrial AAA protease Yme1p restores F0-ATPase subunit accumulation in an *oxa1* deletion mutant of *Saccharomyces cerevisiae*. J. Biol. Chem. ***275***, 23471-5.

Lenaz, G., Bovina, C., d'Aurelio, M., Fato, R., Formiggini, G., Genova, M.L., Giuliano, G., Merlo Pich, M., Paolucci, U., Parenti Castelli, G., and Ventura, B. (2002). Role of mitochondria in oxidative stress and aging. Ann. N. Y. Acad. Sci. ***959***, 199-213.

Leonhard, K., Guiard, B., Pellecchia, G., Tzagoloff, A., Neupert, W., and Langer, T. (2000). Membrane protein degradation by AAA proteases in mitochondria: Extraction of substrates from either membrane surface. Mol. Cell ***5***, 629-38.

Levine, R.L., Garland, D., Oliver, C.N., Amici, A., Climent, I., Lenz, A.G., Ahn, B.W., Shaltiel, S., and Stadtman, E.R. (1990). Determination of carbonyl content in oxidatively modified proteins. Methods Enzymol. ***186***, 464-78.

Li, C., Tao, Y.P., and Simon, L.D. (2000). Expression of different-size transcripts from the *clpP-clpX* operon of *Escherichia coli* during carbon deprivation. J. Bacteriol. ***182***, 6630-7.

Liberton, M., Howard Berg, R., Heuser, J., Roth, R., and Pakrasi, H.B. (2006). Ultrastructure of the membrane systems in the unicellular cyanobacterium *Synechocystis* sp. strain PCC 6803. Protoplasma ***227***, 129-38.

Lichtenthaler, H.K. and Welburn A.R. (1983). Determination of total carotenoids and chlorophyll a and b of leaf extracts in different solvents. Biochem. Soc. Trans. ***603***, 591-2.

Lindahl, M., Spetea, C., Hundal, T., Oppenheim, A.B., Adam, Z., and Andersson, B. (2000). The thylakoid FtsH protease plays a role in the light-induced turnover of the photosystem II D1 protein. Plant Cell ***12***, 419-31.

Lindahl, M., Tabak, S., Cseke, L., Pichersky, E., Andersson, B., and Adam, Z. (1996). Identification, characterization, and molecular cloning of a homologue of the bacterial FtsH protease in chloroplasts of higher plants. J. Biol. Chem. ***271***, 29329-34.

Lindahl, M., Yang, D.-H., and Andersson, B. (1995). Regulatory proteolysis of the major light-harvesting chlorophyll a/b protein of photosystem II by a light-induced membrane-associated enzymic system. Europ. J. Biochem. ***231***, 503-9.

Logan, D.C. (2006). The mitochondrial compartment. J. Exp. Bot. ***57***, 1225-43.

Long, S.P., Humphries, S., and Falkowski, P.G. (1994). Photoinhibition of photosynthesis in nature. Ann. Rev. Plant Physiol. Plant Mol. Biol. ***45***, 633-62.

Ludtke, S.J., Chen, D.H., Song, J.L., Chuang, D.T., and Chiu, W. (2004). Seeing GroEL at 6A resolution by single-particle electron cryomicroscopy. Structure ***12***, 1129-36.

Lupinkova, L. and Komenda, J. (2004). Oxidative modifications of the photosystem II D1 protein by reactive oxygen species: From isolated protein to cyanobacterial cells. Photochem. Photobiol. ***79***, 152-62.

Maeda, S., Badger, M.R., and Price, G.D. (2002). Novel gene products associated with NdhD3/D4-containing NDH-1 complexes are involved in photosynthetic CO_2 hydration in the cyanobacterium, *Synechococcus* sp. PCC7942. Mol. Microbiol. ***43***, 425-35.

Mairhofer, M., Steiner, M., Mosgoeller, W., Prohaska, R., and Salzer, U. (2002). Stomatin is a major lipid-raft component of platelet alpha granules. Blood ***100***, 897-904.

Malaga-Trillo, E., Laessing, U., Lang, D.M., Meyer, A., and Stuermer, C.A. (2002). Evolution of duplicated reggie genes in Zebrafish and Goldfish. J. Mol. Evol. ***54***, 235-45.

Mann, N.H., Novac, N., Mullineaux, C.W., Newman, J., Bailey, S., and Robinson, C. (2000). Involvement of an FtsH homologue in the assembly of functional photosystem I in the cyanobacterium *Synechocystis* sp. PCC 6803. FEBS Lett. ***479***, 72-7.

Marcus, L., Hartnett, J., and Storts D. R. (1996). The pGEM®-T and pGEM®-T Easy vector systems. Promega Notes Magazine ***58***, 36

Marder, J.B., Goloubinoff, P., and Edelman, M. (1984). Molecular architecture of the rapidly metabolized 32-kilodalton protein of photosystem II. Indications for COOH-terminal processing of a chloroplast membrane polypeptide. J. Biol. Chem. ***259***, 3900-8.

Martinez-Yamout, M., Legge, G.B., Zhang, O., Wright, P.E., and Dyson, H.J. (2000). Solution structure of the cysteine-rich domain of the *Escherichia coli* chaperone protein DnaJ. J. Mol. Biol. ***300***, 805-18.

Matsubara, S. and Chow, W.S. (2004). Populations of photoinactivated photosystem II reaction centers characterized by chlorophyll a fluorescence lifetime *in vivo*. Proc. Natl. Acad. Sci. USA ***101***, 18234-9.

Matsuyama, S., Akimaru, J., and Mizushima, S. (1990). SecE-dependent overproduction of SecY in *Escherichia coli* - Evidence for interaction between two components of the secretory machinery. FEBA Lett. ***269***, 96-100.

Mattoo, A.K., Hoffman-Falk, H., Marder, J.B., and Edelman, M. (1984). Regulation of protein metabolism: Coupling of photosynthetic electron transport to *in vivo* degradation of the rapidly metabolized 32-kilodalton protein of the chloroplast membranes. Proc. Natl. Acad. Sci. USA ***81***, 1380-4.

Maxwell, D.P., Wang, Y., and McIntosh, L. (1999). The alternative oxidase lowers mitochondrial reactive oxygen production in plant cells. Proc. Natl. Acad. Sci. USA ***96***, 8271-6.

McClung, J.K., Danner, D.B., Stewart, D.A., Smith, J.R., Schneider, E.L., Lumpkin, C.K., Dell'Orco, R.T., and Nuell, M.J. (1989). Isolation of a cDNA that hybrid selects antiproliferative mRNA from rat liver. Biochem. Biophys. Res. Commun. ***164***, 1316-22.

McClung, J.K., Jupe, E.R., Liu, X.T., and dell'Orco, R.T. (1995). Prohibitin: Potential role in senescence, development, and tumor suppression. Exp. Gerontol. ***30***, 99-124.

McClung, J.K., King, R.L., Walker, L.S., Danner, D.B., Nuell, M.J., Stewart, C.A., and dell'Orco, R.T. (1992). Expression of prohibitin, an antiproliferative protein. Exp. Gerontol. ***27***, 413-7.

Melis, A. (1999). Photosystem II damage and repair cycle in chloroplasts: What modulates the rate of photodamage ? Trends Plant Sci. ***4***, 130-5.

Menand, B., Marechal-Drouard, L., Sakamoto, W., Dietrich, A., and Wintz, H. (1998). A single gene of chloroplast origin codes for mitochondrial and chloroplastic methionyl-tRNA synthetase in *Arabidopsis thaliana*. Proc. Natl. Acad. Sci. USA ***95***, 11014-9.

Mi, H., Endo, T., Schreiber, U., Ogawa, T., and Asada, K. (1992). Electron donation from cyclic and respiratory flows to the photosynthetic intersystem chain is mediated by pyridine nucleotide dehydrogenase in the cyanobacterium *Synechocystis* PCC 6803. Plant Cell Physiol. ***33***, 1233-7.

Millar, A.H., Sweetlove, L.J., Giege, P., and Leaver, C.J. (2001). Analysis of the *Arabidopsis* mitochondrial proteome. Plant Physiol. ***127***, 1711-27.

Miriagou, V., Carattoli, A., Tzelepi, E., Villa, L., and Tzouvelekis, L.S. (2005). IS26-associated In4-type integrons forming multiresistance loci in enterobacterial plasmids. Antimicrob. Agents Chemother. ***49***, 3541-3.

Mitsuhara, I., Malik, K.A., Miura, M., and Ohashi, Y. (1999). Animal cell-death suppressors Bcl-x(L) and Ced-9 inhibit cell death in tobacco plants. Curr. Biol. ***9***, 775-8.

Miyao, M. (1994). Involvement of active oxygen species in degradation of the D1 protein under strong illumination in isolated subcomplexes of photosystem II. Biochemistry ***33***, 9722-30.

Montano, M.M., Ekena, K., Delage-Mourroux, R., Chang, W., Martini, P., and Katzenellenbogen, B.S. (1999). An estrogen receptor-selective coregulator that potentiates the effectiveness of antiestrogens and represses the activity of estrogens. Proc. Natl. Acad. Sci. USA ***96***, 6947-52.

Moon, B.Y., Higashi, S., Gombos, Z., and Murata, N. (1995). Unsaturation of the membrane lipids of chloroplasts stabilizes the photosynthetic machinery against low-temperature photoinhibition in transgenic tobacco plants. Proc. Natl. Acad. Sci. USA ***92***, 6219-23.

Mori, H. and Ito, K. (2001). The Sec protein-translocation pathway. Trends Microbiol. ***9***, 494-500.

Morrow, I.C. and Parton, R.G. (2005). Flotillins and the PHB domain protein family: Rafts, worms and anaesthetics. Traffic ***6***, 725-40.

Mulder, N.J., Apweiler, R., Attwood, T.K., Bairoch, A., Barrell, D., Bateman, A., Binns, D., Biswas, M., Bradley, P., Bork, P., Bucher, P., Copley, R.R., Courcelle, E., Das, U., Durbin, R., Falquet, L., Fleischmann, W., Griffiths-Jones, S., Haft, D., Harte, N., Hulo, N., Kahn, D., Kanapin, A., Krestyaninova, M., Lopez, R., Letunic, I., Lonsdale, D., Silventoinen, V., Orchard, S.E., Pagni, M., Peyruc, D., Ponting, C.P., Selengut, J.D., Servant, F., Sigrist, C.J., Vaughan, R., and Zdobnov, E.M. (2003). The InterPro Database, 2003 brings increased coverage and new features. Nucleic Acids Res. ***31*** , 315-8.

Mullineaux, C. (1999). The thylakoid membranes of cyanobacteria: Structure, dynamics and function. Functional Plant Biol. ***26***, 671-7.

Mullineaux, C.W. and Emlyn-Jones, D. (2005). State transitions: An example of acclimation to low-light stress. J. Exp. Bot. ***56*** , 389-93.

Munekage, Y., Hashimoto, M., Miyake, C., Tomizawa, K., Endo, T., Tasaka, M., and Shikanai, T. (2004). Cyclic electron flow around photosystem I is essential for photosynthesis. Nature ***429***, 579-82.

Murata, N. (1969). Control of excitation transfer in photosynthesis. I. Light-induced change of chlorophyll a fluorescence in *Porphyridium cruentum*. Biochim. Biophys. Acta ***172***, 242-51.

Musatov, A., Ortega-Lopez, J., and Robinson, N.C. (2000). Detergent-solubilized bovine cytochrome c oxidase: Dimerization depends on the amphiphilic environment. Biochemistry ***39***, 12996-3004.

Müller, P., Li, X.P., and Niyogi, K.K. (2001). Non-photochemical quenching. A response to excess light energy. Plant Physiol. ***125***, 1558-66.

Nadimpalli, R., Yalpani, N., Johal, G.S., and Simmons, C.R. (2000). Prohibitins, stomatins, and plant disease response genes compose a protein superfamily that controls cell proliferation, ion channel regulation, and death. J. Biol. Chem. ***275***, 29579-86.

Nakai, M., Sugita, D., Omata, T., and Endo, T. (1993). SecY protein is localized in both the cytoplasmic and thylakoid membranes in the cyanobacterium *Synechococcus* PCC7942. Biochem. Biophys. Res. Commun. ***193***, 228-34.

Nakai, T., Mera, Y., Yasuhara, T., and Ohashi, A. (1994). Divalent metal ion-dependent mitochondrial degradation of unassembled subunits 2 and 3 of cytochrome c oxidase. J. Biochem. ***116***, 752-8.

Nakai, T., Yasuhara, T., Fujiki, Y., and Ohashi, A. (1995). Multiple genes, including a member of the AAA family, are essential for degradation of unassembled subunit 2 of cytochrome c oxidase in yeast mitochondria. Mol. Cell. Biol. ***15***, 4441-52.

Nakamura, Y., Kaneko, T., Hirosawa, M., Miyajima, N., and Tabata, S. (1998). CyanoBase, a www database containing the complete nucleotide sequence of the genome of *Synechocystis* sp. strain PCC6803. Nucleic Acids Res. ***26***, 63-7.

Neumann-Giesen, C., Falkenbach, B., Beicht, P., Claasen, S., Luers, G., Stuermer, C.A., Herzog, V., and Tikkanen, R. (2004). Membrane and raft association of reggie-1/flotillin-2: Role of myristoylation, palmitoylation and oligomerization and induction of filopodia by overexpression. Biochem. J. ***378***, 509-18.

Ng, W.O., Grossman, A.R., and Bhaya, D. (2003). Multiple light inputs control phototaxis in *Synechocystis* sp. strain PCC 6803. J. Bacteriol. ***185***, 1599-607.

Nield, J. (1997). Structural characterisation of photosystem II. Ph.D. thesis, University of London, UK.

Nijtmans, L.G., Artal, S.M., Grivell, L.A., and Coates, P.J. (2002). The mitochondrial PHB complex: Roles in mitochondrial respiratory complex assembly, ageing and degenerative disease. Cell. Mol. Life Sci. ***59***, 143-55.

Nijtmans, L.G., de Jong, L., Artal Sanz, M., Coates, P.J., Berden, J.A., Back, J.W., Muijsers, A.O., van der Spek, H., and Grivell, L.A. (2000). Prohibitins act as a membrane-bound chaperone for the stabilization of mitochondrial proteins. EMBO J. ***19***, 2444-51.

Nilsson, R., Brunner, J., Hoffman, N.E., and van Wijk, K.J. (1999). Interactions of ribosome nascent chain complexes of the chloroplast-encoded D1 thylakoid membrane protein with cpSRP54. EMBO J. ***18***, 733-42.

Nishiyama, Y., Allakhverdiev, S.I., and Murata, N. (2006). A new paradigm for the action of reactive oxygen species in the photoinhibition of photosystem II. Biochim. Biophys. Acta ***1757***, 742-9.

Nishiyama, Y., Allakhverdiev, S.I., Yamamoto, H. , Hayashi, H., and Murata, N. (2004). Singlet oxygen inhibits the repair of photosystem II by suppressing the translation elongation of the D1 protein in *Synechocystis* PCC 6803. Biochemistry ***43***, 11321-30.

Nishiyama, Y., Yamamoto, H., Allakhverdiev, S.I. , Inaba, M., Yokota, A., and Murata, N. (2001). Oxidative stress inhibits the repair of photodamage to the photosynthetic machinery. EMBO J. ***20***, 5587-94.

Niwa, H., Tsuchiya, D., Makyio, H., Yoshida, M., and Morikawa, K. (2002). Hexameric ring structure of the ATPase domain of the membrane-integrated metalloprotease FtsH from *Thermus thermophilus* HB8. Structure ***10***, 1415-23.

Nixon, P.J., Barker, M., Boehm, M., de Vries, R., and Komenda, J. (2005). FtsH-mediated repair of the photosystem II complex in response to light stress. J. Exp. Bot. ***56***, 357-63.

Nixon, P.J., Trost, J.T., and Diner, B.A. (1992). Role of the carboxy terminus of polypeptide D1 in the assembly of a functional water-oxidizing manganese cluster in photosystem II of the cyanobacterium *Synechocystis* sp. PCC 6803: Assembly requires a free carboxyl group at C-terminal position 344. Biochemistry ***31***, 10859-71.

Niyogi, K.K. (1999). Photoprotection revisited: Genetic and molecular approaches. Annu. Rev. Plant Physiol. Plant Mol. Biol. ***50***, 333-59.

Niyogi, K.K., Li, X.P., Rosenberg, V., and Jung, H.S. (2005). Is PsbS the site of non-photochemical quenching in photosynthesis? J. Exp. Bot. ***56***, 375-82.

Norling, B., Mirzakhanian, V., Nilsson, F., Morre, D.J., and Andersson, B. (1994). Subfractional analysis of cyanobacterial membranes and isolation of plasma membranes by aqueous polymer two-phase partitioning. Anal. Biochem. ***218***, 103-11.

Norling, B., Zak, E., Andersson, B., and Pakrasi, H. (1998). 2D-isolation of pure plasma and thylakoid membranes from the cyanobacterium *Synechocystis* sp. PCC 6803. FEBS Lett. ***436***, 189-92.

Novy, R., Drott, D., Yaeger, K., and Mierendorf, R. (2001). Overcoming the codon bias of ***E. coli*** for enhanced protein expression. Newsletter of Novagen, Inc. ***12***, 1-3.

Nuell, M.J., Stewart, D.A., Walker, L., Friedman, V., Wood, C.M., Owens, G.A., Smith, J.R., Schneider, E.L., dell' Orco, R., Lumpkin, C.K., Danner, D.B., and McClung, J.K. (1991). Prohibitin, an evolutionarily conserved intracellular protein that blocks DNA synthesis in normal fibroblasts and HeLa cells. Mol. Cell. Biol. ***11***, 1372-81.

Ogawa, T. (1991b). Cloning and inactivation of a gene essential to inorganic carbon transport of *Synechocystis* PCC6803. Plant Physiol. ***96***, 280-4.

Ogawa, T. (1991a). A gene homologous to the subunit-2 gene of NADH dehydrogenase is essential to inorganic carbon transport of *Synechocystis* PCC6803. Proc. Natl. Acad. Sci. USA ***88***, 4275-9.

Ogawa, T. and Kaplan, A. (2003). Inorganic carbon acquisition systems in cyanobacteria. Photosynth. Res. ***77***, 105-15.

Ogura, T., Inoue, K., Tatsuta, T., Suzaki, T., Karata, K., Young, K., Su, L.H., Fierke, C.A., Jackman, J.E., Raetz, C.R., Coleman, J. , Tomoyasu, T., and Matsuzawa, H. (1999). Balanced biosynthesis of major membrane components through regulated degradation of the committed enzyme of lipid A biosynthesis by the AAA protease FtsH (HflB) in *Escherichia coli*. Mol. Microbiol. ***31***, 833-44.

Ogura, T., Tomoyasu, T., Yuki, T., Morimura, S., Begg, K.J., Donachie, W.D., Mori, H., Niki, H., and Hiraga, S. (1991). Structure and function of the *ftsH* gene in *Escherichia coli*. Res. Microbiol. ***142***, 279-82.

Ogura, T. and Wilkinson, A.J. (2001). AAA+ superfamily ATPases: Common structure - diverse function. Genes Cells ***6***, 575-97.

Ohad, I., Keren, N., Zer, H., Gong, H., Mor, T.S. , Gal, A., Tal, S., and Domovich, Y. (1994). Light-induced degradation of the PSII reaction centre D1 protein *in vivo*: An integrative approach. *In*: Baker, Bowyer (eds). Photoinhibition of photosynthesis. Bios Scientific Publishers, Oxford, UK. 161-77.

Ohad, I., Kyle, D.J., and Arntzen, C.J. (1984). Membrane protein damage and repair: Removal and replacement of inactivated 32-kilodalton polypeptides in chloroplast membranes. J. Cell Biol. ***99***, 481-5.

Ohkawa, H., Pakrasi, H.B., and Ogawa, T. (2000). Two types of functionally distinct NAD(P)H dehydrogenases in *Synechocystis* sp. strain PCC6803. J. Biol. Chem. ***275***, 31630-4.

Ohnishi, N., Allakhverdiev, S.I., Takahashi, S., Higashi, S., Watanabe, M., Nishiyama, Y., and Murata, N. (2005). Two-step mechanism of photodamage to photosystem II: Step 1 occurs at the oxygen-evolving complex and step 2 occurs at the photochemical reaction center. Biochemistry ***44***, 8494-9.

Okamoto, S., Ikeuchi, M., and Ohmori, M. (1999). Experimental analysis of recently transposed insertion sequences in the cyanobacterium *Synechocystis* sp. PCC 6803. DNA Res. ***6***, 265-73.

Omata, T. and Ogawa, T. (1986). Biosynthesis of a 42-kD polypeptide in the cytoplasmic membrane of the cyanobacterium *Anacystis nidulans* strain R2 during adaptation to low CO_2 concentration. Plant Physiol. ***80***, 525-30.

Omata, T. and Ogawa, T. (1985). Changes in the polypeptide composition of the cytoplasmic membrane in the cyanobacterium *Anacystis nidulans* during adaptation to low carbon dioxide conditions. Plant Cell Physiol. ***26***, 1075-81.

Omata, T., Price, G.D., Badger, M.R., Okamura, M., Gohta, S., and Ogawa, T. (1999). Identification of an ATP-binding cassette transporter involved in bicarbonate uptake in the cyanobacterium *Synechococcus* sp. strain PCC 7942. Proc. Natl. Acad. Sci. USA ***96***, 13571-6.

Panichkin, V.B., Arakawa-Kobayashi, S., Kanaseki, T., Suzuki, I., Los, D.A., Shestakov, S.V., and Murata, N. (2006). Serine/threonine protein kinase SpkA in *Synechocystis* sp. strain PCC 6803 is a regulator of expression of three putative pilA operons, formation of thick pili, and cell motility. J. Bacteriol. *188*, 7696-9.

Paschen, S.A., Rothbauer, U., Kaldi, K., Bauer, M.F., Neupert, W., and Brunner, M. (2000). The role of the TIM8-13 complex in the import of Tim23 into mitochondria. EMBO J. ***19***, 6392-400.

Peltier, G. and Cournac, L. (2002). Chlororespiration. Annu. Rev. Plant. Biol. ***53***, 523-50.

Peschek, G.A., Obinger, C., and Paumann, M. (2004). The respiratory chain of blue-green algae (cyanobacteria). Physiol. Plant. ***120***, 358-369.

Piper, P.W. and Bringloe, D. (2002). Loss of prohibitins, though it shortens the replicative life span of yeast cells undergoing division, does not shorten the chronological life span of G_0-arrested cells. Mech. Ageing Dev. ***123***, 287-95.

Piper, P.W., Jones, G.W., Bringloe, D., Harris, N., MacLean, M., and Mollapour, M. (2002). The shortened replicative life span of prohibitin mutants of yeast appears to be due to defective mitochondrial segregation in old mother cells. Aging Cell ***1***, 149-57.

Prasil, O., Adir, N., and Ohad, I. (1992). Dynamics of PSII: Mechanism of photoinhibition and recovery processes. *In*: Barber (ed), The photosystems: Structure, function and molecular biology. Elsevier Science Publishers, Amsterdam, The Netherlands. 295-8.

Prentki, P. and Krisch, H.M. (1984). *In vitro* insertional mutagenesis with a selectable DNA fragment. Gene ***29***, 303-13.

Price, M.P., Thompson, R.J., Eshcol, J.O., Wemmie, J.A., and Benson, C.J. (2004). Stomatin modulates gating of acid-sensing ion channels. J. Biol. Chem. ***279***, 53886-91.

Qiu, X.B., Shao, Y.M., Miao, S., and Wang, L. (2006). The diversity of the DnaJ/Hsp40 family, the crucial partners for Hsp70 chaperones. Cell. Mol. Life Sci. ***63***, 2560-70.

Rao, M.V. and Davis, K.R. (1999). Ozone-induced cell death occurs via two distinct mechanisms in *Arabidopsis*: The role of salicylic acid. Plant J. ***17***, 603-14.

Reuter, W. and Müller, C. (1993). New trends in photobiology: Adaptation of the photosynthetic apparatus of cyanobacteria to light and CO_2. J. Photochem. Photobiol. B Biol. ***21***, 3-27.

Rintamäki, E., Kettunen, R., and Aro, E.M. (1996). Differential D1 dephosphorylation in functional and photodamaged photosystem II centers. Dephosphorylation is a prerequisite for degradation of damaged D1. J. Biol. Chem. ***271***, 14870-5.

Rippka, R., Deruelles, J., Waterbury, J.B., Herdman, M., and Stanier, R. (1979). Genetic assignments, strain histories and properties of pure cultures of cyanobacteria. J. Gen. Microbiol. ***111***, 1-61.

Rippka, R. and Herdman, M. (1992). Catalogue of strains. Pasteur Culture Collection of cyanobacterial strains in axenic culture.

Rivera-Milla, E., Stuermer, C.A., and Malaga-Trillo, E. (2006). Ancient origin of reggie (flotillin), reggie-like, and other lipid-raft proteins: Convergent evolution of the SPFH domain. Cell. Mol. Life Sci. ***63***, 343-57.

Robson, A. and Collinson, I. (2006). The structure of the Sec complex and the problem of protein translocation. EMBO Rep. ***7***, 1099-103.

Roise, D. and Schatz, G. (1988). Mitochondrial presequences. J. Biol. Chem. ***263***, 4509-11.

Rokka, A., Suorsa, M., Saleem, A., Battchikova, N., and Aro, E.M. (2005). Synthesis and assembly of thylakoid protein complexes: Multiple assembly steps of photosystem II. Biochem. J. ***388***, 159-68.

Rose, R.E. (1988). The nucleotide sequence of pACYC184. Nucleic Acids Res. ***16***, 355

Rosegrant, M.W., Sombilla, M.A., and Perez, N. (1995). Food, agriculture and the environment. Discussion paper No. 5

Rostoks, N., Schmierer, D., Kudrna, D., and Kleinhofs, A. (2003). Barley putative hypersensitive induced reaction genes: Genetic mapping, sequence analyses and differential expression in disease lesion mimic mutants. Theor. Appl. Genet. ***107***, 1094-101.

Roy, L.M. and Barkan, A. (1998). A SecY homologue is required for the elaboration of the chloroplast thylakoid membrane and for normal chloroplast gene expression. J. Cell Biol. ***141***, 385-95.

Ruban, A.V., Young, A.J., and Horton, P. (1993). Induction of nonphotochemical energy dissipation and absorbance changes in leaves (evidence for changes in the state of the light-harvesting system of photosystem II *in vivo*). Plant Physiol. ***102***, 741-50.

Ruprecht, J. and Nield, J. (2001). Determining the structure of biological macromolecules by transmission electron microscopy, single particle analysis and 3D reconstruction. Prog. Biophys. Mol. Biol. ***75***, 121-64.

Rusch, S.L. and Kendall, D.A. (1995). Protein transport via amino-terminal targeting sequences: Common themes in diverse systems. Mol. Membr. Biol. ***12***, 295-307.

Rögner, M., Chisholm, D.A., and Diner, B.A. (1991). Site-directed mutagenesis of the *psbC* gene of photosystem II: Isolation and functional characterization of CP43-less photosystem II core complexes. Biochemistry ***30***, 5387-95.

Saikawa, N., Akiyama, Y., and Ito, K. (2004). FtsH exists as an exceptionally large complex containing HflK/C in the plasma membrane of *Escherichia coli*. J. Struct. Biol. ***146***, 123-9.

Salter, A.H., Virgin, I., Hagman, A., and Andersson, B. (1992). On the molecular mechanism of light-induced D1 protein degradation in photosystem II core particles. Biochemistry ***31***, 3990-8.

Salzer, U., Ahorn, H., and Prohaska, R. (1993). Identification of the phosphorylation site on human erythrocyte band 7 integral membrane protein: Implications for a monotopic protein structure. Biochim. Biophys. Acta ***1151***, 149-52.

Salzer, U. and Prohaska, R. (2001). Stomatin, flotillin-1, and flotillin-2 are major integral proteins of erythrocyte lipid rafts. Blood ***97***, 1141-3.

Sambrook, J., Fritsch, E.F., and Maniatis, T. (1989). Molecular cloning: A laboratory manual. Second edition. Cold Spring Harbor Laboratory Press, New York, USA.

Samuel, B.U., Mohandas, N., Harrison, T., McManus, H., Rosse, W., Reid, M., and Haldar, K. (2001). The role of cholesterol and glycosylphosphatidylinositol-anchored proteins of erythrocyte rafts in regulating raft protein content and malarial infection. J. Biol. Chem. ***276***, 29319-29.

Samuelson, J.C., Chen, M., Jiang, F., Moller, I., Wiedmann, M., Kuhn, A., Phillips, G.J., and Dalbey, R.E. (2000). YidC mediates membrane protein insertion in bacteria. Nature ***406***, 637-41.

Santos, D. and de Almeida, D.F. (1975). Isolation and characterization of a new temperature-sensitive cell division mutant of *Escherichia coli* K-12. J. Bacteriol. ***124***, 1502-7.

Saraste, M. (1999). Oxidative phosphorylation at the fin de siecle. Science ***283***, 1488-93.

Sato, T., Saito, H., Swensen, J., Olifant, A., Wood, C., Danner, D., Sakamoto, T., Takita, K., Kasumi, F., Miki, Y., Skolnick, M., and Nakamura, Y. (1992). The human prohibitin gene located on chromosome 17q21 is mutated in sporadic breast cancer. Cancer Res. ***52***, 1643-6.

Schatz, G. and Dobberstein, B. (1996). Common principles of protein translocation across membranes. Science ***271***, 1519-26.

Schatz, P.J. and Beckwith, J. (1990). Genetic analysis of protein export in *Escherichia coli*. Annu. Rev. Genet. ***24***, 215-48.

Schneppenheim, R., Budde, U., Dahlmann, N., and Rautenberg, P. (1991). Luminography - a new, highly sensitive visualization method for electrophoresis. Electrophoresis ***12***, 367-72.

Schroeder, W.T., Stewart-Galetka, S., Mandavilli, S., Parry, D.A., Goldsmith, L., and Duvic, M. (1994). Cloning and characterization of a novel epidermal cell surface antigen (ESA). J. Biol. Chem. ***269***, 19983-91.

Schulte, T., Paschke, K.A., Laessing, U., Lottspeich, F., and Stuermer, C.A. (1997). Reggie-1 and reggie-2, two cell surface proteins expressed by retinal ganglion cells during axon regeneration. Development ***124***, 577-87.

Schägger, H., Cramer, W.A., and von Jagow, G. (1994). Analysis of molecular masses and oligomeric states of protein complexes by blue native electrophoresis and isolation of membrane protein complexes by two-dimensional native electrophoresis. Anal. Biochem. ***217***, 220-30.

Schägger, H. and von Jagow, G. (1991). Blue-native electrophoresis for isolation of membrane protein complexes in enzymatically active form. Anal. Biochem. ***199***, 223-31.

Scotti, P.A., Urbanus, M.L., Brunner, J., de Gier, J.W., von Heijne, G., van der Does, C., Driessen, A.J., Oudega, B., and Luirink, J. (2000). YidC, the *Escherichia coli* homologue of mitochondrial Oxa1p, is a component of the Sec translocase. EMBO J. ***19***, 542-9.

Sedensky, M.M., Siefker, J.M., and Morgan, P.G. (2001). Model organisms: New insights into ion channel and transporter function. Stomatin homologues interact in *Caenorhabditis elegans*. Am. J. Physiol. Cell Physiol. ***280***, C1340-8.

Shacter, E., Williams, J.A., Lim, M., and Levine, R.L. (1994). Differential susceptibility of plasma proteins to oxidative modification: Examination by western blot immunoassay. Free Radic. Biol. Med. ***17***, 429-37.

Shen, J.R. and Inoue, Y. (1993). Binding and functional properties of two new extrinsic components, cytochrome c-550 and a 12-kDa protein, in cyanobacterial photosystem II. Biochemistry ***32***, 1825-32.

Sherman, D.M., Troyan, T.A., and Sherman, L.A. (1994). Localization of membrane proteins in the cyanobacterium *Synechococcus* sp. PCC7942 (radial asymmetry in the photosynthetic complexes). Plant Physiol. ***106***, 251-62.

Shibata, M., Katoh, H., Sonoda, M., Ohkawa, H., Shimoyama, M., Fukuzawa, H., Kaplan, A., and Ogawa, T. (2002). Genes essential to sodium-dependent bicarbonate transport in cyanobacteria: Function and phylogenetic analysis. J. Biol. Chem. ***277***, 18658-64.

Shibata, M., Ohkawa, H., Kaneko, T., Fukuzawa, H., Tabata, S., Kaplan, A., and Ogawa, T. (2001). Distinct constitutive and low-CO_2-induced CO_2 uptake systems in cyanobacteria: Genes involved and their phylogenetic relationship with homologous genes in other organisms. Proc. Natl. Acad. Sci. USA ***98***, 11789-94.

Shikanai, T., Munekage, Y., and Kimura, K. (2002). Regulation of proton-to-electron stoichiometry in photosynthetic electron transport: Physiological function in photoprotection. J. Plant Res. ***115***, 3-10.

Shipton, C.A. and Barber, J. (1991). Photoinduced degradation of the D1 polypeptide in isolated reaction centers of photosystem II: Evidence for an autoproteolytic process triggered by the oxidizing side of the photosystem. Proc. Natl. Acad. Sci. USA ***88***, 6691-5.

Short, J.M., Fernandez, J.M., Sorge, J.A., and Huse, W.D. (1988). Lambda ZAP: A bacteriophage lambda expression vector with *in vivo* excision properties. Nucleic Acids Res. ***16***, 7583-600.

Shotland, Y., Shifrin, A., Ziv, T., Teff, D., Koby, S., Kobiler, O., and Oppenheim, A.B. (2000). Proteolysis of bacteriophage lambda cII by *Escherichia coli* FtsH (HflB). J. Bacteriol. ***182***, 3111-6.

Sigrist, C.J., Cerutti, L., Hulo, N., Gattiker, A., Falquet, L., Pagni, M., Bairoch, A., and Bucher, P. (2002). PROSITE: A documented database using patterns and profiles as motif descriptors. Brief Bioinform. ***3***, 265-74.

Silva, P., Choi, Y.J., Hassan, H.A., and Nixon, P.J. (2002). Involvement of the HtrA family of proteases in the protection of the cyanobacterium *Synechocystis* PCC 6803 from light stress and in the repair of photosystem II. Philos. Trans. R. Soc. Lond. B. Biol. Sci. ***357***, 1461-7; discussion 1467-70.

Silva, P. and Nixon, P.J. (2001). Identification of possible assembly and repair factors in photosystem two preparations of *Synechocystis* sp. PCC 6803: A new model for D1 turnover. Proceedings 12th International Congress on Photosynthesis. Canberra, Australia.

Silva, P., Thompson, E., Bailey, S., Kruse, O., Mullineaux, C.W., Robinson, C., Mann, N.H., and Nixon, P.J. (2003). FtsH is involved in the early stages of repair of photosystem II in *Synechocystis* sp PCC 6803. Plant Cell ***15***, 2152-64.

Simons, K. and Ehehalt, R. (2002). Cholesterol, lipid rafts, and disease. J. Clin. Invest. ***110***, 597-603.

Sippola, K. and Aro, E.M. (2000). Expression of *psbA* genes is regulated at multiple levels in the cyanobacterium *Synechococcus* sp. PCC 7942. Photochem. Photobiol. ***71***, 706-14.

Small, I., Peeters, N., Legeai, F., and Lurin, C. (2004). Predotar: A tool for rapidly screening proteomes for N-terminal targeting sequences. Proteomics ***4***, 1581-90.

Smith, D. and Howe, C.J. (1993). The distribution of photosystem I and photosystem II polypeptides between the cytoplasmic and thylakoid membranes of cyanobacteria. FEMS Microbiol. Lett. ***110***, 341-7.

Snedden, W.A. and Fromm, H. (1997). Characterization of the plant homologue of prohibitin, a gene associated with antiproliferative activity in mammalian cells. Plant Mol. Biol. ***33***, 753-6.

Snyers, L., Umlauf, E., and Prohaska, R. (1998). Oligomeric nature of the integral membrane protein stomatin. J. Biol. Chem. ***273***, 17221-6.

Sokolenko, A., Pojidaeva, E., Zinchenko, V., Panichkin, V., Glaser, V.M., Herrmann, R.G., and Shestakov, S.V. (2002). The gene complement for proteolysis in the cyanobacterium *Synechocystis* sp. PCC 6803 and *Arabidopsis thaliana* chloroplasts. Curr. Genet. ***41***, 291-310.

Spence, E., Bailey, S., Nenninger, A., Moller, S.G., and Robinson, C. (2004). A homolog of Albino3/OxaI is essential for thylakoid biogenesis in the cyanobacterium *Synechocystis* sp. PCC6803. J. Biol. Chem. ***279***, 55792-800.

Spetea, C., Hundal, T., Lohmann, F., and Andersson, B. (1999). GTP bound to chloroplast thylakoid membranes is required for light-induced, multienzyme degradation of the photosystem II D1 protein. Proc. Natl. Acad. Sci. USA ***96***, 6547-52.

Spetea, C., Keren, N., Hundal, T., Doan, J.M., Ohad, I., and Andersson, B. (2000). GTP enhances the degradation of the photosystem II D1 protein irrespective of its conformational heterogeneity at the Q_B site. J. Biol. Chem. ***275***, 7205-11.

Stanier, R.Y. (1973). The biology of blue-green algae. Autotrophy and heterotrophy in unicellular blue-green algae. Botanical Monographs (Oxford) ***9***, 501-18.

Stanier R. Y. , Kunisawa R. , Mandel M. , and Cohen-Bazire G. (1971). Purification and properties of unicellular blue-green algae (order Chroococcales). Bacteriol. rev. ***35***, 171-205.

Steglich, G., Neupert, W., and Langer, T. (1999). Prohibitins regulate membrane protein degradation by the m-AAA protease in mitochondria. Mol. Cell. Biol. ***19***, 3435-42.

Stewart, G.W. (2004). Hemolytic disease due to membrane ion channel disorders. Curr. Opin. Hematol. ***11***, 244-50.

Stewart, G.W. (1997). Stomatin. Int. J. Biochem. Cell Biol. ***29***, 271-4.

Stewart, G.W., Hepworth-Jones, B.E., Keen, J.N., Dash, B.C., Argent, A.C., and Casimir, C.M. (1992). Isolation of cDNA coding for an ubiquitous membrane protein deficient in high Na+, low K+ stomatocytic erythrocytes. Blood ***79***, 1593-601.

Studier, F.W. and Moffatt, B.A. (1986). Use of bacteriophage T7 RNA polymerase to direct selective high-level expression of cloned genes. J. Mol. Biol. ***189***, 113-30.

Styring, S., Virgin, I., Ehrenberg, A., and Andersson, B. (1990). Strong light photoinhibition of electron-transport in photosystem II - Impairment of the function of the 1st quinone acceptor, Q_A. Biochim. Biophys. Acta ***1015***, 269-78.

Summons, R.E., Jahnke, L.L., Hope, J.M., and Logan, G.A. (1999). 2-Methylhopanoids as biomarkers for cyanobacterial oxygenic photosynthesis. Nature ***400***, 554-7.

Sun, L., Liu, L., Yang, X.J., and Wu, Z. (2004). Akt binds prohibitin 2 and relieves its repression of MyoD and muscle differentiation. J. Cell Sci. ***117***, 3021-9.

Suorsa, M., Regel, R.E., Paakkarinen, V., Battchikova, N., Herrmann, R.G., and Aro, E.M. (2004). Protein assembly of photosystem II and accumulation of subcomplexes in the absence of low molecular mass subunits PsbL and PsbJ. Eur. J. Biochem. ***271***, 96-107.

Suzuki, S., Ferjani, A., Suzuki, I., and Murata, N. (2004). The SphS-SphR two component system is the exclusive sensor for the induction of gene expression in response to phosphate limitation in *Synechocystis*. J. Biol. Chem. ***279***, 13234-40.

Taghi-Kilani, R., Gyurek, L.L., Millard, P.J., Finch, G.R., and Belosevic, M. (1996). Nucleic acid stains as indicators of *Giardia muris* viability following cyst inactivation. Int. J. Parasitol ***26***, 637-46.

Takahashi, A., Kawasaki, T., Wong, H.L., Suharsono, U., Hirano, H., and Shimamoto, K. (2003). Hyperphosphorylation of a mitochondrial protein, prohibitin, is induced by calyculin A in a rice lesion-mimic mutant cdr1. Plant Physiol. ***132***, 1861-9.

Takeda, T., Yokota, A., and Shigeoka, S. (1995). Resistance of photosynthesis to hydrogen peroxide in algae. Plant Cell Physiol. ***36***, 1089-95.

Tamoi, M., Murakami, A., Takeda, T., and Shigeoka, S. (1998). Acquisition of a new type of fructose-1,6-bisphosphatase with resistance to hydrogen peroxide in cyanobacteria: Molecular characterization of the enzyme from *Synechocystis* PCC 6803. Biochim. Biophys. Acta ***1383***, 232-44.

Tannert, A., Pohl, A., Pomorski, T., and Herrmann, A. (2003). Protein-mediated transbilayer movement of lipids in eukaryotes and prokaryotes: The relevance of ABC transporters. Int. J. Antimicrob. Agents ***22***, 177-87.

Tatsuta, T., Model, K., and Langer, T. (2004). Formation of membrane-bound ring complexes by prohibitins in mitochondria. Mol. Biol. Cell ***16***, 248-59.

Tatsuta, T., Model, K., and Langer, T. (2005). Formation of membrane-bound ring complexes by prohibitins in mitochondria. Mol. Biol. Cell ***16***, 248-59.

Taura, T., Baba, T., Akiyama, Y., and Ito, K. (1993). Determinants of the quantity of the stable SecY complex in the *Escherichia coli* cell. J. Bacteriol. ***175***, 7771-5.

Tavernarakis, N. and Driscoll, M. (1997). Molecular modeling of mechanotransduction in the nematode *Caenorhabditis elegans*. Annu. Rev. Physiol. ***59***, 659-89.

Tavernarakis, N., Driscoll, M., and Kyrpides, N.C. (1999). The SPFH domain: Implicated in regulating targeted protein turnover in stomatins and other membrane-associated proteins. Trends Biochem. Sci. ***24***, 425-7.

Taylor, L.A. and Rose, R.E. (1988). A correction in the nucleotide sequence of the Tn903 kanamycin-resistance determinant in pUC4K. Nucleic Acids Res. ***16***, 358

Terashima, M., Kim, K.M., Adachi, T., Nielsen, P.J., Reth, M., Kohler, G., and Lamers, M.C. (1994). The IgM antigen receptor of B lymphocytes is associated with prohibitin and a prohibitin-related protein. EMBO J. ***13***, 3782-92.

Terauchi, K. and Ohmori, M. (1999). An adenylate cyclase, Cya1, regulates cell motility in the cyanobacterium *Synechocystis* sp. PCC 6803. Plant Cell Physiol. ***40***, 248-51.

Tetenkin, V.L., Golitsin, V.M., and Gulyaev, B.A. (1998). Stress protein of cyanobacteria CP36: Interaction with photoactive complexes and formation of supramolecular structures. Biochemistry (Moscow) ***63***, 584-91.

Thompson, J.D., Higgins, D.G., and Gibson, T.J. (1994). CLUSTAL W: Improving the sensitivity of progressive multiple sequence alignment through sequence weighting, position-specific gap penalties and weight matrix choice. Nucleic Acids Res. ***22***, 4673-80.

Thompson, L.K. and Brudvig, G.W. (1988). Cytochrome b-559 may function to protect photosystem II from photoinhibition. Biochemistry ***27***, 6653-8.

Thornton, L.E., Ohkawa, H., Roose, J.L., Kashino, Y., Keren, N., and Pakrasi, H.B. (2004). Homologs of plant PsbP and PsbQ proteins are necessary for regulation of photosystem II activity in the cyanobacterium *Synechocystis* 6803. Plant Cell ***16***, 2164-75.

Tichy, M., Lupinkova, L., Sicora, C., Vass, I., Kuvikova, S., Prasil, O., and Komenda, J. (2003). *Synechocystis* 6803 mutants expressing distinct forms of the photosystem II D1 protein from *Synechococcus* 7942: Relationship between the *psbA* coding region and sensitivity to visible and UV-B radiation. Biochim. Biophys. Acta ***1605***, 55-66.

Tilman, D., Cassman, K.G., Matson, P.A., Naylor, R., and Polasky, S. (2002). Agricultural sustainability and intensive production practices. Nature ***418***, 671-7.

Towbin, H., Staehelin, T., and Gordon, J. (1979). Electrophoretic transfer of proteins from polyacrylamide gels to nitrocellulose sheets: Procedure and some applications. Proc. Natl. Acad. Sci. USA ***76***, 4350-4.

Trebst, A. (1978). Plastoquinones in photosynthesis. Philos. Trans. R. Soc. Lond. B Biol. Sci. ***284***, 591-9.

Tyystjärvi, E. and Aro, E.M. (1996). The rate constant of photoinhibition, measured in lincomycin-treated leaves, is directly proportional to light intensity. Proc. Natl. Acad. Sci. USA ***93***, 2213-8.

Tzagoloff, A., Barrientos, A., Neupert, W., and Herrmann, J.M. (2004). Atp10p assists assembly of Atp6p into the F0 unit of the yeast mitochondrial ATPase. J. Biol. Chem. ***279***, 19775-80.

Umlauf, E., Csaszar, E., Moertelmaier, M., Schuetz, G.J., Parton, R.G., and Prohaska, R. (2004). Association of stomatin with lipid bodies. J. Biol. Chem. ***279***, 23699-709.

Umlauf, E., Mairhofer, M., and Prohaska, R. (2006). Characterization of the stomatin domain involved in homo-oligomerization and lipid raft association. J. Biol. Chem. ***281***, 23349-56.

van de Meene, A.M., Hohmann-Marriott, M.F., Vermaas, W.F., and Roberson, R.W. (2006). The three-dimensional structure of the cyanobacterium *Synechocystis* sp. PCC 6803. Arch. Microbiol. ***184***, 259-70.

van der Heiden, M.G., Choy, J.S., van der Weele, D.J., Brace, J.L., Harris, M.H., Bauer, D.E., Prange, B., Kron, S.J., Thompson, C.B., and Rudin, C.M. (2002). Bcl-x(L) complements *Saccharomyces cerevisiae* genes that facilitate the switch from glycolytic to oxidative metabolism. J. Biol. Chem. ***277***, 44870-6.

van Heel, M., Gowen, B., Matadeen, R., Orlova, E.V., Finn, R., Pape, T., Cohen, D., Stark, H., Schmidt, R., Schatz, M., and Patwardhan, A. (2000). Single-particle electron cryo-microscopy: Towards atomic resolution. Q. Rev. Biophys. ***33***, 307-69.

van Heel, M., Harauz, G., Orlova, E.V., Schmidt, R., and Schatz, M. (1996). A new generation of the IMAGIC image processing system. J. Struc. Biol. ***116***, 17-24.

Vasil'ev, S., Brudvig, G.W., and Bruce, D. (2003). The X-ray structure of photosystem II reveals a novel electron transport pathway between P680, cytochrome b559 and the energy-quenching cation, Chl_Z+. FEBS Lett. ***543***, 159-63.

Vass, I., Styring, S., Hundal, T., Koivuniemi, A., Aro, E.M., and Andersson, B. (1992). Reversible and irreversible intermediates during photoinhibition of photosystem II. Stable reduced Q_A species promote chlorophyll triplet formation. Proc. Natl. Acad. Sci. USA ***89***, 1408-12.

Vermaas, W.F.J., Ikeuchi, M., and Inoue, Y. (1988). Protein composition of the photosystem II core complex in genetically engineered mutants of the cyanobacterium *Synechocystis* sp. PCC 6803. Photosynth. Res. ***17***, 97-113.

Volonte, D., Galbiati, F., Li, S., Nishiyama, K., Okamoto, T., and Lisanti, M.P. (1999). Flotillins/cavatellins are differentially expressed in cells and tissues and form a hetero-oligomeric complex with caveolins *in vivo*. Characterization and epitope-mapping of a novel flotillin-1 monoclonal antibody probe. J. Biol. Chem. ***274***, 12702-9.

Wada, H., Gombos, Z., and Murata, N. (1994). Contribution of membrane lipids to the ability of the photosynthetic machinery to tolerate temperature stress. Proc. Natl. Acad. Sci. USA ***91***, 4273-7.

Walsh, P., Bursac, D., Law, Y.C., Cyr, D., and Lithgow, T. (2004). The J-protein family: Modulating protein assembly, disassembly and translocation. EMBO Rep. ***5***, 567-71.

Wang, H.L., Postier, B.L., and Burnap, R.L. (2004). Alterations in global patterns of gene expression in *Synechocystis* sp. PCC 6803 in response to inorganic carbon limitation and the inactivation of *ndhR*, a LysR family regulator. J. Biol. Chem. ***279***, 5739-51.

Wang, K.J., Wang, R.T., and Zhang, J.Z. (2004). Identification of tumor markers using two-dimensional electrophoresis in gastric carcinoma. World J. Gastroenterol. ***10***, 2179-83.

Watson, A., Mazumder, A., Stewart, M., and Balasubramanian, S. (1998). Technology for microarray analysis of gene expression. Curr. Opin. Biotechnol. ***9***, 609-14.

Weiner, M.P., Anderson, C., Jersepth, B., Wells, S., and Johnson-Browne, B. (1994). Studier pET system vectors and hosts. Strategies ***7***, 41-3.

Westphal, S., Heins, L., Soll, J., and Vothknecht, U.C. (2001). *Vipp1* deletion mutant of *Synechocystis*: A connection between bacterial phage shock and thylakoid biogenesis? Proc. Natl. Acad. Sci. USA ***98***, 4243-8.

Wilkins, M.R., Gasteiger, E., Bairoch, A., Sanchez, J.C., Williams, K.L., Appel, R.D., and Hochstrasser, D.F. (1999). Protein identification and analysis tools in the ExPASy server. Methods Mol. Biol. ***112***, 531-52.

Williams, J.G.K. (1988). Construction of specific mutations in photosystem II photosynthetic reaction center by genetic-engineering methods in *Synechocystis* 6803. Methods Enzymol. ***167***, 766-78.

Wilson, A., Ajlani, G., Verbavatz, J.M., Vass, I., Kerfeld, C.A., and Kirilovsky, D. (2006). A soluble carotenoid protein involved in phycobilisome-related energy dissipation in cyanobacteria. Plant Cell ***18***, 992-1007.

Wingler, A., Lea, P.J., Quick, W.P., and Leegood, R.C. (2000). Photorespiration: Metabolic pathways and their role in stress protection. Philos. Trans. R. Soc. Lond. B Biol. Sci. ***355***, 1517-29.

Xu, Z., Horwich, A.L., and Sigler, P.B. (1997). The crystal structure of the asymmetric GroEL-GroES-(ADP)7 chaperonin complex. Nature ***388***, 741-50.

Yamaoka, T., Satoh, K., and Katoh, S. (1978). Photosynthetic activities of a thermophilic blue-green alga. Plant Cell Physiol. ***19***, 943-54.

Yao, D., Kieselbach, T., Komenda, J., Promnares, K., Prieto, M.A., Tichy, M., Vermaas, W., and Funk, C. (2007). Localization of the small cab-like proteins in photosystem II. J. Biol. Chem. ***282***, 267-76.

Yeremenko, N., Kouril, R., Ihalainen, J.A., d'Haene, S., van Oosterwijk, N., Andrizhiyevskaya, E.G., Keegstra, W., Dekker, H.L., Hagemann, M., Boekema, E.J., Matthijs, H.C.P., and Dekker, J.P. (2004). Supramolecular organization and dual function of the IsiA chlorophyll-binding protein in cyanobacteria. Biochemistry ***43***, 10308-13.

Yoshihara, S., Suzuki, F., Fujita, H., Geng, X.X., and Ikeuchi, M. (2000). Novel putative photoreceptor and regulatory genes required for the positive phototactic movement of the unicellular motile cyanobacterium *Synechocystis* sp. PCC 6803. Plant Cell Physiol. ***41***, 1299-304.

Yoshimura, H., Yoshihara, S., Okamoto, S., Ikeuchi, M., and Ohmori, M. (2002). A cAMP receptor protein, SYCRP1, is responsible for the cell motility of *Synechocystis* sp. PCC 6803. Plant Cell Physiol. ***43***, 460-3.

Yousef, N., Pistorius, E.K., and Michel, K.-P. (2003). Comparative analysis of *idiA* and *isiA* transcription under iron starvation and oxidative stress in *Synechococcus elongatus* PCC 7942 wild-type and selected mutants. Arch. Microbiol. ***180***, 471-83.

Zahn, R., Perrett, S., and Fersht, A.R. (1996). Conformational states bound by the molecular chaperones GroEL and SecB: A hidden unfolding (annealing) activity. J. Mol. Biol. ***261***, 43-61.

Zak, E., Norling, B., Maitra, R., Huang, F., Andersson, B., and Pakrasi, H.B. (2001). The initial steps of biogenesis of cyanobacterial photosystems occur in plasma membranes. Proc. Natl. Acad. Sci. USA ***98***, 13443-8.

Zhang, J.Z., Abbud, W., Prohaska, R., and Ismail-Beigi, F. (2001a). Overexpression of stomatin depresses GLUT-1 glucose transporter activity. Am. J. Physiol. Cell Physiol. ***280***, C1277-83.

Zhang, J.Z., Hayashi, H., Ebina, Y., Prohaska, R., and Ismail-Beigi, F. (1999a). Association of stomatin (band 7.2b) with GLUT1 glucose transporter. Arch. Biochem. Biophys. ***372***, 173-8.

Zhang, L., Paakkarinen, V., Suorsa, M., and Aro, E.M. (2001b). A SecY homologue is involved in chloroplast-encoded D1 protein biogenesis. J. Biol. Chem. ***276***, 37809-14.

Zhang, L., Paakkarinen, V., van Wijk, K.J., and Aro, E.M. (2000). Biogenesis of the chloroplast-encoded D1 protein: Regulation of translation elongation, insertion, and assembly into photosystem II. Plant Cell ***12***, 1769-82.

Zhang, L., Paakkarinen, V., van Wijk, K.J., and Aro, E.M. (1999b). Co-translational assembly of the D1 protein into photosystem II. J. Biol. Chem. ***274***, 16062-7.

Zhang, P., Battchikova, N., Jansen, T., Appel, J., Ogawa, T., and Aro, E.M. (2004). Expression and functional roles of the two distinct NDH-1 complexes and the carbon acquisition complex NdhD3/NdhF3/CupA/Sll1735 in *Synechocystis* sp. PCC 6803. Plant Cell ***16***, 3326-40.

Zhang, P., Battchikova, N., Paakkarinen, V., Katoh, H., Iwai, M., Ikeuchi, M., Pakrasi, H.B., Ogawa, T., and Aro, E.M. (2005). Isolation, subunit composition and interaction of the NDH-1 complexes from *Thermosynechococcus elongatus* BP-1. Biochem J. ***390***, 513-20.

Zhang, X. and Studier, F.W. (1997). Mechanism of inhibition of bacteriophage T7 RNA polymerase by T7 lysozyme. J. Mol. Biol. ***269***, 10-27.

Zhu, Y., Paszty, C., Turetsky, T., Tsai, S., Kuypers, F.A., Lee, G., Cooper, P., Gallagher, P.G., Stevens, M.E., Rubin, E., Mohandas, N., and Mentzer, W.C. (1999). Stomatocytosis is absent in "stomatin"-deficient murine red blood cells. Blood ***93***, 2404-10.

Zolla, L. and Rinalducci, S. (2002). Involvement of active oxygen species in degradation of light-harvesting proteins under light stresses. Biochemistry ***41***, 14391-402.

Zorick, T.S. and Echols, H. (1991). Membrane localization of the HflA regulatory protease of *Escherichia coli* by immunoelectron microscopy. J. Bacteriol. ***173***, 6307-10.

Zouni, A., Witt, H.T., Kern, J., Fromme, P., Krauss, N., Saenger, W., and Orth, P. (2001). Crystal structure of photosystem II from *Synechococcus elongatus* at 3.8 A resolution. Nature ***409***, 739-43.

Zurawski, G., Bohnert, H.J., Whitfeld, P.R., and Bottomley, W. (1982). Nucleotide sequence of the gene for the M(r) 32,000 thylakoid membrane protein from *Spinacia oleracea* and *Nicotiana debneyi* predicts a totally conserved primary translation product of M(r) 38,950. Proc. Natl. Acad. Sci. USA ***79***, 7699-703.